DOCTOR OF PHILOSOPHY

GPR55 and N-acyl Amino Acids

Penman, June

Award date:
2013

DOCTOR OF PHILOSOPHY

GPR55 and N-acyl Amino Acids

June Penman

2013

University of Dundee

GPR55 and N-acyl Amino Acids

June Penman

A thesis submitted to the University of Dundee in candidature for the degree of Doctor of Philosophy, December 2013.

Some of nature's beauty is hidden from the naked eye.
Science provides the tools to allow us to see.

i. TABLE OF CONTENTS

ii. LIST OF FIGURES

iii. LIST OF TABLES

iv. ACKNOWLEDGEMENTS

My choice to attend Dundee University as a mature student was both a daunting and exciting prospect and one that I look back on with fond memories. Although predominantly an individual's work, a PhD requires support from many others – so here I take a moment to thank you.

Firstly thanks go to my supervisor Dr Andy Irving - It has been an adventure; you allowed me bench space and the freedom to carry out my experiments. The encouragement to travel, for conferences, to places I had never visited before – Dublin, Copenhagen, Lund and Freiburg. I even attempted the German I had learnt years ago!!! "Ich danke Ihnen".

Dr Chris Henstridge, you gave me the foundation stone onto which I built this thesis without your help and support at the beginning I would not have achieved my goals. Dr Ashley Dorning and Dr Amy Alexander; what can I say, we were the Three Musketeers. Through the highs and lows you were both there with words of support and possibly more importantly home baking (never underestimate the power of chocolate cookies!!!). Without your support I would not have made it to the end. I can think of no-one better to have gone through this process with. Dr Phil Coates, my second supervisor, thank you for all your help and support throughout my PhD studies.

Xiao Luo as you finish your Masters I wish you every success with your future PhD studies. It was a pleasure to have met you – your smile is infectious. The numerous Honours and summer vacation students over the years; Claire, Darragh, Faith, Natalia, Allison, Miriam, Lisa, Alana, Cara, Avi, Janki, Viola, Alice, Alex and Dmitry you all kept me young. I wish you all successful careers whatever you go on to do.

Yasaman Malekizadeh – As my PhD ends I wish you good luck for your PhD journey; it is a shame I will not be there to share your success. Your cheery nature is a tonic. Dr Mary Palmer – your words of advice and encouragement, hugs and smiles kept me going. Our chats across the lab bench will be missed. I wish you every success in your bee research.

Andrew Carnegie is quoted to have said - "There is little success where there is little laughter" therefore my thanks also go to Dr Dayne Beccano-Kelly - I am amazed I got

any work done with all the laughing but you knew better! Dr Carl Holmgren – your knowledge is immense allowing for great conversations. I thank you for sharing your love of Scandanavian Noir now I have time to watch them something I very much look forward too. Dr Selma Dadak - your kind words and encouragement kept me going in the early days. To the newest members of the lab Dr Monica Tapia Pacheco, Orla Haugh and Gemma McGregor - best wishes for your future experiments. Absolute pleasure to have met you all - I wish each of you years of success with your research careers.

To those in the Medical Research Institute who help with any problem: Dr Dianne Peden, Helen Callachan, Catherine Cavanagh. My monitoring committee: Professors Tim Hales, Keith Matthews and Drs Andy South and Chris Connolly. A special thanks to Karen-Anne Bollan and Dr Michelle Cooper - no problem was ever too much. Both of you always made time to help with warm smiles, kind words and the knowledge you ladies have is immense. Last but by no means least Lynn Dyer you looked after me through undergraduate and now postgraduate studies. Your smile, cheery hello and encouragement lift the spirit. I cannot thank each of you enough.

To my funding body: the Caledonian Research Fund - this PhD could not have been undertaken without this award.

To my friends: Kath – we went through undergrad together and your support through my PhD encouraged me so much. I wish you every success with your medical career. Cath, Dean Catriona, James, Euan, my god-daughter Eleanor, Jimmy and Mary – you were all there to remind me of ‘normal’ life. To my family: Mum and Dad - you always gave words of encouragement and support. Moreover you probably know as much about GPR55 as I do!!! My sister, Susan and brother-in-law Tom you invited me for dinner on numerous occasions - these were relaxing times giving a nice break from my PhD. My Auntie Janet and Uncle Ken you never ever doubted me for one minute. Finally, to my niece, Jessica (Boo), you inspired me to succeed with your desire to read my chapter book. Therefore, this thesis is for you Boo I hope that in a small way it will inspire you to reach for the stars whatever career path you may choose in the future.

v. STUDENT DECLARATION

I, the undersigned declare that the candidate is the author of the thesis; that, unless otherwise stated, all references cited have been consulted by the candidate; that the work of which the thesis is a record has been done by the candidate and that it has not been previously accepted for a higher degree: provided that if the thesis is based upon joint research, the nature and extent of the candidate's individual contribution shall be defined.

Miss June Penman

December 2013

vi. SUPERVISOR DECLARATION

I certify that June Penman has completed nine terms in the Medical Research Institute, University of Dundee, carrying out research work under my supervision. June has fulfilled the conditions of Ordinance 39 at the University of Dundee and is therefore eligible to submit the following thesis in application for the degree of Doctor of Philosophy.

Dr Andrew J Irving

December 2013

vii. SUMMARY

G-protein coupled receptor 55 (GPR55) is a novel lipid sensing receptor activated by the endogenous lipid, lysophosphatidylinositol (LPI) and is reported as a putative cannabinoid receptor. However GPR55 shares limited homology with the two cloned cannabinoid receptors (CB_1 and CB_2) but does exhibit some cannabinoid sensitivity. Recently a family of bioactive lipids, the N-acyl amino acids, are gaining interest due to their structural similarity to endocannabinoids (naturally occurring CB_1 and CB_2 agonists). N-acyl amino acids have little or no affinity for either CB_1 or CB_2 and many have no known biological target at present.

This study used a subset of N-acyl amino acids; possessing either a serine or glycine head group attached to varying fatty acid chains; to assess these novel lipids as potential GPR55 ligands. Three cell lines were utilised, a stably transfected HEK293 cell line that overexpresses 3xHA N-terminus tagged hGPR55 (hGPR55-HEK293 cells) and control HEK293 cells. In addition, the DU145 a prostate cancer cell line which is reported to endogenously express GPR55 was investigated. N-acyl amino acid challenge activated GPR55 to promote Ca^{2+} mobilisation, CREB phosphorylation, actin cytoskeletal reorganisation and elongation of focal adhesions. Furthermore GPR55-mediated downstream signalling effectors were studied comparing LPI to the orphan lipid; N oleoyl-L-serine (NOSer).

This study highlights that N-acyl amino acids act as GPR55 agonist/partial agonists in hGPR55-HEK293 cells. Both LPI and NOSer exert effects in prostate cancer cells (DU145s) which are GPR55 mediated. GPR55 may exhibit ligand bias as LPI was more efficacious in Ca^{2+} mobilisation. However in the pCREB assay NOSer was more efficacious than LPI. A similar efficacy and potency to either LPI or NOSer was observed in the other assays in both hGPR55-HEK293 and DU145 cells. Furthermore this study is the first where a named GPCR can be assigned for responses that are mediated by NOSer.

viii. ABBREVIATIONS

µM	micromolar
2-AG	2-arachidonoyl glycerol
2-APB	2-Aminoethoxydiphenylborane
AA	arachidonic acid
ABDH4	α/β domain containing hydrolase 4
Abn-CBD	abnormal cannabidiol
ACEA	*N*-(2-Chloroethyl)-5*Z*,8*Z*,11*Z*,14*Z*-eicosatetraenamide
AEA	N-arachidonoylethanolamide
AJA	ajulemic acid
AM251	1-(2,4-Dichlorophenyl)-5-(4-iodophenyl)-4-methyl-N-1-piperidinyl-1H-pyrazole-3-carboxamide
ANOVA	analysis of variance
AR4-2J	pancreatic tumoral cell line
Arp2/3	actin-related protein-2/3
ATF	activating transcription factor
AtT-20	pituitary adenoma cell line
BAPTA-AM	1,2-*Bis*(2-aminophenoxy)ethane-*N*,*N*,*N*',*N*'-tetraacetic acid tetrakis(acetoxymethyl ester)
BK_{Ca}	large conductance Ca^{2+}-activated K^+ channels
BLAST	basic local alignment search tool
Bmx	bone marrow kinase on chromosome X
BV-2	murine microglial cell line
bZIP	basic region leucine zipper

Ca^{2+}	calcium
$[Ca^{2+}]_i$	intracellular calcium
CaMKII	calcium/calmodulin-dependent kinase II
cAMP	cyclic adenosine monophosphate
CB_1	cannabinoid receptor type 1
CB_2	cannabinoid receptor type 2
CBD	cannabidiol
CBP	CREB binding protein
CF-HBS	Ca^{2+} free HEPES buffered saline supplemented with 100 µM EDTA
CHI	closed head injury
CHO	Chinese hamster ovary cells
CID16020046	4-[4,6-Dihydro-4-(3-hydroxyphenyl)-3-(4-methylphenyl)-6-oxopyrrolo[3,4-*c*]pyrazol-5(1*H*)-yl]benzoic acid
CO_2	carbon dioxide
COX	cyclooxygenase
CP 55,940	(-)-*cis*-3-[2-Hydroxy-4-(1,1-dimethylheptyl)phenyl]-*trans*-4-(3-hydroxypropyl)cyclohexanol
$cPLA_2$	cytosolic phospholipase A_2
CRE	cyclic-AMP response element
CREB	cyclic-AMP response element-binding protein
CREM	cyclic-AMP response element modulator
CTCF	corrected total cell-area fluorescence
CTNF	corrected total nuclear fluoresence
DAG	diacylglycerol

DAGL	diacylglycerol lipase
DALN	deasacetyllevonantradol
DDHD1	DDHD domain containing 1
DMEM/F12	Dulbecco's modified eagle medium: Nutrient mixture F-12
DMSO	dimethyl sulfoxide
DRG	dorsal root ganglion neurons
DU145	human prostatic carcinoma cell line
EA.hy926	human vascular endothelial cell line
EAE	experimental autoimmune encephalomyelitis
ECM	extracellular matrix
Edg	endothelial cell differentiation gene
EDTA	ethylenediaminetetraacetic acid
ER	endoplasmic reticulum
ERK1/2	extracellular signal-regulated kinase 1/2
FA	focal adhesion
FAAH	fatty acid amide hydrolase
FCA	Freund's complete adjuvant
FFA	free fatty acid
fMLP	N-formyl-peptide receptor ligand
Fura 2-AM	2-[6-[*bis*[2-[(Acetyloxy)methoxy]-2-oxoethyl]amino]-5-[2-[2-[*bis*[2-[(acetyloxy)methoxy]-2-oxoethyl]amino]-5-methylphenoxy]ethoxy]-2-benzofuranyl]-5-oxazolecarboxylic acid (acetyloxy)methyl ester
GDE	glycerophosphodiesterase

GDP	guanosine diphosphate
GEF	guanine exchange factor
Gö6980	3-[1-[3-(Dimethylamino) propyl]-5-methoxy-1*H*-indol-3-yl]-4-(1*H*-indol-3-yl)-1*H*-pyrrole-2, 5-dione
GPCR	G protein-coupled receptor
GPR119	G protein-coupled receptor 119
GPR120	G protein-coupled receptor 120
GPR18	G protein-coupled receptor 18
GPR23	G protein-coupled receptor 23
GPR35	G protein-coupled receptor 35
GPR40	G protein-coupled receptor 40
GPR41	G protein-coupled receptor 41
GPR43	G protein-coupled receptor 43
GPR55	G protein-coupled receptor 55
GPR92	G protein-coupled receptor 92
G-protein	guanine nucleotide-binding protein
GRKs	G-protein receptor kinases
GTP	guanosine triphosphate
GTPγS	guanosine 5'-O-[gamma-thio] triphosphate
H^+	hydrogen
H1152 dihydrochloride	(*S*)-(+)-2-Methyl-1-[(4-methyl-5-isoquinolinyl) sulfonyl]-hexahydro-1*H*-1,4-diazepine dihydrochloride
HA tag	haemagglutinin tag
HBS	HEPES buffered saline

HEK293 cells	human embryonic kidney 293 cell line
HeLa cells	cervical adenocarcinoma cell line
HEPES	2-[4-(2-hydroxyethyl) piperazin-1-yl] ethanesulfonic acid
hGPR55-HEK293 cells	HEK293 cell line stably overexpressing recombinant human GPR55 protein
HL-60	human promyelocytic leukemia cell line
HMC-1	human mast cell leukaemic cell line
HMVEC	human dermal microvascular endothelial cells
HU-210	(6a*R*)-*trans*-3-(1,1-Dimethylheptyl)-6a,7,10,10a-tetrahydro-1-hydroxy-6,6-dimethyl-6*H*-dibenzo[*b,d*]pyran-9-methanol
HUVEC	human umbilical vein endothelial cells
I_{CRAC}	calcium-release-activated Ca^{2+} channel
IFNγ	interferon gamma
IL-2	interleukin 2
IM9	EBV-transformed human B lymphoblastoid cell line
IP_3	inositol 1, 4, 5-triphosphate
IP_3R	inositol 1, 4, 5-triphosphate receptor
JNK	c-JUN-N-terminal kinase
JWH015	(2-Methyl-1-propyl-1*H*-indol-3-yl)-1-naphthalenylmethanone
JWH133	(6a*R*,10a*R*)-3-(1,1-Dimethylbutyl)-6a,7,10,10a-tetrahydro-6,6,9-trimethyl-6*H*-dibenzo[*b,d*]pyran
KID	kinase inducible domain

KN-62	4-[(2*S*)-2-[(5-isoquinolinylsulfonyl) methylamino]-3-oxo-3-(4-phenyl-1-piperazinyl) propyl] phenyl isoquinolinesulfonic acid ester
LGCC	ligand gated Ca^{2+} channel
LOX	lipoxegenase
LPA	lysophosphatidic acid
LPI	L-α-lysophosphatidylinositol
LPI-PLC	lysophophatidylinositol-phospholipase C
LPS	lipopolysaccharide
LY294002	2-(4-Morpholinyl)-8-phenyl-4*H*-1-benzopyran-4-one hydrochloride
MAGL	monoacylglycerol lipase
MAPK	mitogen activated protein kinase
MCF-7	human breast adenocarcinoma cell line
MDA-MB-231	human breast adenocarcinoma cell line
mDia	mammalian diaphanous
MEF	mouse embryonic fibroblasts
MEK1	mitogen-activated protein kinase kinase 1
MEKK1	mitogen-activated protein kinase kinase kinase 1
mEPSC	mini excitatory postsynaptic currents
min	minute
ML-141	4-[4, 5-Dihydro-5-(4-methoxyphenyl)-3-phenyl-1*H*-pyrazol-1-yl] benzenesulfonamide
mM	millimolar
mTOR	mammalian target of rapamycin

N18TG2	murine neuroblastoma cell line
Na^+	sodium
NADA	N-arachidonoyl dopamine
NAGly	N-arachidonoyl glycine
NAPE	N-arachidonoyl-phosphatidylethanolamine
NAPE-PLD	NAPE-hydrolysing phospholipase D
NASer	N-arachidonoyl-L-serine
NAT	N-acyltransferase
NFAT	nuclear activated factor of T-cells
NG108-15	neuroblastoma x glioma hybrid cell line
nM	nanomolar
NOGly	N-oleoyl glycine
NOSer	N-oleoyl-L-serine
NPGly	N-palmitoyl glycine
NPSer	N-palmitoyl-L-serine
O-1602	5-Methyl-4-[(1*R*,6*R*)-3-methyl-6-(1-cyclohexen-1-yl]-1,3-benzenediol
OEA	N-oleoylethanolamide
oGPCRs	orphan G-protein coupled receptor
OHSC	organotypic hippocampal slice cultures
Orai1	calcium release-activated calcium channel protein 1
P2Y5	lysophosphatidic acid receptor 6
pAKT	phosphorylated AKT
PBS	phosphate buffered solution

PC12	cell line derived from a phaeochromocytoma of the rat adrenal medulla
PC3	human prostatic carcinoma cell line
pCREB	phosphorylated CREB
PD98059	2-(2-Amino-3-methoxyphenyl)-4*H*-1-benzopyran-4-one
PEA	palmitoylethanolamide
PFA	paraformaldehyde
PI	phosphatidylinositol
PI-3 kinase	phosphoinositide 3-kinase
PIP_2	phosphatidylinositol 4, 5-bisphosphate
PKA	protein kinase A
PKB	protein kinase B
PKC	protein kinase C
PLA_1	phospholipase A_1
PLA_2	phospholipase A_2
PLC	phospholipase C
PLD	phospholipase D
PMCA	plasma membrane Ca^{2+} ATPase
PPAR	peroxisome proliferator-activated receptor
PTEN	phosphatase and tensin homolog deleted on chromosome 10
PTPN22	protein tyrosine phosphatase non-receptor type 22
PTX	pertussis toxin
PWR	plasmon waveguide resonance

RAW264.7	murine leukaemic monocyte macrophage cell line
RGS	regulators of G-protein signalling
Rho A	ras homolog gene, family member A
RIN m5F	rat insulinoma cell line
ROCK	Rho associated protein kinase
RyR	ryanodine receptor
S1P	sphingosine 1-phosphate
sec	second
SEM	standard error of the mean
SERCA	sarcoplasmic/endoplasmic reticulum calcium ATPase
SH-SY5Y	human neuroblastoma cell line
siRNA	short interfering ribonucleic acid
SOC	store operated Ca^{2+}
SOCE	store operated Ca^{2+} entry
SR141617A	*N*-(Piperidin-1-yl)-5-(4-chlorophenyl)-1-(2,4-dichlorophenyl)-4-methyl-1*H*-pyrazole-3-carboxamide hydrochloride
SR144528	5-(4-chloro-3-methylphenyl)-1-[(4-methylphenyl)methyl]-N-[(1S,2S,4R)-1,3,3-trimethylbicyclo[2.2.1]hept-2-yl]-1H-pyrazole-3-carboxamide
STIM-1	stromal interacting molecule-1
Syk	spleen tyrosine kinase
TM	transmembrane
TNF-α	tumour necrosis factor-α

TPA	12-O-Tetradecanoylphorbol-13-acetate
Triton™ x-100	4-(1, 1, 3, 3-Tetramethylbutyl) phenyl-polyethylene glycol
TRP	transient receptor potential
TRPC5	transient receptor potential cation channel, subfamily C, member 5
TRPM6	transient receptor potential cation channel, subfamily M, member 6
TRPM7	transient receptor potential cation channel, subfamily M, member 7
TRPM8	transient receptor potential cation channel, subfamily M, member 8
TRPV1	transient receptor potential vanilloid 1
TRPV2	transient receptor potential vanilloid 2
TRPV3	transient receptor potential vanilloid 3
TRPV6	transient receptor potential vanilloid 6
U1026	1, 4-Diamino-2, 3-dicyano-1, 4-*bis* [2-aminophenylthio] butadiene
U73122	1-[6-[[(17β)-3-Methoxyestra-1, 3, 5(10)-trien-17-yl] amino] hexyl]-1*H*-pyrrole-2, 5-Dione
U87	human glioblastoma-astrocytoma, epithelial-like cell line
VGCC	voltage gated Ca^{2+} channel
vGLUT1	vesicular glutamate transporter 1
WIN 55, 212-2	(*R*)-(+)-[2,3-Dihydro-5-methyl-3-(4-morpholinylmethyl)pyrrolo[1,2,3-*de*]-1,4-benzoxazin-6-yl]-1-naphthalenylmethanone mesylate

Y-27632 dihydrochloride	*trans*-4-[(1*R*)-1-Aminoethyl]-*N*-4-pyridinylcyclohexanecarboxamide dihydrochloride
Δ^9-THC	Δ^9-tetrahydrocannabinol

CHAPTER ONE

Introduction

1. INTRODUCTION

1.1. G-protein coupled receptors

Seven transmembrane receptors (7TM) also known as G protein-coupled receptors (GPCRs) constitute a large and diverse family of membrane receptors with around 800 genes encoding GPCRs in the human genome (Fredriksson *et al.*, 2003; Civelli *et al.*, 2013). GPCRs are classified into 5 different groups – Glutamate, Rhodopsin, Adhesion, Frizzled and Secretin (GRAFS) (Fredriksson *et al.*, 2003; Jacoby *et al.*, 2006). The majority of GPCRs are members of the Rhodopsin family which is further subdivided into α, β, γ and δ groups (Fredriksson *et al.*, 2003; Civelli *et al.*, 2013). Over 100 GPCRs are known as orphan GPCRs (oGPCRs) as they have no known ligand (Klabunde and Hessler, 2002; Jacoby *et al.*, 2006). GPCRs allow a plethora of extracellular stimuli, such as lipids, proteins and peptides, biogenic amines, amino acids or ions, to interact with intracellular signalling effectors (Marinissen and Gutkind, 2001). Thereby, allowing cells to interact with their surrounding extracellular environment to promote physiological homeostasis (Dorsam and Gutkind, 2007). GPCRs are known to be important in pathophysiological conditions such as obesity, cardiovascular disease, type II diabetes, Alzheimer's disease, multiple sclerosis and cancer (Marinissen and Gutkind, 2001; Radhika and Dhanasekaran, 2001; Heng *et al.*, 2013). GPCRs are the most important protein family for drug discovery where ~50% of pharmaceuticals target GPCRs either as agonists or antagonists (Klabunde and Hessler, 2002; Rask-Andersen *et al.*, 2011; Garland, 2013).

Many physiological responses that are now known to be mediated by GPCRs were revealed before the receptors eliciting the responses had been discovered. Earl Sutherland's work with cyclic adenosine monophosphate (cAMP); the first second messenger to be characterised (Sutherland and Wosilait, 1955; Sutherland, 1972); and the discovery that guanine nucleotides mediate adenylyl cyclase activation through the action of glucagon on a hormone receptor (Rodbell *et al.*, 1971) were carried out at time when it was not known that GPCRs were the signal transducers. Furthermore several pharmaceuticals were developed and used in the clinic, such as β-blockers and analgesic opiates (now known to act on the β–adrenoceptors and morphine receptors respectively) but the GPCRs involved were still to be isolated (Jacoby *et al.*, 2006). However coupled with the knowledge of ligands such as isoproterenol and adrenaline the β–adrenoceptor was purified through affinity chromatography (Caron *et al.*, 1979; Jacoby *et al.*, 2006) but the structure remained to be determined. In the interim

bacteriorhodopsin and subsequently bovine rhodopsin amino acid sequences were determined and using hydrophobicity plots the proteins were suggested to have similar topologies – the presence of 7TM spanning domains (Ovchinnikov, 1982). Interestingly the structural homology of the β–adrenoceptor was found to have the same 7TM domains and similarities were noted in TM V-VII to the previously elucidated rhodopsin receptor (Dixon *et al.*, 1986). Moreover functional similarities of both receptors highlighted activation of guanine nucleotide exchange factors (Dixon *et al.*, 1986). Rhodopsin was the first GPCR to have its crystal structure determined and this confirmed the presence of 7TM domains (Palczewski *et al.*, 2000). In the last decade crystallography has elucidated a total of 13 GPCR structures from rhodopsin (Palczewski *et al.*, 2000) to the most recent the neurotensin receptor (White *et al.*, 2012). GPCRs share a common topology of seven hydrophobic trans-membrane α-helices, each around 20-30 amino acids in length. Three intracellular and three extracellular loops of hydrophilic amino acid chains link the helices together (Oldham and Hamm, 2008). GPCRs also possess an extracellular amino terminus and a cytoplasmic carboxy terminus (Stadel *et al.*, 1997).

1.1.1. GPCRs, G-proteins and signal transduction

Extracellular stimulation of a GPCR requires heterotrimeric guanine nucleotide-binding proteins (G-proteins) to act as molecular switches to allow the initiation of intracellular signalling (Oldham and Hamm, 2008). G-proteins consist of G_{α}- and $G_{\beta\gamma}$-subunits which elicit effects on downstream effectors. There are 16 genes encoding the 21 G_{α}-subunits, 5 genes encode the 6 G_{β}-subunits and 14 genes encode the 14 G_{γ}-subunits (Milligan and Kostenis, 2006; Oldham and Hamm, 2006). When the G_{α}-subunit of the G-protein has guanosine diphosphate (GDP) bound it associates with an inactive GPCR and the $G_{\beta\gamma}$-subunit. The G_{α}-subunit alone can interact with inactive GPCRs however, when the $G_{\beta\gamma}$-subunit is present the association with the inactive GPCR is stronger (Neer, 1994). Upon ligand binding a conformational change occurs within the transmembrane α–helices of the GPCR leading to a change in the cytoplasmic domains (Oldham and Hamm, 2008). This lowers the affinity of the G_{α}-subunits to bind to GDP and increases their affinity for GTP. In essence the GPCR acts as a guanine nucleotide exchange factor (GEF) hastened by the higher concentration of GTP compared to GDP in the cells (Milligan and Kostenis, 2006). The binding of GTP to the α-subunit leads to a conformational change in that subunit which allows the dissociation of the G_{α}–subunit from both the GPCR and the $G_{\beta\gamma}$-subunits (Neer, 1994; Oldham and Hamm, 2006).

Both the G_{α}-subunit and the $G_{\beta\gamma}$-subunits can then interact with effectors to initiate signalling within the cell (Neer, 1994). Moreover the G_{α}-subunit possesses intrinsic GTPase activity which hydrolyses the terminal γ-phosphate producing GDP. This G_{α}-GDP-subunit now has a high affinity for associating with the $G_{\beta\gamma}$-subunit producing an inactive heterotrimeric G-protein (Svoboda *et al.*, 2004). Furthermore the early biochemical studies of purified G_{α}-subunits found that the rate of the GTPase hydrolysis of GTP to GDP was slower than the rapid turnover seen with physiological processes. This led to the discovery of regulators of G-protein signalling (RGS) proteins. RGS proteins increase the rate of GTPase hydrolysis of the G_{α}-subunits at a faster more physiological rate (Hollinger and Hepler, 2002; Milligan and Kostenis, 2006).

Due to their homological and functional similarities heterotrimeric Gα proteins exist as members of four groups $G_{\alpha s}$, $G_{\alpha i}$, $G_{\alpha q}$ and $G_{\alpha 12/13}$ (Oldham and Hamm, 2008). The $G_{\alpha s}$ group consist of four subtypes $G_{\alpha s(S)}$, $G_{\alpha s(L)}$, $G_{\alpha s(XL)}$ and $G_{\alpha olf}$ (Milligan and Kostenis, 2006). The $G_{\alpha s}$ subtypes are ubiquitously expressed whereas $G_{\alpha olf}$ is expressed in the digestive and urogenital tract and in the CNS in olfactory neurons (Milligan and Kostenis, 2006). $G_{\alpha s}$ stimulates the production of cyclic AMP (cAMP) through the activation of adenylyl cyclase (Kostenis *et al.*, 2005), activates large conductance Ca^{2+} -activated K^{+} channels (BK_{Ca}), tubulin GTPase and c-Src (Milligan and Kostenis, 2006). Furthermore the increase in cAMP activates a small GTPase Rap1 which links $G_{\alpha s}$ activation to the mitogen activated protein kinase (MAPK) pathway (Neves *et al.*, 2002).

The $G_{\alpha i/o}$ family consists of eight subtypes; $G_{\alpha o1}$, $G_{\alpha o2}$, $G_{\alpha i1}$, $G_{\alpha i2}$, $G_{\alpha i3}$, $G_{\alpha z}$, $G_{\alpha t1/2}$ and $G_{\alpha gust}$ (Milligan and Kostenis, 2006). $G_{\alpha i/o}$ proteins are expressed for example in neurons, adrenal chromaffin cells, the heart and taste buds (Milligan and Kostenis, 2006). The $G_{\alpha i}$ family inhibit adenylyl cyclase and therefore inhibit the production of cAMP (Neves *et al.*, 2002). $G_{\alpha i/o}$ proteins also activate K^{+} channels, inhibit Ca^{2+} channels, activate Rap1 mediated MAPK activation and increase tubulin GTPases (Milligan and Kostenis, 2006).

There are five members of the $G_{\alpha q}$ group; $G_{\alpha q}$, $G_{\alpha 11}$, $G_{\alpha 14}$, $G_{\alpha 15}$ and $G_{\alpha 16}$ (Milligan and Kostenis, 2006). $G_{\alpha q}$ proteins are ubiquitously expressed however $G_{\alpha 15/16}$ are expressed in haematopoietic cells (Milligan and Kostenis, 2006). $G_{\alpha q}$ proteins activate

phospholipase C-β (PLC-β) which hydrolyses PIP_2 into IP_3 and DAG. IP_3 then acts upon IP_3 receptors on the endoplasmic reticulum to release Ca^{2+} from this Ca^{2+} store (Neves *et al.*, 2002; Clapham, 2007). $G_{\alpha q}$ can also activate phospholipase D (PLD) through the activation of protein kinase C (PKC) (Neves *et al.*, 2002). Moreover $G_{\alpha q}$ can inhibit two pore K^+ channels (Veale *et al.*, 2007; Shrestha *et al.*, 2010), activate Bruton's tyrosine kinase (Bence *et al.*, 1997; Milligan and Kostenis, 2006) and p63-RhoGEF (Lutz *et al.*, 2005; Milligan and Kostenis, 2006).

Finally members of the $G_{\alpha 12/13}$ family consist of two members $G_{\alpha 12}$ and $G_{\alpha 13}$ and are ubiquitously expressed (Milligan and Kostenis, 2006). $G_{\alpha 12/13}$ proteins activate p115RhoGEF (Kozasa *et al.*, 1998), leukaemia-associated RhoGEF (LARG; Suzuki *et al.*, 2003), PLCε (Kelley *et al.*, 2004; Hains *et al.*, 2006), PLD (Ziembicki *et al.*, 2005) and the membrane-cytoskeletal protein, radixin (Vaiskunaite *et al.*, 2000). However the G_{α}-subunits are not the only way effectors are activated when GPCRs are stimulated (figure 1.1).

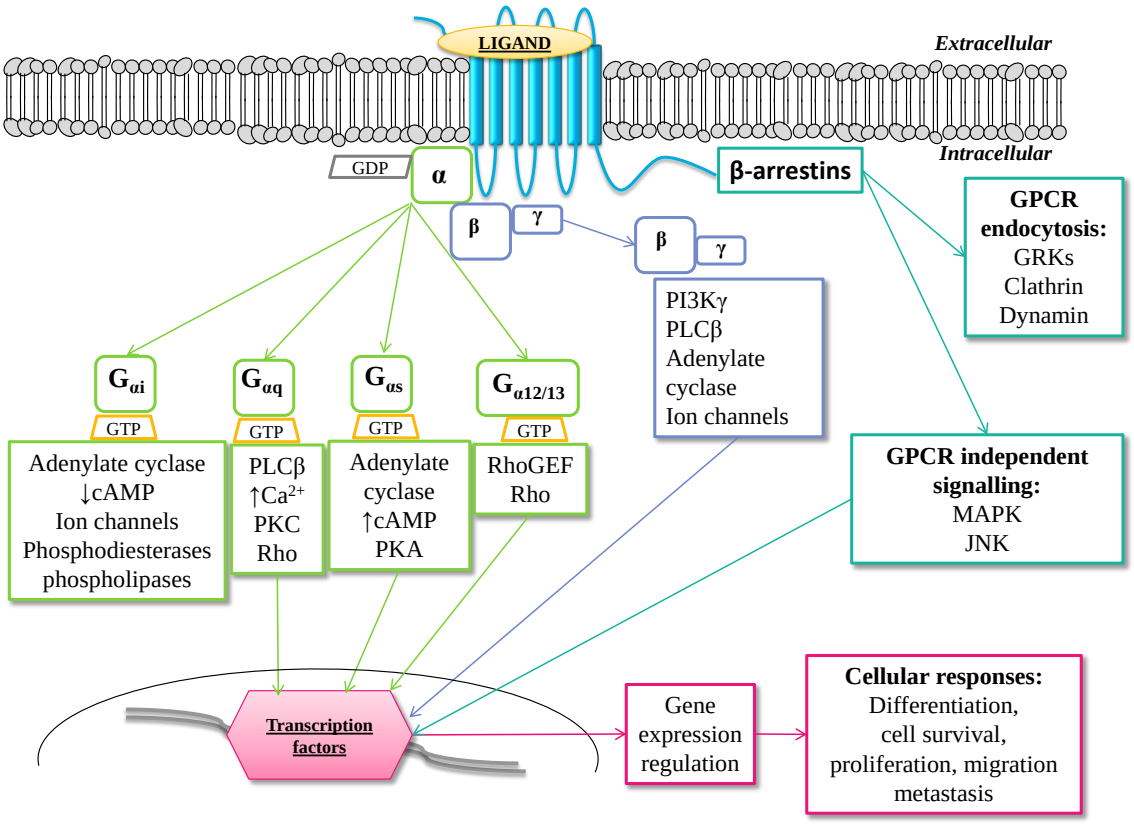

Figure 1.1: Examples of the diverse signalling of seven trans-membrane receptors. *Lipids are one type of ligand that can bind to GPCRs and initiate amplification signalling pathways which result in stimulation of the appropriate effector to regulate physiological homeostasis.*

$G_{\alpha i}$ proteins reduce the level of cAMP as well as exerting effects on ion channels such as Ca^{2+} and K^+ channels. $G_{\alpha q}$ proteins lead to the formation of DAG and IP_3 and then the subsequent release of Ca^{2+}. $G_{\alpha s}$ increases cAMP and $G_{\alpha 12/13}$ signals through the small GTPase Rho. GPCRs were classically known to bind to G-proteins but recent evidence highlights they can also activate β–arrestins to initiate signalling through MAP kinase. GRK, G-protein receptor kinase; MAPK, mitogen activated protein kinase; JNK, c-Jun N-terminal kinase; GDP, guanine diphosphate; PI3K, phosphatidylinositol-3-kinase; PLC, phospholipase C; GTP, guanine triphosphate; cAMP, cyclic adenosine monophosphate; PKA, protein kinase A; GEF, guanine exchange factor. Adapted from Dorsam and Gutkind, 2007; Galandrin et al., 2007.

Originally the $G_{\beta\gamma}$ subunit was thought to only interact with the inactive G_{α}-subunit to inhibit constitutive signalling, and due to its hydrophobicity, to act as an anchor for the heterotrimeric G-protein with the cell membrane (Milligan and Kostenis, 2006). However this hypothesis was contested when muscarinic GPCRs in the heart which activate K^+ channels were found to require $G_{\beta\gamma}$-subunits to promote single channel conductance (Logothetis *et al.*, 1987). Further evidence found $G_{\beta\gamma}$-subunits are also required for breast cancer (MD-MBA-231) cell proliferation and migration towards serum (Tang *et al.*, 2011). Serum-induced growth of MD-MBA-231 breast cancer cells decreased when the $G_{\beta\gamma}$-subunits were inhibited. However proliferation of a non-tumorigenic breast epithelial cell line (MCF10A) was unaffected by $G_{\beta\gamma}$-subunit activation suggesting that the effects on proliferation by $G_{\beta\gamma}$ occur only in tumour cells (Tang *et al.*, 2011). Furthermore inhibiting $G_{\beta\gamma}$-subunits reduced lung metastasis and tumour formation *in vivo* where MDA-MB-231 cells had been injected into the tail vein of mice. Angiogenesis and leukocyte infiltration were also inhibited in primary breast tumours when $G_{\beta\gamma}$ dimers were blocked (Tang *et al.*, 2011). $G_{\beta\gamma}$-subunits from the $G_{\alpha i}$-subunit are also important for chemoattractant neutrophil chemotaxis mediated by phosphoinositide-3 kinase (PI-3 kinase) activation (Lehmann *et al.*, 2008). Furthermore $G_{\beta\gamma}$-subunits can activate PLC (Boyer *et al.*, 1992), Tsk and Btk tyrosine kinase (Langhans-Rajasekaran *et al.*, 1995) and MAPK (Faure *et al.*, 1994). Therefore $G_{\beta\gamma}$-subunits are also important signalling mediators.

Finally, recent research suggests signalling through GPCRs can also occur independently of G-proteins. β-arrestins are now recognised as playing a role in GPCR signalling. There are four β-arrestin subtypes expressed in mammals; β-arrestin1, β-arrestin2 and two visual arrestins – rod-arrestin and cone-arrestin (Coffa *et al.*, 2011). Classically β-arrestins were merely considered to terminate GPCR-mediated signalling

by desensitisation, sequestration and downregulation of the activated GPCR (Luttrell and Lefkowitz, 2002). To initiate β-arrestin's role in desensitisation G-protein coupled receptor kinases (GRKs) are activated after docking with a ligand bound GPCR (Gurevich *et al.*, 2012). GRKs then phosphorylate serine and threonine residues on the carboxyl terminus of an activated GPCR thereby increasing the affinity of GPCR to interact with β-arrestins in a process known as homologous desensitisation (Luttrell and Lefkowitz, 2002; Gurevich *et al.*, 2012). Additionally second messengers can phosphorylate other protein kinases such as protein kinase A (PKA) and protein kinase C (PKC) which can also phosphorylate the cytoplasmic loops and/or serine and threonine resides on the GPCR carboxy terminus also leading to a subsequent interaction with β-arrestins (Luttrell and Lefkowitz, 2002). Unlike GRK phosphorylation which requires an agonist to be bound to the targeted GPCR, PKA and PKC can also phosphorylate unoccupied GPCRs in a process known as heterologous desensitisation (Luttrell and Lefkowitz, 2002). The presence of the β–arrestin disrupts G-protein coupling with the GPCR therefore desensitising the receptor. The GPCR-β-arrestin complex can now interact with 2-AP an adaptor protein which links the GPCR-β-arrestin complex with clathrin (Luttrell and Lefkowitz, 2002). Clathrin is a structural protein component of clathrin-coated pits which promote endocytosis of the ligand bound GPCR (Goodman *et al.*, 1996; Gagnon *et al.*, 1998; Luttrell and Lefkowitz, 2002). Finally the presence of dynamin at the neck of the invaginated membrane allows the clathrin-coated pit to be 'pinched off' where it then internalises promoting GPCR sequestration (Damke *et al.*, 1994; Rappoport *et al.*, 2008; Delom and Fessart, 2011). In studies where a mutant inactive dynamin is present AP-2 still associates with clathrin coated pits however they remain at the cell membrane (Damke *et al.*, 1994). GPCR downregulation occurs when sequestered GPCRs are either targeted into early endosomes for recycling back into the cell membrane or targeted to acidic lysosomes for degradation (Gagnon *et al.*, 1998; Luttrell and Lefkowitz, 2002). Previously β-arrestins from β-adrenoceptors have been reported to dissociate close to the membrane allowing the receptors to recycle quickly. However the vasopressin receptors which recycle slowly were found to remain associated with β-arrestins in endosomes. Furthermore when the c-termini of each receptor type was exchanged the β-adrenoceptors were then targeted to endosomes and the vasopressin receptors were found to dissociate from β-arrestins at the cell membrane (Oakley *et al.*, 1999). Therefore the resensitisation of the activated GPCRs may be dictated by the interaction

between the c-termini of a receptor and the recruited β-arrestin (Oakley *et al.*, 1999; Luttrell and Lefkowitz, 2002).

Recent evidence however suggests that β-arrestins can also initiate signalling through MAPK (Daaka *et al.*, 1998; Shenoy *et al.*, 2006; Yang *et al.*, 2012), JNK (McDonald *et al.*, 2000; Marinissen and Gutkind, 2001), p38 MAPK (Yang *et al.*, 2012) and AKT (Beaulieu *et al.*, 2005; Yang *et al.*, 2012). HEK293 cells transfected with mutant forms of β-arrestin and dynamin inhibited isoproterenol activated β-adrenoceptor ERK1/2 phosphorylation suggesting that endocytosis of the β–adrenoceptors is necessary to initiate MAPK signalling (Daaka *et al.*, 1998). Immunocytochemical studies revealed angiotensin II stimulated the angiotensin II type 1_A (AT_{1A}) receptors which promoted β-arrestin2 to act as a scaffold protein for Raf1 and MEK1 in COS-7 cells. Therefore protein complexes consisting of AT_{1A} receptor, β-arrestin2, Raf1, MEK1 and ERK2 were recruited to endosomes (Luttrell *et al.*, 2001). The retention of β-arrestin-ERK1/2 in endosomes increases the cytosolic whilst lowering the nuclear concentration of phosphorylated ERK1/2 mediated by AT_{1A} receptor activation (Tohgo *et al.*, 2002). A subsequent study highlighted that angiotensin II stimulation of AT_{1A} receptor promoted β-arrestin mediated phosphorylation of ERK1/2. This led to the initiation of protein synthesis therefore providing evidence that β-arrestins can mediate transcriptional regulation (DeWire *et al.*, 2008). However the phosphorylation of eukaryotic translation initiation factor 4E (eIF4E) was not directly via ERK1/2 but by the downstream Mnk1 protein (DeWire *et al.*, 2008).

G-protein and β-arrestin dependent signalling may act synergistically as AT_{1A} receptors treated with angiotensin II require both activation of $G_{\alpha q}$ and β-arrestin1 to promote the formation of stress fibres which are Rho mediated (Barnes *et al.*, 2005). $G_{\alpha q}$ or β-arrestin1 alone could not activate RhoA and only when both signalling mediators were activated was an increase in RhoA-mediated stress fibres observed (Barnes *et al.*, 2005). Therefore cell signalling has come a long way from the canonical the concept of one GPCR-one signalling pathway, to the possibility that GPCRs activate multiple signalling pathways which may be G-protein dependent or independent therefore allowing for the possibility of “ligand bias”, where different ligands can promote distinct signalling events.

1.1.2. Ligand bias

Traditional receptor theory dictated that an agonist bound GPCR signals via one pathway leading to a known outcome regardless of the agonist (Clarke and Bond, 1998; Kenakin *et al.*, 2012). Therefore intrinsic efficacy (sometimes referred to as intrinsic activity) is a measure of the effect induced by agonist-receptor activation which was the same for all agonists of a given receptor (Clarke and Bond, 1998). Furthermore full agonists are defined as having a high intrinsic efficacy where maximal responses to the ligand are produced (Urban *et al.*, 2007). Partial agonists have a lower intrinsic efficacy which leads to submaximal responses being produced. Inverse agonists act on constitutive signalling to reduce the intrinsic efficacy. A neutral antagonist whilst having affinity (the ability to bind to the receptor) blocks the effect of agonists but has no intrinsic efficacy (Urban *et al.*, 2007). However evidence disputes the simplicity of this model as GPCRs have the ability to initiate multiple signalling pathways and different agonists can promote activation of these with differing intrinsic efficacies, a phenomenon known as functional selectivity or ligand bias (Clarke and Bond, 1998; Kenakin *et al.*, 2012). Ligand bias leads to GPCRs adopting altered conformations dependent on the particular ligand that is bound to the GPCR. Stabilised conformational changes in the cannabinoid receptor type 1 (CB_1) were observed with plasmon waveguide resonance (PWR) spectroscopy. It was observed that both WIN 55,212-2 and CP 55,940 bind to CB_1 producing altered PWR spectra suggesting that the CB_1 had adopted different structural conformations with these ligands. Moreover $G_{\alpha i1}$ binding to the receptor promoted different affinities and efficacies (WIN 55,212-2 being lower than CP 55,940) depending on the ligand that was bound to the receptor suggesting that ligand bias of the $G_{\alpha i1}$ protein could occur (Georgieva *et al.*, 2008). It is also known that ligand bias can lead to the recruitment of not only various G-proteins but also β-arrestins (Kenakin, 2011; Wacker *et al.*, 2013). Another study has also reported that CB_1 activated by either CP 55,940 or HU210 promoted differences in gene transcription mediated by AP-1 activation. Each ligand could differentially stabilise the receptor, therefore recruiting different G_{α}-proteins, leading to divergence in the associated signalling and consequent differential promotion of AP-1 activation (Bosier *et al.*, 2008). To this end it is important to consider more than one signalling outcome when testing GPCR ligands. The ligand may be inactive in one signalling pathway but may be potent in a different signalling pathway (Urban *et al.*, 2007). Initially many studies were carried out in recombinant systems overexpressing a receptor of interest and the promiscuity of signalling was thought to be due to the increased receptor

number (Kenakin, 2011). However there is growing evidence in endogenously expressing systems that ligand bias occurs. Furthermore it may be that a ligand can act as an agonist and antagonist at the same GPCR. The somatostatin sst2A receptor can be activated by the synthetic ligands SOM230 or KE108 in endogenously expressing pancreatic cells (AR4-2J) to inhibit adenylyl cyclase, whilst at the same time acts as an antagonist of Ca^{2+} mobilisation and ERK1/2 phosphorylation (Cescato *et al.*, 2010), highlighting the importance of testing novel ligands in different signalling pathways. Furthermore in this study the synthetic ligands promoted effects that varied from the endogenous agonist where the natural ligand SS-14 activated ERK1/2 by two separate pathways ($G_{\alpha i}$ and $G_{\alpha 14}$) where $G_{\alpha 14}$ was antagonised by SOM230 and KE108 (Cescato *et al.*, 2010) therefore differences in ligand bias may occur between endogenous and synthetic ligands in similar cells activating the same receptor (Kenakin *et al.*, 2012). The responses elicited by a GPCR may also be dependent on the cellular environment for example the composition of the membrane, the extracellular and intracellular environments and other GPCRs and proteins that may exert an influence (Clarke and Bond, 1998; Bosier *et al.*, 2010). Therefore agonist activity may differ depending on the cell type that the receptor is present in (Kenakin *et al.*, 2012).

Allosteric modulators can also influence the signalling by GPCRs. These are binding sites distinct from the orthosteric (primary) binding site. Receptor conformation will be altered when a ligand binds to the allosteric site therefore changing the affinity and efficacy of the ligand that binds to the orthosteric site and the subsequent G-protein that is recruited (Bosier and Hermans, 2007). CB_1 receptors when a ligand is bound to the allosteric site are noted as having a higher affinity for a ligand at the orthosteric site however the efficacy is lowered (Price *et al.*, 2005). Furthermore ligand binding in the allosteric site may alter the GPCR signalling even if a ligand is not present in the orthosteric site (Bosier *et al.*, 2010). Therefore allosteric ligands may influence GPCR signalling in their own right or by modulating the effects of the orthosteric ligand.

An understanding of the intricate signalling of the receptor of interest should lead to more specific therapeutics which can act on the pathway responsible without affecting other signalling pathways. Therefore this could lead to the development of novel and more specific ligands. In the long term this coupled with testing at orphan receptors can only enhance modern drug discovery.

1.1.3. Orphan GPCRs

Early studies had led to the characterisation of the first second messenger; cyclic adenosine monophosphate (cAMP) linking the effects from receptor activation to intracellular effectors (Jacoby *et al.*, 2006). There was great success in the clinic with therapeutics in areas of cardiovascular disease, asthma, allergy, pain and epilepsy even though the isolation and sequencing of GPCRs had not taken place (Jacoby *et al.*, 2006). In 1979 the β_2 adrenoceptor was purified and was found to be functional allowing for the characterisation of GPCRs (Jacoby *et al.*, 2006). As molecular techniques advanced, methods based on hybridisation probes (Bunzow *et al.*, 1988) or degenerate polymerase chain reaction (Libert *et al.*, 1989) proved to be highly successful and led to the discovery of numerous orphan G-protein coupled receptors (oGPCRs). Orphan GPCRs have no cognate endogenous ligand assigned to them and therefore still require characterisation. Of the 701 receptors that make up the human Rhodopsin GPCR family around 100 of them remain oGPCRs which present potential for future drug targets by pharmaceutical companies (Stadel *et al.*, 1997; Schlyer and Horuk, 2006; Civelli *et al.*, 2013).

In an attempt to find the endogenous ligands for the growing number of oGPCRs reverse pharmacology was adopted. This technique required the oGPCR to be transfected into a host cell where it is known that there is no endogenous expression of the target receptor. Tissue fractions from regions adjacent to where the receptor is expressed or libraries of endogenous ligands would then be tested on the transfected cells in a variety of signalling assays (Stadel *et al.*, 1997). The deorphanisation of the HT_{1A} serotonin receptor (Fargin *et al.*, 1988) and a D_2 dopamine receptor (Bunzow *et al.*, 1988) were the first to be achieved using reverse pharmacology. Now high throughput screening assays can test numerous ligands from libraries with oGPCRs leading to faster ligand-GPCR pairings. However it is important that more than one signalling assay is tested as ligand bias may occur and potential ligands could be missed in high throughput screening (Southern *et al.*, 2013).

Interestingly, in 1992 the cannabinoid receptor type 1 (CB_1), although not technically an oGPCR, was used to bait fractions from porcine brain whereby anandamide (AEA), a fatty acid amide, was found to displace a radiolabelled cannabinoid probe; [^{3}H]HU-243 (Devane *et al.*, 1992). Therefore, AEA was not only the first mammalian natural

cannabinoid (endocannabinoid) to be discovered but was also the first lipid mediator to be identified using reverse pharmacology (Civelli *et al.*, 2013).

1.2. Overview of the endocannabinoid system

The first medicinal use of the marijuana plant *Cannabis sativa* occurred in China around 5000 years ago. Emperor Shen Nung prescribed *C. sativa* to his subjects for ailments such as rheumatism, absent mindedness and dysmenorrhoea (Hanus, 2009). *C. sativa* was recorded in the first Chinese pharmacopeia; Shen Nung pen ts'ao ching (Divine Husbandman's Materia Medica), with a warning that consuming too many seeds would lead to seeing demons (Zuardi, 2006; Hanus, 2009) pertaining to the psychoactive effects of cannabis. The effects of cannabis were also noted as "Protracted taking may make one fat, strong and never senile." (Russo, 2007). Therefore, suggesting a role for cannabinoids in obesity, immune function and neuroprotection. However it was not until the latter decades of the 20th Century that the most intense research on the molecular mechanisms and chemical structures of phytocannabinoids, endocannabinoids, synthetic analogues and cannabinoid receptors have taken place.

1.2.1. Cannabinoid receptors

The discovery in the mid-1960s of the main active constituent of *C. sativa*, the phytocannabinoid Δ^9-tetrahydrocannabinol (Δ^9-THC), was to open the field of cannabinoid research (Gaoni and Mechoulam, 1964). The lipophilic nature of Δ^9-THC was initially thought to exert effects by disrupting the cell membrane however, by the end of the decade stereoisomers of Δ^9-THC led to the hypothesis that Δ^9-THC was acting upon a target in the cell membrane (Mechoulam and Gaoni, 1967). It would be another twenty years before the discovery and cloning of the first cannabinoid receptor. Cannabinoid receptor type 1 (CB_1) was elucidated from rat brain (Devane *et al.*, 1988) and autoradiography with a labelled cannabinoid ligand ([^{3}H]CP 55,940) further confirmed the location of CB_1 in the brain (Herkenham *et al.*, 1990). CB_1 is predominantly localised in the cerebellum, cerebral cortex, hippocampus, hypothalamus, limbic system and basal ganglia (Moldrich and Wenger, 2000). CB_1 is the most abundantly expressed GPCR in the mammalian brain at the mRNA level and is responsible for the 'high' associated with cannabis use (Herkenham *et al.*, 1990; Begg *et al.*, 2005). The lack of toxicity of cannabinoids may be attributed to absence of CB_1 from the brain stem (Iversen, 2003). Furthermore CB_1 is also expressed in the periphery, including skeletal muscle (Cavuoto *et al.*, 2007), immune system (Galiègue

et al., 1995; Small-Howard *et al.*, 2005), gastrointestinal tract (Pertwee *et al.*, 1996), placenta (Park *et al.*, 2003), cardiovascular system (Liu *et al.*, 2000), testis (Gerard *et al.*, 1991) and prostate (Ruiz-Llorente *et al.*, 2003). A second cannabinoid receptor (CB_2) was elucidated from macrophages in the marginal zone of the spleen (Munro *et al.*, 1993). The two cannabinoid receptors share a 44% homology with each other and a 68% similarity in the transmembrane region (Munro *et al.*, 1993). Whereas CB_1 is localised mainly in the central nervous system, CB_2 is predominantly localised in the periphery such as in the spleen (Lee *et al.*, 2001) and in different types of immune cells. CB_1 receptors are also expressed in immune cells but are between 10 to 100 times lower than seen for CB_2 receptors (Galiègue *et al.*, 1995). It was found that levels of CB_2 mRNA were B cells > natural killer cells > monocytes > neutrophils > cluster of differentiation CD8+ cells > CD4+ cells (Galiègue *et al.*, 1995; Lee *et al.*, 2001). However there is also growing evidence of CB_2 expression in the central nervous system, including microglia in the human cerebellum (Núñez *et al.*, 2004), the rat cerebellum, brainstem and modest levels in the cortex (van Sickle *et al.*, 2005), vasculature of both human cerebral endothelial cells (Golech *et al.*, 2004) and rat Purkinje cells (Ashton *et al.*, 2006). The initial discovery of cannabinoid receptors in mammals promoted the question; do endogenous ligands exist that can activate these receptors?

1.2.2. Endocannabinoids, endogenous CB_1 and CB_2 ligands

Δ^9-THC being lipophilic suggested that an endogenous ligand for the cannabinoid receptors might also be a lipid. In 1992, the first endogenous cannabinoid ligand (endocannabinoid) was isolated from porcine brain, this was a fatty acid amide and named anandamide (AEA) after the Sanskrit word “ananda”, meaning “inner bliss” (Devane *et al.*, 1992). AEA binds to CB_1 (Devane *et al.*, 1992) and CB_2 (as a partial agonist at both receptors) (Bayewitch *et al.*, 1995; Howlett *et al.*, 2002) and also to the transient receptor potential vanilloid 1 cation channel; $TRPV_1$ (Zygmunt *et al.*, 1999; Smart *et al.*, 2000). Within three years a second endocannabinoid, 2-arachidonoyl-glycerol (2-AG) was isolated from canine gut (Mechoulam *et al.*, 1995) and a subsequent study in the same year isolated 2-AG in rat brain (Sugiura *et al.*, 1995). 2-AG is suggested to be the more important endocannabinoid as lower levels of AEA are reported in the brain suggesting that it may not be as physiologically important as 2-AG (Sugiura *et al.*, 2000). Indeed the abundance of 2-AG in rat brains is suggested to be 170 times higher than AEA (Stella *et al.*, 1997). 2-AG acts as an agonist of both CB_1

(Mechoulam *et al.*, 1995) and CB_2 (Mechoulam *et al.*, 1995; Gonsiorek *et al.*, 2000). Other endocannabinoids, all derivatives of arachidonic acid, have since been discovered and include; N-arachidonoyl dopamine (NADA) a $CB_1 > CB_2$ agonist (Bisogno *et al.*, 2000; Huang *et al.*, 2002), the ester of ethanolamine and arachidonic acid, O-arachidonoyl ethanolamine (virodhamine) a CB_1 partial agonist/antagonist and CB_2 agonist (Porter *et al.*, 2002) and the 2-AG analogue, 2-arachindonoyl glycerol ether (noladin ether) a CB_1 (Hanus *et al.*, 2001) and CB_2 agonist (Shoemaker *et al.*, 2005). There is some controversy as to whether noladin ether is a true central nervous system (CNS) endocannabinoid with some groups reporting this lipid in the brain (Hanus *et al.*, 2001; Fezza *et al.*, 2002) however, this is disputed by other groups. Upon testing of various mammalian brain regions the presence of noladin ether was not found (Oka *et al.*, 2003; Richardson *et al.*, 2007).

The endocannabinoids are synthesised on demand when intracellular Ca^{2+} is elevated, either by depolarisation or the action of phospholipase C (PLC) promoting the subsequent release of Ca^{2+} from stores (Kano *et al.*, 2009). The endocannabinoids AEA and 2-AG, whilst sharing a similar structure, are synthesised by different enzymes (Iversen, 2003). AEA is synthesised from the phospholipid precursor N-arachidonoyl-phosphatidylethanolamine (NAPE). N-acyltransferase (NAT) is Ca^{2+}-dependent enzyme which transfers arachidonic acid from phosphatidylcholine to the headgroup of phosphatidylethanolamine to produce NAPE (Cadas *et al.*, 1996). The requirement of Ca^{2+} is thought to be a rate limiting factor in the synthesis of NAPE and therefore AEA (Jin *et al.*, 2007). The increase in Ca^{2+} activates a D-type phosphodiesterase; NAPE-hydrolyzing phospholipase D (NAPE-PLD) which hydrolyses NAPE to form AEA and phosphatidic acid (Di Marzo *et al.*, 1994; Cadas *et al.*, 1997). Recently a Ca^{2+} independent NAT (rat LRAT-like protein; RLP-1) has been discovered and is expressed in the testis (Jin *et al.*, 2007). The physiological significance of the Ca^{2+} independent NAT is unknown at present but the localisation in the testis suggest that it may be important for AEA synthesis in that tissue (Okamoto *et al.*, 2007). The generation of NAPE-$PLD^{(-/-)}$ mice challenged whether the NAPE-PLD enzymatic pathway is required for AEA synthesis. NAPE-$PLD^{(-/-)}$ mice have AEA concentrations that are similar to wild-type littermates suggesting alternative biosynthesising enzymes must exist (Leung *et al.*, 2006). Another AEA synthesising pathway has been described starting with NAPE as the precursor. The two-step AEA synthesising pathway begins with the double-O-deacylation of NAPE by α/β domain containing hydrolase 4(ABDH4) to form

glycerophospho-AEA. This glycerophospho-AEA is then acted upon by glycerophosphodiesterase (GDE1) to generate AEA (Simon and Cravatt, 2008). A subsequent study using double knockout NAPE-PLD$^{(-/-)}$/GDE$^{(-/-)}$ mice partially disrupted AEA formation suggesting yet another synthesising pathway must exist for the generation of AEA (Simon and Cravatt, 2010). In brain and macrophage RAW264.7 cells AEA synthesis occurs from the precursor NAPE in a two-step process. This pathway requires the activation of phospholipase C (PLC) to generate phospho-AEA followed by subsequent activation of protein tyrosine phosphatase non-receptor type 22 (PTPN22) to generate AEA. However some less AEA was observed in the brain extracts from PTPN22$^{(-/-)}$ mice compared to wild type littermates therefore suggesting that other phosphatases may exist for the conversion of phospho-AEA to AEA (Liu *et al.*, 2006). AEA can be either transported across the membrane by diffusion through the membrane leaflet or through a membrane based transporter. There is still controversy as to the exact mechanism of AEA release and cellular uptake (Fowler, 2013).

Rapid termination of signalling occurs by degradation of AEA through the activation of the membrane bound enzyme, fatty acid amide hydrolase (FAAH) (Dainese *et al.*, 2014). FAAH can degrade AEA into arachidonic acid and ethanolamine (Di Marzo *et al.*, 1994). FAAH$^{(-/-)}$ mice have higher levels of AEA in the brain than wild type littermates suggesting that this enzyme is degrading the endocannabinoid (Cravatt and Lichtman, 2002). AEA can also be metabolised by cyclooxygenase-2 (COX-2) and lipoxygenase (LOX) enzymes in particular 12-LOX and 15-LOX (Woodward *et al.*, 2008; Yates and Barker, 2009).

As with AEA an increase in intracellular Ca^{2+} is required for 2-AG synthesis (Stella *et al.*, 1997). 2-AG is synthesised from phospholipid precursors through the hydrolysis of PIP_2 by PLC to produce diacylglycerol (DAG; Stella *et al.*, 1997). Diacylglycerol lipase (DAGL) α and DAGLβ are the enzymes which hydrolyse DAG at the sn-1 position to produce 2-AG (Stella *et al.*, 1997; Bisogno *et al.*, 2003). Moreover in mice lacking either DAGLα or DAGLβ the concentration of 2-AG in the brain is decreased by ~80% and ~50% respectively and is decreased by ~90% in the liver of DAGLβ$^{(-/-)}$ (Gao *et al.*, 2010). Furthermore a specific lysophosphatidylinositol-phospholipase C (LPI-PLC) present in porcine platelets and rat brain can also metabolise LPI (2-

arachidonoyl LPI) into the endocannabinoid 2-AG (Tsutsumi *et al.*, 1994; Kobayashi *et al.*, 1996).

2-AG metabolism can occur with FAAH but is thought to be less important as studies in $FAAH^{(-/-)}$ mice had increased AEA levels but 2-AG concentrations remained the same (Lichtman *et al.*, 2002). Alternatively 2-AG is a substrate for the serine hydrolase monoacylglycerol lipase (MAGL). *In vivo* studies in rats found that 2-AG is metabolised by MAGL into arachidonic acid and glycerol (Dinh *et al.*, 2002). Importantly MAGL in the brain is expressed in similar regions to CB_1 (Dinh *et al.*, 2002). When MAGL was overexpressed in neurons which were stimulated with NMDA/carbachol the synthesis of both AEA and 2-AG increased, however 2-AG levels were decreased in the neurons overexpressing MAGL. Moreover AEA levels in HeLa cells were similar to the levels in neurons transfected with the vector alone (Dinh *et al.*, 2002). However adenoviral vector-mediated gene transfer of MAGL into HeLa cells did not hydrolyse AEA or palmitoylethanolamine (PEA); a structural analogue of AEA (Dinh *et al.*, 2002). 2-AG is also a substrate for leukocyte-type 12-lipoxygenase (LOX; Kozak *et al.*, 2002) and for cyclooxygenases (COX), in particular COX-2 (Kozak *et al.*, 2000).

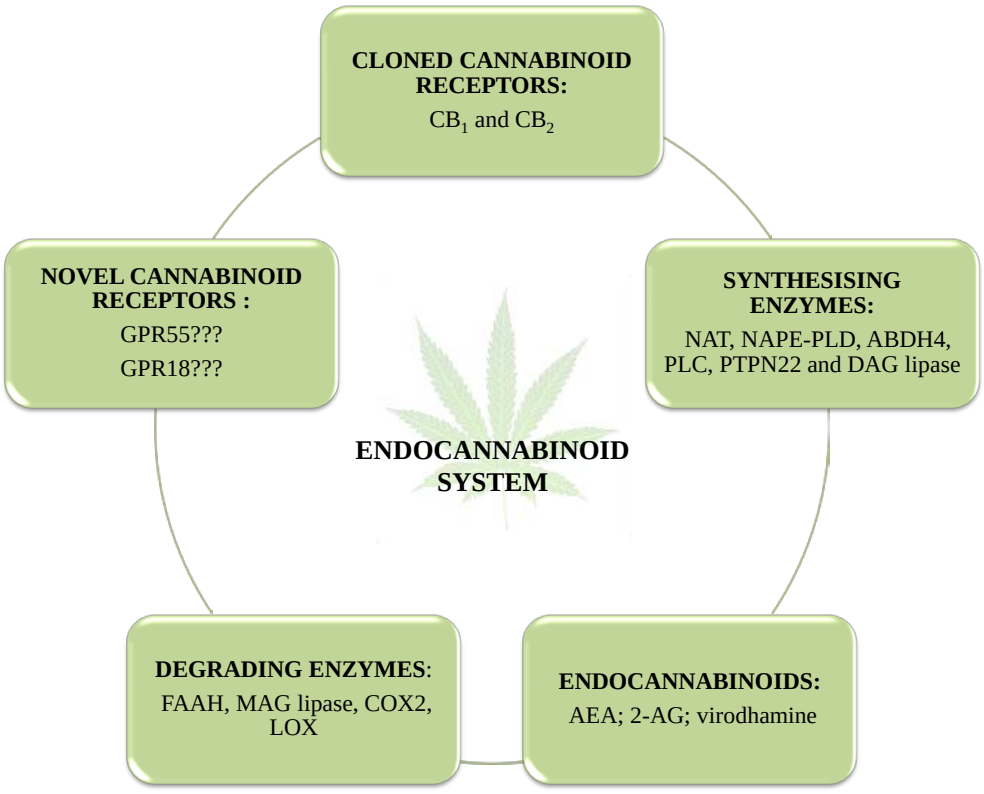

Figure 1.2: Overview of the endocannabinoid system. *Two cloned cannabinoid receptors; CB_1 and CB_2 along with the endogenous lipids, the endocannabinoids, which are produced on*

demand and enzymes for the synthesis and degradation of the endocannabinoids. Furthermore there is growing evidence of potential novel cannabinoid receptors such as GPR55 and GPR18.

1.2.3. Cannabinoid receptor signalling

The classical cannabinoid receptors are members of the GPCR Rhodopsin class A α-group (Civelli *et al.*, 2013) and therefore recruit G-proteins. CB_1 can inhibit adenylyl cyclase and therefore lower the concentration of the second messenger, cAMP (Howlett and Fleming, 1984). Four isoforms of adenylyl cyclase (I, V, VI and VIII) are reported to be inhibited by CB_1 signalling via $G_{\alpha i/o}$ (Rhee *et al.*, 1998). In contrast, CB_1 activation can stimulate three isoforms of adenylyl cyclase (II, IV and VII) which the authors suggest is mediated by $G_{\beta\gamma}$ subunits from the $G_{\alpha i/o}$ protein (Rhee *et al.*, 1998).

There is some controversy as to whether CB_1 receptors can promote Ca^{2+} mobilisation and this may depend on the cellular environment. 2-AG applied to CB_1 receptors is reported to promote Ca^{2+} mobilisation in two neuronal cell lines, NG108-15 cells and N18TG2 cells (Sugiura *et al.*, 1997). In contrast 2-AG does not induce Ca^{2+} mobilisation in the CB_1-HEK293 cells. However the synthetic cannabinoid WIN 55,212-2 can promote Ca^{2+} mobilisation which is $G_{\alpha q}$ mediated in CB_1-HEK293 cells (Lauckner *et al.*, 2005). A subsequent study in rat insulinoma β-cells (RIN m5F) showed that the CB_1 agonist arachidonoyl-chloro-ethanolamide (ACEA) can promote Ca^{2+} mobilisation, which may be $G_{\alpha q}$ mediated (De Petrocellis *et al.*, 2007).

Cannabinoid receptors are also reported to signal via kinase signalling pathways. CB_1, like many GPCRs, can promote activation of MAPK (Bouaboula *et al.*, 1995; Galve-Roperh *et al.*, 2002). Application of CP-55940 to the human astrocytoma cell line U373 MG which endogenously expresses CB_1 receptors and CHO-CB_1 cells promotes the phosphorylation of ERK1/2 (Bouaboula *et al.*, 1995). Furthermore CB_1 stably transfected HEK293 cells demonstrate ERK1/2 phosphorylation when challenged with either AEA or HU-210 (Liu *et al.*, 2000). Endothelial cells (ECV304) which endogenously express CB_1 when treated with HU-210 and AEA were also found to promote the phosphorylation of ERK1/2 (Liu *et al.*, 2000) Other members of the MAPK family are activated by CB_1, including p38 MAPK (Galve-Roperh *et al.*, 2002) and c-JUN-N-terminal kinase (JNK; Liu *et al.*, 2000; Rueda *et al.*, 2000). CB_1 also promotes the phosphorylation of AKT in stably transfected CHO cells or U373 MG

cells (Gómez del Pulgar *et al*., 2000). Signalling to AKT through CB_1 was dependent on $G_{\alpha i/o}$ proteins and PI-3-kinase (Gómez del Pulgar *et al*., 2000).

N-type Ca^{2+} channels can be inhibited in the neuroblastoma-glioma cell line (NG108-15) that have been challenged with WIN 55,212-2 (Mackie and Hille, 1992). N and P/Q type Ca^{2+} channels are inhibited in cultured rat hippocampal neurons through CB_1 (Twitchell *et al*., 1997). Also in AtT-20 cells stably expressing CB_1, AEA inhibits Q-type Ca^{2+} channels. These effects were sensitive to PTX and are therefore likely to be mediated by $G_{\alpha i/o}$ proteins (Mackie *et al*., 1995). Furthermore CB_1 receptors located in cat cerebral arterial smooth muscle cells stimulated with either WIN 55,212-2 or AEA can inhibit L-type Ca^{2+} channels. The modulation of the Ca^{2+} channels can be promoted through the activation of $G_{\alpha i/o}$ proteins (Gebremedhin *et al*., 1999). L-type Ca^{2+} channels are also activated in N18TG2 neuroblastoma cells challenged with the cannabinoid agonist, deasacetyllevonantradol (DALN) which was sensitive to SR141716A a CB_1 antagonist (Rubovitch *et al*., 2002). Furthermore inwardly rectifying K^+ channels were activated in AtT-20 cells that were transfected with CB_1 receptors (Felder *et al*., 1995; Mackie *et al*., 1995).

As with CB_1, activation of CB_2 receptors can inhibit adenylyl cyclase and this effect is sensitive to PTX application suggesting that $G_{\alpha i/o}$ proteins are involved (Bayewitch *et al*., 1995). Also forskolin induced cAMP accumulation was inhibited in CHO cells stably transfected with CB_2 receptors and mediated by $G_{\alpha i/o}$ proteins (Felder *et al*., 1995). However CB_2 receptor activation does not couple to ion channels as reported for CB_1. WIN 55,212-2 applied to CHO cells stably expressing CB_2 receptors did not affect K^+ currents (Felder *et al*., 1995). PLA_2, PLC and PLD activation along with Ca^{2+} mobilisation did not occur in CHO-CB_2 cells these cells (Felder *et al*., 1995). Furthermore in AtT-20 cells stably expressing CB_2 receptors treatment with WIN 55,212-2 did not inhibit the Ca^{2+} current (Felder *et al*., 1995). In contrast some cell lines do exhibit CB_2 receptor-mediated Ca^{2+} mobilisation; RIN m5F cells challenged with JWH133 demonstrate CB_2 receptor-mediated Ca^{2+} mobilisation (De Petrocellis *et al*., 2007). Furthermore 2-AG promoted Ca^{2+} mobilisation in HL-60 cells which was attenuated by application of the CB_2 antagonist, SR144528 and sensitive to PTX (Sugiura *et al*., 2000). CB_2 activation can also lead to changes in gene transcription, CP-55940 applied to the human pro-myelomonocytic cell line, HL60 promoted activation of ERK1/2 and subsequent immediate early gene Krox-24 expression

(Bouaboula *et al*., 1996). Activation of CB_2 receptors in HL-60 cells did not promote the phosphorylation of AKT (Gómez del Pulgar *et al*., 2000). However recent studies dispute this and CB_2 receptors in human prostatic carcinoma PC3 cells activate AKT (Sánchez *et al*., 2003). Therefore CB_2 receptor-mediated AKT phosphorylation may be cell type specific.

1.2.4. Non CB_1/CB_2 cannabinoid sensitive receptors

1.2.4.1. Transient receptor potential vanilloid 1

The transient receptor potential vanilloid 1 ($TRPV_1$) is a non-selective cation channel, but has a preference for Ca^{2+} over other cations (Vriens *et al.*, 2009). Originally $TRPV_1$ was found to be activated by capsaicin, noxious heat ($> 43^oC$) and protons (pH < 5.9) (Caterina *et al.*, 1997; Tominaga *et al.*, 1998; Vriens *et al.*, 2009) and is localised to small and medium primary sensory neurons (Caterina *et al.*, 1997). Interestingly $TRPV_1$ and CB_1 receptors are co-localised in cultured dorsal root ganglion neurons (Ahluwalia *et al.*, 2000), cholinergic myenteric neurons (Coutts *et al.*, 2002; Anavi-Goffer and Coutts, 2003) and several brain regions such as the basal ganglia and hippocampus (Cristino *et al.*, 2006). Previously it was shown with capsacin that the $TRPV_1$ binding site is located intracellularly (Jung *et al.*, 1999). AEA has also been shown to act intracellularly to activate $TRPV_1$ (De Petrocellis *et al.*, 2001). Endogenous ligands that have activity at vanilloid receptors are known as endovanilloids (Starowicz *et al.*, 2007). AEA acting at $TRPV_1$ was first observed in patch clamp experiments in either whole cell or isolated membranes of HEK293 cells transfected with rat $TRPV_1$. AEA, acting as a partial agonist, induced an inward current which was sensitive to the $TRPV_1$ antagonist, capzaspine (Zygmunt *et al.*, 1999). AEA sensitivity at $TRPV_1$ was further confirmed when screening ~1000 bioactive compounds for $TRPV_1$ activity in the FLIPR Ca^{2+} assay (Smart *et al.*, 2000). Smart *et al*., (2000) also observed AEA acting as a partial agonist, similarly to that reported by Zygmunt *et al*., (1999), inducing inward currents in HEK293 cells transfected with human $TRPV_1$. Whilst AEA can activate both CB_1 and $TRPV_1$ it is reported that 2-10 fold higher concentrations of AEA are required to activate $TRPV_1$ compared to concentrations required to mediated CB_1 responses (Starowicz *et al.*, 2007). Also the endocannabinoid NADA activates both rat and human $TRPV_1$ expressed in HEK293 cells. Furthermore the release of substance P and calcitonin gene-related peptide in dorsal root ganglion (DRG) cells is attributed to NADA activating $TRPV_1$ (Huang *et*

al., 2002). However the endocannabinoid 2-AG does not activate $TRPV_1$ (Zygmunt *et al.*, 1999).

1.2.4.2. Peroxisome proliferator-activated receptors

Peroxisome proliferator-activated receptors are nuclear receptor transcription factors of which there are three subtypes PPAR-α, -γ and -δ/β. Activated PPARs heterodimerise with nuclear retinoid X receptors and bind to PPAR response elements to promote gene transcription (O'Sullivan, 2007). PPARs have a diverse range of functions such as lipid metabolism, cell differentiation and survival and inflammatory responses (Michalik *et al.*, 2006). PPARs can be activated by a various ligands; free fatty acids, eicosanoids and prostaglandins (Berger and Moller, 2002). There is also growing evidence that PPARs can be activated by cannabinoids (O'Sullivan, 2007).

1.2.4.3. Novel cannabinoid receptors

Evidence suggests that there are at least three additional cannabinoid receptors; in the brain (Di Marzo *et al.*, 2000; Breivogel *et al.*, 2001; Begg *et al.*, 2005), in the cardiovascular system (Járai *et al.*, 1999; Begg *et al.*, 2005) and the immune system (Rao and Kaminski, 2006). Both AEA and WIN55212-12 applied to $CB_1^{(-/-)}$ mouse brain were observed to stimulate [^{35}S]GTPγS binding mediated by an unknown GPCR which did not bind Δ^9THC (Breivogel *et al.*, 2001). Moreover structural analogues of AEA were ineffective at promoting [^{35}S]GTPγS binding in brain membranes derived from $CB_1^{(-/-)}$ mice (Breivogel *et al.*, 2001). The effects of AEA induced [^{35}S]GTPγS binding in $CB_1^{(-/-)}$ brain membranes were unaffected by CB_1 (SR141716A) or CB_2 (SR144528) antagonists (Di Marzo *et al.*, 2000). The localisation of the WIN 55,212-2 sensitive receptor only partially overlaps with regions where CB_1 is found (Breivogel *et al.*, 2001). This suggests that the WIN 55,212-2 sensitive receptor has a divergent pharmacology and physiological role when compared to CB_1 and CB_2 receptors.

Vasodilatation of the mesenteric arteries has been observed with Abn-CBD and may act on a novel anadamide receptor which is distinct from CB_1 and CB_2 (Offertáler *et al.*, 2003). The existence of this novel anadamide receptor was further confirmed with physiological studies in $CB_1^{(-/-)}/CB_2^{(-/-)}$ mice where Abn-CBD could still exert vasodilation of the mesenteric arteries (Járai *et al.*, 1999). The hypothesis at the time was that an orphan GPCR could be responsible for the effects and attention turned to the G protein-coupled receptor 55 (GPR55). However when Abn-CBD was applied to

GPR55$^{(-/-)}$ mice and compared to wild type littermates it was discovered that the effect remained suggesting that GPR55 was not responsible (Johns *et al.*, 2007). More recently another oGPCR has been suggested as the Abn-CBD receptor, G protein-coupled receptor 18 (GPR18) (McHugh *et al.*, 2010). Interestingly, GPR18 and GPR55 share some pharmacology (Ross, 2009).

Cannabinoid receptors may have a role in the suppression of the immune response in T-cells derived from the spleen (Brown, 2007). Splenocytes derived from double knockout mice ($CB_1^{(-/-)}/CB_2^{(-/-)}$) treated with Δ^9THC, cannabinol, and HU-210 show increases in intracellular Ca^{2+} ($[Ca^{2+}]_i$) when compared to wild-type littermates. Furthermore mobilisation of Ca^{2+} was sensitive to CB_1 and CB_2 antagonists but was CB_1 and CB_2 independent suggesting a novel target for these cannabinoid ligands is present in splenocytes (Rao and Kaminski, 2006). In addition, the phytocannabinoid cannabidiol (CBD) is able to suppress the production of pro-inflammatory cytokines interleukin 2 (IL-2) and IFN-γ. Interestingly this effect is also seen in spleens derived from $CB_1^{(-/-)}/CB_2^{(-/-)}$ mice suggesting that a novel cannabinoid receptor may mediate the effects. The authors propose that there may be a role for GPR55 (Kaplan *et al.*, 2008) which is interesting as high levels of GPR55 mRNA have been detected in the spleen (Baker *et al.*, 2006; Ryberg *et al.*, 2007; Oka, *et al.*, 2010). This provides further evidence that GPR55 may have a role in immune function.

1.3. G-protein coupled receptor 55

In 1999 the orphan G-protein coupled receptor 55 (GPR55) was discovered *in silico*, and subsequently cloned, through the use of homology searches of previously discovered GPCRs using BLAST (basic local alignment search tool) of the expressed sequence tags database (Sawzdargo *et al.*, 1999). GPR55 is a 7TM spanning receptor containing 319 amino acids and the gene is mapped to chromosome 2q37 (Sawzdargo *et al.*, 1999). GPR55 has attracted much recent attention as it is thought to be sensitive to certain cannabinoid ligands and has been proposed to be a novel cannabinoid receptor (Pertwee *et al.*, 2010).

1.3.1. GPR55 pharmacology

Cannabinoid activation of GPR55 was first described in two industrial patents (Brown and Wise, 2001; Drmota *et al.*, 2004). In the first patent from GlaxoSmithKline a yeast based assay highlighted that reporter gene activity is increased in the presence of

AM251 when GPR55 is expressed (Brown and Wise, 2001). The second patent from AstraZeneca further confirmed that GPR55 was sensitive to synthetic cannabinoid ligands, phytocannabinoids and the endocannabinoids AEA, 2-AG, and virodhamine. Furthermore some N-acyl amides were reported to activate GPR55 in GTPγS assays (Drmota *et al*., 2004). AstraZeneca confirmed their findings in a key publication in the British Journal of Pharmacology suggesting that GPR55 is a novel cannabinoid receptor (Ryberg *et al.*, 2007). However, controversy remains as to whether endocannabinoids, such as AEA, 2-AG and virodhamine can activate GPR55. Some research groups report that endocannabinoids can activate GPR55 (Ryberg *et al.*, 2007; Lauckner *et al.*, 2008; Sharir *et al.*, 2012), however, other groups do not reiterate these findings (Oka *et al.*, 2007; Henstridge *et al.*, 2009). A beta-arrestin study also highlighted that endocannabinoids only weakly activated GPR55 (Yin *et al.*, 2009). Finally there is also controversy as to whether palmitoylethanolamine (PEA), a structural analogue of AEA, activates GPR55. Some groups find that low nanomolar potencies of PEA activate GPR55 (Ryberg *et al.*, 2007), whilst others found no difference when PEA was applied to hGPR55-HEK293 cells and compared to control HEK293 cells (Oka *et al.*, 2007; Lauckner *et al.*, 2008). Furthermore GPR55 does not possess the classic cannabinoid binding pocket (Petitet *et al.*, 2006). Therefore the binding sites for the same ligand will be different between CB_1/CB_2 and GPR55 (Garland, 2013). However, emerging data suggests that the endogenous lipid, L-α-lysophosphatidylinoisitol (LPI) is the natural ligand for GPR55. In 2007 a Japanese group first revealed that LPI could activate GPR55 (Oka *et al.*, 2007). Interestingly a subsequent publication from the same group demonstrated that LPI containing an arachidonic fatty acid chain was the most biologically active LPI species in GPR55-mediated Ca^{2+} mobilisation and ERK1/2 phosphorylation assays (Oka *et al.*, 2009). The activity of LPI at GPR55 has now been confirmed by a number of groups (Henstridge *et al*., 2009; Kapur *et al*., 2009; Yin *et al*., 2009).

The synthetic cannabinoid ligand, O-1602 is also a putative GPR55 ligand. It was first noted as a GPR55 agonist when tested in a [^{35}S]GTPγS binding assay where it activated the receptor in a concentration dependent manner (Drmota *et al*., 2004; Johns *et al*., 2007). However it remains controversial as to whether O-1602 activates GPR55. O-1602 activation does not promote ERK1/2 phosphorylation or Ca^{2+} mobilisation assays in hGPR55-HEK293 cells (Oka *et al.*, 2009). Furthermore O-1602 does not effect β-arrestin redistribution (Kapur *et al.*, 2009). However O-1602 can promote GPR55-

mediated inhibition of osteoclastogenesis, an effect that was not observed in GPR55$^{(-/-)}$ mice (Whyte *et al.*, 2012). Also O-1602 decreases the contractility of colonic strips which is blocked in GPR55$^{(-/-)}$ mice when compared to control wild-type littermates (Ross *et al.*, 2012). These data suggest that O-1602 exhibits varying effects on GPR55 depending on the cell type being studied.

Cannabidiol (CBD) is an antagonist for GPR55 and many researchers find that CBD can antagonise GPR55 responses to LPI (Ryberg *et al.*, 2007; Whyte *et al.*, 2009). However CBD is known to act at various targets; CBD has affinity for the Abn-CBD receptor in the vasculature (Járai *et al.*, 1999) therefore suggesting that it may also be an antagonist for GPR18 (McHugh *et al.*, 2010). CBD is also reported to be a CB_1 and CB_2 antagonist in [^{35}S]GTPγS binding assays *in vitro* suggesting that *in vivo* CBD may effect more than just GPR55 (Thomas *et al.*, 2007). However this is contrary to previous data which ruled out CBD-induced activation of cannabinoid receptors in glioma (U87) cell migration (Vaccani *et al.*, 2005). CBD may also act at $TRPV_1$ to promote antihyperalgesic effects (Costa *et al.*, 2004) and CBD activates PPARγ promoting 3T3-L1 differentiation into adipocytes (O'Sullivan and Kendall, 2010). Therefore the development of more GPR55 specific antagonists is required to help clarify the role of GPR55 in normal and pathological states. Recently CID16020046 was identified in a high throughput screen and discovered to be a selective GPR55 antagonist against LPI induced Ca^{2+} mobilisation, ERK1/2 phosphorylation and transcription factor activation in HEK293 cells stably transfected with GPR55. These effects were not observed in CB_1 and CB_2 transfected HEK293 cells. Furthermore CID16020046 also was effective in endogenous GPR55 expressing cells with similar potencies to that noted in the recombinant cells (Kargl *et al.*, 2013). The generation of more specific antagonists like CID16020046 will help the research field gain a better understanding of the physiological role of GPR55.

1.3.2. Localisation of GPR55

GPR55, when compared to the two classical cannabinoid receptors, shares only 13.5% and 14.5% homology with CB_1 and CB_2 respectively (Oka *et al.*, 2007). Phylogenetically CB_1 and CB_2 are members of the Rhodopsin class A α-group whereas GPR55 is a member of the class A δ-group (Civelli *et al.*, 2013). Furthermore, when GPR55 was subjected to a homology search using the GenBank database it highlighted that GPR55 shared a higher level of homology with GPCRs which are members of the

rhodopsin Class A δ-group purinoreceptors; GPR35 (37%), GPR92 (30%), P_2Y_5 (30%), GPR23 (29%) (Baker *et al.*, 2006). Interestingly the endogenous lipid lysoposphatidic acid (LPA) has been reported to activate GPR35 (Oka, *et al.*, 2010), GPR92 (Kotarsky *et al.*, 2006; Lee *et al.*, 2006), P_2Y_5 (Pasternack *et al.*, 2008; Lee *et al.*, 2009) and GPR23 (Noguchi *et al.*, 2003; Lee *et al.*, 2007) but does not activate GPR55 (Oka *et al.*, 2007; Henstridge *et al.*, 2009). Furthermore other lysophospholipids; lysophsophatidylserine, lysophosophatidylcholine and lysophsophatidylethanolamine do not induce GPR55-mediated ERK1/2 phosphorylation (Oka *et al.*, 2007). Interestingly, other notable members of the rhodopsin Class A δ-group are the free fatty acid receptors; GPR40 (Briscoe *et al.*, 2003) which is sensitive to medium to longer chain fatty acids, GPR41 and GPR43 (Brown *et al.*, 2003), which are sensitive to shorter chain fatty acids with 6 or less carbons. Also the putative Abn-CBD receptor which also is activated by the lipid N-arachidonoyl glycine (NAGly), GPR18 (McHugh *et al.*, 2010) is located within the δ-group (Civelli *et al.*, 2013). Therefore GPR55 is clustered in phylogenetic proximity to a number of novel lipid sensing receptors.

GPR55 mRNA is expressed in various brain regions, including caudate, putamen (Sawzdargo *et al.*, 1999), hippocampus, frontal cortex, cerebellum, striatum, hypothalamus and brain stem (Ryberg *et al.*, 2007). GPR55 mRNA was also detected in the adrenal glands, spleen, jejunum and ileum (Ryberg *et al.*, 2007). There is evidence of GPR55 mRNA in microglia (Pietr *et al.*, 2009), large diameter dorsal root ganglion (Lauckner *et al.*, 2008), bone (Whyte *et al.*, 2009) and in metastatic cancer cells (Ford *et al*., 2010; Andradas *et al*., 2011) including the prostate cancer cell line; DU145 (Piñeiro *et al.*, 2011).

1.3.3. GPR55 signal transduction

There is a great deal of controversy as to whether cannabinoids activate GPR55. However there is consensus that the membrane derived lipid lysophosphatidylinositol (LPI) is an endogenous ligand for GPR55. Originally LPI was found to activate ERK1/2 in a screening assay that had also looked at several cannabinoid ligands (Oka *et al.*, 2007). Whilst the cannabinoid ligands had shown no difference when compared to control HEK293 cells, HEK293 cells transiently transfected with human GPR55 were found to increase the phosphorylation of ERK1/2 when LPI was applied (Oka *et al.*, 2007).

Around the same time, Ca^{2+} mobilisation and the activation of the transcription factor, nuclear factor of activated T-cells (NFAT) had been studied and the signalling pathway elucidated, further confirming the effects of LPI activation on GPR55 (Henstridge *et al.*, 2009). As mentioned previously LPI with an arachidonic fatty acid chain induced the most potent effects on Ca^{2+} mobilisation and ERK1/2 phosphorylation (Oka *et al.*, 2009). Two heterotrimeric G-proteins have been implicated in GPR55-mediated signalling (Lauckner *et al.*, 2008; Henstridge *et al.*, 2009). GPR55-mediated activation of $G_{\alpha 13}$ was first reported in the GlaxoSmithKline patent application (Brown and Wise, 2001). The second G-protein associated with GPR55 is $G_{\alpha q}$ which is involved in the mobilisation of Ca^{2+} (Lauckner *et al.*, 2008; Obara *et al.*, 2011). In endothelial cells AEA promoted GPR55-mediated Ca^{2+} mobilisation is distinct requiring the activation of PI3K-Bmx-PLCγ signalling. Moreover integrin clustering is necessary to release the inhibition of GPR55 Ca^{2+} signalling, mediated by CB_1 activation (Waldeck-Weiermair *et al.*, 2008). It remains to be determined if $G_{\alpha 13}$ or $G_{\alpha q}$ are required for Ca^{2+} mobilisation in endothelial cells.

GPR55 can also act on several kinase signalling pathways such as MAPK, PI-3-kinase and AKT. Initially LPI was found to promote GPR55-mediated ERK1/2 phosphorylation but several cannabinoids tested at the same time had no effect (Oka *et al.*, 2007). Recently evidence reported that certain cannabinoid ligands phosphorylate ERK1/2 by activating GPR55 (Henstridge *et al.*, 2010; Anavi-Goffer *et al.*, 2012). Furthermore Anavi-Goffer *et al.*, (2012) report that SR141716A can both activate and inhibit GPR55-mediated ERK1/2 phosphorylation. They describe for the first time that there may be an orthosteric and allosteric binding site present on GPR55. Previously AM251 and SR141716A, CB_1 antagonists are reported as agonists of GPR55 (Kapur *et al.*, 2009; Yin *et al.*, 2009; Henstridge *et al.*, 2010). However SR141716A can also act as a GPR55 antagonist (Lauckner *et al.*, 2008; Piñeiro *et al.*, 2011). The discovery of a potential allosteric site on GPR55 may help to explain the discrepancies with SR141716A (Anavi-Goffer *et al.*, 2012). The aforementioned studies were carried out in recombinant GPR55 over-expressing systems however ERK1/2 phosphorylation is also reported in cell-types endogenously expressing GPR55. Murine BV2 microglia cells treated with interferon γ (INFγ) produced a concentration-dependent increases in LPI induced ERK1/2 phosphorylation (Pietr *et al.*, 2009). ERK phosphorylation is also reported in some cancer cells treated with LPI (Andradas *et al.*, 2011; Piñeiro *et al.*, 2011). Another kinase thought to be downstream of GPR55 is AKT. Modulation of

GPR55 expression in breast and glioblastoma cancer cells did not alter AKT phosphorylation suggesting it is not required for the proliferation of these cancer cell types (Andradas *et al.*, 2011). However when LPI was applied to prostate cancer cells GPR55 mediated AKT phosphorylation was observed (Piñeiro *et al.*, 2011). Overall GPR55 has the ability to influence multiple signalling pathways when activated. These include signalling to transcription factors such as NFAT (Henstridge *et al.*, 2009), CREB and NFκB (Henstridge *et al.*, 2010) suggesting GPR55 may be important for transcription of genes such as c-Fos (Andradas *et al.*, 2011).

1.3.4. (Patho)physiology of GPR55

The pathophysiological role of GPR55 has still to be fully elucidated. Several studies are now highlighting pathologies where GPR55 may be important. GPR55 is thought to have a role in cancer (Ford *et al.*, 2010; Andradas *et al.*, 2011; Piñeiro *et al.*, 2011), immune regulation (Pietr *et al.*, 2009; Balenga *et al.*, 2011), pain modulation (Staton *et al.*, 2008; Schuelert and McDougall, 2011), diabetes, obesity (Moreno-Navarrete *et al.*, 2012) and osteoarthritis (Whyte *et al.*, 2009). The lack of GPR55-specific antagonists has made deciphering GPR55 pathophysiology difficult at the present time. To overcome this problem the use of siRNA targeting GPR55 has helped to decipher the effects that are mediated by GPR55. This has been successful in studies with prostate cancer cells where increases in AKT and ERK1/2 phosphorylation and Ca^{2+} mobilisation are all mediated by GPR55 (Piñeiro *et al.*, 2011). However siRNA applied to breast cancer cells did not lower the endogenous level of GPR55 in the cells however when the cells were transiently transfected with GPR55 and then siRNA was applied the GPR55 level lowered suggesting that the siRNA was lowering the expression of the transfected GPR55 (Ford *et al.*, 2010). Many other studies have employed GPR55 siRNA to gain an understanding of the effect GPR55 has in areas as diverse as neuroprotection (Kallendrusch *et al.*, 2013), breast and brain cancer proliferation (Andradas *et al.*, 2011) and Ca^{2+} mobilisation in endothelial cells (Waldeck-Weiermair *et al.*, 2008). Another method for deciphering GPR55 mediated effects is to use $GPR55^{(-/-)}$ mice. $GPR55^{(-/-)}$ mice were generated and have allowed assessment of inflammatory pain (Staton *et al.*, 2008). The knockout mice have also highlighted that GPR55 is necessary for regulating increases in bone mass (Whyte *et al.*, 2009). These mice are valuable tools in understanding the physiological processes mediated by GPR55 and allow an understanding of the effects GPR55 has on human physiology (Hall *et al.*, 2009).

1.3.4.1. GPR55 and cancer

GPR55 is expressed in several types of cancer derived from the brain, cervix, pancreas (Andradas *et al.*, 2011), breast (Ford *et al.*, 2010; Andradas *et al.*, 2011), skin (Andradas *et al.*, 2011; Pérez-Gómez *et al.*, 2013), blood (Oka *et al.*, 2010), ovaries and prostate (Piñeiro *et al.*, 2011). GPR55-mediated cancer cell proliferation is induced by LPI with the MAPK pathway playing an important role especially in aggressive cancer (Andradas *et al.*, 2011). Early studies with LPI reported that the lipid was synthesised by PLA_2 in k-ras oncogene transformed fibroblasts where the concentration rose to three times that observed in normal fibroblasts (Falasca and Corda, 1993). A subsequent study highlighted that k-ras oncogene transformed rat thyroid cells were also found to have an accumulation of LPI due to the increased activity of PLA_2 (Falasca and Corda, 1994). Moreover LPI accumulated in the extracellular medium of neoplastic fibroblasts and was found to promote the proliferation of these cells an effect that was not observed in normal fibroblasts (Falasca, *et al.*, 1998). LPI was also found to accumulate in the ascites of women with ovarian cancer (Xiao *et al.*, 2001; Sutphen *et al.*, 2004). Late stage and recurrent ovarian cancer samples were found to have higher concentrations of unsaturated LPI (Shen *et al.*, 2001). These results suggested that LPI is being released from cancer cells into the tumour microenvironment and then could promote effects in an autocrine manner on at the time an unknown membrane target. Therefore late stage ovarian cancer cells that have GPR55 present may have exacerbated effects, such as proliferation, due to their tumour microenvironments (ascites) containing the more biologically active LPI species which could then act upon GPR55 present in the cells that are releasing LPI. Furthermore the prostate cancer cell line, DU145 confirmed LPI was generated in cancer cells through the activation of cytosolic PLA_2 ($cPLA_2$). Application of $cPLA_2$-siRNA decreased the proliferation of PC3 prostate cells, using an anchorage independent assay, when compared to scrambled cPLA2-siRNA but could be recovered by exogenous application of LPI. Furthermore [^{3}H]-LPI when applied to PC3 cells accumulated in the extracellular medium and further experiments concluded that the ABCC1 transporter was involved in the release of LPI from the cytosol as knockdown of ABCC1 inhibited the accumulation of [^{3}H]-LPI in the extracellular medium. Therefore LPI is thought to act in an autocrine manner to augment the effects of LPI on the PC3 prostate cancer cells (Piñeiro *et al.*, 2011). Proliferation mediated by GPR55 has also been observed in breast cancer and glioblastoma cell lines and correlated with an increase in the percentage of cells exhibiting the proliferation marker, Ki67 (Andradas *et al.*, 2011). Indeed this effect was also observed *in vivo* where there

was an increase in proliferation of cells in a xenograft glioblastoma assay (Andradas *et al.*, 2011). Overall the presence of GPR55 increased the proliferative effect in several cancer cell types and this was reversed with GPR55 knockdown. However one study has reported contradictory effects where application of O-1602 and AEA-induced GPR55 activation which was anti-proliferative in cholangiocarcinoma both *in vitro* and *in vivo* (Huang *et al.*, 2011). The effects were found to require $G_{\alpha 12}$, JNK, lipid rafts and the FAS receptor suggesting that either the discrepancies may be due to the effects being cell type specific or may be due to ligand biased signalling via GPR55 in this cell type.

Furthermore two breast cancer cell lines; MCF-7 and MDA-MB-231 were found to express GPR55 mRNA. Higher GPR55 mRNA expression was found in the MDA-MB-231 cells which are known to have a higher metastatic capability than the MCF-7 cells (Ford *et al.*, 2010). The authors observed the MCF-7 cells did not migrate towards serum and LPI had no effect in a Boyden chamber assay. However increasing the expression of GPR55 by transiently transfecting GPR55 cDNA into MCF-7 cells led to the development of a migratory phenotype more typical of the MDA-MB-231 cells, whereby the cells could now migrate towards the serum an effect which was enhanced when LPI was present. Furthermore the invasiveness of MCF-7 cells was greater when GPR55 expression was increased by prior transient transfection of GPR55. The MDA-MB-231 cells also exhibited an elongated phenotype which exhibited polarity when plated on grooved substrata. These results suggest GPR55 is important for polarity, migration and invasion in breast cancer cells (Ford *et al.*, 2010).

1.3.4.2. GPR55 and the immune system

Staton *et al.* (2008) studied neuropathic and inflammatory pain using GPR55 knockout mice and wild type controls. Levels of both pro-inflammatory and anti-inflammatory cytokines were found to increase in $GPR55^{(-/-)}$ when compared to $GPR55^{(+/+)}$. These results suggest that GPR55 has a role in the regulation of the production of certain cytokines (Staton *et al.*, 2008). Mast cells are mediators of inflammatory events and as such are important in inflammatory mediated angiogenesis. Mast cells activated by the phorbol ester; 12-O-Tetradecanoylphorbol-13-acetate (TPA) promoted the release of nerve growth factor. This concentration of TPA induced nerve growth factor was lower when cannabinoid like ligand palmitoylethanolamine (PEA) was applied to human mastocytic cells (HMC-1). However neither CB_1 or CB_2 were expressed in HMC-1

cells (Cantarella *et al.*, 2011). Previously PEA has been reported to be a GPR55 agonist (Ryberg *et al.*, 2007). Application of GPR55 siRNA did not lower the TPA induced concentration of nerve growth factor in HMC-1 cells challenged with PEA suggesting that PEA induced GPR55 activation promotes an anti-inflammatory effect by inhibiting the release of nerve growth factor in HMC-1 cells (Cantarella *et al.*, 2011).

Recent studies utilising western blotting techniques have shown that p38 mitogen activated protein kinase (p38 MAPK) and activating transcription factor 2 (ATF2) are both phosphorylated when treated with 1 μM LPI. The study utilised stably transfected hGPR55-HEK293 cells and IM9 lymphoblastoid cells. The IM9 cells are derived from B-cells which are immune cells found in the spleen and that the group found to endogenously express GPR55 mRNA (Oka, *et al.*, 2010). Treatment with GPR55 siRNA reduced the level of p38 MAPK and ATF2 phosphorylation in these cells suggesting that the phosphorylation is dependent on GPR55 (Oka, *et al.*, 2010).

GPR55 expression is also found in human neutrophil (HL60) cells. To allow effective neutrophil migration GPR55 and CB_2 are reported to act in a synergistic manner in the HL60 cells. Application of both AM251 (GPR55 agonist) and 2-AG (CB_2 agonist) increased the migration observed with HL60 cells compared to either agonist alone. Moreover an elongated migratory phenotype was only observed when both agonists were applied together. The migration was sensitive to both GPR55 and CB_2 antagonism. Furthermore the two receptors also promote cross talk to inhibit the formation of reactive oxygen species and neutrophil degranulation. Moreover the crosstalk between GPR55 and CB_2 is mediated by the small Rho GTPases (Balenga *et al.*, 2011).

Recently GPR55 is suggested to possibly play a role in multiple sclerosis. $GPR55^{(+/+)}$ and $GPR55^{(-/-)}$ mice with a C57BL/6 genetic background were immunised with myelin oligodendrocyte glycoprotein 35-55 peptide (MOG_{35-55}) to promote experimental autoimmune encephalomyelitis (EAE); a model of multiple sclerosis. The $GPR55^{(-/-)}$ mice were less susceptible to the development of EAE than wild type littermates. The development of EAE was lower in female $GPR55^{(-/-)}$ mice when compared to both wild type littermates and male $GPR55^{(-/-)}$ mice. The authors also report that changing the genetic background can influence the disease severity. The ABH genetic background for $GPR55^{(-/-)}$ mice followed the trend of female mice having

a lower severity of EAE but this was not as prominent as had been seen with the mice of with a C57BL/6 genetic background (Sisay *et al.*, 2013).

1.3.4.3. GPR55 and pain

GPR55 has been highlighted to play a role in mediating sensitivity to pain. Hyperalgesia to mechanical stimuli after the application of Freund's complete adjuvant (FCA) was not observed for two weeks after the injection of FCA in male $GPR55^{(-/-)}$ mice. Moreover partial ligation of the sciatic nerve in both male and female GPR55(-/-) mice did not promote hyperalgesia to mechanical stimuli for four weeks. Furthermore GPR55 knockout animals displayed a resistance to inflammatory and neuropathic pain (Staton *et al.*, 2008). GPR55 is a suggested target inducing pro-nociception in a rat chronic constriction injury (CCI) model. Application of O-1602 was found to increase the pain sensitivity of the rat paw in this neuropathic pain model (Breen *et al.*, 2012). Furthermore in a rat model of arthritis, application of O-1602 decreased nociception of the knee joint (Schuelert and McDougall, 2011). The O-1602 anti-nociceptive effects were mediated by un-myelinated C-fibres and were unaffected by application of the antagonists to CB_1 and CB_2; AM281 and AM630 respectively. Moreover, application of O-1918 the Abn-CBD antagonist prior to application of O-1602 increased the sensitivity to pain suggesting that a novel target is mediating the effect with one possibility being GPR55 (Schuelert and McDougall, 2011). However a caveat of the study is that O-1602 can also target the Abn-CBD receptor and therefore the effects may be mediated by GPR18 (McHugh *et al.*, 2010). Therefore further work using GPR55 knockout animals would be required to confirm if GPR55 plays a role in these pain models.

Recent evidence reports that GPR55 has a pro-nociceptive effect in peripheral sensory neurons *in vivo* (Gangadharan *et al.*, 2013). LPI challenge in $G_{\alpha 13}{}^{(-/-)}$ and $G_{\alpha q}{}^{(-/-)}$ mice highlighted these G-proteins were important for the LPI induced mechanical hypersensitivity. However the loss of mechanical hypersensitivity was greater in these mice than observed in the $GPR55^{(-/-)}$ mice suggesting that the LPI-induced sensitivity to pain in sensory neurons are only partially mediated by GPR55. Moreover LPI partially lowered cancer associated pain in $GPR55^{(-/-)}$ mice (Gangadharan *et al.*, 2013). Interestingly GPR55 can be extruded from cancer cells into the tumour microenvironment therefore sensory neurons in the vicinity of the tumour could potentially be activated by this increase in LPI concentration (Piñeiro *et al.*, 2011).

Finally in contrast to the previous reports of GPR55 mediated pro-nociception, a recent study highlights that anti-nociception in mice treated with PEA and AM251 followed by an injection of formalin may be attributed to GPR55, however knockout mice would be required to substantiate this (Naderi *et al.*, 2012).

1.3.4.4. GPR55 and bone

GPR55 mRNA is expressed in osteoclasts (bone resorption) and osteoblasts (bone formation) cells derived from humans or mice (Whyte *et al.*, 2009). GPR55 mediated the inhibition of O-1602-induced osteoclastogenesis as this effect was not observed in $GPR55^{(-/-)}$ mice. LPI and O-1602 promoted osteoclast polarisation and bone resorption by GPR55 activating Rho and ERK1/2 signalling. The activation of Rho and ERK1/2 was not observed in osteoclasts derived from GPR55 knockout mice. There were subtle differences as LPI induced ERK1/2 phosphorylation which was decreased in cells pre-treated with cannabidiol (CBD). However the CBD decrease in ERK1/2 phosphorylation was not significant. Furthermore Rho activation was increased with O-1602 and LPI however prior treatment with CBD was found to significantly lower the O-1602 induced Rho activation. In contrast the LPI increased Rho activation but was not significantly lowered with CBD pre-treatment. The authors noted that ligand bias may promote these signalling differences (Whyte *et al.*, 2009). O-1602 and LPI-induced Rho activation was mediated through GPR55 as osteoclasts derived from $GPR55^{(-/-)}$ mice exhibited Rho levels that were decreased compared to wild type osteoclasts (Whyte *et al.*, 2009). Furthermore bone volume was increased due to a decrease in bone resorption in male $GPR55^{(-/-)}$ mice. The authors noted that there was an increase in the number of osteoclasts but they were found to be inactive. Interestingly these effects are present in an osteopetrotic phenotype. GPR55 may therefore have a role in osteoporosis, arthritis and bone cancer pain (Ross, 2011).

1.3.4.5. GPR55 and the cardiovascular system

Originally, as mentioned before, studies with mesenteric arteries had highlighted that Abn-CBD could activate a novel cannabinoid receptor to promote vasodilatation as these effects remained in double knockout mice $CB_1^{(-/-)}/CB_2^{(-/-)}$ (Járai *et al.*, 1999; Offertáler *et al.*, 2003). This novel receptor was primarily considered to be GPR55 but was then discounted as the vasodilatation remained in $GPR55^{(-/-)}$ mice (Johns *et al.*, 2007). GPR55 has since been visualised in mesenteric arterial smooth muscle cells through the use of T1117 a fluorescent tetramethylrhodamine attached to AM251 (Daly

et al., 2010). Whilst AM251 is an antagonist of CB_1 receptors (Pertwee, 2006) it is also an agonist of GPR55 (Henstridge *et al.*, 2010). Ca^{2+} mobilisation occurred when T1117 was applied to hGPR55-HEK293 cells an effect that was attenuated in control HEK293 cells. However T1117 was found to be inactive at CB_1 receptors (Daly *et al.*, 2010). Furthermore application of O-1602 prior to application of T1117 reduced the fluorescence observed suggesting that O-1602 had internalised GPR55 before T1117 was applied. GPR55 was found to be localised to the three layers of the arteries; the tunica media, adventitia and endothelium (Daly *et al.*, 2010).

In human umbilical vein endothelial cells (HUVEC), GPR55 is reported to mediate Ca^{2+} mobilisation. However the GPR55 mediated Ca^{2+} mobilisation in HUVEC cells depends on the configuration of integrins in the cell membrane. When integrins were clustered GPR55 mediated Ca^{2+} mobilisation was seen as the inhibition that had previously been exerted by the CB_1 receptor was diminished (Waldeck-Weiermair *et al.*, 2008). AEA applied in the presence of extracellular Ca^{2+} was found to initiate signalling through CB_1 which activated spleen tyrosine kinase (Syk) which then inhibits PI-3-kinase; which is required for GPR55 signalling to occur. It is the action of integrin clustering which then negatively regulates Syk promoting the uncoupling of CB_1 and the β1 integrin thereby allowing AEA-induced GPR55 mediated Ca^{2+} mobilisation to occur in the HUVEC cells (Waldeck-Weiermair *et al.*, 2008). Furthermore LPI applied to HUVEC cells promoted the mobilisation of Ca^{2+} and membrane hyperpolarisation which was augmented when GPR55 expression was increased by transient transfection and was diminished when GPR55-siRNA was present (Bondarenko *et al.*, 2010). Previously LPI was found to be increased in bradykinin stimulated endothelial cells through the activation of PLA_2 (Kaya *et al.*, 1989). This could allow LPI to act in an autocrine manner on targets in the endothelial cells. Moreover the depolarising current in endothelial cells was GPR55-independent. LPI can exert direct effects by acting on ion channels and therefore may have a role in membrane potential. LPI triggered the hyperpolarisation of endothelial cells by acting directly on intermediate conductance Ca^{2+} activated K^+ (IK_{Ca}) channels (Bondarenko *et al.*, 2011). Furthermore LPI can also act on endothelial large-conductance Ca^{2+} and voltage-gated K^+ (BK_{Ca}) channels suggesting that LPI effects in endothelial cells are partially mediated by GPR55 with LPI induced ion channel activation also playing a role (Bondarenko *et al.*, 2011).

More recently GPR55 mRNA was expressed in rat neonatal ventricular cardiomyocytes and divergent signalling events were dependent on GPR55 localisation. Application of LPI extracellularly to GPR55 located at the cell membrane promotes depolarisation that is Ca^{2+} independent. However application of LPI to intracellular GPR55 hyperpolarises the cardiomyocyte membrane and was found to be Ca^{2+} dependent. The effects of LPI were antagonised by the application of a novel GPR55 antagonist ML-193 (Kotsikorou *et al.*, 2013; Yu *et al.*, 2013; Zhao and Abood, 2013).

Angiogenesis may also be GPR55-mediated by a novel N-acyl amino acid; N-arachidonoyl-L-serine, an 'endocannabinoid-like' lipid (Zhang *et al.*, 2010). Migration of endothelial cells was partially reduced when GPR55-siRNA was present and the tube formation was also partially inhibited with GPR55 knockdown (Zhang *et al.*, 2010). Application of O-1918 inhibited the tube formation when GPR55 was present but had no effect when GPR55 was knocked down (Zhang *et al.*, 2010). O-1918 has previously been reported as inhibiting the effects of the Abn-CBD receptor in endothelial cells (Offertáler *et al.*, 2003). However, it remains to be determined if O-1918 is a GPR55 antagonist.

1.3.4.6. GPR55 and the nervous system

The role of GPR55 in the brain is still in its infancy at the present time. However research is beginning to reveal pathologies where GPR55 may be of importance. GPR55 mRNA is expressed in the central nervous system (high to low abundance) in the frontal cortex, striatum, hypothalamus, brain stem, hippocampus, cerebellum and spinal cord and is localised in regions where CB_1 was also present (Ryberg *et al.*, 2007). Whereas another study reported GPR55 mRNA in the striatum > hippocampus > forebrain > cortex > cerebellum (Wu *et al.*, 2013). Furthermore LPI is present in brain (37.5 nmol/g tissue). Furthermore the second most common LPI composition in the rat brain contains the arachidonic fatty acid which is reported as the most potent form to activate GPR55 (Oka *et al.*, 2009). Recently GPR55 expression was reported to be co-localised with vesicular glutamate transporter 1 (vGLUT1), the synaptic vesicle protein in the CA1 region of the hippocampus. Acute hippocampal slices when treated with LPI were found to increase miniature excitatory postsynaptic currents (mEPSCs) in neurons in CA1 pyramidal cells and was sensitive to the GPR55 antagonist CBD (Sylantyev *et al.*, 2013). Moreover presynaptic Ca^{2+} mobilisation was required for the mEPSCs as store depletion abolished the responses. GPR55 activation associated with

neurotransmitter release and did not affect Ca^{2+} mobilisation postsynaptically (Sylantyev *et al.*, 2013). This emerging data suggests that GPR55 may be important in synaptic plasticity.

Microglia are the macrophages of the brain and are known to express cannabinoid receptors (Walter *et al.*, 2003). Quantitative real time polymerase chain reaction (qPCR) was employed by Pietr *et al.*, (2009) to compare the levels of CB_1, CB_2 and GPR55 mRNA in both primary mouse microglial and in BV-2 cells. A low level of expression of CB_1 receptors were found in the BV-2 cells, (Pietr *et al.*, 2009) which correlates with the low expression of CB_1 previously seen in primary microglial (Walter *et al.*, 2003). There were higher levels of expression of both CB_2 and GPR55 receptors in both types of cells. It was found that when the BV-2 cells were treated with INF-γ to produce 'primed' cells there was an increase in the level of GPR55 mRNA expression. However, this was not seen in the primary microglial cells (Pietr *et al.*, 2009). The BV-2 cell line when treated with LPS ('activated' cells) lead to both the CB_2 and GPR55 mRNA expression levels being lowered (Pietr *et al.*, 2009). Therefore this is in agreement with previous studies where the expression of CB_2 mRNA is dependent on the activation state of microglia (Lee *et al.*, 2001; Carlisle *et al.*, 2002). In a recent study conditioned media from LPS activated BV-2 cells was applied to SH-SY5Y neuroblastoma cells. Application of Abn-CBD and O-1602 to these SH-SY5Y cells promoted protection against microglial induced neurotoxicity however it remains to be determined if this protection is mediated by GPR55 (Janefjord *et al.*, 2013).

Immunohistochemical studies report that GPR55 is also expressed in large diameter (>35 μm) dorsal root ganglion (DRG) neurons. Application of LPI promoted the mobilisation of Ca^{2+} in the large DRG neurons. Furthermore activation of GPR55 inhibits the M-current suggesting that GPR55 may have a role in promoting neuronal excitability (Marrion, 1997; Lauckner *et al.*, 2008). In a model of neurodegeneration using rat organotypic hippocampal slice cultures (OHSC) GPR55 activated by LPI was found to protect the dentate gyrus cells and decrease the number of activated microglia (Kallendrusch *et al.*, 2013). Immunocytochemical labelling of degenerating neurons and activated microglia were found to be decreased in OHSC which had been lesioned with NMDA prior to application of LPI when compared to NMDA lesion alone. Moreover higher concentrations of LPI decreased the microglial numbers whereas lower concentrations were found to protect the neurons with little or no effect on the number

of microglia present (Kallendrusch *et al.*, 2013). GPR55 is reported to be important for motor co-ordination as $GPR55^{(-/-)}$ mice did not perform as well as wild type littermates in a rotarod test. Also $GPR55^{(-/-)}$ mice were found to produce more footslips when walking on parallel rods (Wu *et al.*, 2013). However $GPR55^{(-/-)}$ mice retained the ability to learn and therefore improved in the rotarod test with training. Both knockout mice and wild type littermates did not exert differences in anxiety/depression, grip strength, fear conditioning or auditory function each of which could have affected the rotarod test highlighting that motor co-ordination was affected but was not due to lack of grip strength or vestibular disturbance (Wu *et al.*, 2013). Furthermore LPI was found to promote [^{35}S]GTPγS binding in the prefrontal cortex and the hippocampus. The receptor that LPI binds to in this study was not determined however the authors speculate that it may be GPR55 due to the presence of GPR55 mRNA in the brain (Rojo *et al.*, 2012). Therefore further studies with $GPR55^{(-/-)}$ animals would help to confirm this hypothesis.

1.3.4.7. GPR55 and the gastrointestinal system

GPR55 mRNA was found in regions of the gastrointestinal (GI) tract; the ileum (Ryberg *et al.*, 2007; Lin *et al.*, 2011; Li *et al.*, 2013), jejunum (Ryberg *et al.*, 2007), duodenum (Lin *et al.*, 2011) and colon (Lin *et al.*, 2011; Li *et al.*, 2013). GPR55 was localised to the mesenteric neurons of the colon (Li *et al.*, 2013). GPR55 expression was higher in the ileum and to a lesser extent in the colon and duodenum when the gut had been subjected to lipopolysaccharide (LPS) to induce inflammation of the gut (Lin *et al.*, 2011). In one study O-1602 was applied to neutrophils derived from wild type mice and was observed to inhibit the neutrophil chemotaxis. When O-1602 was applied to neutrophils derived from $GPR55^{(-/-)}$ mice the inhibition of neutrophil chemotaxis to the bacterial peptide N-formyl-peptide receptor ligand (fMLP) remained suggesting that the effect was not mediated by GPR55 (Schicho *et al.*, 2011) but through an unknown target possibly GPR18 (McHugh *et al.*, 2012). However in studies looking at contraction of the gut GPR55 mediated effects were found. Using electric field stimulation to induce neurogenic effects in colonic strips derived from $GPR55^{(-/-)}$ mice O-1602 was found to decrease contractility compared to colonic strips derived from either double $CB_1^{(-/-)}/CB_2^{(-/-)}$ mice or wild type controls (Ross *et al.*, 2012). Therefore GPR55 mediated neurogenic activity slowed gut contractions in colonic strips when challenged with O-1602 (Ross *et al.*, 2012). A subsequent study also confirmed that O-1602 slowed the gut transit times and led to a slower rate of peristaltic expulsion in wild

type mice. Therefore suggesting that the slowing of gut motility are GPR55-mediated as GPR55$^{(-/-)}$ mice had a shorter transit time and peristaltic expulsion was faster (Li *et al.*, 2013).

1.3.4.8. GPR55 in energy metabolism

Plasma LPI levels are found to be higher in obese patients when compared to lean patients. Moreover GPR55 expression is higher in the visceral and subcutaneous adipose tissue from the obese patients. Studies on Type II diabetics also highlighted that GPR55 expression is increased in visceral adipose tissue (Moreno-Navarrete *et al.*, 2012). Visceral adipose tissue is correlated with the development of insulin resistance which then leads to Type II diabetes, cardiovascular disease, obesity which ultimately lead to metabolic syndrome (Lebovitz and Banerji, 2005). Furthermore GPR55 protein is expressed in pancreatic β-cells, the insulin secreting cells. GPR55 however is not expressed in pancreatic α and δ-cells (Romero-Zerbo *et al.*, 2011). Activation of GPR55 with both synthetic and endogenous agonists promotes the release of insulin in clonal pancreatic β (BRIN-BD11) cells which was dependent on Ca^{2+} mobilisation and partially via cAMP with increased insulin release when glucose was also present (glucose stimulated insulin secretion). Abn-CBD was found to be the most potent and selective for GPR55. However AM251, O-1602 and the N-acyl amides; OEA and PEA also stimulated insulin release by activating GPR55 but these effects were less GPR55 specific suggesting that other targets are also present in the BRIN-BD11 cells (McKillop *et al.*, 2013). Moreover a previous study also reported that O-1602 promoted insulin release in pancreatic β-cells stimulated with glucose. The authors confirmed that Abn-CBD also activated GPR55 in murine derived pancreatic islet cells which decreased glucose concentrations and increased insulin release. The insulin release was lowered in GPR55$^{(-/-)}$ mice suggesting that GPR55 mediated the increases in insulin secretion (Romero-Zerbo *et al.*, 2011). Another set of researchers found that lipid storage induced by O-1602 was GPR55 independent as GPR55$^{(-/-)}$ mice exhibited a higher food intake when compared to wild type littermates (Díaz-Arteaga *et al.*, 2012). More specific GPR55 agonists would be of benefit in better understanding GPR55 and energy metabolism. However GPR55 is a promising target for type II diabetes research.

1.4. Lipid signalling

Originally lipids were described as structural components of the lipid bilayer of cells (Singer and Nicolson, 1971). Lipids are hydrophobic molecules that play an important

role in biological membranes providing a barrier between external environments and the internal cytosolic region of cells (Singer and Nicolson, 1972; Piomelli *et al.*, 2007). It is now acknowledged that membrane lipids are also important precursors for the synthesis of bioactive lipids. Bioactive lipids have the ability to activate signalling pathways by, for example, lipid binding and subsequent activation of GPCRs (Wenk, 2005). Imbalances in bioactive lipids have consequences in the progression of several diseases such as autoimmunity, inflammation, obesity and cancer to name but a few (Wymann and Schneiter, 2008; Hu *et al.*, 2009). Lysophospholipids are thought to have the potential as biomarkers for the diagnosis of certain gynaecological cancers (Xiao *et al.*, 2001; Sutphen *et al.*, 2004). Interestingly, LPA/LPI species that contain unsaturated fatty acid chains are more prominent in women with late stage or a re-occurrence of ovarian cancer (Shen *et al.*, 2001). Indeed, both lysophosphatidic acid (LPA) and L-α-lysophospatidylinositol (LPI) occur at elevated levels in the ascites of women with ovarian cancer when compared to healthy controls (Sutphen *et al.*, 2004). However, more recent studies have started to uncover a role for bioactive lipids in cell signalling. Several bioactive lipids are known to act upon GPCRs to initiate intracellular signalling.

1.4.1. Sphingosine-1-phosphate

Sphingosine 1-phosphate (S1P) is a bioactive lipid which is synthesised intracellularly from phosphorylation of sphingosine by sphingosine kinases; sphingosine kinase 1 and 2 (Spiegel and Milstien, 2003). S1P is then pumped out of the cell through ABCC transporters where it can then act in an autocrine or paracrine manner on receptors in the membrane in a process known as ‘inside-out signalling’ (Kunkel *et al.*, 2013). Degradation of S1P requires the actions of S1P lysase or S1P phophatases (Ishii *et al.*, 2004; Kunkel *et al.*, 2013). S1P is stored at high concentrations in platelets and released when they are activated (Yatomi *et al.*, 1995; Moolenaar, 1999; Ishii *et al.*, 2004). The concentration of S1P in blood ranges from 200 nM - 800 nM and it is bound to serum albumin and lipoproteins (Ishii *et al.*, 2004). Originally S1P had been observed to cell growth by an as yet unknown target (Zhang *et al.*, 1991). However Lee *et al.*, (1998) transfected the clone of endothelial cell differentiation gene (Edg) 1 into HEK293 cells as these cells do not endogenously express Edg1. Several lipids from serum such as LPA and LPI were then tested and only S1P was found to induce changes in morphology in Edg1 transfected HEK293 cells (Lee *et al.*, 1998). This study deorphanised the Edg1 receptor and highlighted S1P as a bioactive lipid (Lee *et al.*, 1998). Subsequent studies led to the discovery of another four orphan S1P receptors all

of which belong to the subset of Edg GPCRs. To date a total of five S1P receptors exist, $S1P_{1-5}$ (Spiegel and Milstien, 2003). Three other receptors are part of the Edg family of receptors but are not activated by S1P, rather by another bioactive lipid known as lysophosphatidic acid; LPA (Meyer zu Heringdorf and Jakobs, 2007).

1.4.2. Lysophsophatidic acid

LPA is a mitogenic bioactive lipid which acts on GPCRs (Ishii *et al.*, 2009). LPA is known to act extracellularly on at least 6 GPCRs. The first three LPA receptors are similar sharing a homology of 50-57% (Noguchi *et al.*, 2003; Ishii *et al.*, 2009). LPA_{1-3} are members of the Edg group of GPCRs and as such are phylogenetically related to the S1P receptors. Activation of LPA_{1-3} induces signalling that promotes activation of MAPK, mobilisation of Ca^{2+} and inhibition of cyclic AMP (Noguchi *et al.*, 2003). Studies on $LPA_1^{(-/-)}$ and $LPA_2^{(-/-)}$ revealed that other LPA receptors must exist. This led through reverse pharmacological approaches to the discovery and subsequent cloning of LPA_4/GPR23 (Noguchi *et al.*, 2003); LPA5/GPR92 (Lee *et al.*, 2006) and LPA_6/P_2Y_5 (Pasternack *et al.*, 2008). These receptors are structurally distinct from LPA_{1-3} receptors, being more related to the purinergic GPCR cluster. Activated platelets, adipocytes and neurons produce LPA (Ishii *et al.*, 2004). LPA is derived from the biosynthesis of membrane phospholipids by three synthesis pathways; the phospholipase A_1 (PLA_1) and secretory PLA_2 deacylating phosphatidic acid, lyso-PLD or autotaxin catalysis of lysophosphatidylcholine or by phosphorylation of 2-AG by acylglycerol kinase (Meyer zu Heringdorf and Jakobs, 2007). Metabolism of LPA is via dephosphorylation with a lipid phosphate phosphatase (Brindley and Pilquil, 2009). LPA plays a role in several biological processes such as neurite retraction (Lee *et al.*, 2007; Yanagida *et al.*, 2007), cell survival, wound healing (Ishii *et al.*, 2004) and cancer progression (Mukherjee *et al.*, 2012). LPA in the blood is bound to serum albumin and lipoproteins (Ishii *et al.*, 2004). Physiologically LPA in serum ranges between 100 nM and 25 µM (Tigyi and Miledi, 1992; Ishii *et al.*, 2004). Furthermore LPA is present at higher levels in the ascites and serum of ovarian cancer patients when compared to control patients (Sedláková *et al.*, 2011). It was found that 90% of patients with early stage I ovarian cancer had elevated levels of LPA. LPA_2 and LPA_3 were found to be up-regulated in ovarian cancer patients and were absent in control individuals (Sedláková *et al.*, 2011). Interestingly LPA acts on the non-EDG receptors GPR23, GPR92 and P_2Y_5 which are phylogenetically closest to GPR55 (Fredriksson *et al.*,

2003; Baker *et al.*, 2006). Furthermore LPA is structurally similar to LPI however, unlike LPI it does not activate GPR55 (Oka *et al.*, 2007; Henstridge *et al.*, 2009).

1.4.3. L-α-lysophosphatidylinositol

LPI is a product from the hydrolysis of cell membrane-derived phosphatidylinositol (PI) where a free fatty acid is released resulting in the generation of LPI (Yamashita *et al.*, 2013). In the 1960s the acylation of LPI by acyl CoA to form PI was described (Keenan and Hokin, 1964). By the early 1980s activated platelets were found to generate LPI by PI deacylation through the actions of phospholipase A_2; PLA_2 (Billah and Lapetina, 1982). PLA hydrolyses the acyl bond of the membrane derived lipid, phosphatidylinositol at either the sn-1 or sn-2 position to generate a free fatty acid and LPI (Bonventre, 1992). With PLA_1 or PLA_2 cleaving the fatty acid chains at either the sn-1 or sn-2 position respectively. PLA_1 is localised both extracellularly and intracellularly. An increase in Ca^{2+} is required to stimulate the PLA_1 DDHD domain containing 1 (DDHD1) which in turn hydrolyses PI forming LPI and its activity can be modulated by phospholipase D acting on phophatidic acid (Yamashita *et al.*, 2010). Arachidonic acid being polyunsaturated is in general found at the sn-2 position as would other polyunsaturated fatty acids (Yamashita *et al.*, 1997). Therefore as 2-arachidonyl LPI is the most potent LPI species to act on GPR55 and it is thought to be generated by hydrolysis of the fatty acid chain at the sn-1 position by intracellular PLA_1 (Yamashita *et al.*, 2010). Cytosolic $PLA_{2\alpha}$ isoform may also be responsible for the formation of LPI species (Mariggiò *et al.*, 2006; Piñeiro *et al.*, 2011). Once LPI has been generated the lipid can be further metabolised. LPI can be acylated to form PI via 1 acyl- or 2 acyl-LPI acyltransferase. Furthermore a specific LPI-PLC present in porcine platelets and rat brain can also metabolise LPI (2-arachidonoyl LPI) into the endocannabinoid 2-AG (Tsutsumi *et al.*, 1994; Kobayashi *et al.*, 1996). LPI can also be metabolised by phospholipase D (autotaxin) to form LPA in activated platelets (Aoki *et al.*, 2002; Piñeiro and Falasca, 2012; Yamashita *et al.*, 2013).

LPI as a signalling mediator was first observed in pancreatic islets where application of LPI promoted insulin release (Metz, 1986). Around the same time studies with macrophage RAW 264.7 cells treated with lipid X were found to accumulate LPI (Zoeller *et al.*, 1987). Also hepatocytes treated with 1,25-dihydroxyvitamin D displayed increases in cytosolic Ca^{2+} which was promoted by the deacylation of PI by PLA_2 to form LPI. When LPI was applied directly to hepatocytes Ca^{2+} mobilisation

was reported suggesting that LPI was mediating the 1,25-dihydroxyvitamin D induced Ca^{2+} mobilisation (Baran and Kelly, 1988). LPI was also discovered to be synthesised by PLA_2 in k-ras oncogene transformed fibroblasts where the concentration rose to three times of that observed in normal fibroblasts (Falasca and Corda, 1993). A subsequent study highlighted that k-ras oncogene transformed rat thyroid cells were also found to have an accumulation of LPI due to the increased activity of PLA_2 (Falasca and Corda, 1994). Moreover LPI accumulated in the extracellular medium of neoplastic fibroblasts and was found to promote the proliferation of these cells an effect that was not observed in normal fibroblasts (Falasca *et al.*, 1998). It is now known that LPI concentrations from the plasma of healthy females is ~1.5 µM (Sutphen *et al.*, 2004). Moreover the levels of LPI can increase significantly in late stage ovarian cancer patients or those with recurring ovarian cancer (Sutphen *et al.*, 2004). However the target for LPI was still unknown.

The first study to uncover a molecular target for LPI was discovered when assessing the neuroprotective effect of lysophospholipids. Application of LPI, 30 min before ischemia, promoted ~95% protection to hippocampal neurons *in vivo* in rats subjected to transient global forebrain ischemia. Moreover *in vitro* glutamate induced neuronal cell death which was decreased in cultured cerebral granular cells treated with LPI. The authors suggested that LPI may be acting upon 2 pore-domain K^+ channels; TREK and TRAAK, to promote the neuroprotection (Blondeau *et al.*, 2002) as LPI had been reported as a strong activator of TREK and TRAAK (Maingret, 2000). LPI is also reported to activate members of the transient receptor potential family of cation channels. Lysophospholipids including LPI induced Ca^{2+} mobilisation through the activation of TRPC5 (Flemming *et al.*, 2006) and also modulates the temperature sensitivity required for TRPM8 (normally <25^{o}C) activation to a physiological relevant 37^{o}C for channels expressed inside the body (Andersson *et al.*, 2007). In the same year Ca^{2+} mobilisation and ERK1/2 phosphorylation were found to be induced by LPI through an oGPCR; GPR55 (Oka *et al.*, 2007). A plethora of papers followed; each confirming the effects of LPI on the activation of GPR55 not only in recombinant cell lines (Oka *et al.*, 2007, 2009; Henstridge *et al.*, 2009, 2010; Andradas *et al.*, 2011) but also in cells that were shown to endogenously express GPR55 (Lauckner *et al.*, 2008; Waldeck-Weiermair *et al.*, 2008; Pietr *et al.*, 2009; Whyte *et al.*, 2009; Ford *et al.*, 2010; Andradas *et al.*, 2011; Piñeiro *et al.*, 2011; Pérez-Gómez *et al.*, 2013).

1.4.4. Free fatty acids

Free fatty acids (FFA) and lysophospholipids are the product of the action of PLA enzymes on the membrane derived lipids. Evidence is growing that free fatty acids (FFA) can act on three FFA receptors; GPR40, GPR43 and GPR41 which were cloned in 1997 (Sawzdargo *et al.*, 1997) and are now known as FFA_{1-3} respectively. FFA_1 is activated by medium and long chain FFAs; C6-22 (Briscoe *et al.*, 2003; Stoddart *et al.*, 2008). Whereas FFA_2 and FFA_3 are activated by short chain FFAs; C1-6 (Brown *et al.*, 2003; Stoddart *et al.*, 2008). FFA_1 is expressed in pancreatic β-cells and when activated leads to insulin release. Overstimulation can lead to β–cell dysfunction therefore FFA_1 is of interest as a therapeutic target pathologies such as obesity and type II diabetes (Costanzi *et al.*, 2008). FFA_2 and FFA_3 are expressed in pancreatic α- and β-cells moreover FFA_2 is expressed in adipocytes and some immune cells. FFA_2 and FFA_3 may be a therapeutic target for metabolic syndrome and inflammatory bowel diseases however this is speculative as there is disparity in results from animal studies at the present time (Offermanns, 2013). Recently another two GPCRs can be activated by FFAs; GPR84 is activated by medium chain FFAs (C9-14) and GPR120 being activated by long chain FFAs (C14-22) however both these GPCRs share little homology with FFA_{1-3} (Stoddart *et al.*, 2008). GPR84 expression is up-regulated in tumour necrosis factor-α (TNF-α) stimulated adipocytes or in cultures where macrophages are present suggesting that GPR84 may be important in the development of inflammation induced insulin resistance in adipocytes (Nagasaki *et al.*, 2012). Recently mice lacking GPR120 become obese and insulin resistant when fed a high fat diet. Also a mutation of the GPR120 gene (p.R270H) within the European population predisposes those who express it to become obese. Furthermore GPR120 is up-regulated in obese individuals (Ichimura *et al.*, 2012). Overall the FFA receptors are an emerging research field that offer potential novel therapeutic targets for metabolic disorders such as obesity and type II diabetes.

1.4.5. N-acyl amino acids

There is a growing interest in the 'endocannabinoid-like' N-acyl amino acids. They are a family of more than 70 endogenous lipids and have a molecular structure that is similar to the two major endocannabinoids; AEA and 2-AG (figure 1.3; Bradshaw *et al.*, 2009). The N-acyl amino acids despite being structurally similar to the endocannabinoids are found to have little or no affinity for cannabinoid receptors or $TRPV_1$ (Sheskin *et al.*, 1997; Milman *et al.*, 2006; Smoum *et al.*, 2010). N-acyl amino

acids possess a fatty acid chain that is saturated, mono-saturated or unsaturated conjugated to an amino acid head group (Bradshaw *et al.*, 2009; Tan *et al.*, 2010). Furthermore many of the N-acyl amino acids remain orphans where the biological target and therefore their physiological function remains to be determined (Bradshaw *et al.*, 2009). These lipids are of particular interest as they may be important endogenous activators of as yet unknown oGPCRs.

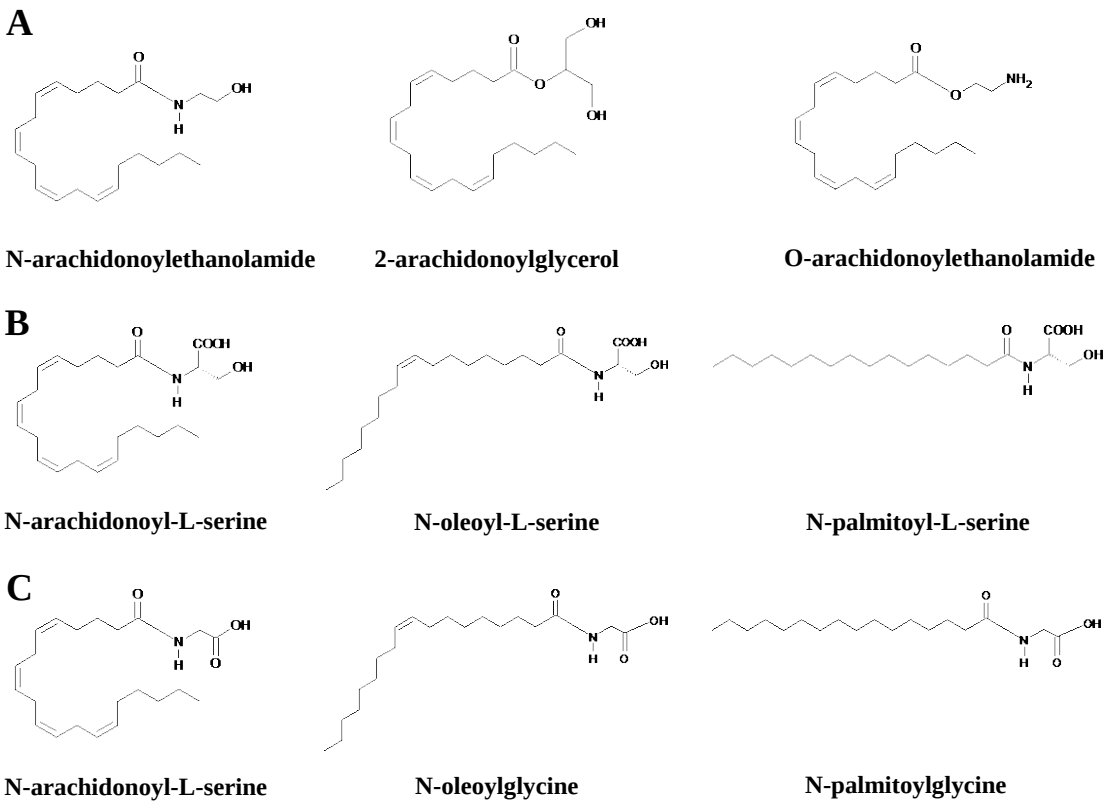

Figure 1.3: Endocannabinoids and structurally related N-acyl amino acids. *Chemical structures of the following families are **A**, endocannabinoids; **B**, N-acyl serines; **C**, N-acyl glycines. Note that the structure of the endocannabinoids is similar to the N-acyl amino acids.*

1.4.5.1. N-arachidonoyl glycine

The most studied N-acyl amino acid is N-arachidonoyl glycine (NAGly). Originally synthetic NAGly was generated in the laboratory as a structural analogue of AEA and was found to have little affinity for CB_1 or CB_2 (Sheskin *et al.*, 1997; Huang *et al.*, 2001). However NAGly is reported to activate several GPCRs; GPR18 (Kohno *et al.*, 2006; Yin *et al.*, 2009; McHugh *et al.*, 2010, 2012; Caldwell *et al.*, 2013), GPR72 (Hannedouche and Roy, 2010) and as a GPR92 partial agonist (Oh *et al.*, 2008). NAGly does not activate $TRPV_1$ as Ca^{2+} influx was not observed in $TRPV_1$-HEK293

cells (Huang *et al.*, 2001) Endogenous NAGly was extracted from bovine brain (Huang *et al.*, 2001). Moreover NAGly was expressed in the following rat tissues; spinal cord > small intestine > kidney > glabrous skin > brain and lower expression in testes > lung > liver > blood > spleen and only modest expression in the heart (Huang *et al.*, 2001). The widespread distribution of NAGly would suggest it may have a role in several physiological functions.

At present most research on NAGly has been focused on pain and inflammation. Recent evidence highlights NAGly as having a role in pain and inflammation which is independent of cannabinoid receptors. NAGly was found to inhibit formalin induced pain in rats and to lower inflammation (Huang *et al.*, 2001). Also a rat model of inflammatory pain; where Freund's complete adjuvant (FCA) was injected into the paw and reported to reduce mechanical allodynia and thermal hyperalgesia when the rats were treated with NAGly. This decrease in pain sensitivity was insensitive to cannabinoid antagonists (Succar *et al.*, 2007). Furthermore neuropathic pain is alleviated in rats with partial sciatic nerve ligation when NAGly is present highlighting an analgesic action. Both arachidonic acid and glycine the metabolic products of NAGly did not affect mechanical allodynia. The decrease in NAGly-induced mechanical allodynia was not sensitive to cannabinoid antagonists (Vuong *et al.*, 2008). Recent evidence suggests that NAGly treatment in an *in vivo* model of peritonitis decreases the migration of leukocytes to sites of inflammation. NAGly was also reported to increase the production of prostaglandin J and lipoxin A4 *in vitro* therefore NAGly may contribute to the resolution of inflammation (Burstein *et al.*, 2011).

Three biosynthesising pathways have been suggested for NAGly. The first *in situ* NAGly synthesis occurs in rat brain from the precursors of arachidonic acid (AA) and glycine in a two-step process. The enzyme arachidonyl-CoA synthetase is localised to brain, platelets and the aorta and is specific for AA conversion into arachidonyl-coenzymeA (arachidonoyl-CoA). The conjugation of glycine to arachidonyl-CoA requires a second enzyme; acyl-coenzyme A: glycine N-acyltransferase (Huang *et al.*, 2001). The second pathway involves the oxidation of AEA. In a two-step enzymatic process alcohol dehydrogenases which oxidises ethanolamine of AEA to produce N-arachidonoyl glycinal, an aldehyde intermediate which is then oxidised by an aldehyde dehydrogenase to form NAGly (Burstein *et al.*, 2000). Recent evidence suggests that FAAH may be part of the NAGly biosynthesis pathway through the hydrolysis of AEA

which generates arachidonic acid. This arachidonic acid can then be conjugated glycine to produce NAGly. Applying a FAAH inhibitor (URB 597) or using $FAAH^{(-/-)}$ mice promoted an increase in AEA but decreased NAG levels suggesting that FAAH is required for the biosynthesis of NAGly in vivo through the degradation of AEA (Bradshaw *et al.*, 2009).

1.4.5.2. N-arachidonoyl-L-serine

Other arachidonic acid derived N-acyl amino acids have been extracted from the mammalian brain including N-arachidonoyl GABA, N-arachidonoyl alanine (Huang *et al.*, 2001) and N-arachidonoyl serine (Milman *et al.*, 2006). N-arachidonoyl-L-serine (NASer) was isolated from bovine brain and found to have a structure similar to AEA differing only in the head group, a serine instead of an ethanolamine (Milman *et al.*, 2006). *In vitro*, NASer can activate large conductance Ca^{2+} potassium channels (BK_{Ca}) (Godlewski *et al.*, 2009) and N-type Ca^{2+} channels in sympathetic neurons (Guo *et al.*, 2008). However there is some controversy as to whether NASer activates cannabinoid receptors and TRPV1. Originally NASer was found to bind weakly to CB_1 with a dissociation constant greater than 10 µM which was less than 1% of the response produced by the structural analogue AEA. Additionally concentrations up to 30 µM NASer had no effect in displacing radioligand binding to rat CB_2 or $TRPV_1$ receptors (Milman *et al.*, 2006). However recent studies report that a decrease in oedema and lesion volume in mice treated with NASer after a closed head injury (CHI) are mediated by CB_2, $TRPV_1$ and partially mediated by BK_{Ca} (Cohen-Yeshurun *et al.*, 2011). The NASer mediated neuroprotection after CHI required phosphorylation of ERK1/2 and AKT and a subsequent increase in the anti-apoptotic protein BCL-xL (possibly mediated by CB_2 and $TRPV_1$). Moreover CB_2 activation by NASer decreased the pro-apoptotic protein caspase-3 (Cohen-Yeshurun *et al.*, 2011). Furthermore a subsequent study highlights that NASer promoted the proliferation of neural progenitor cells *in vitro* which was mediated by CB_1, CB_2 and $TRPV_1$. Also the authors note that 96 hr after NASer treatment there is an increase in the expression of both CB_1 and CB_2 suggesting NASer may mediate the initiation of cannabinoid gene transcription (Cohen-Yeshurun *et al.*, 2013).

NASer applied to rat isolated mesenteric arteries and abdominal aorta promoted vasodilatation (Milman *et al.*, 2006) similar to that previously seen with Abn-CBD (Offertáler *et al.*, 2003). The similarity of effects seen between NAS and Abn-CBD

suggest a similar, as yet unknown, target may induce these effects (Milman *et al.*, 2006). Furthermore the endocannabinoid virodhamine (which is structurally similar to NASer) also exerts actions at the Abn-CBD endothelial receptor (Porter *et al.*, 2002). Interestingly NASer is reported as the first endogenous ligand that acts selectively on the Abn-CBD receptor (Milman *et al.*, 2006). It is therefore suggested that NASer may play a role in vascular protection and homeostasis that is independent of CB_1 and CB_2 (Milman *et al.*, 2006). The stereoselectivity of NASer (L-enantiomer is active) suggests that it is mediated via a receptor in the membrane (Milman *et al.*, 2006). Furthermore vasodilatation of the aorta is sensitive to pertussis toxin (PTX), an effect that is not observed in the mesenteric arteries, suggesting that a $G_{\alpha i}/G_{\alpha o}$ linked receptor influences the aortic relaxation.

NASer may also have a role in lowering inflammation as it can inhibit the formation of TNF-α promoted by lipopolysaccharide (LPS) in $CB_1^{(-/-)}$ and $CB_2^{(-/-)}$ knockout mice and in primary murine macrophages (Milman *et al.*, 2006). Moreover zymosan treatment promoted reactive oxygen intermediates which were suppressed in RAW264.7 cells treated with NASer - albeit at a high concentration (76.6 µM; Milman *et al.*, 2006). Furthermore a Boyden chamber assay reported that NASer antagonised the AEA, virodhamine and Abn CBD-induced migration of human neutrophils at a non CB_1/CB_2 target possibly by the Abn-CBD receptor, GPR18 (McHugh *et al.*, 2008).

There is also controversy as to whether NASer activates GPR55. Previous research reports NASer promotes endothelial migration and *in vitro* tube formation which were partially attributed to GPR55 activation. Application of NASer to GPR55 siRNA treated human dermal microvascular endothelial cells **(**HMVEC) lowered phosphorylation of ERK1/2 and Akt compared to control cells (Zhang *et al.*, 2010). As siRNA knockdown is never 100% efficient the remaining responses seen could be either due to incomplete knockdown of all the GPR55 present or may be due to NASer acting on another as yet unknown target in these cells. For example NASer could act on a GPCR which is sensitive to PTX as was observed in the aorta (Milman *et al.*, 2006). In another study however, utilising hGPR55-HEK293 cells in a GTPγS assay it was reported that NASer did not exert agonist or antagonist effects (Cohen-Yeshurun *et al.*, 2011).

1.4.5.3. N oleoyl-L-serine

N-oleoyl-L-serine (NOSer) is similar in structure to NASer with the exception of the fatty acid chain being oleic rather than the arachidonic. NOSer is an orphan lipid that is suggested to act through a $G_{\alpha i/o}$ protein-coupled receptor. It is present in murine bone and the lipid acts to phosphorylate ERK1/2 (Smoum *et al.*, 2010). The lipid was also found in other mouse tissues such as the brain and the spleen and was found to be 10 fold greater and 10 fold less respectively than seen in distal femoral metaphysis. Concentrations of 10 μM were unable to bind to either CB_1 or CB_2 in experiments using rat brain synaptosomal membranes or in transfected cells. This was further confirmed in osteoblast cells that were deficient of CB_1 and CB_2. NOSer may have a role in osteoporosis as ovariectomised mice treated with NOSer exhibited recovery of bone loss via increases in bone formation and inhibiting bone loss (Smoum *et al.*, 2010).

1.4.5.4. N-oleoyl glycine

N-oleoyl glycine (NOGly) was originally thought to be an intermediate in the N-acyl amide, oleamide, synthesis pathway. When either oleamide or NOGly was administered to rats the concentration of oleamide was found to increase in the animals treated with oleamide. However rats treated with NOGly did not have increased concentrations of oleamide suggesting that NOGly is not required to produce oleamide. Furthermore when oleamide and NOGly were administered to rats both compounds were found to promote hypothermia and to decrease locomotion suggesting that NOGly is also a bioactive lipid (Chaturvedi and Driscoll, 2006). NOGly is reported to be synthesised by the conjugation of oleoyl-CoA and glycine through the action of mitochondrial protein cytochrome *c* in the presence of hydrogen peroxide (Mueller and Driscoll, 2007). Cytochrome *c* is also required for the synthesis of NAGly and NASer with arachidonoyl-CoA and either glycine or serine as substrates. These studies highlight a potential *in vivo* biosynthesis for certain N-acyl amino acids (McCue *et al.*, 2008, 2009).

1.5. Ca^{2+} signalling

1.5.1. Overview of Ca^{2+} signalling

In the late 19th Century Sydney Ringer serendipitously discovered that extracellular Ca^{2+} played a role in the contraction of an isolated heart (Ringer, 1883). Ca^{2+} research did not progress a great deal until ~1940's when Heilbrunn developed the hypothesis that Ca^{2+} acted as an intracellular messenger whereby Ca^{2+} was released from an

unknown internal store that he referred to as the "rigid cortex". However it was dismissed as unconventional by the scientific community at the time (Petersen *et al.*, 2005). Today it is widely acknowledged that Ca^{2+} is an important intracellular second messenger (Petersen *et al.*, 2005). Ca^{2+} concentration in quiescent cells is ~0.1 µM but increasing to ~1 µM in activated cells. The range in concentration coupled with spatial (location of Ca^{2+} transients) and temporal (frequency of oscillatory Ca^{2+} transient) aspects of the Ca^{2+} signal generated allow diversity in Ca^{2+}-mediated cellular processes. Ca^{2+} plays a role in many physiological processes such as fertilisation, muscle contraction, neuronal signalling, gene transcription, proliferation and apoptosis (Berridge *et al.*, 1998). To ensure Ca^{2+} homeostasis, cells have developed Ca^{2+} signalling that is both dynamic and meticulously regulated (Berridge *et al.*, 1998).

1.5.2. Regulation of Ca^{2+} signalling

Ca^{2+} must be regulated as high concentrations are toxic to the cell (Berridge *et al.*, 1998). Therefore cells regulate Ca^{2+} signalling by producing transient responses whereby Ca^{2+} is released from intracellular stores and then quickly sequestered back again (Berridge *et al.*, 1998). Agonist binding of GPCRs or tyrosine receptor kinases leads to the activation of phospholipase C (PLC) isoforms: PLCβ and PLCγ respectively (Berridge *et al.*, 2003; Clapham, 2007). PLC cleaves phosphatidylinositol 4, 5-bisphosphate (PIP_2) to produce inositol 1, 4, 5-triphosphate (IP_3) and diacylglycerol (DAG), whereby IP_3 translocates through the cytosol and binds to IP_3 receptors located on the membrane of the endoplasmic reticulum (ER) leading to the subsequent release of Ca^{2+} (Clapham, 2007). Also localised to the ER are ryanodine receptors (RyR). Ca^{2+}, as a natural ligand of RyR, promotes Ca^{2+} induced Ca^{2+} release (CICR) allowing Ca^{2+} to be released from the lumen of the ER (Clapham, 2007). Paradoxically, high concentrations of Ca^{2+} negatively feedback on IP_3 and RyR closing the channels (Clapham, 2007). Plasma membrane Ca^{2+} ATPases (PMCA) channel and the Na^{+} /Ca^{2+} exchanger localised in the cell membrane removes the Ca^{2+} from the cell (Bootman *et al.*, 2001). However the stores that are depleted must be replenished and cells use a mechanism known as store operated calcium entry (SOCE) to achieve this (Berridge *et al.*, 1998; Bugaj *et al.*, 2005). Depletion of the ER Ca^{2+} store induces signals to initiate store operated Ca^{2+} entry (SOCE) through store operated Ca^{2+} (SOC) channels located on the plasma membrane (Cheng *et al.*, 2011). The Ca^{2+} release-activating current (I_{CRAC}) is a member of the SOC family of Ca^{2+} entry channels (Cheng *et al.*, 2011) and is highly selective for Ca^{2+} over other divalent cations (Yeromin *et al.*,

2004). I_{CRAC} is activated by a decrease in ER luminal Ca^{2+} and is unaffected by the increases in cytosolic Ca^{2+} levels. Therefore a Ca^{2+} sensor must exist to regulate I_{CRAC}.

Initially stromal interacting molecules (STIM) were identified in *Drosophilia melanogaster* and then subsequently in HeLa cells (Clapham, 2007). RNA interference of STIM 1 was found to influence the I_{CRAC} in HEK293 cells. The authors noted that the influence on I_{CRAC} in HEK293 cells overexpressing STIM 1 generated only 17% increase in the SOC current therefore they suggest that STIM 1 while having a role in SOCE was not the Ca^{2+} channel (Roos *et al.*, 2005). Subsequent evidence observed that STIM are proteins located on the inside of the ER to act as Ca^{2+} sensors (Roos *et al.*, 2005; Zhang *et al.*, 2005). Depletion of Ca^{2+} from the ER leads to STIM translocating to a region of the ER which is situated close to the plasma membrane (Zhang *et al.*, 2005; Wu *et al.*, 2006; Park *et al.*, 2009). Orai1 is a protein localised to the plasma membrane and was identified as being important in I_{CRAC} and SOCE (Feske *et al.*, 2006). Subsequent studies identified Orai1 as the pore subunit of CRAC (Prakriya *et al.*, 2006). Depletion of Ca^{2+} from the ER leads to the translocation of Orai1 to a plasma membrane at junctions with the ER (Park *et al.*, 2009). This allows STIM to bind and activate the Orai1 channels (Park *et al.*, 2009). The Ca^{2+} influx from the extracellular environment must be sequestered back into the stores. Sarcoplasmic/endoplasmic reticulum Ca^{2+} ATPases (SERCA) pumps this free cytosolic Ca^{2+} back into the ER (Clapham, 2007). The stores are predominately in the endoplasmic reticulum but Ca^{2+} can also be stored in the mitochondria and nucleus (figure 1.4; Bootman *et al*., 2001; Clapham, 2007).

LPI was reported to activate GPR55 to promote Ca^{2+} mobilisation in hGPR55-HEK293 cells, an effect that was ablated in control HEK293 cells (Oka *et al.*, 2007). A plethora of papers was to follow confirming GPR55-mediated elevation of intracellular Ca^{2+} in a variety of cell types; either recombinant GPR55-overexpressing cells or endogenously expressing cells. These include hGPR55-HEK293 cells (Oka *et al.*, 2007; Lauckner *et al.*, 2008; Henstridge *et al.*, 2009, 2010), human umbilical vein derived endothelial cell (HUVEC) line; EA.hy926 (Waldeck-Weiermair *et al.*, 2008) the neuronal cell line; PC12 cells (Obara *et al.*, 2011), prostate cancer cell line; PC-3 (Piñeiro *et al.*, 2011) and in cardiomyocytes (Yu *et al.*, 2013). Furthermore some cannabinoid ligands; Δ^9THC, JWH015, AM251 and SR141716A are also reported to activate GPR55 to promote Ca^{2+} mobilisation (Lauckner *et al.*, 2008; Henstridge *et al.*, 2010).

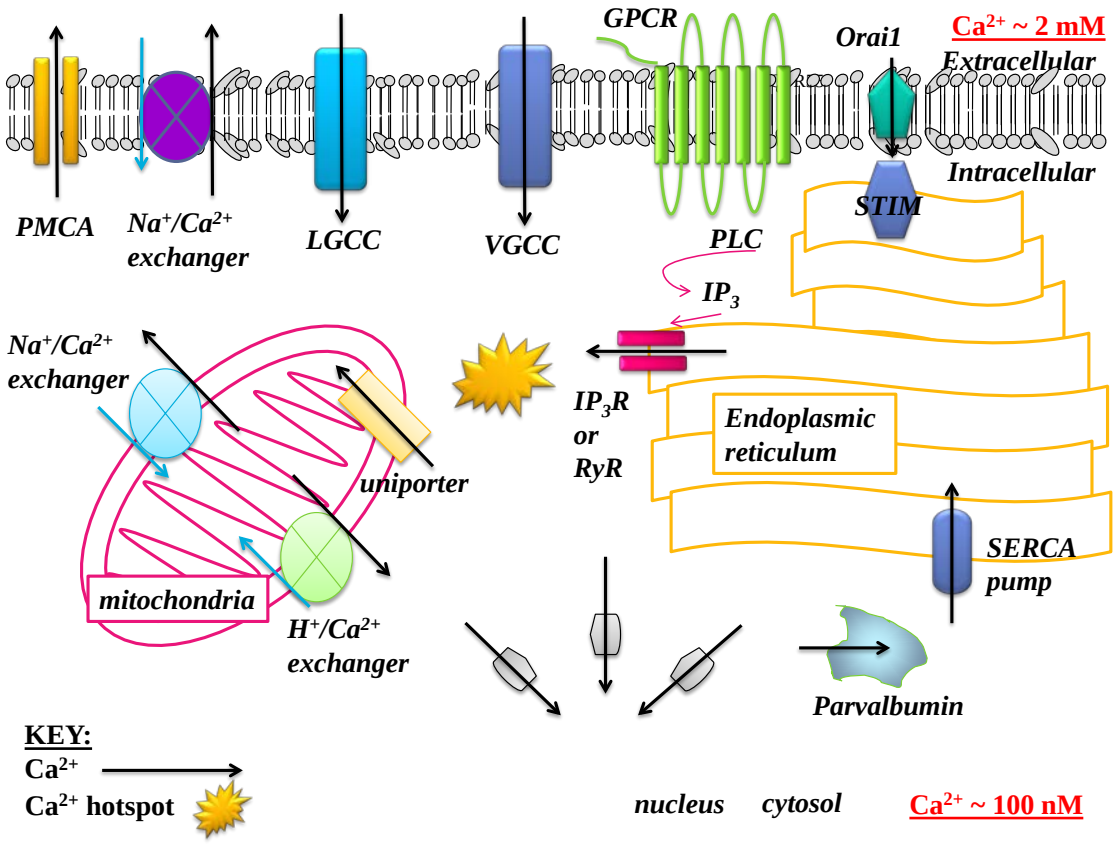

Figure 1.4: Summary of homeostatic regulation of cellular Ca^{2+}. *Ca^{2+} homeostasis is essential for the survival of the cell. Ca^{2+} can enter the cell through Ca^{2+} channels in the cell membrane such as voltage activated channels and the ligand activated channels. Activated GPCRs lead to the formation of IP_3 through PLC hydrolysis of PIP_2. IP_3 acts on the IP_3 receptors in the ER and releases Ca^{2+}. This leads to a Ca^{2+} hotspot which attracts mitochondria whereby the uniport channel sequesters the Ca^{2+}. Removal of Ca^{2+} also occurs through the PMCA and the Na^+/Ca^{2+} exchanger in the cell membrane. ER replenishment occurs when STIM and Orai bind leading to SOCE. The increase in Ca^{2+} is sequestered into the ER through the SERCA pump. Ca^{2+} can also enter the nucleus via the nuclear pores where it can be stored. Ca^{2+} is also bound to parvalbumin a Ca^{2+} binding protein. Release of Ca^{2+} can also occur by a Na^+/Ca^{2+} and H^+/Ca^{2+} exchanger in mitochondria. Each of these events ensures that intracellular Ca^{2+} remains low compared to the extracellular concentration. Ca^{2+}, calcium; Na^+, sodium; H^+, hydrogen; PMCA, plasma membrane Ca^{2+} ATPase; LGCC, ligand gated Ca^{2+} channel; VGCC, voltage gated Ca^{2+} channel; GPCR, G-protein coupled receptor; Orai, Ca^{2+} release-activated calcium channel protein 1; STIM, stromal interaction molecule; PLC, phospholipase C; IP_3, inositol trisphosphate; RyR, ryanodine receptor; SERCA, sarcoendoplasmic reticulum calcium transport ATPase. Modified from Carafoli, 2003.*

1.6. Cyclic AMP response element binding protein

CREB is a 43 kDa transcription factor that binds to a cyclic AMP response element (CRE) conserved (5'-TGACGTCA-3') region on the promoter of genes to regulate their transcription (Kwok *et al.*, 1994; Johannessen *et al.*, 2004; Carlezon *et al.*, 2005). CREB is a member of the basic region leucine zippers (bZIPs) family of transcription factors and is a closely related to cyclic AMP response element modulator (CREM) and activating transcription factor; ATF1 (Sands and Palmer, 2008). CREB is found to exist as either monomers or dimers with the latter being required to initiate transcription (Yamamoto *et al.*, 1988). CREB can form either homo- or heterodimers with other members of the bZIPs (the leucine rich region unzips to allow dimerisation). CREB phosphorylation increases the number of dimers in the cell thereby improving transcription efficiency (Yamamoto *et al.*, 1988). The basic region is important for CREB to bind to DNA and phosphorylation of serine 133 (Gonzalez and Montminy, 1989) in the kinase inducible domain; KID (Sands and Palmer, 2008) recruits CREB binding protein (CBP) a co-transcriptional regulator and the CBP paralogue p300 (Chrivia *et al.*, 1993; Kwok *et al.*, 1994; Cha-Molstad *et al.*, 2004) allowing transcriptional regulation to occur.

1.6.1. Signalling associated with CREB phosphorylation

Multiple signalling pathways have been implicated where extracellular stimuli such as stress signals, neurotransmitters, lipids and fluxes of ions act upon cell surface channels or receptors and promote the phosphorylation of CREB (residue serine 133) in the nucleus to initiate gene expression (Euskirchen *et al.*, 2004). These signalling pathways include PKA (Dash *et al.*, 1991), mitogen activated protein kinase (MAPK) (Impey *et al.*, 1998), Ca^{2+}/CaMKII (Sheng *et al.*, 1990; Impey *et al.*, 1998) and AKT/PKB (Du and Montminy, 1998). Therefore multiple signalling pathways may converge and ultimately lead to CREB phosphorylation and subsequent regulation of gene transcription. GPR55-mediated CREB phosphorylation has been reported in hGPR55-HEK293 cells treated with the CB1 inverse agonist/antagonists; AM251 and SR141716A and LPI (Henstridge *et al.*, 2010).

1.6.2. Kinases and phosphatases - key players in phosphorylation signal transduction events

The most common form of post-translational modification in eukaryotic signal transduction is phosphorylation (Ubersax and Ferrell, 2007). Phosphorylation is a

reversible process where substrates have a phosphate group added by kinases. A second group of enzymes known as phosphatases act in an opposing manner to kinases (by removing phosphate groups) to regulate signal transduction therefore, allowing phosphorylation to act as a molecular switch (Hunter, 1995; Bononi *et al.*, 2011).

CREB is phosphorylated on serine 133 and is then activated where it leads to regulation of transcription of genes (Arias *et al.*, 1994). Therefore after CREB has been phosphorylated it must be regulated this occurs through the action of phosphatases. Two nuclear localised protein serine/threonine phosphatases; PP1 (Hagiwara *et al.*, 1992) and PP2A (Wadzinski *et al.*, 1993) are reported to dephosphorylate CREB. Using okadaic acid at concentrations above 10 nM the Hagiwara study highlights that PP1 was required to dephosphorylate pCREB in forskolin-stimulated PC12 cells (Cohen *et al.*, 1989; Hagiwara *et al.*, 1992). However a subsequent study reports that PP2A is the dominant phosphatase required to dephosphorylate pCREB (Wadzinski *et al.*, 1993). Using rat liver nuclear extracts which were PKA stimulated, the presence of okadaic acid inhibited the dephosphorylation of CREB and enhanced the transcription mediated by the phosphoenolpyruvate carboxykinase (PEPCK) promoter. Furthermore a specific inhibitor for PP1, heat-stable protein inhibitor-2, when applied to the rat liver nuclear extracts had no effect on gene transcription mediated PEPCK. Therefore in rat liver cells, PP2A is the phosphatase required to dephosphorylate pCREB (Wadzinski *et al.*, 1993). These data suggest that the phosphatase required to dephosphorylate CREB may be cell-type specific.

Additionally a recent study highlights that phosphate and tensin homolog deleted on chromosome 10 (PTEN) phosphatase has been found to be co-localised with CREB in HeLa and mouse embryonic fibroblasts (Gu *et al.*, 2011). The group reported a direct interaction between CREB and PTEN phosphatase and found that deletion of PTEN in $PTEN^{(-/-)}$ MEF cells led to c-Myc and Bcl2 gene expression both of which require CREB activation for transcription. This was reversed in $PTEN^{(+/+)}$ MEFs where these cell survival genes had lower expression in quantitative PCR when compared to $PTEN^{(-/-)}$ MEFs (Gu *et al.*, 2011).

CREB activation can also be regulated by phosphatases acting upon kinase upstream of the transcription factor. As mentioned one of the main kinase signalling pathway required for CREB phosphorylation is MAPK (Impey *et al.*, 1998). MAPK (ERK1/2) is

a serine/threonine kinase where MAPK kinase (MEK1/2) phosphorylates both a threonine and tyrosine to activate the protein (Pouysségur *et al.*, 2002). Therefore, if either one of the phosphates or both are removed this renders ERK1/2 inactive. Either tyrosine specific, serine/threonine specific phosphatases (such as PP2A) have the ability to remove one of the phosphate groups (Alessi *et al.*, 1995). Furthermore dual specificity protein phosphatases can also remove both of the phosphate groups on the ERK1/2 protein subsequently inactivating the protein and inhibiting the signalling via that pathway (Keyse, 2000; Kondoh and Nishida, 2007).

PP2A is also implicated in the regulation of AKT by dephosphorylating the active protein (Bononi *et al.*, 2011). Therefore this protein phosphatase can regulate CREB both directly and indirectly.

1.7. Focal adhesion proteins and the actin cytoskeleton

Cell movement is important from our conception, throughout life and in some cases hastens our death. The ability for cells to migrate is important in many cellular processes. These include the movement of cells in gastrulation to sites where they differentiate into tissues and organs in the developing embryo, fibroblasts migrating to a wound where they migrate to each other to initiate the healing, immune cells infiltrating sites of inflammation and infection. However aberrant migration of cells can lead to certain pathologies such as metastasis of cancer cells (Ridley *et al.*, 2003). The actin cytoskeleton is required for not only the shape of the cell but is essential for cell motility, cytokinesis and phagocytosis and also has a role in the movement of intracellular components (Nobes and Hall, 1995). Migration of cells is a highly dynamic process where the leading edge of the cell is characterised by the formation of lamellipodia and filopodia, which contain focal adhesions and stress fibres. Focal adhesions are complexes of more than 50 proteins (Zamir and Geiger, 2001; Zaidel-Bar *et al.*, 2003). Assembly and disassembly of focal adhesions is important at the leading and retracting edge of cells respectively. These events lead to the polarity of the cell to allow directed migration (Zaidel-Bar *et al.*, 2003). Furthermore polymerisation of the actin cytoskeleton is also required (Machesky and Hall, 1997).

1.7.1. Vinculin, a focal adhesion protein

Focal adhesions (FAs), areas where the cell binds to the ECM were first visualised by electron microscopy (Abercrombie *et al.*, 1971). FAs tend to form just behind the

leading edge in motile cells although they are also prominent in stationary cells (Burridge and Chrzanowska-Wodnicka, 1996; Smilenov, 1999). FAs are only a few microns long and attach the actin cytoskeleton to the extracellular matrix (ECM) (Zamir and Geiger, 2001). Vinculin is 117 kDalton focal adhesion protein which intracellularly associates with the ECM-integrins and with cadherin cell-cell interactions (Ziegler *et al.*, 2006). However vinculin should not just be considered a linker protein as there are many binding sites for other proteins within vinculin (Ziegler *et al.*, 2006). These include Arp2/3 required for actin polymerisation in lamellipodia and is important in cell spreading, the Diaphanous-related formin mDia, and the actin regulatory proteins Ena/VASP suggested to be responsible for growth of stress fibres at the FAs (Endlich *et al.*, 2007). Another vinculin binding protein is zyxin which is suggested to be responsible for the retraction dependent formation of FAs from focal complexes at migrating edge of the lamellipodia (Zaidel-Bar *et al.*, 2003). Furthermore PIP_2 can bind to vinculin where it crosslinks vinculin to other proteins such as paxillin to promote the formation of focal contacts (Zamir and Geiger, 2001). Cell migration begins with the formation of small adhesions known as focal complexes which are dot-like structure. These then mature into focal adhesions which are elongated in appearance (Carisey and Ballestrem, 2011). Both focal complexes and FAs contain vinculin (Zaidel-Bar *et al.*, 2003). Vinculin when activated has an open conformation which allows the binding of the actin cytoskeleton to the vinculin tail and talin to the vinculin head. Talin binds and activates the integrins which form into clusters which leads to the enlargement of the FA (Humphries *et al.*, 2007). It is reported that mouse embryonic fibroblasts from vinculin$^{(-/-)}$ mice are smaller and less adhesive than wild type littermates. Moreover the fibroblasts from the knockout animals also migrate faster than wild type littermates however re-introduction of vinculin reversed these effects (Carisey and Ballestrem, 2011).

Contraction of stress fibres generates force which acts on FAs leading to their elongation (Kaverina *et al.*, 2002; Endlich *et al.*, 2007). Focal complexes are mediated by rac1 and cdc42 and mature into FAs when Rho is activated (Kaverina *et al.*, 2002). Also mechanical cues from the extracellular environment lead to the control of the spatiotemporal aspects of FA assembly, disassembly and reorganisation which is mediated by vinculin to control the polarity of the migrating cell (Carisey *et al.*, 2013). Therefore vinculin is at the fore-front of focal adhesion regulation (Carisey and Ballestrem, 2011).

1.7.2. Rho signalling and the actin cytoskeleton

The actin cytoskeleton shows directionality in the way it is polymerised which is important for migration and cell movement in response to chemical stimuli as would be seen with cancer metastasis and immune cells moving to sites of inflammation (Machesky and Hall, 1997). Stress fibres are highly organised bundles of polymerised F-actin (by the action of actin bundling proteins; α-actinin) to form the actin-myosin contractile system (Katoh *et al.*, 2001, 2007). Stress fibres terminate in focal adhesions where the fibre interacts with the vinculin tail (Humphries *et al.*, 2007). α-actinin also interact with vinculin therefore regulating not only stress fibres but also FAs (Katoh *et al.*, 2007).

The small Rho GTPases such as Rho, rac and cdc42 have specific roles in the migration of cells (figure 1.5). Rac activation promotes the formation of lamellipodia by actin polymerisation. Actin stress fibres within the lamellipodia have a uniform polarity and the barbed (growing) end is at the leading edge of the lamellipodia (Cramer *et al.*, 1997). In a process known as "treadmilling" actin monomers of G-actin are polymerised at the barbed end at the cell periphery with subsequent release of G-actin monomers from the interior end of the actin fibre (Wehrle-Haller and Imhof, 2003). The small Rho GTPase, cdc42, is responsible for filopodia formation (Small *et al.*, 1999). Filopodia have stress fibres which are parallel to each other (Ridley *et al.*, 2003). The bundling of the actin cytoskeleton that leads to the formation of stress fibres is well documented as being mediated by Rho (Machesky and Hall, 1997). Rho is also reported to be required for the formation of focal adhesion complexes (Ridley and Hall, 1992; Nobes and Hall, 1995). Nobes and Hall (1995), state that two distinct pathways, each signalling through Rho, exist for either the formation of stress fibres or for the creation of focal adhesion complexes. Previous studies have reported that increases in the stress fibres were observed in fibroblasts treated with LPA (Ridley and Hall, 1992; Amano *et al.*, 1997). The authors also noted that focal adhesion proteins were increased in cells treated with LPA (Ridley and Hall, 1992). One set of researchers injected an inactive catalytic domain of the Rho binding domain and attenuated the formation of stress fibres and blocked the creation of focal adhesion complexes suggesting that Rho and ROCK are important in mediating the formation of stress fibres and focal adhesion complexes (Amano *et al.*, 1997). As GPR55 activates Rho, rac and cdc42 (Ryberg *et al.*, 2007) it suggests that GPR55 may be important for both cytoskeletal reorganisation and FA formation. Recently breast cancer cells have a migratory phenotype that is

mediated by GPR55 although the exact Rho GTPases remain to be determined (Ford *et al.*, 2010). Furthermore GPR55 mediated polarisation of neutrophils required signalling via Rho (Balenga *et al.*, 2011). Therefore GPR55 may mediate the generation of cytoskeletal components required for the migration of cells.

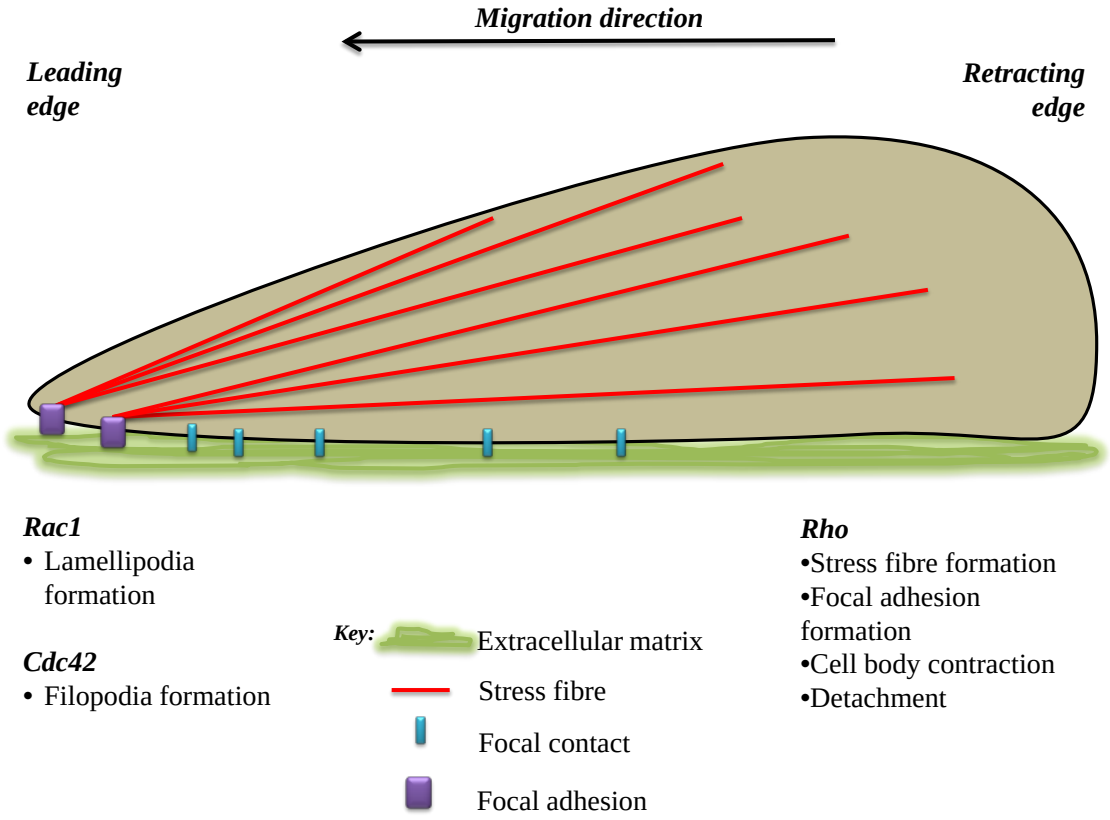

Figure 1.5: Rho GTPases play important roles in cell migration. *Differing Rho GTPase family members (Rac1, Cdc42 and Rho) induce varying effects in cells that lead to cell polarisation and subsequent migration. Bundles of actin filaments make up stress fibres and attach to focal adhesion complexes allowing the attachment of the cell to the extracellular matrix.*

1.8. Project aims

The main aims of this study were:

- To assess a novel group of lipids, the N-acyl amino acids, in a recombinant stably overexpress human GPR55 cell line (hGPR55-HEK293 cells) in a variety of signalling assays; Ca^{2+} mobilisation, CREB phosphorylation, cytoskeletal reorganisation and changes in FAs.

- To evaluate the signalling induced by GPR55 activation by either LPI or NOSer by the use of pharmacological inhibitors in the signalling assays above to attempt to elucidate the signalling pathways involved.

- To assess GPR55 signalling in an endogenous setting when activated by either LPI or NOSer utilising the previously characterised endogenously GPR55 expressing prostate cancer cell line, DU145. Furthermore using pharmacological inhibitors to assess the signalling pathways mediated by GPR55 in DU145 cells.

CHAPTER TWO

Materials and Methods

2.1. MATERIALS

2.1.1. Cell culture: Plasticware and general reagents

Bioquote Limited, York, UK.

- Cell Permeable Rho Inhibitor

cDNA Resource Center, Missouri University of Science and Technology USA.

- Plasmids encoding Gα13 (Q226L/D294N)

Fisher Scientific, Loughborough, UK.

- Parafilm
- Falcon™ Bacteriological Petri Dishes with Lid; 30 mm

Greiner bio-one, Stonehouse, UK.

- 25cm² TC treated flask with filter cap (T_{25} TC flask)
- 75cm² TC treated flask with filter cap
- Culture dish, Tissue culture treated, 35mm
- Culture dish, Tissue culture treated, 60mm
- 24 well Tissue culture treated plate with lid, sterile
- Cryo.s™, 2 ml, polypropylene, round bottom, internal thread, sterile
- Serological pipette PS, 5ml, ST, 1/10 GRADS
- Pipette tips; 10 µl, 200 µl, 1000 µl
- Sample container 25x90mm, 30ml, Conical skirted bottom
- 15ml polypropylene centrifuge tube with conical base

Life Technologies, Paisley, UK.

- Dulbecco Modified Eagle Medium / F-12
- Phosphate Buffered Solution
- Lipofectamine™ 2000

- Opti-MEM® Reduced Serum Medium, no Phenol Red

Merck Millipore Darmstadt, Germany.

- Millex-GP, 0.22 µm, polyethersulfone, 33 mm, gamma sterilized

Roche Diagnostics Limited, West Sussex, UK.

- G418 solution

Sera Labs International, West Sussex, UK.

- Heat inactivated foetal bovine serum South American origin

Sigma Aldrich, Dorset, UK.

- Trypsin EDTA solution
- L-glutamine solution
- Poly-D-lysine
- Sodium hydroxide
- HEPES
- EDTA
- Paraformaldehyde
- Dimethyl sulphoxide
- Serum replacement 2
- Triton™ x-100
- Dow Corning® high-vacuum silicone grease
- Phorbol 12-myristate 13-acetate

Thermo Fisher Scientific, Waltham, MA, USA.

- Nalgene™ Cryo 1°C freezing container cat no 5100-0001

Tocris Bioscience, Bristol, UK.

- Fura-2-AM

VWR, Lutterworth, Leicestershire, UK.

- Sucrose
- Glucose
- Sodium Chloride
- Potassium Chloride
- Calcium Chloride
- Magnesium Chloride
- Coverglasses, round, 9 mm
- Ethanol

2.1.2. Cell lines

- Human Embryonic Kidney 293-AD (HEK293) cells; Life Technologies, Paisley, UK.
- Stable cell line over-expressing human 3xHA-GPR55 (hGPR55-HEK293 cells); Advantagen, Dundee, UK.
- DU145 prostate cancer cell line; Division of Cancer Research, University of Dundee, Dundee, UK.

2.1.3. siRNA

Dharmacon Thermo Scientific, Loughborough, UK.

- DharmaFECT 1 Transfection Reagent
- siGENOME ON TARGET plus SMARTpool duplex siRNA fragments. The siRNA consisted of four individual targeted fragments (21 nucleotides) as follows:

Human GPR55-siRNA

GCUACUACUUUGUCAUCAA

AAGAACAGGUGGCCCGAUU

GAGAAACAGCUUUAUCGUA

GAAUUCCGCAUGAACAUCA

2.1.4. Antibodies

Antibody	Supplier	Dilution
Mouse anti-HA	Covance Inc., Alnwick Northumberland, UK.	1:1000
Mouse anti-phosphoCREB (serine 133) clone 10E9	Millipore, Upstate, Billerica, MA, USA.	1:250
Mouse anti-vinculin	Sigma Aldrich, Dorset, UK.	1:500
Alexa fluor® 546-conjugated phalloidin	Molecular Probes®, Life technologies, Paisley, UK.	1:250
Alexa Fluor® 488 donkey anti-mouse	Molecular Probes®, Life technologies, Paisley, UK.	1:500
Cy 3 donkey anti-mouse	Jackson Immunoresearch Laboratories Incorporated, West Grove, PA, USA.	1:500

2.1.5. Lipids and other ligands

Generic name Chemical name	**Chemical Structure**	**Supplier**
AM251 1-(2,4-Dichlorophenyl)-5-(4-iodophenyl)-4-methyl-N-1-piperidinyl-1H-pyrazole-3-carboxamide	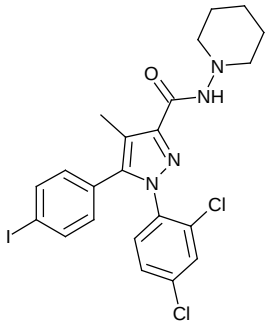	Abcam biochemicals ® Cambridge, UK.
L-α-Lysophosphatidylinositol sodium salt from *Glycine max* (soybean) 1-Acyl-sn-glycero-3-phospho-(1-D-myo-inositol)	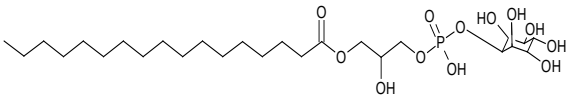	Sigma Aldrich, Dorset, UK
N- arachidonoyl-L-serine 1-(5Z,8Z,11Z,14Z-eicosatetraenoyl)-L-serine, (S)-3-hydroxy-2-(5Z,8Z,11Z,14Z)-eicosatetraenamidopropanoate, (S)-3-hydroxy-2-arachidonamidopropanoate	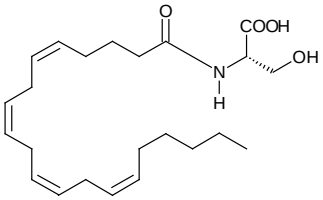	Avanti Polar Lipids, Alabaster, AL, USA
N-oleoyl L-serine 1-(9Z-octadecenoyl)-L-serine (S)-3-hydroxy-2-(9Z)-octadecenamidopropanoate (S)-3-hydroxy-2-oleoamidopropanoate	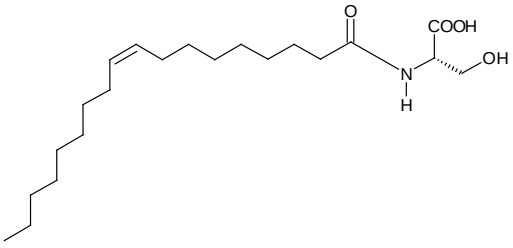	Avanti Polar Lipids, Alabaster, AL, USA

Generic name Chemical name	**Chemical Structure**	**Supplier**
N-palmitoyl L-serine 1-hexadecanoyl-L-serine, (S)-3-hydroxy-2-hexadecanamidopropanoate (S)-3-hydroxy-2-palmitamidopropanoate	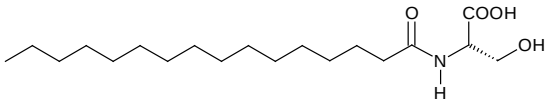	Avanti Polar Lipids, Alabaster, AL, USA
N arachidonoyl glycine N-[1-oxo-5Z,8Z,11Z,14Z-eicosatetraenyl]-glycine	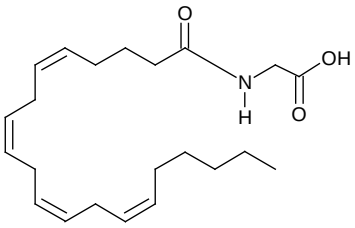	Avanti Polar Lipids, Alabaster, AL, USA
N oleoyl glycine N-(9Z-octadecenoyl)-glycine	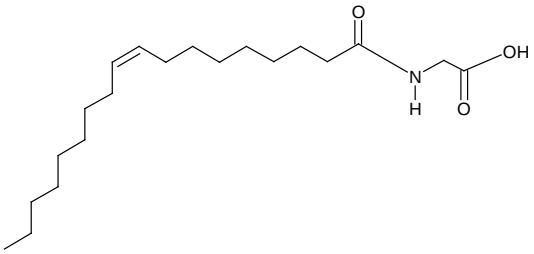	Avanti Polar Lipids, Alabaster, AL, USA
N palmitoyl glycine N-(1-oxohexadecyl)-glycine	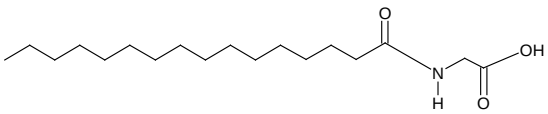	Avanti Polar Lipids, Alabaster, AL, USA
12-O-Tetradecanoylphorbol 13-acetate Phorbol 12-myristate 13-acetate; 4β,9α,12β,13α,20-Pentahydroxytiglia-1,6-dien-3-one 12-tetradecanoate 13-acetate	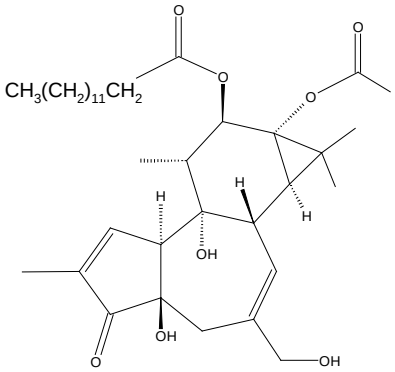	Sigma Aldrich, Dorset, UK

2.1.6. Inhibitors

Generic name Chemical name	**Chemical Structure**	**Supplier**
2-APB (2-Aminoethoxydiphenylborane)	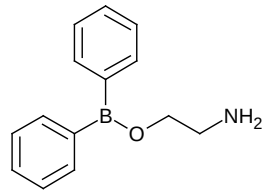	Tocris Bioscience, Bristol, UK.
BAPTA-AM 1,2-*Bis*(2-aminophenoxy)ethane-*N*,*N*,*N*',*N*'-tetraacetic acid tetrakis(acetoxymethyl ester)	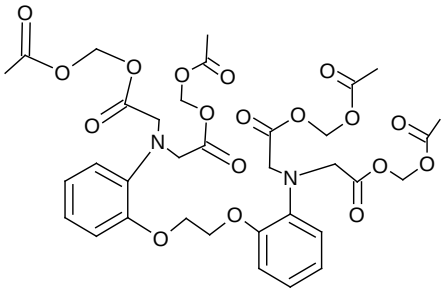	Tocris Bioscience, Bristol, UK.
Gö6980 2-[1-(3-Dimethylaminopropyl)-5-methoxyindol-3-yl]-3-(1H-indol-3-yl) maleimide	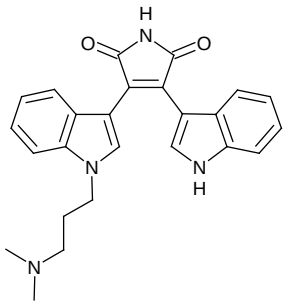	Calbiochem, Merck Chemicals, Nottingham, UK
H1152 dihydrochloride (*S*)-(+)-2-Methyl-1-[(4-methyl-5-isoquinolinyl)sulfonyl]-hexahydro-1*H*-1,4-diazepine dihydrochloride	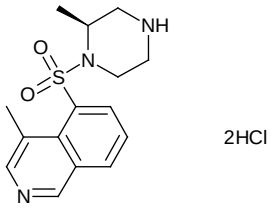	Tocris Bioscience, Bristol, UK.

Generic name Chemical name	**Chemical Structure**	**Supplier**
KN-62 4-[(2*S*)-2-[(5-isoquinolinylsulfonyl) methylamino]-3-oxo-3-(4-phenyl-1piperazinyl) propyl] phenyl isoquinolinesulfonic acid ester	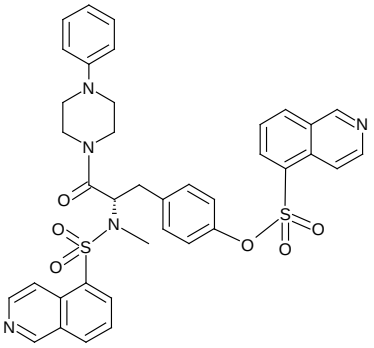	Tocris Bioscience, Bristol, UK.
LY294002 hydrochloride 2-(4-Morpholinyl)-8-phenyl-4*H*-1-benzopyran-4-one hydrochloride	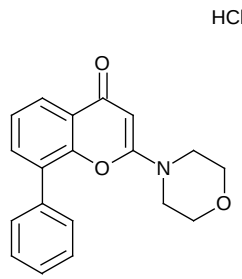	Tocris Bioscience, Bristol, UK.
ML-141 4-[4,5-Dihydro-5-(4-methoxyphenyl)-3-phenyl-1*H*-pyrazol-1-yl]benzenesulfonamide	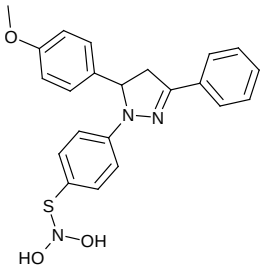	Tocris Bioscience, Bristol, UK.
PD98059 2-(2-Amino-3-methoxyphenyl)-4*H*-1-benzopyran-4-one	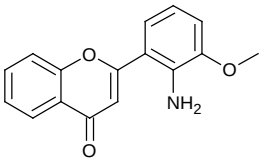	Tocris Bioscience, Bristol, UK.

Generic name Chemical name	**Chemical Structure**	**Supplier**
Rapamycin (3*S*,6*R*,7*E*,9*R*,10*R*,12*R*,14*S*,15*E*,17*E*,19-*E*,21*S*,23*S*,26*R*,27*R*,34a*S*)-9,10,12,13,14,21,22,23,24,25,26,27,32,33,34,34a-Hexadecahydro-9,27-dihydroxy-3-[(1*R*)-2-[(1*S*,3*R*,4*R*)-4-hydroxy-3-methoxycyclohexyl]-1-methylethyl]-10,21-dimethoxy-6,8,12,14,20,26-hexamethyl-23,27-epoxy-3*H*-pyrido[2,1-*c*][1,4]oxaazacyclohentriacontine-1,5,11,28,29(4*H*,6*H*,31*H*)-pentone	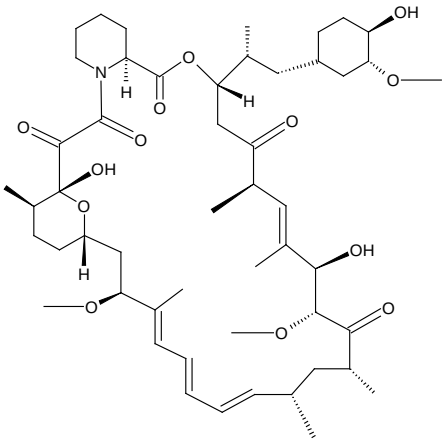	Tocris Bioscience, Bristol, UK
Thapsigargin (3*S*,3a*R*,4*S*,6*S*,6A*R*,7*S*,8*S*,9b*S*)-6-(Acetyloxy)-2,3,3a,4,5,6,6a,7,8,9b-decahydro-3,3a-dihydroxy-3,6,9-trimethyl-8-[[(2*Z*)-2-methyl-1-oxo-2-butenyl]oxy]-2-oxo-4-(1-oxobutoxy) azuleno[4,5-*b*]furan-7-yl octanoate	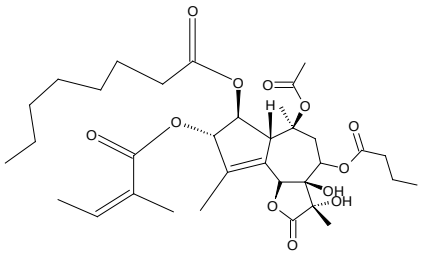	Tocris Bioscience, Bristol, UK
U0126 1,4-Diamino-2,3-dicyano-1,4-*bis*[2-aminophenylthio]butadiene	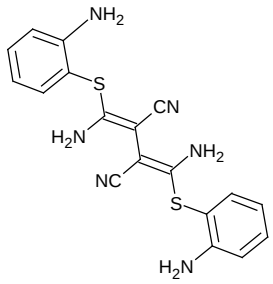	Calbiochem, Merck Chemicals, Nottingham, UK
U0124 1,4-Diamino-2,3-dicyano-1,4-bis[2-methylthio]butadiene	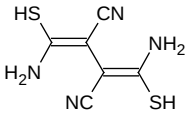	Calbiochem, Merck Chemicals, Nottingham, UK

Generic name **Chemical name**	**Chemical Structure**	**Supplier**
U73122 1-[6-[[(17β)-3-Methoxyestra-1,3,5(10)-trien-17-yl]amino]hexyl]-1*H*-pyrrole-2,5-dione	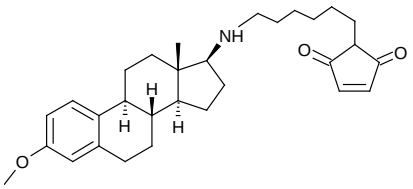	Tocris Bioscience, Bristol, UK
Wortmannin (1*S*,6b*R*,9a*S*,11*R*,11b*R*) 11-(Acetyloxy)-1,6b,7,8,9a,10,11,11b-octahydro-1-(methoxymethyl)-9a,11b-dimethyl-3*H*-furo[4,3,2-*de*]indeno[4,5,-*h*]-2-*h*]-2-benzopyran-3,6,9-trione	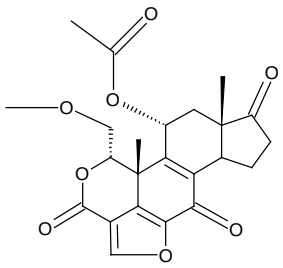	Calbiochem, Merck Chemicals, Nottingham, UK
Y27632 dihydrochloride *trans*-4-[(1*R*)-1-Aminoethyl]-*N*-4-pyridinylcyclohexanecarboxamide dihydrochloride	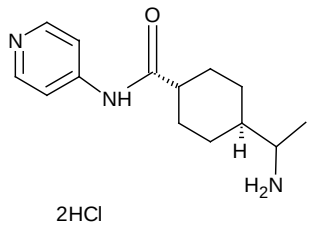 2HCl	Tocris Bioscience, Bristol, UK
YM-254890	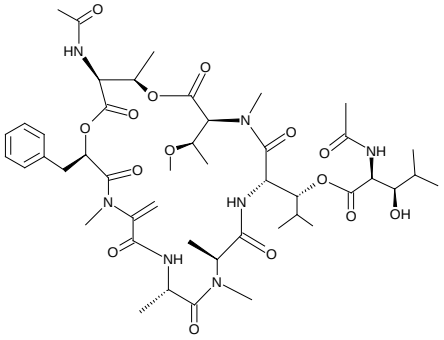	Astellas Pharma Inc Osaka, Japan

2.1.7. Antagonist

Generic name Chemical name	**Chemical Structure**	**Supplier**
(-)-Cannabidiol 2-[(1*R*,6*R*)-3-Methyl-6-(1-methylethe-nyl)-2-cyclohexen-1-yl]-5-pentyl-1,3-benzenediol	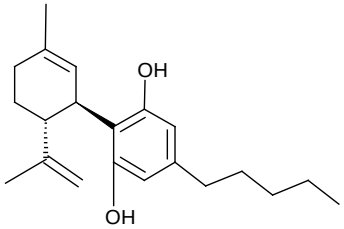	Tocris Bioscience, Bristol, UK

2.2. METHODS

2.2.1. Cell Culture Protocols

2.2.1.1. Resuscitation of frozen cells

HEK293, the stable cell line over-expressing human 3xHA-GPR55 (hGPR55-HEK293 cells) and DU145 cells were stored in the -80^{o}C freezer until required. All cell culture products were filtered using Millex-GP, 0.22 µm, polyethersulfone, 33 mm, gamma sterilized filters. DMEM medium containing 10% heat inactivated foetal bovine serum and 2 mM L-glutamine was warmed in a humidified incubator, 37^{o}C and 5% CO_2, prior to cells being resuscitated. Next, 7 ml of serum-containing medium was filtered into a T_{25} tissue culture flask at the same time the cells were quickly warmed (to avoid damage to the cells). The cells were then put into the medium in the flask and left to settle for around 2 hr. The medium was removed at this point and fresh serum-containing medium was added to the settled cells to reduce the amount of DMSO present in the flask. Cells were then left to grow; if necessary media were changed every 2-3 days until the cells reached 80-90% confluency.

2.2.1.2. Cell maintenance

HEK293 and DU145 cells were maintained in DMEM supplemented with 10% heat inactivated foetal bovine serum and 2 mM L-glutamine. They were kept in a humidified atmosphere of 5% CO_2 and 37^{o}C. hGPR55-HEK293 cells were selected for using the neomycin antibiotic; G418 (500 µg/ml). Cells were passaged once they reached around 80-90% confluency. Initially, they were washed once with phosphate buffer solution (PBS) to remove serum. The cells were then incubated with 0.5 ml trypsin until they detached from the base of the flask. The flasks were checked under a

light microscope to ensure that the cells were detached and the flask was gently tapped on the side to release any that were still attached. Finally 3 ml of serum-containing medium was added to the flask; the presence of the serum inactivates the trypsin stopping its protease effects from further damaging the cells. Two sterile T_{25} tissue culture flasks had 4 ml of serum-containing medium added and then 1 ml of the passaged cells was added to these flasks and kept in a humidified atmosphere of 5% CO_2 and 37^{o}C.

Borosilicate glass coverslips (9 mm; ~200) were placed in a 30 ml sample container and 70% ethanol was added until the coverslips were covered. They were gently mixed (5 min) to allow the ethanol to sterilise all the coverslips. The ethanol was then aspirated and dH_20 was filtered onto the coverslips where they were gently mixed then the dH_2O was aspirated. This washing process was carried out twice to ensure the removal of all the ethanol. Poly-D-lysine (20 µg/ml) was added to filtered dH_20 (20 ml) in the sample container with the coverslips. The coverslips were then rotated for 1 hr to ensure even coating prior to the poly-D-lysine solution being aspirated. The coverslips were then rinsed and stored in sterile water for up to a week. Poly-D-lysine coated coverslips were dried and placed in petri dishes ~ 20 coverslips in a culture dish (60 mm); serum-containing medium (4 ml) was added to the dishes prior to the addition of passaged cells (1 ml) which were left to settle for 24 hr in a humidified atmosphere of 5% CO_2 and 37^{o}C. The cells were then serum-starved for 12-16 hr before the commencement of experiments.

2.2.1.3. Freezing down cells

Cells were grown to 80-90% confluency and then washed with PBS which was then aspirated. Next, cells were treated with 0.5 ml of trypsin until they had detached from the bottom of the flask after which 4 ml of serum containing medium was added. Each flask of detached cells was then transferred to a centrifuge tube (15 ml) and spun down at 1000 rpm for 5 min. The supernatant was aspirated and the pellet was re-suspended in 0.75 ml of filtered serum-containing medium which was supplemented with 10% DMSO. Cryotubes containing the re-suspended cells were then placed in the Nalgene™ Cryo 1^{o}C freezing container to allow a slow freezing process to occur (to limit any damage occurring to the cells) and was placed in the -80^{o}C freezer. After 24 hr the cryotubes were removed from the freezing container and kept in the -80^{o}C freezer until required.

2.2.1.4. Preparation of transient transfections

24 hr prior to the transient transfection – cells were plated as above onto poly-D-lysine coated coverslips. They were placed in a humidified environment for 24 hr to settle and were ~ 70% confluent. On the transfection day; 2 µl of Lipofectamine™ 2000 (2 mg/ml) was added to 98 µl of OptiMEM® in one Eppendorf tube. In a second Eppendorf tube 2 µl of cDNA (1 mg/ml) was added to 98 µl of OptiMEM. Both Eppendorf tubes were mixed by gently pipetting the mixture up and down several times. They were left for 5 min. After which the cDNA mix was added to the Lipofectamine™ 2000 mix and again gently pipetted up and down 4-5 times to mix well. This was left for 20 min (to allow time for cDNA-liposome complexes to form) prior to the cDNA-liposome complexes being added dropwise to the coverslips (which were now in 0.8 ml of serum-free medium). The cells/cDNA mix were then placed in a humidified environment and left for 15-20 hr before the commencement of experiments.

2.2.1.5. Preparation of siRNA transient transfection

3 µl of Dharmafect1 was added to an Eppendorf tube and 97 µl of serum-free was added and gently pipetted up and down five times. In another Eppendorf tube 5 µl of the required siRNA (20 µM) was added and then 95 µl of serum-free medium was gently pipetted up and down five times to ensure even distribution. These Eppendorf tubes were then left for 15 min. The contents of the siRNA eppendorf tubes was then added to the Dharmafect1 containing Eppendorf tubes and these were then gently pipetted up and down five times ensuring that no bubbles were present. These tubes were then left for a further 20 min. 0.8 ml of serum-free medium that contained 1:50 of serum replacement 2 was added to the dishes. Each set of siRNA mix was added to the coverslips in a drop wise manner onto each coverslip before gently moving the dish from side to side to allow good dispersal of the mix. The final concentration of 100 nM of siRNA was achieved. Cells were placed in a humidified atmosphere for between 60-72 hr before commencement of experiments.

2.2.2. Experimental Protocols

2.2.2.1. Calcium (Ca^{2+}) imaging

Variations in intracellular calcium $[Ca^{2+}]_i$ concentration were measured using a digital epifluorescence imaging system (Perkin Elmer, Emeryville, CA, USA) mounted on an Olympus BX50WI microscope (Olympus, Tokyo, Japan). Cells plated on poly-D-lysine coverslips were placed in serum-free medium overnight. These cells were loaded

with a ratiometric dye, Fura-2-AM (6 µM) for 60 min before the commencement of experiments. Cells were then washed in HEPES buffered saline (HBS in mM: NaCl 135; KCl 5; $MgCl_2$ 1; $CaCl_2$ 1; HEPES 10; Glucose 10; pH 7.4). A coverslip containing loaded cells was then placed in a Falcon™ Petri dish (30 mm) attached with high vacuum grease to ensure stability during perfusion with HBS. Typically ligands were perfused for a 5 min period at a rate of 2 ml/min. Ratiometric images pairs (350 nm and 380 nm excitation) were acquired at 2-5 sec intervals. Effects of ligands on the F_{350}/F_{380} ratio, which is proportional to the $[Ca^{2+}]_i$, were determined for individual cells in a given field.

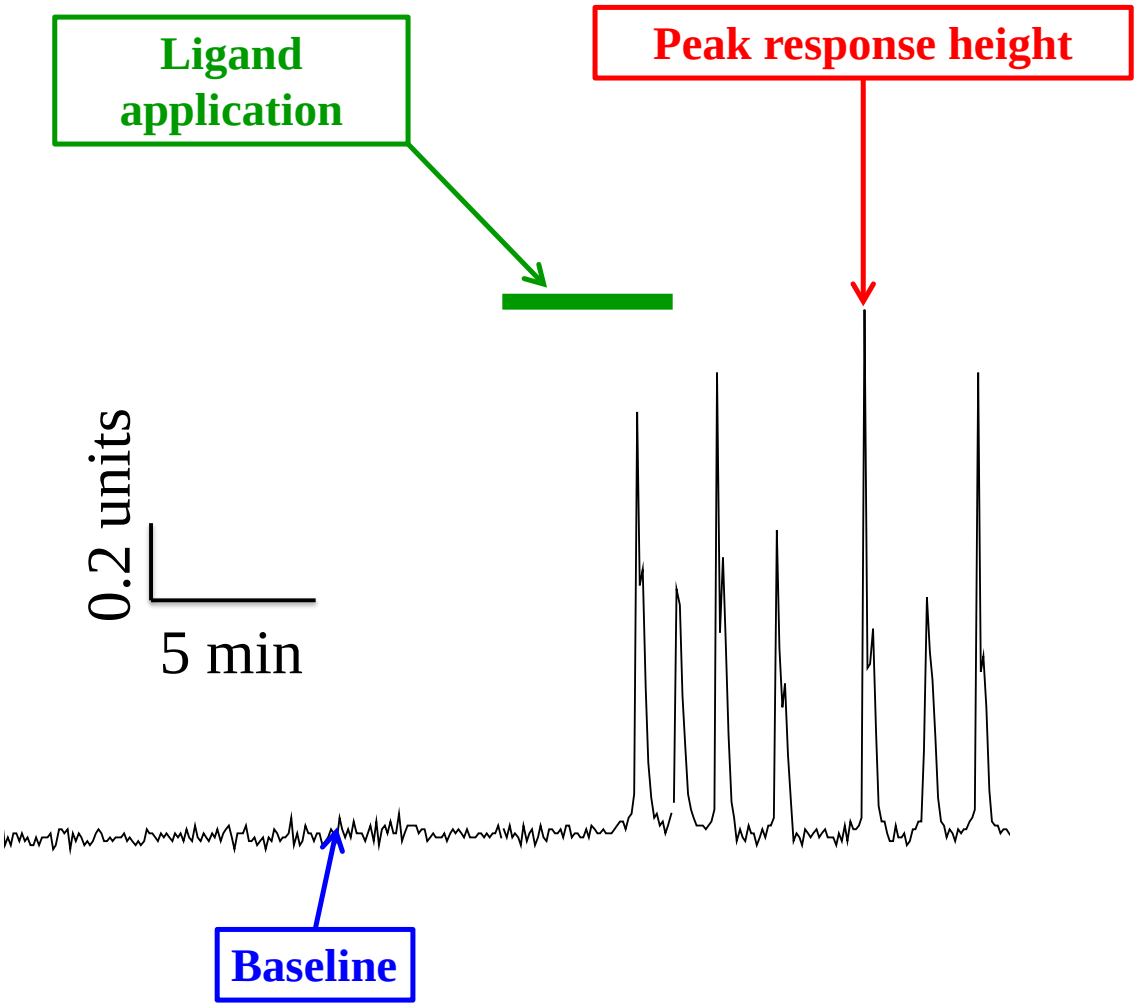

Figure 2.1: Example Ca^{2+} trace of single cell recording. *The highest peak response ratio value within 15 min of ligand application is measured (red arrow) along with a baseline ratio value (blue arrow) which is subtracted to give the response height.*

For analysis, baseline ratio values obtained prior to drug addition were subtracted from peak responses. Raw data was analysed with Metafluor® offline (Molecular Devices

(UK) Ltd, Wokingham, UK) software whereby background recordings were removed. Traces were then transferred to Origin 7 software (OriginLab Corporation, Stoke Mandeville, UK) where mean peak response data was measured within 15 min of ligands being applied (5 min ligand application and 10 min wash). The response height measured the highest point reached in the 15 min stated above. The baseline height was measured as the mean value within 5 min before the application of ligands (figure 2.1).

Peak response measurements were made in Origin. Having transferred the Metafluor data with the background removed into Origin as a single ASCII (in file tab) make the graph by plotting the line graph. When this is minimised the raw data table can be seen (figure 2.2A). From this data table highlight all the cells from time of ligand application until 15 min later - this accounts for the 5 min ligand application and 10 min washout (figure 2.2B). Highlight the Statistic tab and click on descriptive statistics and then click on statistics on columns. In the cell column delete any cells which have shown constitutive activity and then moving to the right find the Max(Y) column and copy and paste this into Excel (figure 2.2C). Now going back to the raw data highlight 5 min of data prior to the application of the ligand and work out the average – this corresponds to the baseline value. Ensure that any cell removed previously is also removed from the baseline values.

The following calculation was used:

Peak response = response height - baseline height.

Peak response data was analysed using GraphPad Prism 4, (GraphPad Software, Inc., La Jolla, CA, USA) to generate both sigmoidal concentration response curves and histograms.

A

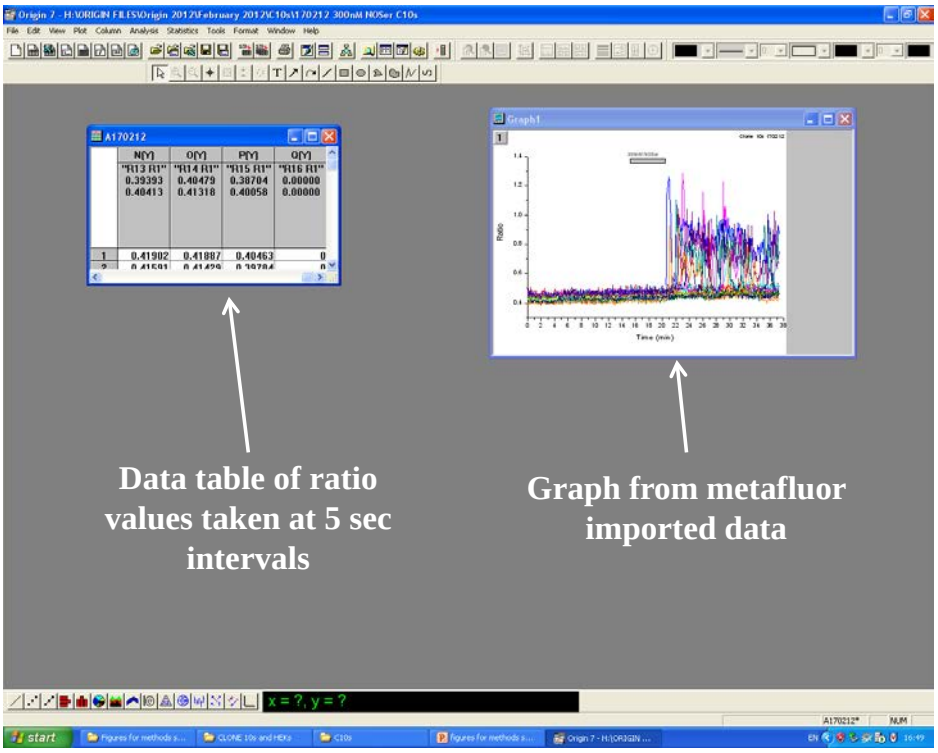

B

Column A = Time
Column B onwards = individual cells

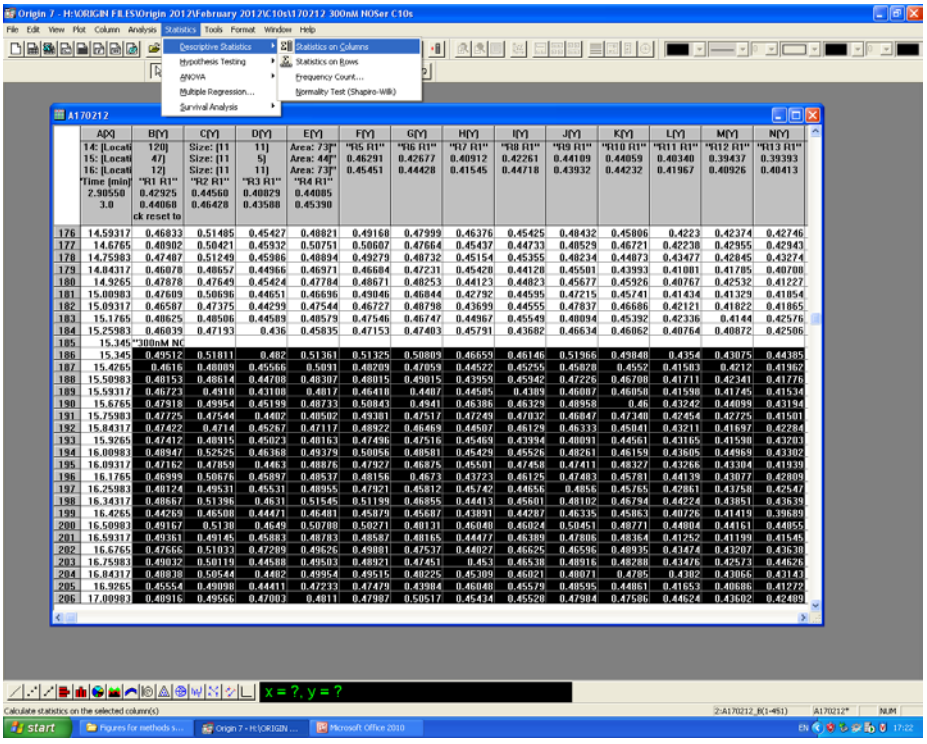

1. Highlight data from drug addition to 10 min after the wash begins

2. Click on Statistics tab. Highlight descriptive statistics. Followed by Statistics on columns.

C

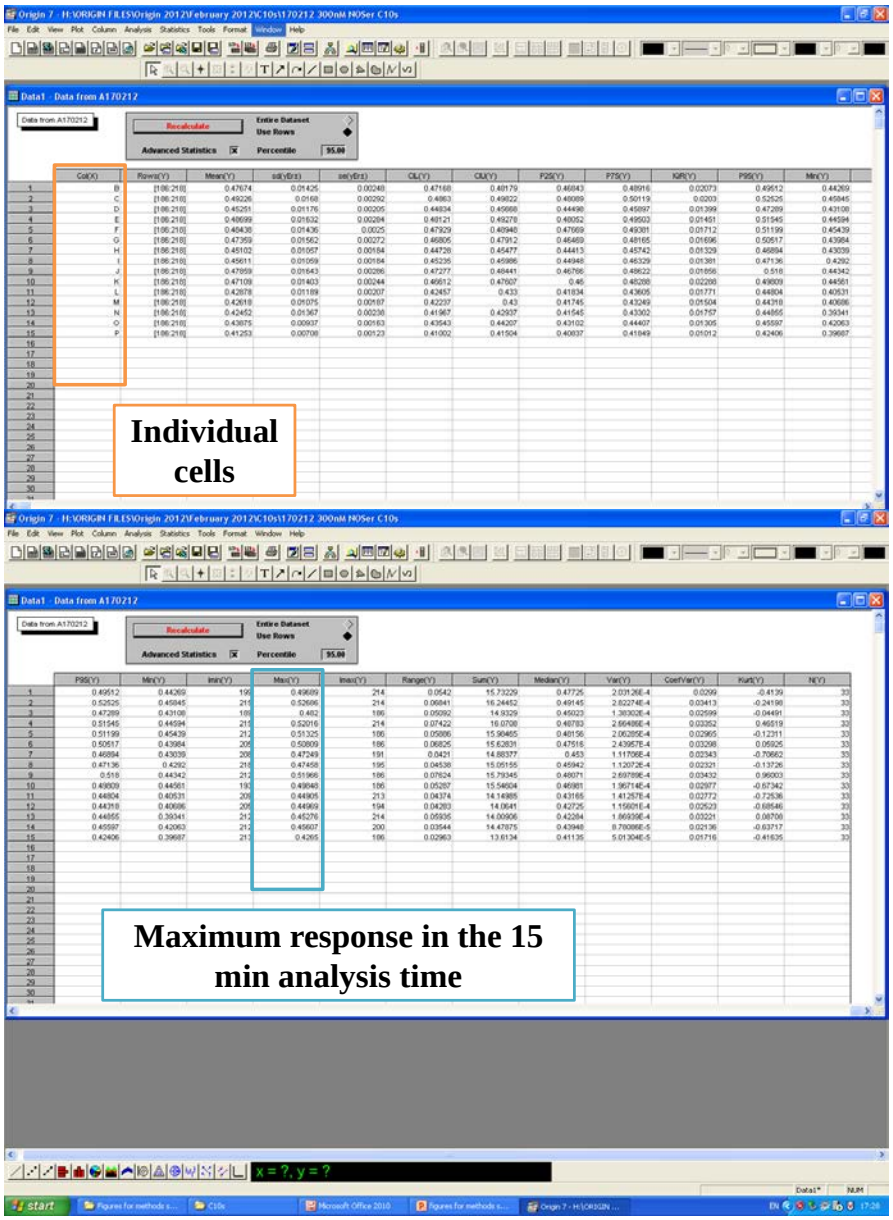

Figure 2.2: Ca^{2+} analysis with Origin. *The Ca^{2+} data is analysed in Metafluor with the background removed and then imported as a single ASCII into Origin and a graph produced.* ***A****, when the graph is minimised the raw data values are revealed.* ***B****, Raw data is highlighted from time when drug applied to 10 mins into wash. Using the statistics button the descriptive statistics on columns is plotted.* ***C****, Descriptive statistics for each cell and the Max(Y) column highlighted.*

2.2.2.2. Confocal microscopy

2.2.2.2.1. Phosphorylation of cAMP Response Element Binding Protein (pCREB)

HEK293, hGPR55-HEK293 and DU145 cells were plated on poly-D-lysine coated coverslips and placed overnight in serum-free medium in a humidified incubator (37^{o}C; 5% CO_2). Cells were treated with ligands diluted in HBS and placed a dry incubator (37^{o}C) for 25 min. In experiments where inhibitors were applied, the cells were treated

with the inhibitor for 30 min prior to co-application of the inhibitor and ligand for a further 25 min. Cells were fixed and permeabilised with ice cold methanol, in a -20 ^{o}C freezer for 10 min. Fat-free powdered milk was dissolved in HBS to a final concentration of 5% and was then applied to the cells and left at room temperature for 20 min. After which the cells were washed 3 times with HBS to ensure all the milk solution is removed. Mouse anti-phosphoCREB diluted in HBS (1:250) was applied for 60 min. The cells were then washed 3 times with HBS. The secondary antibody Alexa fluor® 488 donkey anti-mouse diluted in HBS (1:500) was then applied for 30 min. Cells were washed as above and maintained in glucose-free HBS. Images were acquired and processed using a laser scanning confocal imaging system (Zeiss LSM510; Carl Zeiss Microscopy Ltd, Cambridge, UK) which incorporates an upright Axioskop FS2 microscope (Carl Zeiss, Oberkochen, Germany) using a 40x water immersion objective.

Nuclear fluorescence measurements were performed with Image J freeware (http://imagej.nih.gov/ij/). To allow the measurements to be made ensure that the analyse tab is open and the set measurements box visible. Ensure that the following boxes are ticked area, min & max gray values, integrated density, mean gray value and add to overlay (figure 2.3).

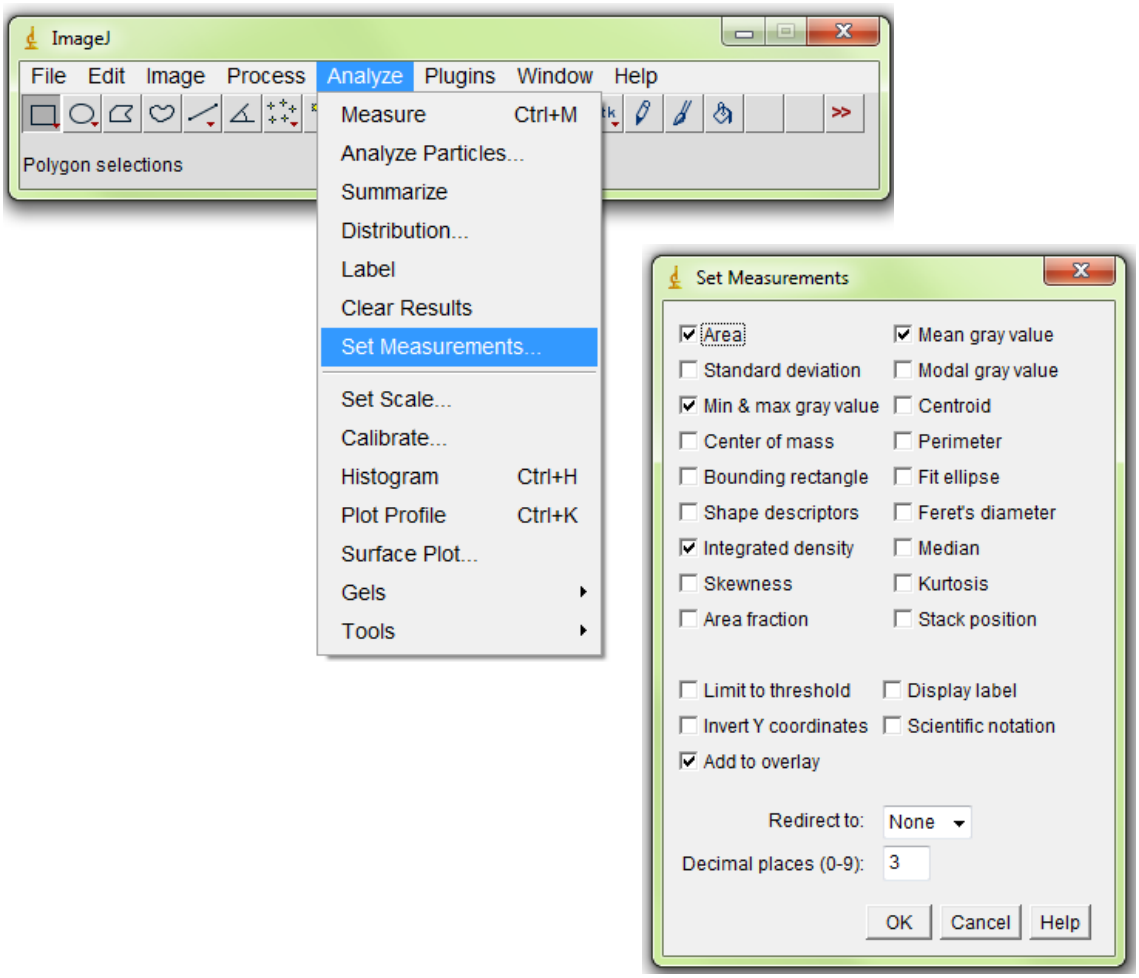

Figure 2.3: Measurement settings in Image J freeware. *Open the analyse tab and click on set measurements. Ensure that the area, min & max gray values, integrated density, mean gray value and add to overlay are all ticked then click on OK.*

The analysis was carried out on the raw data image acquired from using Zeiss LSM 510 Laser-sharp software. For each image, defined nuclei were traced using a bright-field image - use > key to visualise the bright-field, to highlight the nuclear membrane and then the measurement recorded with the fluorescent image present - use < key to visualise the fluorescent image. To record the results press the 'm' key. Three background regions devoid of cells were also analysed to allow a mean background reading to be calculated (figure 2.4).

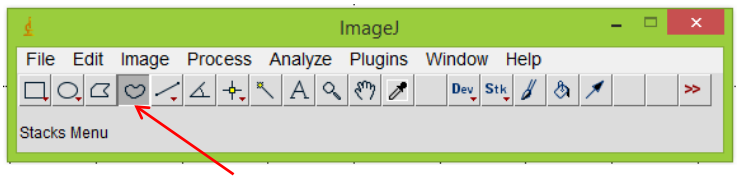

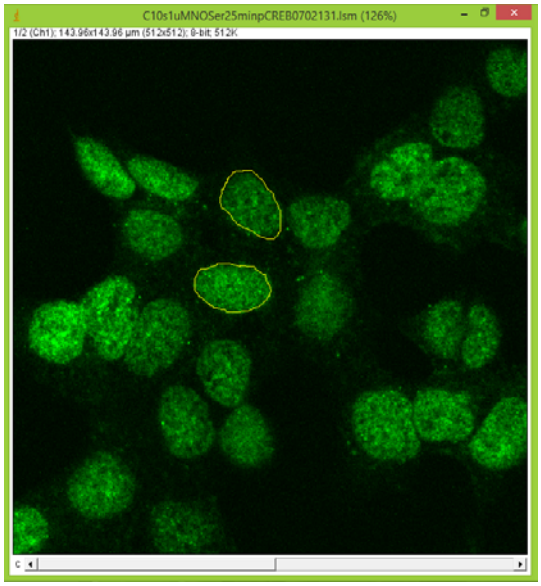

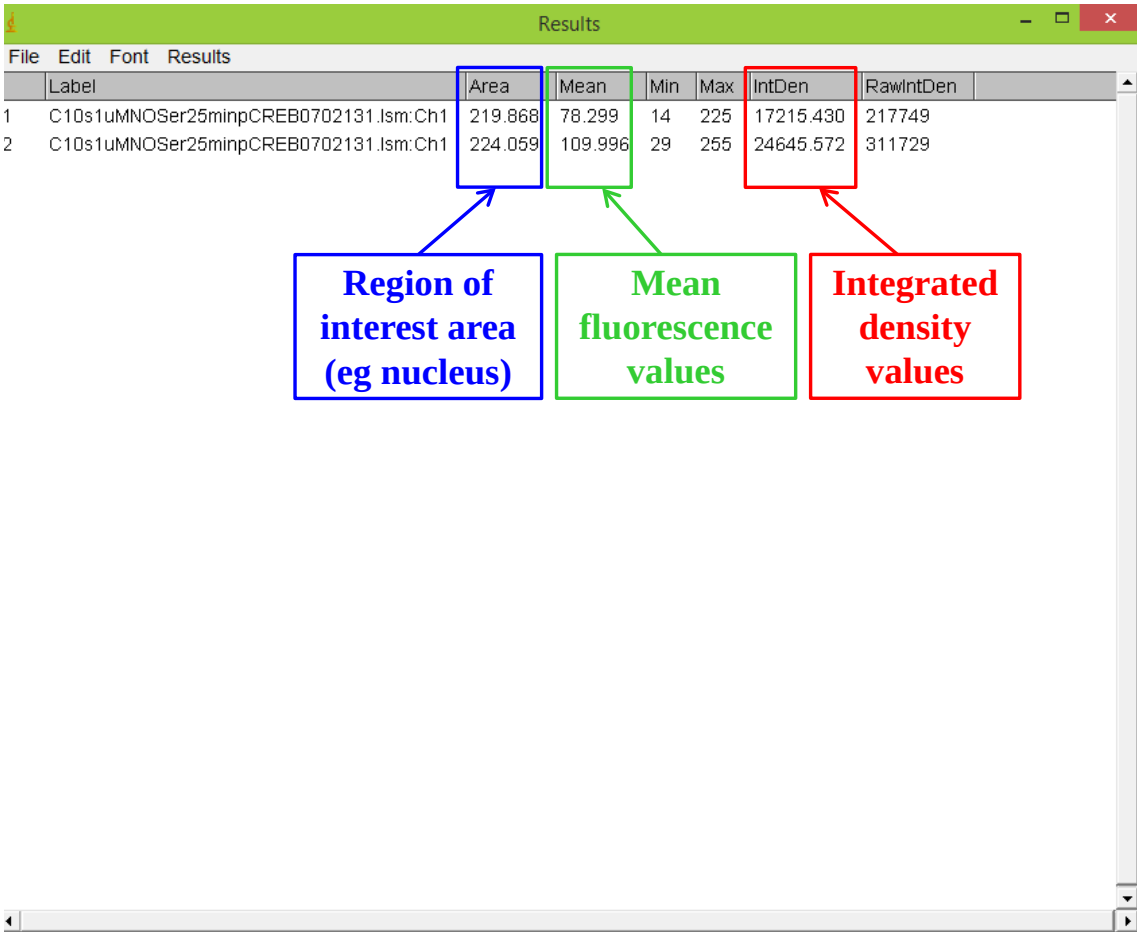

Figure 2.4: Analysis of nuclear phosphorylated CREB using Image J. *Click on the irregular icon and using the brightfield image draw either in a background region void of cells or round the nuclear membrane. Change to the fluorescent image and press 'm' to record the results.*

Measurements were derived from fluorescent image where the corrected Total Nuclear Fluorescence (CTNF) for individual nuclei was calculated as follows:

CTNF = Integrated Density - (Area of the nucleus x mean background reading).

Where, the integrated density is the product of the area of the nuclei and the mean grey level intensity value. The latter value is the sum of all the pixels in the region divided by the number of pixels that are present in the selected area giving a value for the fluorescence intensity within the nucleus. The area of the nuclei x mean background reading is therefore equivalent to the background integrated density value (or background fluorescence intensity). Thus, CTNF is fluorescence intensity within a nucleus minus background fluorescence intensity (Gavet & Pines, 2010; Potapova *et al*., 2011). For the compilation of concentration-response curves each point was calculated by CTNF minus the mean DMSO CTNF value from 25 nuclei per experiment then normalised to 1 µM LPI for 2-3 experiments. This data was then transferred to GraphPad Prism 4 to allow the compilation of concentration-response curves. Data on the histograms was derived by calculation of the CTNF which was then normalised to that obtained with the 1 µM LPI mean CTNF value. This data was transferred to GraphPad Prism 4 and histograms were compiled.

2.2.2.2.2. Cytoskeletal reorganisation assay

Cells were plated on poly-D-lysine coated coverslips and placed overnight in serum-free medium in a humidified atmosphere (37^{o}C; 5% CO_2). HEK293 cells, hGPR55-HEK293 cells or DU145 cells were transferred into individual wells in 24 well plates with 1 ml of serum-free medium for 30 min and kept in a humidified atmosphere. Subsequently the ligands were added to the serum-free well at the appropriate final concentration for 30 or 60 min; HEK293 and hGPR55-HEK293 or DU145 respectively. In experiments where inhibitors were applied, the cells were treated with the inhibitor for 30 min prior to co-application of the inhibitor and ligand for a further 30 or 60 min; hGPR55-HEK293 and DU145 cells respectively. Cells were fixed in 4% paraformaldyhyde (PFA) supplemented with 200 mM sucrose for 10 min, then permeabilised with 0.2% triton X-100 for 10 min. F-actin was labelled using Alexa Fluor® 546-conjugated phalloidin which was diluted in HBS (1:500) and applied for 30 min at room temperature. Cells were then washed 3 times with HBS and maintained in glucose-free HBS. Cells were examined using a laser scanning confocal microscope

(Zeiss LSM510) as described previously. Changes in actin structure were not directly quantified, and are displayed as images (figure 2.5).

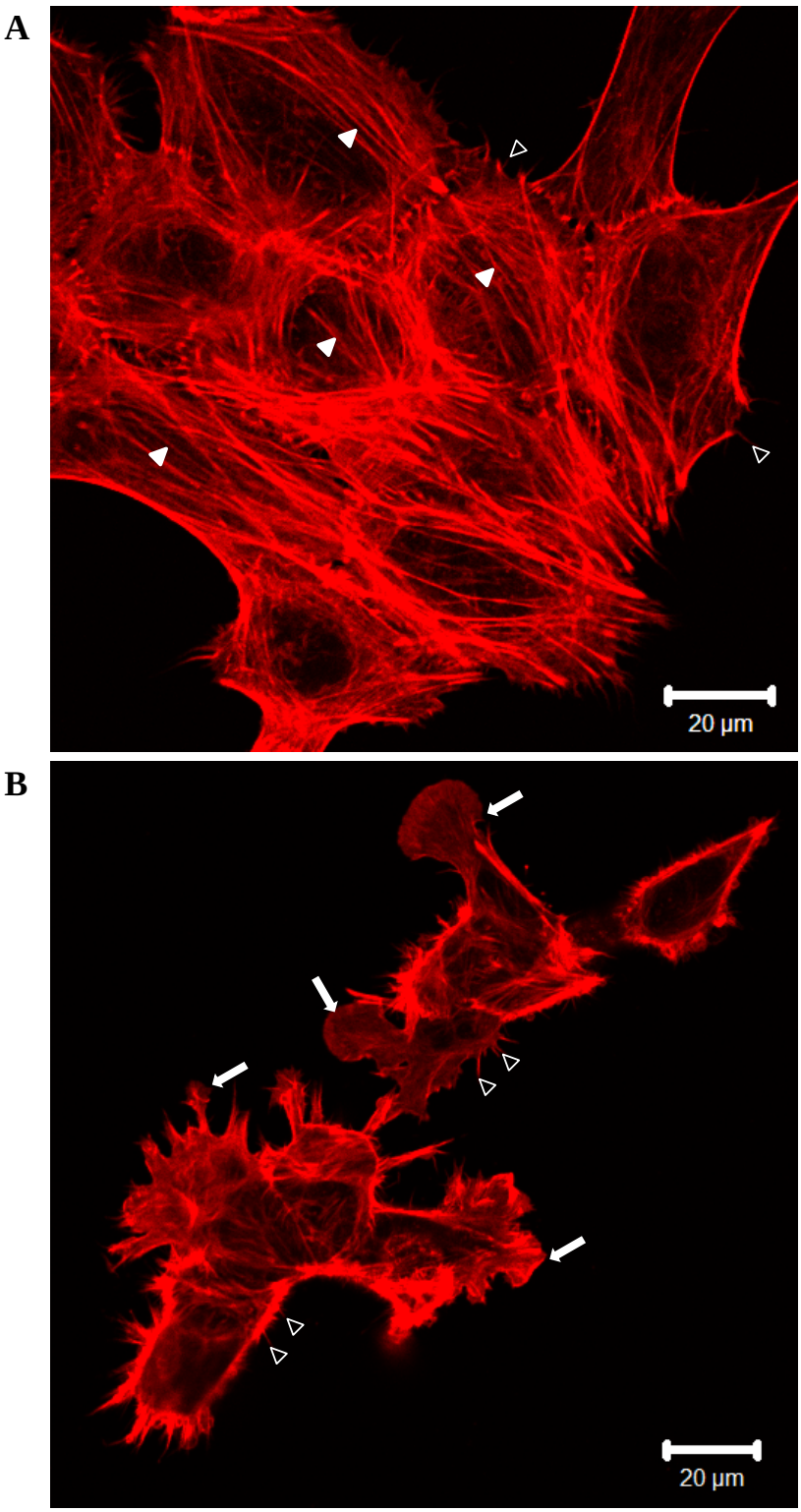

Figure 2.5: Example confocal microscopy images depicting cytoskeletal reorganisation. *Confocal images highlighting* ***A,*** *Stress fibres which are depicted by the closed arrowheads and filopodia depicted by the open arrowheads.* ***B,*** *Lamellipodia are depicted by the arrows.*

2.2.2.2.3. Focal adhesion (FA) protein assay

Cells were plated on poly-D-lysine coated coverslips and placed overnight in serum-free medium in a humidified atmosphere (37^{o}C; 5% CO_2). Cells were transferred into 1 ml of serum-free medium in individual wells of a 24 well plate for 30 min in a humidified atmosphere prior to commencement of experiments. The ligands were then applied for 30 or 60 min; HEK293 and hGPR55-HEK293 or DU145 respectively. In experiments where inhibitors were applied, the cells were treated with the inhibitor for 30 min prior to co-application of the inhibitor and ligand for a further 30 or 60 min; hGPR55-HEK293 and DU145 cells respectively. Cells were fixed in 4% PFA supplemented with 200 mM sucrose for 10 min, then permeabilised with 0.2 % triton X-100 for 10 min. Mouse anti-vinculin diluted in HBS (1:500) was applied for 60 min. The cells were then washed 3 times with HBS. A fluorescently-conjugated secondary antibody, Alexa fluor® 488 donkey-anti mouse, was diluted in HBS (1:500) and then applied for 30 min. After which the cells were washed as above and stored in glucose-free HBS. Cells were then examined using a laser scanning confocal microscope (Zeiss LSM510) as described previously.

FA lengths were measured using LSM 510 Laser-sharp software (Carl Zeiss Microscopy Ltd, Cambridge, UK). A measure tool in the overlay tab was used to record µm lengths; using LSM 510 Laser-sharp software click on the overlay button then click on the ruler icon and then the line icon. Now drag over the FA and record the measurement (figure 2.6). This data was then transferred to GraphPad Prism 4 where either concentration response curves or histograms were compiled. For concentration response curves the mean control (DMSO) value was removed from the lipid-induced FA length.

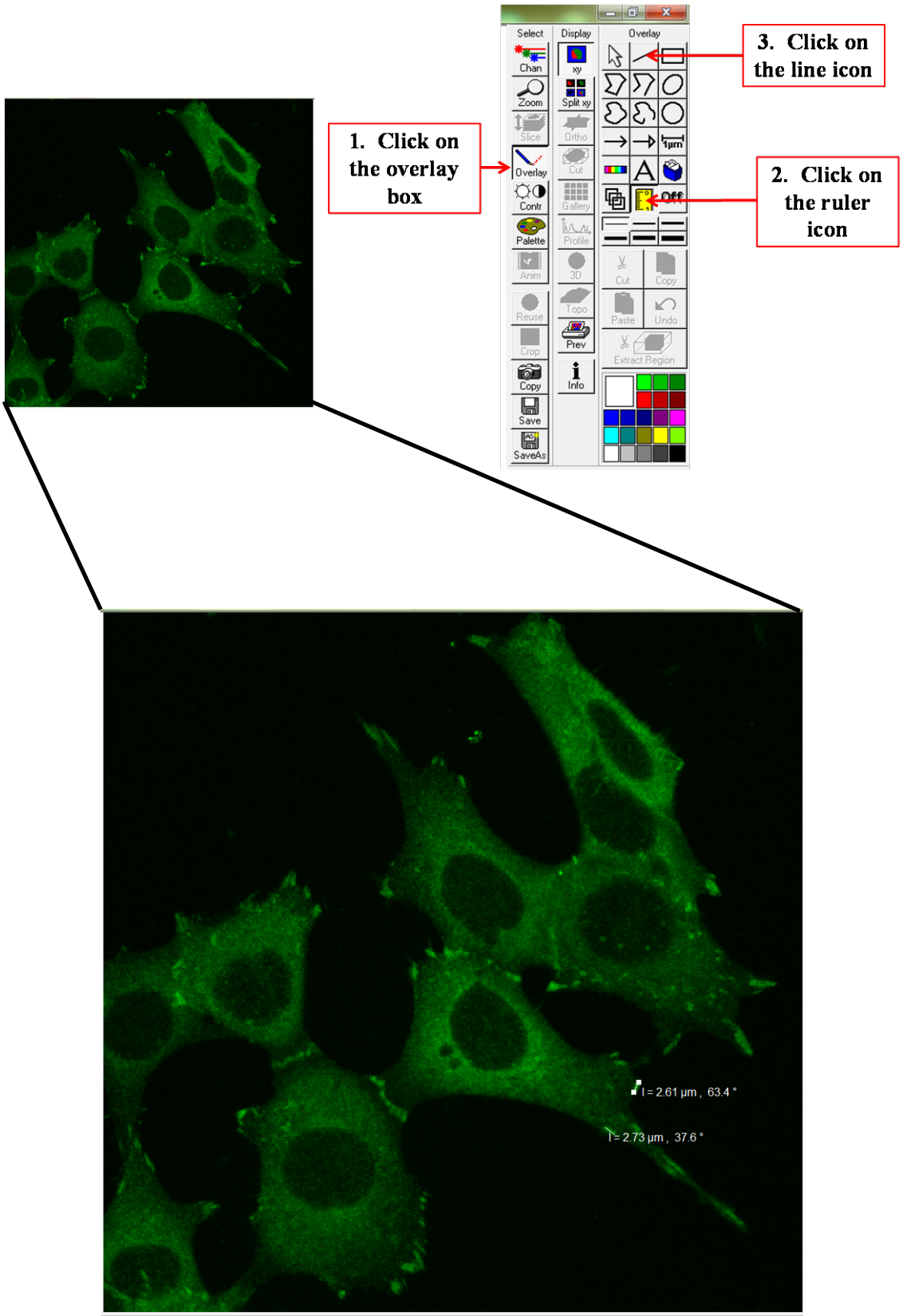

***Figure 2.6:* Analysis of FA length.** *Clicking on the overlay icon on the right of the screen leads to the opening of the window to reveal the ruler and line icons. After clicking all three icons the mouse can be dragged over the FA and the length recorded.*

2.2.2.2.4. HA immunoreactivity

hGPR55-HEK293 cells were fixed with 4% PFA containing 200 mM sucrose at room temperature for 10 min. Cells were then incubated for 60 min with mouse anti-HA (1:1000) in HBS. The cells were then washed 3 times with HBS, after which a conjugated secondary antibody, Alexa fluor® 488 anti-rabbit (1:500) was applied for 30 min. Cells were washed 3 times with HBS. Cells were examined using a laser scanning confocal microscope (Zeiss LSM510) as described previously.

Fluorescence measurements were performed with Image J freeware. The analysis was carried out on the raw data image acquired from using Zeiss LSM 510 Laser-sharp software. For each image, the outline of the cell area was traced using a bright-field image as a guide (similar to pCREB analysis). Three background regions devoid of cells were also analysed. Measurements were derived from fluorescent image where the Corrected Total Cell-area Fluorescence (CTCF) was calculated as follows:

CTCF = Integrated Density - (Area of cell region x mean background reading).

This data was then transferred to GraphPad Prism 4 to allow the compilation of histograms.

2.2.3. Statistical analysis

2.2.3.1. Ca^{2+} studies

Histogram data was analysed with unpaired Student t-tests to compare the two data sets. $P < 0.05$ was considered significant. Data were typically obtained from 10 cells per field obtained from a minimum of two experiments unless otherwise stated.

2.2.3.2. pCREB studies

Statistical analyses were performed using one-way ANOVA followed by a Bonferroni *post hoc* test for multiple comparisons. $P < 0.05$ was considered significant. Data were typically obtained from three experiments unless otherwise stated.

2.2.3.3. FA studies

Statistical analyses were performed using either one-way ANOVA followed by a Bonferroni *post hoc* test for multiple comparisons or a two-way ANOVA followed by a Bonferroni *post hoc* test for multiple comparisons. $P < 0.05$ was considered significant. hGPR55-HEK293 cells: Data was typically obtained from a minimum of at least two

experiments. DU145 cells: Data were typically obtained from a minimum of at least two experiments unless otherwise stated.

2.2.3.4. HA immunoreactivity

Statistical analyses were performed using one-way ANOVA followed by a Bonferroni *post hoc* test for multiple comparisons. $P < 0.05$ was considered significant. Data were typically obtained from a minimum of at least three experiments.

CHAPTER THREE

N-acyl Amino Acids and GPR55-Mediated Ca^{2+} Signalling

3.1. INTRODUCTION

In 2007 the first report of LPI activating GPR55 to promote Ca^{2+} mobilisation in hGPR55-HEK293 cells, an effect that was not observed in control HEK293 cells, was published (Oka *et al.*, 2007). A plethora of papers were to follow confirming that GPR55can elevate intracellular Ca^{2+} levels in a variety of cell types; either recombinant GPR55-overexpressing cells or endogenously expressing cells. These include hGPR55-HEK293 cells (Oka *et al.*, 2007; Lauckner *et al.*, 2008; Henstridge *et al.*, 2009, 2010), human umbilical vein derived endothelial cell (HUVEC) line; EA.hy926 (Waldeck-Weiermair *et al.*, 2008) the neuronal cell line; PC12 cells (Obara *et al.*, 2011), prostate cancer cell line; PC-3 (Piñeiro *et al.*, 2011) and in cardiomyocytes (Yu *et al.*, 2013). Furthermore some cannabinoid ligands; Δ^9THC, JWH015, AM251 and SR141716A are also reported to stimulate GPR55-mediated Ca^{2+} mobilisation (Lauckner *et al.*, 2008; Henstridge *et al.*, 2010).

In HEK293 cells transiently expressing recombinant GPR55, JWH015 and Δ^9THC induced GPR55 mediated Ca^{2+} mobilisation required $G_{\alpha 12}$ and Rho (Lauckner *et al.*, 2008). The requirement for $G_{\alpha 12}$ family of G-proteins and Rho was confirmed in a separate study where signalling via the $G_{\alpha 13}$-Rho-ROCK axis was associated with GPR55-mediated Ca^{2+} mobilisation (Henstridge *et al.*, 2009). However in prostate cancer cells (PC-3) Ca^{2+} mobilisation mediated by GPR55 did not require ROCK signalling (Piñeiro *et al.*, 2011). Furthermore it was also reported that PLC, and Ca^{2+} release form stores was involved in GPR55-mediated Ca^{2+} mobilisation (Lauckner *et al.*, 2008; Henstridge *et al.*, 2009) and there was a requirement for an intact actin cytoskeleton (Lauckner *et al.*, 2008). Additionally the presence of extracellular Ca^{2+} was also found to be necessary to promote the formation of GPR55-mediated oscillatory Ca^{2+} transients in hGPR55-HEK293 cells (Henstridge *et al.*, 2009). A second G-protein; $G_{\alpha q}$ was also reported for GPR55-promoted Ca^{2+} mobilisation in both hGPR55-HEK293 cells and phaeochromocytoma (PC12) cells (Lauckner *et al.*, 2008; Obara *et al.*, 2011). In endothelial cells AEA can promote GPR55-mediated Ca^{2+} mobilisation, but this is a distinct system, requiring the activation of PI3K-Bmx-PLCγ signalling for this effect. Moreover, integrin clustering mediated by CB_1 activation is necessary to release the inhibition of GPR55 Ca^{2+} signalling (Waldeck-Weiermair *et al.*, 2008). It remains to be determined if $G_{\alpha 13}$ or $G_{\alpha q}$ are required for Ca^{2+} mobilisation in endothelial cells. A more recent study revealed that application of LPI to cardiomyocytes promoted increases in intracellular Ca^{2+} which were sensitive to the GPR55 novel antagonist ML-

193. The authors also reported that the localisation of GPR55 in cardiomyocytes influenced the signalling required for Ca^{2+} mobilisation. GPR55 localised at the plasma membrane acted to release Ca^{2+} from stores via IP_3 receptors and this was further augmented by Ca^{2+} induced Ca^{2+} release promoted by the activation of ryanodine receptors. However GPR55 located on cardiomyocyte lysosomal membranes increased intracellular Ca^{2+} by activating acidic-like Ca^{2+} stores via the endo-lysosomal NAADP-sensitive two-pore Ca^{2+}-permeable ion channels followed by subsequent activation of ryanodine receptors (Yu *et al.*, 2013).

In this study a novel set of 'endocannabinoid-like' lipids were tested for their effects on intracellular Ca^{2+} homeostasis and their ability to activate GPR55. Such 'endocannabinoid-like' lipids, including N-acyl amino acids, are of interest as whilst they have an endocannabinoid structure they are unable to activate the classical cannabinoid receptors (CB_1 and CB_2), but have interesting biological actions. Many of these lipids remain orphans at the present time, with no known molecular target. To investigate whether these lipids can activate GPR55, their actions were compared in hGPR55-HEK293 cells and control HEK293 cells. Subsequent experiments utilised pharmacological inhibitors to study the signalling pathways underlying their effects on Ca^{2+} signalling.

3.2. RESULTS

3.2.1. L-α-Lysophophatidylinositol promotes Ca^{2+}mobilisation in hGPR55-HEK293 cells.

Firstly, the endogenous GPR55 ligand LPI was tested to allow for validation of the Ca^{2+} assay (Oka *et al.*, 2007; Henstridge *et al.*, 2009). Several different cell types with either recombinant or native expression of GPR55 have been observed to induce Ca^{2+} mobilisation when challenged with LPI (Lauckner *et al.*, 2008; Waldeck-Weiermair *et al.*, 2008; Henstridge *et al.*, 2009; Obara *et al.*, 2011).

hGPR55-HEK293 cells were loaded with Fura 2-AM (6 μM) for 60 min prior to being placed on a digital epifluorescent imaging system at 30-34^{o}C. Treatment with 100 nM, 300 nM or 1 μM LPI (5 min) led to the generation of oscillatory Ca^{2+} transients (figure 3.1Ai-iii), whereby the frequency and number of Ca^{2+} transients, along with the number of responsive cells, increased with higher LPI concentrations. In hGPR55-HEK293 cells the mean LPI-mediated peak response was concentration-dependent (figure 3.1B)

with an EC_{50} of 183 ± 8 nM (95% confidence limits). Little or no response to LPI (1 µM) was observed in control HEK293 cells (figure 3.1Aiv) in comparison with hGPR55-HEK293 cells (mean, peak LPI response in hGPR55-HEK293 cells = 0.77 ± 0.059 ratio units, HEK293 cells = 0.031 ± 0.022 ratio units, n = 32 cells, P < 0.001, figure 3.2C). These data suggest that LPI induced Ca^{2+} mobilisation is mediated by GPR55.

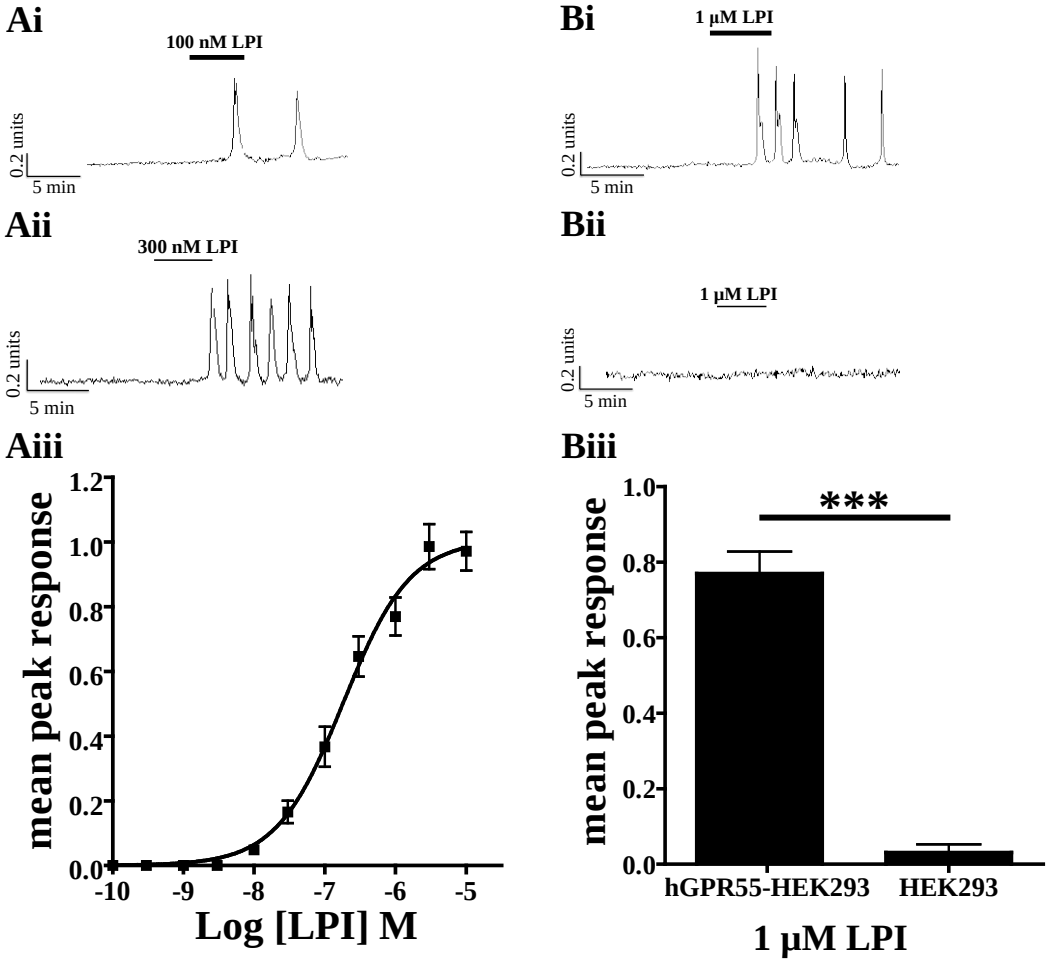

Figure 3.1: Treatment of hGPR55-HEK293 cells with LPI promotes oscillatory Ca^{2+} transients. *Ligands were perfused over the cells at a rate of 2 ml/min for 5 min.* ***Ai****, representative Ca^{2+} trace from an hGPR55-HEK293 cell treated with 100 nM LPI;* ***Aii****, representative Ca^{2+} trace from an hGPR55-HEK293 cell treated with 300 nM LPI; note oscillatory Ca^{2+} transients are formed which are concentration dependent.* ***Aiii****, representative Ca^{2+} trace from an hGPR55-HEK293 cell treated with 1 µM LPI;* ***Aiv****, representative Ca^{2+} trace from a HEK293 cell treated with 1 µM LPI; note that Ca^{2+} transients were not observed.* ***B****, LPI concentration response curve in hGPR55-HEK293 cells. Data are the mean, peak response ± SEM derived from 32 cells, from 3 independent experiments.* ***C****, histogram comparing responses in hGPR55-HEK293 cells and control HEK293 cells. Note the responses*

*are ablated in HEK293 cells. Data are the mean, peak response ± SEM of 32 cells from 3 independent experiments. Student's unpaired two-tailed t-test; ***P < 0.001.*

3.2.2. N-acyl serines induce Ca^{2+} mobilisation in hGPR55-HEK293 cells.

Having validated the Ca^{2+} assay with LPI, the next experiments were to test if three novel N-acyl serine lipids could induce Ca^{2+} mobilisation in hGPR55-HEK293 cells. Three lipids were chosen each with a serine head group but with varying fatty acid chain saturation and length; NASer (C20:4; polyunsaturated), NOSer (C18:1; monounsaturated) and NPSer (C16:0; saturated).

Various concentrations of NASer, up to a maximum concentration of 10 µM, were perfused over hGPR55-HEK293 cells at a rate of 2 ml/min over a 5 min period. NASer (100 nM) when applied to hGPR55-HEK293 cells induced just a single Ca^{2+} transient (figure 3.2Ai). However when NASer (1 µM) challenged hGPR55-HEK293 cells it was observed to increase both the height of the peak response and the number of oscillatory Ca^{2+} transients produced (figure 3.2Aii). The mean, peak Ca^{2+} response was concentration-dependent with an EC_{50} of 256 ± 18 nM (95% confidence limits) (figure 3.3B). To test if these results were GPR55-mediated NASer (3 µM) was first applied to hGPR55-HEK293 cells where robust oscillatory Ca^{2+} transients were produced (figure 3.2Aiii). Next NASer (3 µM) was applied to HEK293 cells where no effect was observed (responses to NASer (3 µM) hGPR55-HEK293 cells = 0.771 ± 0.037 ratio units, HEK293 cells = 0.024 ± 0.024 ratio units, n = 32 cells, P < 0.001, figure 3.2C).

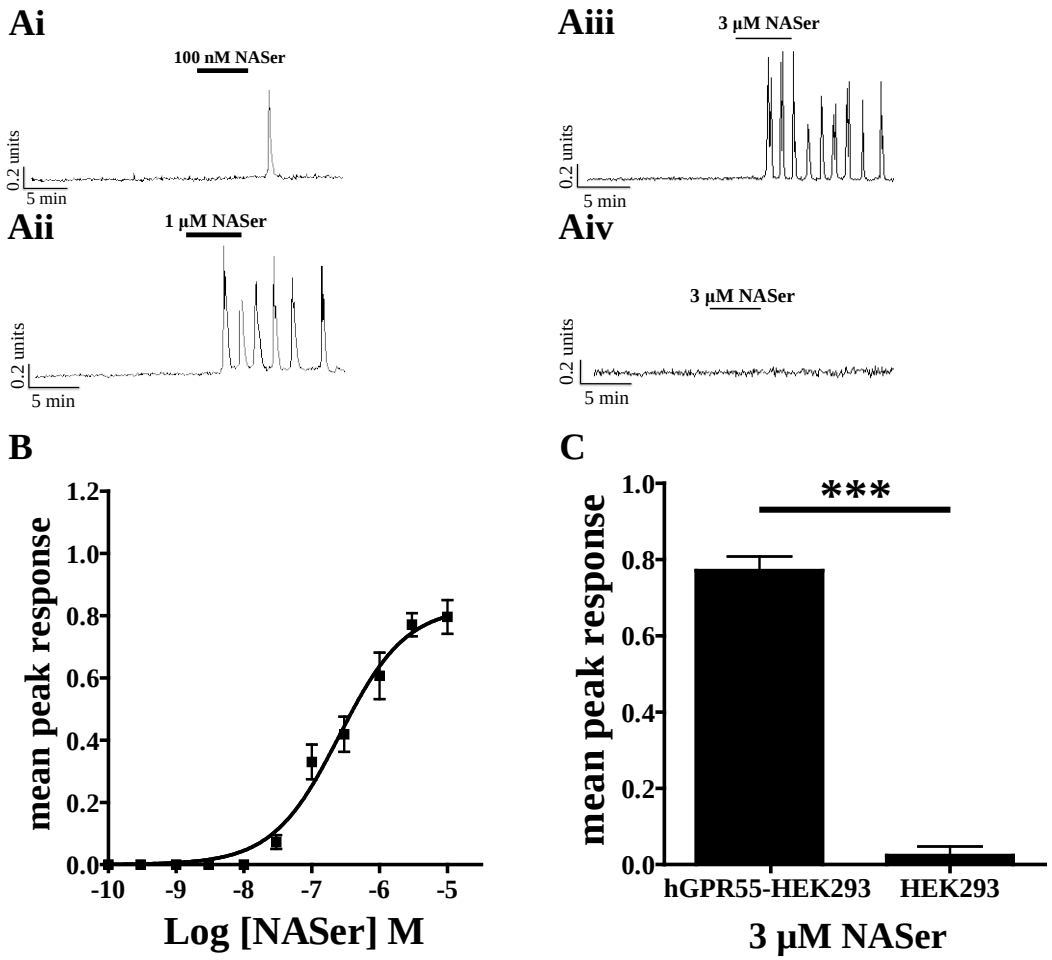

Figure 3.2: NASer-mediated Ca^{2+} responses in hGPR55-HEK293 cells. ***Ai****, representative Ca^{2+} trace from an hGPR55-HEK293 cell treated with 100 nM NASer; note a small delay in response and the formation of a single Ca^{2+} transient when NASer was perfused over the cells at 2 ml/min for 5 min.* ***Aii****, representative Ca^{2+} trace from an hGPR55-HEK293 cell treated with 1 µM NASer; note oscillatory Ca^{2+} transients when NASer was perfused over the cells.* ***Aiii****, representative Ca^{2+} trace from an hGPR55-HEK293 cell treated with 3 µM NASer; note the increased frequency of oscillatory Ca^{2+} transients.* ***Aiv****, representative Ca^{2+} trace from a HEK293 cell treated with 3 µM NASer; note, Ca^{2+} responses were ablated.* ***B****, concentration-response response curve for NASer illustrating the mean, peak Ca^{2+} response in hGPR55-HEK293 cells. Data are the mean, peak response ± SEM derived from 32 cells, from 3 independent experiments.* ***C****, histogram of mean peak Ca^{2+} responses in hGPR55-HEK293 cells and HEK293 cells challenged with 3 µM NASer. Data are the mean peak response ± SEM of 32 cells from 3 independent experiments. Student's unpaired two-tailed t-test; ***P < 0.001.*

Next we investigated the effects of NOSer. Treatment of hGPR55-HEK293 cells with NOSer (100 nM) also induced Ca^{2+} transients that were oscillatory (figure 3.3Ai). Higher NOSer concentrations (1-10 µM) promoted a greater peak response and

increased the frequency of oscillations (figure 3.3Aii and iii). NOSer-induced Ca^{2+} responses were concentration-dependent with an EC_{50} of 253 ± 4 nM (95% confidence limits) (figure 3.3B). HEK293 cells when challenged with NOSer (10 µM) did not produce Ca^{2+} transients but rather a small 'bump-like' increase in the Ca^{2+} ratio (hGPR55-HEK293 cells = 0.767 ± 0.066 ratio units, HEK293 cells = 0.13 ± 0.021 ratio units, n = 32 cells, P < 0.001; figure 3.3C).

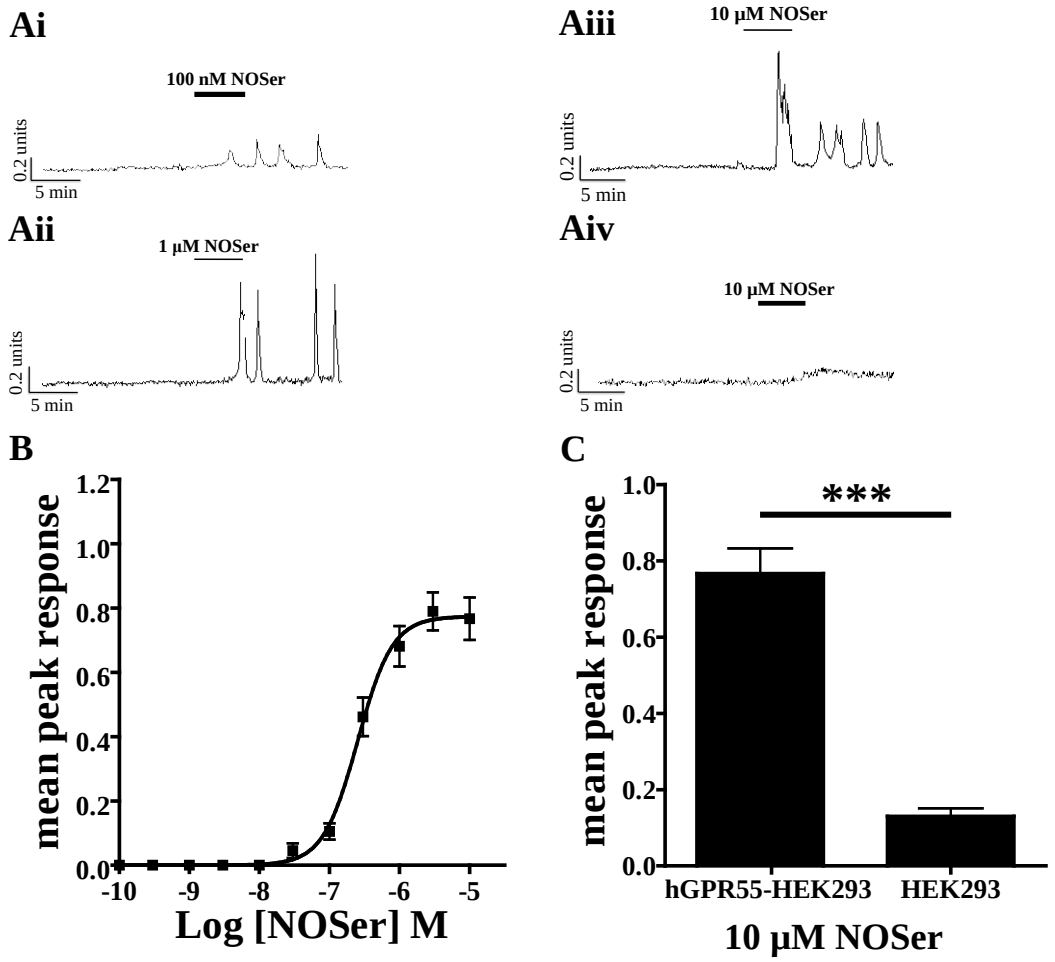

Figure 3.3: NOSer promotes oscillatory Ca^{2+} transients in hGPR55-HEK293 cells. ***Ai****, representative Ca^{2+} trace from an hGPR55-HEK293 cell treated with 100 nM NOSer; note the formation of small oscillatory Ca^{2+} transient when NOSer was perfused over the cells at 2 ml/min for 5 min.* ***Aii****, representative Ca^{2+} trace from an hGPR55-HEK293 cell treated with 1 µM NOSer; note oscillatory Ca^{2+} transients when NOSer was perfused over the cells.* ***Aiii****, representative Ca^{2+} trace from an hGPR55-HEK293 cell treated with 10 µM NOSer.* ***Aiv****, representative Ca^{2+} trace from a HEK293 cell treated with 10 µM NOSer; note, transient Ca^{2+} responses were ablated but a small bump-like response is observed.* ***B****, concentration-response response curve for NOSer illustrating the mean, peak Ca^{2+} response in hGPR55-HEK293 cells. Data are the mean, peak response ± SEM derived from 32 cells, from 3 independent experiments.* ***C****, histogram of mean peak Ca^{2+} responses in hGPR55-HEK293 cells and*

*HEK293 cells challenged with 10 µM NOSer. Data are the mean peak response ± SEM of 32 cells from 3 independent experiments. Student's unpaired two-tailed t-test; ***P < 0.001.*

Next hGPR55-HEK293 cells were challenged with NPSer (100 nM). Ca^{2+} responses to NPSer were single Ca^{2+} transients with a delayed initiation (figure 3.4Ai). Increasing the concentration of NPSer (1-10 µM) led to faster responses, an increase in the peak response and the appearance of Ca^{2+} oscillations (figure 3.4Aii and iii). NPSer-mediated Ca^{2+} responses were concentration-dependent with an EC_{50} of 314 ± 12 nM (95% confidence limits) (figure 3.5B). To determine whether these responses were likely to be mediated by GPR55 responses to a high concentration of NPSer (10 µM) were compared between hGPR55-HEK293 cells and control, HEK293 cells (figure 3.4Aiii and iv). Responses in the latter cells were not observed (hGPR55-HEK293 cells = 0.647 ± 0.045 ratio units, HEK293 cells = 0.036 ± 0.023 ratio units, n = 32 cells, P < 0.001, figure 3.4C).

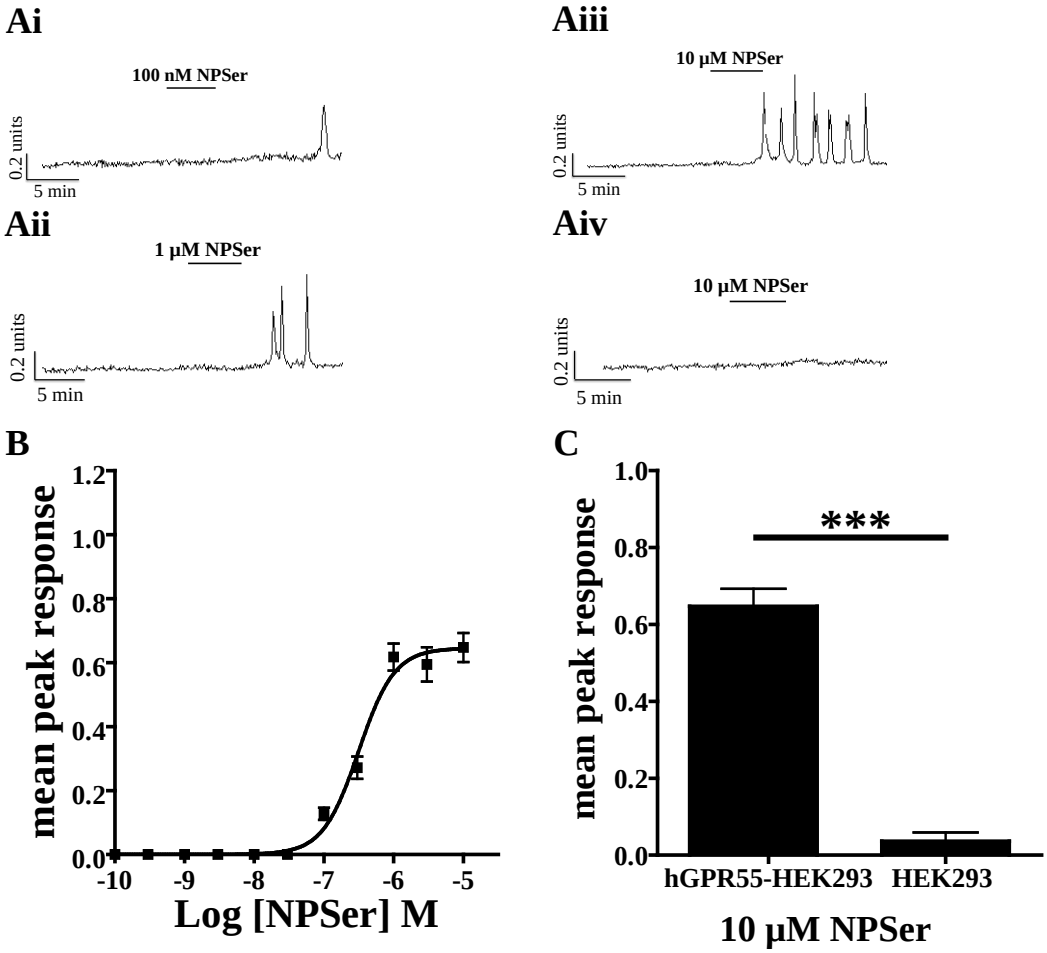

***Figure 3.4: Oscillatory Ca^{2+} transients are promoted when NPSer is applied to hGPR55-HEK293 cells. Ai**, representative Ca^{2+} trace from an hGPR55-HEK293 cell treated with 100*

nM NPSer; note a delay in response and the formation of a single Ca^{2+} transient when NPSer was perfused over the cells at 2 ml/min for 5 min. ***Aii****, representative Ca^{2+} trace from an hGPR55-HEK293 cell treated with 1 µM NPSer; note faster initiation of Ca^{2+} transients when NPSer was perfused over the cells.* ***Aiii****, representative Ca^{2+} trace from an hGPR55-HEK293 cell treated with 10 µM NPSer; note the increased frequency of oscillatory Ca^{2+} transients.* ***Aiv****, representative Ca^{2+} trace from a HEK293 cell treated with 10 µM NPSer; note, transient Ca^{2+} responses were ablated.* ***B****, concentration-response response curve for NPSer illustrating the mean peak Ca^{2+} response in hGPR55-HEK293 cells. Data are the mean, peak response ± SEM derived from 32 cells, from 3 independent experiments.* ***C****, histogram of mean peak Ca^{2+} responses in hGPR55-HEK293 cells and HEK293 cells challenged with 10 µM NPSer. Data are the mean peak response ± SEM of 32 cells from 3 independent experiments. Student's unpaired two-tailed t-test; ***P < 0.001.*

3.2.3. N-acyl glycines induce a more modest Ca^{2+} response in hGPR55-HEK293 cells.

These experiments were to investigate if a different amino acid head group influenced N-acyl amino acid -mediated Ca^{2+} mobilisation in hGPR55-HEK293 cells. Three novel N-acyl glycines with either an arachidonic, oleic or palmitic fatty acid chain were studied.

Treatment of hGPR55-HEK293 cells with NAGly (300 nM) promoted a single, delayed Ca^{2+} transient (figure 3.5Ai). Higher concentrations of NAGly (3-10µM) promoted a faster onset Ca^{2+} response that was also oscillatory (figure 3.5Aii and iii). Ca^{2+} responses were concentration-dependent with an EC_{50} of 908 ± 63 nM (figure 3.5B). No response to NAGly (10 µM) was observed in control HEK293 cells (response to 10 µM NAGly in hGPR55-HEK293 cells = 0.551 ± 0.059 ratio units, HEK293 cells = 0.003 ± 0.003 ratio units, n = 32 cells, P < 0.001, figure 3.5Aiv and C).

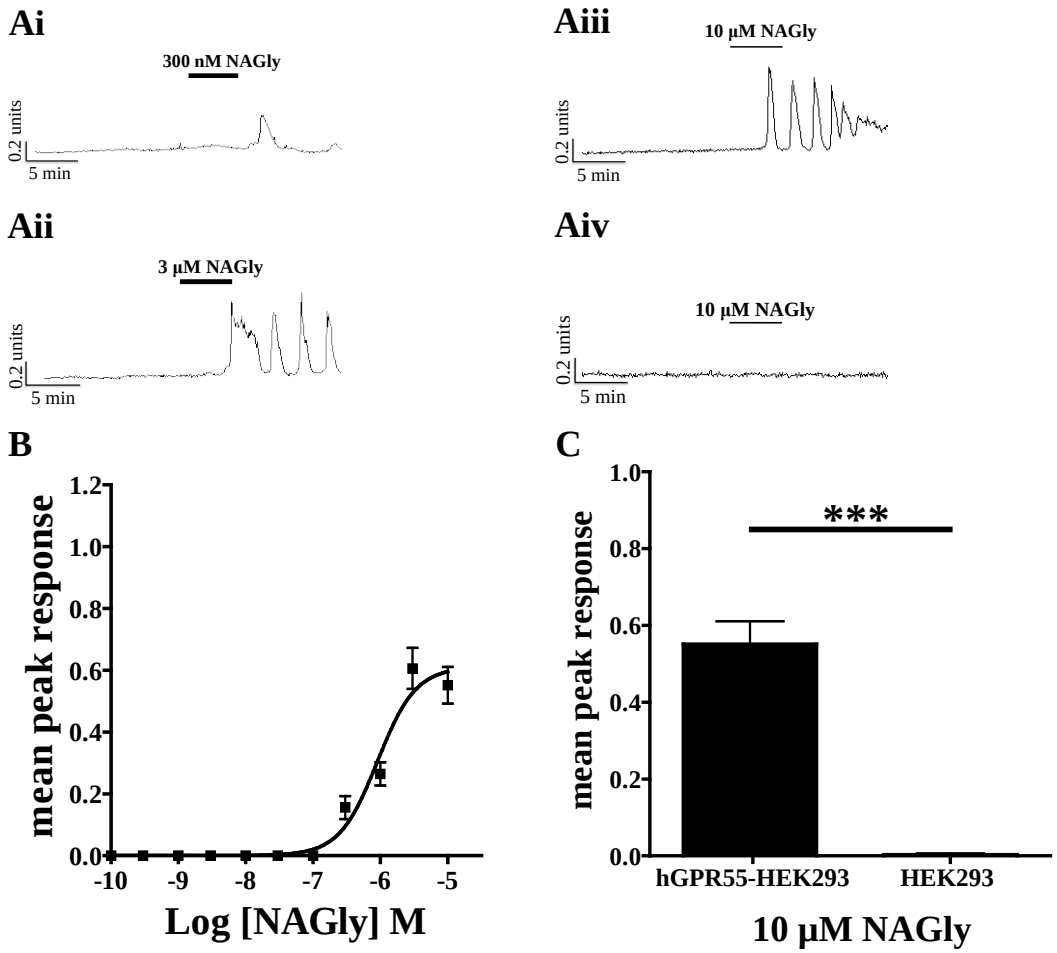

Figure 3.5: NAGly induces oscillatory Ca^{2+} transients in hGPR55-HEK293 cells. *NAGly was perfused over hGPR55-HEK293 cells are a rate of 2 ml/min.* ***Ai****, representative Ca^{2+} trace from an hGPR55-HEK293 cell treated with 300 nM NAGly; note a small delay in response and the formation of a single Ca^{2+} transient.* ***Aii****, representative Ca^{2+} trace from an hGPR55-HEK293 cell treated with 3 µM NAGly; note oscillatory Ca^{2+} transients when NAGly was perfused over the cells.* ***Aiii****, representative Ca^{2+} trace from an hGPR55-HEK293 cell treated with 10 µM NAGly; note the increased frequency of oscillatory Ca^{2+} transients which is concentration dependent.* ***Aiv****, representative Ca^{2+} trace from a HEK293 cell treated with 10 µM NAGly; note, Ca^{2+} responses were ablated.* ***B****, concentration-response response curve for NAGly illustrating the mean, peak Ca^{2+} response in hGPR55-HEK293 cells. Data are the mean, peak response ± SEM derived from 32 cells, from 3 independent experiments.* ***C****, histogram of mean, peak Ca^{2+} responses in hGPR55-HEK293 cells and HEK293 cells challenged with 10 µM NAGly. Data are the mean, peak response ± SEM of 32 cells from 3 independent experiments. Student's unpaired two-tailed t-test; ***P < 0.001.*

Exposure of hGPR55-HEK293 to NOGly (300 nM) produced modest, delayed Ca^{2+} transients (figure 3.6Ai). Increasing NOGly concentrations (1-3µM) promoted larger,

more oscillatory Ca^{2+} transients (EC_{50} of 347 ± 12 nM (95% confidence limits); figure 3.6Aii, iii and B), although the effects were smaller than those seen with the other lipids at equivalent concentrations. NOGly (3 µM) applied to HEK293 generated a very small Ca^{2+} elevation (response to NOGly (3 µM) in hGPR55-HEK293 cells = 0.372 ± 0.051 ratio units, HEK293 cells = 0.072 ± 0.028 ratio units, n = 32 cells, P < 0.001; figure 3.6Aiv and C). The small 'bump-like' response profile in HEK293 cells was similar to that seen with NOSer suggesting that the oleic acid tail may interact with an unknown target in HEK293 cells.

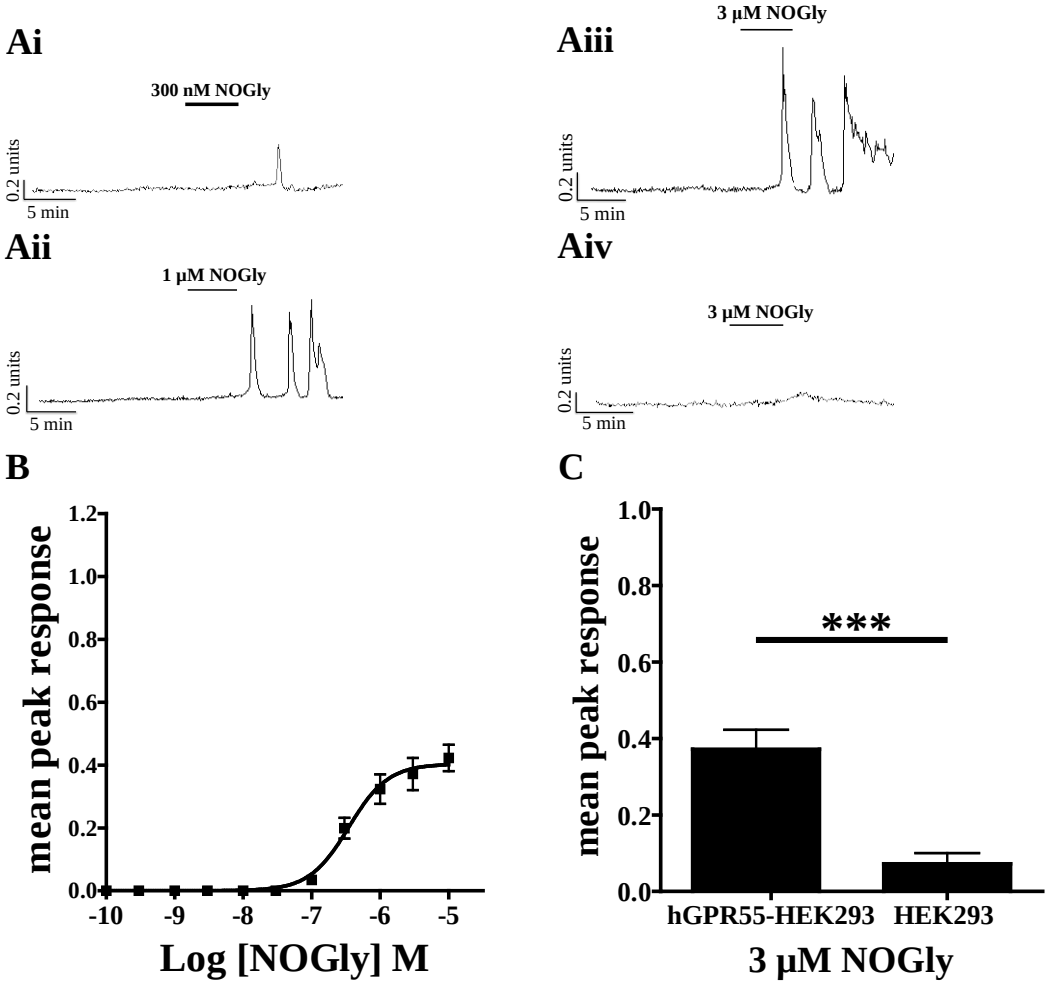

Figure 3.6: Oscillatory Ca^{2+} transients are promoted when NOGly is applied to hGPR55-HEK293 cells. *NOGly was perfused over hGPR55-HEK293 cells are a rate of 2 ml/min.* ***Ai****, representative Ca^{2+} trace from an hGPR55-HEK293 cell treated with 300 nM NOGly; note a small delay in response and the formation of a single Ca^{2+} transient.* ***Aii****, representative Ca^{2+} trace from an hGPR55-HEK293 cell treated with 1 µM NOGly; note oscillatory Ca^{2+} transients when NOG was perfused over the cells.* ***Aiii****, representative Ca^{2+} trace from an hGPR55-HEK293 cell treated with 3 µM NOGly; note the increased peak response of the oscillatory Ca^{2+} transients which is concentration dependent.* ***Aiv****, representative Ca^{2+} trace from a*

HEK293 cell treated with 3 µM NOGly; note, Ca^{2+} responses were ablated but a small bump-like response is observed. ***B****, concentration-response response curve for NOGly illustrating the mean, peak Ca^{2+} response in hGPR55-HEK293 cells. Data are the mean, peak response ± SEM derived from 32 cells, from 3 independent experiments.* ***C****, histogram of mean, peak Ca^{2+} responses in hGPR55-HEK293 cells and HEK293 cells challenged with 3 µM NOGly. Data are the mean, peak response ± SEM of 32 cells from 3 independent experiments. Student's unpaired two-tailed t-test; ***P < 0.001.*

Finally hGPR55-HEK293 cells challenged with NPGly (300 nM) displayed very little effect with the majority of cells producing no response (figure 3.7Ai). Higher concentrations of NPGly (3-10 µM) generated small Ca^{2+} transients in cells (figure 3.7Aii-iii) with a lower maximal response in relation to the other lipids (figure 3.7B). NPGly (10 µM) did not induce Ca^{2+} responses in control HEK293 cells (response to NPGly (10 µM) in hGPR55-HEK293 cells = 0.064 ± 0.027 ratio units, HEK293 cells = 0.004 ± 0.004 ratio units, n = 32 cells, $P < 0.05$, figure 3.7Aiv and C). These data suggest that whilst the NPGly induced Ca^{2+} responses in hGPR55-HEK293 cells were small they may be GPR55-mediated.

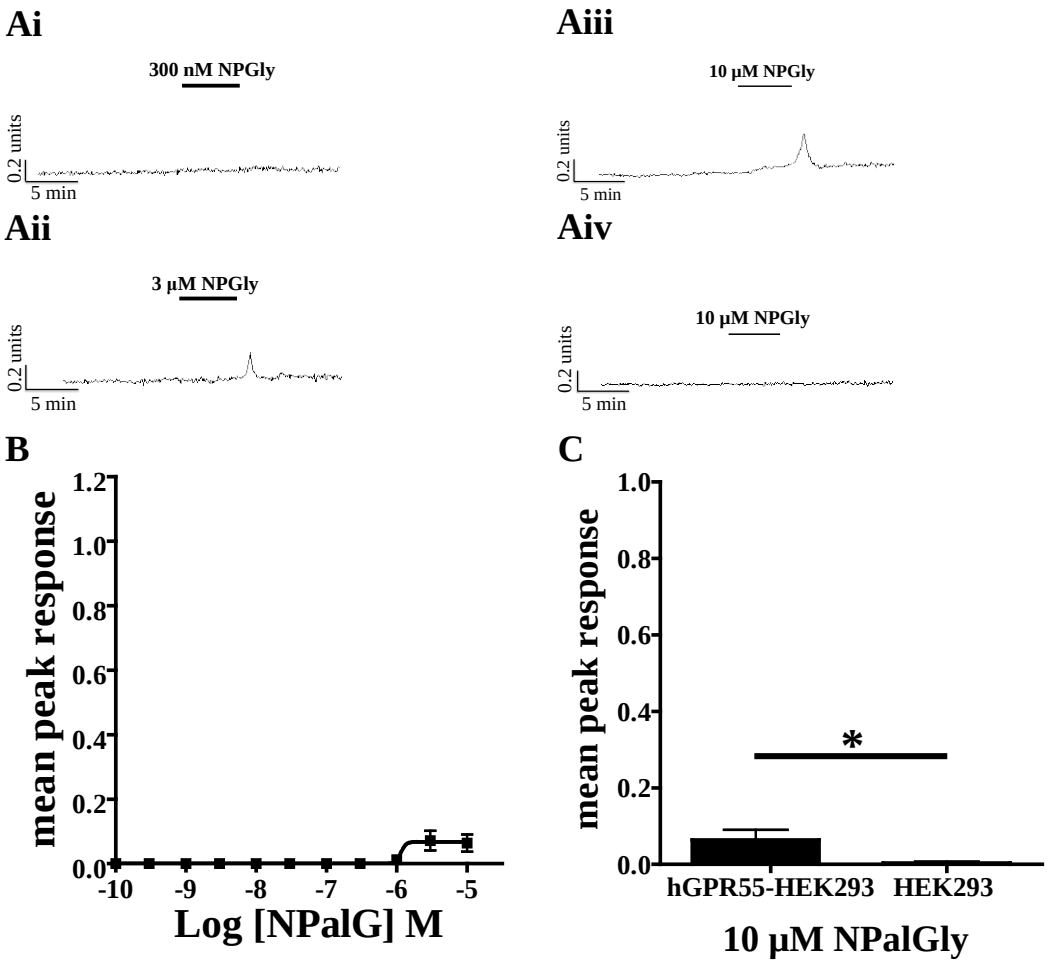

Figure 3.7: Ca^{2+} transients are promoted when NPGly is applied to hGPR55-HEK293 cells. ***Ai****, representative Ca^{2+} trace from an hGPR55-HEK293 cell treated with 300 nM NPGly, showing no response.* ***Aii****, representative Ca^{2+} trace from an hGPR55-HEK293 cell treated with 3 µM NPGly; note a slightly delayed and small Ca^{2+} transient when NPGly was perfused over the cells.* ***Aiii****, representative Ca^{2+} trace from an hGPR55-HEK293 cell treated with 10 µM NPGly; note a similarly delayed and small Ca^{2+} transient when NPGly was perfused over the cells.* ***Aiv****, representative Ca^{2+} trace from a HEK293 cell treated with 10 µM NPGly; note, transient Ca^{2+} responses were ablated.* ***B****, concentration-response response curve for NPGly illustrating the mean, peak Ca^{2+} response in hGPR55-HEK293 cells. Data are the mean, peak response ± SEM derived from 32 cells, from 3 independent experiments.* ***C****, histogram of mean peak Ca^{2+} responses in hGPR55-HEK293 cells and HEK293 cells challenged with 10 µM NPGly. Data are the mean, peak response ± SEM of 32 cells from 3 independent experiments. Student's unpaired two-tailed t-test; *P < 0.05.*

LPI remains the most potent and efficacious lipid when compared to the N-acyl amino acids. NASer and NOSer produced a similar E_{max} which was ~20 % lower than that seen with LPI (figure 3.8A). NASer and NOSer had similar EC_{50} values and were the most potent of all the N-acyl amino acids studied (table 3.1). NPSer had the lowest potency and efficacy of the three N-acyl serines. Presence of a glycine head group resulted in a reduced efficacy when compared to either LPI or the N-acyl serines. The lower E_{max} produced by NAGly and NOGly suggests they may be partial agonists of GPR55 (figure 3.8B). NAGly was found to be the least potent of the N-acyl amino acids studied (table 3.1). NOGly whilst having a similar potency was found to be less efficacious than NPSer. NOGly was ~50% less efficacious than either NASer or NOSer. NPGly promoted a small increase in $[Ca^{2+}]_i$ at 3 and 10 μM concentrations but lower concentrations were found to have no effect in hGPR55-HEK293 cells. Overall these data suggest that the presence of the serine head group increases the potency and efficacy of the mean Ca^{2+} peak responses in hGPR55-HEK293 cells when compared to lipids with a glycine head group. The lower efficacy of the N-acyl glycines suggests that these lipids act as partial agonists at GPR55 in the Ca^{2+} assay.

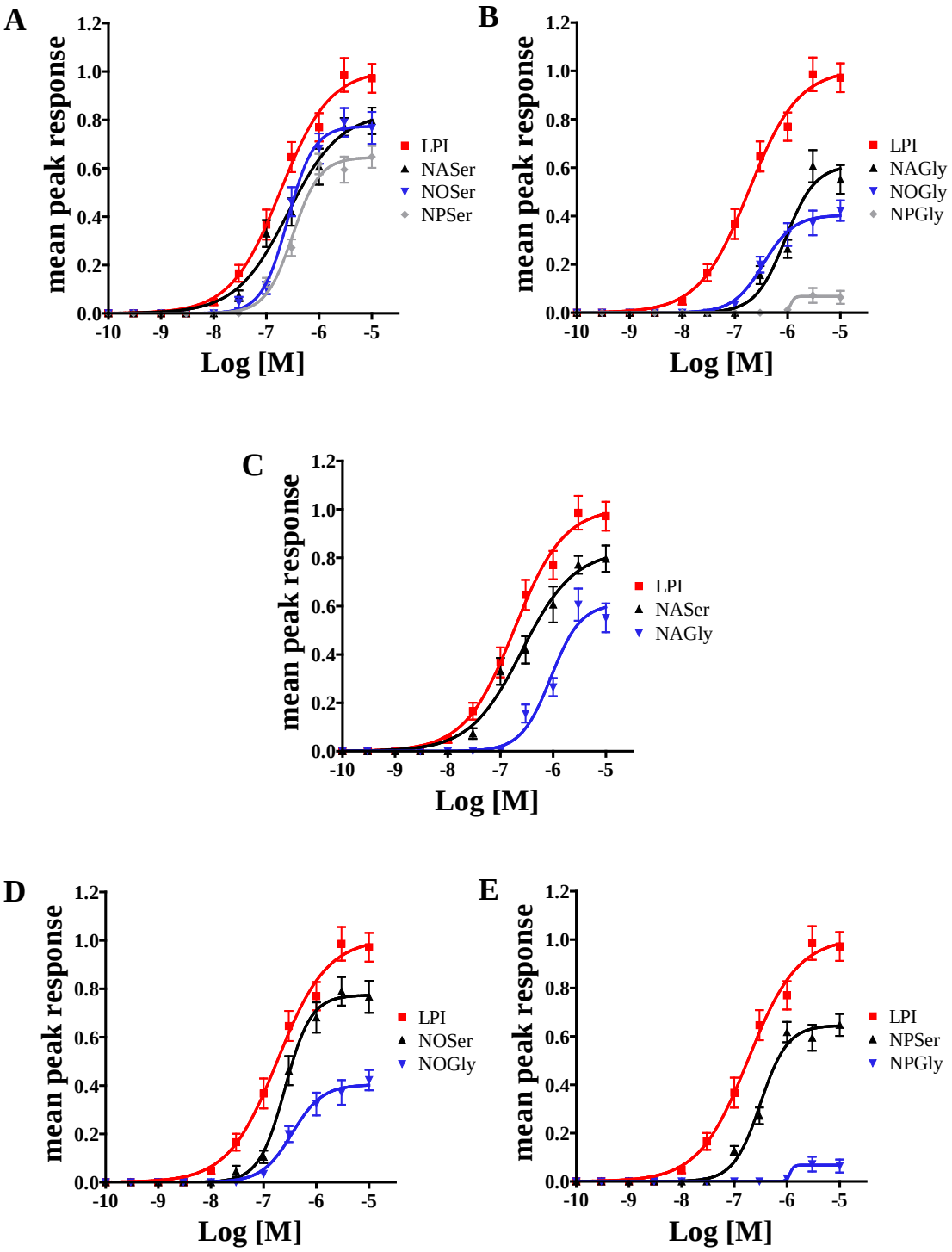

Figure 3.8: Pooled concentration-response data for Ca^{2+} responses to lipids in hGPR55-HEK293 cells*. LPI is depicted in red on all graphs.* ***A****, comparison of the lipids that contain a serine head group.* ***B****,* ***c****omparison of lipids that contain a glycine head group.* ***C****, N-acyl amino acids with an arachidonic (C20:4) fatty acid chain.* ***D****, N-acyl amino acids that contain an oleic (C18:1) fatty acid chain.* ***E****, N-acyl amino acids that have a palmitic (C16:0) fatty acid chain. Data are the mean, peak response ± SEM of 32 cells from 3 independent experiments.*

Ligand	EC_{50} (nM)
LPI	183 ± 8
NASer	256 ± 18
NOSer	253 ± 4
NPSer	314 ± 12
NAGly	908 ± 63
NOGly	347 ± 12
NPGly	nd

Table 3.1: Relative potencies of the N-acyl amino acids compared to LPI. *Results derived from three independent experiments. nd = not determined. EC_{50} values (95% confidence limits).*

3.2.4. Ca^{2+} signalling in hGPR55-HEK293 cells.

As NOSer was the most potent and efficacious of the N-acyl amino acids it was used to elucidate the cell signalling events that underlie the oscillatory Ca^{2+} responses in hGPR55-HEK293 cells. In particular we studied the origin of the NOSer-mediated Ca^{2+} response in hGPR55-HEK293 cells. BAPTA-AM is a membrane permeable Ca^{2+} chelator which is preferentially selective for Ca^{2+} over other divalent cations. In control experiments, NOSer induced oscillatory Ca^{2+} transients in hGPR55-HEK293 (figure 3.9Ai). However, when BAPTA-AM (50 µM) was applied for 20 min prior to co-application with NOSer for a further 5 min, responses were inhibited by 87.1 ± 4.83% (control NOSer = 0.547 ± 0.043 ratio units, BAPTA-AM + NOSer = 0.073 ± 0.009 ratio units, n = 30 cells, $P < 0.001$, figure 3.9B and C). These results suggest that free cytosolic Ca^{2+} is required for NOSer-induced Ca^{2+} responses in hGPR55-HEK293 cells.

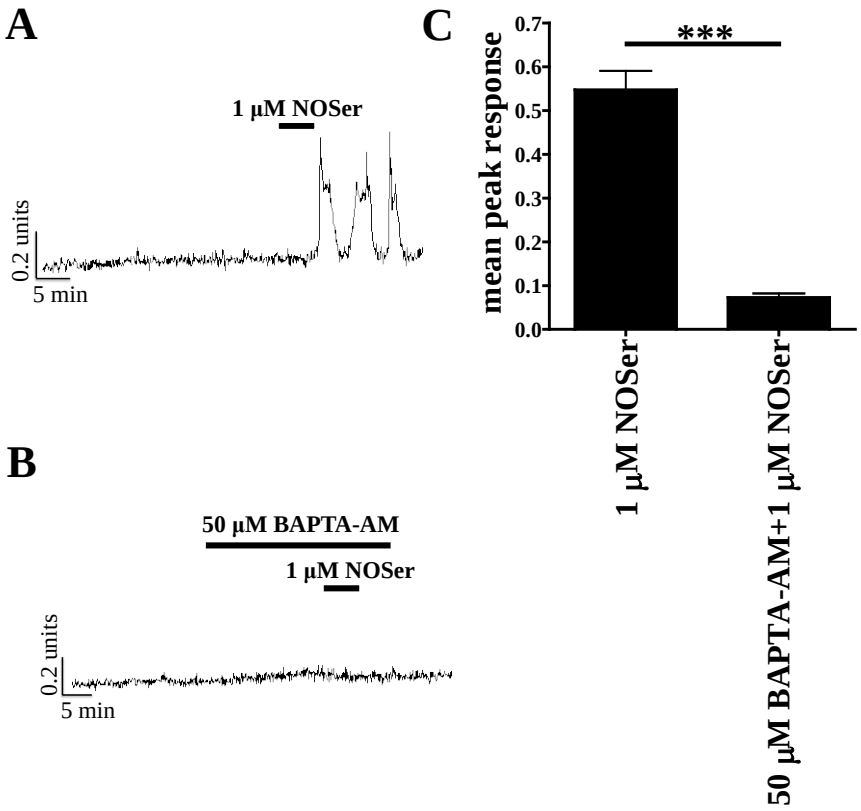

Figure 3.9: Chelation of Ca^{2+} reduces the mobilisation of Ca^{2+} in hGPR55-HEK293 cells. *The membrane permeant Ca^{2+} chelator, BAPTA-AM was applied for 20 min prior to the co-application of NOSer.* ***A****, representative Ca^{2+} trace from an hGPR55-HEK293 cell challenged with 1 µM NOSer.* ***B****, representative Ca^{2+} trace from an hGPR55-HEK293 cell treated with 50 µM BAPTA (20 min) prior to co-application with 1 µM NOSer (5 min); note the loss of Ca^{2+} transients.* ***C****, histogram of pooled mean Ca^{2+} responses of hGPR55-HEK293 cells treated either with NOSer alone or in the presence of BAPTA-AM. Data are the mean, peak response ± SEM; n = 30 cells derived from two independent experiments. Student's unpaired two-tailed t-test; ***P < 0.001.*

GPCR-mediated Ca^{2+} signalling often requires a release of Ca^{2+} from intracellular stores associated with Ca^{2+} influx through channels located in the plasma membrane (SOCE). Re-uptake of Ca^{2+} into stores is via the ATP driven SERCA pump (Clapham, 2007). The plant alkaloid thapsigargin can inhibit irreversibly the SERCA pump (Thastrup *et al.*, 1990; Lytton *et al.*, 1991), which leads to the depletion of Ca^{2+} from the ER. This is associated with the influx of Ca^{2+} across the cell membrane by ATP driven PMCA or Na^{+}/Ca^{2+} exchanger (Bootman *et al.*, 2001). Therefore the effects of thapsigargin (2 µM) on NOSer responses in hGPR55-HEK293 cells were investigated. In control cells, NOSer (1 µM) promoted Ca^{2+} transients in hGPR55-HEK293 cells (figure 3.10Ai).

Treatment with thapsigargin induced an elevation in $[Ca^{2+}]_i$ followed by a slow decrease which did not return to baseline levels even after thapsigargin was washed out. Subsequent addition of NOSer after a 20 min wash did not induce any Ca^{2+} response in hGPR55-HEK293 cells (figure 3.10Aii).

Oscillatory activity requires a release of Ca^{2+} from an intracellular Ca^{2+} store and SOCE to promote influx of Ca^{2+} across the plasma membrane which is sequestered back into the store whereby it can be released in the next wave of Ca^{2+} release (Uhlén and Fritz, 2010). Responses to NOSer in the absence of extracellular Ca^{2+} exhibited a single Ca^{2+} transient with no oscillatory activity. Subsequent addition of HBS supplemented with Ca^{2+} (1.8 mM) promoted the reinstatement of Ca^{2+} oscillations suggesting that Ca^{2+} influx through SOC channels located in the plasma membrane is required for this activity (figure 3.10B) . These data suggest that Ca^{2+} responses to NOSer in hGPR55-HEK293 cells involve Ca^{2+} release from the ER and influx of extracellular Ca^{2+}.

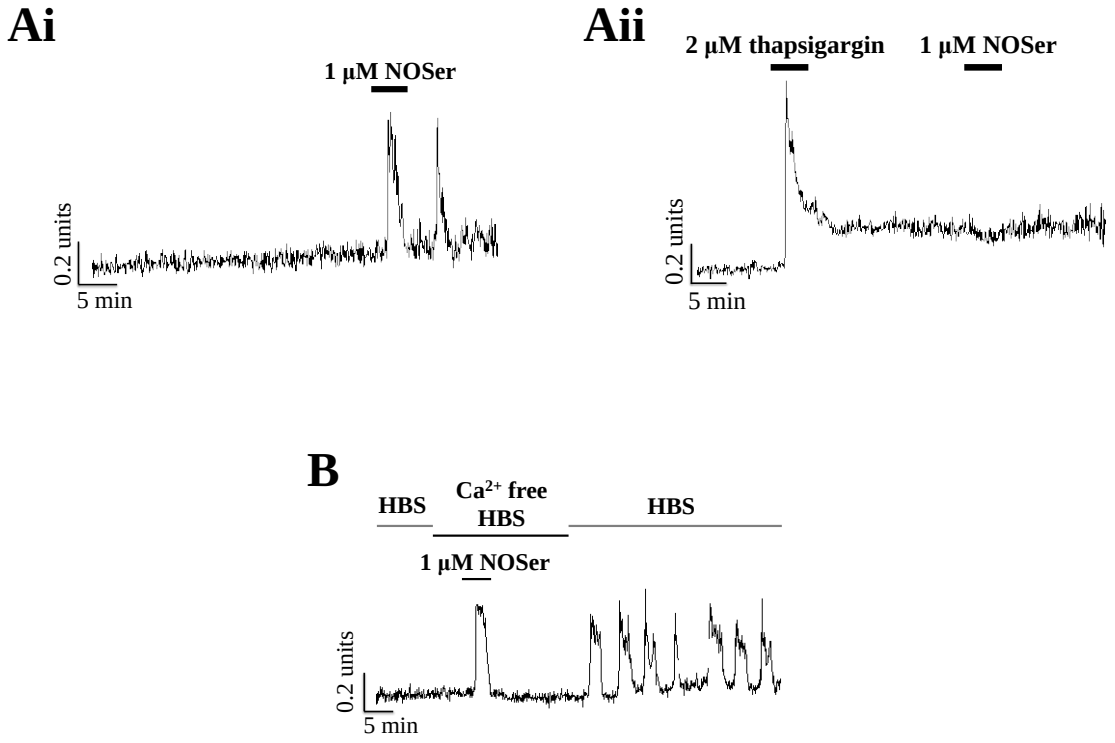

Figure 3.10: Role of Ca^{2+} stores and extracellular Ca^{2+} in NOSer-mediated responses. *The source of Ca^{2+} mobilisation in hGPR55-HEK293 cells was investigated. Thapsigargin was applied to deplete Ca^{2+} from stores.* ***Ai****, representative Ca^{2+} trace from an hGPR55-HEK293 cell challenged with 1 µM NOSer; note Ca^{2+} transients were produced.* ***Aii****, representative Ca^{2+} trace from an hGPR55-HEK293 cell treated with 2 µM thapsigargin and 1 µM NOSer; note the formation of a single Ca^{2+} transient suggesting Ca^{2+} release from the ER. Ca^{2+}*

remained elevated and subsequent application of NOSer did not induce Ca^{2+} transients. ***B****, representative Ca^{2+} trace from an hGPR55-HEK293 cell perfused with Ca^{2+} free HBS supplemented with 100 µM EDTA for 5 min prior to addition of 1 µM NOSer; a single Ca^{2+} transient was formed. Readdition of HBS containing 1.8 mM Ca^{2+} promoted oscillatory Ca^{2+} transients.*

Having ascertained that Ca^{2+} release from the ER was important for the intracellular Ca^{2+} response the upstream mediators ROCK and PLC were studied. Previous work by Henstridge and colleagues suggest that both ROCK and PLC activation are necessary for the mobilisation of intracellular Ca^{2+} in hGPR55-HEK293 cells challenged with LPI (Henstridge *et al.*, 2009). ROCK has two isoforms; therefore both isoforms were studied in their ability to mobilise Ca^{2+} in hGPR55-HEK293 cells when challenged with NOSer (1 µM). ROCK I and II are targeted by the use of Y-27632 dihydrochloride (Ishizaki *et al.*, 2000; Tamura *et al.*, 2005) and ROCK II by the use of H1152 dihydrochloride (Tamura *et al.*, 2005). Pre-treatment of hGPR55-HEK293 cells with the ROCK I and ROCK II inhibitor, Y-27632 (10 µM; 20 min) prior to co-application with NOSer (1 µM; 5 min) reduced the peak Ca^{2+} response by 53.9 ± 19.2% relative to that observed with NOSer alone (NOSer = 0.458 ± 0.061 ratio units, Y-27632 + NOSer = 0.245 ± 0.05 ratio units, n = 30 cells, $P < 0.01$, figure 3.11Ai-iii). The role of the ROCK II isoform was tested by utilising the selective ROCK II inhibitor, H1152. H1152 (1 µM; 20 min) was applied to hGPR55-HEK293 cells prior to the co-application of NOSer (1 µM; 5 min), subsequent responses were reduced in amplitude by 29.3 ± 9.5% relative to control (NOSer = 0.763 ± 0.063 ratio units, H1152 + NOSer = 0.543 ± 0.064 ratio units, n = 30 cells, $P < 0.05$, figure 3.11Bi-iii). These results highlight that ROCK signalling is important in hGPR55-HEK 293 cells treated with NOSer. The inhibition of Ca^{2+} peak response appears more pronounced with cells treated with Y-27632 compared to H1152. This may be due to Y-27632 blocking the two isoforms of ROCK whereas H1152 blocks the ROCK II isoform only.

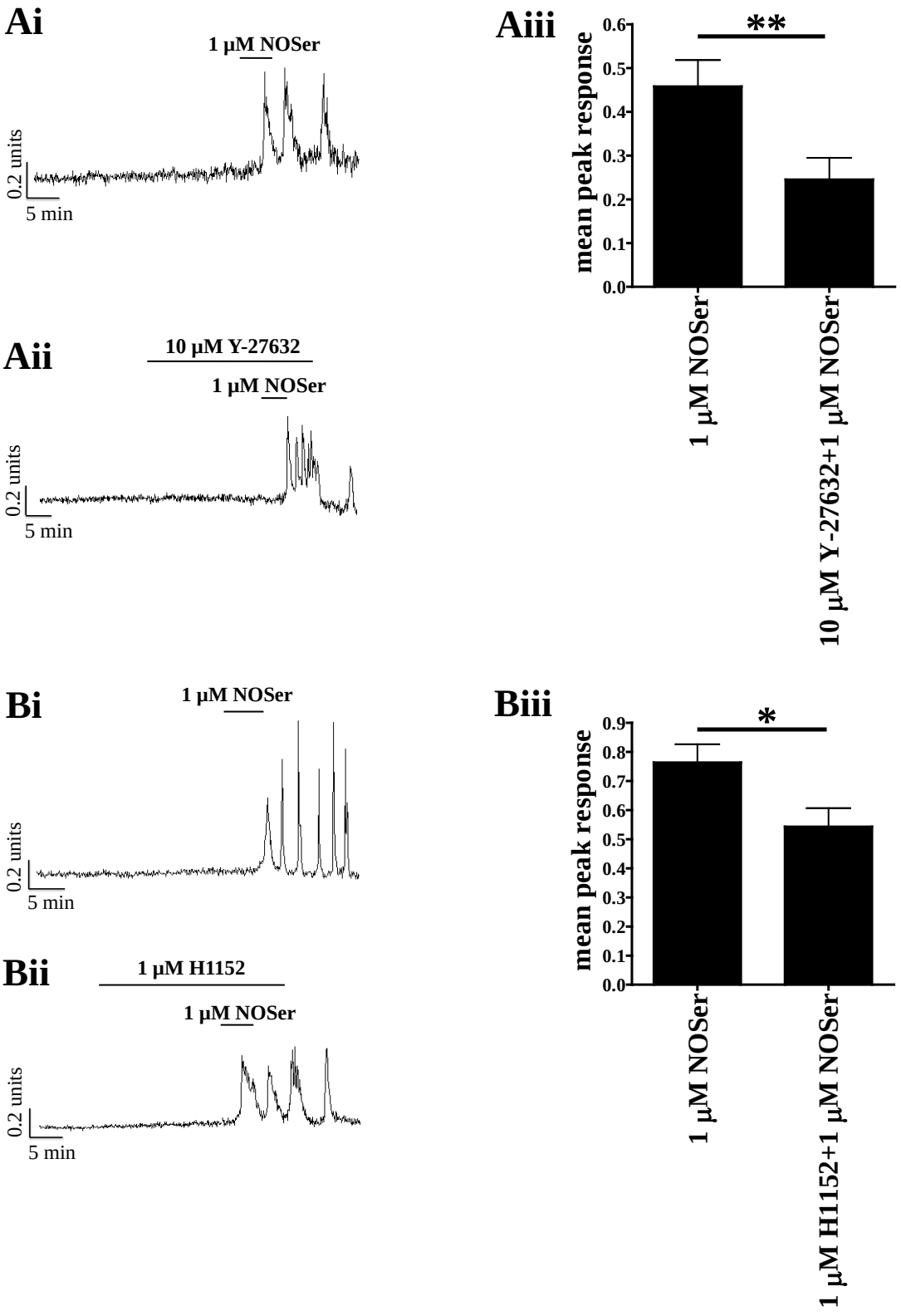

Figure 3.11: ROCK signalling is required for NOSer-induced Ca^{2+} mobilisation in hGPR55-HEK293 cells. *Two different ROCK inhibitors were applied to hGPR55-HEK293 cells for 20 min prior to co-application of the inhibitor with 1 µM NOSer.* ***Ai****, representative Ca^{2+} trace from an hGPR55-HEK293 cell challenged with 1 µM NOSer.* ***Aii****, representative Ca^{2+} trace from an hGPR55-HEK293 cell treated with 10 µM Y-27632; ROCK I and II inhibitor (20 min)*

prior to co-application with 1 µM NOSer (5 min); note the peak response is lowered in the presence of the Y-27632. ***Aiii****, histogram of mean, peak* Ca^{2+} *responses in hGPR55-HEK293 cells treated with either NOSer alone or co-applied with Y-27632.* ***Bi****, representative* Ca^{2+} *trace from an hGPR55-HEK293 cell challenged with 1 µM NOSer.* ***Bii****, representative* Ca^{2+} *trace from an hGPR55-HEK293 cell treated with 1 µM H1152; ROCK II inhibitor (20 min) prior to co-application with 1 µM NOSer (5 min); note the peak response is lowered in the presence of H1152.* ***Biii****, histogram of pooled mean* Ca^{2+} *responses in hGPR55-HEK293 cells challenged with either NOSer alone or co-applied with H1152. Data are the mean, peak response ± SEM; n = 30 cells derived from two independent experiments. Student's unpaired two-tailed t-test; *P < 0.05; **P < 0.01.*

PLC is required to catalyse the hydrolysis of PIP_2 into IP_3 and DAG. IP_3 then diffuses within the cytoplasm and activates IP_3 receptors on the ER to promote the release of Ca^{2+} (Berridge *et al.*, 2003). Therefore NOSer was co-applied with the PLC inhibitor, U73122 (1 µM) after an initial 20 min application of U73122. Responses to NOSer in the presence of U73122 had a lower peak Ca^{2+} response of 66.5% relative to control (NOSer = 0.879 ± 0.054 ratio units, U73122 + NOSer = 0.294 ± 0.062 ratio units, n = 15 cells, P < 0.05, figure 3.12Bi-iii). Also it was noted that fewer cells responded when U73122 was present. These results suggest that NOSer-mediated Ca^{2+} mobilisation involves PLC activation in hGPR55-HEK293 cells. Higher concentrations of U73122 (3-5 µM) generated direct effects on Ca^{2+} levels, thus could not be evaluated further.

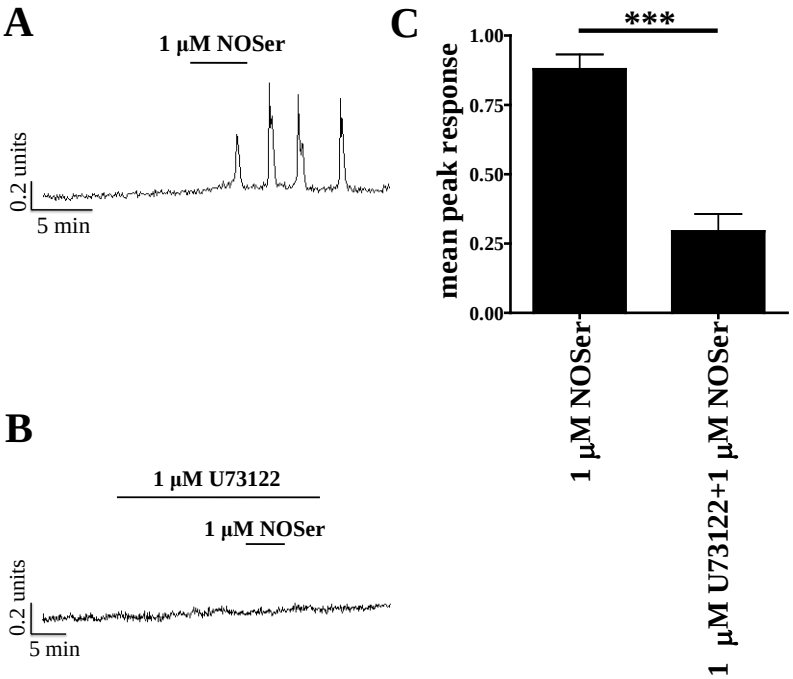

Figure 3:12: PLC is required for NOSer-mediated Ca^{2+} responses in hGPR55-HEK293 cells. *Application of the PLC inhibitor, 1 µM U73122, lowered the Ca^{2+} responses.* ***A****, representative Ca^{2+} trace from an hGPR55-HEK293 cell challenged with 1 µM NOSer.* ***B****, representative Ca^{2+} trace from an hGPR55-HEK293 cell treated with 1 µM U73122 (20 min) prior to co-application with 1 µM NOSer (5 min); note the lower peak response.* ***C****, histogram of pooled mean Ca^{2+} responses of hGPR55-HEK293 cells treated either with NOSer alone or in the presence of the PLC inhibitor. Data are the mean, peak responses ± SEM; n = 15 cells derived from one experiment. Student's unpaired two-tailed t-test; *P < 0.05.*

3.3. DISCUSSION

3.3.1. N-acyl amino acid and Ca^{2+} mobilisation in hGPR55-HEK293 cells.

LPI-induced Ca^{2+} mobilisation is known to be mediated by GPR55 in various cell types and expression systems (Oka *et al.*, 2007; Lauckner *et al.*, 2008; Henstridge *et al.*, 2009; Obara *et al.*, 2011). This study highlighted that all the N-acyl amino acids promoted the mobilisation of Ca^{2+} in hGPR55-HEK293 cells. Little or no effect was observed in control HEK293 cells challenged with the N-acyl amino acids suggesting that Ca^{2+} mobilisation was GPR55-mediated. LPI remains the most efficacious and potent ligand tested when compared to the N-acyl amino acids in this Ca^{2+} assay. The N-acyl amino acids that contain a serine head group were found to be more efficacious and more potent than those that possess a glycine head group with the same fatty acid chain. To date the N-acyl amino acids utilised in this study have not been characterised in relation their GPR55 activity with the exception of NASer and NAGly.

This is the first study to highlight that NASer-induced Ca^{2+} mobilisation is GPR55-mediated. Previous research, however, has provided conflicting reports as to whether NASer activates GPR55. Effects of NASer promoting endothelial migration and *in vitro* tube formation were attributed in part to GPR55. Application of NASer (10 nM-10 µM) to GPR55 siRNA treated human dermal microvascular endothelial cells **(**HMVEC) also lowered phosphorylation of ERK1/2 and Akt compared to control cells (Zhang *et al.*, 2010). As siRNA knockdown is never 100% efficient the remaining responses seen could be either due to incomplete silencing of GPR55 or may be due to NASer acting on another, as yet unknown, target in these cells. In another study utilising hGPR55-HEK293 cells, a GTPγS assay highlighted that NASer did not exert agonist or antagonist effects when binding to GPR55 (Cohen-Yeshurun *et al.*, 2011). Such discrepancies could be due to different cell types being utilised and therefore

responses may be cell-type specific. Also hGPR55-HEK293 cells may produce differing results due to variations in laboratory culturing methods or passage number.

To date this is the first study to highlight that NAGly, acting as a partial GPR55 agonist, can induce Ca^{2+} mobilisation in hGPR55-HEK293 cells. In contrast, two previous studies have observed that the effects of NAGly do not involve GPR55 activation. In one study hGPR55-HEK293 cells were reported to promote weak migration when challenged with NAGly (0.1 nM–10 μM). This was concentration-independent and similar effects were observed with the GPR55 agonist, LPI. The authors however report that GPR18 mediated the NAGly-induced migration in the murine microglial cell line (BV2) and hGPR18-HEK293 cells (McHugh *et al.*, 2010). It should be noted that the cells in the McHugh study were not placed in serum free medium prior to the experiments which may explain why migratory responses were not seen (Marazzi *et al.*, 2011). In another study the NAGly-induced lowering of intraocular pressure in a murine model of glaucoma was not GPR55-mediated, as GPR55 $^{(-/-)}$ mice exhibited similar results to wild type mice. Interestingly, GPR18 was observed to mediate the NAGly-induced lowering of intraocular pressure (Caldwell *et al.*, 2013). Emerging evidence highlights that NAGly can activate several GPCRs; GPR18 (Kohno *et al.*, 2006; Yin *et al.*, 2009; McHugh *et al.*, 2010, 2012; Caldwell *et al.*, 2013), GPR72 (Hannedouche and Roy, 2010) and GPR92 as a partial agonist (Oh *et al.*, 2008). However in two independent β–arrestin assays, NAGly was inactive at GPR18 (Yin *et al.*, 2009; Southern *et al.*, 2013). This discrepancy may be due to the sensitivity of β–arrestins assays being lower than that of signalling assays where amplification of signal occurs as the pathway is activated. Another explanation may be that NAGly exerts a ligand bias where signalling via β-arrestins does not occur. Therefore testing the ligand in other assays/cell types provides evidence that NAGly activates GPR18 (Caldwell *et al.*, 2013). This study however adds another GPCR to the repertoire of known GPCRs that are activated by NAGly.

NOSer was found to promote concentration-dependent, oscillatory Ca^{2+} transients in hGPR55-HEK293 cells, but not in control HEK293 cells. These data suggest that the Ca^{2+} responses in this study are likely to be GPR55-mediated. This is the first study to assign a GPCR for the orphan lipid, NOSer. A previous study of osteoblast proliferation reported NOSer effects to be sensitive to pertussis toxin (PTX) suggesting that it acts through an unknown $G_{\alpha i/o}$ sensitive GPCR (Smoum *et al.*, 2010). However, PTX treatment of GPR55-containing membranes was found to produce no effect in a

GTPγS binding assay when compared to untreated GPR55-containing membranes therefore suggesting that GPR55 does not signal through $G_{\alpha i/o}$ (Ryberg *et al.,* 2007). These data suggest that NOSer induces effects through GPR55 however; there is also another as yet unknown GPCR target for NOSer that is sensitive to $G_{\alpha i/o}$ proteins.

The structurally similar NOGly was originally thought of as an intermediate in the production of the sleep-inducing lipid amide, oleamide (Merkler *et al.*, 2004). However recent evidence suggests that NOGly may also be a biologically active signalling molecule (Chaturvedi and Driscoll, 2006) but the target for this lipid remains unknown. This study observed weak activity at GPR55 suggesting that NOGly may be a GPR55 partial agonist.

NPSer promoted Ca^{2+} mobilisation in hGPR55-HEK293 cells. Little is known about this lipid, eg synthesis and localisation, therefore further work will be required to elucidate a physiological role. NPGly is structurally similar to NPSer and is known to act on an unknown PTX-sensitive GPCR in both primary cultured dorsal root ganglion cells and a hybrid neuroblastoma x dorsal root ganglion cell line; F-11 to promote Ca^{2+} mobilisation (Rimmerman *et al.,* 2008). NPGly was found to promote a small increase in $[Ca^{2+}]_i$ in hGPR55-HEK293 cells with a threshold concentration of 3 μM. The presence of the glycine head group conjugated to a palmitic fatty acid chain has diminished GPR55- activity when compared to NPSer.

3.3.2. NOSer-induced formation of oscillatory Ca^{2+} transients requires PLC, ROCK, Ca^{2+} release from the ER and extracellular Ca^{2+}.

Activation of a GPCR can initiate the formation of IP_3 and DAG from PLC-induced PIP_2 hydrolysis. IP_3 translocates and acts on IP_3 receptors to promote the mobilisation of Ca^{2+} from the ER. Released Ca^{2+} can then act upon SOCs in the plasma membrane allowing the opening of the channel and an influx of Ca^{2+} into the cell. Ca^{2+} can act as an agonist of IP_3 receptors therefore allowing high levels of Ca^{2+} to negatively feedback in the IP_3 receptor to close the channel leading to the formation of a Ca^{2+} transient (Finch *et al.*, 1991). Ca^{2+} at low μM concentrations is reported to activate a second type of Ca^{2+} channel on the ER, the ryanodine receptor; RyR (Clapham, 2007). Therefore the presence of a Ca^{2+} buffer would be expected to influence the Ca^{2+} induced activation of IP_3 receptors (Dargan and Parker, 2003). Application of BAPTA-AM, the membrane permeable Ca^{2+} chelator inhibited NOSer-induced oscillatory Ca^{2+} transients

in hGPR55-HEK293 cells. One possibility is that the chelation of free cytosolic Ca^{2+} lowered the concentration of Ca^{2+} available to activate IP_3 or RyR receptors or led to Ca^{2+} store depletion. These data suggest that free cytosolic Ca^{2+} is important for Ca^{2+} mobilisation in NOSer challenged hGPR55-HEK293 cells.

Previous studies highlighted a requirement for both Ca^{2+} release from stores (Lauckner *et al.*, 2008; Henstridge *et al.*, 2009) and extracellular Ca^{2+} influx for GPR55-mediated Ca^{2+} signalling (Henstridge *et al.*, 2009). Extracellular Ca^{2+} was not required for GPR55-mediated Ca^{2+} transients when hGPR55-HEK293 cells treated with cannabinoid ligands (Lauckner *et al.*, 2008). Cannabinoid ligands (Δ^9THC and JWH015) were applied to hGPR55-HEK293 cells in either 0 or 2 mM Ca^{2+} Ringer's solution Ca^{2+} responses were similar suggesting that extracellular Ca^{2+} was not required (Lauckner *et al.*, 2008). However, a subsequent study revealed that extracellular Ca^{2+} was required for LPI-induced oscillatory Ca^{2+} transients in hGPR55-HEK293 (Henstridge *et al.*, 2009). A single Ca^{2+} transient occurred in the presence of Ca^{2+} free HBS supplemented with 100 µM EDTA but subsequent Ca^{2+} oscillations were ablated. This suggests that intracellular Ca^{2+} stores are depleted and cannot refill when extracellular Ca^{2+} is absent (Bird and Putney, 2005). Interestingly, the reintroduction of 1.8 mM Ca^{2+} containing HBS led to the reinstatement of oscillatory Ca^{2+} transients (Henstridge *et al.*, 2009) suggesting that Ca^{2+} from the extracellular media is entering the cell and subsequently refilling the ER through the SERCA pump. Indeed, application of thapsigargin, a selective inhibitor of SERCA (Thastrup *et al.*, 1990; Lytton *et al.*, 1991) promoted a sustained elevation of $[Ca^{2+}]_i$ in hGPR55-HEK293 cells. Upon subsequent application of NOSer no responses were observed, suggesting that the oscillatory Ca^{2+} transients require refilling of the ER.

GPR55 is reported to signal via the $G_{\alpha 13}$-Rho-ROCK pathway to promote Ca^{2+} mobilisation in hGPR55-HEK293 cells challenged with LPI (Henstridge *et al.*, 2009). Recent evidence suggests that an intact actin cytoskeleton is necessary for Ca^{2+} signalling to occur in astrocytes (Sergeeva *et al.*, 2000), fibroblasts (Ribeiro *et al.*, 1997) and hGPR55-HEK293 cells (Lauckner *et al.*, 2008). Rho-ROCK signalling is important for cytoskeletal reorganisation in cells (Amano *et al.*, 1997; Hall, 1998; Katoh *et al.*, 2001). As with LPI, activation of ROCK was involved in NOSer-induced GPR55-mediated Ca^{2+} mobilisation in hGPR55-HEK293 cells.

In summary this study has identified novel N-acyl amino acids that promote oscillatory Ca^{2+} transients in hGPR55-HEK293 cells. Ca^{2+} oscillations were absent in HEK293 cells challenged with the N-acyl amino acids suggesting that Ca^{2+} mobilisation is GPR55-mediated. Furthermore, the NOSer-induced mobilisation of Ca^{2+} required free cytosolic Ca^{2+}, ROCK, PLC, Ca^{2+} release from the ER, and the presence extracellular Ca^{2+} (figure 3.13). Together this study introduces a novel group of lipids that are structurally similar to the endocannabinoids which activate GPR55 to promote Ca^{2+} mobilisation.

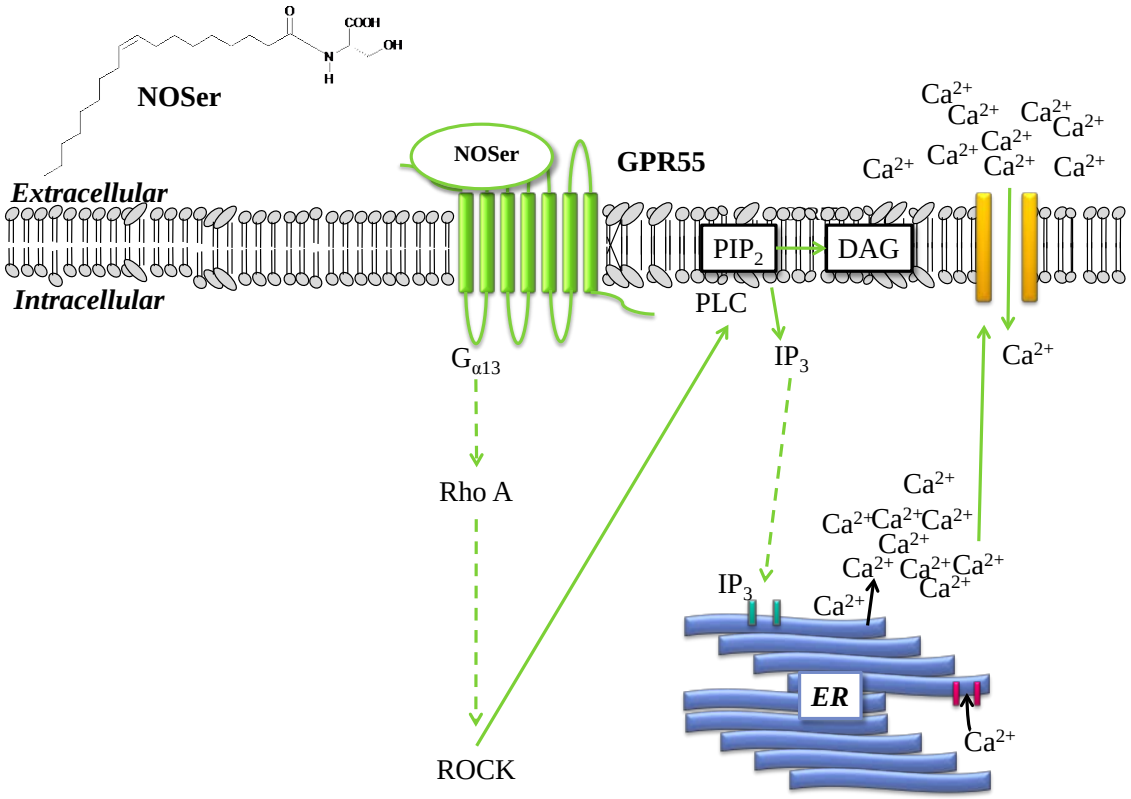

Figure 3.13: Summary of signalling cascade required to promote Ca^{2+} mobilisation. *hGPR55-HEK293 cells were challenged with NOSer. Upon NOSer activation of GPR55 it is suggested that $G_{\alpha 13}$ is activated and leads to phosphorylation of the small GTPase RhoA. ROCK phosphorylation leads to the activation of PLC which metabolises membrane bound PIP_2 into IP_3 and DAG. IP_3 translocates to act on IP_3 receptors in ER membrane and promotes the release of Ca^{2+}. Increases in Ca^{2+} lead to Ca^{2+} induced Ca^{2+} release by opening SOC localised in the plasma membrane. NOSer, N-oleoyl-L-serine; GPR55, G-protein coupled receptor 55; RhoA, Ras homolog gene, family member A; ROCK, Rho associated protein kinase; PLC, Phospholipase C; PIP_2, phosphatidylinositol 4, 5-bisphosphate; DAG, diacylglycerol; IP_3, inositol 1, 4, 5-triphosphate; Ca^{2+}, calcium; ER, endoplasmic reticulum. Solid arrows = signalling effectors; dashed arrows = suggested effectors.*

To provide further evidence that the N-acyl amino acids are GPR55 agonists other signalling assays were examined. Ca^{2+} signalling is important in homeostatic regulation and plays a role in transcriptional activation (Dolmetsch *et al.*, 1998; Chawla and Bading, 2001). A transcription factor that can be activated by Ca^{2+} signalling is CREB (Chawla and Bading, 2001). In the next chapter GPR55-mediated N-acyl amino acid-induced CREB signalling will be discussed.

CHAPTER FOUR

Further Downstream Signalling Promoted by N-acyl Amino Acids in hGPR55-HEK293 Cells

4.1. INTRODUCTION

GPR55 is known to signal through a plethora of pathways in recombinant overexpressing cell lines or endogenously GPR55 expressing immortalised cells along with primary cell cultures. These pathways include Ca^{2+} mobilisation (Oka *et al.*, 2007; Lauckner *et al.*, 2008; Henstridge *et al.*, 2009; Obara *et al.*, 2011), cytoskeletal reorganisation (Balenga *et al.*, 2011), phosphorylation of ERK1/2 (Oka *et al.*, 2007, 2009; Anavi-Goffer *et al.*, 2012) and p38 MAPK phosphorylation (Oka *et al.*, 2010). Furthermore, subsequent downstream signalling occurs promoting the activation of transcription factors such as nuclear factor of activated T-cells (NFAT; Henstridge *et al.*, 2009), Activating transcription factor 2 (ATF2; Oka *et al.*, 2010) and phosphorylation of cyclic AMP response element binding protein (pCREB; Henstridge *et al.*, 2010). LPI can induce GPR55-mediated pCREB in a concentration dependent manner in hGPR55-HEK293 cells (Henstridge *et al.*, 2010). Both Ca^{2+} (Sheng *et al.*, 1991; Impey *et al.*, 1998) and the MAPK pathway (Impey *et al.*, 1998) can induce pCREB and as mentioned above these are signalling pathways associated with GPR55. However the precise role of these pathways in GPR55-mediated pCREB has not been elucidated.

Many of the effectors that GPR55 can activate are also important for cytoskeletal reorganisation, such as members of Rho small GTPase family which includes RhoA, cdc42 and rac1 (Ryberg *et al.*, 2007). GPR55-mediated signalling through ROCK has also been implicated in cytoskeletal reorganisation (Balenga *et al.*, 2011). Furthermore the authors report that the $G_{\alpha 13}$/Rho/ROCK signalling axis is important for changes in F-actin (the polymerised form of actin) in hGPR55-HEK293 cells (Balenga *et al.*, 2011). LPI is reported to promote GPR55-mediated cytoskeletal reorganisation in the breast cancer cell line; MDA-MB-231 (Ford *et al.*, 2010), hGPR55-HEK293 cells and the neutrophil cell line; HL60 (Balenga *et al.*, 2011). Furthermore the focal adhesion protein, vinculin is known to be activated by $G_{\alpha 13}$ (Buhl *et al.*, 1995) and Rho (Nobes and Hall, 1995; Amano *et al.*, 1997) and as such could potentially be regulated by GPR55-mediated signalling.

This study began by utilising previously characterised GPR55 agonists and novel N-acyl amino acids to examine the activation of pCREB in hGPR55-HEK293 cells. To date, N-acyl amino acids have not been evaluated in a GPR55-mediated pCREB assay. As CREB is a transcription factor downstream of multiple signalling pathways; the

mechanisms by which LPI and NOSer promote pCREB in hGPR55-HEK293 cells were compared. Finally to assess whether LPI or the N-acyl amino acid, NOSer display agonist bias a further two GPR55 assays; a cytoskeletal reorganisation assay and a novel focal adhesion protein assay whereby changes in length of vinculin-containing FAs were assessed. To the best of our knowledge GPR55-mediated changes in FAs have not been previously reported. The potential signalling pathways required for cytoskeletal reorganisation and FA changes were also studied.

4.2. RESULTS

4.2.1. Cyclic AMP response element binding protein

Several studies have reported that the phosphorylation of ERK1/2 can be mediated via GPR55 activation with LPI as a ligand (Oka *et al.*, 2007; Whyte *et al.*, 2009; Obara *et al.*, 2011; Anavi-Goffer *et al.*, 2012). Downstream of ERK1/2 signalling is the transcription factor CREB. Previously an increase in pCREB was observed in western blot studies, where certain cannabinoid ligands activated GPR55 (Henstridge *et al*., 2010). It was observed that AM251, a CB_1 antagonist, was the most efficacious ligand tested (Henstridge *et al*., 2010). Here a novel approach was developed to evaluate this pathway, utilising pCREB immunolabelling and confocal microscopy which allowed the visualisation of increases in pCREB and their cellular location.

4.2.1.1. Application of the synthetic cannabinoid, AM251, promotes nuclear pCREB in hGPR55-HEK293 cells.

Previous western blot studies in hGPR55-HEK293 cells have shown efficacious effects of the synthetic CB_1 antagonist, AM251 on pCREB mediated by GPR55 (Henstridge *et al.*, 2010). Therefore, in order to validate the immunocytochemical pCREB assay for GPR55, AM251 was use as a test ligand. In control hGPR55-HEK293 cells treated with DMSO, pCREB labelling was at low levels. Furthermore, cells treated with the 12-OTetradecanoylphorbol-13-acetate (TPA; 100 nM), a phorbol ester used as a positive control, had marked nuclear pCREB staining. Application of low concentrations of AM251 (10 nM - 30 nM) did not induced pCREB labelling. Higher concentrations of AM251 (100 nM - 10 µM) however promoted concentration-dependent nuclear pCREB expression with an EC_{50} of 256 ± 51 nM (95% confidence limits) (figure 4.1 and B).

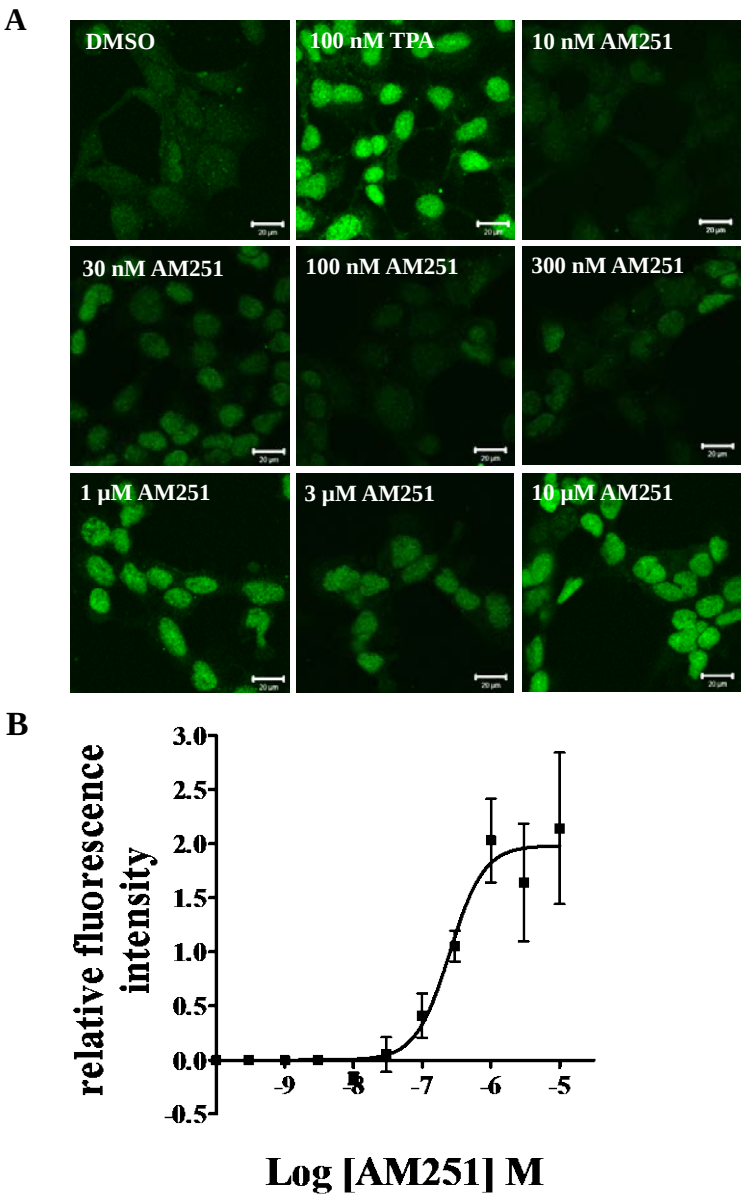

Figure 4.1: AM251 induces nuclear pCREB expression in hGPR55-HEK293 cells. *Varying concentrations of AM251 were applied to hGPR55-HEK293 cells for 25 min. Cells were methanol-fixed and pCREB labelling was visualised using a mouse anti-pCREB (ser 133) primary antibody followed by an Alexa fluor® 488-conjugated secondary antibody.* ***A****, representative confocal images of nuclear pCREB in hGPR55-HEK293 cells illustrating the effects of various concentrations of AM251. Ligand treatments were as follows DMSO, vehicle control; 100 nM TPA, positive control; 10 nM AM251; 30 nM AM251; 100 nM AM251; 300 nM AM251; 1 µM AM251; 3 µM AM251; 10 µM AM251. Scale bars = 20 µm; n = 3. Note that as the concentration of AM251 increases there is an increase in the intensity of nuclear pCREB staining.* ***B****, AM251 concentration-response curve depicting the effects of AM251 on nuclear pCREB fluorescence in hGPR55-HEK293 cells. Note AM251 increases pCREB in a concentration-dependent manner. Fluorescence intensity is the corrected total nuclear*

fluorescence (CTNF) minus the mean DMSO value normalised to that observed with 1 µM LPI. Data are the means ± SEM; n = 3.

4.2.1.2. LPI promotes nuclear pCREB in hGPR55-HEK293 cells.

Next, the effect of LPI, the putative, endogenous ligand for GPR55, on pCREB was evaluated in hGPR55-HEK293 cells. Treatment of hGPR55-HEK293 cells with low concentrations of LPI (10 nM - 30 nM) had little effect on pCREB labelling. However, higher levels (100 nM - 10 µM) promoted concentration-dependent increases in nuclear pCREB with an EC_{50} of 262 ± 54 nM (95% confidence limits) (figure 4.2A and B).

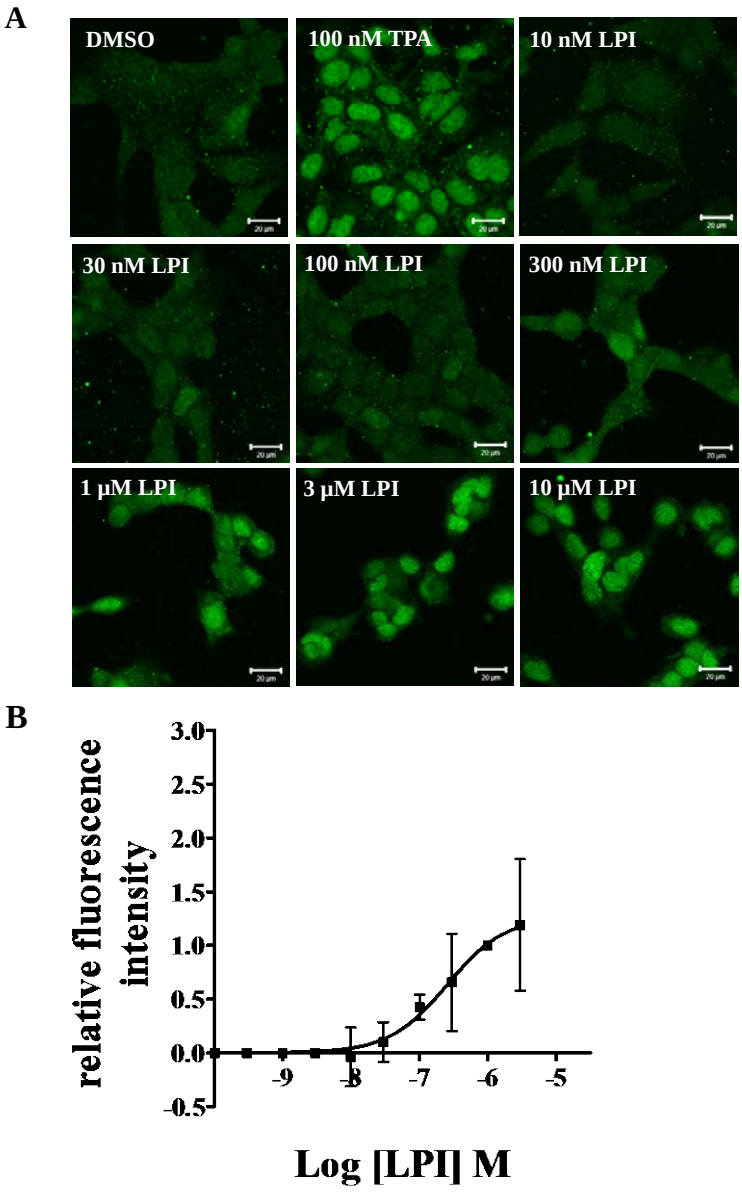

Figure 4.2: LPI promotes nuclear pCREB expression in hGPR55-HEK293 cells. *Various concentrations of LPI were applied to hGPR55-HEK293 cells for 25 min.* ***A****, representative laser scanning confocal images of nuclear pCREB in hGPR55-HEK293 cells illustrating the*

effects of various ligands, including: DMSO, vehicle control; 100 nM TPA, positive control; 10 nM LPI; 30 nM LPI; 100 nM LPI; 300 nM LPI; 1 µM LPI; 3 µM LPI; 10 µM LPI. Scale bars = 20 µm. n = 3. ***B****, LPI concentration-response curve for nuclear pCREB responses in hGPR55-HEK293 cells. Fluorescence intensity is the corrected total nuclear fluorescence (CTNF) minus the mean DMSO value then normalised to 1 µM LPI. Data are the means ± SEM; n = 3.*

4.2.1.3. Pharmacological characterisation of N-acyl serine-evoked pCREB in hGPR55-HEK293 cells.

In the next series of experiments N-acyl amino acid activation of GPR55-pCREB signalling in hGPR55-HEK293 cells was investigated using the N-acyl serines NASer, NOSer and NPSer which have previously been tested in the Ca^{2+} assay. At concentrations below 100 nM NASer had no clear effect on pCREB). However, higher concentrations of NASer (300 nM - 3 µM) induced concentration-dependent increases in nuclear pCREB; the EC_{50} was not calculated as the pCREB response did not reach a maximum level (figure 4.3A and B).

Next hGPR55-HEK293 cells were treated with NOSer (10 nM - 10 µM), which induced a concentration-dependent increase in nuclear pCREB, giving an EC_{50} of 95 ± 29 nM (95% confidence limits) (figure 4.4A and B).

The next ligand tested was NPSer. Treatment of hGRP55-HEK293 cells with NPSer within the range 10 nM - 100 nM produced little effect. However, higher concentrations of NPSer (300 nM - 10 µM) generated pCREB responses which were lower than those previously observed with NAS and NOSer in hGPR55-HEK293 cells (figure 4.5A and B).

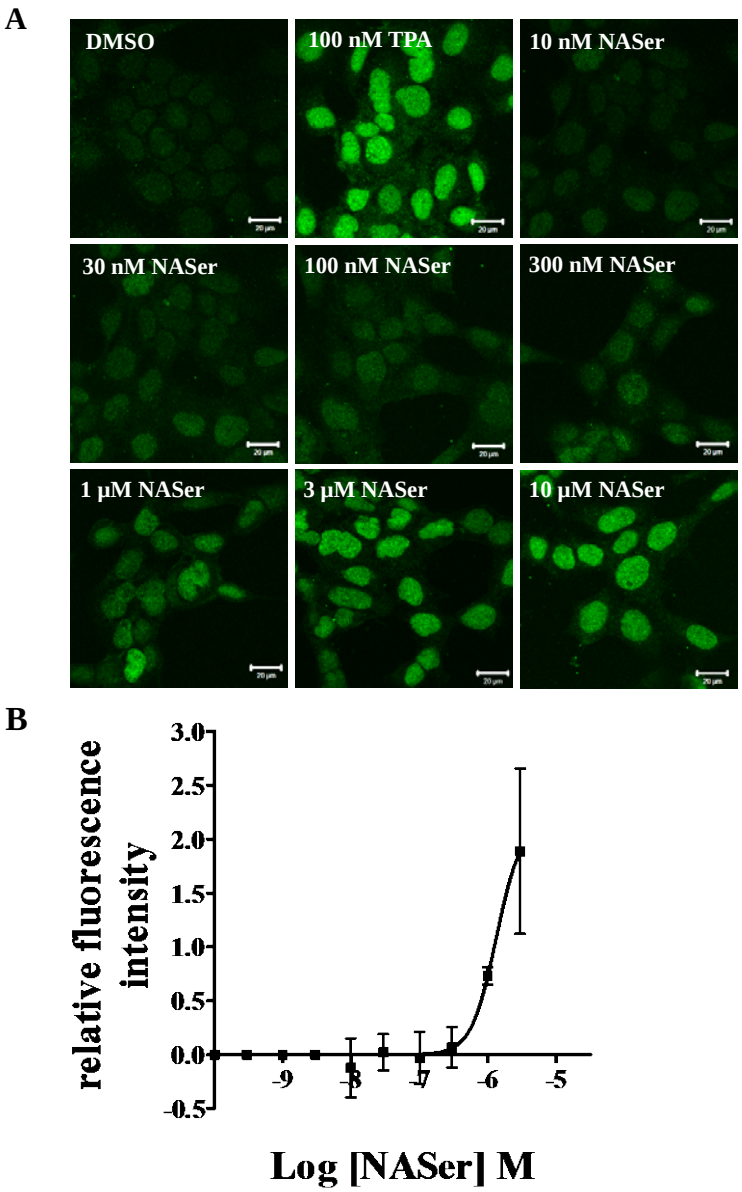

Figure 4.3: ***NASer induces nuclear pCREB in hGPR55-HEK293 cells.*** *Various concentrations of NASer were applied to hGPR55-HEK293 cells for 25 min.* ***A****, representative confocal images of nuclear pCREB in hGPR55-HEK293 cells illustrating the effects of 25 min treatment with the following ligands: DMSO, vehicle control; 100 nM TPA, positive control; 10 nM NASer; 30 nM NASer; 100 nM NASer; 300 nM NASer; 1 µM NASer; 3 µM NASer; 10 µM NASer. Scale bars = 20 µm; n = 3.* ***B****. NASer concentration-response curve for nuclear pCREB in hGPR55-HEK293 cells. Fluorescence intensity is CTNF minus the mean DMSO value then normalised to 1 µM LPI. Data are the means ± SEM; n = 3.*

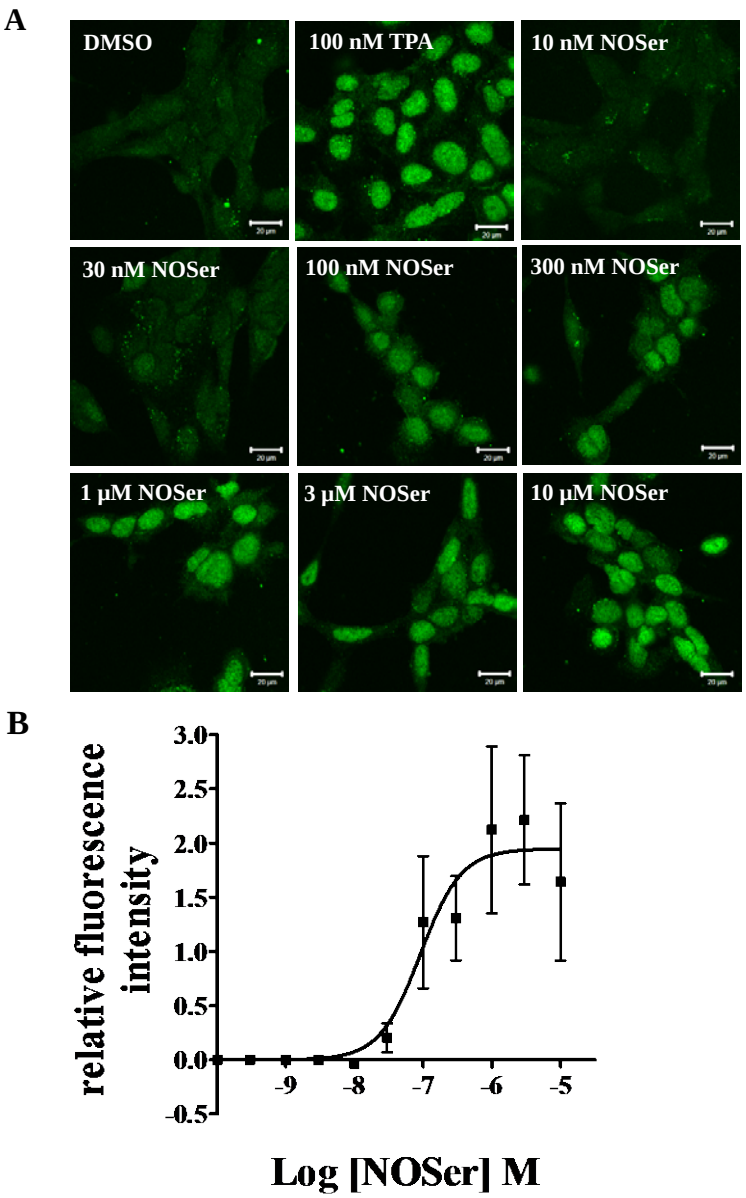

Figure 4.4: NOSer treatment of hGPR55-HEK293 cells promotes the phosphorylation of nuclear CREB. *Various concentrations of NOSer were applied to hGPR55-HEK293 cells for 25 min.* ***A****, representative confocal images of nuclear pCREB in hGPR55-HEK293 cells illustrating the effects 25 min exposure to various ligands., including DMSO, vehicle control; 100 nM TPA, positive control; 10 nM NOSer; 30 nM NOSer; 100 nM NOSer; 300 nM NOSer; 1 µM NOSer; 3 µM NOSer; 10 µM NOSer. Scale bars = 20 µm. n = 3.* ***B****, NOSer concentration-response curve for nuclear pCREB fluorescence in hGPR55-HEK293 cells. Fluorescence intensity is CTNF minus the mean DMSO value. Data are the means ± SEM; n = 3.*

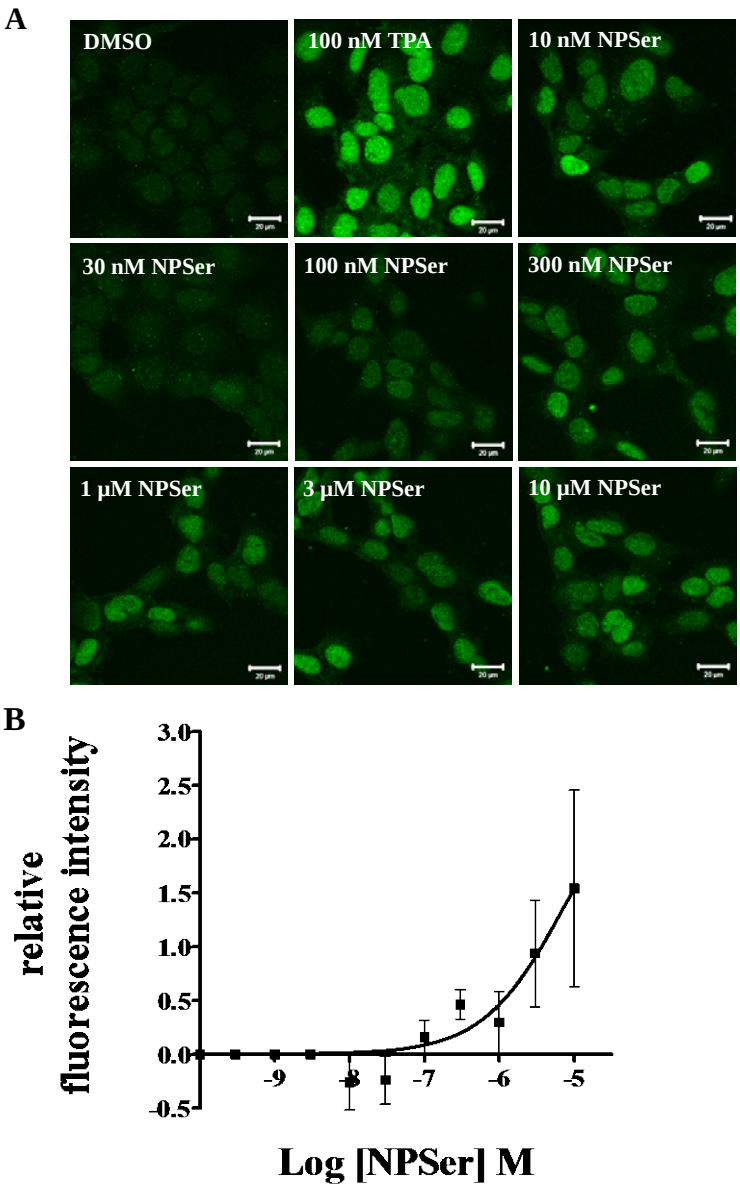

Figure 4.5: NPSer induces nuclear CREB phosphorylation in hGPR55-HEK293 cells. *Various concentrations of NPSer were applied to hGPR55-HEK293 cells for 25 min.* ***A****, representative confocal images of nuclear pCREB labelling in hGPR55-HEK293 cells illustrating the effects of 25 min treatment with various ligands, including DMSO, vehicle control; 100 nM TPA, positive control; 10 nM NPSer; 30 nM NPSer; 100 nM NPSer; 300 nM NPSer; 1 µM NPSer; 3 µM NPSer; 10 µM NPSer. Scale bars = 20 µm. n = 3.* ***B****, NPSer concentration-response curve for nuclear pCREB in hGPR55-HEK293 cells. Fluorescence intensity is CTNF minus the mean DMSO value then normalised to 1 µM LPI. Data are the means ± SEM; n = 3.*

4.2.1.4. Pharmacological characterisation of N-acyl glycine-induced pCREB in hGPR55-HEK293 cells.

In the next experiments a range of N-acyl glycine ligands were evaluated using the GPR55 pCREB assay. Firstly, hGPR55-HEK293 cells were challenged with NAGly at varying concentrations. At 30 nM, NAGly had no clear effects. However, slight increases in nuclear pCREB staining were observed with NAGly treatment between 100 - 300 nM. More marked effects were observed at high concentration (1 - 10 µM), giving an EC_{50} of 848 ± 153nM (95% confidence limits) (figure 4.6A and B).

Secondly pCREB responses to NOGly in hGPR55-HEK293 cells were tested. NOGly (30 nM - 10 µM) produced a concentration-dependent increased in pCREB with an EC_{50} of 1085 ± 264 nM (95% confidence limits) (figure 4.7A and B).

Finally, NPGly was tested in the pCREB assay. Whilst this ligand had little effect in the Ca^{2+} assay it was evaluated for pCREB activity to determine whether it might display agonist-biased signalling. However, NPGly over the concentration range 30 nM - 10 µM generated little or no pCREB response (figure 4.8A and B).

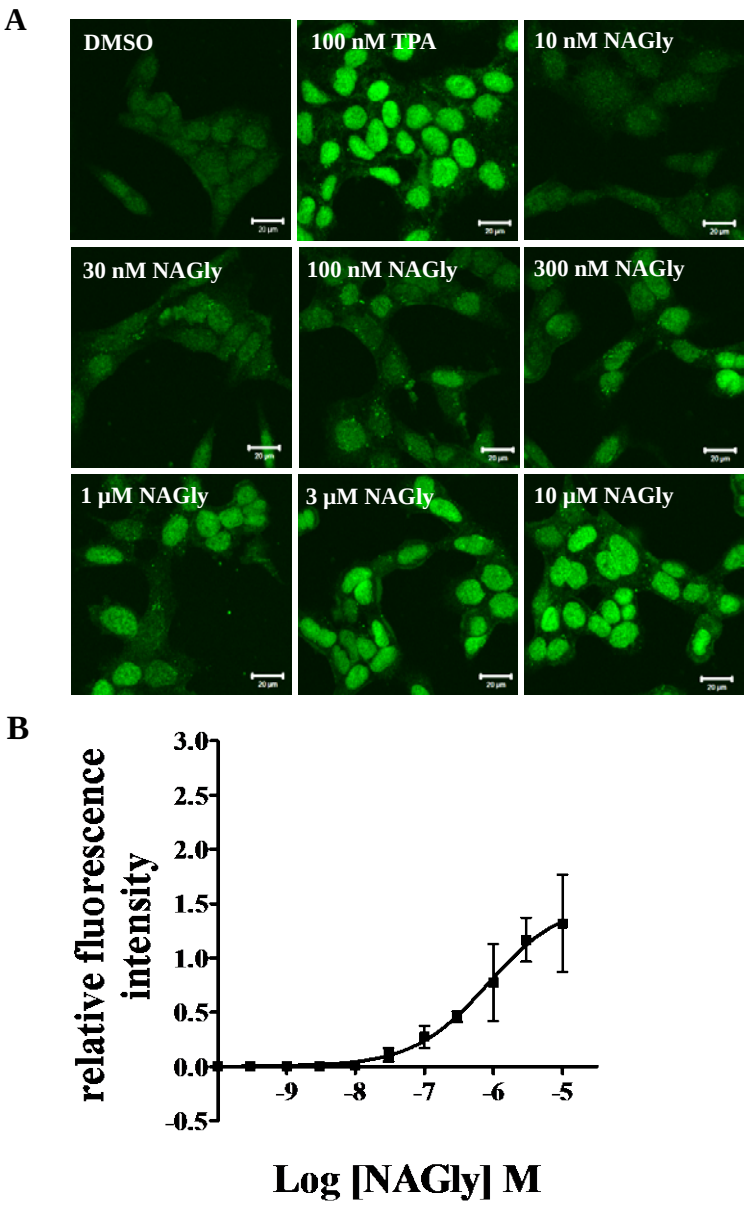

Figure 4.6: NAGly induces nuclear pCREB in hGPR55-HEK293 cells. ***A****, representative confocal images of nuclear pCREB labelling in hGPR55-HEK293 cells treated for 25 min with various ligands, including DMSO, vehicle control; 100 nM TPA, positive control; 10 nM NAGly; 30 nM NAGly; 100 nM NAGly; 300 nM NAGly; 1 µM NAGly; 3 µM NAGly; 10 µM NAGly. Scale bars = 20 µm. n = 3.* ***B****, NAGly concentration-response curve of nuclear pCREB fluorescence in hGPR55-HEK293 cells. Fluorescence intensity is CTNF minus the mean DMSO value then normalised to 1 µM LPI. Data are the means ± SEM; n = 3.*

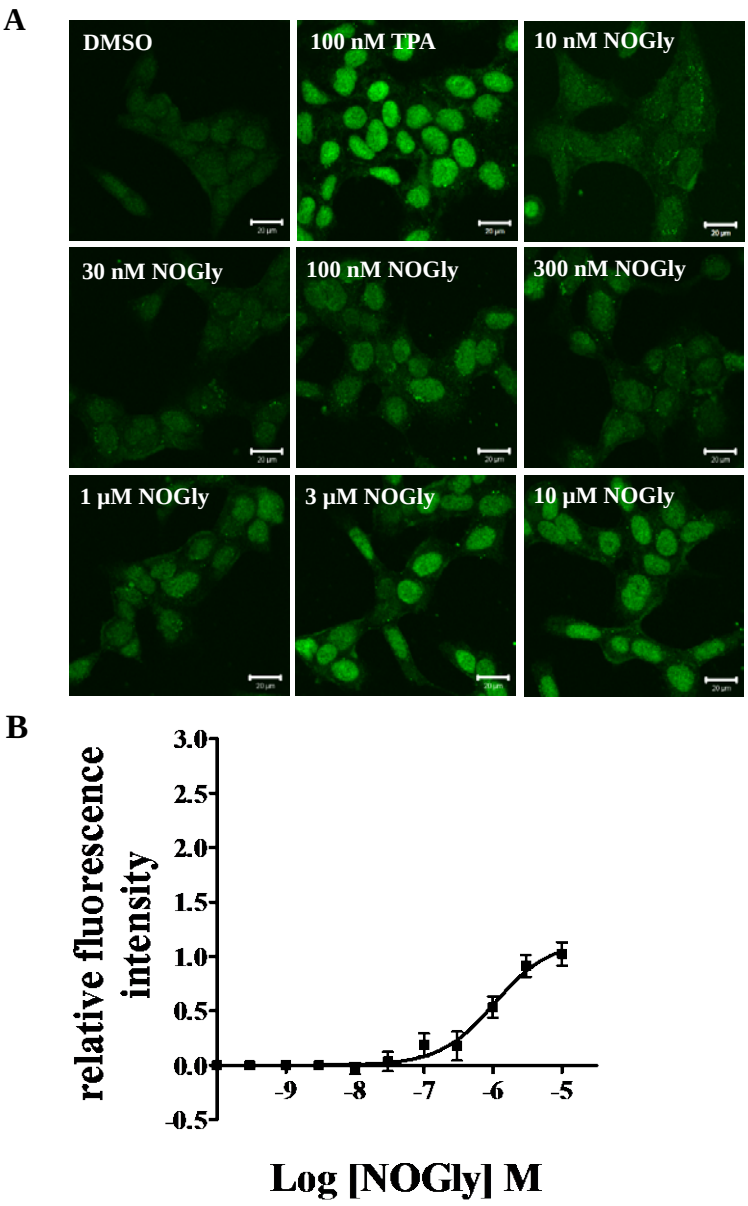

Figure 4.7: NOGly induces nuclear pCREB in hGPR55-HEK293 cells. *Various concentrations of NOGly were applied to hGPR55-HEK293 cells for 25 min.* ***A****, representative confocal images of nuclear pCREB in hGPR55-HEK293 cells illustrating the effects of 25 min treatment with the following ligands, DMSO, vehicle control; 100 nM TPA, positive control; 10 nM NOGly; 30 nM NOGly; 100 nM NOGly; 300 nM NOGly; 1 µM NOGly; 3 µM NOGly; 10 µM NOGly. Scale bars = 20 µm. n = 3.* ***B****, NOGly concentration-response curve for nuclear pCREB labelling in hGPR55-HEK293 cells. Fluorescence intensity is corrected total nuclear fluorescence minus the mean DMSO value then normalised to 1 µM LPI. Data are the means ± SEM; n = 3.*

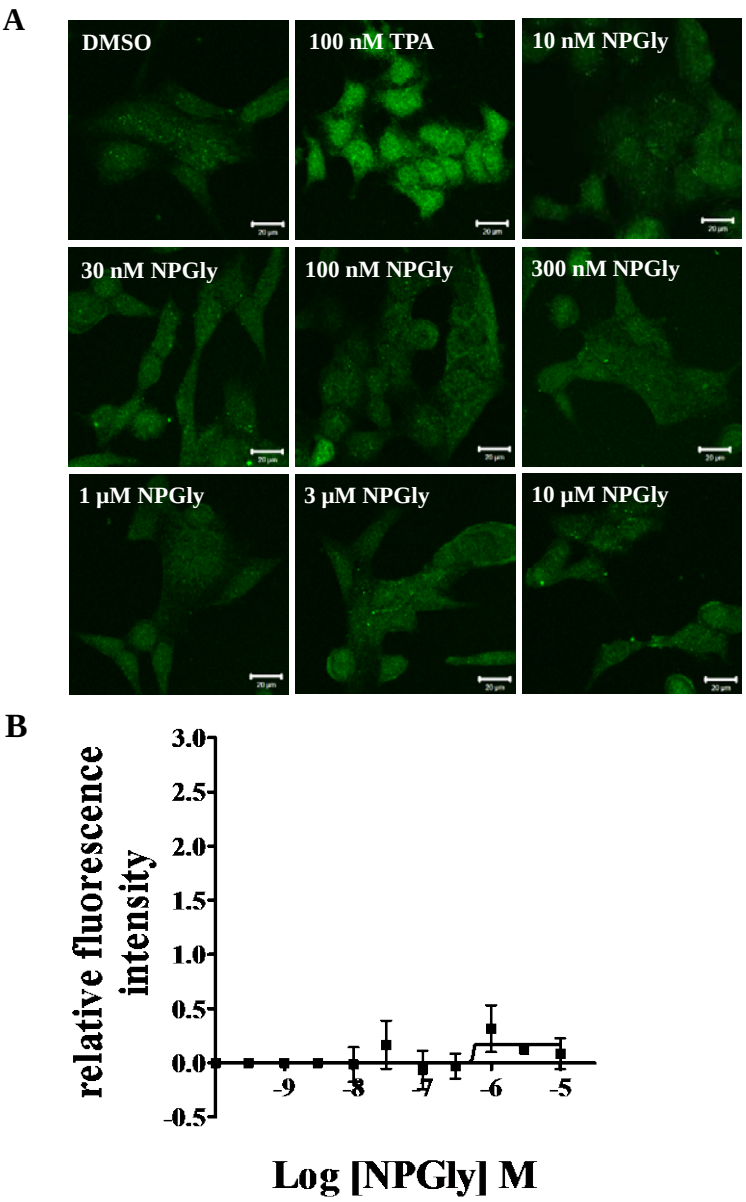

Figure 4.8: Effects of NPGly on nuclear pCREB in hGPR55-HEK293 cells. *Various concentrations of NPGly were applied to hGPR55-HEK293 cells for 25 min.* ***A****, representative confocal images of nuclear pCREB in hGPR55-HEK293 cells illustrating the effects of 25 min treatment with the following compounds, DMSO, vehicle control; 100 nM TPA, positive control; 10 nM NPGly; 30 nM NPGly; 100 nM NPGly; 300 nM NPGly; 1 µM NPGly; 3 µM NPGly; 10 µM NPGly. Scale bars = 20 µm. n = 3.* ***B****, NPGly concentration-response curve for nuclear pCREB fluorescence in hGPR55-HEK293 cells. Fluorescence intensity is CTNF minus the mean DMSO value normalised to 1 µM LPI. Data are the means ± SEM; n = 3.*

4.2.1.5. The relative potencies and efficacy of endogenous N-acyl amino acids-evoked pCREB in hGPR55-HEK293 cells.

AM251 was found to be more efficacious than LPI (figure 4.9) which is in agreement with a previous western blot study using hGPR55-HEK293 cells (Henstridge *et al.*,

2010). NOSer was also found to have a higher E_{max} than LPI. Indeed NOSer was ~30% more efficacious than LPI. In contrast to the Ca^{2+} assay these data suggest that NOSer is more efficacious in the pCREB assay than in the Ca^{2+} mobilisation assay. As noted in the Ca^{2+} assay the serine head group appears to increase the pCREB efficacies compared to the lipids with a glycine head group suggesting that there is no ligand bias with the N-acyl amino acids.

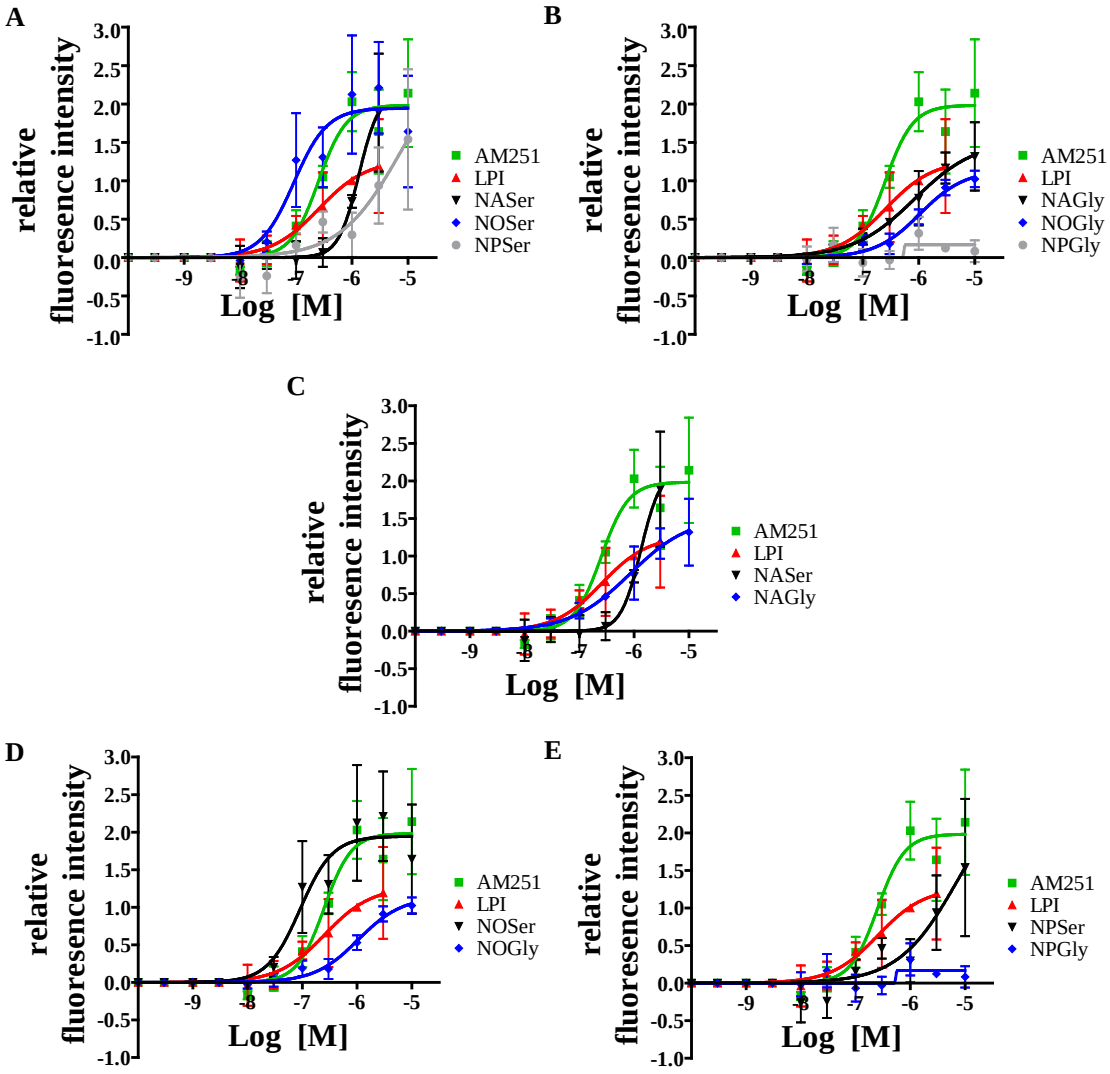

Figure 4.9: Pooled concentration-response data for pCREB responses to lipids in hGPR55-HEK293 cells. ***A****, comparison of the lipids that contain a serine head group.* ***B****, comparison of lipids that contain a glycine head group.* ***C****, comparison of lipids with the arachidonic (C20:4) fatty acid chain.* ***D****, comparison of lipids containing oleic (C18:1) fatty acid chain.* ***E****, comparison of lipids containing palmitic (16:0) fatty acid chain. Note the presence of a glycine head group increases the efficacy in the lipids with either arachidonic or oleic fatty acid chains. NASer and NOSer are more efficacious than LPI. Data are the mean responses ± SEM; n = 3.*

NOSer was found to be the most potent of the ligands tested in the pCREB assay (table 4.1). This was followed by AM251 and LPI; all with EC_{50} values in the low nanomolar range. NOGly was found to have an EC_{50} value which was in the low micromolar range. This was a little unexpected as this lipid had shown similar EC_{50} values in the Ca^{2+} assay to NOSer. These data therefore suggest that NOGly may be exerting some agonist bias when acting on GPR55 in hGPR55-HEK293 cells. NASer, NPSer and NPGly did not produce a clear maximal response within the concentration range tested therefore an EC_{50} could not be calculated. NAGly in both the Ca^{2+} and pCREB assay was found to have an EC_{50} that was in the high nanomolar range.

Ligand	**EC_{50} (nM)**
AM251	256 ± 51
LPI	262 ± 54
NASer	nd
NOSer	95 ± 29
NPSer	nd
NAGly	848 ± 153
NOGly	1085 ± 264
NPGly	nd

Table 4.1: Relative potencies of pCREB compared to LPI. *EC_{50} values for the ligands studied. NASer, NPSer and NPGly were undetermined as their E_{max} values could not be determined. Note the most potent ligands were NOSer, AM251 and LPI. Results are derived from three independent experiments. nd = not determined. EC_{50} values (95% confidence limits).*

4.2.1.6. Endogenous lipids do not promote pCREB signalling in control HEK293 cells.

The endogenous lipoamino acids were tested for pCREB activity in control HEK293 cells. None of the GPR55 lipid ligands generated pCREB responses in HEK293 cells. However, responses were observed with 100 nM TPA; a phorbol ester used as a positive control. Responses to supra-maximal concentrations of GPR55 ligands were compared between hGPR55-HEK293 cells and HEK293 cells. In hGPR55-HEK293 cells a one-way ANOVA highlighted increases in pCREB were significant ($F_{(17,36)}$ = 12.17; P = 0.0001). Moreover Bonferroni *post hoc* analysis revealed that compared to DMSO, vehicle control, all lipids except 3 µM NOGly and 3 µM NPGly were significantly

different. Furthermore 3 µM NPGly pCREB staining was similar to DMSO in hGPR55-HEK293 cells (figure 4.10A). However, no significant effects of the ligands on pCREB were observed in HEK293 cells relative to DMSO control (figure 4.10A and B). These results suggest that the pCREB promoted by the endogenous lipids are GPR55-mediated.

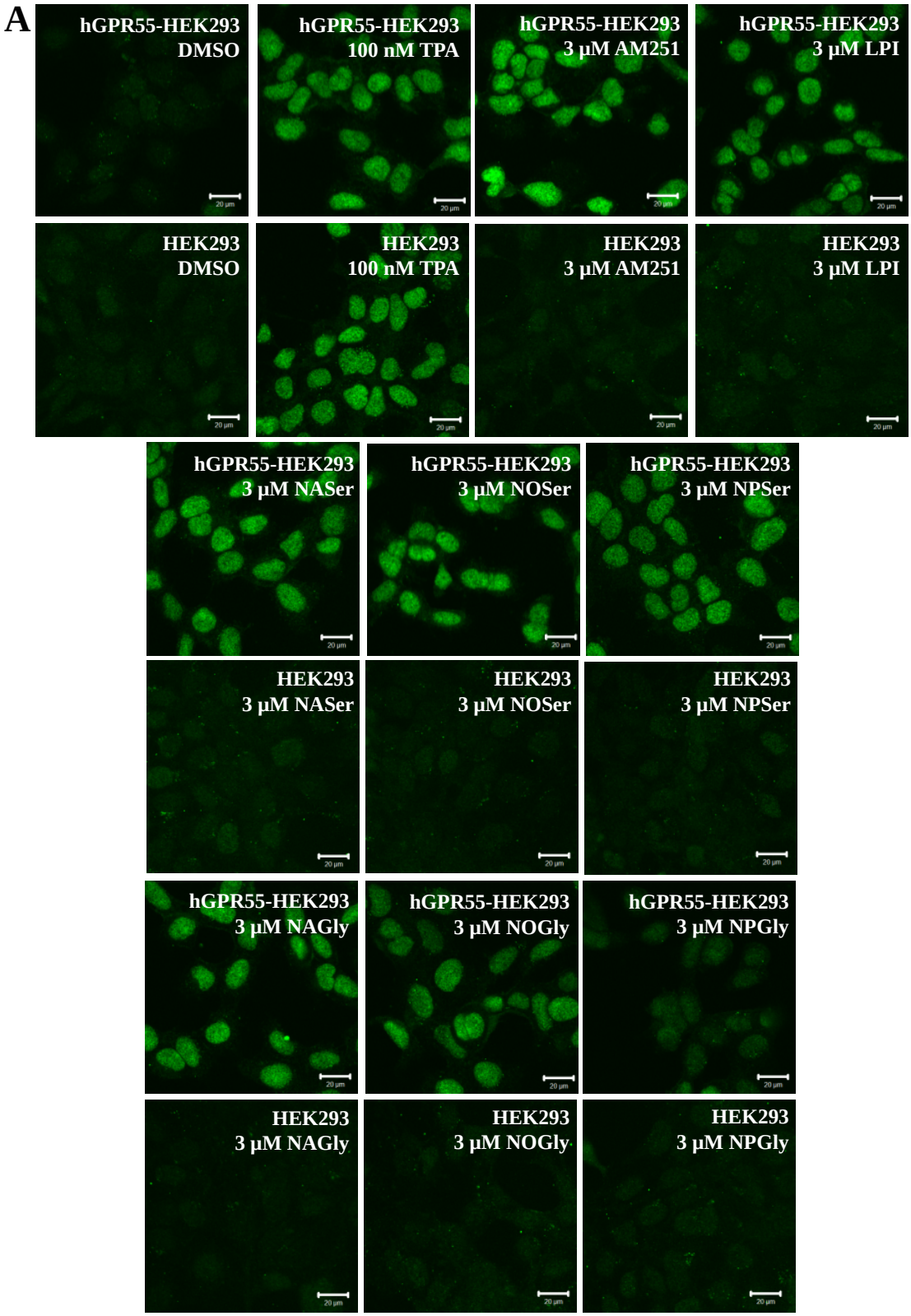

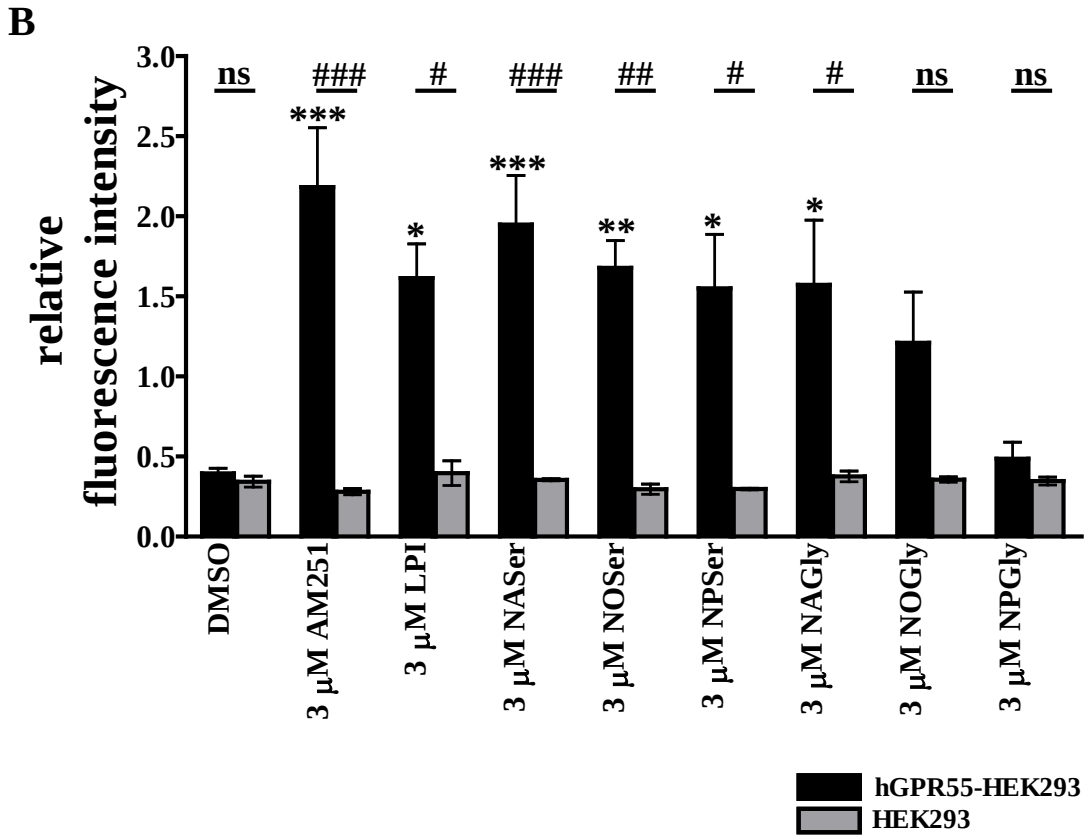

Figure 4.10: A comparison of pCREB responses to GPR55 ligands in hGPR55-HEK293 cells and control HEK293 cells. *Cells were treated with ligands for 25 min.* ***A****, Representative confocal images of hGPR55-HEK293 cells and HEK293 cells exposed to the following treatments: DMSO; 100 nM TPA; 3 µM AM251; 3 µM LPI; 3 µM NASer; 3 µM NOSer; 3 µM NPSer; 3 µM NAGly; 3 µM NOGly; 3 µM NPGly.* ***B****, histogram of pooled data depicting nuclear pCREB responses to various ligands in either hGPR55-HEK293 (black) or HEK293 cells (grey). Note that pCREB responses to GPR55 ligands are absent in HEK293 cells. Data is CTNF normalised to 1 µM LPI. Data are the means ± SEM; n = 3. One-way ANOVA followed by a Bonferroni post hoc test; #P < 0.05; ##P < 0.01; ###P < 0.001; ns = not significant.*

4.2.1.7. $G_{\alpha 13}$, not $G_{\alpha q}$, is required for the phosphorylation of nuclear CREB in hGPR55-HEK293 cells.

Two heterotrimeric G-protein families have been suggested to be involved in GPR55 signalling, including $G_{\alpha 12}$ and $G_{\alpha q}$. For example, the related G proteins $G_{\alpha 12}$ and $G_{\alpha 13}$ have been implicated in the mobilisation of Ca^{2+} in hGPR55-HEK293 cells (Lauckner *et al.*, 2008; Henstridge *et al.*, 2009) However, $G_{\alpha q}$ may also have a role in this pathway in recombinant hGPR55-HEK293 cells (Lauckner *et al.*, 2008) and also the rat

phaeochromocytoma cell line and PC12 cells (Obara *et al.*, 2011) treated with either THC (5 µM) or LPI (10 µM) respectively.

Initially the effects of dominant negative $G_{\alpha 13}$(Q226L/D294N) on responses to LPI and NOSer were investigated. One-way ANOVA highlighted that hGPR55-HEK293 cells transfected with $G_{\alpha 13}$(Q226L/D294N) promoted significant increases across the data set ($F_{(5,6)} = 17.11$; $P = 0.0017$). Bonferroni post hoc analysis revealed that LPI in the presence of $G_{\alpha 13}$(Q226L/D294N) generated a pCREB response which was significantly less than LPI alone. Furthermore, the general trend was that $G_{\alpha 13}$(Q226L/D294N) transfected hGPR55-HEK293 cells treated with NOSer promoted pCREB responses that were lower than NOSer alone however, this was not significant. Both LPI or NOSer in the presence of $G_{\alpha 13}$(Q226L/D294N) and $G_{\alpha 13}$(Q226L/D294N) alone produced pCREB staining that was similar to basal levels (figure 4.11A and B).

The cyclic depsipeptide YM-254890 was derived from culture broth of the bacterium, Chromobacterium sp. QS3666 and had been observed to inhibit platelet aggregation (Taniguchi *et al.*, 2003). Ca^{2+} mobilisation was inhibited when known $G_{\alpha q}$ activated receptors were studied and the effect was found to mediated by YM-254890 inhibiting the exchange of GDP for GTP on $G_{\alpha q}$ following receptor activation (Takasaki *et al.*, 2004; Nishimura *et al.*, 2010). Furthermore LPI-induced Ca^{2+} mobilisation in PC12 cells, which endogenously express GPR55, was inhibited by YM-254890 (Obara *et al.*, 2011). Therefore the $G_{\alpha q}$ inhibitor YM-254890 (1 µM) was used to elucidate if the $G_{\alpha q}$ signalling is required for GPR55 to promote nuclear pCREB. An one-way ANOVA highlighted a significant difference across the data set ($F_{(5,12)} = 17.65$; $P < 0.0001$). *Post hoc* analysis revealed that LPI treated hGPR55-HEK293 cells when compared to other cells treated with LPI in the presence of YM-254890 there was very little difference observed (figure 4.12A and B). Similarly, NOSer alone when compared to YM-254890 co-applied with NOSer showed little difference in pCREB staining. Finally treatment with YM254890 alone had no effect on pCREB levels, producing staining that was similar to that observed with DMSO.

Taken together these data suggest that LPI requires $G_{\alpha 13}$ but not $G_{\alpha q}$ heterotrimeric G-proteins to induce nuclear pCREB in hGPR55-HEK293 cells. These data are in agreement with a previous Ca^{2+} signalling study in hGPR55-HEK293 cells where $G_{\alpha 13}$ was important to promote the mobilisation of Ca^{2+} in cells treated with LPI (Henstridge

et al., 2009). Moreover, NOSer induce pCREB is likely to be $G_{\alpha 13}$ dependent and $G_{\alpha q}$ independent.

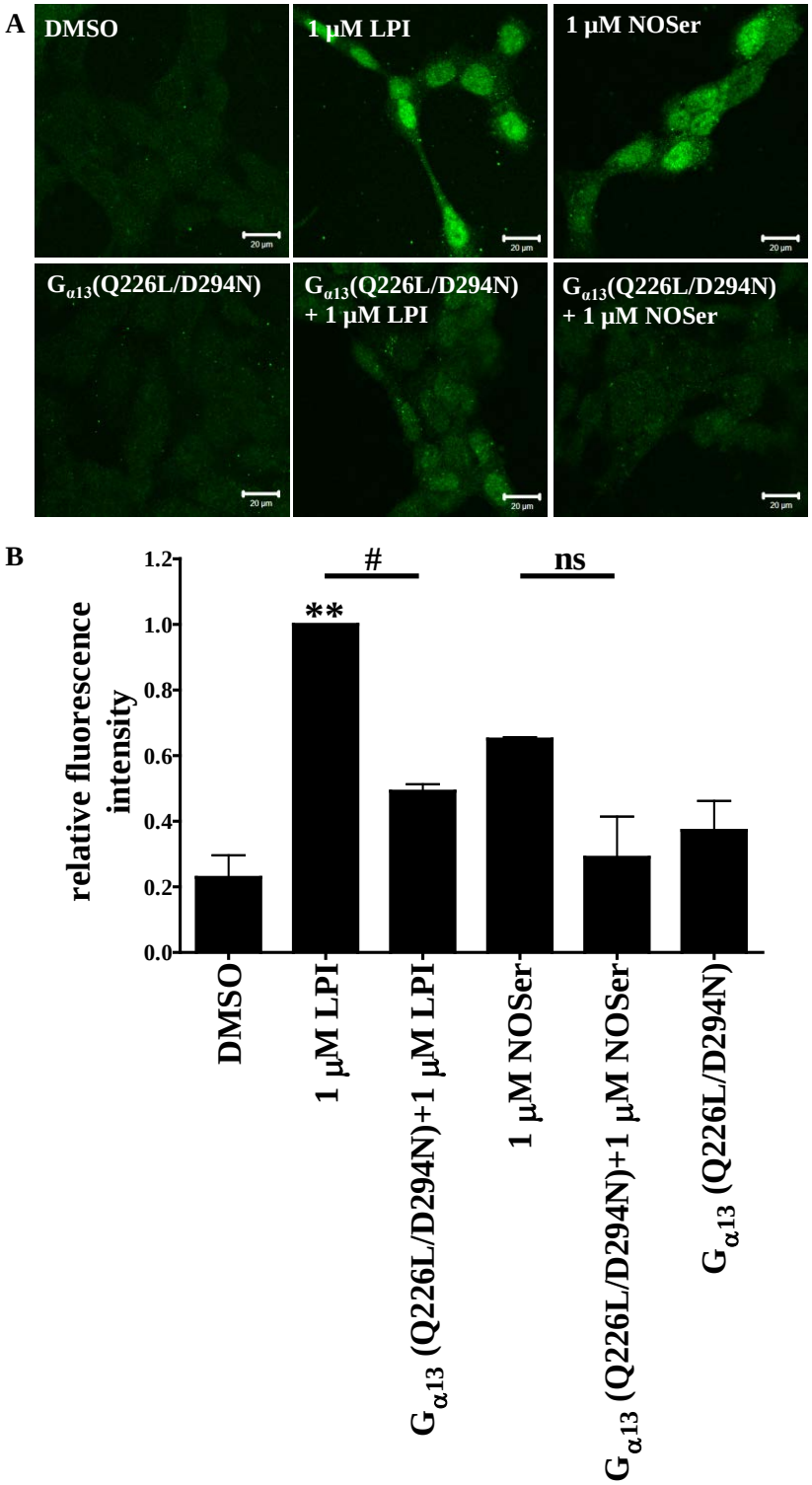

Figure 4.11: $G_{\alpha 13}$ is required for GPR55-mediated CREB activation in hGPR55-HEK293 cells. *Cells were transfected with a dominant negative $G_{\alpha 13}$ cDNA (Q226L/D294N) for 18 hr prior to application of the lipids.* ***A****, representative confocal images of pCREB labelling in*

hGPR55-HEK293 in response to the following treatments: DMSO; 1 µM LPI; 1 µM NOSer; $G_{\alpha 13}$(Q226L/D294N); $G_{\alpha 13}$(Q226L/D294N) + 1 µM LPI; $G_{\alpha 13}$(Q226L/D294N) + 1 µM NOSer. Scale bars = 20 µm; n = 2. ***B****, histogram of pooled data, showing the mean CTNF normalised to 1 µM LPI when hGPR55-HEK293 cells were challenged with either 1 µM LPI or 1 µM NOSer either with or without the presence of $G_{\alpha 13}$(Q226L/D294N). Data are the means ± SEM; n = 2. * = compared to vehicle control. One-way ANOVA with a Bonferroni post hoc test; **P < 0.01; #P < 0.05; ns = not significant.*

4.2.1.8. The Rho-ROCK pathway is required for GPR55-mediated nuclear CREB phosphorylation.

The next set of experiments was designed to study the effect inhibiting Rho had on GPR55-mediated pCREB. Previous work reported that the small G-protein RhoA is downstream of GPR55-mediated signalling through activation of $G_{\alpha 12}$ and $G_{\alpha 13}$ heterotrimeric G-proteins when challenged with either cannabinoid ligands, AEA or O-1602 (Ryberg *et al.*, 2007), or with LPI (Henstridge *et al.*, 2009). Therefore, a membrane permeable Rho inhibitor, CT04 (1 µg/ml) was tested in hGPR55-HEK293 cells to assess the effect of Rho in the promotion of nuclear pCREB. Significant differences were highlighted when testing the data with a one-way ANOVA ($F_{(5,12)}$ = 4.93; P = 0.011). *Post hoc* analysis revealed that CT04 (1 µg/ml) had no effect by itself, relative to vehicle control (DMSO; 0.1%) on nuclear pCREB staining (figure 4.13A and B). Moreover NOSer promoted a significant increase in nuclear pCREB. However, CT04-treated hGPR55-HEK293 cells challenged with LPI exhibited 58.24 ± 22.93% reduced responses when compared to LPI alone. Likewise, responses to NOSer were also inhibited by 48.94 ± 6.5% in the presence of CT04. However the lowering of the lipids response in the presence of CT04 was not significant.

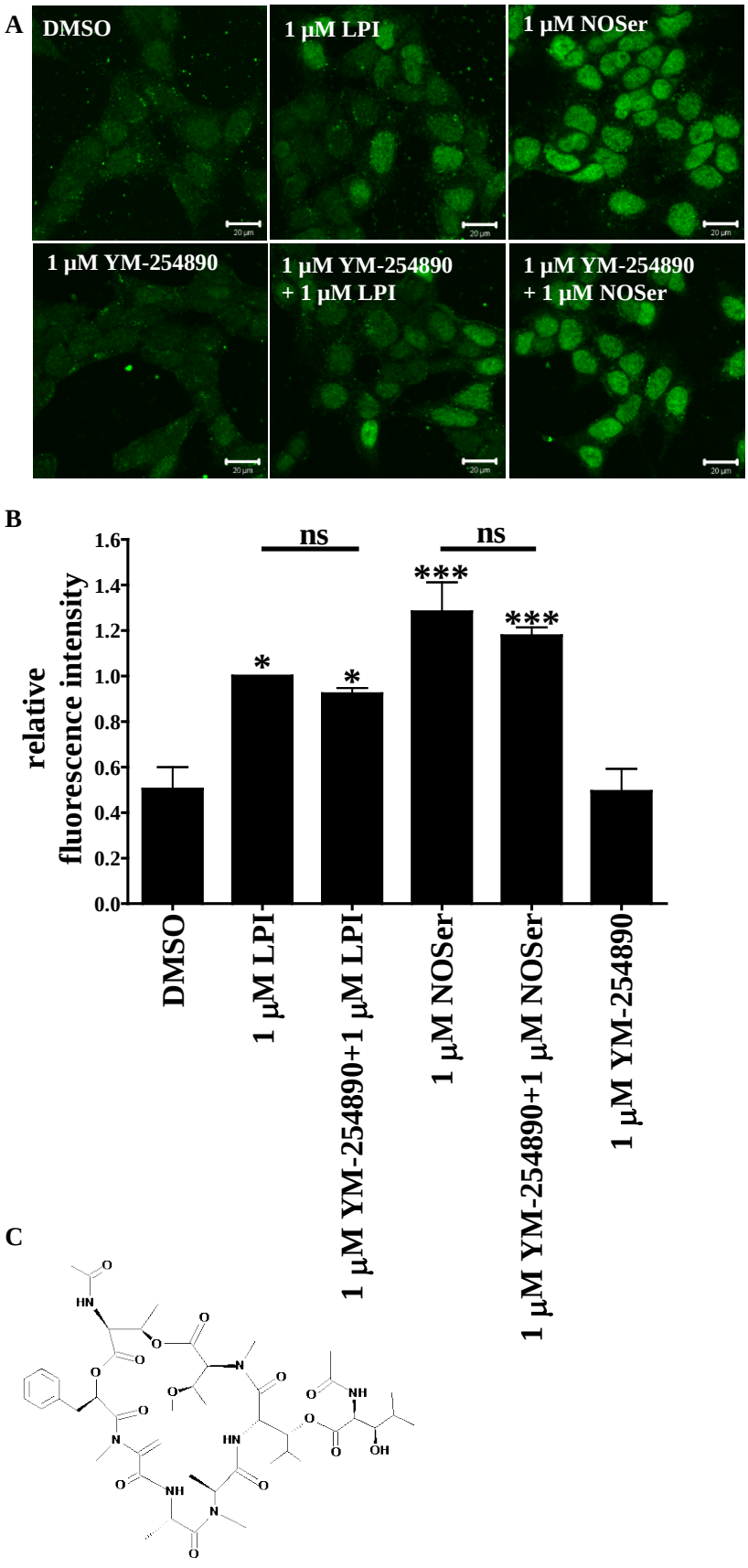

Figure 4.12: $G_{\alpha q}$ is not required for GPR55-mediated CREB phosphorylation in hGPR55-HEK293 cells. *Cells were treated for 30 min with a $G_{\alpha q}$ inhibitor (YM-254890; 1 µM) prior to co-application of inhibitor with LPI or NOSer.* ***A****, representative confocal images of nuclear*

pCREB labelling in hGPR55-HEK293 cells treated as follows: DMSO; 1 µM LPI; 1 µM NOSer; 1 µM YM-254890; 1 µM YM-254890 + 1 µM LPI; 1 µM YM-254890 + 1 µM NOSer. Scale bars = 20 µm; n = 3. ***B****, histogram of pooled data, revealing the mean CTNF normalised to 1 µM LPI of nuclear pCREB fluorescence when hGPR55-HEK293 cells were challenged with either 1 µM LPI or 1 µM NOSer either with or without 1 µM YM-254890.* ***C****, chemical structure of YM-254890. Note the presence of the $G_{\alpha q}$ inhibitor has no significant effect on the responses promoted by the lipids. Data are the means ± SEM; n = 3. * = compared to vehicle control. One-way ANOVA with a Bonferroni post hoc test; *P < 0.05; ***P < 0.001; ns = not significant.*

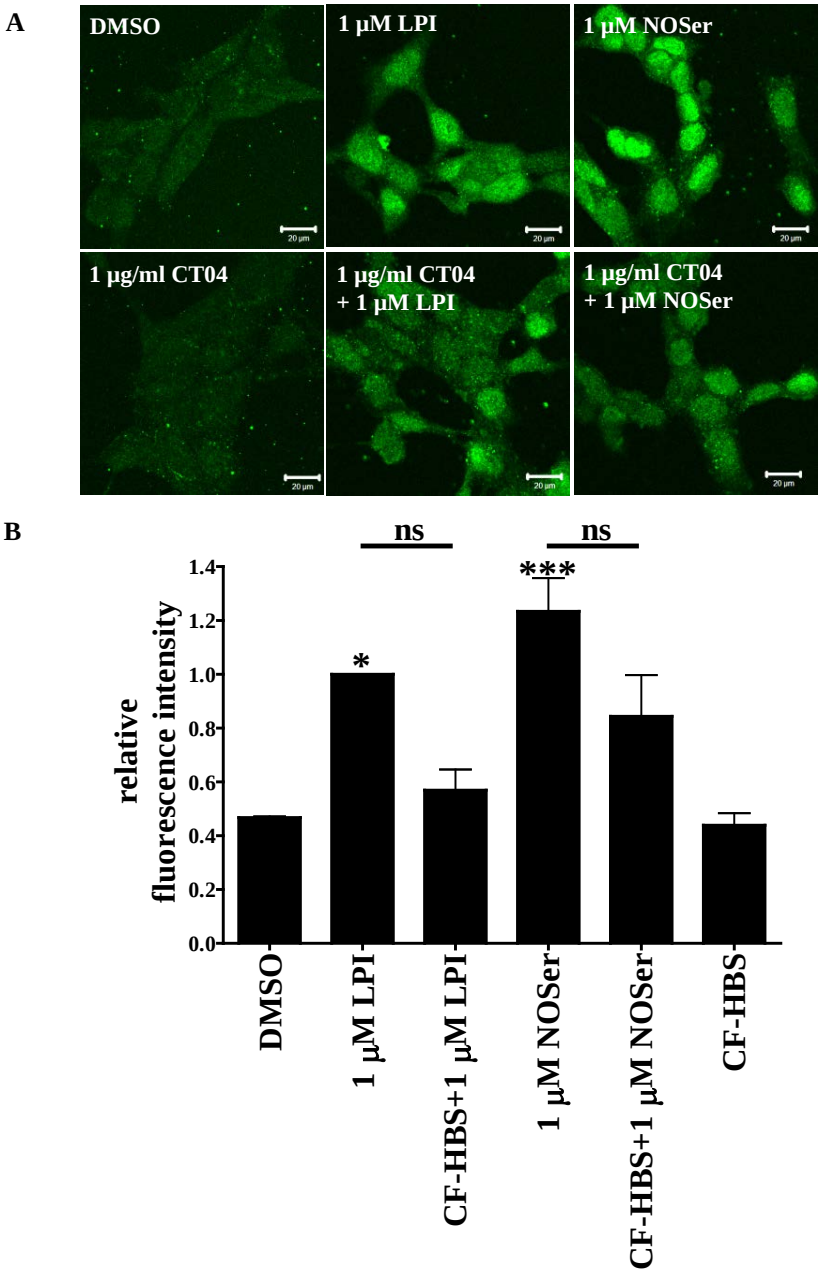

Figure 4.13: Signalling through Rho small GTPases is required for GPR55-mediated pCREB signalling. *hGPR55-HEK293 were treated for 4 hr with a membrane permeant Rho*

inhibitor (CT04; 1 µg/ml) prior to treatment with lipid ligands. ***A****, representative confocal images of nuclear pCREB in cells treated as follows: DMSO; 1 µM LPI; 1 µM NOSer; 1 µg/ml CT04; 1 µg/ml CT04 + 1 µM LPI; 1 µg/ml CT04 + 1 µM NOSer. Scale bars = 20 µm; n = 3.* ***B****, histogram of pooled data, revealing the mean CTNF normalised to 1 µM LPI of nuclear pCREB fluorescence of hGPR55-HEK293 cells challenged as stated. Note NOSer-induced pCREB staining was more robust than LPI-induced pCREB staining. Data are the means ± SEM; n = 3. * = compared to vehicle control. One-way ANOVA with a Bonferroni post hoc test; * < 0.05; ns = not significant.*

Next the effects of inhibition of Rho kinases (ROCK) I and II were investigated using the synthetic inhibitors; Y-27632 dihydrochloride which targets the catalytic site of ROCK I and ROCK II (Ishizaki *et al.*, 2000; Tamura *et al.*, 2005) or H1152 dihydrochloride which blocks ROCK II (Tamura *et al.*, 2005). LPI and NOSer produced a robust increase in pCREB staining that is localised to the nucleus (figure 4.14A). Furthermore an one-way ANOVA highlighted a significant difference across the experimental data ($F_{(5,12)}$ = 36.3; P < 0.0001). *Post hoc* analysis revealed a very highly significant difference to either of the lipids when compared to the lipid in the presence of Y-27632. Furthermore treatment with Y-27632 (10 µM) lowered nuclear pCREB to both LPI and NOSer by 68.44 ± 8.15% and 59.73 ± 7.92%. Y-27632 + LPI and Y27632 + NOSer reduced the nuclear pCREB response to basal levels (figure 4.14A). Moreover by itself, Y-27632 had no effect on pCREB levels (figure 4.14A and B).

One-way ANOVA revealed significant differences within the ROCK II inhibitor data set ($F_{(5,12)}$ = 17.95; P < 0.0001). Bonferroni *post hoc* analysis revealed a general trend whereby CREB phosphorylation was reduced when H1152 (100 nM) was co-applied with LPI by 86.0 ± 9.5% or NOSer by 34.8 ± 27.6% however these effects were not significant. When tested by itself, H1152 alone had no effect on pCREB labelling (figure 4.14D and E). Taken together these data suggest that ROCK I is required to promote nuclear pCREB in hGPR55-HEK293 cells treated with either of the lipids tested. However it is likely that ROCK II is required in hGPR55-HEK293 cells challenged with LPI but may not be so important in cells treated with NOSer.

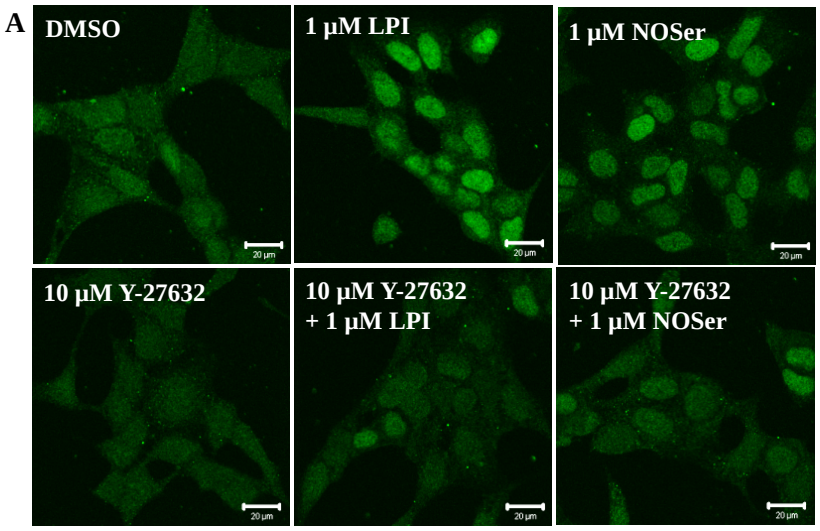
A
DMSO
1 µM LPI
1 µM NOSer
10 µM Y-27632
10 µM Y-27632
+ 1 µM LPI
10 µM Y-27632
+ 1 µM NOSer
20 µm

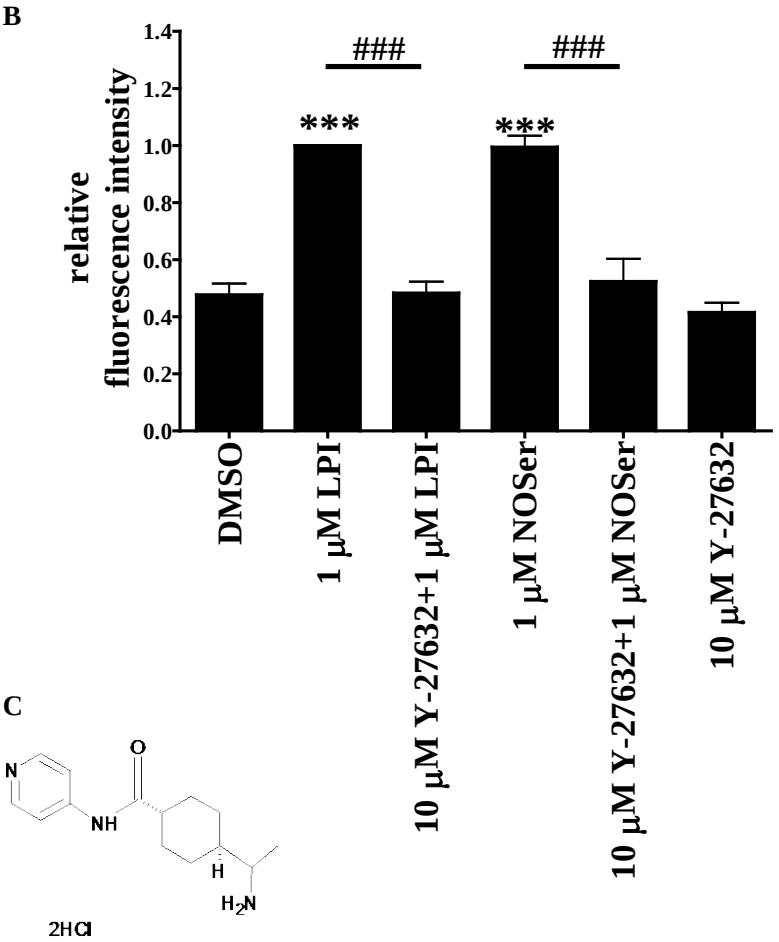
B
relative
fluorescence intensity
1.4
1.2
1.0
0.8
0.6
0.4
0.2
0.0
###
###
***
***
DMSO
1 µM LPI
10 µM Y-27632+1 µM LPI
1 µM NOSer
10 µM Y-27632+1 µM NOSer
10 µM Y-27632

C
N
O
NH
H
H2N
2HCl

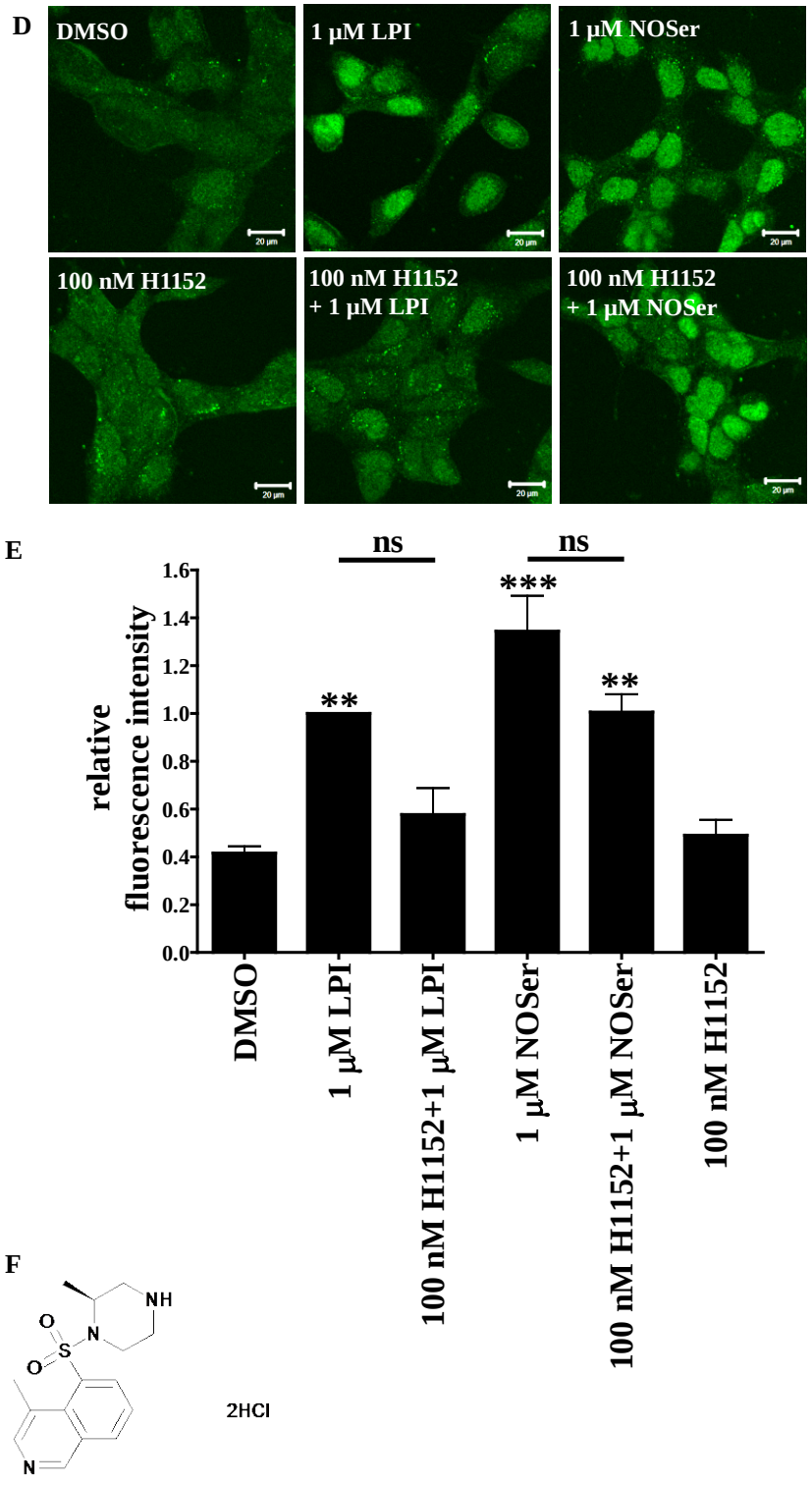

Figure 4.14: A role for ROCK signalling in GPR55-mediated pCREB signalling. *hGPR55-HEK293 cells were treated with ROCK inhibitors (either Y-27632 dihydrochloride; 10 µM or H1152 dihydrochloride; 100 nM) for 30 min prior to co-application of inhibitor and either 1 µM LPI or 1 µM NOSer for a further 25 min.* ***A****, representative confocal images of pCREB labelling in cells following treatment with: DMSO; 1 µM LPI; 1 µM NOSer; 10 µM Y-27632; 10 µM Y-27632 + 1 µM LPI; 10 µM Y-27632 + 1 µM NOSer.* *Scale bars = 20 µm; n = 3.* ***B****, histogram of pooled data, showing the mean CTNF of pCREB normalised to 1 µM LPI,*

hGPR55-HEK293 cells were challenged with either 1 µM LPI or 1 µM NOSer in the absence or presence of 10 µM Y-27632. ***C****, chemical structure of Y-27632 dihydrochloride.* ***D****, representative confocal images of nuclear pCREB in hGPR55-HEK293 cells following treatment with: DMSO; 1 µM LPI; 1 µM NOSer; 100 nM H1152; 100 nM H1152 + 1 µM LPI; 100 nM H1152 + 1 µM NOSer. Scale bars = 20 µm; n = 3.* ***E****, histogram depicting pooled pCREB data, highlighting the mean CTNF normalised to 1 µM LPI for responses to 1 µM LPI or 1 µM NOSer in the presence or absence of 100 nM H1152.* ***F****, chemical structure of H1152 dihydrochloride. Data are the means ± SEM; n = 3. * = compared to vehicle control. One-way ANOVA with a Bonferroni post hoc test; **P < 0.01; ***P < 0.001; ###P < 0.001; ns = not significant.*

4.2.1.9. Does Ca^{2+} play a role in GPR55-mediated pCREB signalling in hGPR55-HEK 293 cells?

Mobilisation of Ca^{2+} is downstream of GPR55 in hGPR55-HEK293 cells treated with either LPI or NOSer. Previous research has shown that Ca^{2+} plays a role in transcriptional regulation; where the amplitude and frequency of transient Ca^{2+} oscillations are important factors (Dolmetsch *et al.*, 1998). As GPR55-mediated Ca^{2+} mobilisation is oscillatory it suggests that Ca^{2+} may play an important role in pCREB in hGPR55-HEK293 cells treated with endogenous lipid ligands. Therefore this next set of experiments was designed to assess if Ca^{2+} is involved in GPR55-mediated pCREB signalling. To study if free cytosolic Ca^{2+} influences nuclear pCREB in hGPR55-HEK293 cells the cell permeable Ca^{2+} chelator, BAPTA-AM (50 µM), was utilised. Treatment with BAPTA-AM (50 µM; 55 min) itself resulted in a small increase in nuclear pCREB labelling, however when applied 30 min before and then in the presence of either of the lipids there was a lowering of nuclear pCREB observed ($F_{(5,6)} = 9.512$; $P = 0.0081$). There is a general trend whereby both LPI and NOSer are inhibited by BAPTA-AM; 78.12 ± 5.46% and 84.90 ± 6.33% respectively. However Bonferroni *post hoc* analysis revealed no significant difference between hGPR55-HEK293 cells treated with lipid alone or in the presence of BAPTA-AM. These data suggest that it is likely that chelation of intracellular Ca^{2+} exerts a small effect on pCREB responses in hGPR55-HEK293 cells treated with the endogenous lipids.

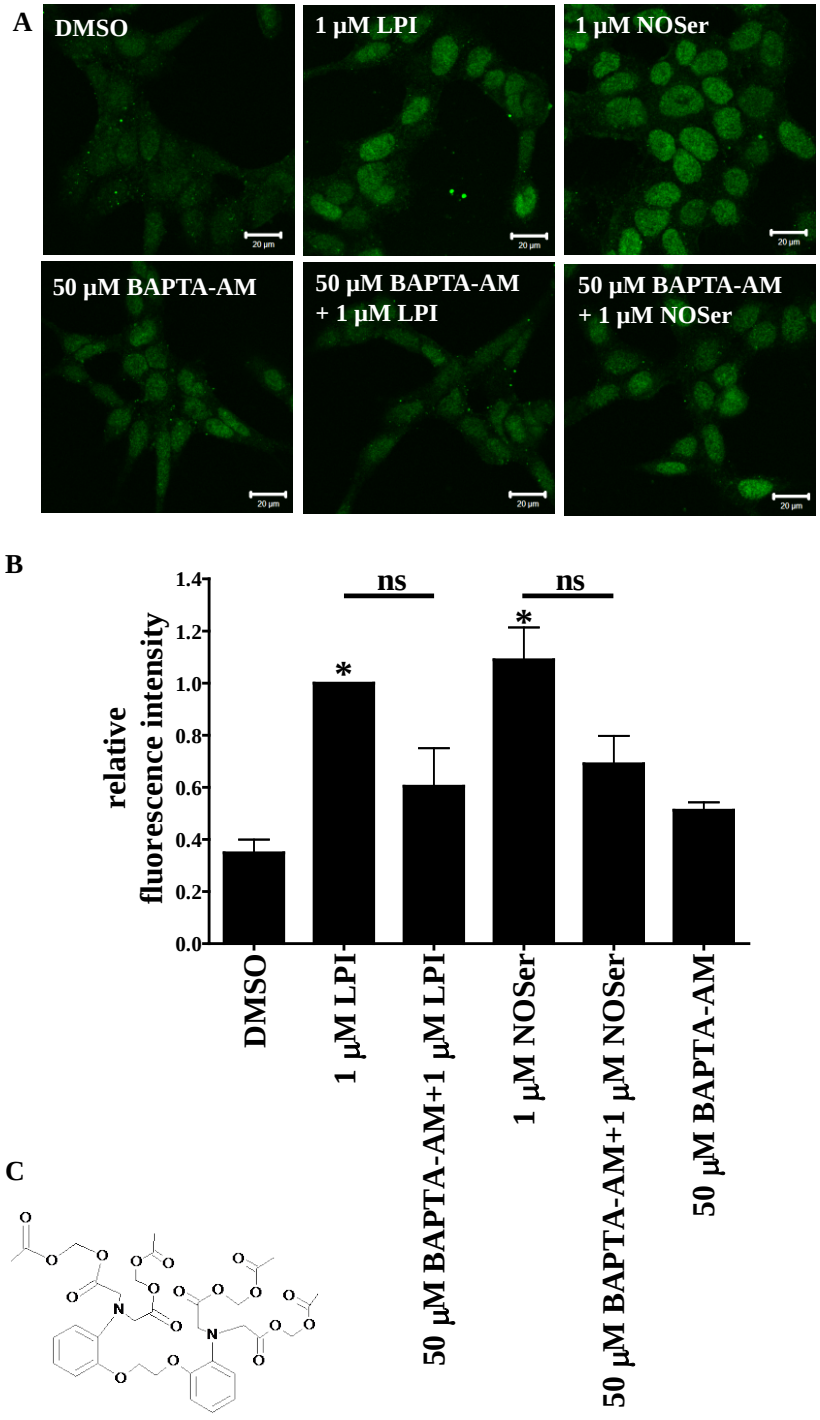

Figure 4.15: Intracellular Ca^{2+} chelation influences GPR55-mediated pCREB signalling. *hGPR55-HEK293 cells were treated for 30 min with a Ca^{2+} chelator (BAPTA-AM; 50 µM) prior to co-application of chelator with lipid.* ***A****, representative confocal images of nuclear pCREB labelling in cells following treatment with, DMSO; 1 µM LPI; 1 µM NOSer; 50 µM BAPTA-AM; 50 µM BAPTA-AM + 1 µM LPI; 50 µM BAPTA-AM + 1 µM NOSer. Scale bars = 20 µm; n = 2.* ***B****, histogram of pooled data, highlighting the mean CTNF normalised to 1 µM LPI for responses to either 1 µM LPI or 1 µM NOSer either in the absence or presence of 50 µM BAPTA-AM. Data are the means ± SEM; n = 2. Note chelation of Ca^{2+} decreases the nuclear pCREB labelling of lipid treated hGPR55-HEK293 cells.* ***C****, chemical structure of*

*BAPTA-AM. * = compared to vehicle control. One-way ANOVA with a Bonferroni post hoc test; *P < 0.05; ns = not significant.*

As oscillatory Ca^{2+} transients in hGPR55-HEK293 cells require extracellular Ca^{2+} (Henstridge *et al.*, 2009) the effects of extracellular Ca^{2+} on GPR55-mediated pCREB activity was studied. Thus hGPR55-HEK293 cells were pre-treated with Ca^{2+}-free HBS supplemented with 100 µM EDTA (CF-HBS) for 5 min prior to application of lipids in CF-HBS for a further 25 min. Analysis with a one-way ANOVA highlighted that there were significant differences across the CF-HBS experimental data ($F_{(5,12)}$ = 13.23; P = 0.0002). Treatment of cells with CF-HBS had no effect on basal pCREB activity (figure 4.16A and B). However, it was noted that cells in CF-HBS had a tendency to become retracted with a rounded morphology during the experiment. Responses to LPI in CF-HBS in hGPR55-HEK293 cells were markedly inhibited by 75.7 ±13.3% and were not significantly different from CF-HBS. Interestingly, in the presence of CF-HBS NOSer responses were inhibited to a lesser extent of 52.1 ±17.5% than observed with LPI. However despite the general trend of CF-HBS inhibiting the lipids, Bonferroni *post hoc* analysis revealed the inhibition was not significant. These data suggest that extracellular Ca^{2+} is likely to be involved in GPR55-mediated pCREB signalling in hGPR55-HEK293 cells treated with either of the lipids. Therefore, extracellular Ca^{2+} may be important for responses to LPI than NOSer.

PLC activation is reported to be required for GPR55-mediated Ca^{2+} mobilisation in hGPR55-HEK293 cells challenged with either cannabinoid ligands (Δ^9THC; JWH015) or LPI (Lauckner *et al.*, 2008; Henstridge *et al.*, 2009). The present study has also highlighted that PLC is required for NOSer-mediated Ca^{2+} mobilisation in hGPR55-HEK293 cells. Therefore the PLC inhibitor, U73122 (1 µM), was used to evaluate whether PLC is involved in GPR55-pCREB signalling in hGPR55-HEK293 cells. One-way ANOVA revealed significant differences within the experimental data ($F_{(5,12)}$ = 21.21; P < 0.0001). Bonferroni *post hoc* analysis highlighted that treatment with U73122 itself (1 µM) did not significantly affect pCREB levels (figure 4.17A and B). However, responses to LPI and NOSer were inhibited in cells treated with co-application of U73122 by 75.6 ±3.5% and 63.7 ±10.1% respectively compared to cells treated with lipid alone. These data suggest that PLC is involved in promoting pCREB in hGPR55-HEK293 cells treated with endogenous lipids.

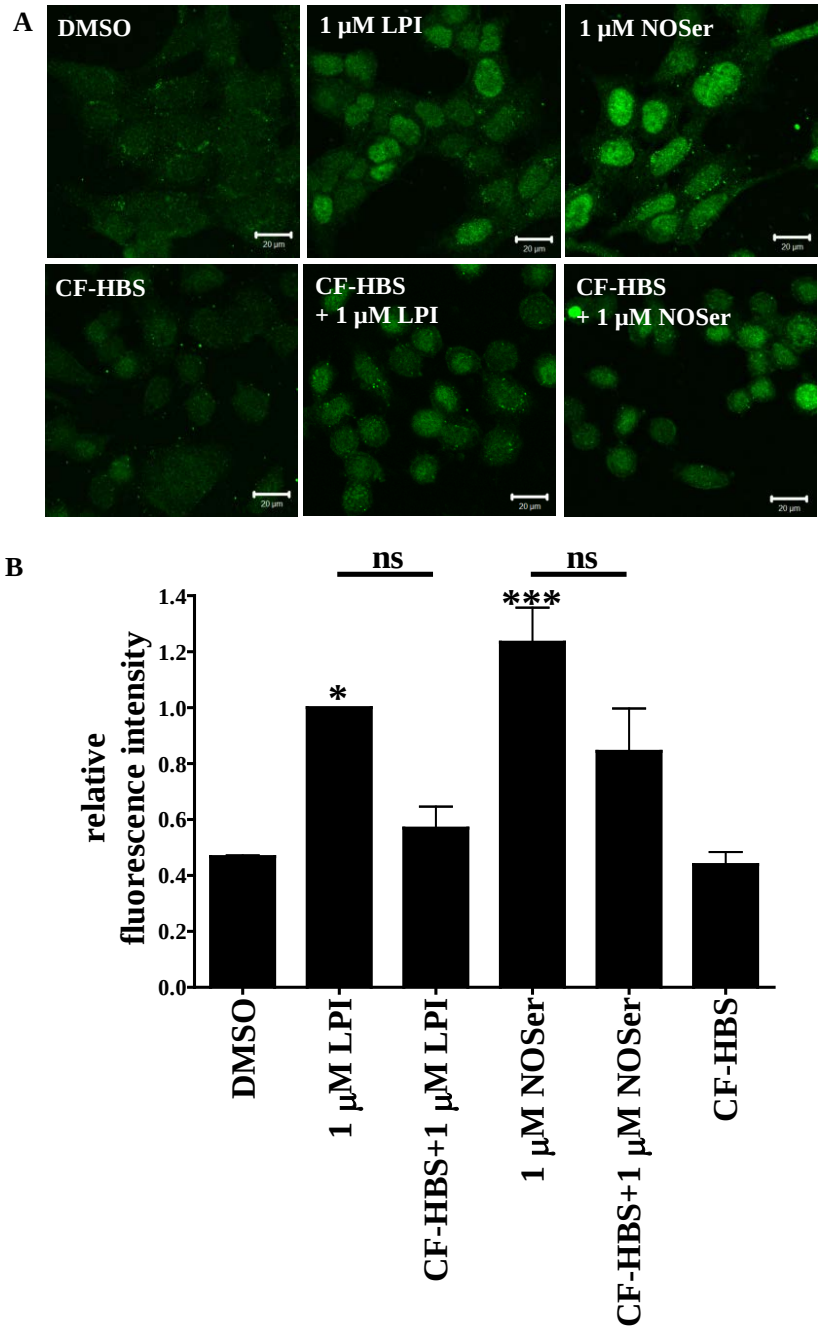

Figure 4.16: A role for extracellular Ca^{2+} in GPR55-mediated pCREB signalling. *hGPR55-HEK293 cells were placed in normal extracellular Ca^{2+} or Ca^{2+} free HBS + 100 µM EDTA (CF-HBS) for 5 min prior to the addition of the appropriate lipid ligand.* ***A****, representative confocal images of nuclear pCREB labelling in cells following treatment with: DMSO; 1 µM LPI; 1 µM NOSer; CF-HBS; CF-HBS + 1 µM LPI; CF-HBS + 1 µM NOSer. Scale bars = 20 µm; n = 3.* ***B****, histogram of pooled data; depicting the mean CTNF normalised to 1 µM LPI of pCREB in hGPR55-HEK293 cells treated with either 1 µM LPI, 1 µM NOSer in HBS or with the lipid in CF-HBS. Note extracellular Ca^{2+} is involved for GPR55-mediated nuclear pCREB activity in hGPR55-HEK293 cells. * = data compared to vehicle control. Data are the means ± SEM; n = 3. One-way ANOVA with a Bonferroni post hoc test; *P < 0.05; ***P < 0.001; ns = not significant.*

CaMKII has been implicated in signalling to CREB (Zanassi *et al.*, 2001) and can be activated by an increase in intracellular Ca^{2+}. Therefore the cell permeable CaMKII inhibitor KN-62 (Tokumitsu *et al.*, 1990) was tested on the hGPR55-HEK293 cells. One-way ANOVA analysis highlighted significant differences within the CAMKII experimental data ($F_{(5,12)} = 11.79$; $P = 0.0003$). Further analysis with a Bonferroni *post hoc* test revealed that cells treated with the CaMKII inhibitor KN-62 (2 μM) alone did not significantly affect basal pCREB levels. However, although the general trend was one whereby lower pCREB responses was observed where the lipids were co-applied with KN-62 however this was not significantly different to lipid alone. It is likely that CAMKII is required to promote nuclear pCREB responses in hGPR55-HEK293 cells challenged with either LPI or NOSer (figure 4.18A and B).

PKC a kinase activated downstream of PLC or via increased Ca^{2+} has been implicated as a signalling mediator leading to CREB phosphorylation (Zanassi *et al.*, 2001). Therefore Gö6983 (1 μM), a cell permeable, selective PKC inhibitor was tested on LPI and NOSer responses in hGPR55-HEK293 cells. One-way ANOVA revealed significant differences across the experimental data ($F_{(5,12)} = 32.31$; $P < 0.0001$). Therefore the data was subjected to a Bonferroni *post hoc* test where it highlighted that treatment with Gö6983 alone did not affect basal pCREB levels (figure 4.19A and B). However, LPI or NOSer when co-applied with Gö6983 exhibited reduced nuclear pCREB responses by 81.1 ± 3.5% and 60.3 ± 5.7% respectively.

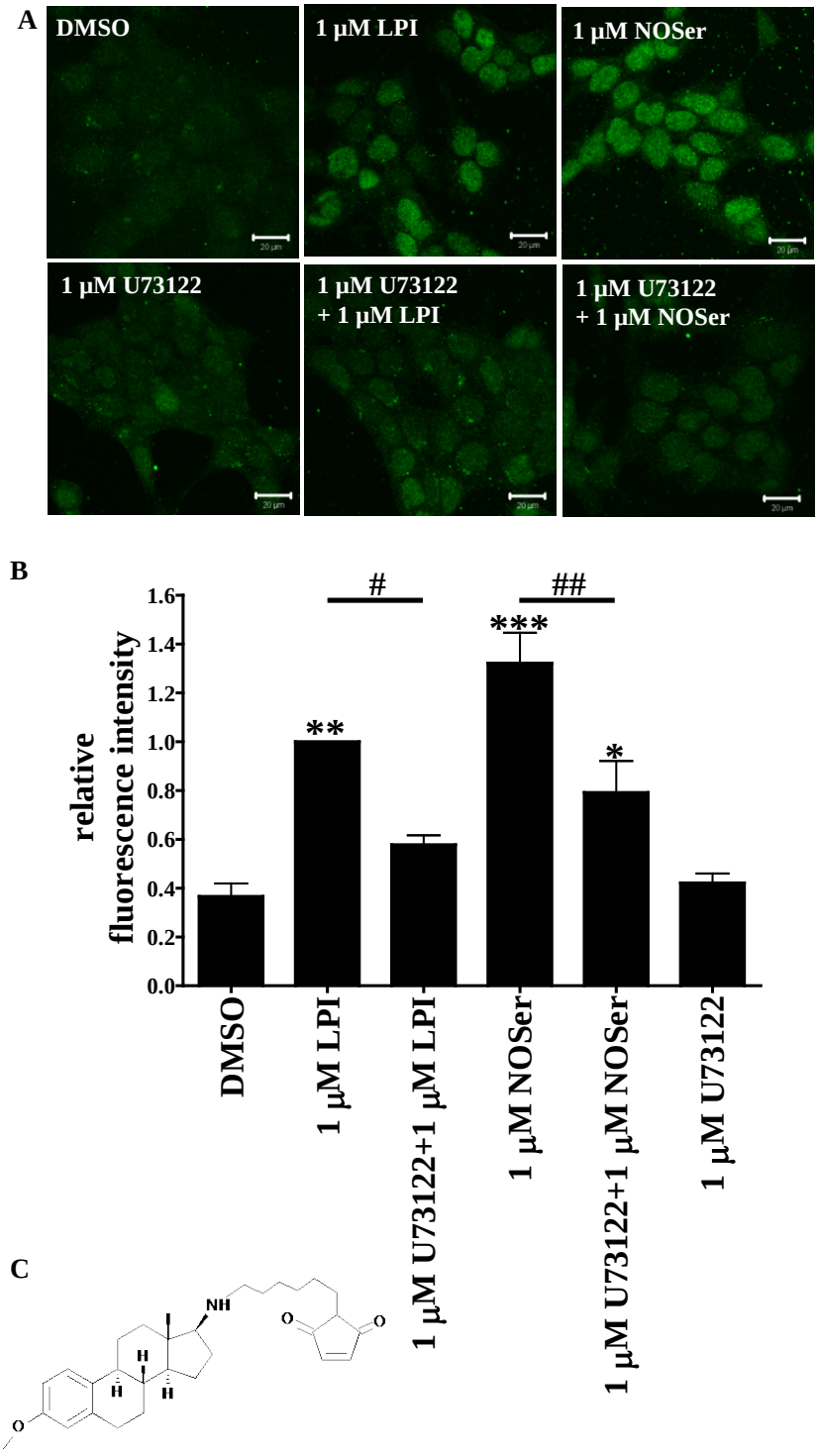

Figure 4.17: A role for PLC in GPR55-mediated nuclear pCREB signalling in hGPR55-HEK293 cells treated with endogenous lipids. *Cells were treated for 30 min with a PLC inhibitor (U73122; 1 µM) prior to co-application of inhibitor with ligand.* ***A****, representative confocal images of nuclear pCREB in hGPR55-HEK293 cells following treatment with: DMSO; 1 µM LPI; 1 µM NOSer; 1 µM U73122; 1 µM U73122 + 1 µM LPI; 1 µM U73122 + 1 µM NOSer. Scale bars = 20 µm. n = 3.* ***B****, histogram of pooled data, showing the mean CTNF normalised to 1 µM LPI of pCREB when hGPR55-HEK293 cells were challenged with either 1*

µM LPI or 1 µM NOSer either with or without co-application of 1 µM U73122. Note inhibition of PLC decreases the immunolabelling of lipid-induced nuclear pCREB. ***C****, structure of U73122. Data are the means ± SEM; n = 3. * = compared to vehicle control. One-way ANOVA with a Bonferroni post hoc test; *P < 0.05; **P < 0.01; ***P < 0.001; #P < 0.05; ##P < 0.01.*

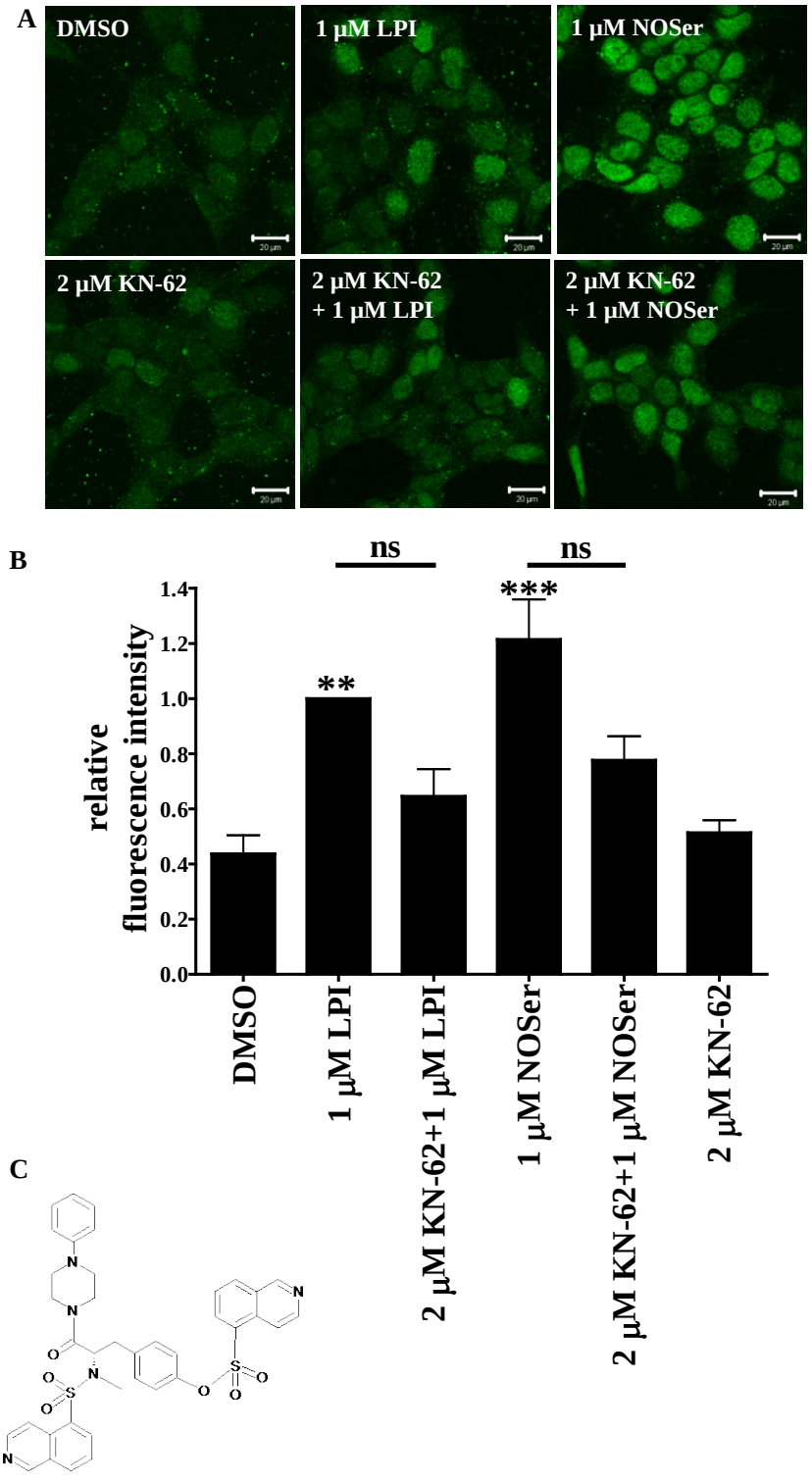

Figure 4.18: CaMKII is involved in GPR55-mediated nuclear pCREB responses in hGPR55-HEK293 cells treated with endogenous lipids. *Cells were treated for 30 min with a CaMKII*

inhibitor (KN-62; 2 µM) prior to co-application of inhibitor with lipid ligands. ***A****, representative confocal images of pCREB in hGPR55-HEK293 cells treated as follows: DMSO; 1 µM LPI; 1 µM NOSer; 2 µM KN-62; 2 µM KN-62 + 1 µM LPI; 2 µM KN-62 + 1 µM NOSer. Scale bars = 20 µm; n = 3.* ***B****, histogram of pooled data, showing the mean pCREB CTNF normalised to 1 µM LPI when hGPR55-HEK293 cells were challenged with either 1 µM LPI or 1 µM NOSer either in the absence or presence of 2 µM KN-62.* ***C****, chemical structure of KN-62. Data are the means ± SEM; n = 75 cells derived from 3 independent experiments. * = compared to vehicle control. One-way ANOVA with a Bonferroni post hoc test; **P < 0.01; ***P < 0.001; ns = not significant.*

4.2.1.10. Phosphoinositide-3 kinase and mammalian Target of Rapamycin (mTOR) promotes pCREB in hGPR55-HEK293 cells challenged with endogenous lipids.

In HUVEC cells GPR55-mediated Ca^{2+} mobilisation requires PI-3 kinase which then activates PLCγ (Falasca *et al.*, 1998; Waldeck-Weiermair *et al.*, 2008). As observed in the present study the broad spectrum PLC inhibitor decreased agonist-stimulated pCREB in hGPR55-HEK293 cells. Although the PLC isoform is unknown it is possible that PI-3 kinase may influence PLC in these cells. Furthermore, PI-3 kinase is an upstream mediator of AKT (Dugourd *et al.*, 2003) and GPR55 is reported to activate AKT in PC3 and DU145 prostate cancer cells (Piñeiro *et al.*, 2011). The AKT/PKB pathway can also promote pCREB (Du and Montminy, 1998; Das *et al.*, 2005). Therefore these experiments were designed to study the effect that PI-3-kinase inhibitors exert on GPR55-mediated pCREB when applied to hGPR55-HEK293 cells. One-way ANOVA analysis highlighted significant differences across the data set ($F_{(5,12)}$ = 13.37; P = 0.0001). Bonferroni *post hoc* analysis revealed that treatment of cells with LY294002 (3 µM) did not affect basal pCREB levels (figure 4.20A and B). However, LPI (1 µM) pCREB responses were inhibited by 91.0 ± 10.3% when co-applied with LY294002 compared to LPI treatment alone but were not significant. Likewise with NOSer (1 µM), responses were significantly inhibited by 74.6 ± 8.0% with LY294002.

To further determine that PI-3 kinase is involved in GPR55-mediated nuclear pCREB signalling, wortmannin, a structurally distinct PI-3 kinase inhibitor was tested. There were significant differences within the experimental data highlighted with one-way ANOVA analysis ($F_{(5,12)}$ = 16.04; P < 0.0001). Wortmannin alone did not affect basal pCREB levels (figure 4.20D and E). However, when wortmannin treatment reduced pCREB responses to LPI or NOSer by 89.2 ± 7.2% and 84.9 ± 7.5% respectively compared with agonist treatments alone.

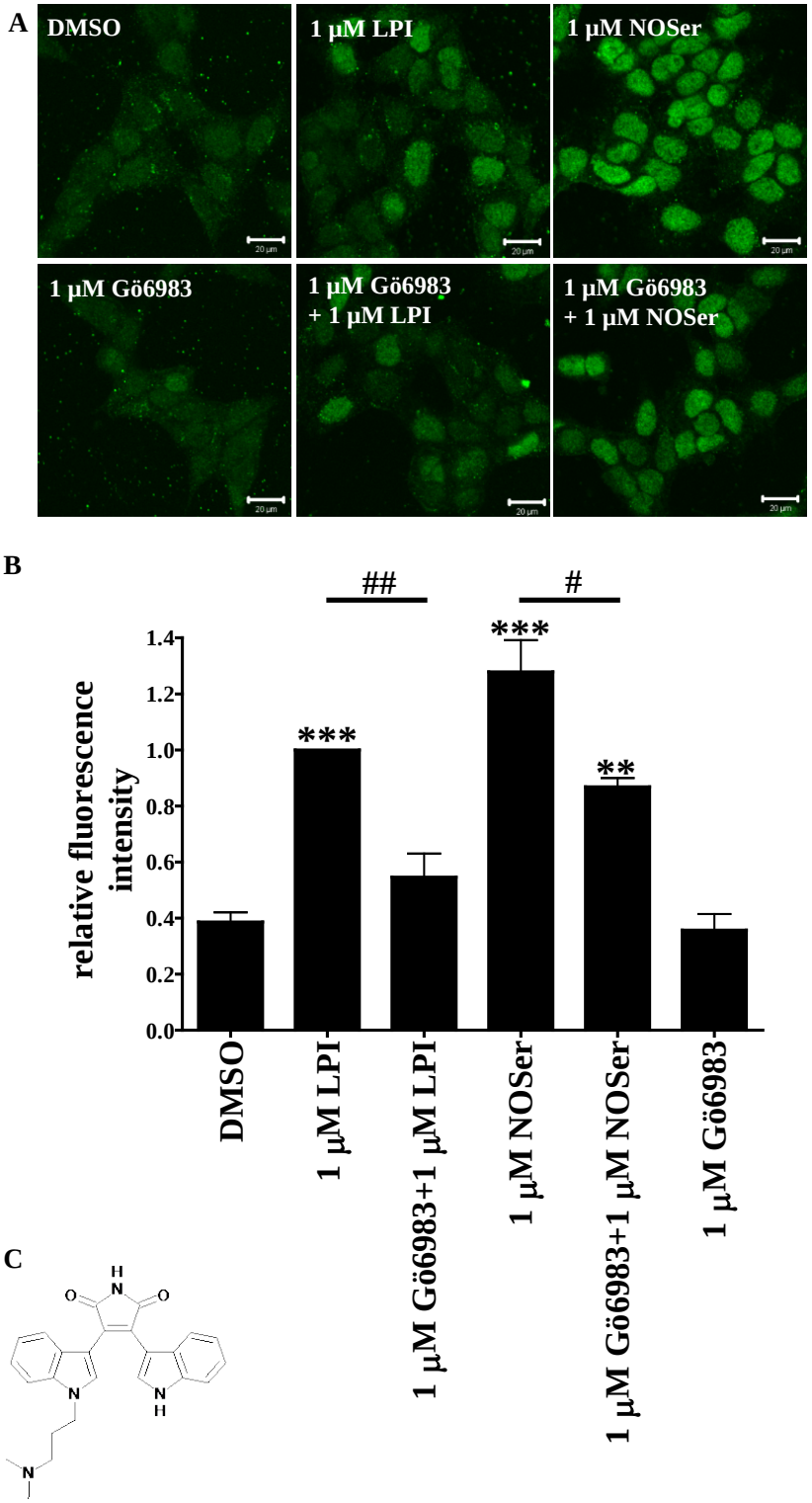

Figure 4.19: PKC is involved in GPR55-mediated pCREB responses in hGPR55-HEK293 cells treated with endogenous lipids. *Cells were treated for 30 min with a PKC inhibitor (Gö6983; 1 µM) prior to co-application of inhibitor with lipid ligands.* ***A****, representative confocal images of nuclear pCREB in hGPR55-HEK293 cells treated as follows****:*** *DMSO; 1 µM LPI; 1 µM NOSer; 1 µM Gö6983; 1 µM Gö6983 + 1 µM LPI; 1 µM Gö6983 + 1 µM NOSer. Scale bars = 20 µm; n = 3.* ***B****, histogram of pooled data, depicting the mean pCREB CTNF*

normalised to 1 µM LPI for hGPR55-HEK293 cells were challenged with either 1 µM LPI or 1 µM NOSer in the absence or presence of 1 µM Gö6983. ***C****, chemical structure of Gö6983. Data are the means ± SEM; n = 75 cells derived from 3 independent experiments. * = compared to vehicle control. One-way ANOVA with a Bonferroni post hoc test; **P < 0.01; ***P < 0.001; # < 0.05; ##P < 0.01.*

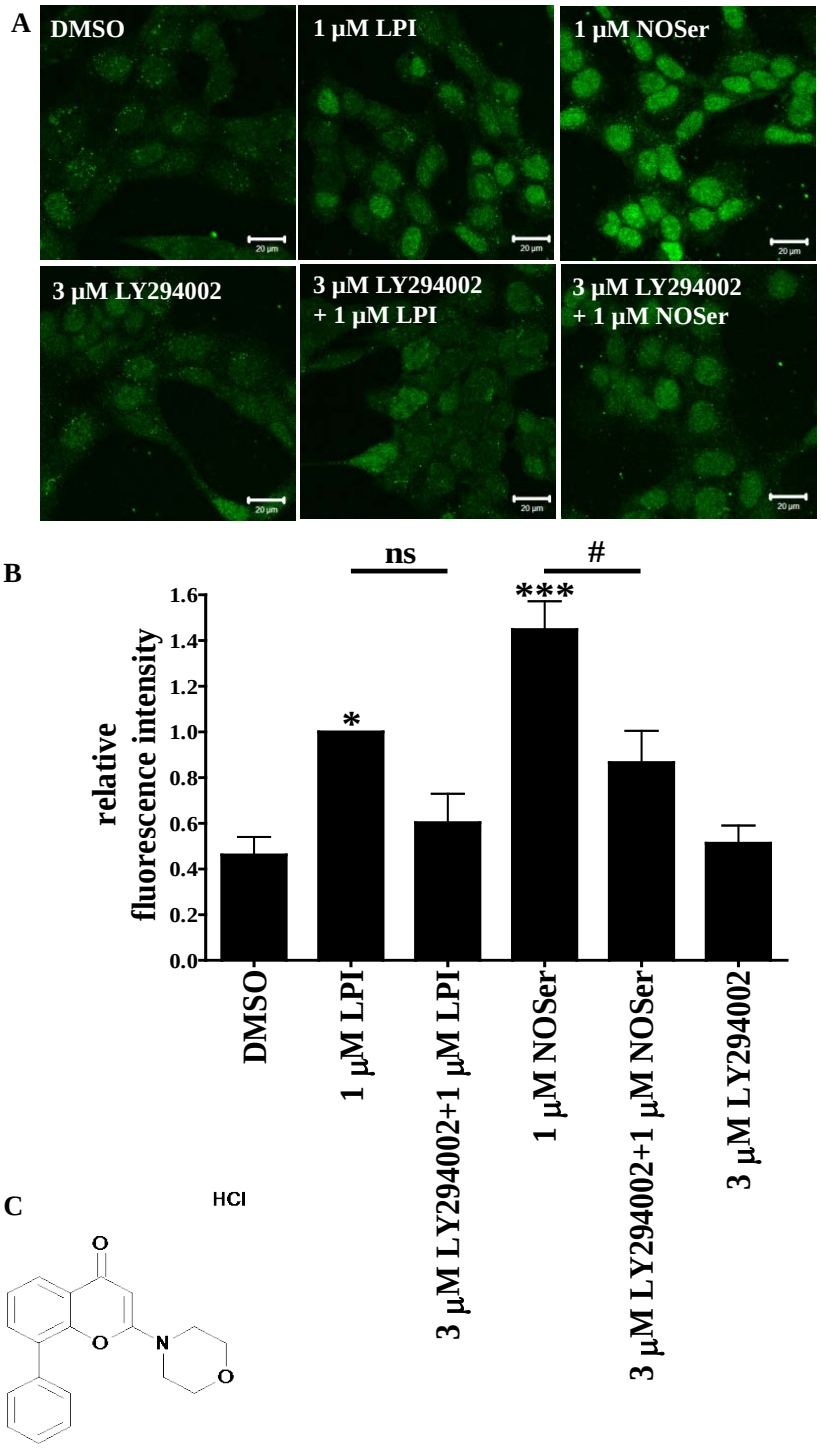

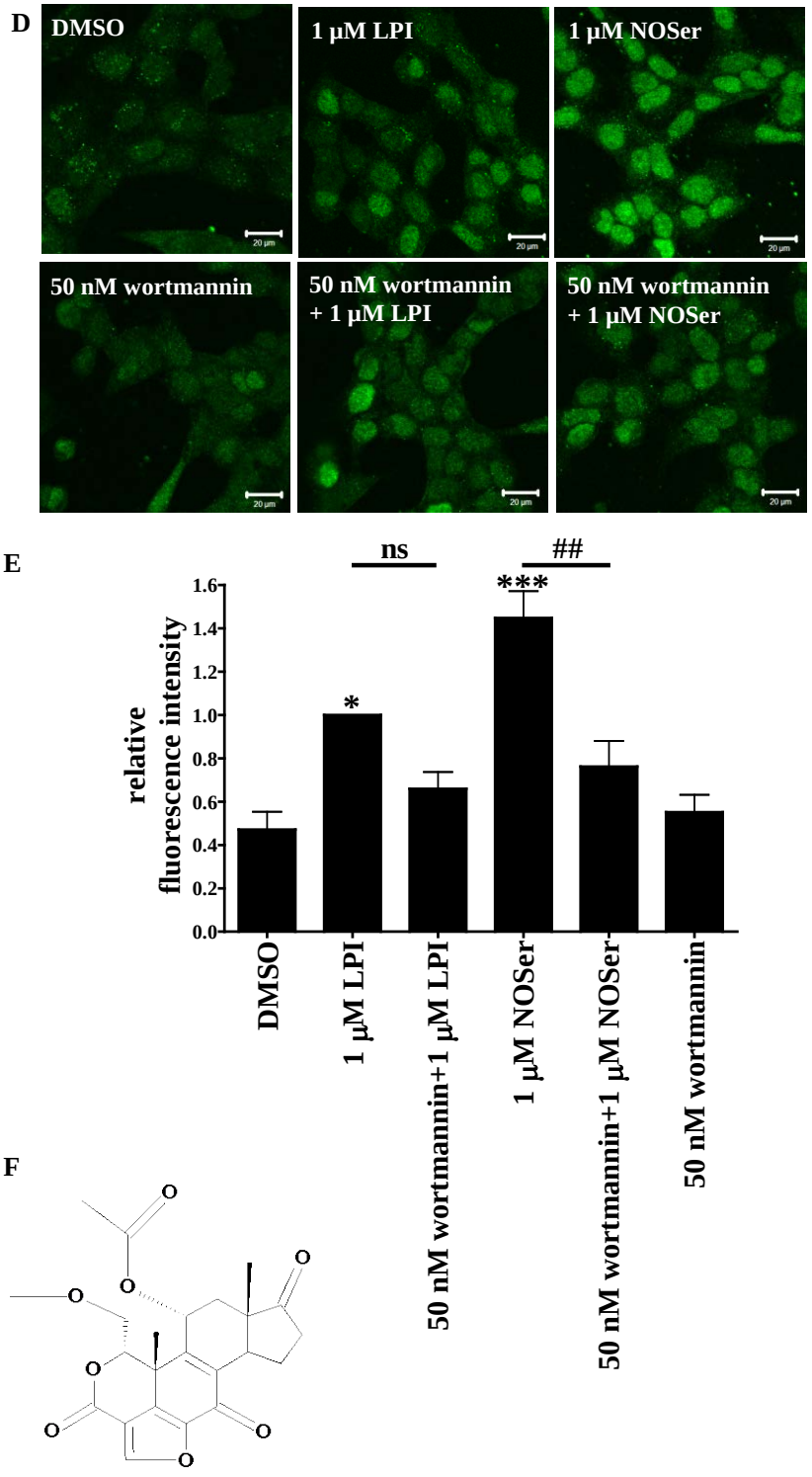

4.20: PI-3 kinase is involved in NOSer induced GPR55-mediated pCREB signalling. *hGPR55-HEK293 cells were treated for 30 min with PI-3 kinase inhibitors (LY294002; 3 µM or wortmannin; 50 nM) prior to co-application of inhibitor with a lipid.* ***A****, representative confocal images of nuclear pCREB in cells following treatment with: DMSO; 1 µM LPI; 1 µM NOSer; 3 µM LY294002; 3 µM LY294002 + 1 µM LPI; 3 µM LY294002 + 1 µM NOSer. Scale bars = 20 µm. n = 3.* ***B****, histogram of pooled data, showing the mean CTNF normalised to 1 µM LPI of nuclear pCREB when hGPR55-HEK293 cells were challenged with either 1 µM LPI*

or 1 µM NOSer either in the presence of absence of 3 µM LY294002. ***C****, chemical structure of LY294002.* ***D****, representative confocal images of hGPR55-HEK293 cells following treatment with DMSO; 1 µM LPI; 1 µM NOSer; 50 nM wortmannin; 50 nM wortmannin + 1 µM LPI; 50 nM wortmannin + 1 µM NOSer. Scale bars = 20 µm; n = 3.* ***E****, histogram of pooled data, highlighting the mean CTNF normalised to 1 µM LPI of nuclear pCREB in hGPR55-HEK 293 cells when treated with either 1 µM LPI or 1 µM NOSer alone or in the presence of 50 nM wortmannin.* ***F****, chemical structure of wortmannin. Note that two structurally distinct PI-3 kinase inhibitors decreased the NOSer-induced nuclear pCREB in hGPR55-HEK293 cells. Data are the means ± SEM; n = 3. * = compared to vehicle control. One-way ANOVA with a Bonferroni post hoc test; *P < 0.05; ***P < 0.001; #P < 0.05; ##P < 0.01; ns = not significant.*

The kinase mTOR is downstream of PI-3 kinase activation and has the ability to regulate AKT phosphorylation and as such may influence pCREB (Vogt, 2001). This is the first study to look at potential GPR55-mediated mTOR effects. One-way ANOVA highlighted a significant difference within the experimental data ($F_{(5,12)}$ = 3.824; P = 0.0265). A Bonferroni *post hoc* test revealed that treatment of cells with rapamycin (50 nM; 55 min) resulted in a slight elevation, but not significant, on pCREB staining relative to vehicle control, basal levels (figure 4.21A and B). Treatment with rapamycin lowered the nuclear pCREB responses to both LPI and NOSer but was not significant. The increase in pCREB responses to the presence of rapamycin alone makes it difficult to decipher the inhibition that is occurring with each of the endogenous lipids. Further experiments would be required to allow a better understanding. However these data suggest that mTOR is not required for GPR55 ligand-induced nuclear pCREB in hGPR55-HEK293 cells.

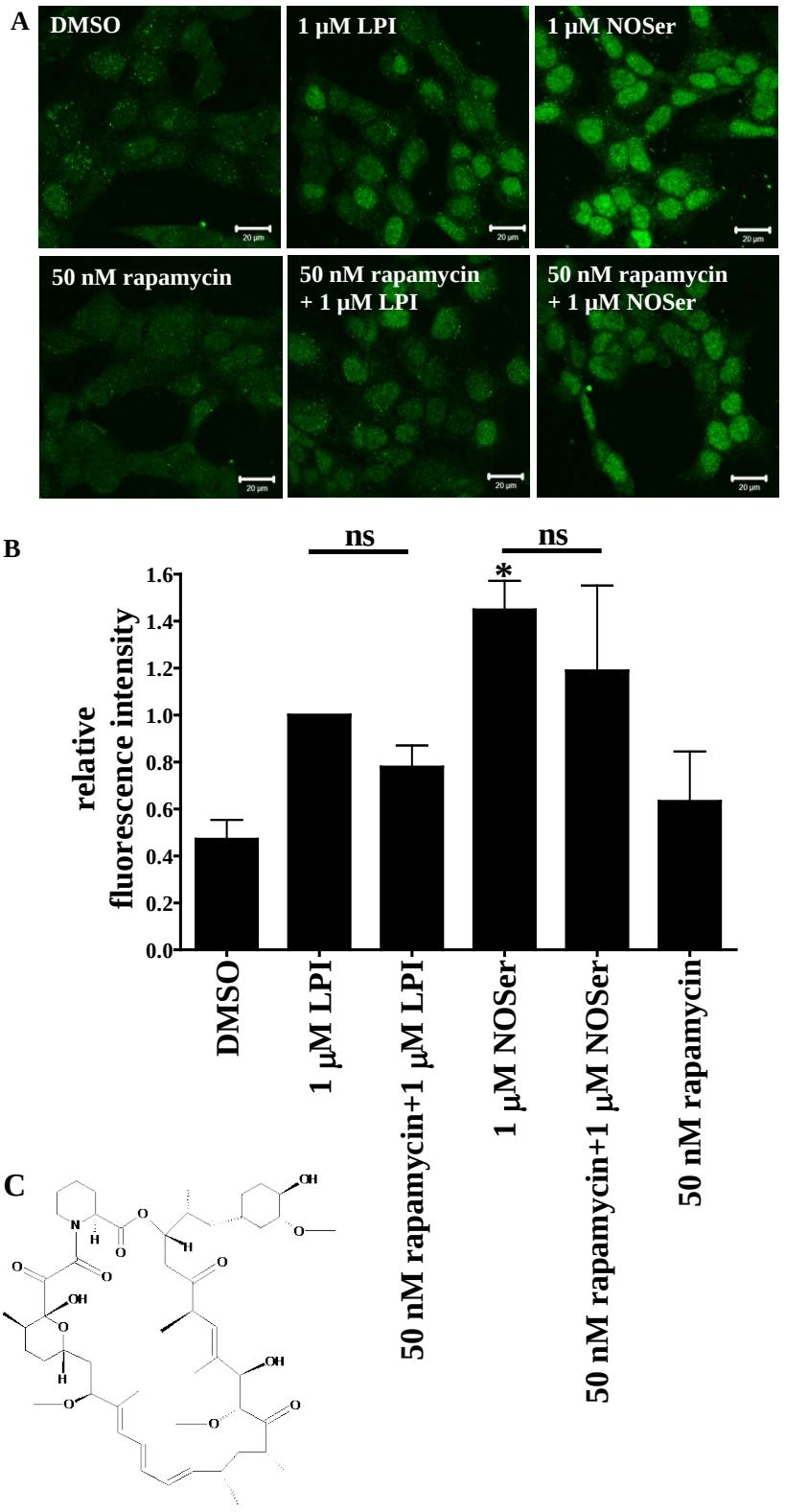

Figure 4.21: A role for mTOR in GPR55-pCREB signalling. *The mTOR inhibitor (rapamycin; 50 nM) was applied to hGPR55-HEK293 cells for 30 min prior to co-application with either of the lipids.* ***A****, representative confocal images of nuclear pCREB labelling in cells following treatment with DMSO; 1 µM LPI; 1 µM NOSer; 50 nM rapamycin; 50 nM rapamycin + 1 µM LPI; 50 nM rapamycin + 1 µM NOSer. Scale bars = 20 µm; n = 2.* ***B****, histogram of pooled data; depicting the mean CTNF normalised to 1 µM LPI of nuclear pCREB in hGPR55-*

*HEK293 cells treated with either 1 µM LPI, 1 µM NOSer or either lipid co-applied with 50 nM rapamycin. * = data compared to vehicle control. Data are the means ±SEM; n = 2. One-way ANOVA with a Bonferroni post hoc test; *P < 0.05; ns = not significant.*

4.2.1.11. The MAP kinase pathway contributes to GPR55-pCREB signalling in hGPR55-HEK293 cells.

Ca^{2+} is one pathway that is associated with pCREB. Other signalling pathways, however can induce pCREB, one of which is MAPK (Wade, 2003). LPI acting via GPR55 can activate the MAP kinase pathway leading to phosphorylation of ERK1/2 (Oka *et al.*, 2007; Henstridge *et al.*, 2010; Anavi-Goffer *et al.*, 2012). Therefore, MEK1/2 inhibitors (protein upstream of ERK1/2) were utilised to study a potential role for MAPK in GPR55-mediated nuclear pCREB signalling in hGPR55-HEK293 cells. A one-way ANOVA highlighted a significant difference within MAPK experimental data ($F_{(8,18)}$ = 7.025; P = 0.0003). The MEK1/2 inhibitors PD98059 (25 µM) or U0126 (5 µM) did not affect basal pCREB staining (figure 4.22A and B). In the presence of PD98059 pCREB responses to LPI or NOSer were inhibited by 86.8 ± 7.2% and 76.2 ± 11.8% respectively. Furthermore the presence of U0126 inhibited pCREB responses to LPI or NOSer by 95.2 ± 3.5% and 68.6 ± 7.9% respectively. These data highlight that LPI was significantly inhibited but in contrast NOSer effects were not significant However NOSer did exert a general trend of inhibiting pCREB when the MEK1/2 inhibitors were present.

To further confirm the MEK1/2 inhibitors results, U0124 (5 µM), an inactive analogue of U0126 was employed. Analysis by one-way ANOVA highlighted significant differences within the experimental data ($F_{(5,12)}$ = 20.30; P < 0.0001). Furthermore a subsequent Bonferroni *post hoc* test revealed that vehicle control produced basal levels of pCREB that was not localised to the nucleus. U0124 by itself did not affect basal pCREB levels (figure 4.22D and E). Responses to LPI and NOSer in the presence of U0124 were also not effected. These results suggest that the MAPK pathway is involved in GPR55-pCREB signalling in hGPR55-HEK293 cells when challenged with LPI and is likely to be important in NOSer induced pCREB.

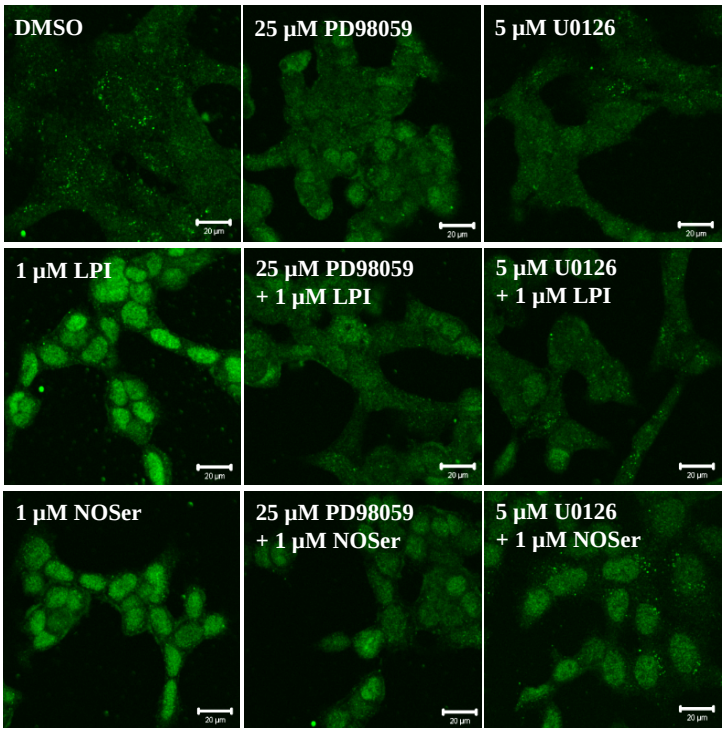
DMSO
25 µM PD98059
5 µM U0126
1 µM LPI
25 µM PD98059
+ 1 µM LPI
5 µM U0126
+ 1 µM LPI
1 µM NOSer
25 µM PD98059
+ 1 µM NOSer
5 µM U0126
+ 1 µM NOSer

B

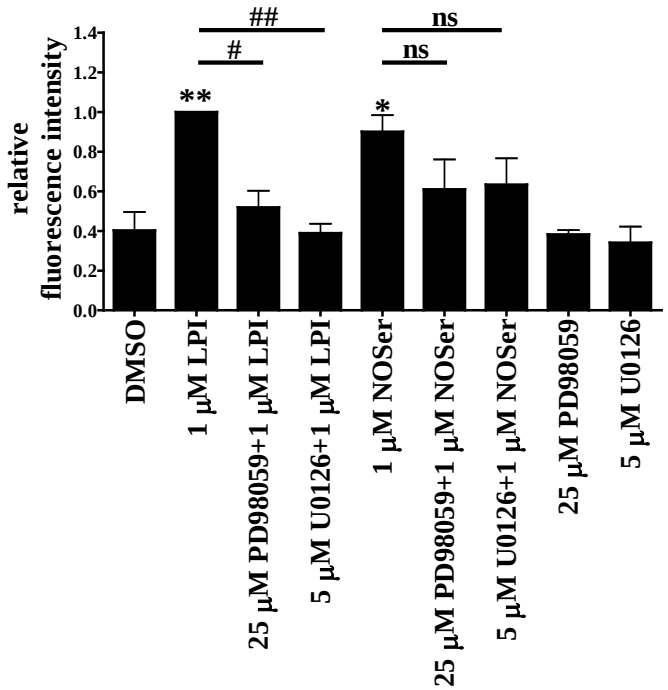
relative fluorescence intensity
0.0
0.2
0.4
0.6
0.8
1.0
1.2
1.4
##
#
ns
ns
**
*
DMSO
1 µM LPI
25 µM PD98059+1 µM LPI
5 µM U0126+1 µM LPI
1 µM NOSer
25 µM PD98059+1 µM NOSer
5 µM U0126+1 µM NOSer
25 µM PD98059
5 µM U0126

Ci

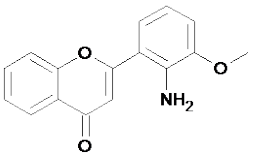
O
O
NH2
O

Cii

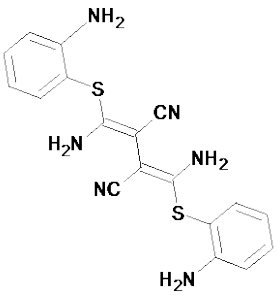
NH2
S
CN
H2N
NH2
NC
S
H2N

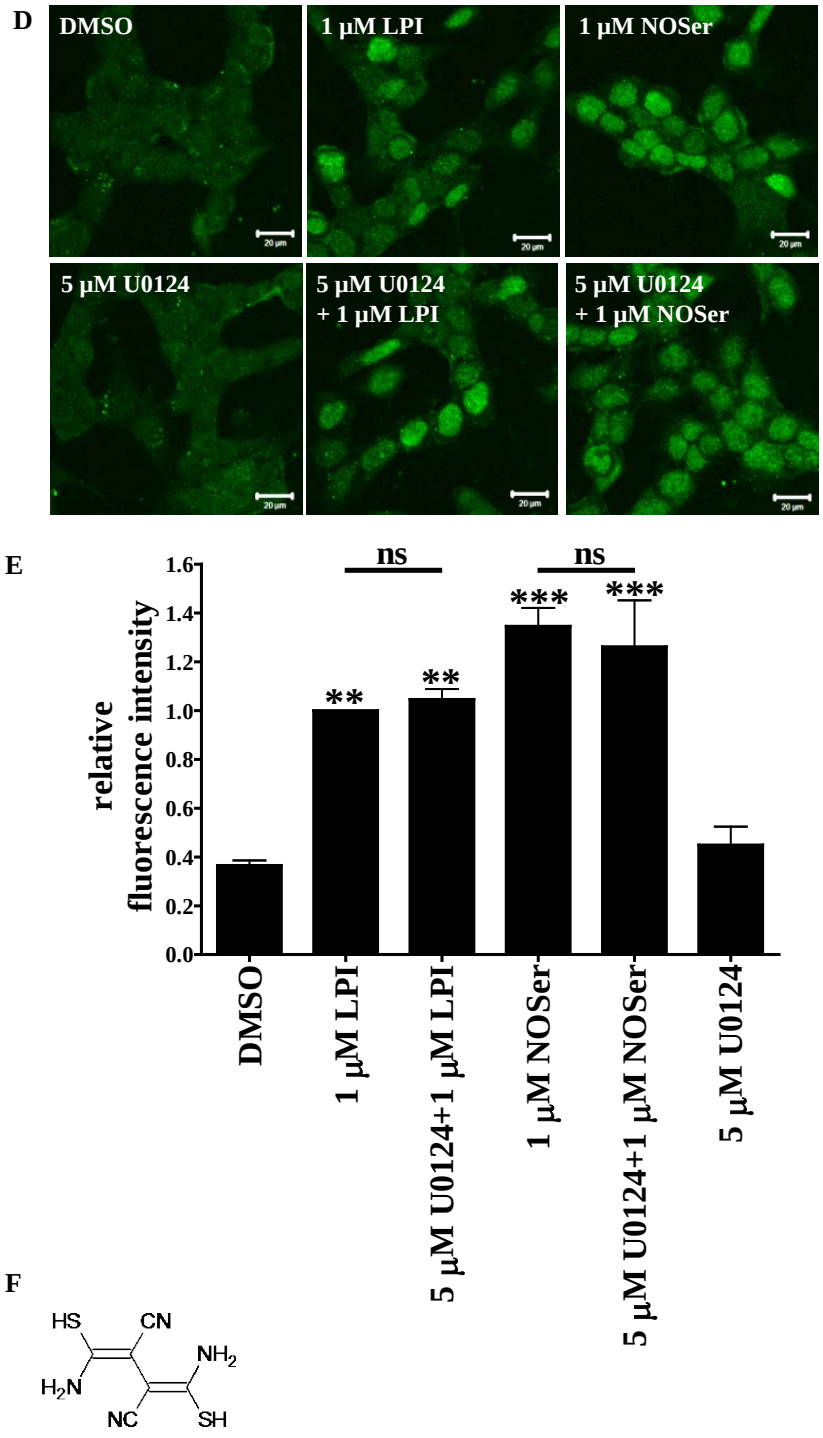

Figure 4.22: MAPK is involved in GPR55-pCREB signalling in hGPR55-HEK293 cells treated with endogenous lipids. *Cells were treated for 30 min with MEK1/2 inhibitors (PD98059; 25 µM or U0126; 5 µM) prior to co-application of inhibitor with lipid ligands. Alternatively cells were treated for 30 min with an inactive form of MEK inhibitor (U0124; 5 µM) prior to the lipids being co-applied.* ***A****, representative confocal images of nuclear pCREB in hGPR55-HEK293 following treatment with DMSO; 25 µM PD98059; 5 µM U0126; 1 µM LPI; 25 µM PD98059 + 1 µM LPI; 5 µM U0126 + 1 µM LPI; 1 µM NOSer; 25 µM PD98059 + 1 µM NOSer; 5 µM U0126 + 1 µM NOSer. Scale bars = 20 µm. n = 3.* ***B****, histogram of*

pooled data, showing the mean CTNF normalised to 1 µM LPI of pCREB in hGPR55-HEK293 cells which were challenged with either 1 µM LPI or 1 µM NOSer either with or without MEK1/2 inhibitors either 25 µM PD98059 or 5 µM U0126. ***C****, chemical structures of the MEK1/2 inhibitors are as follows* ***i****, PD98059;* ***ii****, U0126.* ***D****, representative confocal images of hGPR55-HEK293 cells challenged as follows: DMSO; 1 µM LPI; 1 µM NOSer; 5 µM U0124; 5 µM U0124 + 1 µM LPI; 5 µM U0124 + 1 µM NOSer. Scale bars = 20 µm; n = 3.* ***E****, histogram of pooled data, highlighting the CTNF normalised to 1 µM LPI of pCREB in hGPR55-HEK293 cells challenged with either 1 µM LPI or 1 µM NOSer either alone or in the presence of 5 µM U0124.* ***F****, structure of U0124; an inactive analogue of U0126. Data are the means ± SEM; n = 3. * = compared to vehicle control. One-way ANOVA with a Bonferroni post hoc test; *P < 0.05; **P < 0.01; ***P < 0.001; #P < 0.05; ##P < 0.01; ns = not significant.*

4.2.2. The actin cytoskeleton and the focal adhesion protein, vinculin.

These final sets of experiments were carried out to study effects the endogenous lipids could exert on the actin cytoskeleton or vinculin, a focal adhesion protein. Whilst previous studies have highlighted morphological changes in neutrophils; HL60, hGPR55-HEK293 (Balenga *et al.*, 2011) and the breast cancer cell line; MDA-MB-231 (Ford *et al.*, 2010) when treated with LPI. NOSer has not been studied in a GPR55-mediated cytoskeletal assay. This is also the first study using a novel FA assay to assess changes induced by the two endogenous lipids; LPI and NOSer.

4.2.2.1. Endogenous lipids modulate the actin cytoskeleton and FA length in hGPR55-HEK293 cells.

In order to investigate the effects of GPR55 ligands on the F-actin cytoskeleton, hGPR55-HEK293 cells were treated with Alexa fluor® 546 phalloidin following ligand exposure and subsequent fixation and permeabilisation. Endogenous lipids were applied for various times. Following 10 min ligand treatment, the cytoskeleton of LPI (1 µM) and NOSer (1 µM) challenged hGPR55-HEK293 cells were similar to vehicle control (DMSO) cells (figure 4.23). It should be noted that at each of the time points the control cells had a cell morphology that was flat and spread out. Application of the lipid ligands for 15 min promoted a modest cytoskeletal reorganisation with some stress fibres (depicted by arrowheads) being observed. Longer treatments with either of the endogenous lipids promoted the formation of additional stress fibres (depicted by arrowheads) and morphological changes whereby lamellipodia (depicted by arrows) were observed. These effects were pronounced at 60 min with more of the cells being

observed to have both lamellipodia and stress fibres present. It was observed that as the time was increased the proportion of cells with cytoskeletal reorganisation was increased. However due to the nature of phalloidin whereby it can dissociate with time, no quantitative analysis was carried out.

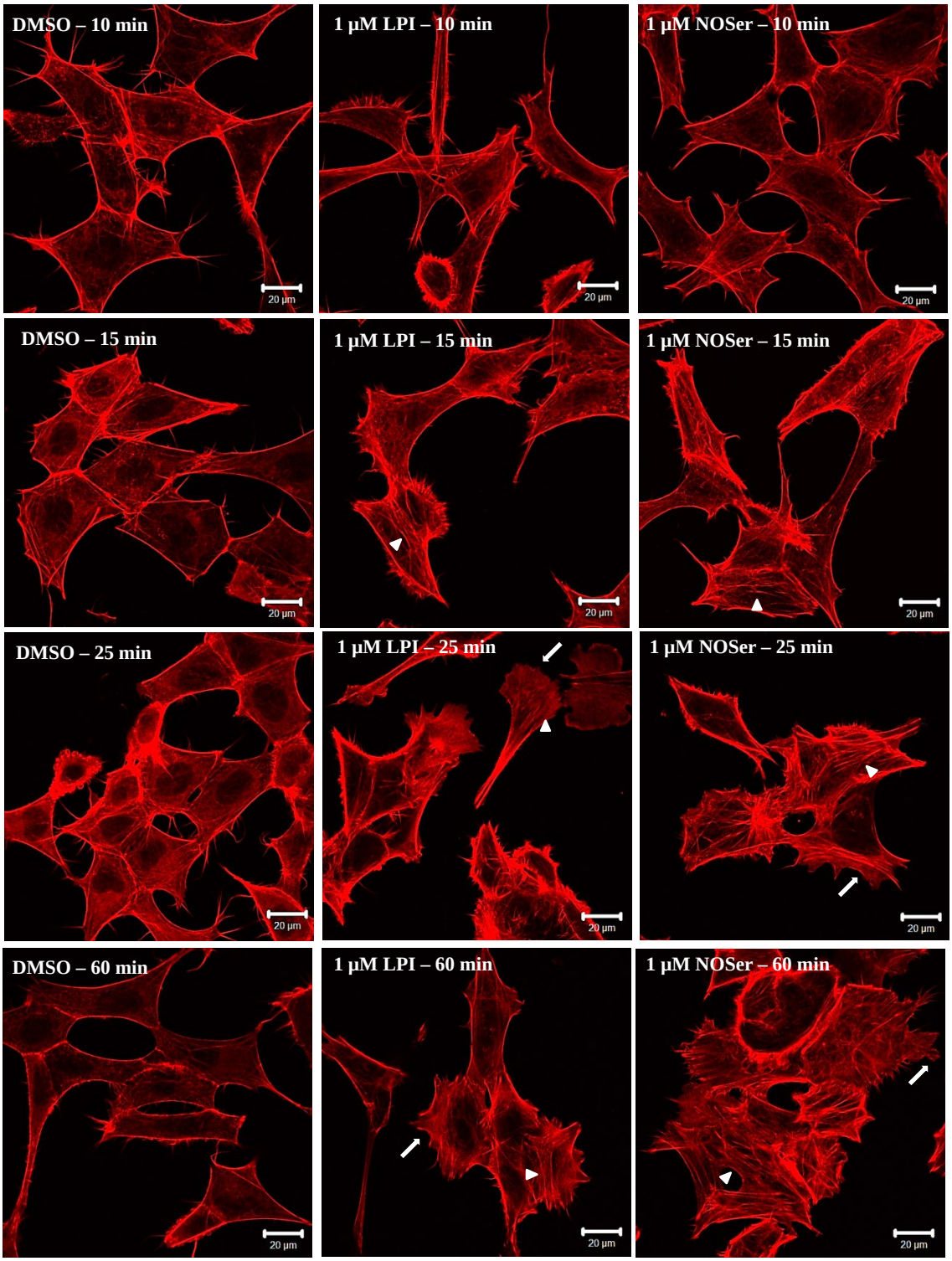

Figure 4.23: Time-dependence of actin cytoskeletal reorganisation in hGPR55-HEK293 cells following exposure to GPR55 ligands. *To visualise the actin cytoskeleton cells were fixed, permeabilised and then incubated with Alexa fluor® 546 phalloidin. DMSO treated cells at all*

the time points have a flattened, spread out morphology. Application of either LPI or NOSer for 15 min promoted a slight cytoskeletal reorganisation with some filopodia present. At 25 min the effects were much more pronounced with the formation of lamellipodia, filopodia and some stress fibres. Notably, stress fibres were more prominent in NOSer treated hGPR55-HEK293 cells, with some lamellipodia are still present with 60 min lipid challenge. Scale bars = 20 µm; n = 3; arrows = lamellipodia; open arrow head = filopodia; arrowheads = stress fibres.

A similar temporal study was carried out investigating structural changes in the expression of the focal adhesion vinculin, assessed using vinculin immunostaining in hGPR55-HEK293 cells. Changes in FA length were measured following treatment with LPI and NOSer (figure 4.24A and B). To determine if there were temporal differences and if lipid presences promoted differences in the FA length a two-way ANOVA was used. This highlighted that there was a significant difference dependant on the time the lipids were applied for ($F_{(8,4)}$ = 3.81; P = 0.0249). Furthermore the presence of the lipids promoted FA length that was significantly different to vehicle control treated cells ($F_{(8,2)}$ = 6.92; P = 0.0074). At 10 min LPI (1 µM) treatment, FA length was increased but not significantly relative to DMSO treated cells (DMSO = 2.62 ± 0.00 µm, LPI = 2.81 ± 0.51 µm, n = 2, figure 4.24A and B). NOSer had no effect FA length (DMSO = 2.62 ± 0.00 µm, NOSer = 2.69 ± 0.01 µm). At 15 min, both lipids were found to promote an increase in the FA length when compared to control cells (DMSO = 2.36 ± 0.16 µm, LPI = 3.41 ± 0.06 µm, NOSer = 3.12 ± 0.37 µm). An increase in FA length was also observed following 25 min ligand exposure (DMSO = 2.29 ± 0.09 µm, LPI = 3.41 ± 0.43 µm, NOSer = 3.45 ± 0.69 µm). However, at 60 min ligand exposure, FA length was similar to control cells (DMSO = 2.47 ± 0.14 µm, LPI = 2.70 ± 0.01 µm, NOSer = 2.55 ± 0.23 µm). Interestingly at 120 min the lipid-mediated changes in FA length were observed again with both LPI and NOSer treated cells with longer FAs than control cells (DMSO = 1.87 ± 0.05 µm, LPI = 2.42 ± 0.24 µm, NOSer = 2.43 ± 0.07 µm). These data highlight the dynamic nature of FA turnover in hGPR55-HEK293 cells. As both lipids produced good responses at 25 min to both cytoskeletal reorganisation and vinculin labelling this time was used for all subsequent experiments using hGPR55-HEK293 cells.

A

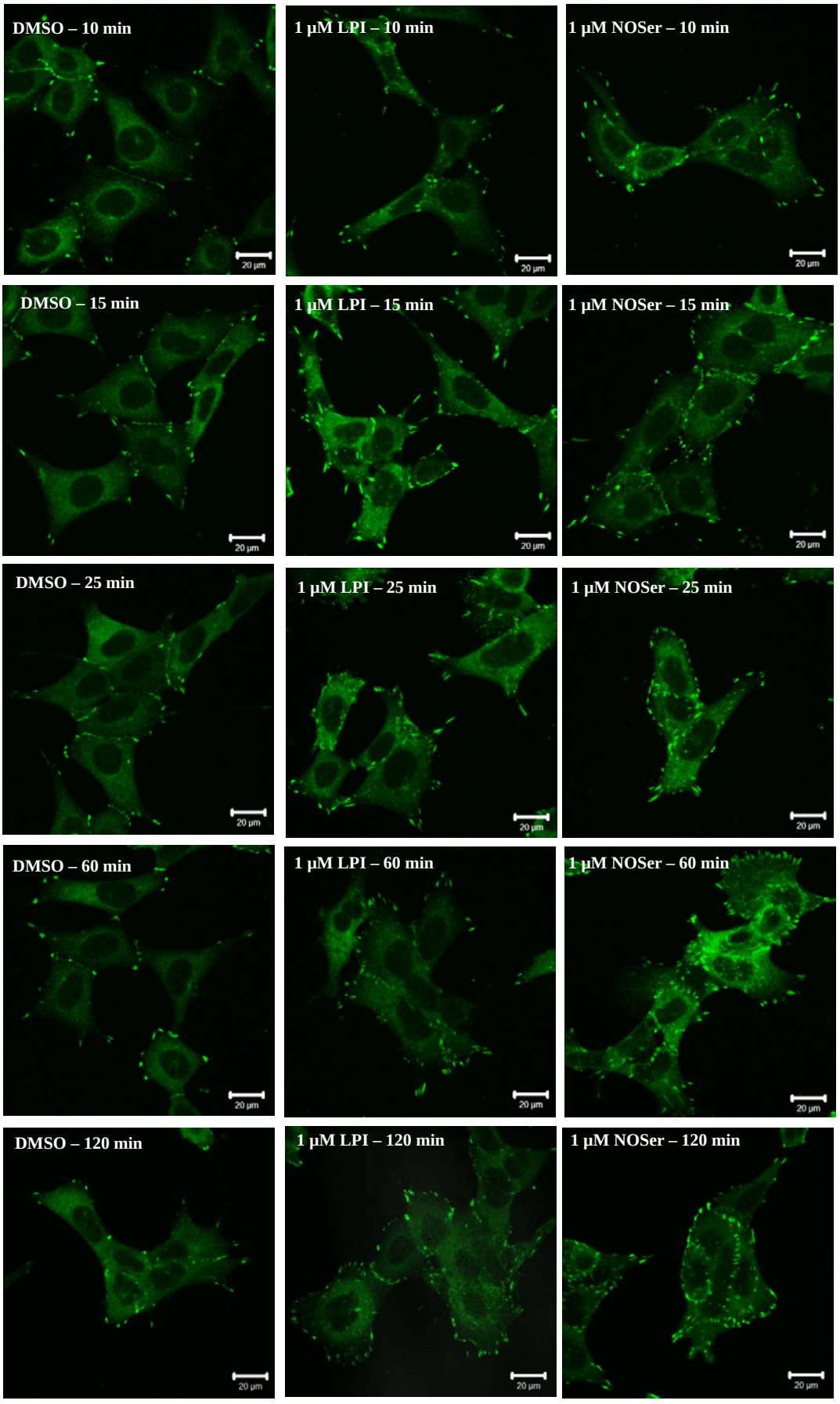
DMSO – 10 min
1 µM LPI – 10 min
1 µM NOSer – 10 min
DMSO – 15 min
1 µM LPI – 15 min
1 µM NOSer – 15 min
DMSO – 25 min
1 µM LPI – 25 min
1 µM NOSer – 25 min
DMSO – 60 min
1 µM LPI – 60 min
1 µM NOSer – 60 min
DMSO – 120 min
1 µM LPI – 120 min
1 µM NOSer – 120 min
20 µm

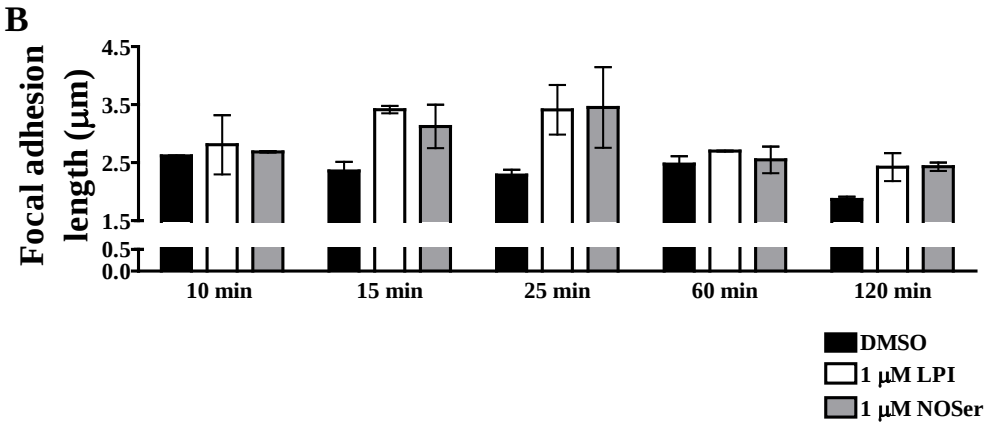

Figure 4.24: Time-course study of changes in vinculin-containing FA length in hGPR55-HEK293 cells challenged with endogenous lipids. *Lipids were applied for times stated and then fixed and permeabilised prior to application of anti-vinculin for 60 min. FA immunostaining was visualised using an anti-vinculin primary antibody followed by Alexa fluor® 488 conjugated secondary antibody.* ***A****, representative confocal images are DMSO (vehicle control), LPI or NOSer. Scale bars = 20 µm; n = 2.* ***B****, histogram of pooled data, depicting vinculin-containing FA length in hGPR55-HEK293 cells treated with either LPI or NOSer. Note FA length was dynamic initially increasing with time and then returning to basal levels at 60 min only to slightly increase again at 120 min. Data are the means ± SEM; n = 2. Two-way ANOVA with a Bonferroni post hoc test.*

4.2.2.2. Endogenous lipid effects on the actin cytoskeleton in hGPR55-HEK293 cells and HEK293 cells.

Next various concentrations of LPI were applied to hGPR55-HEK293 cells. DMSO-treated cells (0.1%; 25 min) exhibited a flat, spread out morphology with some filopodia present. Cells treated with LPI (10 and 30 nM) were also found to have a flat morphology with some filopodia (open arrowheads) and were similar to control cells. Cells treated with higher concentrations of LPI (100 and 300 nM) were retracted and were smaller than observed in control cells with filopodia, lamellipodia (arrows) and stress fibres (solid arrowheads) beginning to be formed. High concentrations of LPI (1 - 10 µM) also produced some stress fibres, filopodia and lamellipodia. The cells were retracted and more rounded-up than the control cells (figure 4.25).

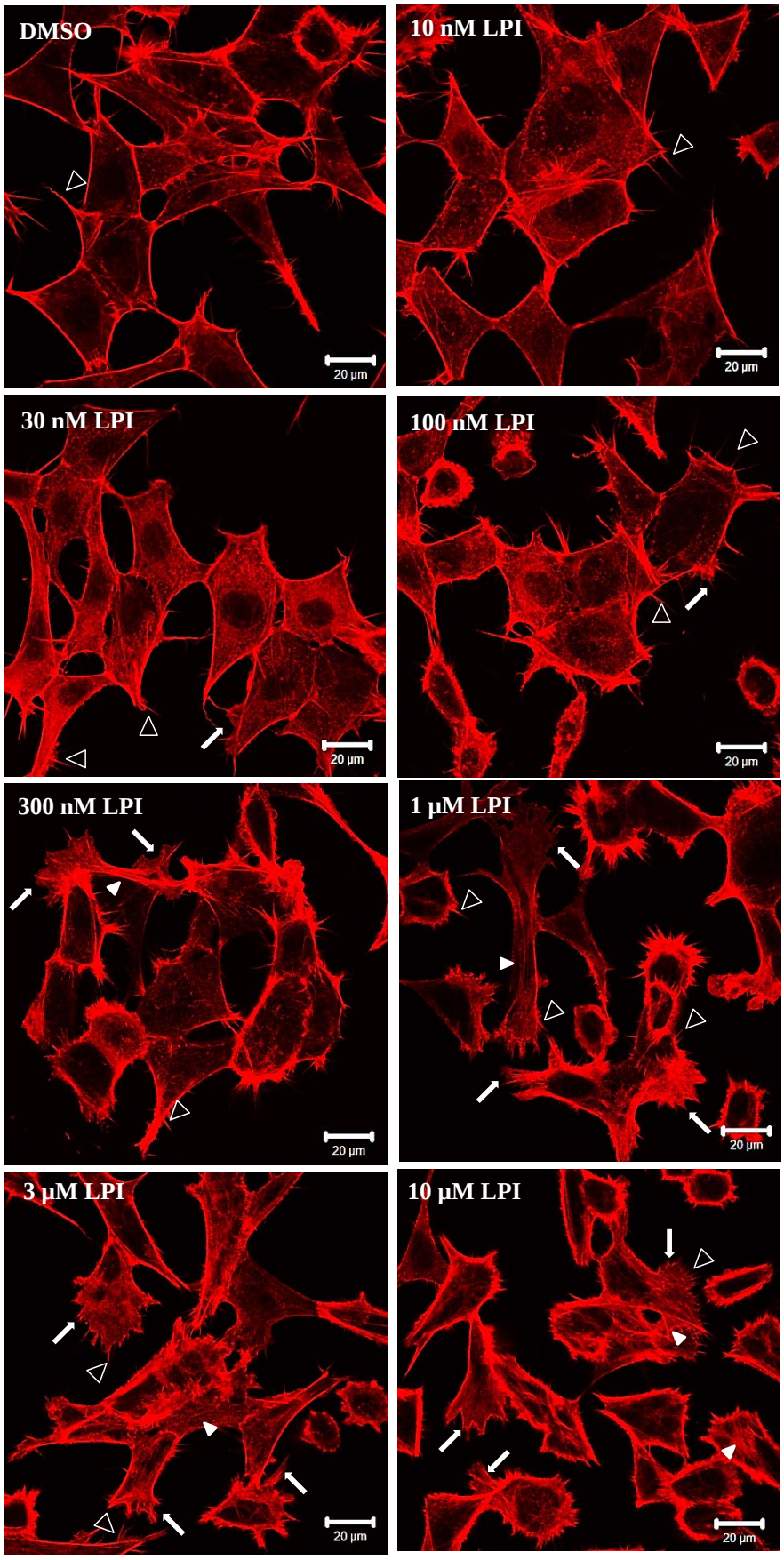

Figure 4.25: LPI-induced F-actin cytoskeletal reorganisation in hGPR55-HEK293 cells. *Cells were treated with LPI or DMSO for 25 min. Representative confocal images of phalloidin labelling are illustrated for DMSO; 10 nM LPI; 30 nM LPI; 100 nM LPI; 300 nM LPI; 1 µM*

LPI; 3 µM LPI; 10 µM LPI. Scale bars = 20 µm; n = 3. Note as the LPI concentration increased the morphology of the hGPR55-HEK293 cells were observed to become retracted and more rounded-up with lamellipodia, filopodia and some stress fibres being produced. Filled arrow head = stress fibres; open arrow head = filopodia; arrows = lamellipodia.

Various concentrations of LPI (10 nM - 10 µM) was applied to hGPR55-HEK293 cells for 25 min. Vinculin-positive FAs were found predominately on the cell periphery. As the LPI concentration increased the number of FAs produced per cell was observed to increase (figure 4.26A). Furthermore, FA length was found to increase with LPI treatment, in a concentration dependent manner with an EC_{50} of 72 ± 10 nM (95% confidence limits) (figure 4.26B).

The next experiments were designed to study the effects of NOSer on both cytoskeletal reorganisation and vinculin-containing FAs. Application of NOSer (10 nM) to hGPR55-HEK293 cells did not affect cell morphology relative to control cells treated with DMSO. At higher concentrations, NOSer (30 nM) led to cytoskeletal reorganisation occurring whereby lamellipodia, some filopodia and stress fibres were observed. As the NOSer concentration was increased (100 nM - 10 µM) the cells retracted and were more rounded than control cells. There was an increase in the expression of lamellipodia, filopodia and stress fibres (figure 4.27). However, the stress fibres were not noticeable at 10 µM.

Next, NOSer (10 nM - 10 µM) was applied to the hGPR55-HEK293 cells to study the effect the lipid had on vinculin-containing FAs (figure 4.28A). As had been observed with LPI the FAs were localised predominantly at the cell periphery. The number of FAs per cell was also observed increase with NOSer concentration. Additionally, the length of the FAs was found to increase in a concentration-dependent manner with an EC_{50} for NOSer of 65 ± 11 nM (95% confidence limits) (figure 4.28B). These data taken together for both LPI and NOSer suggest that cytoskeletal reorganisation and vinculin-containing FA length is affected in a similar manner by both lipids. NOSer was however slightly more potent in both assays.

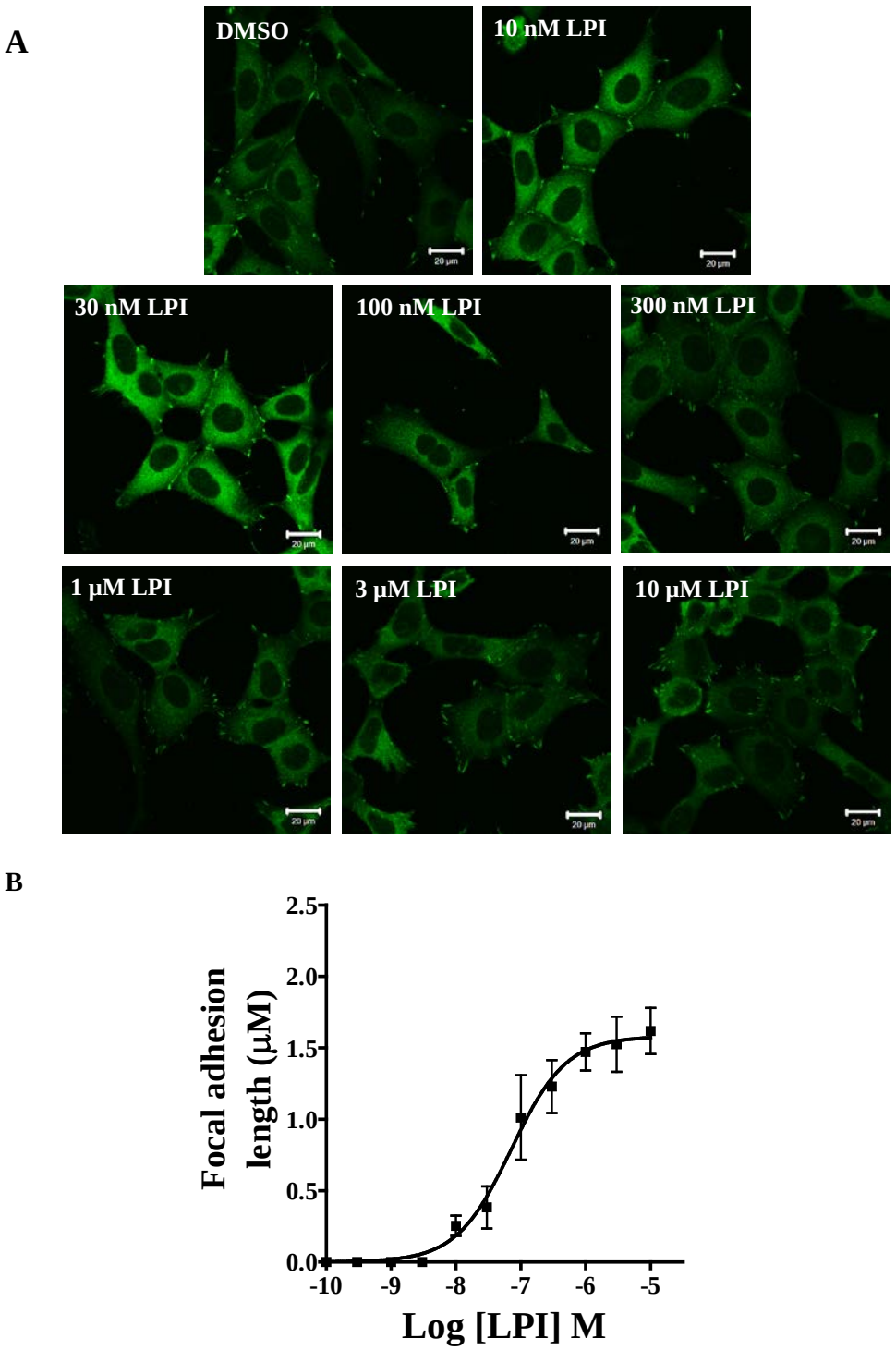

Figure 4.26: LPI modulates vinculin-containing FA length in hGPR55-HEK293 cells. ***A****, Representative confocal images of vinculin labelling illustrating the effect of: DMSO; 10 nM LPI; 30 nM LPI; 100 nM LPI; 300 nM LPI; 1 µM LPI; 3 µM LPI; 10 µM LPI. Scale bars = 20 µm; n = 3.* ***B****, histogram of pooled data, depicting concentration-dependent increases in vinculin-containing FA length. Note, the number of FAs per cell was also observed to increase in a concentration-dependent manner. Data are the means ± SEM; n = 3.*

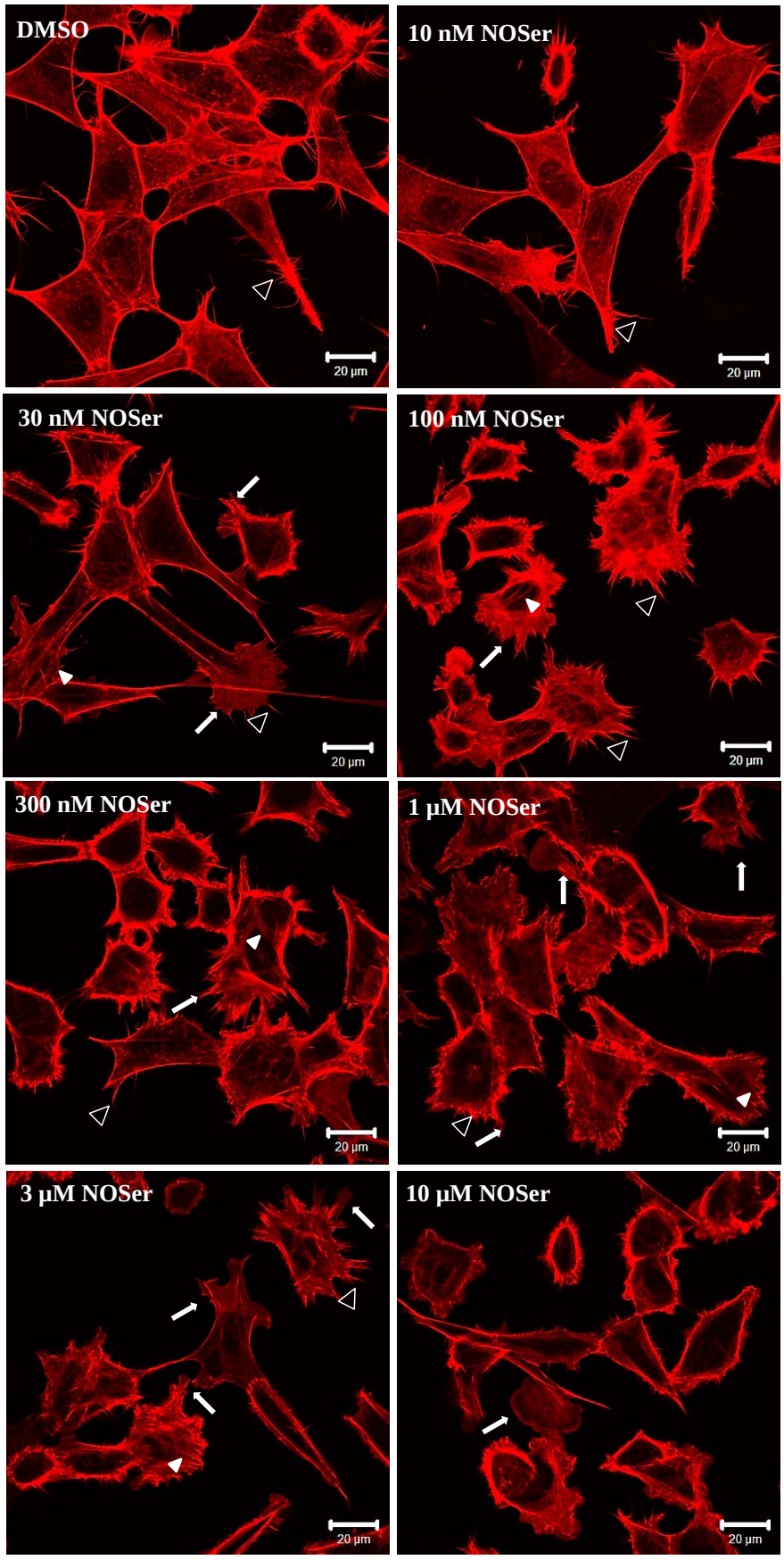

Figure 4.27: NOSer exhibits concentration-dependent cytoskeletal reorganisation in hGPR55-HEK293 cells. *Cells were treated with NOSer or DMSO for 25 min. Representative confocal images of phalloidin labelling are illustrated for: DMSO; 10 nM NOSer; 30 nM*

NOSer; 100 nM NOSer; 300 nM NOSer; 1 µM NOSer; 3 µM NOSer; 10 µM NOSer. Note the NOSer-induced increase in cytoskeletal structures; including filopodia, stress fibres and lamellipodia is concentration-dependent. Scale bars = 20 µm; n = 3. Filled arrow head = stress fibres; open arrow head = filopodia; arrows = lamellipodia.

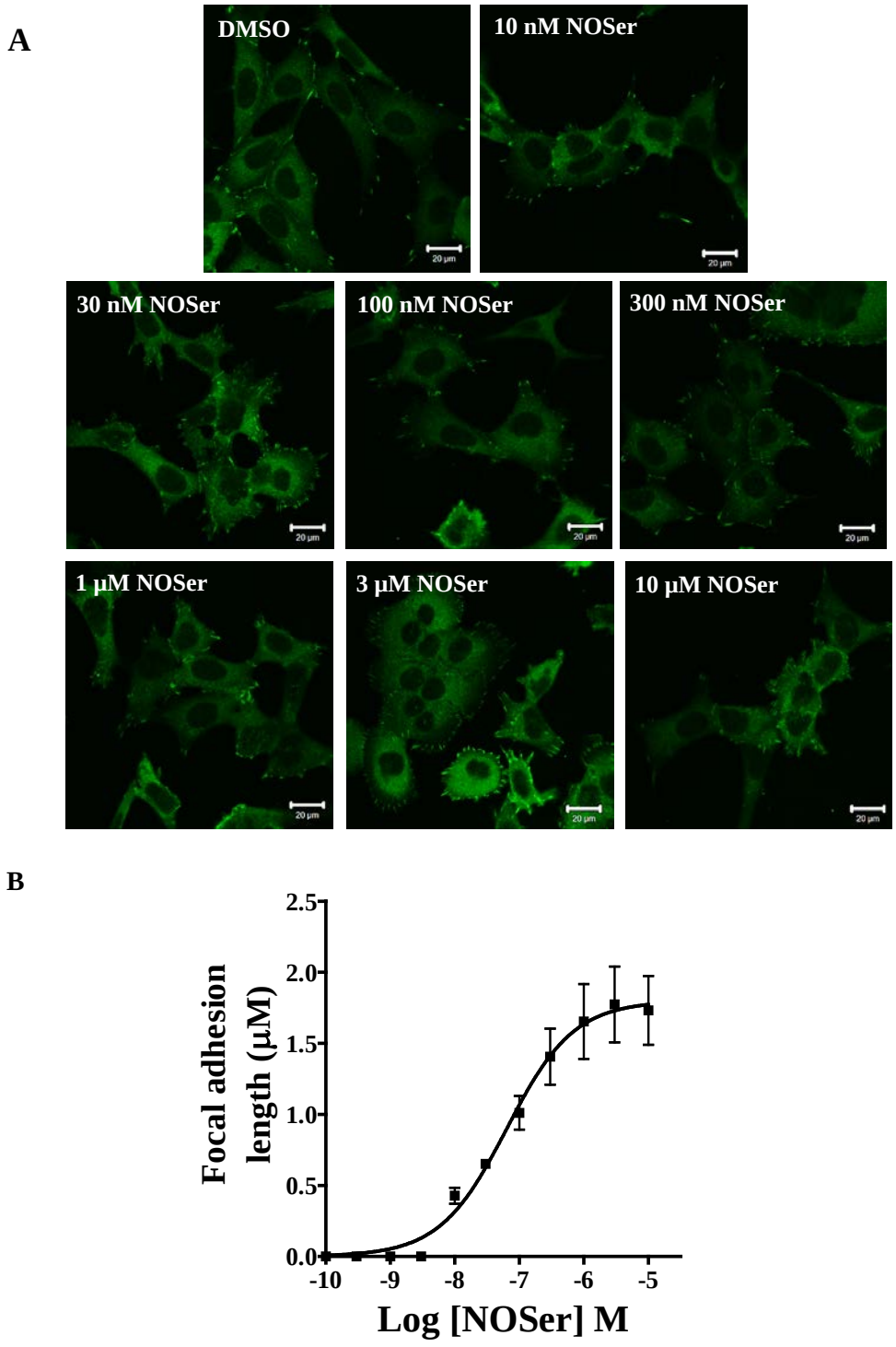

Figure 4.28: NOSer modulates vinculin-containing FAs in hGPR55-HEK293 cells. ***A****, representative confocal images of vinculin labelling illustrating the effect of: DMSO; 10 nM LPI; 30 nM LPI; 100 nM LPI; 300 nM LPI; 1 µM LPI; 3 µM LPI; 10 µM LPI. Scale bars = 20*

µm; n = 3. ***B****, histogram of pooled vinculin-containing FAs length data suggesting increases in NOSer-induced FA length are concentration dependent. Note the number of FAs also increased in a concentration dependent manner. Data are the means ± SEM; n = 3.*

4.2.2.3. Cytoskeletal reorganisation and differences in FA length are GPR55-mediated.

Next we investigated whether the cytoskeletal reorganisation and the differences to the FA length in hGPR55-HEK293 cells induced by LPI and NOSer were mediated by GPR55. To test this hGPR55-HEK293 and HEK293 cells were treated with DMSO (0.1%) as a vehicle control, or submaximal concentrations of either LPI (1 µM) or NOSer (1 µM). DMSO treated hGPR55-HEK293 cells had flattened spread out morphology. LPI or NOSer applied to hGPR55-HEK293 cells exhibited typical cytoskeletal reorganisation with stress fibres, lamellipodia and filopodia being observed (figure 4.29Ai). HEK293 cells treated with DMSO, LPI or NOSer exhibited a cell morphology that was similar to the DMSO treated hGPR55-HEK293 cells (figure 4.29Aii). Vinculin-containing FAs were observed in hGPR55-HEK293 cells treated with DMSO. Application of either LPI or NOSer to hGPR55-HEK293 cells led to an increase in the number of FAs being observed (figure 4.29Bi). However, HEK293 cells were found to have very few FAs present whether treated with DMSO, LPI or NOSer (figure 4.29Bii). There may be some constitutive effects of GPR55 on FAs in hGPR55-HEK293 as they were more prominent in control hGPR55-HEK293 cells than in the control HEK293 cells. Nevertheless, these data suggest that the effects of LPI and NOSer are GPR55-mediated.

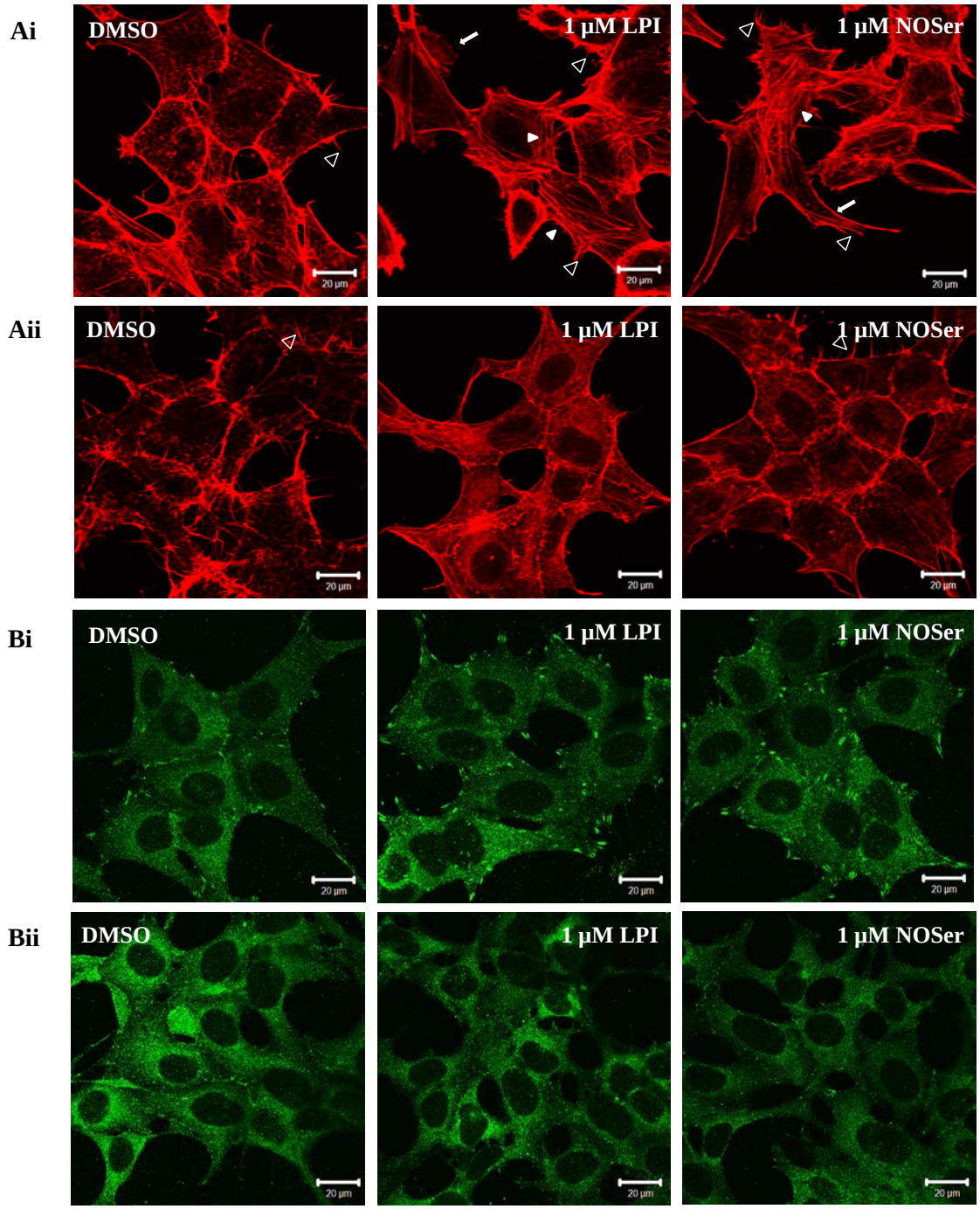

Figure 4.29: Comparison of LPI and NOSer effects on cytoskeletal reorganisation and FAs in hGPR55-HEK293 cells and HEK293 cells. *Both hGPR55-HEK293 cells and HEK293 cells were treated with ligands for 25 min.* ***Ai****, representative confocal images of the actin cytoskeleton in hGPR55-HEK293 cells treated as follows: DMSO; 1 µM LPI; 1 µM NOSer.* ***Aii****, representative confocal images of the actin cytoskeleton in HEK293 cells treated as follows: DMSO; 1 µM LPI; 1 µM NOSer.* ***Bi****, representative confocal images of vinculin-containing FAs in hGPR55-HEK293 cells challenged with: DMSO; 1 µM LPI; 1 µM NOSer.* ***Bii****, representative confocal images of vinculin-containing FAs in HEK293 cells challenged with: DMSO; 1 µM LPI; 1 µM NOSer. Note no clear effects of LPI and NOSer on stress fibres,*

lamellipodia or FAs were observed in HEK293 cells. Arrow = lamellipodia; filled arrowheads = stress fibres; open arrow heads = filopodia. Scale bars = 20 µm; n = 3.

4.2.2.4. $G_{\alpha 13}$ but not $G_{\alpha q}$ mediate changes in the actin cytoskeleton and FAs in hGPR55-HEK293 cells.

These next series of experiments were carried out to elucidate the signalling pathways required for cytoskeletal reorganisation and changes in vinculin-containing FAs. $G_{\alpha 13}$ (Henstridge *et al.,* 2009) and $G_{\alpha q}$ (Lauckner *et al.,* 2008) are reported to be required for Ca^{2+} mobilisation in hGPR55-HEK293 cells therefore both were tested to observe if they affected the actin cytoskeleton or vinculin-containing FAs. Application of LPI (1 µM) or NOSer (1 µM) promoted the formation of stress fibres that were not present in the control cells (figure 4.30). Dominant negative $G_{\alpha 13}$(Q226L/D294N) cDNA transiently transfected into hGPR55-HEK293 cells for 18 hr prior to the commencement of experiments were found to have some stress fibres present and several cells had a retracted and rounded morphology. This may be due to the protocol with the addition of 'foreign' DNA adding stress to the cells. However this needs further investigation with a modification of the protocol to include a transfection control such as GFP, which would highlight if the transfection procedure itself was responsible for the cell rounding. LPI challenged $G_{\alpha 13}$(Q226L/D294N) transfected cells were found to have very few stress fibres present similar to the control $G_{\alpha 13}$(Q226L/D294N) transfected hGPR55-HEK293 cells (figure 4.30E). NOSer applied to $G_{\alpha 13}$(Q226L/D294N) transiently transfected hGPR55-HEK293 cells were found to have some stress fibres however they were found to be similar to $G_{\alpha 13}$(Q226L/D294N)-transfected hGPR55-HEK293 cells. There appeared to be a decrease in stress fibres present in lipid challenged $G_{\alpha 13}$(Q226L/D294N) transfected cells than in non-transfected hGPR55-HEK293 cells; therefore, suggesting that $G_{\alpha 13}$(Q226L/D294N) activation is required for the observed cytoskeletal reorganisation which was either LPI or NOSer-mediated.

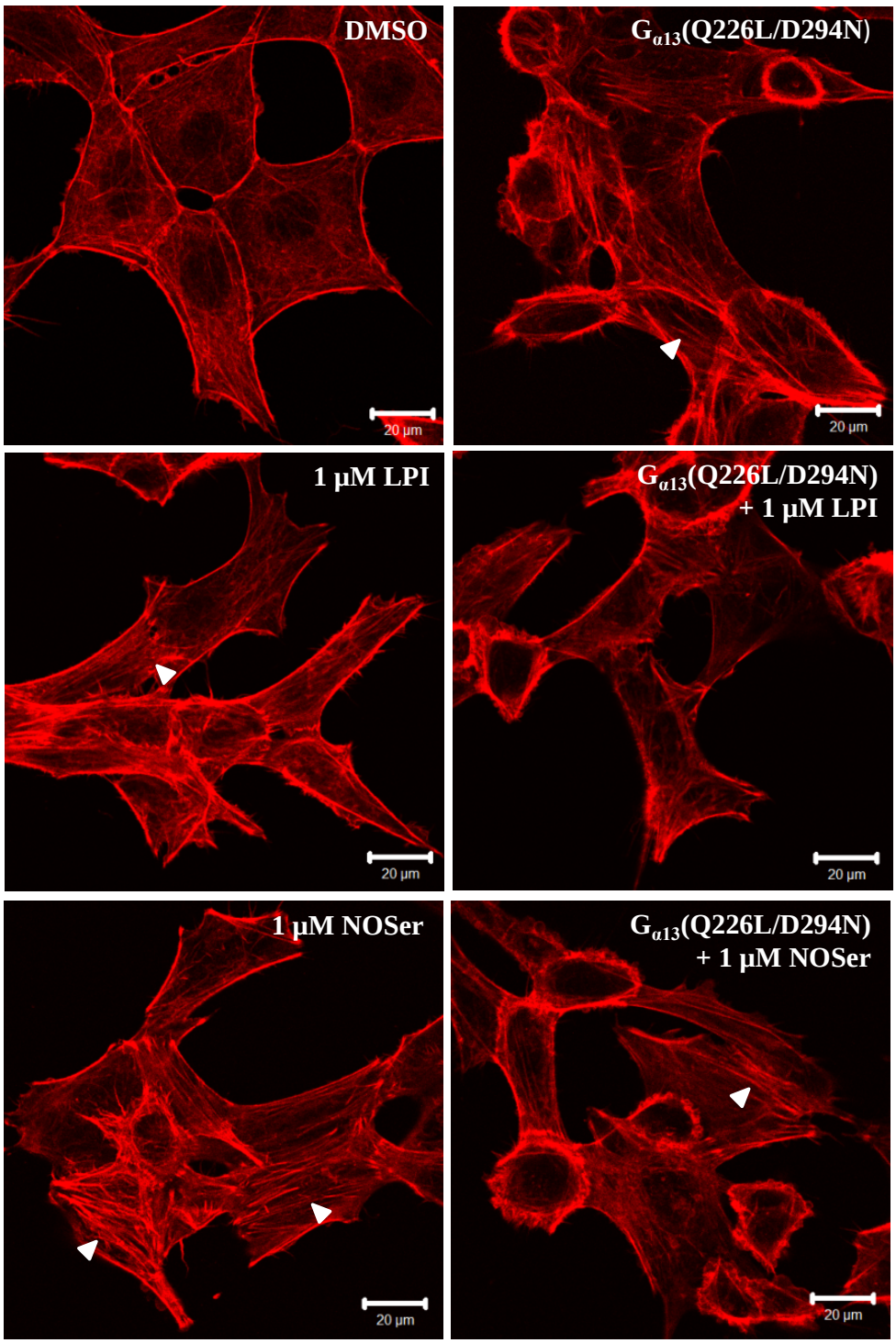

Figure 4.30: $G_{\alpha 13}$ is required for GPR55-mediated cytoskeletal reorganisation. *hGPR55-HEK293 cells were transiently transfected with $G_{\alpha 13}$ for 18 hr prior to the commencement of experiments. The F-actin cytoskeleton was visualised with Alexa Fluor® 546 phalloidin. Representative confocal images of the phalloidin labelling following treatment with: DMSO; $G_{\alpha 13}$(Q226L/D294N); 1 µM LPI; $G_{\alpha 13}$(Q226L/D294N) + 1 µM LPI; 1 µM NOSer; $G_{\alpha 13}$(Q226L/D294N) + 1 µM NOSer. Note the presence of some stress fibres in the $G_{\alpha 13}$ (Q226L/D294N) which were also observed in $G_{\alpha 13}$(Q226L/D294N) + NOSer treated cells. Overall LPI or NOSer was less effective at promoting stress fibres in $G_{\alpha 13}$(Q226L/D294N) transfected cells. Arrowheads = stress fibres; Scale bars = 20 µm; n = 3.*

Previous studies in Swiss 3T3 fibroblast cells have reported that $G_{\alpha 13}$ is required for vinculin-containing FA assembly (Buhl *et al.*, 1995). $G_{\alpha 13}$ activation is important for GPR55-mediated responses therefore $G_{\alpha 13}$(Q226L/D294N) was transiently transfected into hGPR55-HEK293 cells. One-way ANOVA highlighted significant differences between the data sets tested ($F_{(5,12)} = 26.74$; $P < 0.0001$). Bonferroni *post hoc* analysis revealed that application of LPI (1 µM) or NOSer (1 µM) to the hGPR55-HEK293 cells promoted vinculin-containing FA assembly with an increase in both the length of the FAs and the number present compared to control cells (DMSO = 2.09 ± 0.15 µm, LPI = 3.09 ± 0.01 µm, NOSer = 3.19 ± 0.06 µm, n = 3; one-way ANOVA followed with a Bonferroni *post hoc* test, $P < 0.001$, figure 4.31A and B). Transient transfection of $G_{\alpha 13}$(Q226L/D294N) into hGPR55-HEK293 cells did not affect FA length (untransfected DMSO = 2.09 ± 0.15 µm, $G_{\alpha 13}$(Q226L/D294N) = 2.15 ± 0.13 µm, $P > 0.05$). However, responses to LPI or NOSer were reduced, by 64.2 ± 11.6% and 58.4 ± 7.9% respectively, in hGPR55-HEK293 cells transiently transfected with $G_{\alpha 13}$(Q226L/D294N) with shorter FAs than with ligand alone (LPI = 3.09 ± 0.01 µm, $G_{\alpha 13}$(Q226L/D294N) + LPI = 2.50 ± 0.15 µm, NOSer = 3.19 ± 0.06 µm, $G_{\alpha 13}$(Q226L/D294N) + NOSer = 2.61 ± 0.03 µm, $P < 0.01$). These data suggest that whilst the LPI and NOSer-mediated FAs were longer than seen in control cells the effects were dependent on $G_{\alpha 13}$ activation.

Next we investigated the effects of $G_{\alpha q}$ inhibition on GPR55-mediated cytoskeletal changes. Application of the $G_{\alpha q}$ inhibitor YM-254890 (1 µM, 55 min) alone had little effect on the actin cytoskeleton in hGPR55-HEK293 cells and was similar to DMSO treatment (figure 4.32). Treatment with $G_{\alpha q}$ inhibitor for 30 min prior to co-application with either LPI (1 µM) or NOSer (1 µM) did not affect responses to these ligands. Thus cells exhibited a similar change in morphology to the lipid treated cells whereby filopodia, stress fibres and lamellipodia were observed. These data suggest that $G_{\alpha q}$ activation is not required to promote the cytoskeletal changes observed in lipid challenged hGPR55-HEK293 cells.

The effects of the $G_{\alpha q}$ inhibitor were assessed in the FA assay. One-way ANOVA analysis highlights a significant difference ($F_{(5,12)} = 18.2$; $P < 0.0001$). $G_{\alpha q}$ inhibition with YM-254890 (1 µM; 55 min) did not influence FA length (DMSO = 2.17 ± 0.13 µm, YM-254890 = 2.24 ± 0.15 µm, n = 3, one-way ANOVA with a Bonferroni *post hoc* test, $P > 0.05$; figure 4.33A and B). In addition, YM-254890 did not inhibit responses

to LPI (1 µM) and NOSer (1 µM) on FA length (LPI = 3.38 ± 0.13 µm, YM-254890 + LPI = 3.36 ± 0.13 µm, NOSer = 3.42 ± 0.17 µm, YM-254890+NOSer = 3.41 ± 0.15 µm, n = 3, P > 0.05). These data suggest that lipid-induced increases in FA length in hGPR55-HEK293 cells are $G_{\alpha q}$-independent.

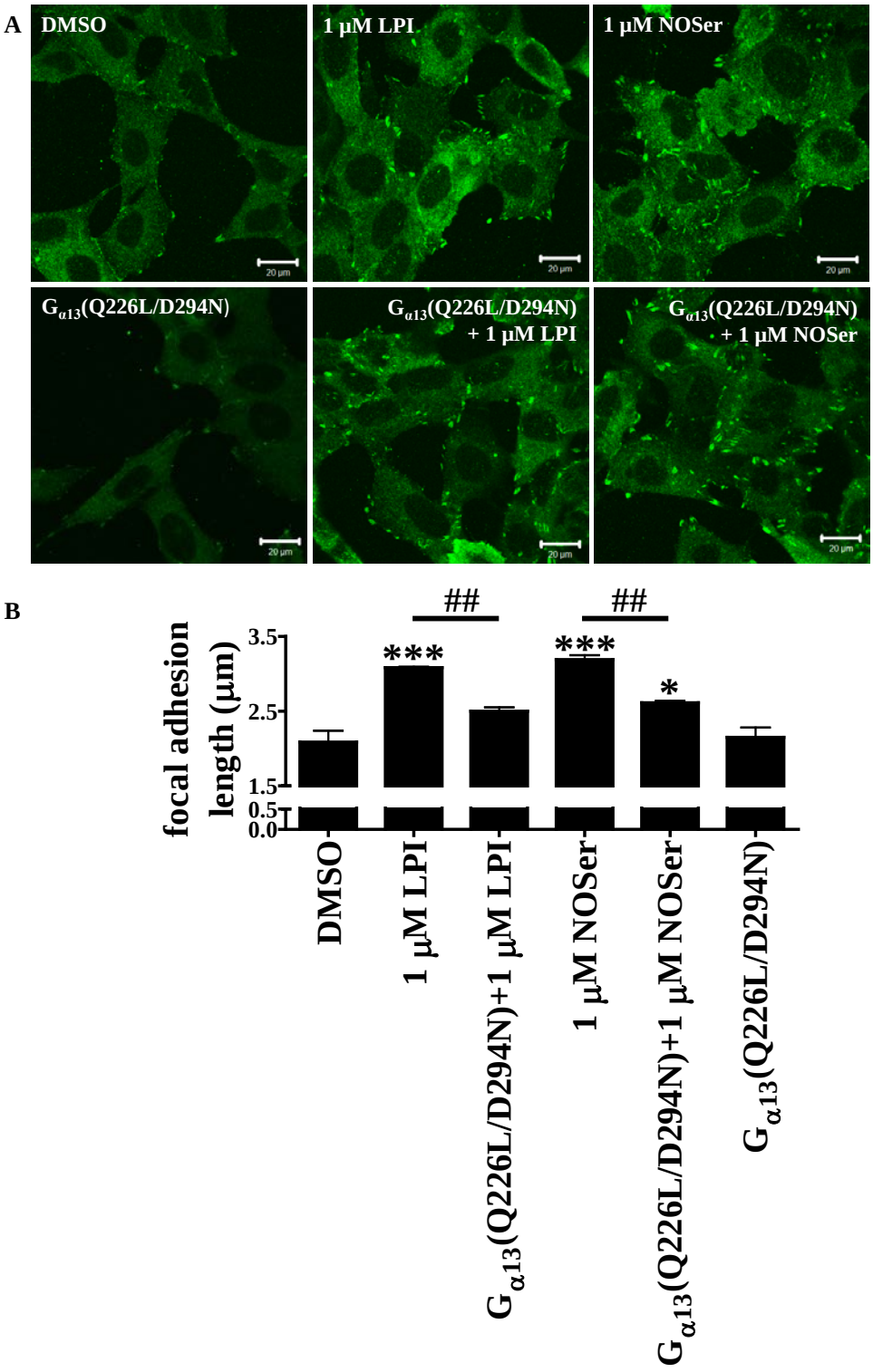

Figure 4.31: A role for $G_{\alpha 13}$ in GPR55-mediated effects on FA length. ***A****, representative confocal images of vinculin labelling in hGPR55-HEK293 cells illustrating the effect of: DMSO; 1 µM LPI; 1 µM NOSer; $G_{\alpha 13}$(Q226L/D294N); $G_{\alpha 13}$(Q226L/D294N) + 1 µM LPI;*

$G_{\alpha 13}$(Q226L/D294N) + 1 µM NOSer. Scale bars = 20 µm; n = 3. ***B****, histogram of pooled data depicting effects vinculin-containing FA length in hGPR55-HEK293 cells. Note that the transient transfection of dominant negative $G_{\alpha 13}$(Q226L/D294N) decreases the length of the lipid-induced FAs when compared to non-transfected cells highlighting the importance of $G_{\alpha 13}$ activation for increasing FA length. * = data compared to vehicle control. Data are the means ± SEM; n = 3. One-way ANOVA with a Bonferroni post hoc test; *P < 0.05; ##P < 0.01; ***P < 0.001.*

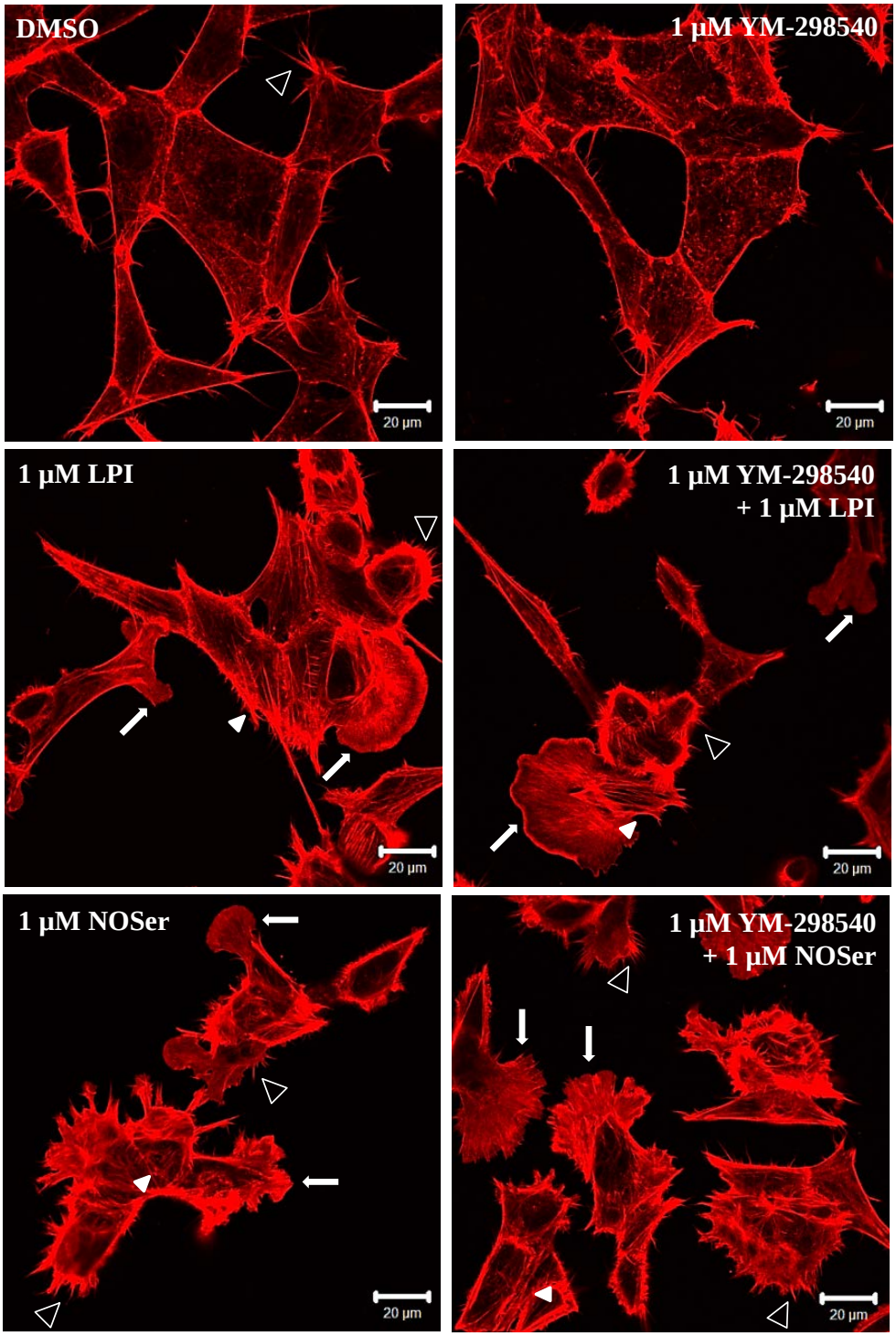

Figure 4.32: $G_{\alpha q}$ does not influence cytoskeletal reorganisation in hGPR55-HEK293 cells treated with endogenous lipids. *The $G_{\alpha q}$ inhibitor (YM-254890; 1 µM) was applied for 30 min*

prior to co-application of inhibitor with lipid ligands. The F-actin cytoskeleton was visualised with Alexa Fluor® 546 phalloidin. Panels show representative confocal images of phalloidin labelling following treatment with: DMSO; 1 µM YM-254890; 1 µM LPI; 1 µM YM-254890 + 1 µM LPI; 1 µM NOSer; 1 µM YM-254890 + 1 µM NOSer. Note the formation of lamellipodia, filopodia and stress fibres in cells treated with either of the lipids. These effects are also observed when the inhibitor is present with either of the lipids suggesting that the effects are not $G_{\alpha q}$-mediated. Scale bars = 20 µm; n = 3; arrows = lamellipodia; solid arrowheads = stress fibres; open arrowhead = filopodia.

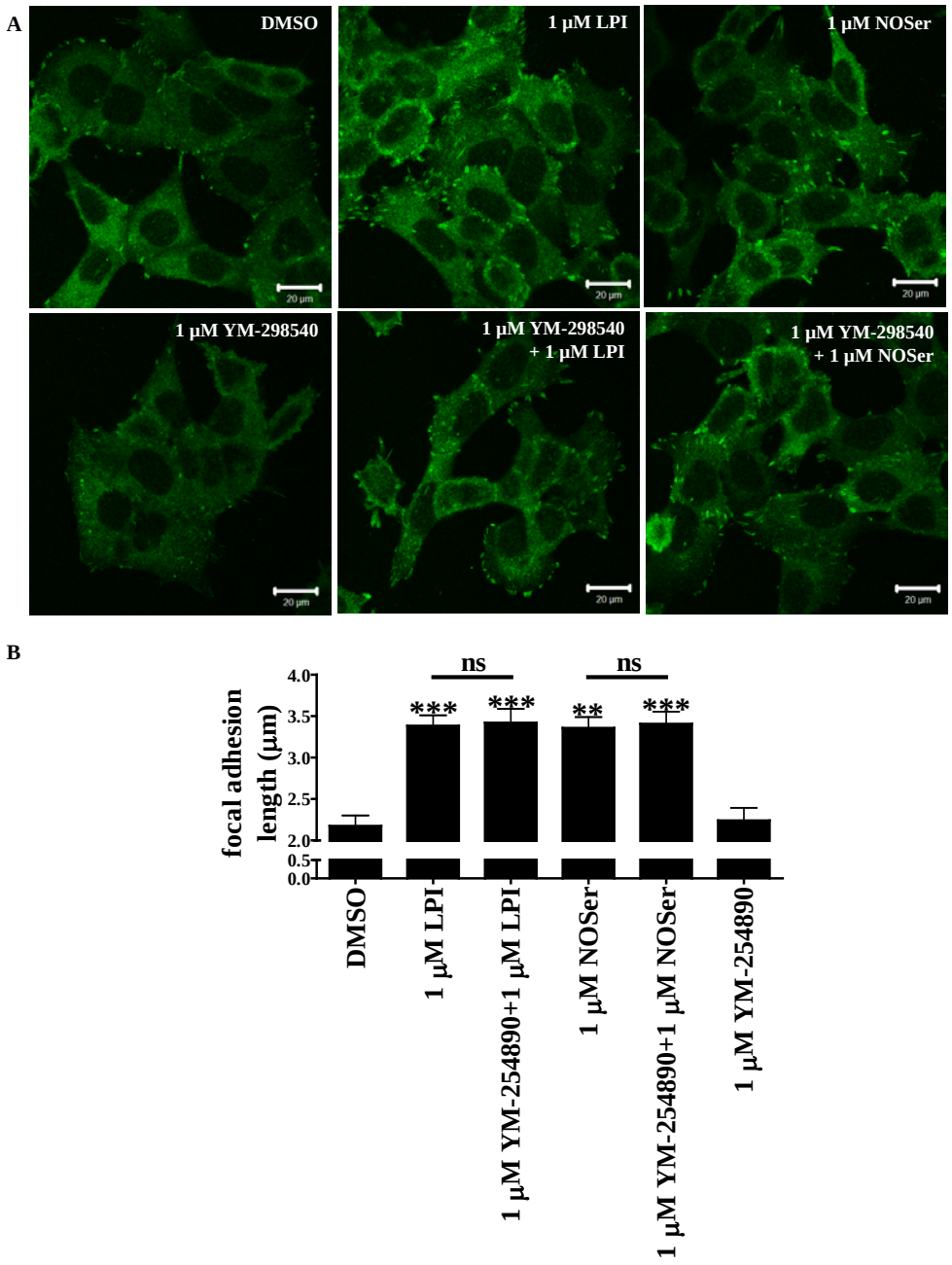

Figure 4.33: GPR55-mediated changes in FA length are $G_{\alpha q}$-independent in hGPR55-HEK293 cells. ***A****, representative confocal images of vinculin labelling illustrating the effect of DMSO; 1 µM LPI; 1 µM NOSer; 1 µM YM-254890; 1 µM YM-254890 + 1 µM LPI; 1 µM YM-*

254890 + 1 µM NOSer. Scale bars = 20 µm; n = 3. Note there is an increase in the FA length and the number of FAs in lipid treated cells. ***B****, histogram of pooled data, depicting vinculin-containing FA length in hGPR55-HEK293 cells. Note* $G_{\alpha q}$ *activation is not required for increasing FA length in lipid challenged cells. * = data compared to vehicle control. Data are the means ± SEM; n = 3. One-way ANOVA with a Bonferroni post hoc test; **P < 0.01; ***P < 0.001; ns = not significant.*

4.2.2.5. Rho-ROCK axis is required for the cytoskeletal reorganisation and FA changes in hGPR55-HEK293 cells.

The Rho-ROCK axis lies downstream of $G_{\alpha 13}$ therefore the cell permeable Rho inhibitor (CT04; 1 µg/ml) was applied to the hGPR55-HEK293 cells for 4 hr prior to the commencement of experiments. Application of the Rho inhibitor for 4 hr had little or no effect on cytoskeletal structure with a cell morphology that was similar to control cells (figure 4.34). Pre-treatment of hGPR55-HEK293 cells with the Rho inhibitor prior to the addition of LPI or NOSer did not prevent the cytoskeletal changes; the cells had retracted and were more rounded than seen with control cells. Lamellipodia and stress fibres were observed in the Rho inhibitor treated cells but these appear to be less robust than seen in with cells treated with lipid alone. These data suggest that the Rho inhibitor at the concentration used in this assay could only partially inhibit GPR55-mediated cytoskeletal changes in hGPR55-HEK293 cells.

Next, the Rho inhibitor (CT04; 1 µg/ml) was now tested in the GPR55-vinculin FA assay. One-way ANOVA analysis revealed a very high significant difference across the data set ($F_{(5,12)}$ = 29.33; P < 0.0001). Rho inhibitor reduced the effects of LPI and NOSer on FA length by 95.1 ± 4.9% and 88.2 ± 5.5% respectively; (LPI = 3.19 ± 0.08 µm, CT04 + LPI = 2.53 ± 0.05 µm, NOSer = 3.28 ± 0.07 µm, CT04 + NOSer = 2.75 ± 0.06 µm, n = 3, one-way ANOVA with a Bonferroni *post hoc* test, P < 0.01, figure 4.35A and B). These data suggest that signalling via Rho is required for the increases in the FA length mediated by the lipids. The inhibition appears to be more robust in LPI treated than NOSer treated hGPR55-HEK293 cells. As this is a general Rho inhibitor acting on Rho A, B and C further studies would be required to understand which of these isoforms mediates the effects seen in both the cytoskeletal reorganisation and the increases in vinculin-containing FA lengths.

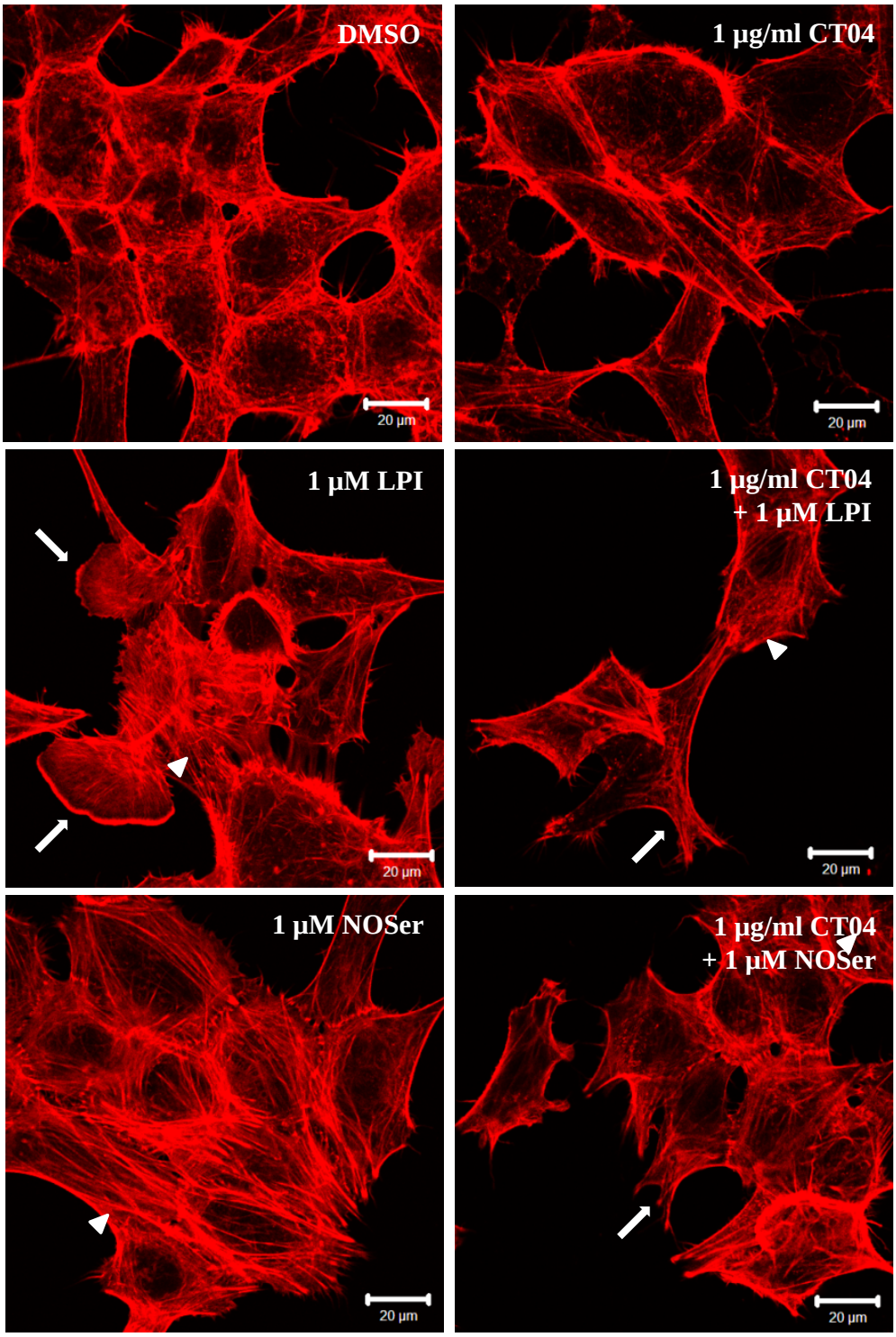

Figure 4.34: A role for Rho activation in GPR55-mediated cytoskeletal reorganisation. *The cell permeant Rho inhibitor CT04 was applied to hGPR55-HEK293 cells for 4 hr prior to addition of lipid ligands. The F-actin cytoskeleton was visualised with Alexa Fluor® 546 phalloidin. Panels show representative confocal images of phalloidin labelling following treatment with: DMSO; 1 µg/ml CTO4; 1 µM LPI; 1 µg/ml CT04 + 1 µM LPI; 1 µM NOSer; 1 µg/ml CT04 + 1 µM NOSer. Note the lipid-induced cytoskeletal reorganisation is decreased in cells pre-treated with the Rho inhibitor. Scale bars = 20 µm; n = 3. Arrowhead = stress fibres; arrows = lamellipodia.*

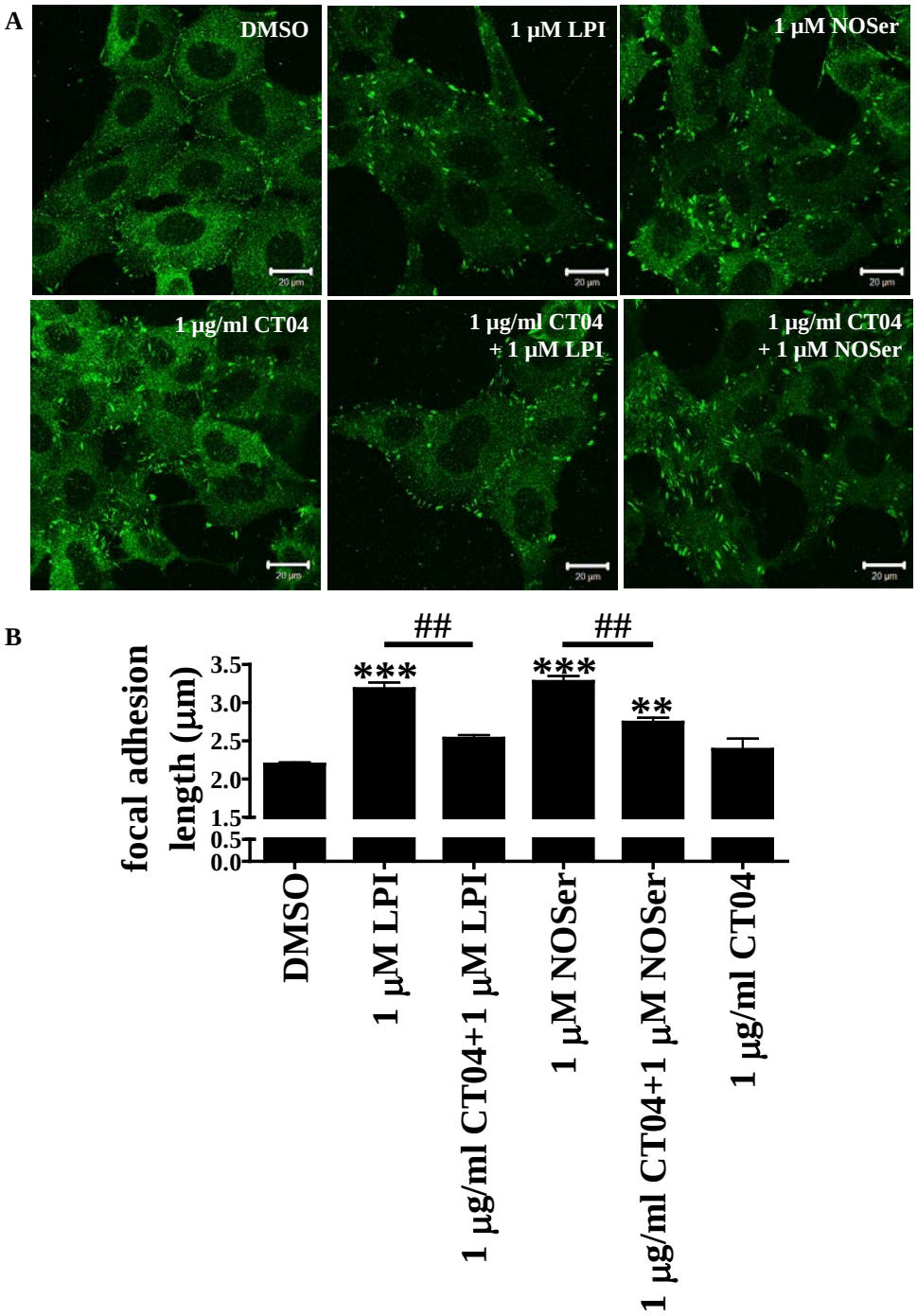

Figure 4.35: Rho is involved in GPR55-mediated changes in FA length. *The Rho inhibitor (CT04) was applied to hGPR55-HEK293 cells 4 hr prior to the commencement of experiments.* ***A****, representative confocal images of vinculin labelling illustrating the effect of: DMSO; 1 µM LPI; 1 µM NOSer; 1 µg/ml CTO4; 1 µg/ml CT04 + 1 µM LPI; 1 µg/ml CT04 + 1 µM NOSer. Scale bars = 20 µm; n = 3.* ***B****, histogram of pooled data highlighting lipid-mediated changes in FA length in hGPR55-HEK293 cells either in the presence or absence of the Rho inhibitor. Note Rho signalling is required for the formation of lipid-treated FAs. * = data compared to vehicle control. Data are the means ± SEM; n = 3. One-way ANOVA with a Bonferroni post hoc test; **P < 0.01; ***P < 0.001; ##P < 0.01.*

Next cdc42 was evaluated, another member of the Rho small GTPase family, which can be activated by GPR55 (Ryberg *et al.*, 2007). Cdc42 is known to be important in the generation of filopodia in Swiss 3T3 fibroblasts (Nobes and Hall, 1995). Therefore a novel cdc42 inhibitor (ML-141; 10 µM) was evaluated in hGPR55-HEK293 cells. Cells treated with the cdc42 inhibitor had a flat, spread out morphology similar to control cells. Co-application of either LPI or NOSer with the cdc42 inhibitor had little effect on lipid-induced reorganisation of the cytoskeleton; the cells had a similar morphology to those treated with lipid alone (figure 4.36). These data suggest that the cdc42 inhibitor (ML-141) did not affect the lipid-induced changes in the F-actin cytoskeleton in hGPR55-HEK293 cells. Filopodia were observed in all cells treated with the ML-141 suggesting that the inhibitor did not affect the filopodia formation in this assay.

Cdc42 is implicated in the formation of vinculin-containing FAs in Swiss 3T3 fibroblasts (Nobes and Hall, 1995) hence the cdc42 inhibitor was also tested in the vinculin assay. One-way ANOVA analysis highlights significant difference in the data set ($F_{(5,12)} = 11.2$; $P = 0.0003$). Furthermore Bonferroni *post hoc* analysis revealed in the presence of the cdc42 inhibitor ML-141 (10 µM), LPI (1 µM) or NOSer (1 µM) mediated FA lengthening was not significantly different with lipids alone (LPI = 3.31 ± 0.08 µm, ML-141 + LPI = 2.99 ± 0.22 µm, NOSer = 3.30 ± 0.13 µm, ML-141 + NOSer = 2.98 ± 0.13 µm, n = 3, $P > 0.05$, figure 4.37A and B). ML-141 (10 µM; 55 min) applied by itself did not significantly affect FA length (DMSO = 2.16 ± 0.12 µm, ML-141 = 2.43 ± 0.13 µm, n = 3, $P > 0.05$). These data suggest that cdc42 activation is not required for the formation of vinculin-containing FAs in hGPR55-HEK293 cells treated with the endogenous lipids.

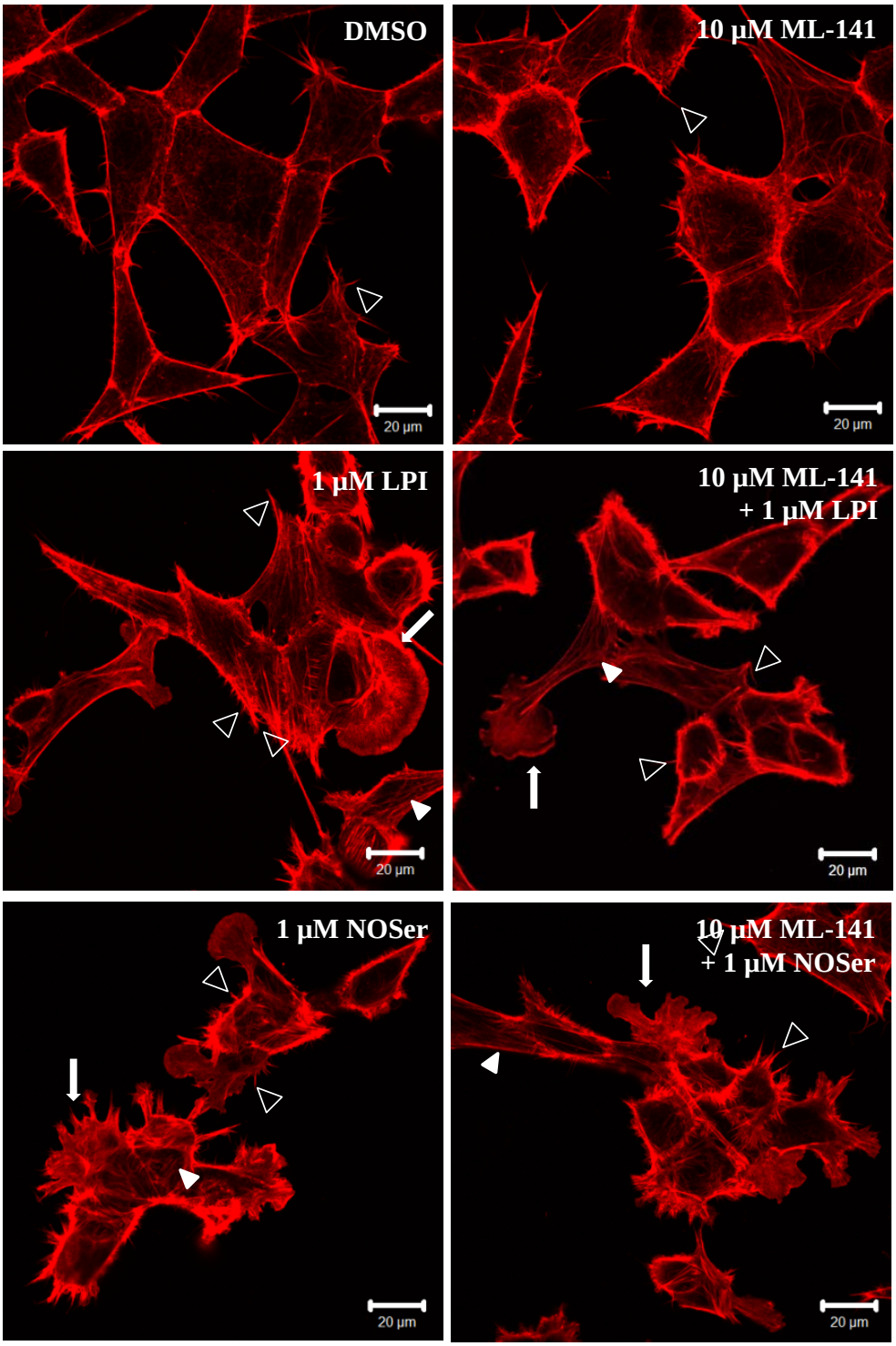

Figure 4.36: Cdc42 is not required for GPR55-mediated cytoskeletal remodelling. *The cdc42 inhibitor (ML-141) was applied to hGPR55-HEK293 cells for 30 min prior to co-application with either of the lipids. The F-actin cytoskeleton was visualised with Alexa Fluor® 546 phalloidin. Panels show representative confocal images of phalloidin labelling following treatment with: DMSO; 10 µM ML-141; 1 µM LPI; 10 µM ML-141 + 1 µM LPI; 1 µM NOSer; 10 µM ML-141 + 1 µM NOSer. Scale bars = 20 µm; n = 3; arrows = lamellipodia; arrowheads = stress fibres; open arrowheads = filopodia.*

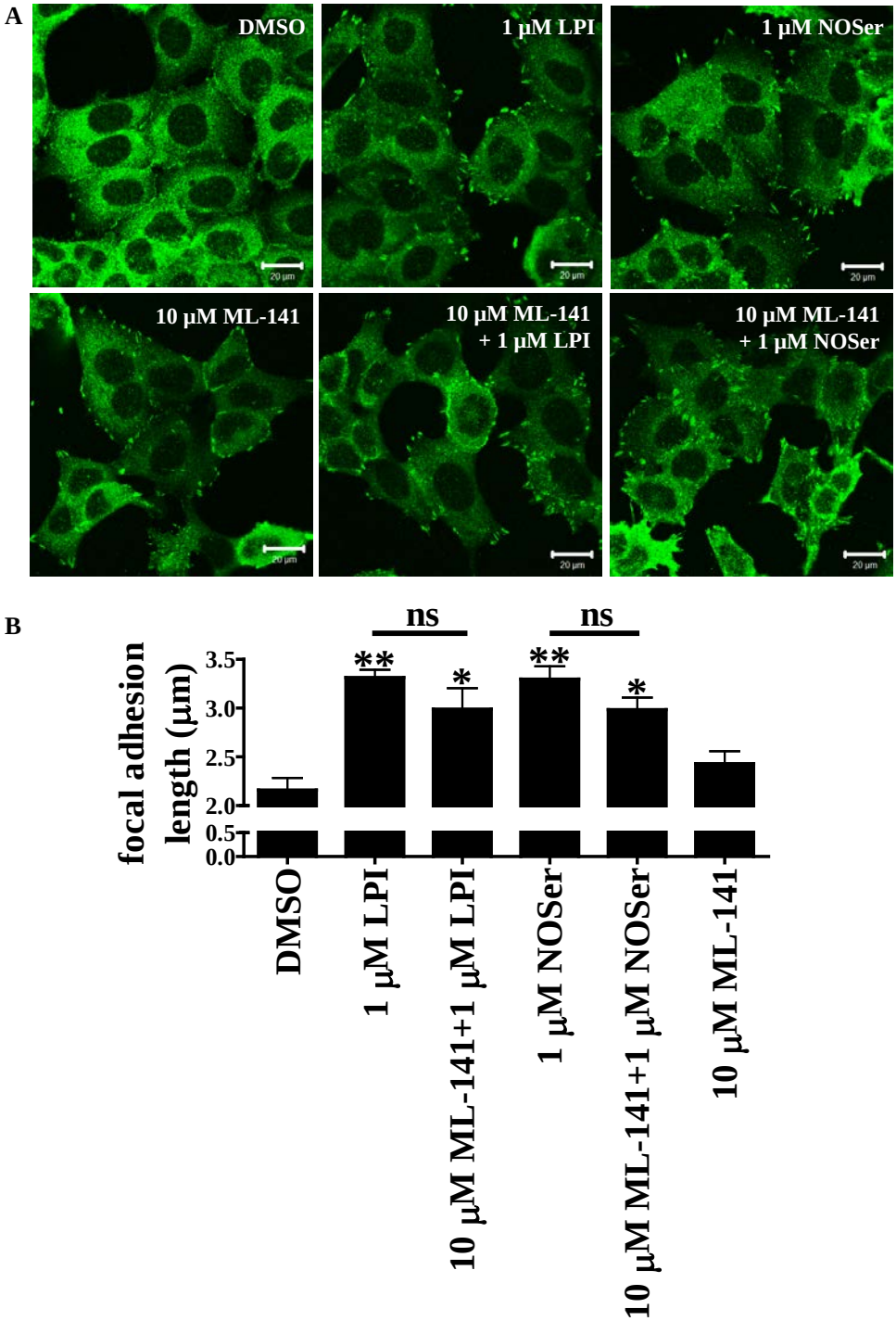

Figure 4.37: GPR55-mediated FA elongation is not effected by cdc42 inhibition. *The cdc42 inhibitor (ML-141; 10 µM) was applied to hGRP55-HEK293 cells for 30 min prior to the co-application with either of the endogenous lipids.* ***A****, representative confocal images of vinculin labelling illustrating the effect of: DMSO; 1 µM LPI; 1 µM NOSer; 10 µM ML-141; 10 µM ML-141 + 1 µM LPI; 10 µM ML-141 + 1 µM NOSer. Scale bars = 20 µm; n = 3.* ***B****, histogram of pooled data, highlighting lipid-mediated changes in FA length in hGPR55-HEK293 cells. Note that inhibition of cdc42 did not affect increases in FA length mediated by either of the lipids. * = data compared to vehicle control. Data are the means ± SEM; n = 3. One-way ANOVA with a Bonferroni post hoc test; *P < 0.05; **P < 0.01; ns = not significant.*

Next the Rho-ROCK signalling axis was investigated as to whether the cytoskeletal reorganisation in hGPR55-HEK293 cells required ROCK signalling, using structurally different ROCK inhibitors. Cells treated with the ROCK I and II inhibitor Y-27632 (10 µM) were retracted and the cell membranes were jagged when compared to control cells (figure 4.38). This was not observed with the ROCK II inhibitor H1152 (100 nM), where H1152 treated cells were similar to control. Pre-treatment of hGPR55-HEK293 cells with either Y-27632 or H1152 for 30 min prior to co-application of either lipid were found to inhibit the LPI and NOSer-induced formation of lamellipodia and stress fibres.

ROCK activation by Rho is known to be an important factor in the formation of FAs (Amano *et al.*, 1997). Therefore the ROCK inhibitors; Y-27632 (10 µM) and H1152 (100 nM) were applied to hGRP55-HEK293 cells for 30 min prior to the application of the lipids. There was a significant differences when the data was subjected to one-way ANOVA analysis ($F_{(8,9)} = 11.55$; $P = 0.0007$). Moreover *post hoc* analysis revealed that FA elongation in response to LPI was reduced in the presence of either Y-27632 or H1152 by 78.2 ± 5.0% and 82.6 ± 6.5% respectively, (LPI = 3.48 ± 0.13 µm, Y-27632 + LPI = 2.03 ± 0.21 µm, H1152 + LPI = 2.23 ± 0.09 µm, n = 3, $P < 0.001$, figure 4.39A and B). Likewise with NOSer, FA elongation was reduced (Y-27632 = 79.2 ± 6.0%; H1152 = 80.2 ± 3.1%) in hGPR55-HEK293 cells that had been treated with the ROCK inhibitors prior to the co-application of lipid (NOSer = 3.42 ± 0.17 µm, Y-27632 + NOSer = 2.17 ± 0.06 µm, H1152 + NOSer = 2.53 ± 0.15 µm). These data suggest that hGPR55-HEK293 cells treated with the endogenous lipids require ROCK activation to increase the FA length. Furthermore increasing the ROCK II inhibitor concentration to 1 µM ablates the vinculin-containing FAs (data not shown) however, at this concentration it can also inhibit CAMKII and cGMP-dependent protein kinase (PKG).

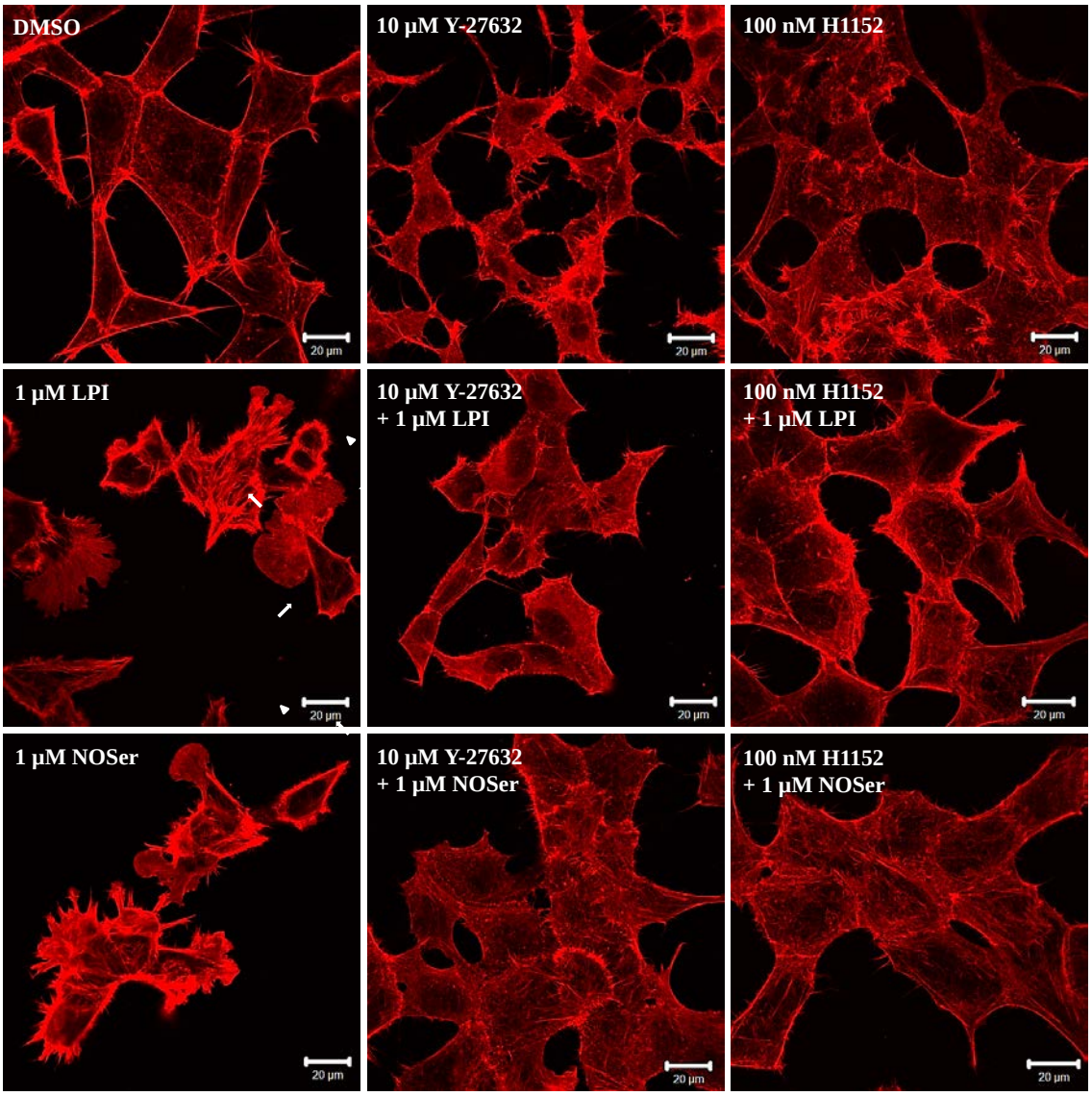

Figure 4.38: Both ROCK I and II are required for GPR55-mediated F-actin cytoskeletal reorganisation. *Two structurally different ROCK inhibitors; the ROCK I and II inhibitor (Y-27632; 10 µM) or the ROCK II inhibitor (H1152; 100 nM) were applied to hGPR55-HEK293 cells for 30 min prior to co-application with the either LPI or NOSer. The F-actin cytoskeleton was visualised with Alexa Fluor® 546 phalloidin. Panels show representative confocal images of phalloidin labelling following treatment with: DMSO; 10 µM Y-27632; 100 nM H1152; 1 µM LPI; 10 µM Y-27632 + 1 µM LPI; 100 nM H1152 + 1 µM LPI; 1 µM NOSer; 10 µM Y-27632 + 1 µM NOSer; 100 nM H1152 + 1 µM NOSer. Note the lipid-induced cytoskeletal reorganisation is prevented in hGPR55-HEK293 cells in the presence of the ROCK inhibitors. Scale bars = 20 µm; n = 3; arrow = lamellipodia; arrowheads = stress fibres.*

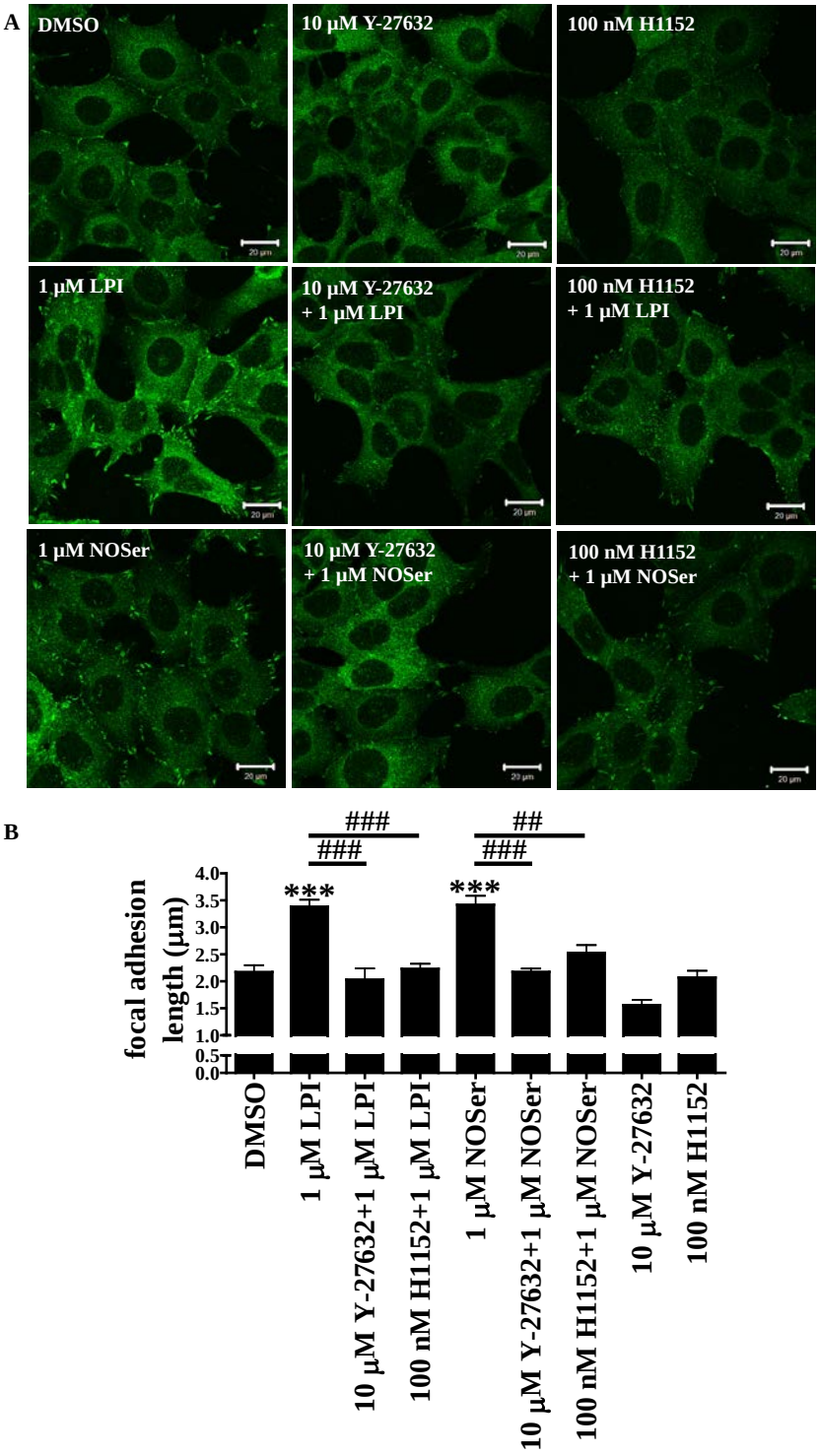

Figure 4.39: ROCK I and II are required for GPR55-mediated FA elongation. *The ROCK I and II inhibitor (Y-27632; 10 µM) or ROCK II inhibitor (H1152; 100 nM) was applied to hGPR55-HEK293 cells prior to co-application with either of the lipids.* ***A****, representative confocal images of vinculin labelling illustrating the effect of: DMSO; 10 µM Y-27632; 100 nM H1152; 1 µM LPI; 10 µM Y-27632 + 1 µM LPI; 100 nM H1152 + 1 µM LPI; 1 µM NOSer; 10 µM Y-27632 + 1 µM NOSer; 100 nM H1152 + 1 µM NOSer. Scale bars = 20 µm; n = 2.* ***B****, histogram of pooled data, highlighting effects on FA length in hGPR55-HEK293 cells. Note the presence of either of the ROCK inhibitors decreases the lipid-induced FA elongation.*

*Furthermore it was observed that Y-27632 applied with either lipid formed fewer FAs per cell. * = data compared to vehicle control. Data are the means ± SEM; n = 2. One-way ANOVA with a Bonferroni post hoc test; ***P < 0.001; ##P < 0.01; ###P < 0.001.*

4.2.2.6. Role of Ca^{2+} signalling in GPR55 effects on the actin cytoskeleton and FA elongation in hGPR55-HEK293 cells.

Next the role of Ca^{2+} signalling in GPR55-mediated FA lengthening was investigated. Firstly the role of PLC was evaluated. Cells treated with the PLC inhibitor U73122 (1 µM; 55 min) led to increased formation of filopodia but were in general flat and spread out (figure 4.40). Treatment of hGPR55-HEK293 with U73122 cells for 30 min prior to co-application with either LPI or NOSer did not prevent the formation of lamellipodia or stress fibres, which were similar to the effects of either the lipid alone. These data suggest that the inhibition of PLC had no effect on the lipid-induced cell rounding and lamellipodia formation mediated by GPR55 in hGPR55-HEK293 cells.

Next the effects of the PLC inhibitor U73122 (1 µM), were studied in the GPR55 FA assay. One-way ANOVA analysis highlighted significant differences between the groups tested ($F_{(5,12)} = 14.55$; $P < 0.0001$). Further analysis with a Bonferroni *post hoc* test revealed that treatment with U73122 did not affect FA length by itself, but significantly inhibited the effects of LPI by 78.0 ± 8.7% (figure 4.41A and B). The PLC inhibitor also inhibited the NOSer on FA length by 63.3 ± 5.6% but was not significant. These data suggest that PLC activation is important for lipid-modulation of FAs in hGPR55-HEK293 cells treated with LPI and is likely to be required FA increases in cells challenged with NOSer.

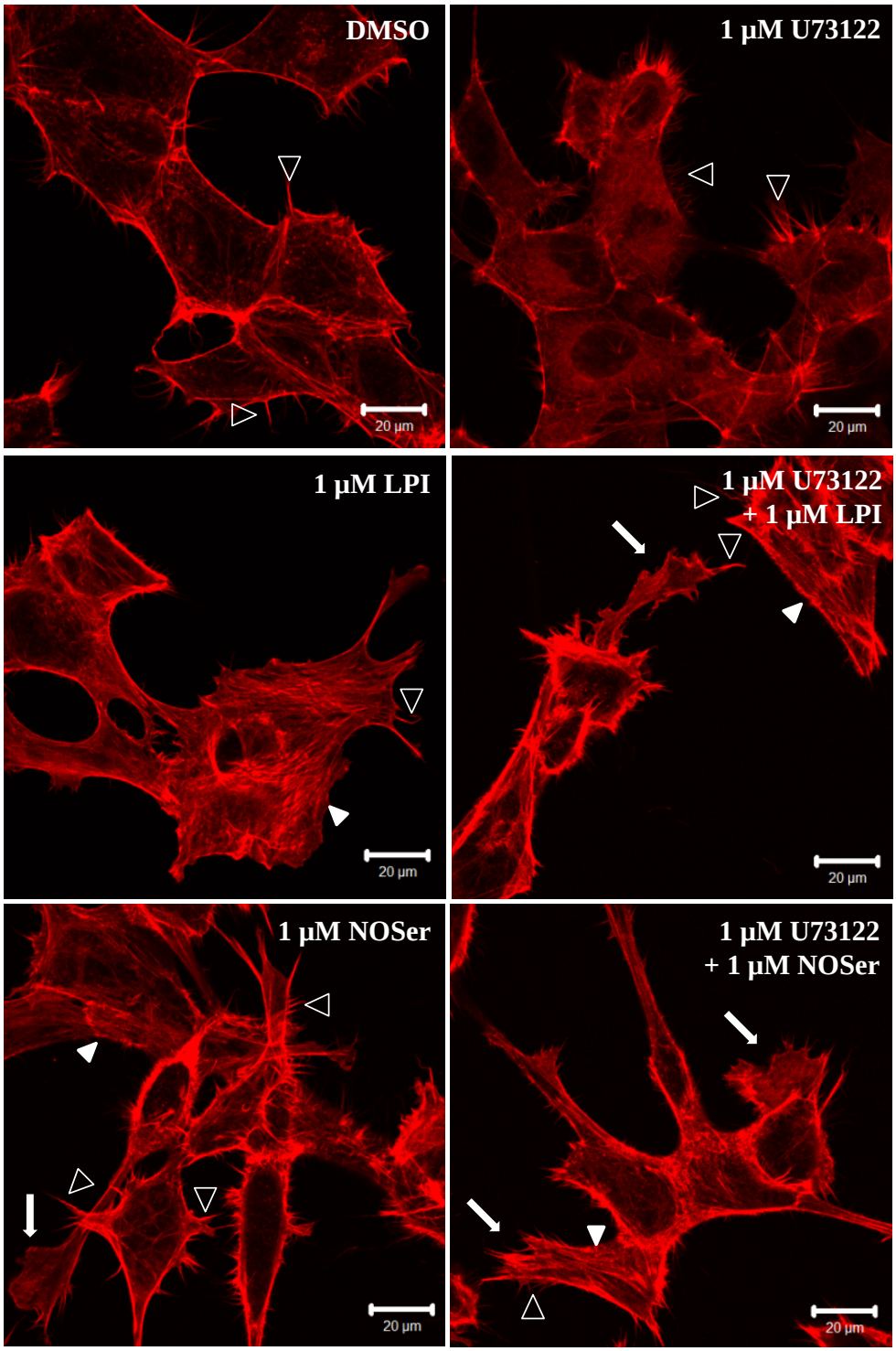

Figure 4.40: Cytoskeletal reorganisation mediated by GPR55 in hGPR55-HEK293 cells does not require PLC activation. *The PLC inhibitor (U73122; 1 µM) was applied to hGPR55-HEK293 cells for 30 min prior to co-application with either LPI or NOSer for a further 25 min. The F-actin cytoskeleton was visualised with Alexa Fluor® 546 phalloidin. Panels show representative confocal images of phalloidin labelling following treatment with: DMSO; 1 µM U73122; 1 µM LPI; 1 µM U73122 + 1 µM LPI; 1 µM NOSer; 1 µM U73122 + 1 µM NOSer. Scale bars = 20 µm; n = 2. Filled arrowheads = stress fibres; arrows = lamellipodia; open arrowheads = filopodia.*

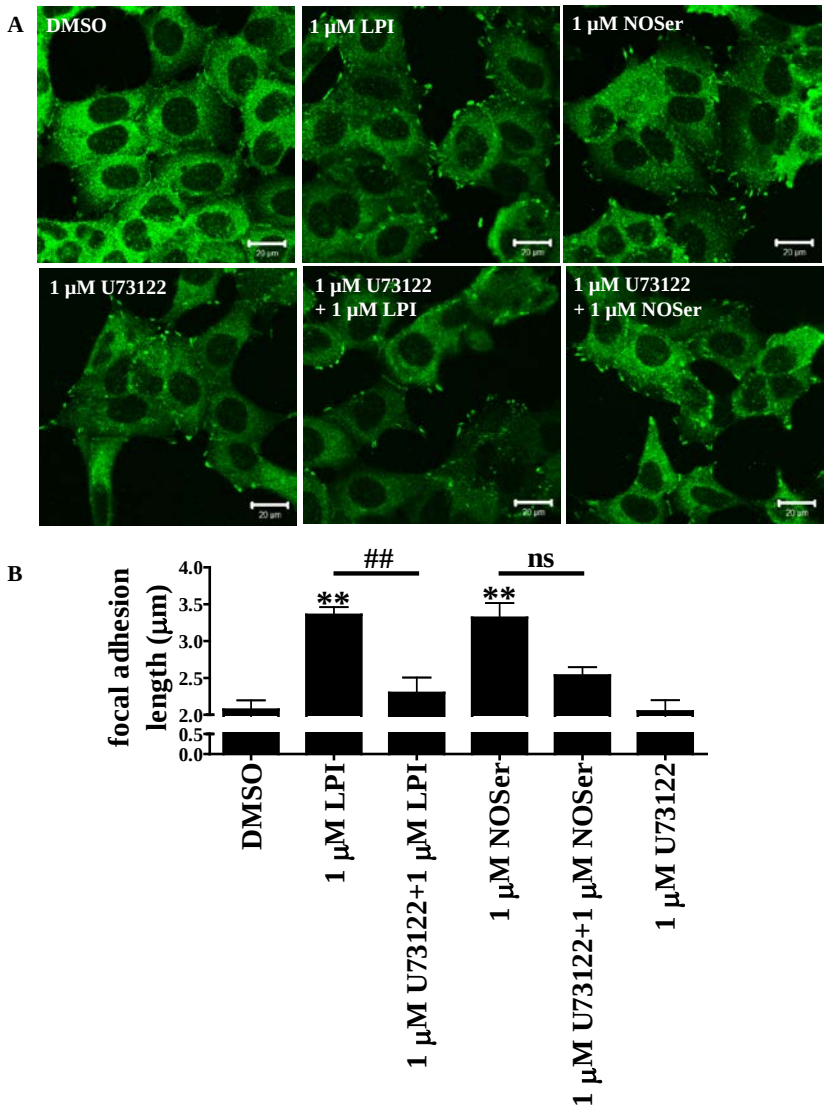

Figure 4.41: PLC is required for GPR55-mediated FA elongation. *The PLC inhibitor (U73122; 1 µM) was applied to hGPR55-HEK293 cells for 30 min prior to co-application with either LPI (1 µM) or NOSer (1 µM).* ***A****, representative confocal images of vinculin labelling illustrating the effect of: DMSO; 1 µM LPI; 1 µM NOSer; 1 µM U73122; 1 µM U73122 + 1 µM LPI; 1 µM U73122 + 1 µM NOSer. Scale bars = 20 µm; n = 3.* ***B****, histogram of pooled data, highlighting vinculin-containing FA length in hGPR55-HEK293 cells. Note the presence of the PLC inhibitor decreases the lipid-induced FA length. * = data compared to vehicle control. Data are means ± SEM; n = 3. One-way ANOVA with a Bonferroni post hoc test; **P < 0.01; ##P < 0.01; ns = not significant.*

4.2.2.7. MAPK influences FA length but does not affect the actin cytoskeleton in hGPR55-HEK293 cells.

The role of MAPK signalling in GPR55-mediated cytoskeletal changes was investigated using MAPK inhibitors. Application of PD98059 (25 µM) induced cell rounding with dense areas of peripheral actin labelling (figure 4.42). However, this was not observed

with U0126 (5 µM), which did not affect the cell morphology and were similar to control cells. LPI or NOSer when applied at 1 µM in the presence of either of the MEK1/2 inhibitors promoted similar cytoskeletal features as had been observed with each lipid alone. These results suggest that MAPK activation is not required for the lipid-induced reorganisation of the F-actin cytoskeleton in hGPR55-HEK293 cells.

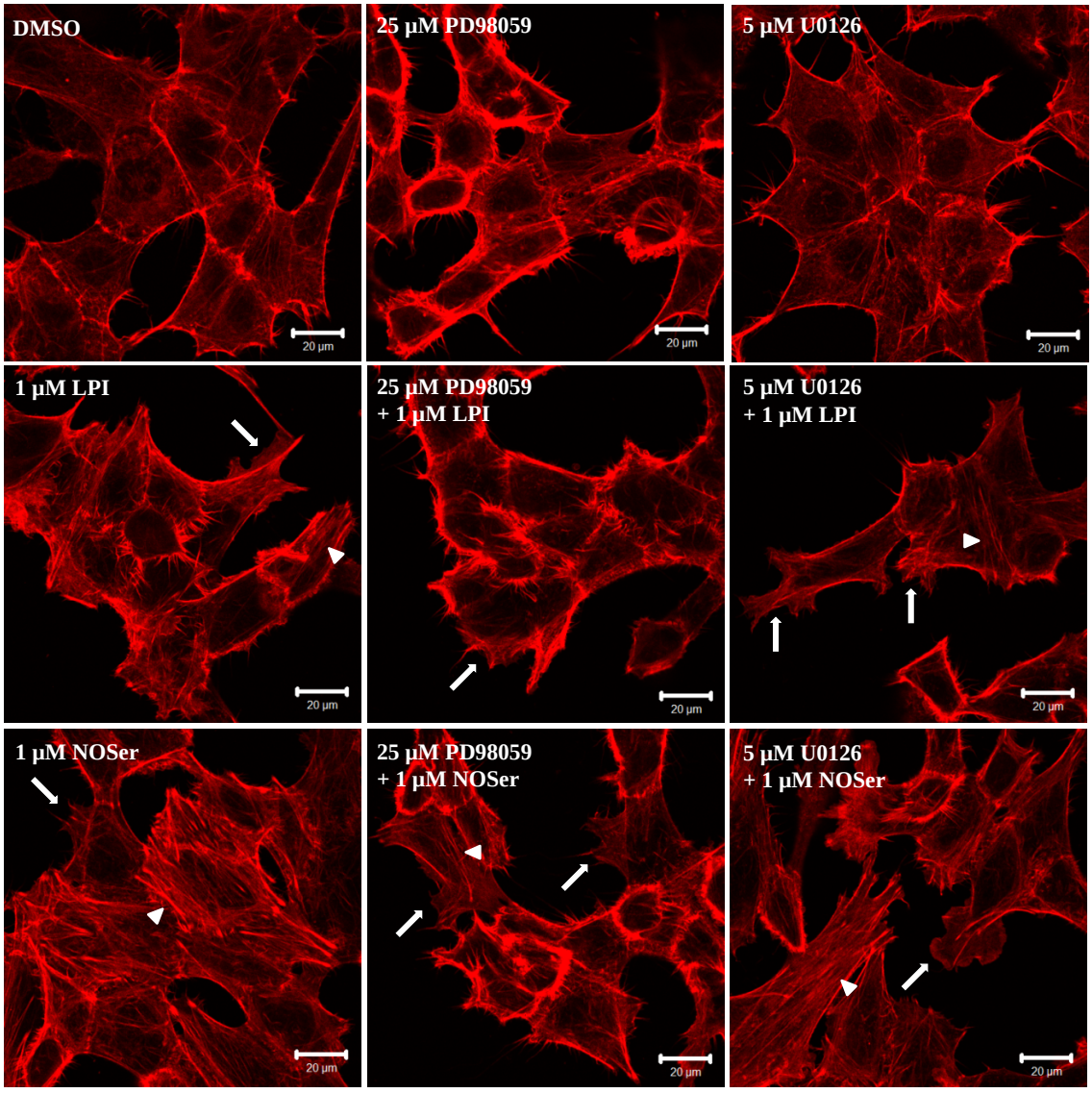

Figure 4.42: MAPK is not required for GPR55-mediated cytoskeletal reorganisation. *Two structurally different MEK1/2 inhibitors; PD98059 (25 µM) and U0126 (5 µM) were applied to hGPR55-HEK293 cells for 30 min prior to the co-application of either LPI (1 µM) or NOSer (1 µM). The F-actin cytoskeleton was visualised with Alexa Fluor® 546 phalloidin. Panels show representative confocal images of phalloidin labelling following treatment with: DMSO; 25 µM PD98059; 5 µM U0126; 1 µM LPI; 25 µM PD98059 + 1 µM LPI; 5 µM U0126 + 1 µM LPI; 1 µM NOSer; 25 µM PD98059 + 1 µM NOSer; 5 µM U0126 + 1 µM NOSer. Note that the MEK1/2 inhibitors did not affect LPI or NOSer induced changes in cytoskeletal reorganisation. Scale bars = 20 µm; n = 3; arrows = lamellipodia; arrowheads = stress fibres.*

The MEK1/2 inhibitors; PD98059 (25 µM) and U0126 (5 µM) were also tested in the GPR55-vinculin assay. Analysis with a one-way ANOVA highlighted that there were significant differences within the groups tested in the presence of the MEK1/2 inhibitors ($F_{(8,18)}$ = 8.227; P = 0.0001). Furthermore *post hoc* analysis revealed that treatment with PD98059 or U0126 (55 min) did not affect FAs, having a similar length to control cells (DMSO = 2.37 ± 0.11 µm, PD98059 = 2.21 ± 0.08 µm, U0126 = 2.36 ± 0.2 µm, n = 3, one-way ANOVA with a Bonferroni *post hoc* test, P > 0.05, figure 4.43A and B). However, pre-treatment with either PD98059 or U0126 prior to co-application with either LPI or NOSer inhibited their actions on FA length in hGPR55-HEK293 cells. LPI was inhibited by 90.7 ± 1.4% and 85.3 ± 13.9% in the presence of PD98059 and U0126 respectively. Furthermore NOSer in the presence of PD98059 and U0126 was inhibited by 86.7 ± 8.3% and 97.1 ± 3.1% respectively; (LPI = 3.45 ± 0.15 µm, PD98059 + LPI = 2.54 ± 0.07 µm, U0126 + LPI = 2.33 ± 0.24 µm, NOSer = 3.43 ± 0.14 µm, PD98059 + NOSer = 2.69 ± 0.22 µm, U0126 + LPI = 2.46 ± 0.17 µm).

An inactive analogue of U0126; U0124 (5 µM) was utilised to confirm that any effects were mediated through MAPK signalling. One-way ANOVA highlighted that there were significant differences within the data set when an inactive MEK1/2 inhibitor ($F_{(5,12)}$ = 10.78; P = 0.0004). Moreover a Bonferroni *post hoc* test revealed that the inactive MEK1/2 inhibitor, U0124, applied to the cells prior to co-application with either LPI or NOSer had no effect (LPI = 3.45 ± 0.15 µm, U0124 + LPI = 3.31 ± 0.11 µm, NOSer = 3.43 ± 0.14 µm, U0124 + NOSer = 3.45 ± 0.15 µm, n = 3, P > 0.05, figure 4.43C and D). These data suggest that the lipid-mediated increases in the length of the vinculin-containing FAs require the activation of MAPK in hGPR55-HEK293 cells challenged with LPI. Furthermore it is likely that MAPK activation is required for FA lengthening in hGPR55-HEK293 cells treated with NOSer.

A

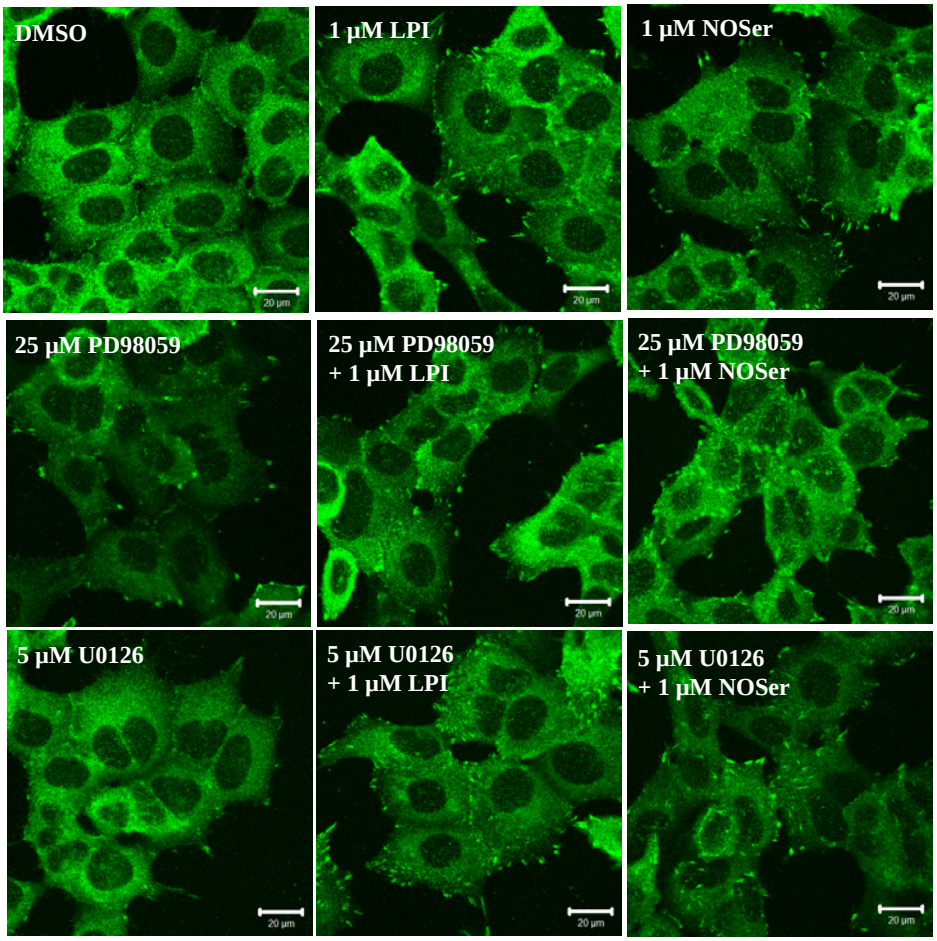
DMSO
1 µM LPI
1 µM NOSer
25 µM PD98059
25 µM PD98059
+ 1 µM LPI
25 µM PD98059
+ 1 µM NOSer
5 µM U0126
5 µM U0126
+ 1 µM LPI
5 µM U0126
+ 1 µM NOSer
20 µm

B

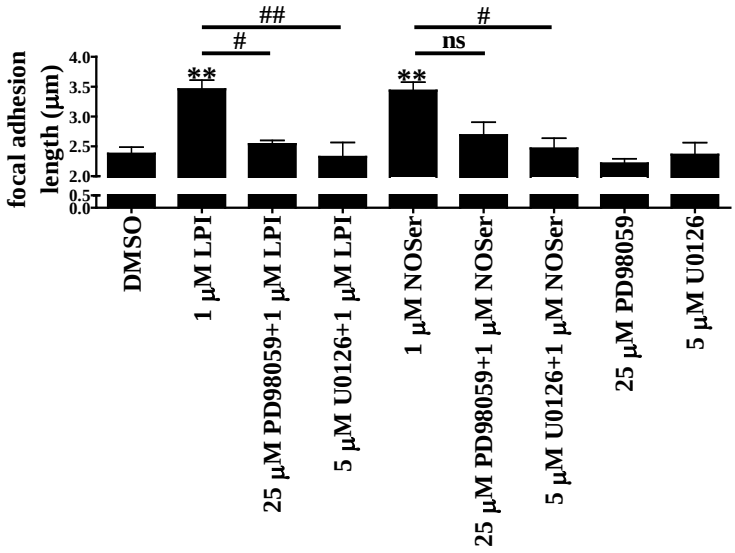
focal adhesion length (µm)
4.0
3.5
3.0
2.5
2.0
0.5
0.0
**
**
##
#
#
ns
DMSO
1 µM LPI
25 µM PD98059+1 µM LPI
5 µM U0126+1 µM LPI
1 µM NOSer
25 µM PD98059+1 µM NOSer
5 µM U0126+1 µM NOSer
25 µM PD98059
5 µM U0126

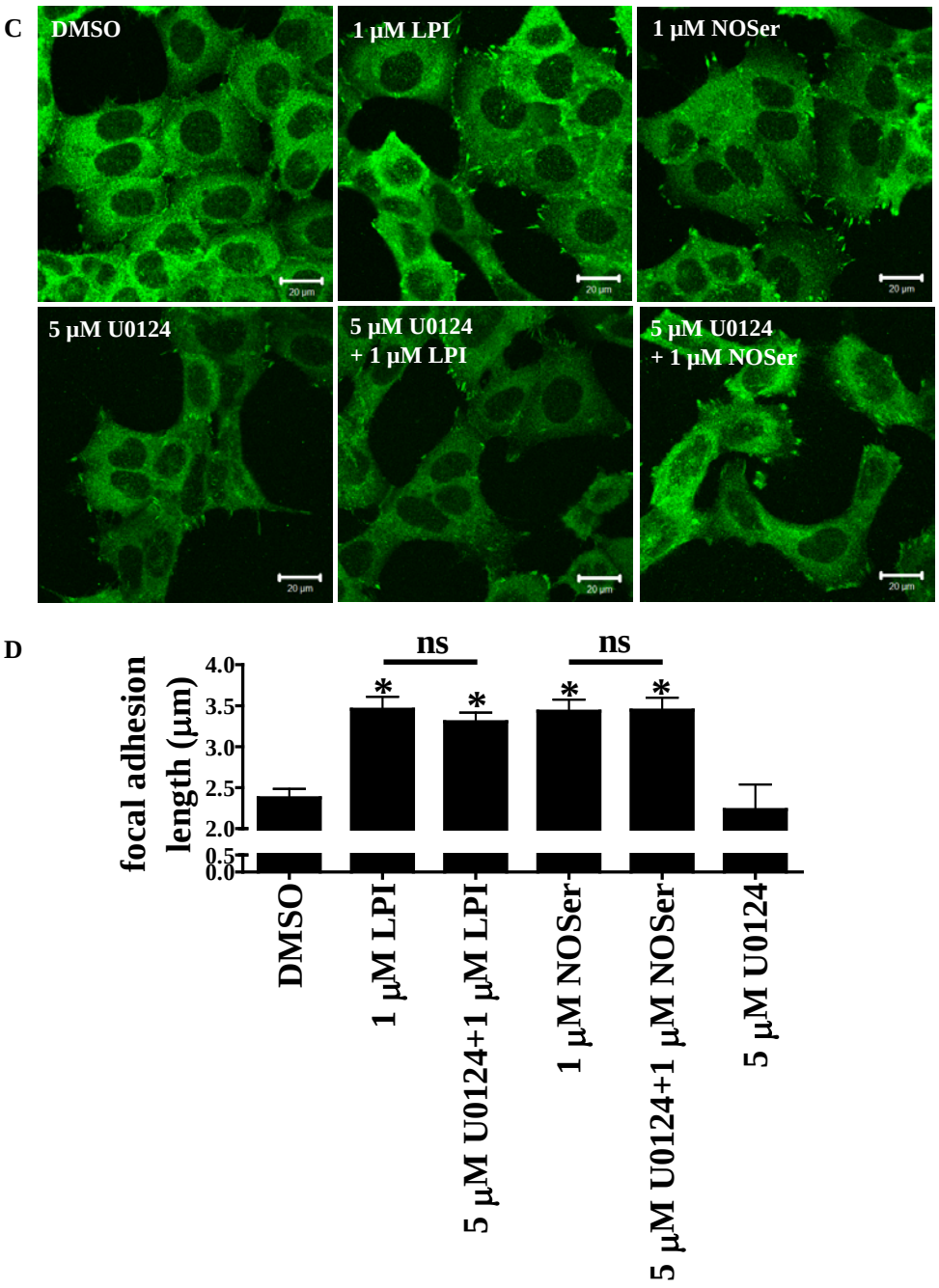

Figure 4.43: MAPK is required for GPR55-mediated increases in FA length. *Two structurally different MEK1/2 inhibitors (PD98059; 25 µM or U0126; 5 µM) or an inactive MEK1/2 inhibitor (U0124; 5 µM) were applied to hGPR55-HEK293 cells for 30 min prior to co-application of with either LPI (1 µM) or NOSer (1 µM).* ***A****, representative confocal images of vinculin labelling illustrating the effect of the active MEK1/2 inhibitors: DMSO; 25 µM PD98059; 5 µM U0126; 1 µM LPI; 25 µM PD98059 + 1 µM LPI; 5 µM U0126 + 1 µM LPI; 1 µM NOSer; 25 µM PD98059 + 1 µM NOSer; 5 µM U0126 + 1 µM NOSer.* ***B****, histogram of pooled MEK1/2 inhibitor data, highlighting effects on vinculin-containing FA length in hGPR55-HEK293 cells. Note that the presence of the active MEK1/2 inhibitors (PD98059 or U0126) leads to an inhibition of lipid-mediated responses.* ***C****, representative confocal images of vinculin labelling highlighting the effect of the inactive MEK1/2 inhibitor: DMSO; 1 µM LPI; 1*

µM NOSer; 5 µM U0124; 5 µM U0124 + 1 µM LPI; 5 µM U0124 + 1 µM NOSer. ***D****, histogram of pooled inactive MEK1/2 inhibitor data, highlighting effects on vinculin-containing FA length in hGPR55-HEK293 cells. Note the presence of 5 µM U0124 does not alter the FA length of lipid-mediated responses. * = data compared to vehicle control. Data are the means ± SEM; n = 3. One-way ANOVA with a Bonferroni post hoc test; *P < 0.05; **P < 0.01; # < 0.05; ## < 0.01; ns = not significant.*

4.2.2.8. PI-3 kinase activation is not required for GPR55-mediated cytoskeletal reorganisation or differences in FA length.

Next we investigated whether PI-3 kinase was involved in GPR55-mediated cytoskeletal reorganisation or differences in FA length. Application of two structurally different PI-3 kinase inhibitors, LY294022 (3 µM) or wortmannin (50 nM), to hGPR55-HEK293 cells did not affect cell morphology or actin cytoskeletal structure relative to control cells (figure 4.44). In addition, PI-3 kinase inhibitors did not affect responses to LPI or NOSer, with a similar reorganisation of the cytoskeleton associated with the appearance of stress fibres and lamellipodia. These data suggest that lipid-induced cytoskeletal reorganisation in hGPR55-HEK293 cells is not mediated through PI-3 kinase activation.

Next, the two structurally distinct PI-3 kinase inhibitors; LY294002 (3 µM) and wortmannin (50 nM) were studied in the GPR55-FA assay. One-way ANOVA highlighted significant differences between the PI3 kinase data set ($F_{(8,18)}$ = 5.834; P = 0.0009). Bonferroni *post hoc* analysis revealed that treatment of hGPR55-HEK293 with either LY294022 or wortmannin did not affect FAs, where they had similar length to the control cells (DMSO = 2.25 ± 0.05 µm, LY294002 = 2.18 ± 0.28 µm, wortmannin = 2.34 ± 0.17 µm, n = 3, one-way ANOVA with a Bonferroni *post hoc* test, P > 0.05, figure 4.45A and B). Treatment with either LY294002 or wortmannin prior to co-application with LPI did not significantly affect LPI-induced changes in FA length (LPI = 3.37 ± 0.14 µm, LY294022 + LPI = 3.02 ± 0.25 µm, wortmannin + LPI = 2.95 ± 0.06 µm). Likewise with NOSer, there was no significant inhibition of responses (NOSer = 3.34 ± 0.23 µm, LY294002 + NOSer = 3.04 ± 0.25 µm, wortmannin + NOSer = 3.21 ± 0.18 µm). These data suggest that activation of PI-3 kinase is not required for the lipid-mediated increases in FA length in hGPR55-HEK293 cells.

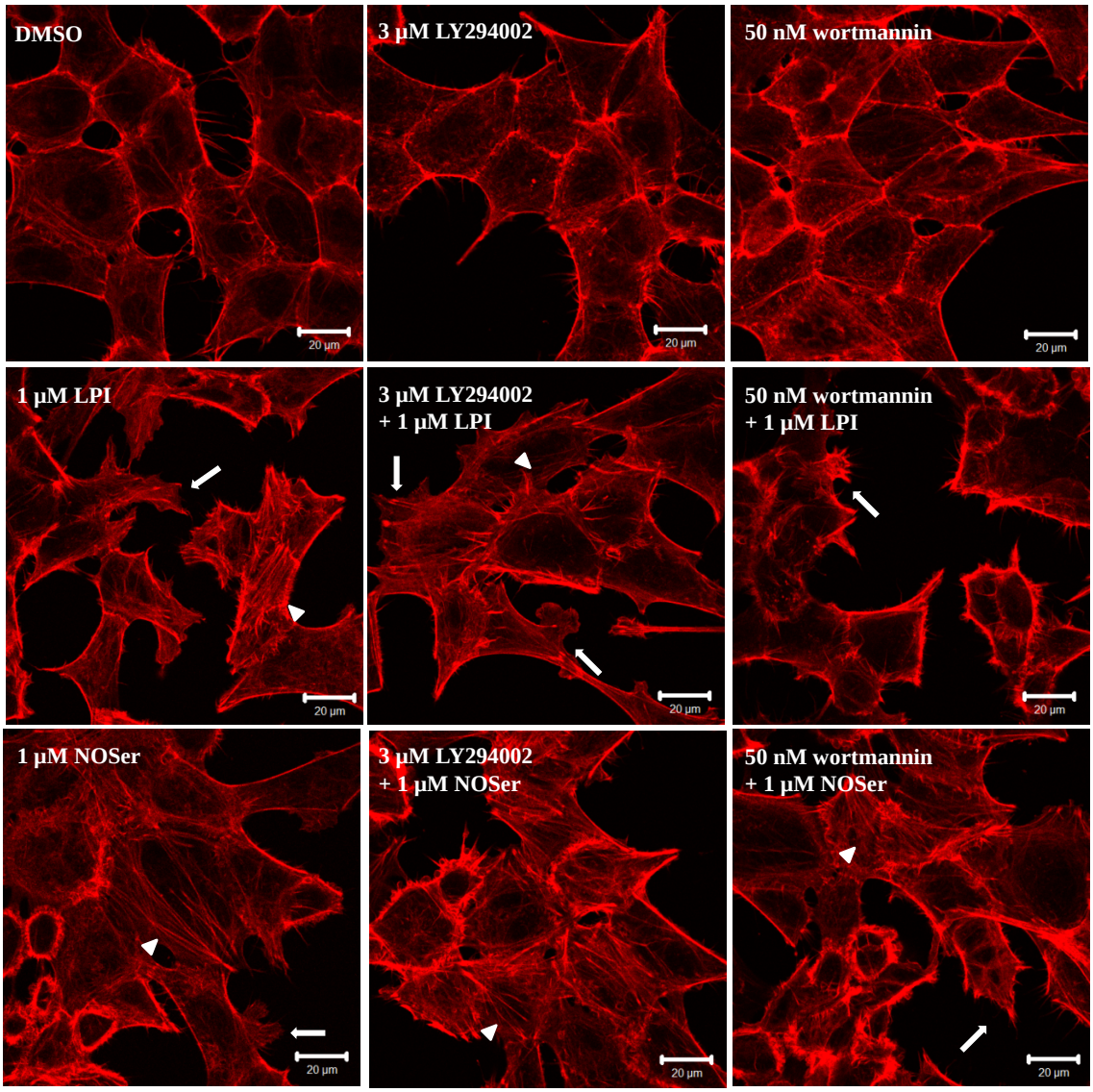

Figure 4.44: GPR55-mediated cytoskeletal reorganisation does not require PI-3 kinase activation. *Two structurally distinct PI-3 kinase inhibitors (LY294022; 3 µM and wortmannin; 50 nM) were applied to hGPR55-HEK293 cells for 30 min prior to co-application with either of the lipids. The F-actin cytoskeleton was visualised with Alexa Fluor® 546 phalloidin. Panels show representative confocal images of phalloidin labelling following treatment with: DMSO; 3 µM LY294002; 50 nM wortmannin; 1 µM LPI; 3 µM LY294002 + 1 µM LPI; 50 nM wortmannin + 1 µM LPI; 1 µM NOSer; 3 µM LY294002 + 1 µM NOSer; 50 nM wortmannin + 1 µM NOSer. Note PI-3 kinase inhibitors did not affect lipid-mediated cell retraction and the formation of lamellipodia and stress fibres. Scale bars = 20 µm; n = 3. Arrows = lamellipodia; arrow heads = stress fibres.*

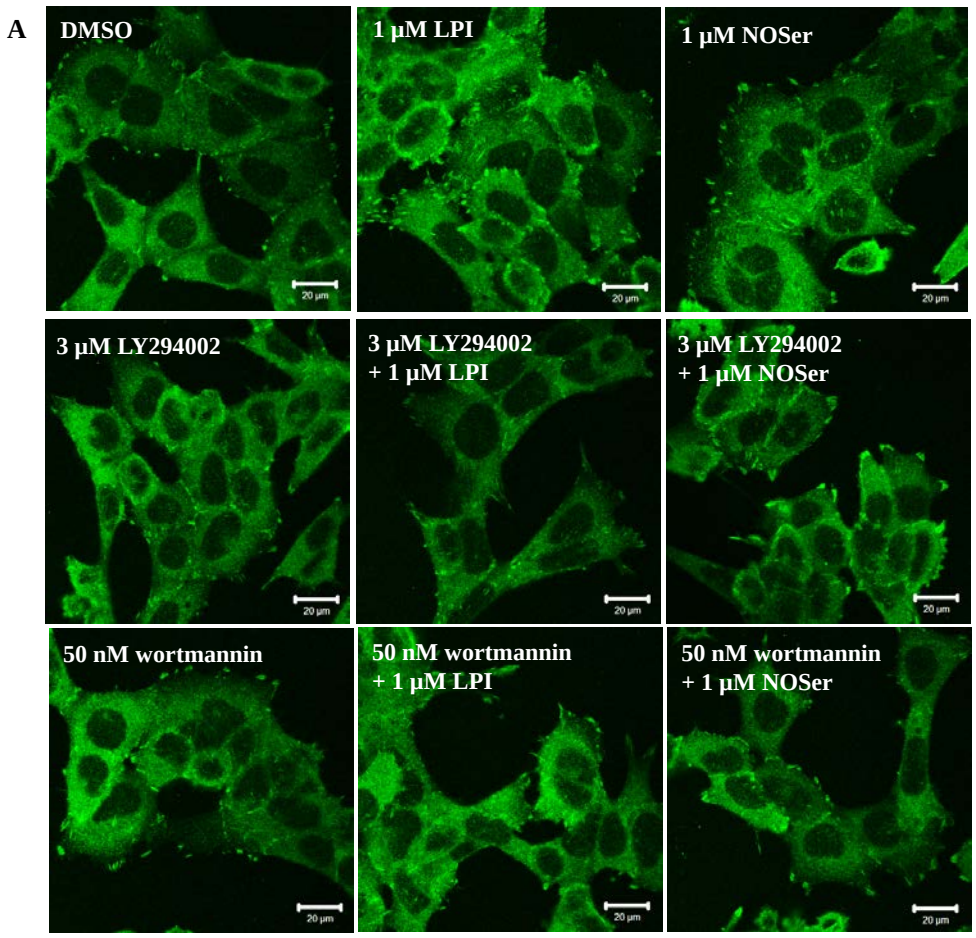

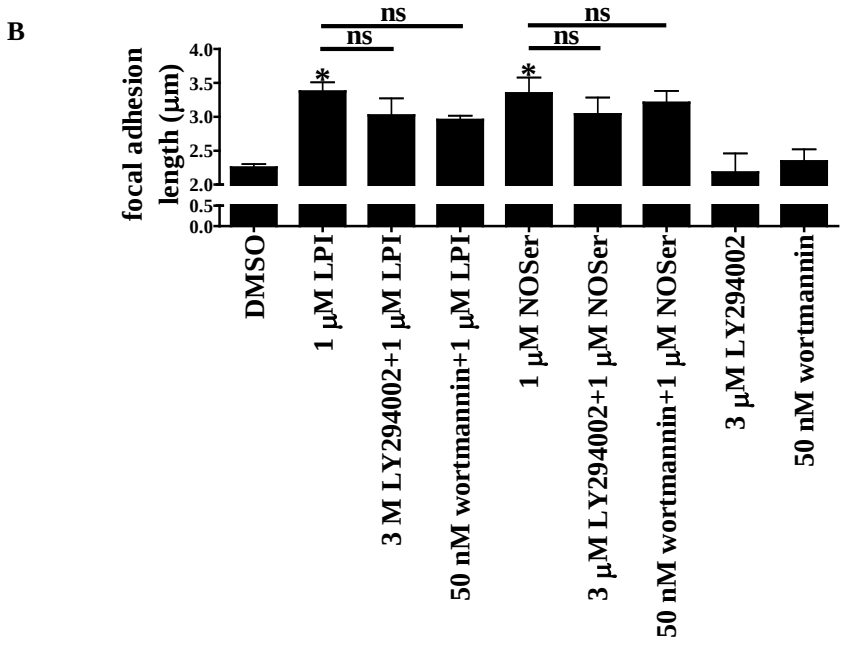

Figure 4.45: GPR55-mediated effects on FA length do not require PI-3 kinase. *Cells were treated for 30 min with PI-3-kinase inhibitors (LY294002; 3 µM or wortmannin; 50 nM) prior to co-application of inhibitor with a lipid.* ***A****, representative confocal images of vinculin labelling illustrating the effect of: DMSO; 3 µM LY294002; 50 nM wortmannin; 1 µM LPI; 3 µM LY294002 + 1 µM LPI; 50 nM wortmannin + 1 µM LPI; 1 µM NOSer; 3 µM LY294002 +*

1 µM NOSer; 50 nM wortmannin + 1 µM NOSer. Scale bars = 20 µm; n = 3. ***B****, histogram of pooled data depicting effects on the length of vinculin-containing FAs in hGPR55-HEK293 cells. Note that inhibiting PI-3 kinase did not influence lipid-induced FA elongation. * = data compared to vehicle control. Data are the means ± SEM; n = 3. One-way ANOVA with a Bonferroni post hoc test; *P < 0.05; ns = not significant.*

4.3. DISCUSSION

4.3.1. GPR55-mediated pCREB in hGPR55-HEK293 cells

This study confirmed that GPR55 signals to CREB not only with previously tested GPR55 agonists; LPI and AM251 (Henstridge *et al.*, 2010) but also with novel N-acyl amino acids. To date only two or the N-acyl amino acids (NAS and NAG) have been studied in relation to GPR55 activation.

In the present study NASer (300 nM - 10 µM) was observed to promote pCREB. Recent evidence has reported that NASer (10 nM - 30 µM) applied for 30 min can promote the phosphorylation of ERK1/2 (pERK), a protein located upstream of CREB, in HUVEC cells (Milman *et al.*, 2006). The authors also observed that this effect was mediated by a $G_{\alpha i/o}$ linked GPCR as PTX abolished the pERK responses. NOSer has also been reported to activate a $G_{\alpha i/o}$ linked GPCR in an osteoblastic cell line (MC3T3 E1) resulting in increased pERK1/2 at a similar time point (30 min) as used in the pCREB assay in this study (Smoum *et al.*, 2010). Therefore, both of the Israeli studies would strongly suggest that their observations are not GPR55-mediated (Milman *et al.*, 2006; Smoum *et al.*, 2010). The present observations, taken together with previous studies, suggest the existence of at least two GPCRs that are sensitive to NASer and NOSer. It is proposed that due to the sensitivity of GPR55 to NASer and NOSer - GPR55 is proposed to be as a novel candidate receptor for both these endogenous lipids.

The pCREB assay utilised in this study also observed that NAGly–induced pCREB was GPR55-mediated. NAGly is reported to activate several GPCRs; GPR18 (Kohno *et al.*, 2006; Yin *et al.*, 2009; McHugh *et al.*, 2010, 2012; Caldwell *et al.*, 2013), GPR72 (Hannedouche and Roy, 2010) and can act as a GPR92 partial agonist (Oh *et al.*, 2008). However prior studies did not find GPR55-mediated migratory effects in a Boyden chamber assay using hGPR55-HEK293 cells treated with NAGly but it should be noted that these cells were not placed in serum free prior to experimentation (McHugh *et al.*, 2010). In another study $GPR55^{(-/-)}$ mice were found to lower the intraocular pressure in

the murine eye to the same extent as wild type mice suggesting that the NAGly-induced response was not GPR55-mediated (Caldwell *et al.*, 2013). Both these studies suggest that the NAGly effects are through activation of GPR18. Interestingly, both GPR55 (Johns *et al.*, 2007) and GPR18 (McHugh *et al.*, 2010) have been considered as the enigmatic abnormal cannabidiol receptor and have an overlapping pharmacology (Ross, 2009). Therefore it is feasible to suggest that the N-acyl amino acids in this study may act as agonists/partial agonists at both these GPCRs, however it remains to be determined if NASer, NOSer, NPSer, NOGly and NPGly can promote GPR18-mediated signalling.

This study also highlighted that some of the N-acyl amino acids may display ligand bias in the hGPR55-HEK293 cells. This is when an agonist has the ability to activate the receptor but exerts a preference as to which downstream signalling pathway is activated (Kenakin, 2011). The responses in the Ca^{2+} mobilisation and pCREB assay differed in potency for LPI (vinculin FA > Ca^{2+} > pCREB assay), NOSer (vinculin FA = pCREB > Ca^{2+} assay) and NOG (Ca^{2+} > pCREB assay) suggesting that these lipids may be demonstrating ligand bias. Previously Henstridge *et al*., 2010, also reported that LPI was more potent in the Ca^{2+} mobilisation (49 ± 4 nM) than in the pCREB assay (630 ± 110 nM). However it was also reported that AM251 was considerably less potent than LPI in a pCREB immunoblot assay; 430 ± 90 nM and 93 ± 10 nM respectively (Henstridge *et al.*, 2010). In contrast this study finds that AM251 was more equipotent than LPI in the pCREB assay.

Ligand	**Ca^{2+} EC_{50} nM**	**pCREB EC_{50} nM**	**Vinculin FAs EC_{50} nM**
LPI	183 ± 8	262 ± 54	72 ± 10
NASer	256 ± 18	nd	nt
NOSer	253 ± 4	95 ± 29	65 ± 11
NPSer	314 ± 12	nd	nt
NAGly	908 ± 63	848 ± 153	nt
NOGly	347 ± 12	1085 ± 264	nt
NPGly	nd	nd	nt
AM251	nt	256 ± 51	nt

Table 4.2: Relative ligand potencies for different GPR55-mediated signalling pathways in hGPR55-HEK293 cells. *EC_{50} values for changes in Ca^{2+}, pCREB and vinculin FA length. Both LPI and NOSer are more potent in the FA and pCREB assays. nt = not tested; nd = not determined (the E_{max} was not achieved therefore the EC_{50} could not be calculated). EC_{50} values (95% confidence limits).*

4.3.1.1. GPR55-modulation of pCREB involves a $G_{\alpha 13}$-Rho-ROCK signalling axis in hGPR55-HEK293 cells.

LPI and NOSer-mediated nuclear pCREB activity in hGPR55-HEK293 cells involves multiple signalling pathways (figure 4.46 and 4.47). $G_{\alpha 13}$ is suggested to be a requirement for Ca^{2+} mobilisation in hGPR55-HEK293 cells (Henstridge *et al.*, 2009). Consistent with this, transient transfection of hGPR55-HEK293 cells with a dominant negative $G_{\alpha 13}$ construct decreased nuclear pCREB labelling. $G_{\alpha q}$-dependent Ca^{2+} mobilisation has also been documented in hGRR55-HEK293 cells (Lauckner *et al.*, 2008). However in this assay nuclear pCREB was found to be $G_{\alpha q}$-independent as application of the $G_{\alpha q}$ inhibitor; YM-254890, did not block the nuclear pCREB response. $G_{\alpha 13}$ is known to activate Rho through an interaction with the guanine exchange factor, p115RhoGEF, therefore linking $G_{\alpha 13}$ directly to Rho activation (Hart *et al.*, 1998). Interestingly cannabinoid ligand treatment of HEK293 cells transiently transfected with GPR55 promoted the activation of RhoA (Ryberg *et al.*, 2007). Recent evidence highlights that hGPR55-HEK293 cells transfected with dominant negative RhoA have abolished Ca^{2+} mobilisation (Lauckner *et al.*, 2008; Henstridge *et al.*, 2009). Indeed, use of the cell permeable C3 transferase, CT04, to inhibit Rho directly, also promote a general trend of inhibiting lipid-induced pCREB responses in hGPR55-HEK293 cells, but was not significant within the number of experiments. However increasing the 'n' number may reveal a significant inhibition of Rho. GPR55 signalling via Rho-ROCK is thought to be required for Ca^{2+} mobilisation (Waldeck-Weiermair *et al.*, 2008; Henstridge *et al.*, 2009), ERK1/2 phosphorylation (Anavi-Goffer *et al.*, 2012) and cytoskeletal reorganisation (Balenga *et al.*, 2011). Hence the cells were treated with inhibitors of ROCK I and II (Y-27632) or ROCK II (H1152). Both ROCK inhibitors were found to lower the nuclear pCREB response to the lipid ligands, suggesting that the $G_{\alpha 13}$-Rho-ROCK signalling axis can promote nuclear pCREB in hGPR55-HEK293 cells. However whilst Y-27632 promoted a very highly significant inhibition of pCREB in hGPR55-HEK293 cells, H1152 was observed to promote a trend of lowering the lipid-mediated pCREB response but at present was not significant. It is likely that

increasing the experimental data will lead to H1152 inhibition of nuclear pCREB in hGPR55-HEK293 cells. These data at present suggest that ROCK I is more important than ROCK II in the signalling to promote pCREB in hGPR55-HEK293 cells challenged with the endogenous lipids.

4.3.1.2. Ca^{2+} is important for pCREB in hGPR55-HEK293 cells treated with endogenous lipids.

As Ca^{2+} mobilisation occurred with both these lipids in hGPR55-HEK293 cells and required ROCK activation, the effect of Ca^{2+} in promoting pCREB was studied. Ca^{2+} is a known signalling mediator for the activation of CREB (Sheng *et al.*, 1990). Chelation of intracellular Ca^{2+} reduced pCREB responses to basal levels, furthermore extracellular Ca^{2+} was also important for lipid-mediated pCREB signalling in hGPR55-HEK293 cells. Following application of a PLC inhibitor, to inhibit the breakdown of PIP_2 into IP_3 and DAG, and therefore the subsequent increase in Ca^{2+} due to the release from the ER, GPR55-mediated pCREB responses were also inhibited, adding further credence to the idea that Ca^{2+} is necessary for pCREB. Ca^{2+}, DAG and the presence of phospholipids, in particular phosphatidylserine, act synergistically to activate PKC (Ganong *et al.*, 1986). Furthermore, fatty acids such as arachidonic or oleic acid may also activate PKC (Shinomura *et al.*, 1991). Applying a PKC inhibitor prior to co-application with either LPI or NOSer to hGPR55-HEK293 cells reduced pCREB staining when compared to either lipid alone. However, the effects were greater against LPI treated cells (68.4 ±7.2% inhibition) than seen with cells treated with NOSer (42.2 ±8.1% inhibition). Whether NOSer can be metabolised, or how quickly, in these cells is not known at present. It could however be plausible for NOSer to breakdown into L-serine and oleic acid with the possibility the latter could act on PKC (Shinomura *et al.*, 1991) and therefore may explain why the NOSer-induced response is decreased to a lesser extent than seen with LPI. A downstream effector of PKC is CaMKII (Waxham and Aronowski, 1993) which is also activated by increases in cytosolic Ca^{2+} (Schwaninger *et al.*, 1993). *In vitro*, the signal produced by Ca^{2+} mobilisation is transferred to the nucleus by CaMKII allowing CREB phosphorylation to occur (Schwaninger *et al.*, 1993). CaMKII phosphorylates CREB at serine residue 133 (Sun *et al.*, 1994) which is known to be important for CREB activation (Gonzalez and Montminy, 1989). CaMKII was found to lower nuclear pCREB in hGPR55-HEK293 cells treated with LPI or NOSer but was not significant. However it is probable that

increasing the experimental data set will promote a significant inhibition by either of the endogenous lipids.

4.3.1.3. MAPK and PI-3-kinase are required phosphorylated in hGPR55-HEK293 cells challenged with endogenous lipids.

GPR55-mediated p44/42 MAPK (ERK1/2) signalling has been reported in several cell types such as hGPR55-HEK293 cells (Oka *et al.*, 2007; Henstridge *et al.*, 2010; Anavi-Goffer *et al.*, 2012); osteoclasts (Whyte *et al.*, 2009); murine microglial cell line BV2 treated with INFγ (Pietr *et al.*, 2009); PC3 and DU145 prostate cancer cell lines and OVCAR3 ovarian cancer cell line (Piñeiro *et al.*, 2011); EVSA-T breast cancer cell line, T98G neuroblastoma cell line and xenografted T98G tumours (Andradas *et al.*, 2011); skin carcinogenesis in mice (Pérez-Gómez *et al.*, 2013). As ERK1/2 is upstream of pCREB and is implicated in GPR55 signalling, the effects of MEK1/2 inhibitors were investigated in hGPR55-HEK293 cells. Application of MEK1/2 inhibitors (either PD98059 or U0126) decreased the LPI (significantly) and NOSer-induced (not significant) nuclear pCREB. It is possible that increasing the experimental data NOSer would be likely to be required to promote nuclear pCREB in hGPR55-HEK293 cells. Furthermore these effects were further confirmed as an inactive MEK1/2 inhibitor (U0124) promoted nuclear pCREB labelling that was similar to endogenous lipids alone.

Activation of PI-3 kinase has been associated with GPR55-mediated Ca^{2+} mobilisation in HUVEC cells (Waldeck-Weiermair *et al.*, 2008; Ross, 2009). Whereby PI-3 kinase acted on PLCγ to promote Ca^{2+} mobilisation (Waldeck-Weiermair *et al.*, 2008). PI-3 kinase is also an important mediator of AKT phosphorylation (Dugourd *et al.*, 2003; Fresno Vara *et al.*, 2004; Steelman *et al.*, 2011) and therefore potentially could influence pCREB through a phosphorylated AKT-dependent signalling pathway (Du and Montminy, 1998). GPR55-mediated AKT phosphorylation occurs in ovarian and prostate cancer cells challenged with LPI (Piñeiro *et al.*, 2011) thus GPR55 could signal through PI-3 kinase and promote pCREB. Therefore in this study two structurally different PI-3-kinase inhibitors were applied to hGPR55-HEK293 cells. Inhibition of PI-3 kinase was found to lower nuclear pCREB labelling in hGPR55-HEK293 cells induced by the endogenous lipids. Whilst these effects were significant in NOSer challenged cells; LPI treated cells produced a general trend where pCREB responses were lower in the present of the PI-3 kinase inhibitors suggesting that this pathway is

likely to be important in LPI-mediated signalling. Furthermore mTOR signalling was found to not be required in the lipid-induced nuclear pCREB signalling in hGPR55-HEK293 cells. These data suggest that PI-3-kinase activation plays a role in pCREB signalling in hGPR55-HEK293 cells, which may involve AKT phosphorylation. It however, remains unknown whether AKT is phosphorylated downstream of GPR55 in hGPR55-HEK293 cells.

4.3.1.4. Summary of GPR55 signalling pathways required to promote nuclear pCREB.

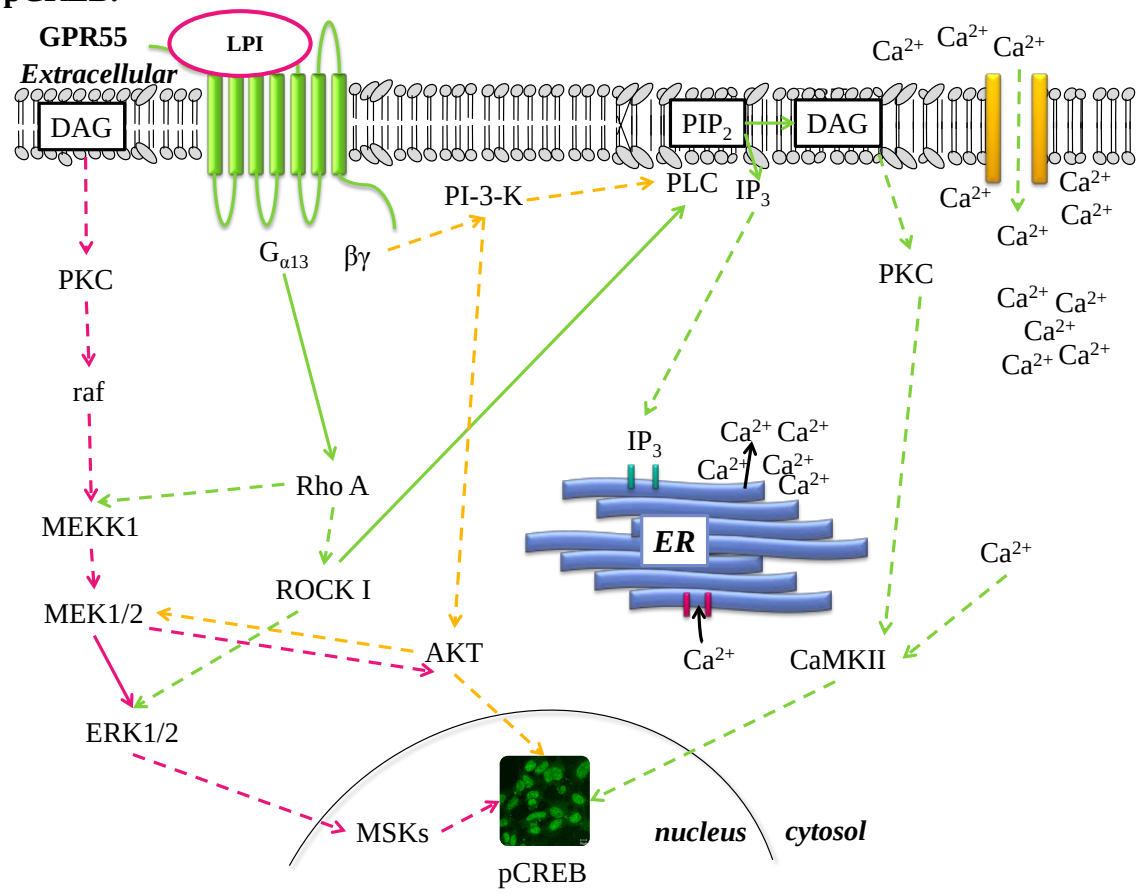

Figure 4.46: Proposed signalling pathways required to promote pCREB in hGPR55-HEK293 cells when challenged with LPI. *Multiple signalling pathways can promote pCREB in LPI challenged hGPR55-HEK293 cells. Potential cross-talk can occur between Ca^{2+} mobilisation, MAPK and PI-3 kinase signalling pathways. LPI, L-α-lysophosphatidylinositol; NOSer, N-oleoyl-L-serine; RhoA, Ras homolog gene, family member A; ROCK, Rho associated protein kinase; PLC, Phospholipase C; PIP_2, phosphatidylinositol 4, 5-bisphosphate; DAG, diacylglycerol; IP3, inositol 1, 4, 5-triphosphate; ER, endoplasmic reticulum; PKC, protein kinase C; CAMKII, Ca^{2+}/calmodulin dependent protein kinase II; mTOR = mammalian Target of Rapamycin; raf = proto-oncogene c-RAF; MEKK1 = mitogen activated protein kinase kinase 1; MEK1 = mitogen activated protein kinase 1; ERK1/2 = extracellular signal-regulated*

protein kinases 1 and 2; MSKs = mitogen- and stress-activated kinases. Green arrows = Ca^{2+} signalling pathway; orange arrows = PI-3 kinase signalling pathway; pink arrows = MAPK signalling pathway. Solid arrows = signalling effectors; dashed arrows = suggested effectors.

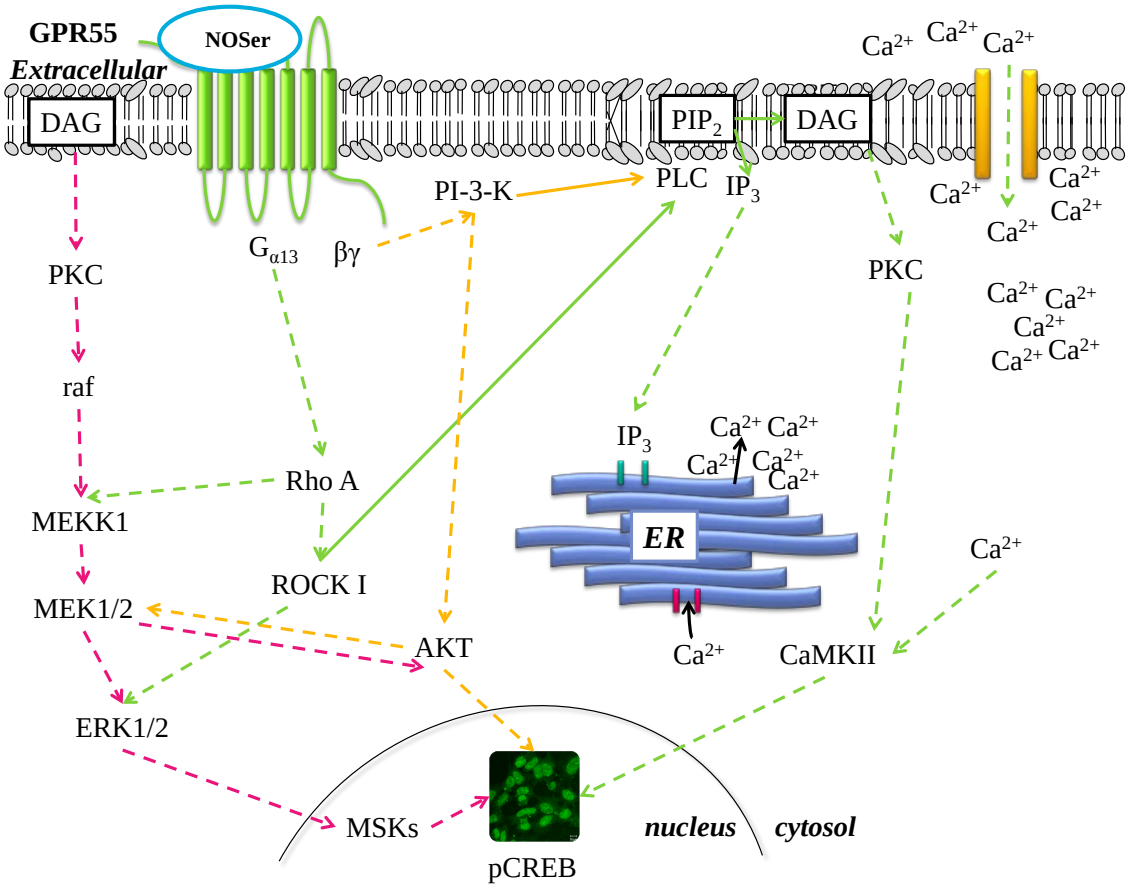

Figure 4.47: Proposed signalling pathways required to promote pCREB in NOSer challenged hGPR55-HEK293 cells. *Multiple signalling pathways can promote pCREB in NOSer challenged hGPR55-HEK293 cells. Potential cross-talk can occur between Ca^{2+} mobilisation, MAPK and PI-3 kinase signalling pathways. LPI, L-α-lysophosphatidylinositol; NOSer, N-oleoyl-L-serine; RhoA, Ras homolog gene, family member A; ROCK, Rho associated protein kinase; PLC, Phospholipase C; PIP_2, phosphatidylinositol 4, 5-bisphosphate; DAG, diacylglycerol; IP3, inositol 1, 4, 5-triphosphate; ER, endoplasmic reticulum; PKC, protein kinase C; CAMKII, Ca^{2+}/calmodulin dependent protein kinase II; mTOR = mammalian Target of Rapamycin; raf = proto-oncogene c-RAF; MEKK1 = mitogen activated protein kinase kinase 1; MEK1 = mitogen activated protein kinase 1; ERK1/2 = extracellular signal-regulated protein kinases 1 and 2; MSKs = mitogen- and stress-activated kinases. Green arrows = Ca^{2+} signalling pathway; orange arrows = PI-3 kinase signalling pathway; pink arrows = MAPK signalling pathway. Solid arrows = signalling effectors; dashed arrows = suggested effectors.*

4.3.2. The actin cytoskeleton and vinculin.

4.3.2.1. Cytoskeletal reorganisation occurs in hGPR55-HEK293 cells challenged with endogenous lipids.

In this study both LPI and NOSer promoted the formation of stress fibres, filopodia and lamellipodia in hGPR55-HEK293 cells (figure 4.48). The formation of stress fibres and FAs requires the activation of Rho (Ridley and Hall, 1992; Katoh *et al.*, 2007). However the formation of the sheet-like lamellipodia at the leading edge of a polarised cell is thought to be mediated by the activation of Rac1, whilst the formation of filopodia (the finger like protrusions) are mediated by cdc42 (Nobes and Hall, 1995). Interestingly, GPR55 can activate each of these small GTPases; RhoA, cdc42 and rac1 (Ryberg *et al.*, 2007). In this study the $G_{\alpha 13}$-Rho-ROCK signalling axis was found to be required for cytoskeletal reorganisation in hGPR55-HEK293 cells treated with either LPI or NOSer. Previous studies have highlighted that the GPR55-activated small G-proteins; RhoA, rac2 and cdc42 are important in cytoskeletal reorganisation in neutrophil (HL60) cells (Balenga *et al.*, 2011). Using F-actin staining with phalloidin to observe cytoskeletal changes the authors applied LPI, AM251 or the endocannabinoid 2-AG and found that each could exert cytoskeletal changes in neutrophils (Balenga *et al.*, 2011). However they also noted that the migratory, elongated type response in HL60 cells was only observed when GPR55 and CB_2 agonists; LPI and 2-AG respectively, were applied together and suggest that CB_2 and GPR55 may act synergistically (Balenga *et al.*, 2011). An alternative study highlighted that cytoskeletal changes were observed in MDA-MB-231 breast cancer cells treated with LPI where they become elongated, a phenotype associated with migration (Ford *et al.*, 2010). This study however was not directed at effects on cell polarity as the hGPR55-HEK293 cells were surrounded by the lipids in petri dishes, leading to an even concentration around the cells. This would explain why the lamellipodia and filopodia were observed in several directions in the hGPR55-HEK293 cells.

4.3.2.2. $G_{\alpha 13}$-Rho-ROCK signalling axis is required for cytoskeletal reorganisation and changes in FA length via GPR55 in hGPR55-HEK293 cells.

This is the first study demonstrating that vinculin-containing FAs can be modulated by GPR55, where LPI or NOSer induced increases in the length of the vinculin-containing FAs. As observed with cytoskeletal reorganisation in hGPR55-HEK293 cells, effects on FAs were mediated by the $G_{\alpha 13}$-Rho-ROCK signalling axis. hGPR55-HEK293 cells treated with Y-27632, a ROCK I and II inhibitor were found to have fewer mature FAs

than cells inhibited by ROCK II alone especially in NOSer challenged hGPR55-HEK293 cells. This suggests that ROCK I may be more important for the reduction of FAs in hGPR55-HEK293 cells in NOSer treated cells. Whereas, inhibition of the lipid-induced stress fibres occurred with either of the ROCK inhibitors. Studies in fibroblasts where cells were transfected with siRNA for ROCK I were found to have a complete loss of stress fibres and vinculin whereas cells transfected with ROCK II siRNA do not lose the stress fibres or vinculin FAs. Therefore the two ROCK isoforms have distinct roles in fibroblasts (Yoneda *et al.*, 2005). This may also be the case for the vinculin-containing FAs in the hGPR55-HEK293 cells. Further experiments with ROCK I and II siRNAs would help in understanding the differences these two proteins are exerting in hGPR55-HEK293 cells especially in relation to the FAs.

4.3.2.3. Inhibition of cdc42 has no effect on the actin cytoskeleton or FAs in hGPR55-HEK293 cells.

The Rho family G protein, cdc42, is thought to play a role in filopodia formation. It was reported that microinjection of cdc42 into fibroblasts leads to the formation of filopodia and vinculin-containing FAs at the periphery of cells, where they are associated with filopodia (Nobes and Hall, 1995). However, in this study the application of cdc42 did not affect the formation of filopodia induced by the lipids. There was also no effect on the length of the vinculin-containing FAs in hGPR55-HEK293 cells whereby cdc42 had been inhibited. This could be a cell type specific response where cdc42 is not required for cytoskeletal reorganisation in hGPR55-HEK293 cells but is required in fibroblasts (Nobes and Hall, 1995).

4.3.2.4. Ca^{2+} mobilisation is important for FA length but has no effect on cytoskeletal reorganisation.

GPR55 is linked to the activation of PLC to induce both the mobilisation of Ca^{2+} and pCREB in hGPR55-HEK293 cells. Therefore any potential role involving PLC in cytoskeletal reorganisation or changes in FA length were studied through the application of U73122; a PLC inhibitor. Previously PLC is reported to be important for the reorganisation of the cytoskeleton whereby application of U73122 (10 μM) or PLC siRNA to DU145 prostate cancer cells was found to inhibit the formation of lamellipodia and filopodia in response to serum (Jones *et al.*, 2005). This however is in contrast to the present study where the application of U73122 did not appear to affect the formation of stress fibres or lamellipodia in hGPR55-HEK293 cells treated with LPI

or NOSer, suggesting that Ca^{2+} is not involved in cytoskeletal reorganisation in hGPR55-HEK293 cells treated with either LPI or NOSer. It may be that the U73122 concentration in this study was not high enough to fully block PLC and all its downstream effects; however, higher concentrations of U73122 were found to have non-specific effects and therefore could not be tested.

Both Ca^{2+} and PKC (both of which are downstream of PLC) have previously been implicated in vinculin phosphorylation (Werth and Pastan, 1984). Also PLC has been reported to effect vinculin FA length in papillary renal cells treated with bradykinin (Márquez *et al.*, 2008). In this study vinculin-containing FAs were shorter when hGPR55-HEK293 cells were treated with U73122, a PLC inhibitor. These data suggest that Ca^{2+} is important for changes in vinculin-containing FA length but has no effect on the cytoskeleton in hGPR55-HEK293 cells. The activation of PLC is required for FA increases in length in hGPR55-HEK293 cells treated with LPI and is likely to be responsible for increases in FA length in NOSer challenged cells.

4.3.2.5. MAPK is involved in GPR55-mediated effects on FA length, but not changes in the actin cytoskeleton in hGPR55-HEK293 cells.

In this study MAPK signalling was found to be important for GPR55-mediated FA elongation. A requirement for ERK1/2 in the formation of FAs is controversial as some studies find ERK1/2 is necessary for their formation (Fincham *et al.*, 2000; Pullikuth and Catling, 2010) whilst others argue that ERK1/2 activation leads to their disassembly (Webb *et al.*, 2004). In the present study the GPR55-mediated FA elongation was inhibited by MEK1/2 blockers. Moreover LPI was found to be more effectively blocked than NOSer challenged hGPR55-HEK293 cells. Furthermore this pathway was not involved in actin cytoskeletal changes induced by LPI or NOSer in the hGPR55-HEK293 cells.

In conclusion, this study has highlighted that the N-acyl amino acids exert GPR55-mediated effects on pCREB in hGPR55-HEK293 cells. Furthermore multiple signalling pathways are required for GPR55-pCREB signalling, including Ca^{2+}, MAPK and potentially AKT. LPI and NOSer were further characterised in two other GPR55-mediated assays; an F-actin cytoskeletal reorganisation assay and a novel FA assay studying the changes in length of vinculin-containing FAs. Signalling through the Rho-ROCK pathway was found to be important for both cytoskeletal reorganisation and

changes in FA length (figure 4.49 and 4.50). However, Ca^{2+} and the MAPK pathways were also found to be important in changes in FA length but had little or no effect on cytoskeletal reorganisation in hGPR55-HEK293 cells. Although some of the signalling pathways such as Ca^{2+}, Rho-ROCK and MAPK are required for FA formation and pCREB (figure 4.48). The two outcomes are thought to be separate as FA formation is likely to be by focal contacts translocating to peripheral regions and combining to form larger focal adhesions rather than being gene regulated. The time scale of ligand treatment (25 min) is not long enough for gene regulation to play a role, if pCREB were to be involved, as this normally requires several hours for gene transcription to occur. It remains to be determined if these GPR55-mediated N-acyl amino acid effects have a physiological role in a native system. Therefore having established that N-acyl amino acids can activate multiple GPR55-mediated signalling cascades in recombinant human GPR55 over-expressing cells, the next chapter shall explore the actions of N-acyl amino acids and LPI-induced in cells which endogenously expresses GPR55.

4.3.2.6. Signalling pathways required for F-actin cytoskeletal reorganisation and FA formation in hGPR55-HEK293 cells.

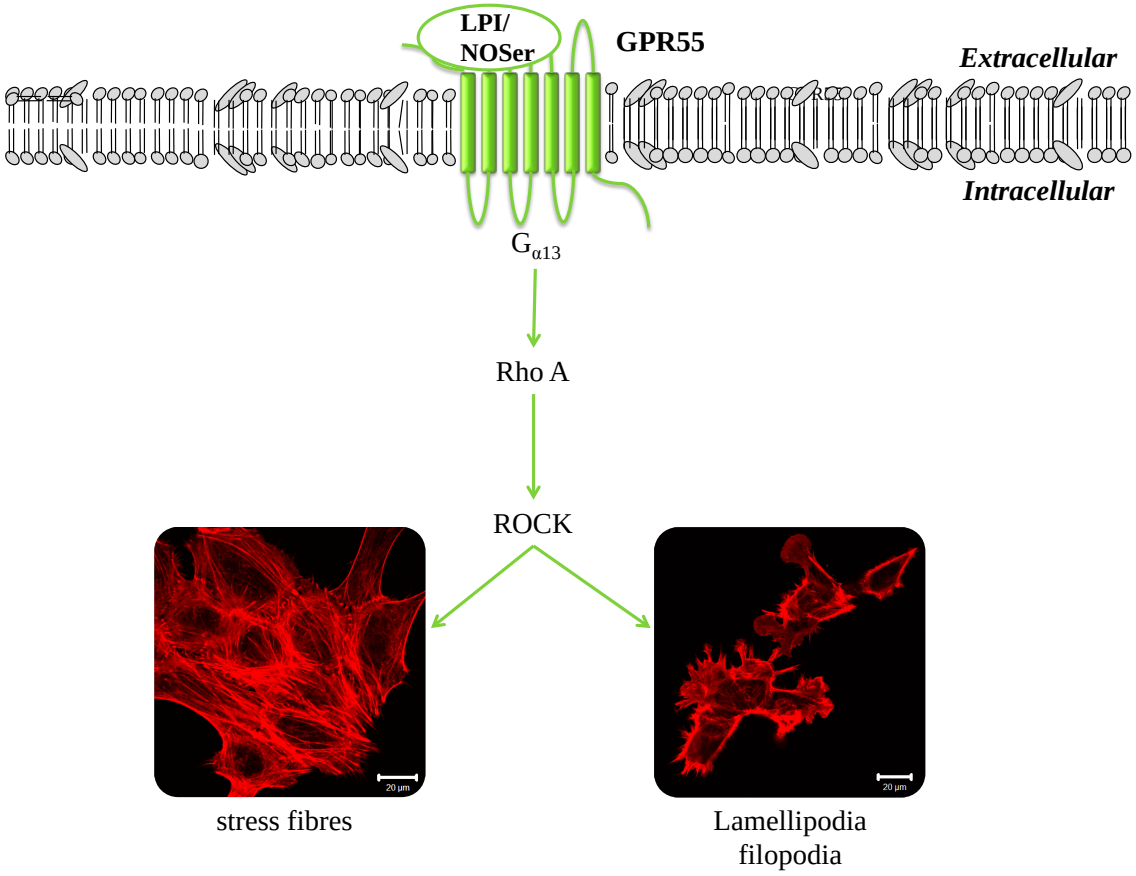

Figure 4.48: Proposed signalling pathways required to promote F-actin reorganisation in hGPR55-HEK293 cells. *Lipid induced F-actin cytoskeletal reorganisation which promotes the*

formation of stress fibres, lamellipodia and filopodia occur in hGPR55-HEK293 cells. These effects are mediated through the $G_{\alpha 13}$-Rho-ROCK signalling axis.

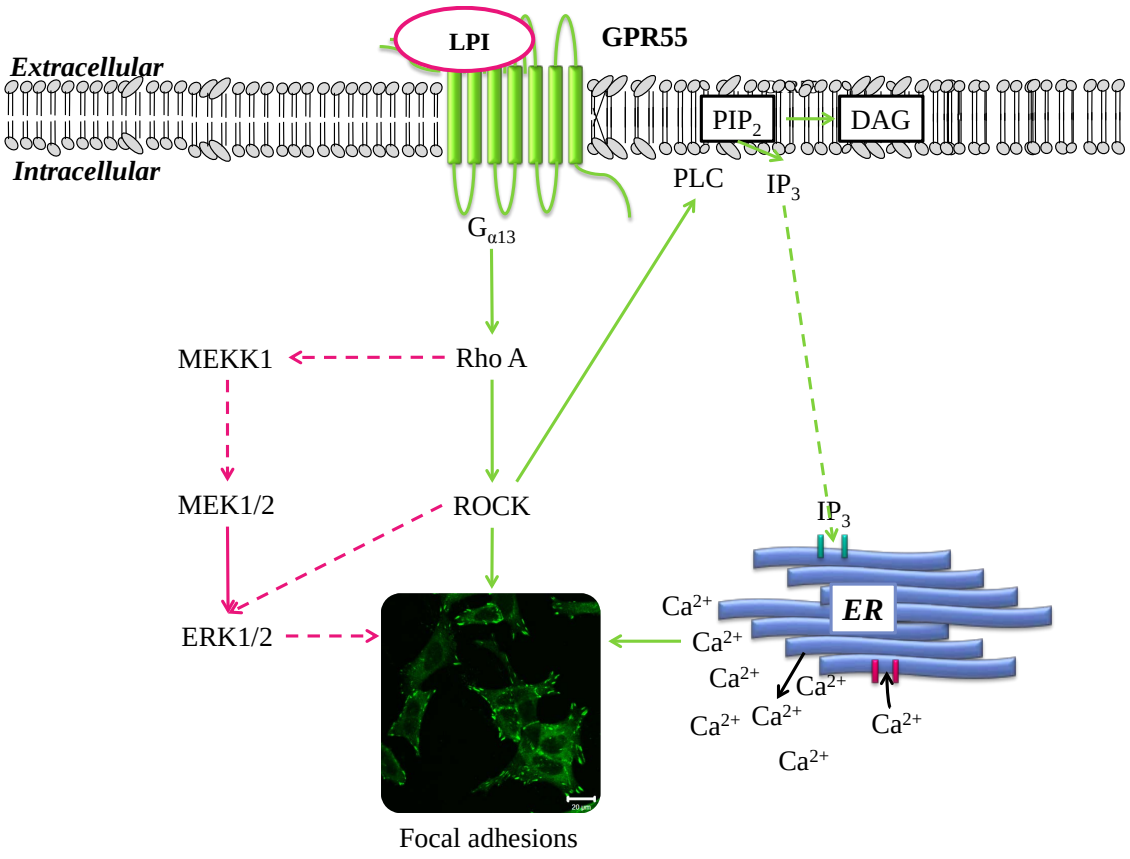

Figure 4.49: Proposed signalling pathways required to promote the formation of LPI-induced FAs in hGPR55-HEK293 cells. *LPI-induced vinculin-containing FAs require the activation of multiple signalling pathways. $G_{\alpha 13}$ but not $G_{\alpha q}$ is required for the FA formation. Rho-ROCK signalling is important but in this study cdc42 did not promote the formation of FAs. PLC activation is required which would lead to the subsequent release of Ca^{2+} from the ER. Ca^{2+} is important for the formation of FAs. Note the dashed line highlights possible interactions.*

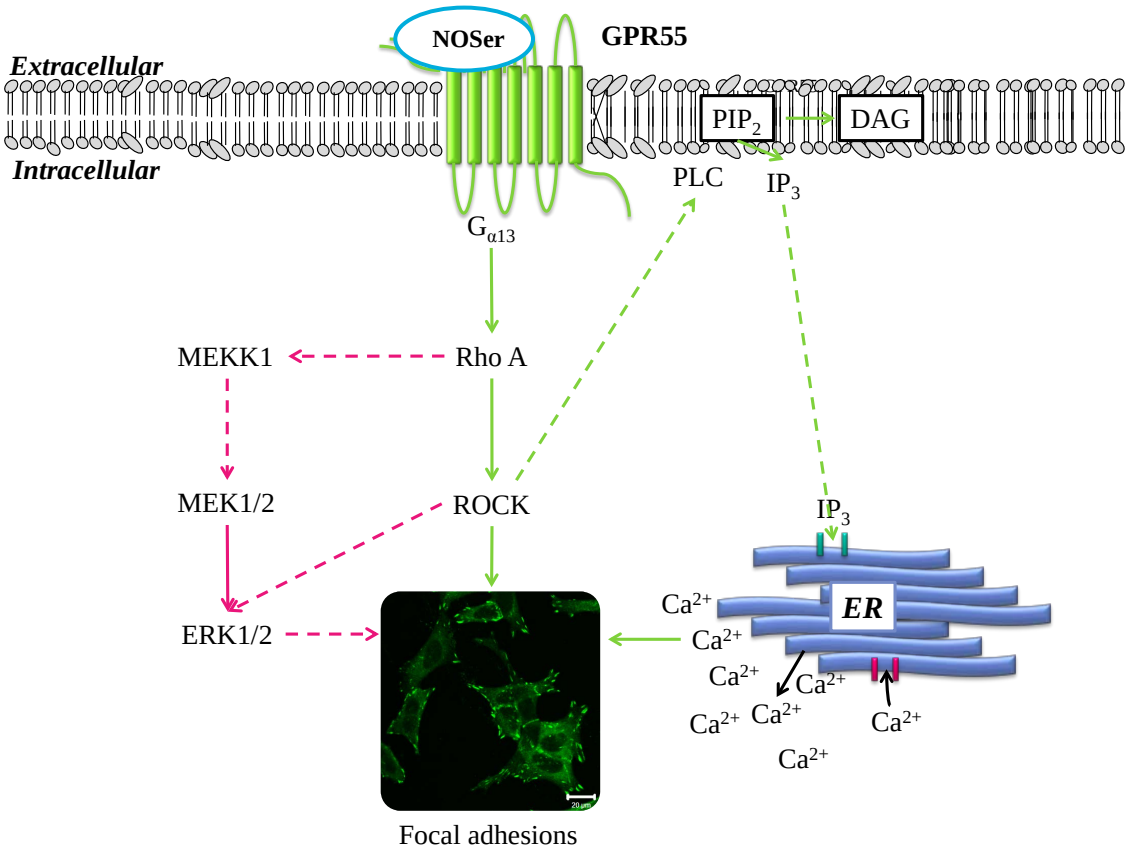

Figure 4.50: Proposed signalling pathways required to promote the formation of FAs in hGPR55-HEK293 cells challenged with NOSer. *NOSer-induced vinculin-containing FAs require the activation of multiple signalling pathways. $G_{\alpha 13}$ but not $G_{\alpha q}$ is required for the FA formation. Rho-ROCK signalling is important but in this study cdc42 did not promote the formation of FAs. PLC activation is likely to be required and would therefore lead to the subsequent release of Ca^{2+} from the ER. Ca^{2+} is important for the formation of FAs. Note the dashed line highlights possible interactions.*

4.3.3. Summary of individual pCREB signalling pathways in hGPR55-HEK293 cells.

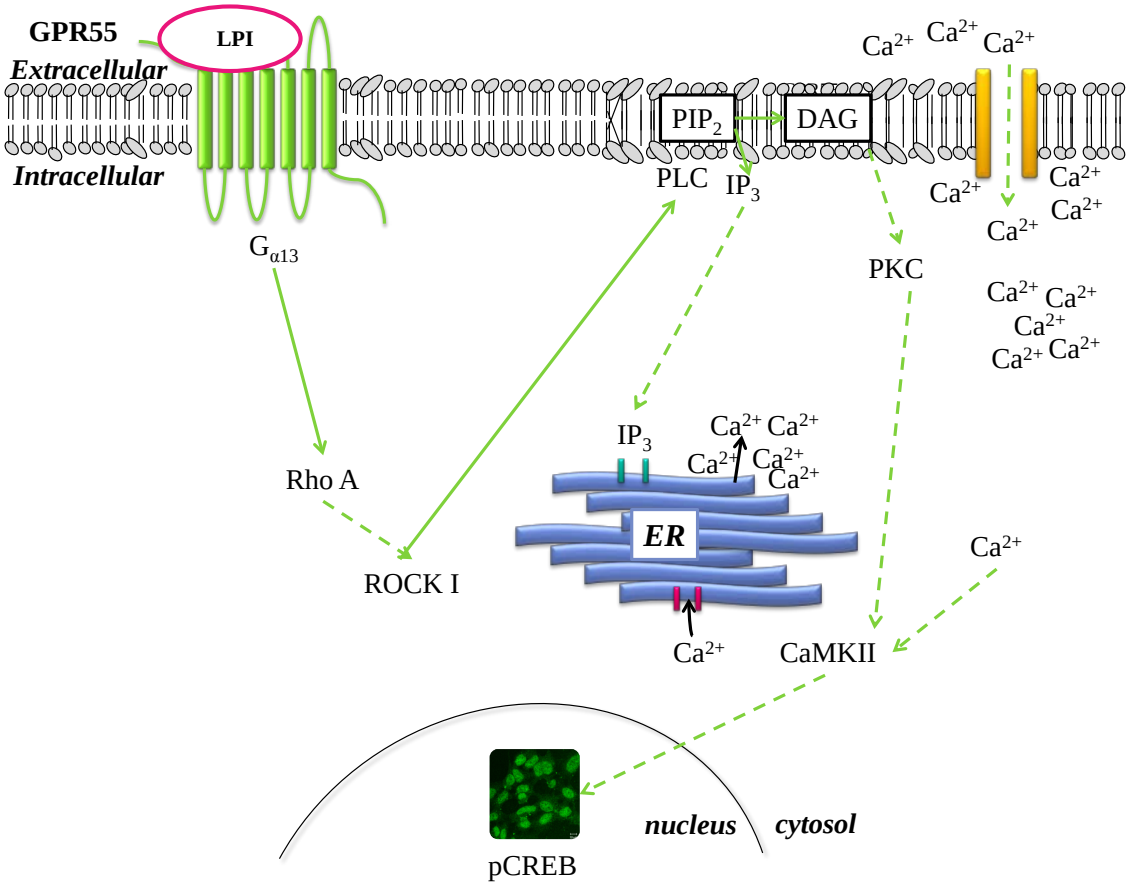

Figure 4.51: Proposed LPI-induced Ca^{2+} signalling cascade required for pCREB in hGPR55-HEK293 cells. *LPI was found to require Ca^{2+} mobilisation to induce nuclear pCREB. Endogenous lipid binding of GPR55 initiates the activation of $G_{\alpha 13}$ which in turn is likely to activate RhoA whereby ROCK I is phosphorylated. Moreover is is likely that ROCK II is als required for pCREB. Phosphorylation of PLC initiates the hydrolysis of PIP_2 into DAG and IP_3. IP_3 translocates to IP_3 receptors on the ER allowing promoting the release of Ca^{2+}. DAG and/or Ca^{2+} activated PKC. PKC and Ca^{2+} can act upon CAMKII which can then phosphorylate CREB. LPI, L-α-lysophosphatidylinositol; RhoA, Ras homolog gene, family member A; ROCK, Rho associated protein kinase; PLC, Phospholipase C; PIP_2, phosphatidylinositol 4, 5-bisphosphate; DAG, diacylglycerol; IP3, inositol 1, 4, 5-triphosphate; ER, endoplasmic reticulum; PKC, protein kinase C; CAMKII, Ca^{2+}/calmodulin dependent protein kinase II.*

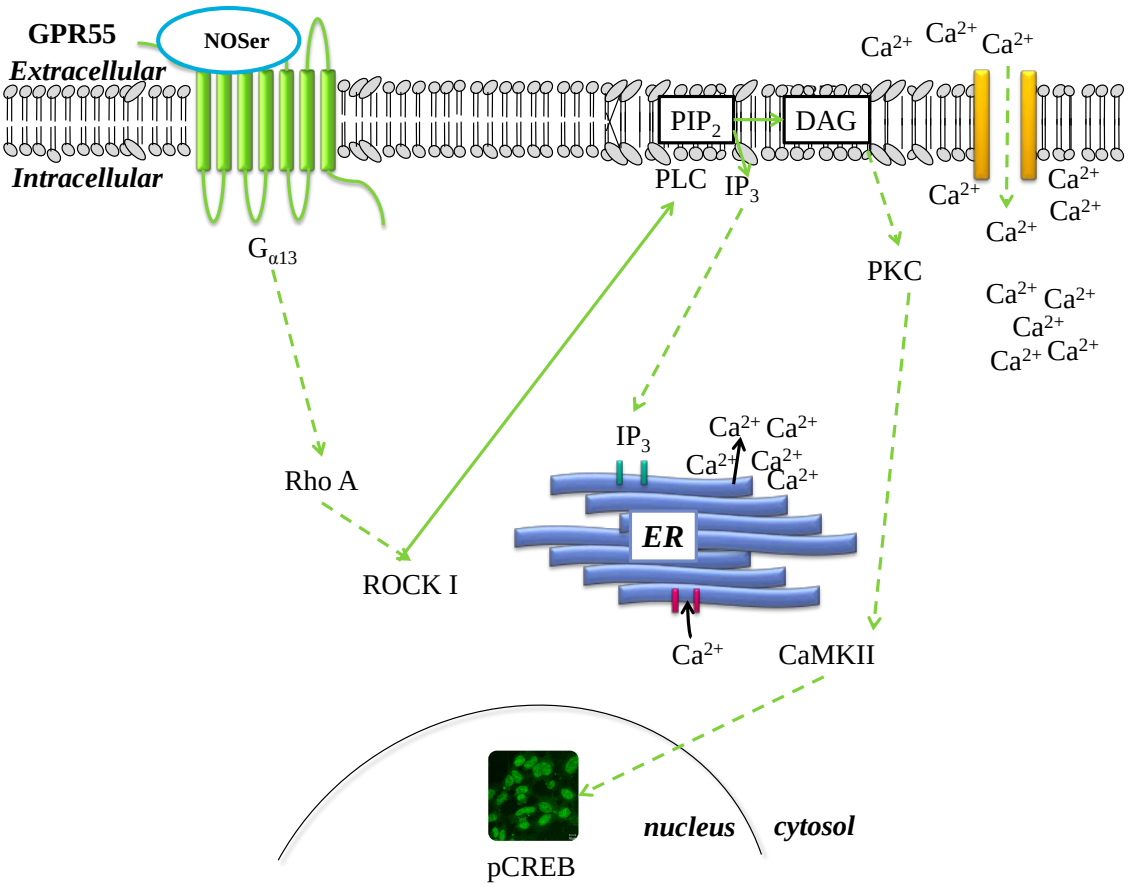

Figure 4.52: Proposed Ca^{2+} signalling cascade required for pCREB in NOSer challenged hGPR55-HEK293 cells. *NOSer was found to require Ca^{2+} mobilisation to induce nuclear pCREB. Endogenous lipid binding of GPR55 is likely to initiate the activation of $G_{\alpha 13}$ which in turn is likely to activate RhoA whereby ROCK I is phosphorylated. Phosphorylation of PLC initiates the hydrolysis of PIP_2 into DAG and IP_3. IP_3 translocates to IP_3 receptors on the ER allowing promoting the release of Ca^{2+}. DAG and/or Ca^{2+} activated PKC. It is also likely that PKC and Ca^{2+} can act upon CAMKII which can then phosphorylate CREB. NOSer, N-oleoyl-L-serine; RhoA, Ras homolog gene, family member A; ROCK, Rho associated protein kinase; PLC, Phospholipase C; PIP_2, phosphatidylinositol 4, 5-bisphosphate; DAG, diacylglycerol; IP3, inositol 1, 4, 5-triphosphate; ER, endoplasmic reticulum; PKC, protein kinase C; CAMKII, Ca^{2+}/calmodulin dependent protein kinase II.*

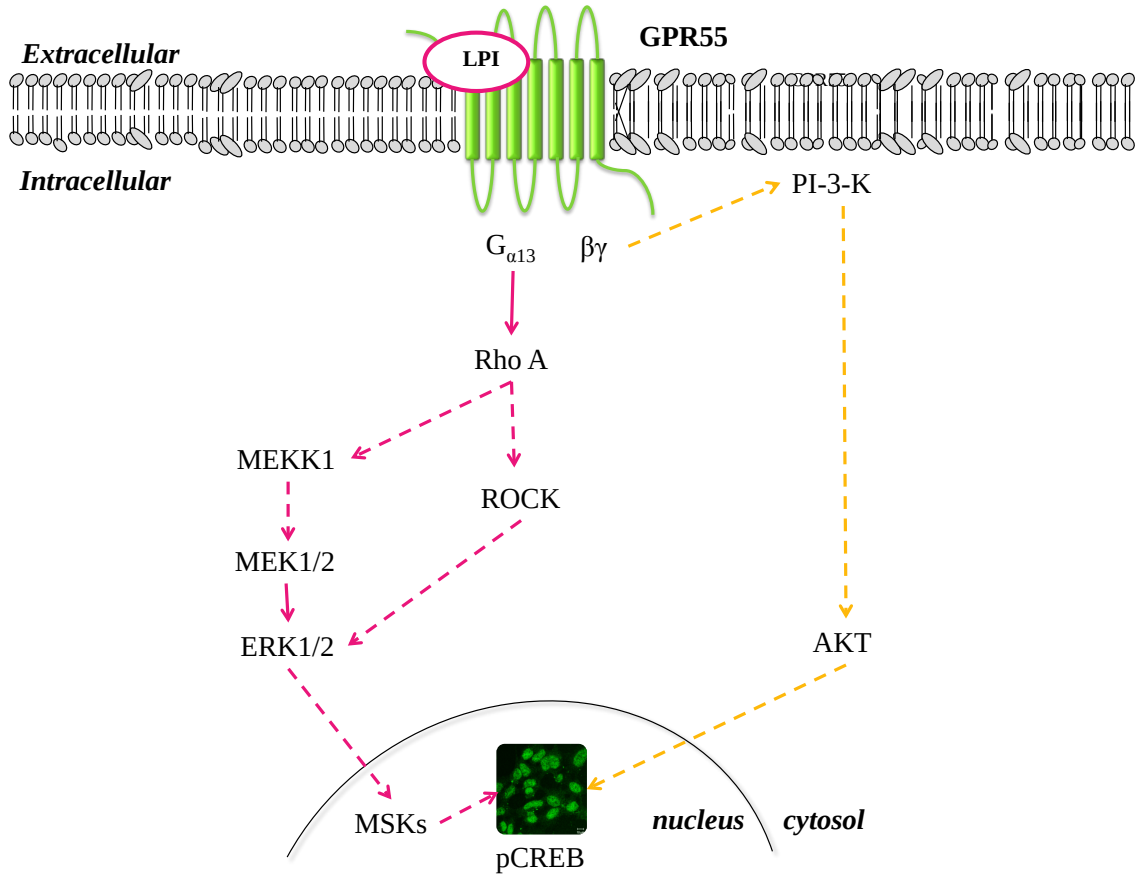

Figure 4.53: Proposed LPI-induced signalling cascades required promoting nuclear pCREB with MAPK and PI-3 kinase signalling pathways. *$G_{\alpha 13}$ acting on RhoA could lead to the phosphorylation of MEKK1 which in turn can phosphorylate MEK1/2. MEK1/2 subsequently phosphorylates ERK1/2 which translocates into the nucleus to phosphorylate CREB. Alternatively Rho phosphorylates ROCK which then subsequently phosphorylates ERK1/2. PI-3 kinase could be activated by the βγ subunits of the $G_{\alpha 13}$ -protein which can then phosphorylate AKT and ultimately CREB. Solid arrows = signalling effectors; dashed arrows = suggested effectors. Pink arrows = MAPK signalling pathway; orange arrows = PI-3 kinase signalling pathway.*

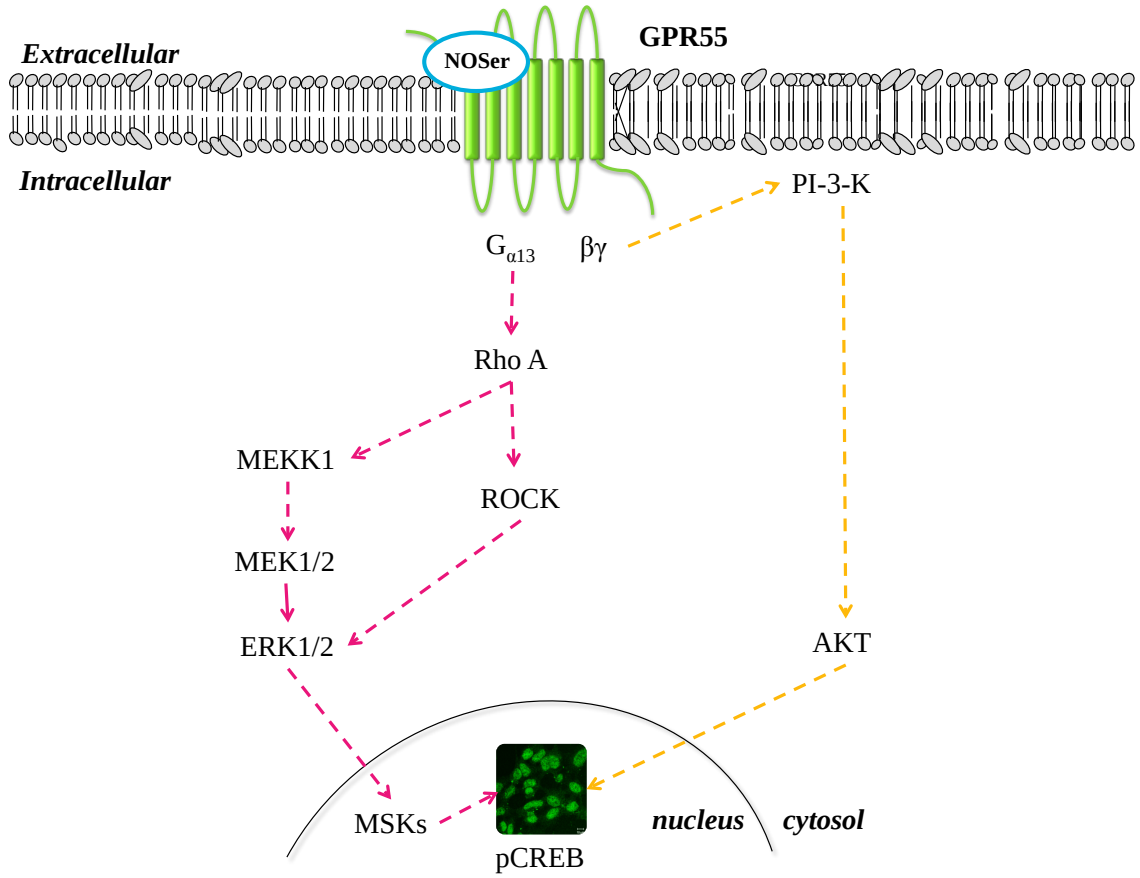

Figure 4.54: Proposed signalling cascades required to promote NOSer-induced nuclear pCREB with MAPK and PI-3 kinase signalling pathways. *$G_{\alpha 13}$ acting on RhoA could lead to the phosphorylation of MEKK1 which in turn can phosphorylate MEK1/2. MEK1/2 subsequently phosphorylates ERK1/2 which translocates into the nucleus to phosphorylate CREB. Alternatively Rho phosphorylates ROCK which then subsequently phosphorylates ERK1/2. PI-3 kinase could be activated by the βγ subunits of the $G_{\alpha 13}$ -protein which can then phosphorylate AKT and ultimately CREB. Solid arrows = signalling effectors; dashed arrows = suggested effectors. Pink arrows = MAPK signalling pathway; orange arrows = PI-3 kinase signalling pathway.*

CHAPTER FIVE

Endogenous Lipid Mediated Effects in the Prostate Cancer Cell Line, DU145. A Potential Role for GPR55?

5.1. INTRODUCTION

GPR55 is known to be expressed in metastatic cancer cells such as prostate cancer cells lines; PC3 and DU145 (Piñeiro *et al.*, 2011). In a study of two breast cancer cell lines; MCF-7 and MDA-MB-231 the authors observed higher GPR55 mRNA expression in the latter cells, which had a higher metastatic capability (Ford *et al.*, 2010). The MCF-7 cells did not migrate towards serum in a Boyden chamber assay. However the transient transfection of GPR55 cDNA into MCF-7 cells led to the development of a migratory phenotype, where the cells could now migrate towards the serum, suggesting GPR55 may play a role migration (Ford *et al.*, 2010). GPR55 is also reported to be expressed at higher levels in aggressive cancer cells suggesting it may play a detrimental role in cancer (Andradas *et al.*, 2011). Indeed the authors found that the increased expression of GPR55 correlated with the patients who had the worst prognosis (Andradas *et al.*, 2011). It was also noted that GPR55-mediated ERK1/2 signalling is necessary for carcinoma proliferation in both cell lines and xenograft studies using glioblastoma cells (Andradas *et al.*, 2011). Furthermore malignant cancer growth in skin carcinomas was found to be GPR55-mediated (Pérez-Gómez *et al.*, 2013). GPR55 was also involved in growth of prostate cancer PC3 cells in soft agar as GPR55 knockdown inhibited the effect (Piñeiro *et al.*, 2011). Another study however has reported that AEA exerted anti-proliferative effects in cholangiocarcinoma which was GPR55-mediated through $G_{\alpha 12}$ proteins (Huang *et al.*, 2011). These differences suggest that effects on cell growth may be cell type specific.

GPR55 is reported to signal through the $G_{\alpha 12}$ family of heterotrimeric G proteins, whose members consist of $G_{\alpha 12}$ and $G_{\alpha 13,}$ and are involved in many aspects of oncogenesis (Worzfeld *et al.*, 2008). Studies with prostate cancer cells have highlighted that there is an up-regulation of $G_{\alpha 12}$ in invasive prostate cancer cell lines including DU145 cells (Kelly *et al.*, 2006). Rho proteins which can be activated by either $G_{\alpha 12/13}$ or $G_{\alpha q}$ which are also required for prostate cancer growth (Dorsam and Gutkind, 2007). Interestingly these proteins are associated with GPR55 (Lauckner *et al.*, 2008; Henstridge *et al.*, 2009).

The lysophospholipid, LPI had been found to increase in the extracellular medium of epithelial (Falasca and Corda, 1994) and fibroblast cells (Falasca *et al.*, 1998) suggesting that LPI could act as an autocrine mediator on the cells that had released the lipid. More recently LPI was found to be increased in the ascites fluid and plasma from

women with ovarian cancer compared to women with benign tumours or healthy volunteers (Xiao *et al.*, 2001; Sutphen *et al.*, 2004) suggesting LPI is present in the ascites surrounding the tumours. Furthermore, LPI is generated in DU145 cells via cytosolic PLA_2 whereby it can exit the cell through an ABCC1 transporter; allowing LPI to act in an autocrine manner on cells in the tumour microenvironment (Piñeiro *et al.*, 2011). Therefore both LPI and GPR55 appear to be important factors in some cancer pathophysiologies.

This study was to characterise LPI and the novel, endogenous GPR55 ligand NOSer in a native GPR55-expressing prostate cancer cell line; DU145. Firstly, GPR55-mediated Ca^{2+} mobilisation in the DU145 cells was studied. LPI and NOSer were then evaluated using the pCREB assay; where several pharmacological inhibitors were used to elucidate the signalling pathways required to promote pCREB. Finally the F-actin cytoskeleton and FAs were assessed using DU145 cells challenged with either LPI or NOSer. To the best of our knowledge this is the first study to report NOSer effects in DU145 cells. Also this is the first study to determine the effects of both LPI and NOSer-induced pCREB, F-actin and vinculin responses in these cells.

5.2. RESULTS

5.2.1. Endogenous lipids promote GPR55-mediated Ca^{2+} mobilisation in DU145 prostate cancer cells.

Recent evidence has highlighted GPR55-mediated Ca^{2+} mobilisation in DU145 cells challenged with 10 µM LPI (Piñeiro *et al.*, 2011). In this study DU145 cells treated with LPI (100 nM) had no effect on the mobilisation of Ca^{2+} (figure 5.1Ai). Perfusion of LPI (3 µM), however, was found to promote a single Ca^{2+} transient in DU145 cells (figure 5.1Aii). Mean peak Ca^{2+} responses were concentration-dependent (figure 5.1B), however an EC_{50} could not be calculated as the responses did not reach E_{max} within the concentration range tested (100 nM - 10 µM; figure 5.1B). LPI (1 µM) perfused over DU145 cells that were transiently transfected with mouse CB_2-siRNA (69 hr) produced a single Ca^{2+} transient (figure 5.1Ci). However DU145 cells that had been transiently transfected with human GPR55-siRNA (69 hr) and challenged with LPI (1 µM) produced a Ca^{2+} transient peak response that was reduced by 33.9 ± 19.4% compared with the CB_2-siRNA treated cells (figure 5.1Cii). DU145 cells treated with GPR55-siRNA produced mean peak Ca^{2+} responses that were lower than seen with control CB_2-siRNA treated cells (CB_2-siRNA = 0.22 ± 0.03 ratio units, GPR55-siRNA = 0.134

± 0.02 ratio units, n = 45, Student's unpaired two-tailed t-test, P < 0.05, figure 5.1D). These data suggests that LPI-induced Ca^{2+} mobilisation in DU145 cells are at least in part GPR55-mediated.

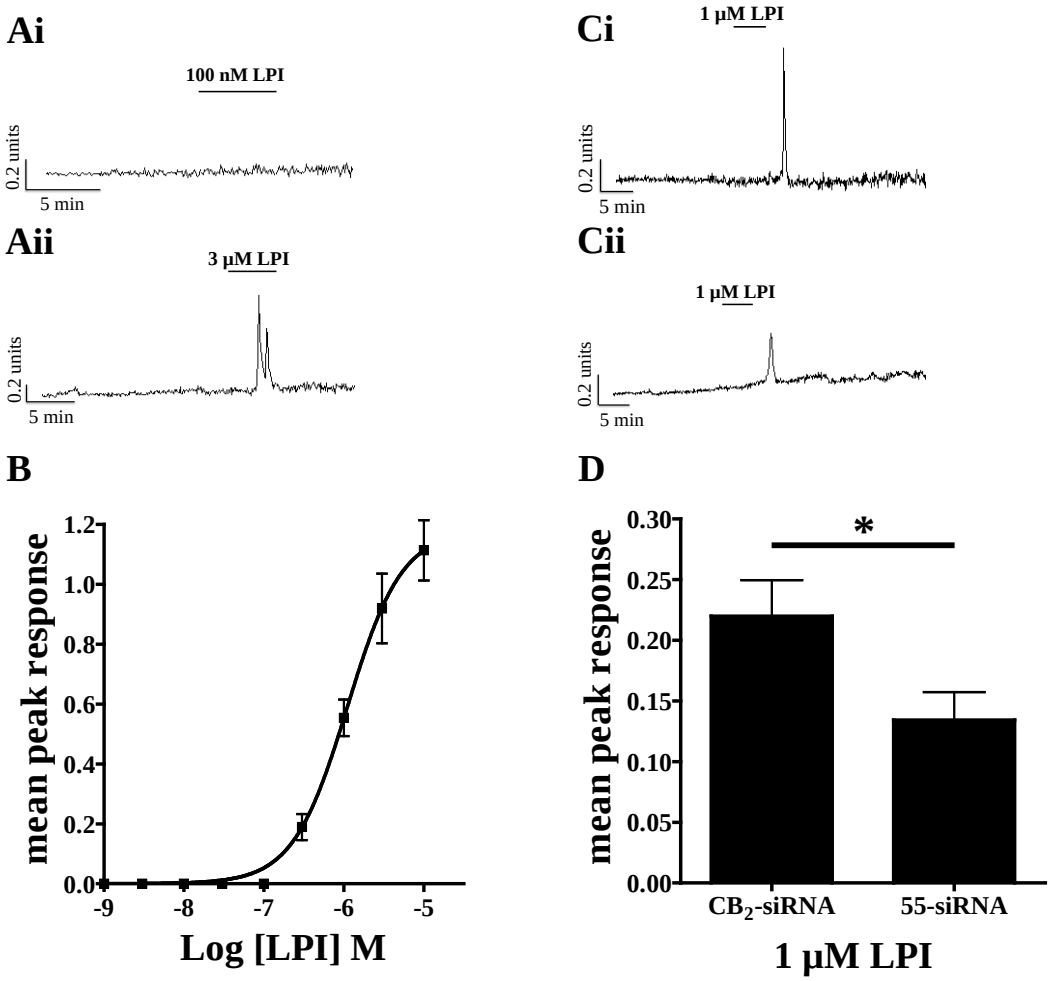

Figure 5.1: LPI-induced Ca^{2+} mobilisation in DU145 cells. ***A****, representative Ca^{2+} traces from DU145 cells treated with LPI at* ***i****, 100 nM;* ***ii****, 3 µM.* ***B****, LPI concentration-response curve in DU145 cells. Data are the mean peak response ± SEM derived from 30 cells from 3 independent experiments.* ***C****, representative Ca^{2+} trace from DU145 cells transiently transfected for 69 hr with* ***i****, CB_2-siRNA;* ***ii****, GPR55-siRNA and then treated with 1 µM LPI.* ***D****, histogram of pooled data, depicting mean Ca^{2+} peak responses from DU145 cells transiently transfected either CB_2- or 55-siRNA and perfused with 1 µM LPI. Note the mean Ca^{2+} response was significantly decreased in the GPR55-siRNA transfected cells when compared to control CB_2-siRNA transfected cells. Data are the mean, peak response ± SEM of 45 cells from 2 independent experiments. Student's unpaired two-tailed t-test; *P < 0.05.*

Having confirmed that LPI promoted Ca^{2+} mobilisation in DU145 cells, the effects of NOSer were studied. DU145 cells challenged with NOSer (1 µM) did not promote Ca^{2+} transients but were found to produce a small 'bump'-like response (figure 5.2Ai).

Increasing the concentration of NOSer (10 µM) was observed to produce a single Ca^{2+} transient (figure 5.2Aii). The augmentation of mean peak Ca^{2+} responses was observed as NOSer concentrations were increased (100 nM - 10 µM). However an E_{max} was not reached in this concentration range therefore the EC_{50} could not be calculated (figure 5.2B). Mean, peak Ca^{2+} responses were also observed to be lower in comparison with LPI responses at equivalent concentrations. DU145 cells transiently transfected with human CB_2-siRNA (69 hr) challenged with NOSer (10 µM) promoted a single Ca^{2+} transient (figure 5.2Ci). DU145 cells transiently transfected with human GPR55-siRNA (69 hr) and then challenged with NOSer (10 µM) were found to produce a single Ca^{2+} transient however, the mean peak Ca^{2+} responses were found to lower than the control CB_2-siRNA treated DU145 cells (figure 5.2Cii). NOSer (10 µM) perfused over DU145 cells transiently transfected with GPR55-siRNA reduced the mean, peak Ca^{2+} transients by 58.1 ± 6.2% when compared to control CB_2-siRNA transfected cells (CB_2-siRNA = 0.282 ± 0.04, GPR55-siRNA = 0.123 ± 0.024, n = 45 cells, Student's unpaired two-tailed t-test, $P < 0.001$, figure 5.2Ci, ii and D). These data suggest that NOSer-induced Ca^{2+} peak responses are at least in part GPR55-mediated. However, it is also observed that NOSer was not as efficacious as LPI at promoting Ca^{2+} mobilisation in DU145 cells suggesting ligand bias where signalling through Ca^{2+} is less effective when GPR55 is activated with NOSer.

5.2.1.1. The GPR55 antagonist CBD partially lowers Ca^{2+} mobilisation in DU145 cells.

To further confirm that GPR55 was mediating the Ca^{2+} mobilisation occurring in DU145 cells the purported GPR55 antagonist CBD (1 µM) was utilised (Ryberg *et al.*, 2007; Whyte *et al.*, 2009). As LPI (3 µM) was found to produce a sub-maximal response in DU145 cells it was used for all subsequent inhibitor experiments. LPI applied in the presence of CBD was observed to lower the mean peak Ca^{2+} response by 28.98 ± 7.7% in DU145 cells when compared with LPI alone (LPI = 0.911 ± 0.028 ratio units, CBD + LPI = 0.668 ± 0.059 ratio units, n = 43 cells, $P < 0.001$, Student's unpaired two-tailed t-test, figure 5.3B and C).

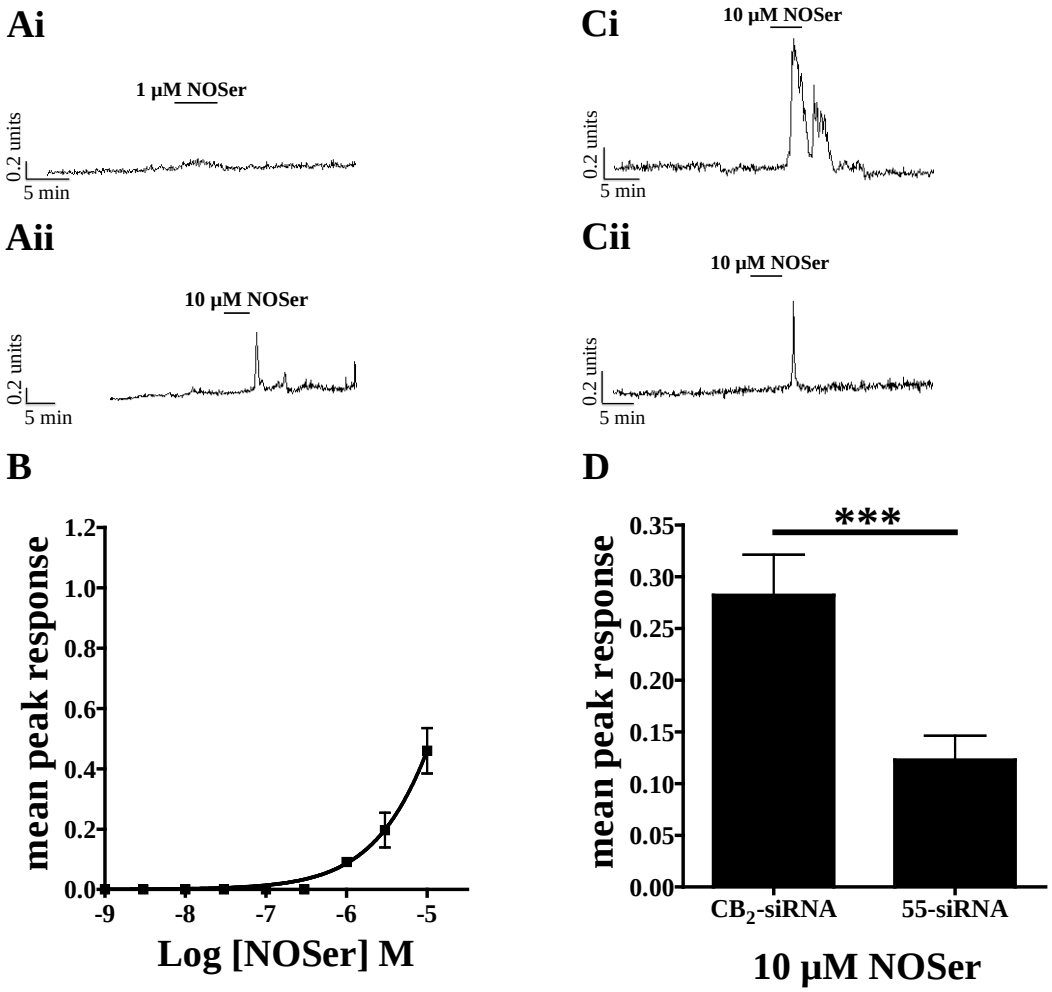

Figure 5.2: NOSer promotes Ca^{2+} mobilisation in DU145 cells. *NOSer was perfused at a rate of 2 ml/min over DU145 cells.* ***A****, representative Ca^{2+} traces from DU145 cells treated with NOSer at* ***i****, 1 µM;* ***ii****, 10 µM.* ***B****, NOSer concentration-response curve in DU145 cells. Data are the mean peak response ± SEM derived from 30 cells from 3 independent experiments.* ***C****, representative Ca^{2+} trace from DU145 cells transiently transfected for 69 hr with* ***i****. CB_2-siRNA;* ***ii****. GPR55-siRNA and then treated with 10 µM NOSer.* ***D****, histogram of pooled data, depicting mean Ca^{2+} peak responses from DU145 cells transiently transfected either CB_2 or 55 siRNA and perfused with 10 µM NOSer. Note the mean Ca^{2+} response was significantly decreased in the GPR55-siRNA transfected cells when compared to control CB_2-siRNA transfected cells. Data are the mean peak response ± SEM of 45 cells from 2 independent experiments. Student's unpaired two-tailed t-test; *P < 0.05.*

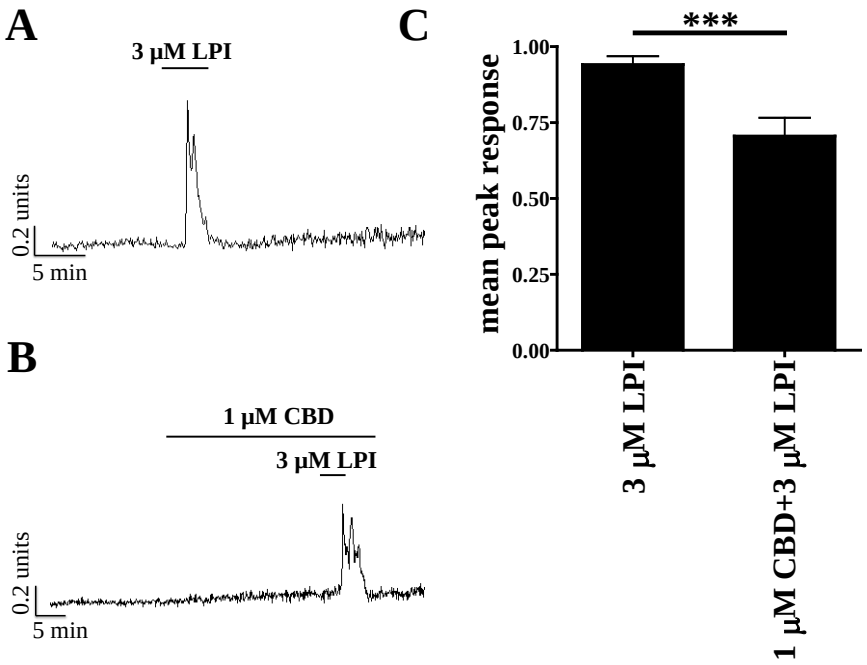

Figure 5.3: CBD antagonises LPI-induced Ca^{2+} mobilisation in DU145 cells. *DU145 cells were perfused with 1 µM CBD (20 min) prior to co-application with 3 µM LPI (5 min).* ***A****, representative Ca^{2+} trace from DU145 cells challenged with 3 µM LPI.* ***B****, representative Ca^{2+} trace from DU145 cells treated with 1 µM CBD and 3 µM LPI.* ***C****, histogram of pooled data, depicting mean peak Ca^{2+} responses from DU145 cells treated with either 3 µM LPI alone or in the presence of 1 µM CBD. Analysis revealed that the presence of CBD significantly decreased the LPI-induced Ca^{2+} response. Data are the mean peak response ± SEM of 43 cells from 2 independent experiments. Student's unpaired two-tailed t-test followed by a Bonferroni post hoc test; ***P < 0.001.*

5.2.1.2. LPI-induced Ca^{2+} transients require $G_{\alpha q}$ in DU145 cells.

Previous studies have highlighted that $G_{\alpha q}$ can induce the mobilisation of Ca^{2+} through GPR55 activation in transiently transfected hGPR55-HEK293 cells (Lauckner *et al.*, 2008). Therefore the $G_{\alpha q}$ inhibitor, YM-254890 (1 µM) was applied to DU145 cells in the presence of LPI (3 µM). When LPI (3 µM) was co-applied with YM-254890 (1 µM) responses were markedly reduced by 66.3 ± 11.6%. Only slight increases in Ca^{2+} ratio were observed, with a clear Ca^{2+} transient induced in just one cell (LPI = 1.096 ± 0.092 ratio units, YM-254890 + LPI = 0.364 ± 0.04 ratio units, n = 58 cells, Student's unpaired two-tailed t-test, P < 0.001, figure 5.4C). These data suggest that LPI mediates the mobilisation of Ca^{2+} in DU145 cells via activation of the heterotrimeric G-protein, $G_{\alpha q}$.

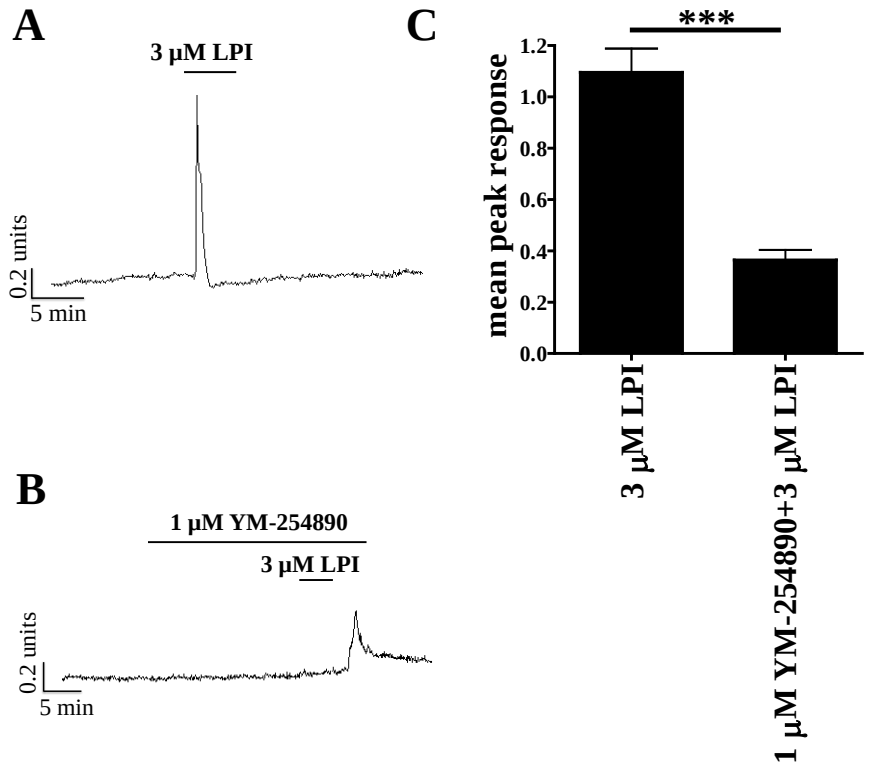

Figure 5.4: LPI-mediated Ca^{2+} signalling is through the activation of $G_{\alpha q}$ in DU145 cells. *The $G_{\alpha q}$ inhibitor YM-254890 (1 µM) was perfused over the DU145 cells for 20 min prior to a five minute co-application with 3 µM LPI followed by a final 5 min application of YM-254890 during washout.* ***A****, representative Ca^{2+} trace from DU145 cells treated with 3 µM LPI.* ***B****, representative Ca^{2+} trace of the responding DU145 cell treated with the co-application of 1 µM YM-254890 and 3 µM LPI.* ***C****, histogram of pooled data depicting mean, peak Ca^{2+} response data whereby the presence of YM-254890 decreases the LPI-mediated Ca^{2+} response in DU145 cells. The analysis revealed a significant decrease in mean Ca^{2+} responses in DU145 cells when the $G_{\alpha q}$ inhibitor was present with LPI. Data are the mean peak response ± SEM of 58 cells from 3 independent experiments. Student's unpaired two-tailed t-test; ***P < 0.001.*

5.2.1.3. ROCK signalling is not required for Ca^{2+} mobilisation in DU145 cells.

$G_{\alpha q}$ along with activating PLCβ (Takashima *et al.*, 2008) can activate RhoA (Vogt *et al.*, 2003), which is known to exert many of its actions via ROCK (Fujisawa *et al.*, 1996; Matsui *et al.*, 1996). In the hGPR55-HEK293 cells we showed that both isoforms of ROCK are important for Ca^{2+} mobilisation. Therefore the same two ROCK inhibitors; Y27632 (ROCK I and II inhibitor) and H1152 (ROCK II inhibitor), were tested in the DU145 cells. Y-27632 (10 µM) applied to DU145 cells prior to co-application with LPI (3 µM) had no effect on the mean, peak Ca^{2+} response (LPI = 0.738 ± 0.044 ratio units, Y-27632 + LPI = 0.748 ±0.044 ratio units, n = 36 cells, Student's unpaired two-tailed t-test, P > 0.05, figure 5.5Ai, ii and B). Likewise, H1152

applied to DU145 cells prior to co-application with LPI did not alter the Ca^{2+} mean peak responses when compared to LPI alone (LPI = 0.862 ± 0.050, H1152 + LPI = 0.839 ± 0.052, n = 46 cells, Student's unpaired two-tailed t-test, P > 0.05, figure 5.5Ci, ii and D).

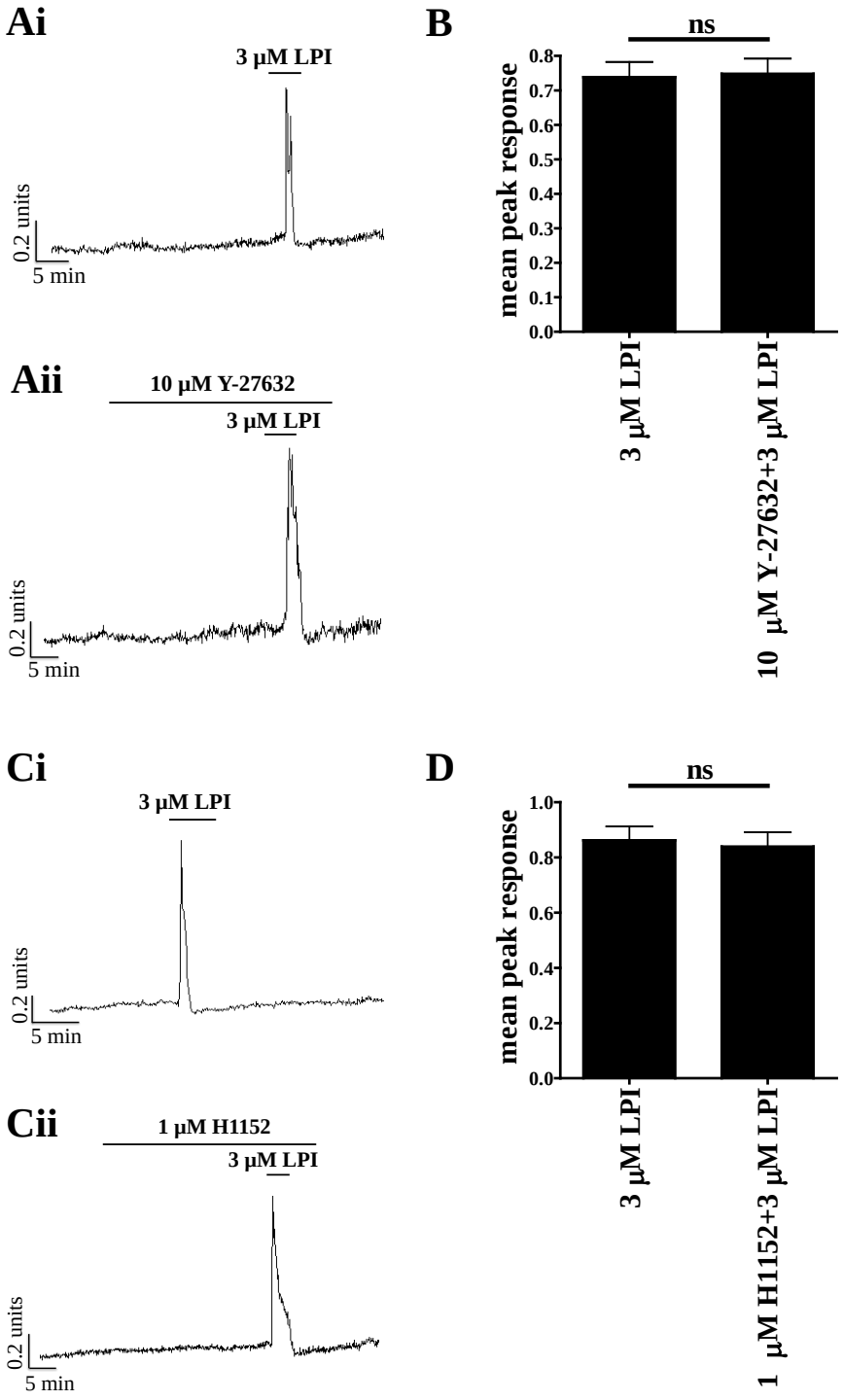

Figure 5.5: LPI-induced Ca^{2+} mobilisation does not require ROCK signalling. *DU145 cells were treated with ROCK inhibitors for 20 min prior to co-appplication with LPI.* ***A****, representative Ca^{2+} traces from DU145 cells challenged with either* ***i****, 3 µM LPI or* ***ii****, 3 µM LPI in the presence of 10 µM Y-27632.* ***B****, histogram of pooled data depicting mean peak Ca^{2+}*

response data from DU145 cells with either perfusion of LPI or LPI in the presence of Y-27632. Data are the mean, peak response ± SEM of 36 cells from 2 independent experiments. ***C****, representative* Ca^{2+} *trace from DU145 cells perfused with either* ***i****, 3 μM LPI or* ***ii****, 3 μM LPI in the presence of 1 μM H1152.* ***D****, histogram of pooled data, highlighting the mean, peak* Ca^{2+} *response data of DU145 cells treated with either LPI alone or LPI in the presence of H1152. Data are the mean, peak response ± SEM of 46 cells from 3 independent experiments. Note that the mean peak* Ca^{2+} *response hGPR55-HEK293 cells was unaffected by the presence of either ROCK II inhibitor. Student's unpaired two-tailed t-test; ns = not significant.*

The effects of ROCK inhibitors were also tested against NOSer (10 μM). However, responses to NOSer in the presence of Y-27632 (10 μM) were similar in magnitude to NOSer alone (NOSer = 0.670 ± 0.035, Y-27632 + NOSer = 0.737 ± 0.051, n = 30 cells, Student's unpaired two-tailed t-test, P > 0.05, figure 5.6Ai, ii, B). Likewise, responses to NOSer in the presence of H1152 (1 μM) were similar in magnitude to NOSer alone (NOSer = 0.723 ± 0.045, H1152 + NOSer = 0.795 ± 0.043, n = 20 cells, Student's unpaired two-tailed t-test, P > 0.05, figure 5.6Ci, ii, D). These data are in agreement with Falasca's group whereby ROCK signalling is not required for LPI-induced Ca^{2+} mobilisation in DU145 cells (Piñeiro *et al.*, 2011).

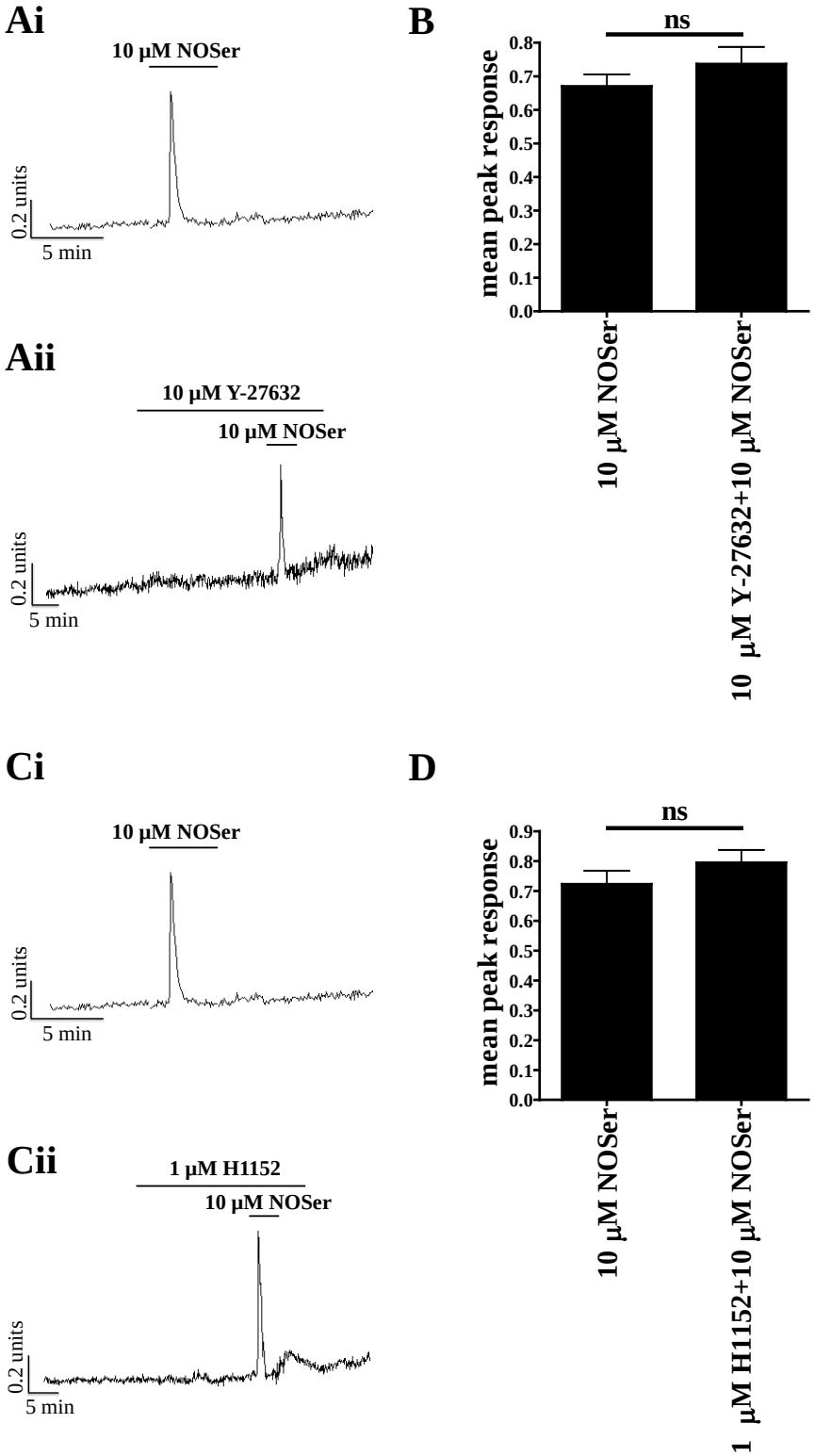

Figure 5.6: ROCK signalling is not required for NOSer-mediated Ca^{2+} mobilisation in DU145 cells. *ROCK inhibitors were applied to DU145 cells for 20 min prior to co-application with LPI.* ***A****, representative Ca^{2+} trace from DU145 cells challenged with either* ***i****. 10 µM NOSer or* ***ii****. 10 µM NOSer in the presence of 10 µM Y-27632.* ***B****, histogram of pooled data, the mean peak Ca^{2+} response data of DU145 cells perfused with NOSer or NOSer in the*

presence of Y-27632. Data are the mean peak response ±SEM of 30 cells from 2 independent experiments. ***C****, representative Ca^{2+} trace from DU145 cells perfused with either* ***i****, 10 µM NOSer or* ***ii****, 10 µM NOSer in the presence of 1 µM H1152.* ***D****, histogram of pooled data, depicting mean peak Ca^{2+} response data of DU145 cells treated with either NOSer alone or NOSer in the presence of H1152. Note there is no difference in the Ca^{2+} responses seen with NOSer in the presence of either ROCK inhibitor. Data are the mean, peak response ± SEM of 20 cells from 2 independent experiments. Student's unpaired two-tailed t-test; ns = not significant.*

5.2.1.4. Role of intracellular Ca^{2+} stores in GPR55-mediated Ca^{2+} responses in DU145 cells.

$G_{\alpha q}$ is also known to promote the mobilisation of Ca^{2+} through the activation of PLCβ (Takashima *et al.*, 2008). Also PLC is reported to be required for GPR55-mediated Ca^{2+} mobilisation (Lauckner *et al.*, 2008; Henstridge *et al.*, 2009). Therefore, U73122 (1 µM), a broad spectrum PLC inhibitor was applied to DU145 cells. Responses to LPI when applied in the presence of U73122 were reduced by 41.9% when compared to treatment with LPI alone (LPI = 0.844 ± 0.077, U73122 + LPI = 0.490 ± 0.120, n = 17 cells, Student's unpaired two-tailed t-test, $P < 0.05$, figure 5.7Ai, ii and B). Likewise, treatment with U73122 (20 min) also inhibited responses to NOSer by 48.2 ± 16.5%, relative to NOSer alone (NOSer = 0.470 ± 0.055, U73122 + NOSer = 0.233 ± 0.037, n = 28 cells, Student's unpaired two-tailed t-test, $P < 0.001$, figure 5.7Ci, ii, D). These data suggest that $G_{\alpha q}$-PLC signalling is important for LPI and NOSer-induced Ca^{2+} mobilisation.

As PLC is required in Ca^{2+} signalling in DU145 cells the effect of inhibition of IP_3 receptors was studied. PLC is the enzyme responsible for the hydrolysis of PIP_2 into IP_3 and DAG (Clapham, 2007). IP_3 can translocate from the cell membrane and act on IP_3 receptors on the ER which promotes the release of Ca^{2+} through the opened IP_3 receptor (Clapham, 2007). 2-APB is an antagonist of IP_3 receptors (Maruyama *et al.*, 1997) but can also interact with some TRP channels such as $TRPV_{1\text{-}3}$ (Colton and Zhu, 2007), $TRPV_6$ (Kovacs *et al.*, 2012) $TRPM_6$ and $TRPM_7$ (Li *et al.*, 2006) at concentrations >100 µM. Therefore 30 µM was used in an attempt to preferentially target IP_3 receptors. Application of NOSer in the presence of 2-APB (30 µM) inhibited Ca^{2+} responses by 69.5% in comparison with those observed with NOSer alone (NOSer = 0.720 ± 0.042 ratio units, 2-APB + NOSer = 0.220 ± 0.052 ratio units, n = 22 cells,

Student's unpaired two-tailed t-test, $P < 0.001$, figure 5.8A-C). These data suggest that IP_3 receptors may be required for the mobilisation of Ca^{2+} in DU145 cells.

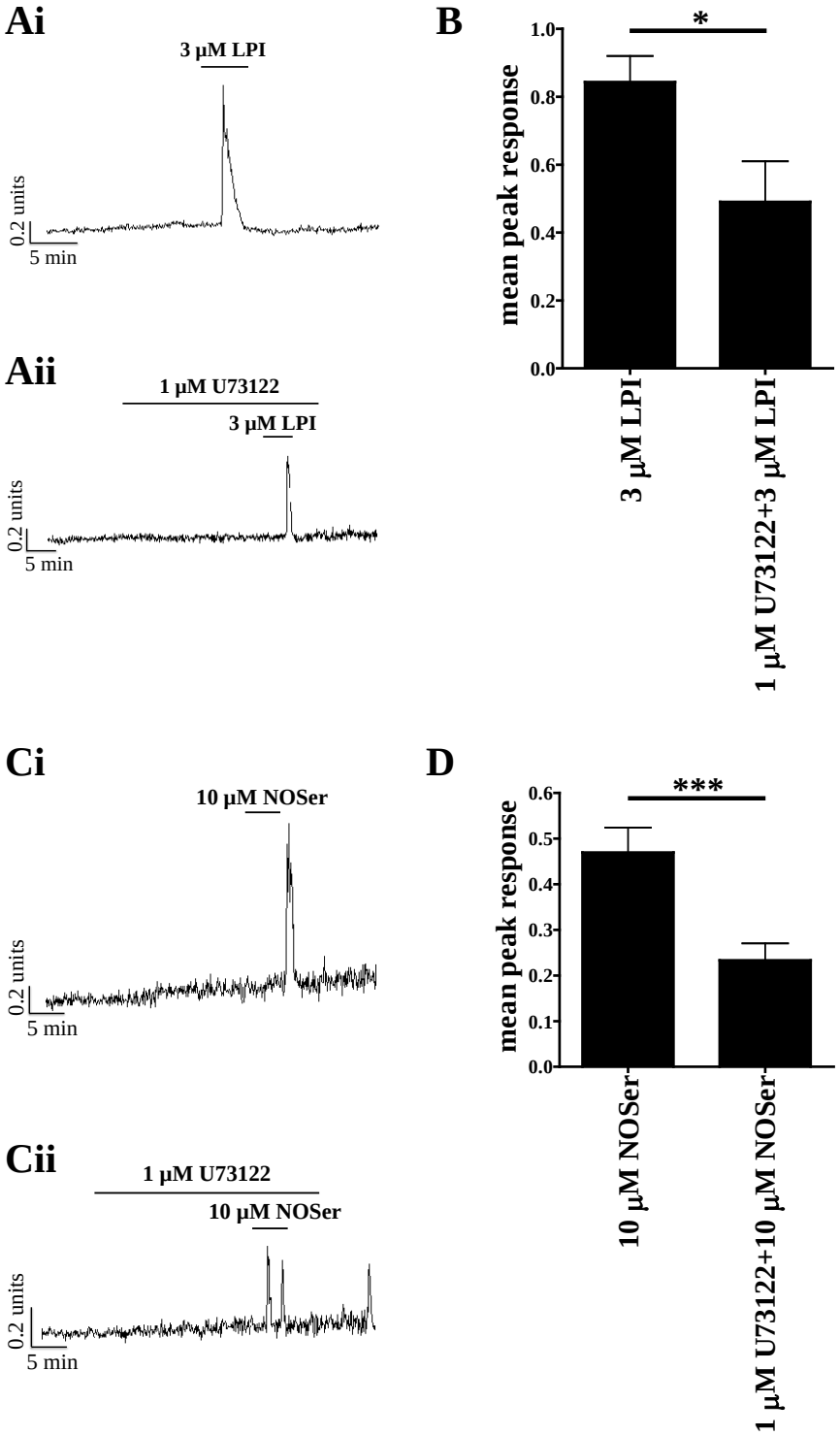

Figure 5.7: Endogenous lipids signal through PLC to promote Ca^{2+} mobilisation in DU145 cells. *The PLC inhibitor U73122 (1 µM) was applied to DU145 cells prior to the co-application of the inhibitor with either LPI or NOSer.* ***A****, representative Ca^{2+} trace from DU145 cells challenged with either* ***i****, 3 µM LPI or* ***ii****, 1 µM U73122 and 3 µM LPI.* ***B****,*

histogram of pooled data depicting the mean, peak Ca^{2+} response highlighting that the responses to LPI are decreased when the PLC inhibitor is present. The analysis revealed a significant decrease in mean Ca^{2+} responses when the PLC inhibitor was present with LPI. Data are the mean, peak response ± SEM of 17 cells from 1 experiment. ***C****, representative Ca^{2+} trace from DU145 cells treated with 10 µM either* ***i****, NOSer or* ***ii****, 10 µM NOSer applied in the presence of 1 µM U73122.* ***D****, histogram of pooled data, depicting the mean peak Ca^{2+} response data whereby NOSer applied in the presence of the PLC inhibitor produced mean peak Ca^{2+} responses that were decreased when compared to NOSer alone. The analysis revealed a significant decrease in mean Ca^{2+} peak responses when the PLC inhibitor was present with NOSer. Data are the mean, peak response ± SEM of 28 cells from 2 independent experiments. Student's unpaired two-tailed t-test; *P < 0.05; ***P < 0.001.*

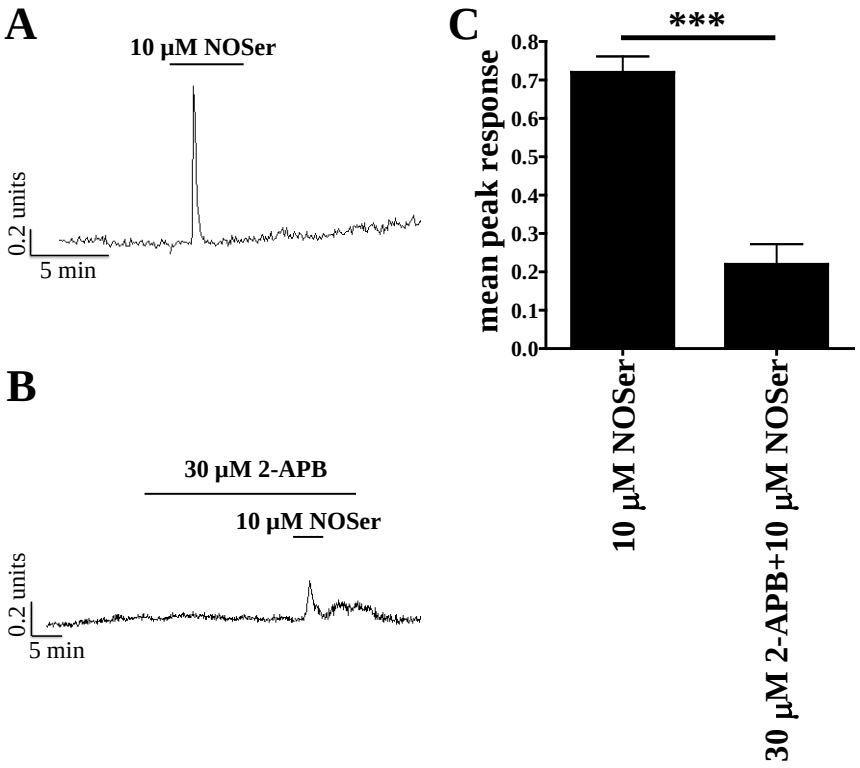

Figure 5.8: IP_3 receptors play a role in Ca^{2+} mobilisation in DU145 cells. *Cells were treated with 2-APB (30 µM) for 20 min prior to co-application with NOSer (5 min).* ***A****, representative Ca^{2+} traces from DU145 cells challenged with* ***i****, 10 µM NOSer or* ***ii****, 30 µM 2-APB co-applied with 10 µM NOSer.* ***B****, histogram of pooled data, for the mean, peak Ca^{2+} response highlighting that responses to NOSer are significantly decreased when the lipid is applied with the IP_3/TRP channel antagonist. Data are the mean peak response ± SEM of 22 cells from 1 experiment. Student's unpaired two-tailed t-test; ***P < 0.001.*

5.2.2. Endogenous lipids, CREB phosphorylation and DU145 cells.

The next sets of experiments were designed to study the effect LPI and NOSer had on pCREB in DU145 cells. In hGPR55-HEK293 cells pCREB labelling increased and was localised to the nucleus when the cells were challenged with the GPR55 lipid ligands. The signalling pathways required for pCREB signalling in hGPR55-HEK293 cells were also studied in the DU145 cells.

5.2.2.1. LPI and NOSer induce nuclear pCREB in DU145 prostate cancer cells.

LPI, as a natural ligand for GPR55 was applied to DU145 cells in the pCREB assay. Cells treated with DMSO (0.1%) were found to have low levels of pCREB but there was some nuclear labelling observed, suggesting a low level of constitutive activation (figure 5.9A). In the presence of TPA (100 nM) there was a pronounced increase in nuclear pCREB labelling in all cells. Low concentrations of LPI (10 nM and 30 nM) did not affect pCREB levels, being similar to DMSO control. However, as the LPI concentration was increased (100 nM - 10 µM range) nuclear pCREB labelling increased along with an increase in the number of cells that responded, giving an EC_{50} of 222 ± 45 nM (95% confidence limits) (figure 5.9B).

Next the effects of NOSer were investigated in DU145 cells. Increasing NOSer concentrations (10 nM - 10 µM) promoted a corresponding increase in nuclear pCREB labelling with 10 µM producing pCREB responses that were similar to TPA (figure 5.10A and B). As a clear E_{max} was not observed within the concentration range (10 nM - 10 µM) the EC_{50} could not be calculated.

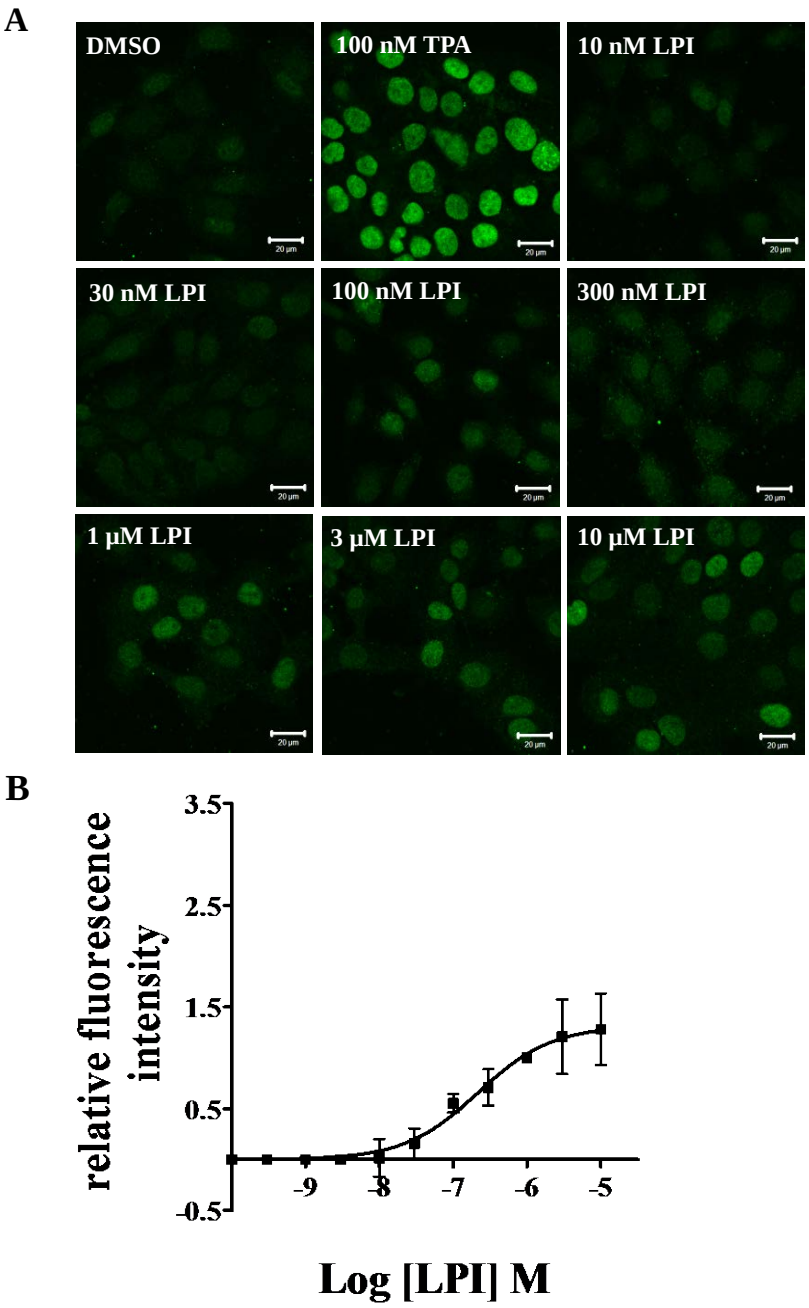

Figure 5.9: LPI promotes concentration-dependent increases in nuclear pCREB in DU145 cells. *Increasing concentrations of LPI were applied to the prostate cancer cell line, DU145 for 25 min.* ***A****, representative confocal images of nuclear pCREB in DU145 cells illustrating the effects of the following treatments: DMSO, vehicle control; 100 nM TPA, positive control; 10 nM LPI; 30 nM LPI; 100 nM LPI; 300 nM LPI; 1 µM LPI; 3 µM LPI; 10 µM LPI. Scale bars = 20 µm. n = 3.* ***B****, concentration-response curve of nuclear pCREB in DU145 cells challenged with LPI. Fluorescence intensity was calculated as CTNF normalised relative to 1 µM LPI. Data are the means ± SEM; n = 3.*

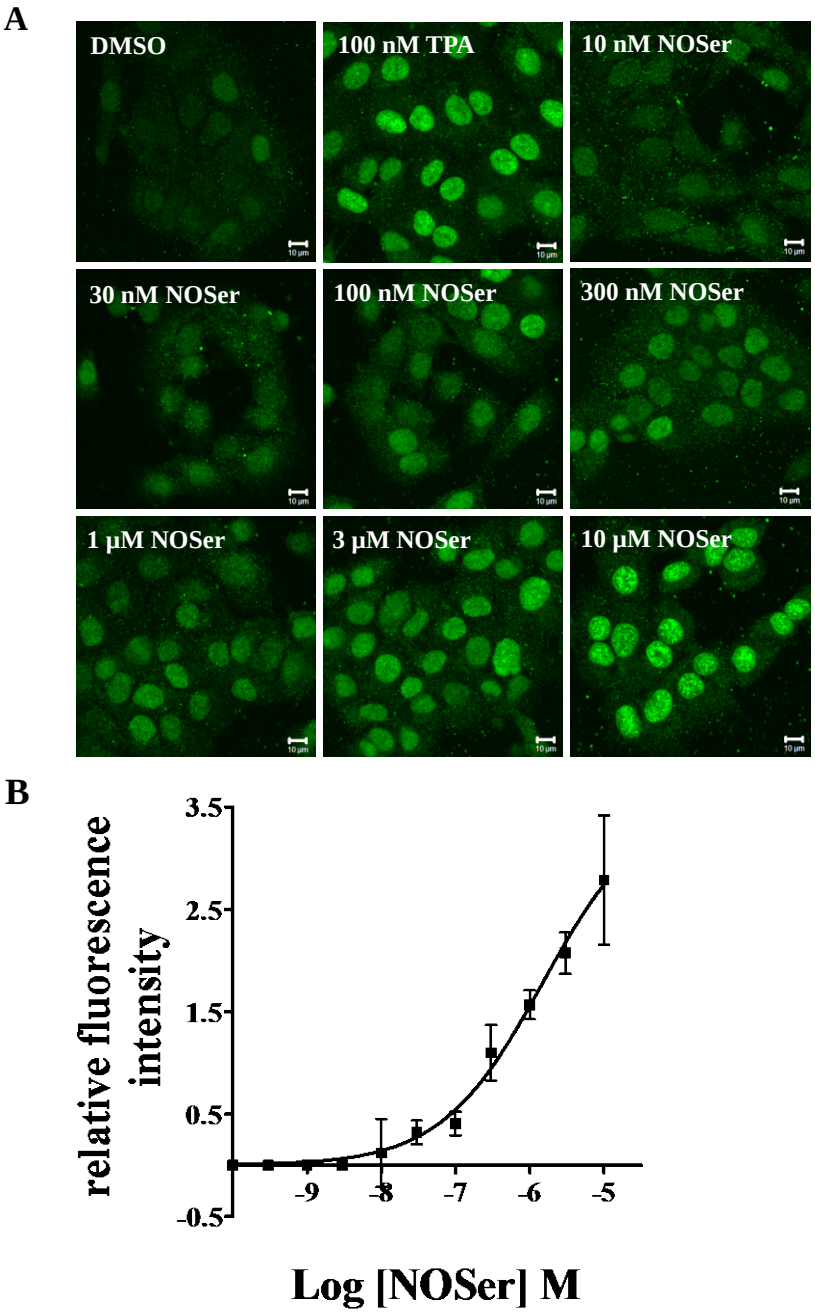

Figure 5.10: NOSer treatment of DU145 prostate cells promotes the phosphorylation of nuclear CREB. *Increasing concentrations of NOSer were applied to the prostate cancer cell line, DU145 for 25 min.* ***A****, representative confocal images of nuclear pCREB in DU145 cells illustrating the effects of the following treatments: DMSO, vehicle control; 100 nM TPA, positive control; 10 nM NOSer; 30 nM NOSer; 100 nM NOSer; 300 nM NOSer; 1 µM NOSer; 3 µM NOSer; 10 µM NOSer. Scale bars = 20 µm. n = 3.* ***B****, concentration-response curve of nuclear pCREB labelling in DU145 cells challenged with increasing concentrations of NOSer. Fluorescence intensity was calculated as CTNF normalised relative to 1 µM LPI. Data are the mean ± SEM; n = 3.*

5.2.2.2. A role for G_{13} and G_q in LPI and NOSer-mediated pCREB responses in DU145 cells.

In the next series of experiments the effects of dominant negative $G_{\alpha 13}$(Q226L/D294N) on LPI and NOSer-mediated pCREB responses were evaluated. One-way ANOVA analysis revealed that there was no significant difference across the experimental data ($F_{(5,12)}$ = 1.286; P = 0.03323). DU145 cells transfected with $G_{\alpha 13}$(Q226L/D294N) showed elevated pCREB levels relative to control. These data suggest that the transient transfection may have stressed the cells and promoted pCREB responses even in the absence of agonist treatment. This may have masked the true inhibition of $G_{\alpha 13}$ in DU145 cells challenged with LPI or NOSer. It is very difficult to interpret this due to pCREB induction with $G_{\alpha 13}$(Q226L/D294N) which is not significantly different to LPI or NOSer responses.

Although $G_{\alpha q}$ was not required to promote pCREB staining in hGPR55-HEK293 cells it has been implicated in both GPR55-mediated Ca^{2+} signalling (Lauckner *et al.*, 2008) and ERK1/2 phosphorylation (Obara *et al.*, 2011). Interestingly the present study suggests that GPR55-mediated Ca^{2+} mobilisation in DU145 cells involved $G_{\alpha q}$ activation. Therefore the $G_{\alpha q}$ inhibitor YM-254890 (1 μM) was tested to elucidate if GPR55-mediated $G_{\alpha q}$ signalling can promote nuclear pCREB in DU145 cells. Analysis using a One-way ANOVA revealed that there were significant differences within the experimental data ($F_{(5,12)}$ = 13.49; P = 0.0001). Responses to LPI or NOSer were inhibited by 97.7 ± 4.1% or 62.8 ± 15.5% respectively in the presence of YM-254890 (figure 5.12A and B). In control experiments, similar pCREB labelling was observed in DU145 cells treated with either DMSO or $G_{\alpha q}$ inhibitor alone. These data suggest that $G_{\alpha q}$ is important for the promotion of pCREB in NOSer challenged DU145 cells and likely to be required in LPI treated cells.

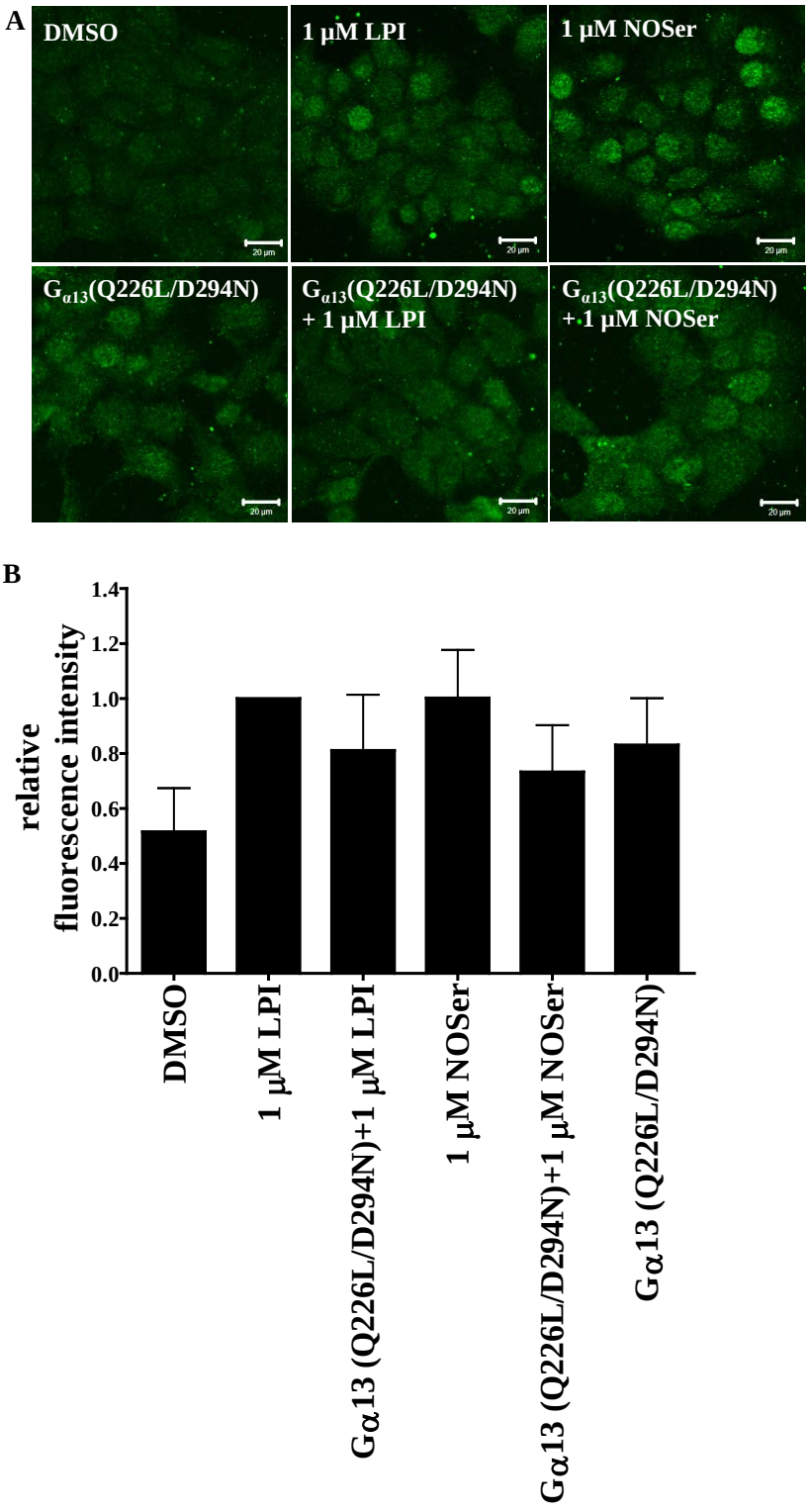

Figure 5.11: A role for $G_{\alpha 13}$ in promoting nuclear pCREB in DU145 cells. *Cells were treated with a dominant negative $G_{\alpha 13}$ (Q226L/D294N) cDNA for 18 hr prior to application of the lipids.* ***A****, representative confocal images of nuclear pCREB in DU145 cells treated as follows DMSO; 1 µM LPI; 1 µM NOSer; $G_{\alpha 13}$(Q226L/D294N); $G_{\alpha 13}$(Q226L/D294N) + 1 µM LPI; $G_{\alpha 13}$(Q226L/D294N) + 1 µM NOSer. Scale bars = 20 µm, n = 3.* ***B****, histogram of pooled data, showing the mean CTNF when DU145 cells were challenged with either 1 µM LPI or 1 µM*

NOSer either with or without $G_{\alpha 13}$(Q226L/D294N). These data are the mean CTNF normalised to 1 µM LPI. Data are the means ± SEM; n = 3. One-way ANOVA.

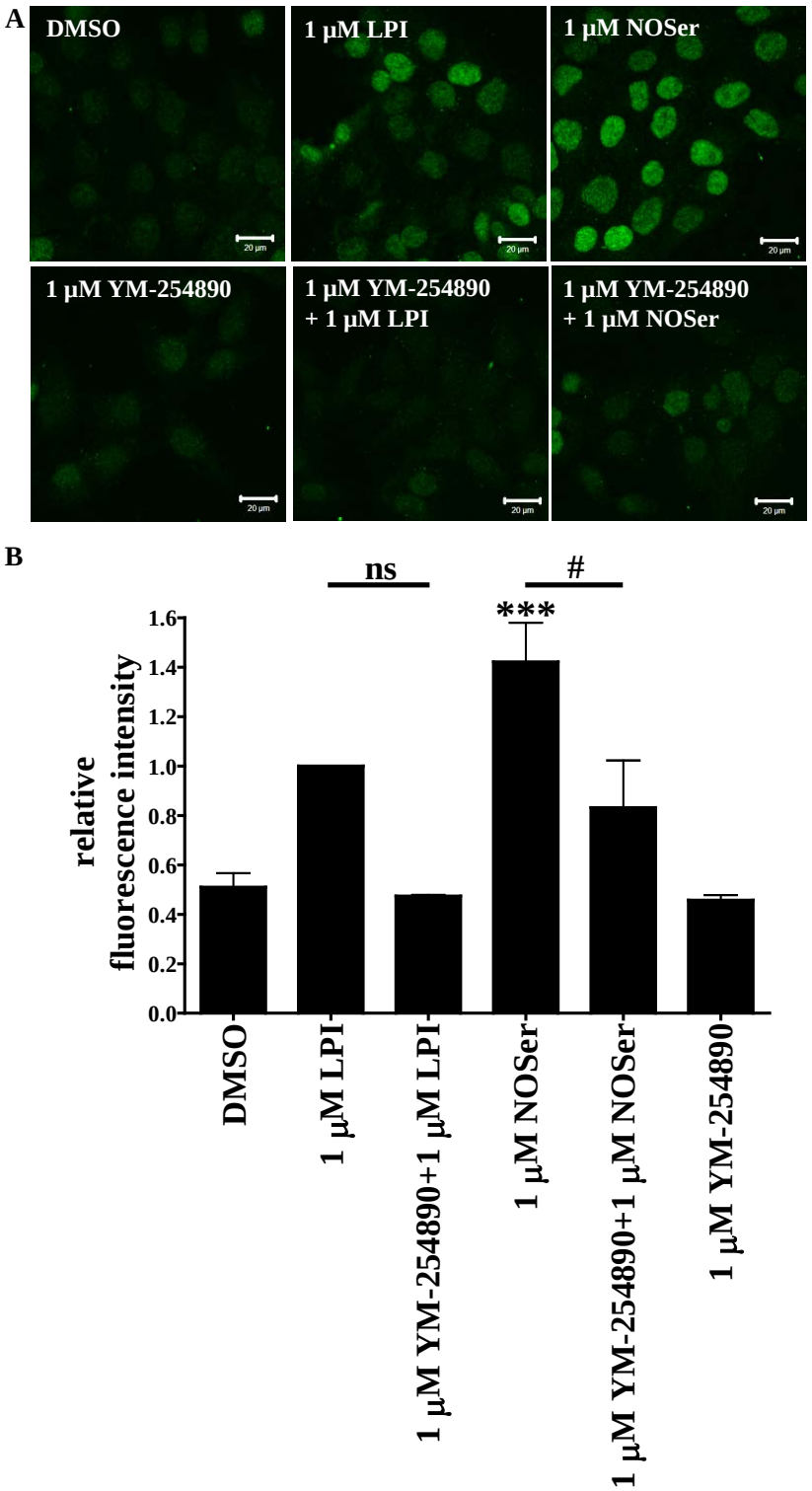

Figure 5.12: $G_{\alpha q}$ signalling is required for endogenous lipid induced nuclear pCREB in DU145 cells. ***A****, representative confocal images of nuclear pCREB labelling in DU145 cells are as follows DMSO; 1 µM LPI; 1 µM NOSer; 1 µM YM-254890; 1 µM YM-254890 + 1 µM LPI; 1 µM YM-254890 + 1 µM NOSer.* ***B****, histogram of pooled data, showing the percentage*

*mean of nuclear pCREB fluorescence intensity when DU145 cells were challenged with either 1 μM LPI or 1 μM NOSer either in the presence or absence of 1 μM YM-254890. Analysis revealed that lipid challenge in the presence of the $G_{\alpha q}$ inhibitor promoted pCREB which was significantly decreased when compared to NOSer alone. * = data compared to vehicle control. Data are the means ±SEM; n = 3. One-way ANOVA followed by a Bonferroni post hoc test; ***P < 0.001; #P < 0.05; ns = not significant.*

5.2.2.3. Rho and ROCK are required to induce nuclear pCREB in DU145 cells.

Both $G_{\alpha 13}$ and $G_{\alpha q}$ have been previously reported to activate RhoA (Chikumi *et al*., 2002; Vogt *et al*., 2003). Furthermore GPR55-mediated Rho activation is required for Ca^{2+} mobilisation (Henstridge *et al*., 2009) and, in the present study, for pCREB in hGPR55-HEK293 cells. Therefore the effects of the cell permeable Rho inhibitor (CT04; 1 μg/ml) were tested on pCREB responses. A one-way ANOVA highlighted significant differences within the CT04 experimental data ($F_{(5,12)}$ = 10.57; P = 0.0005). CT04 did not increase pCREB levels when compared to basal levels (5.13A and B). CT04 was applied to DU145 cells for 4 hr prior to lipid challenge was found to lower pCREB responses to both LPI and NOSer by 59.9 ± 16.0% and 71.5 ± 4.4% respectively. These data suggest that Rho activation is required to promote pCREB labelling in DU145 cells when challenged with either LPI or NOSer.

In the present study ROCK signalling was required to promote nuclear pCREB in the stably transfected hGPR55-HEK293 cells when they were challenged with either LPI or NOSer. Therefore the ROCK inhibitors, Y-27632 (10 μM) and H1152 (100 nM), were tested in the DU145 cells with the same endogenous lipids. A one-way ANOVA highlighted significant differences within the Y-27632 data set ($F_{(5,12)}$ = 12.00; P = 0.0002). Furthermore a Bonferroni *post hoc* test revealed that treatment with Y-27632 had no effect by itself (figure 5.14A and B). However Y-27632 co-applied with 1 μM LPI markedly inhibited responses by 86.2 ± 8.2% and significantly decreased responses by 63.6 ± 16.6% when co-applied with 10 μM.

H1152 was also tested with the DU145 cells. Analysis with a one-way ANOVA revealed significant differences within the H1152 experimental data ($F_{(5,12)}$ = 11.29; P = 0.0003). A Bonferroni *post hoc* test highlighted that treatment with H1152 lowered pCREB responses to LPI and significantly inhibited responses to 10 μM NOSer by 120.7 ± 5.5% and 66.5 ± 8.3% respectively. However H1152 has no effect by itself

(figure 5.14D and E). These data suggest that NOSer challenged DU145 cells require ROCK activation to promote pCREB. Furthermore ROCK is likely to be required by DU145 cells challenged with LPI. This highlights a difference in signalling as NOSer and LPI-mediated Ca^{2+} mobilisation did not require ROCK signalling in the DU145 cells.

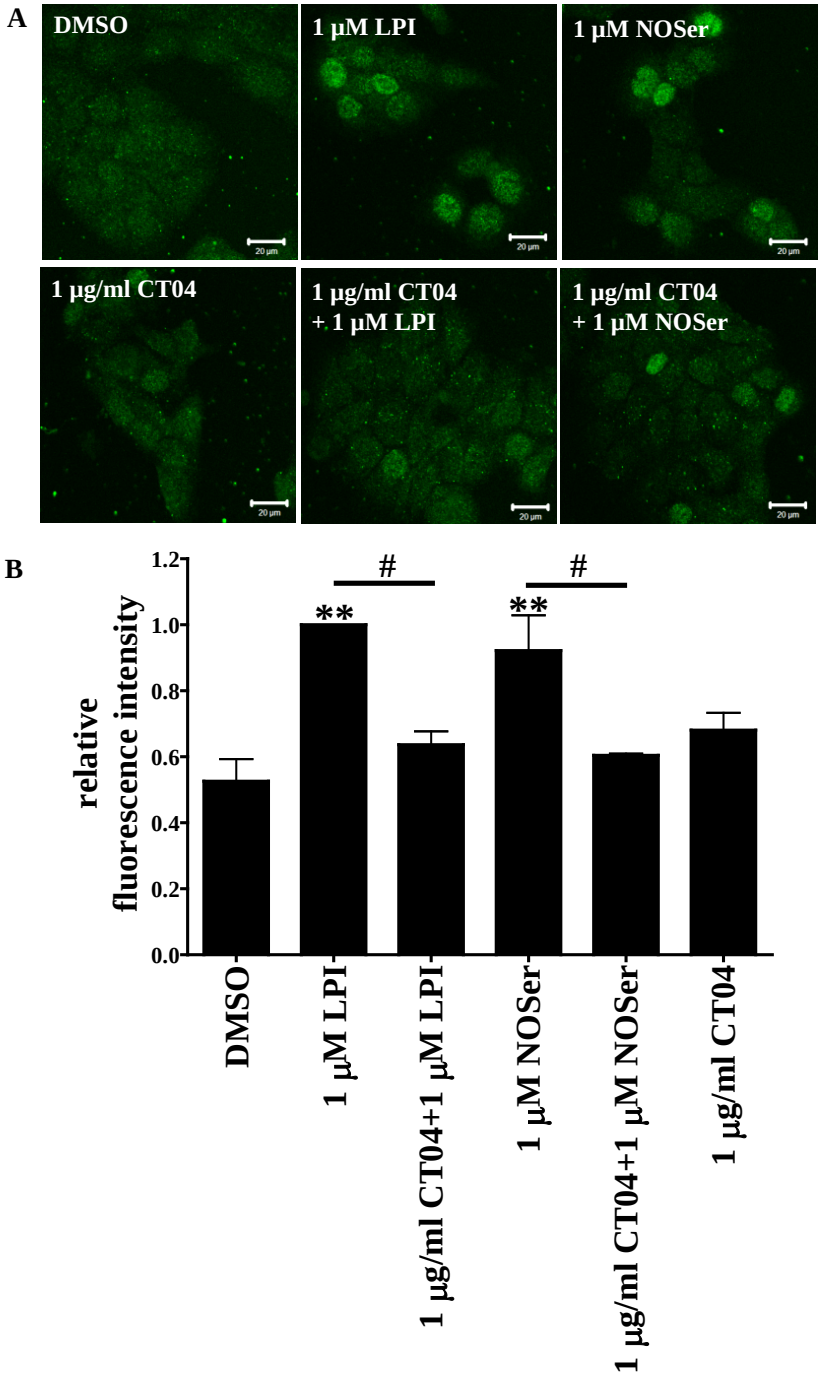

Figure 5.13: Signalling through Rho is required for LPI and NOSer-mediated pCREB responses in DU145 cells. *Cells were treated for 4 hr with a membrane permeant Rho inhibitor (1 µg/ml CT04) prior to treatment with lipid.* ***A****, representative confocal images of nuclear pCREB in hGPR55-HEK293 cells are as follows: DMSO; 1 µM LPI; 1 µM NOSer; 1 µg/ml*

CT04; 1 µg/ml CT04 + 1 µM LPI; 1 µg/ml CT04 + 1 µM NOSer. Scale bars = 20 µm; n = 3. ***B****, histogram of pooled data displaying the mean nuclear pCREB fluorescence when DU145 cells were challenged with either 1 µM LPI or 1 µM NOSer either in the presence of absence of the Rho inhibitor. Analysis revealed that the presence of the Rho inhibitor significantly decreased the effects of lipid challenge in DU145 cells. The data is CTNF normalised to 1 µM LPI. Data are the means ± SEM; n = 3. * = compared to vehicle control. One-way ANOVA followed by a Bonferroni post hoc test; **P < 0.01; #P < 0.05.*

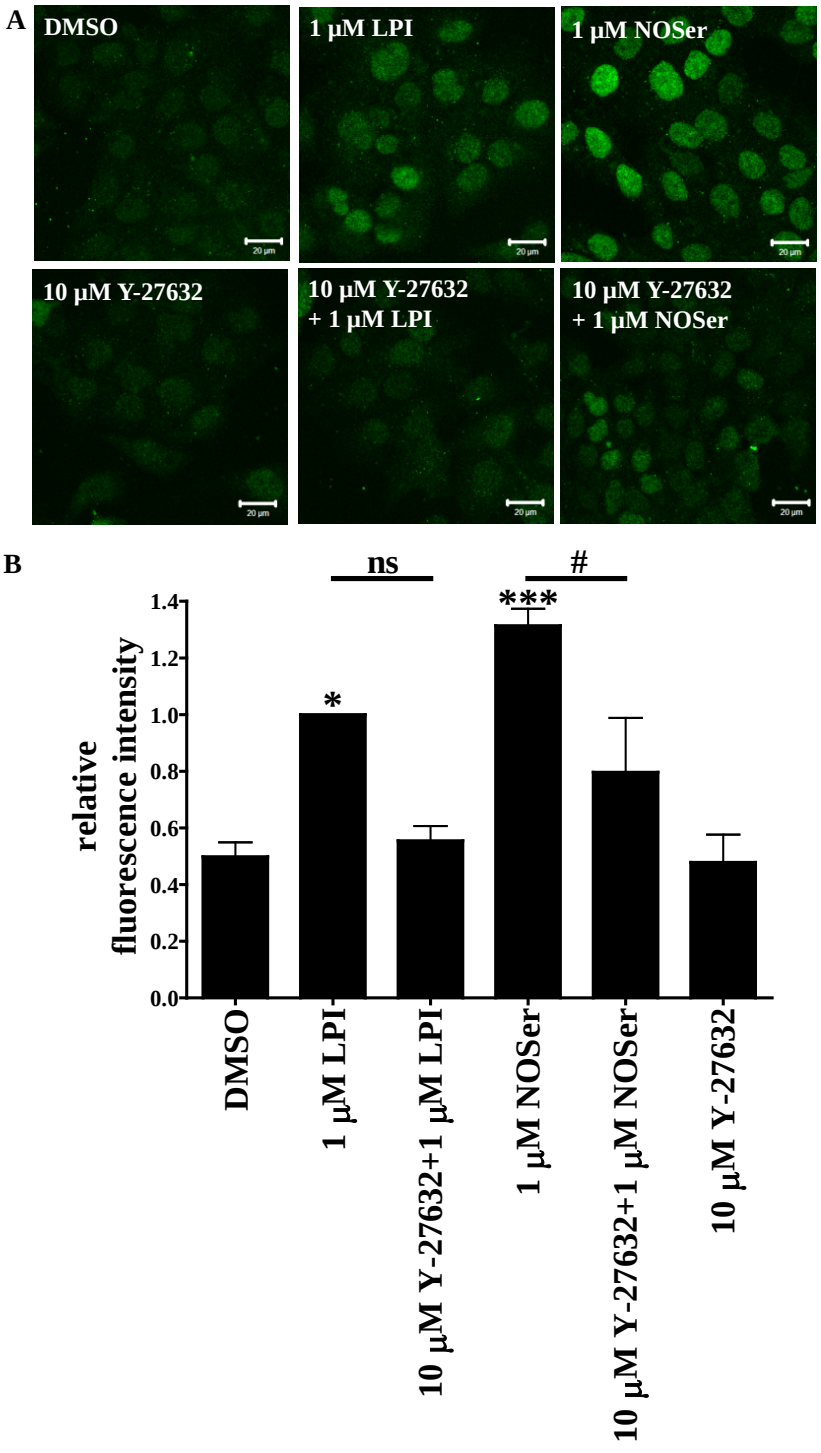

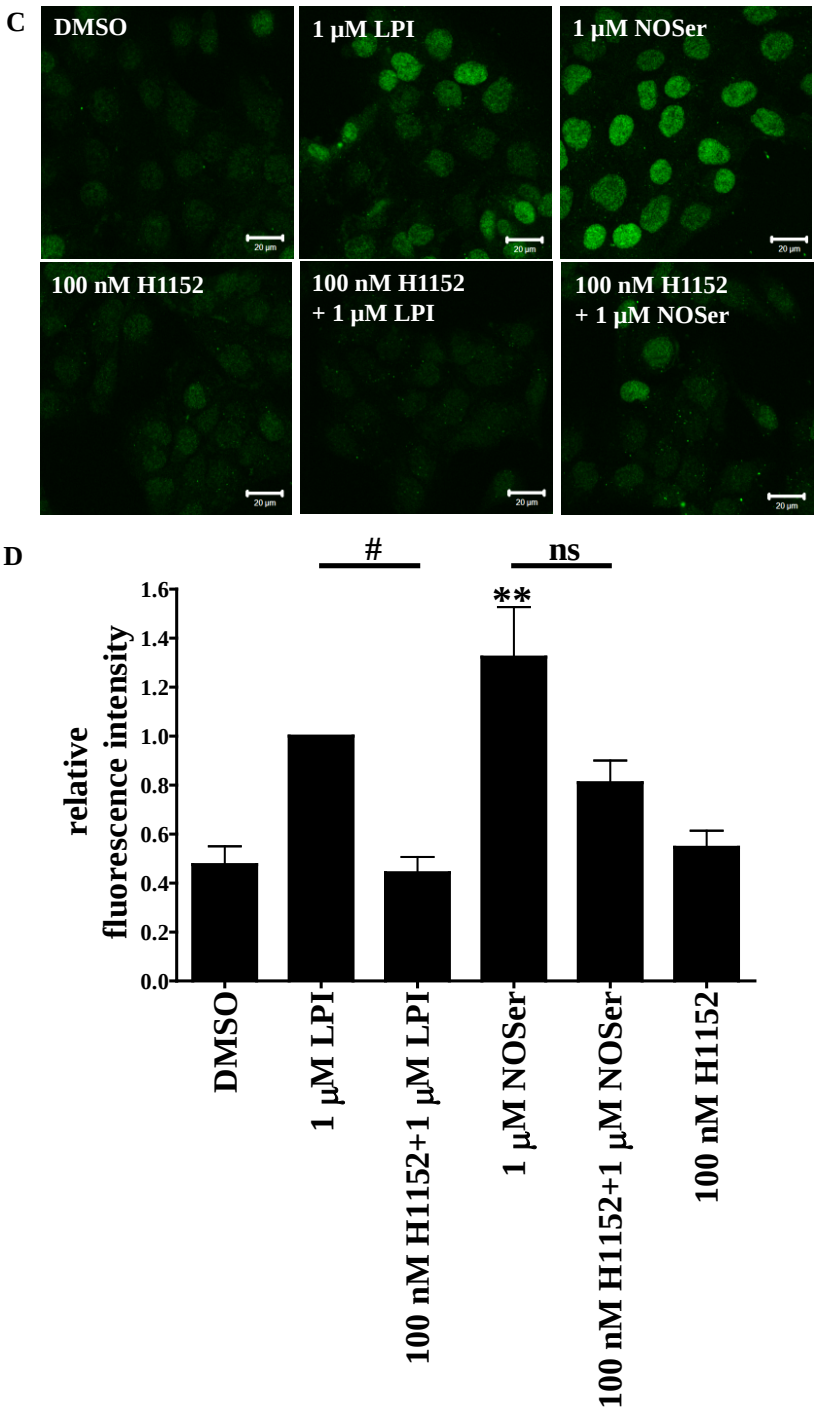

Figure 5.14: ROCK signalling is required to promote nuclear pCREB in DU145 cells. ***A****, representative confocal images of nuclear pCREB labelling are DMSO; 1 µM LPI; 1 µM NOSer; 10 µM Y-27632; 10 µM Y-27632 + 1 µM LPI; 10 µM Y-27632 + 1 µM NOSer. Scale bars = 20 µm; n = 3.* ***B****, histogram of pooled data, highlighting the CTNF of nuclear pCREB fluorescence when DU145 cells were challenged with either 1 µM LPI, 1 µM NOSer or the lipids in the presence of 10 µM Y-27632. Analysis revealed the ROCK I and II inhibitor (Y-27632; 10 µM) decreases the nuclear pCREB labelling in lipid challenged DU145 cells.* ***C****, representative confocal images of nuclear pCREB labelling are DMSO; 1 µM LPI; 1 µM NOSer; 100 nM H1152; 100 nM H1152 + 1 µM LPI; 100 nM H1152 + 1 µM NOSer. Scale*

bars = 20 µm; n = 3. ***D****, histogram of pooled data showing the CTNF of nuclear pCREB in DU145s challenged with 1 µM LPI or 1 µM NOSer alone or co-applied with 100 nM H1152. Analysis revealed presence of the ROCK II inhibitor decreased the lipid-induced pCREB labelling in the DU145 cells. * = data compared to vehicle control. Data are means ± SEM; n = 3. One-way ANOVA followed by a Bonferroni post hoc test. *P < 0.05; **P < 0.01; ***P < 0.001; #P < 0.05; ns = not significant.*

5.2.2.4. The role of Ca^{2+} homeostasis in nuclear pCREB responses to endogenous lipids in DU145s.

The next sets of experiments were to determine if increases in Ca^{2+} were a required for LPI and NOSer-mediated pCREB responses in DU145 cells. This study previously demonstrated that in hGPR55-HEK293 cells, Ca^{2+} plays a role in promoting GPR55-mediated pCREB labelling. LPI can also promote Ca^{2+} mobilisation in DU145 cells however NOSer was much less effective at inducing Ca^{2+} mobilisation than seen with LPI. Therefore the role of lipid-induced Ca^{2+} signalling in promoting pCREB in DU145 cells was studied. A one-way ANOVA highlighted significant differences in the BAPTA-AM experimental data set ($F_{(5,12)} = 6.69$; $P = 0.0034$). A Bonferroni *post hoc* test revealed that in the presence of BAPTA-AM, neither LPI nor NOSer was able to stimulate any additional increase in pCREB levels (figure 5.15A and B). These data suggest that the chelation of intracellular Ca^{2+} may interfere with LPI and NOSer-mediated pCREB. However the direct effect of BAPTA-AM on pCREB levels masks this effect.

Does the presence of extracellular Ca^{2+} effect pCREB responses in DU145s treated with exogenous lipids? In order to address this, cells were placed in Ca^{2+} free HBS supplemented with 100 µM EDTA (CF-HBS) for 5 min prior to the addition of lipids in CF-HBS applied for 25 min. Cells in CF-HBS had a tendency to retract, become rounded and in general have a less flattened morphology in CF-HBS. A one-way ANOVA was performed but did not find any significant differences with the data set ($F_{(5,6)} = 4.664$; $P = 0.0438$). The pCREB responses to both LPI and NOSer in CF-HBS were lowered (figure 5.16A and B). These data suggest that the extracellular Ca^{2+} is likely to be important for lipid promoted nuclear pCREB in DU145 cells.

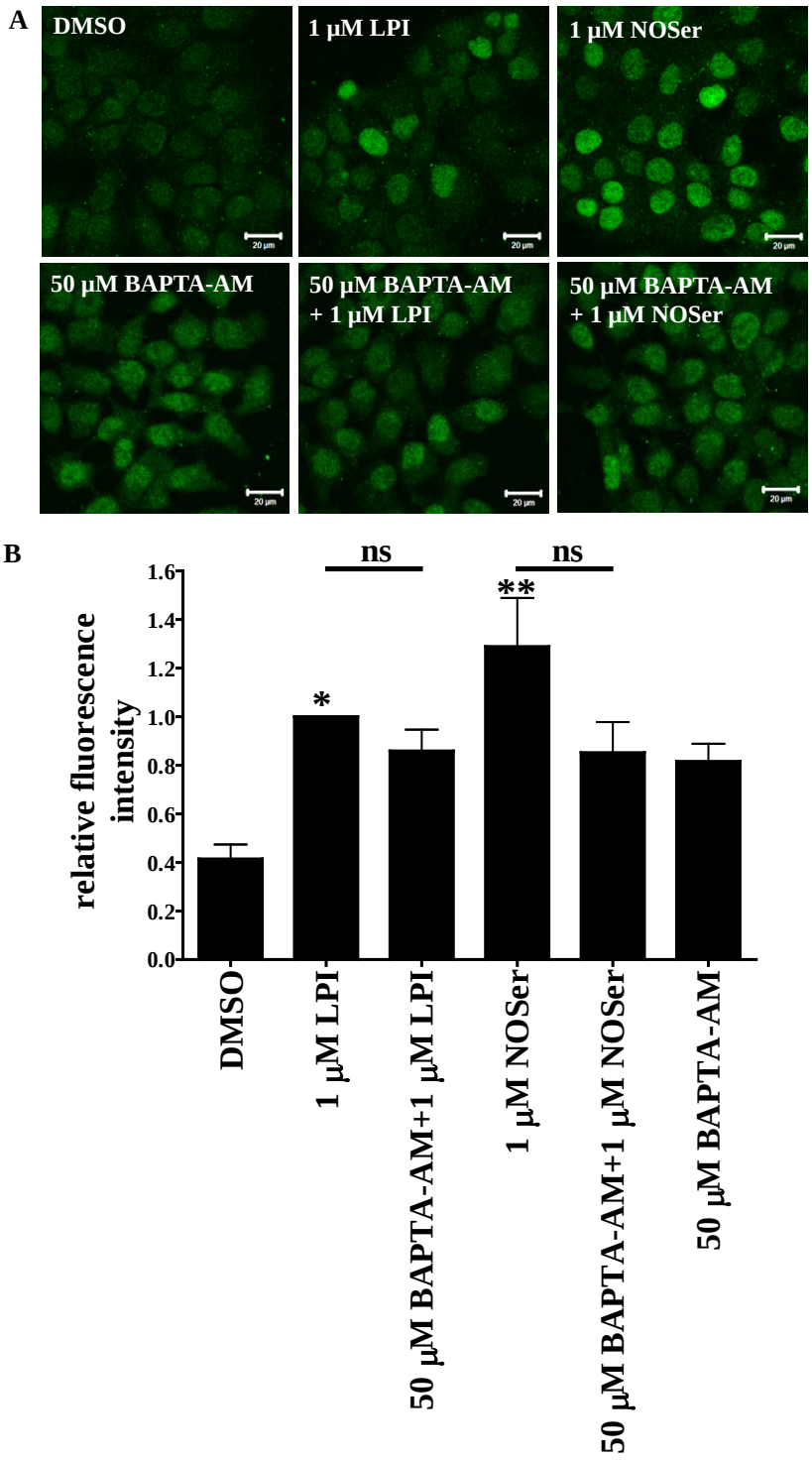

Figure 5.15: Effects of BAPTA-AM on LPI and NOSer-mediated nuclear pCREB signalling in DU145 cells. ***A****, representative confocal images of nuclear pCREB labelling in DU145 cells are as follows DMSO; 1 µM LPI; 1 µM NOSer; 50 µM BAPTA-AM; 50 µM BAPTA-AM + 1 µM LPI; 50 µM BAPTA-AM + 1 µM NOSer.* ***B****, histogram of pooled data, showing the percentage mean of nuclear pCREB fluorescence intensity when DU145 cells were challenged with either 1 µM LPI or 1 µM NOSer either in the presence of 50 µM BAPTA-AM or alone. Analysis revealed that both LPI and NOSer-induced pCREB responses were not significantly decreased when* Ca^{2+} *was chelated. However LPI-induced pCREB responses whilst they were*

*lower were not significantly different when the Ca^{2+} was chelated. * = data compared to vehicle control. Data are the means ± SEM; n = 3. One-way ANOVA followed by a Bonferroni post hoc test; *P < 0.05; **P < 0.01; ns = not significant.*

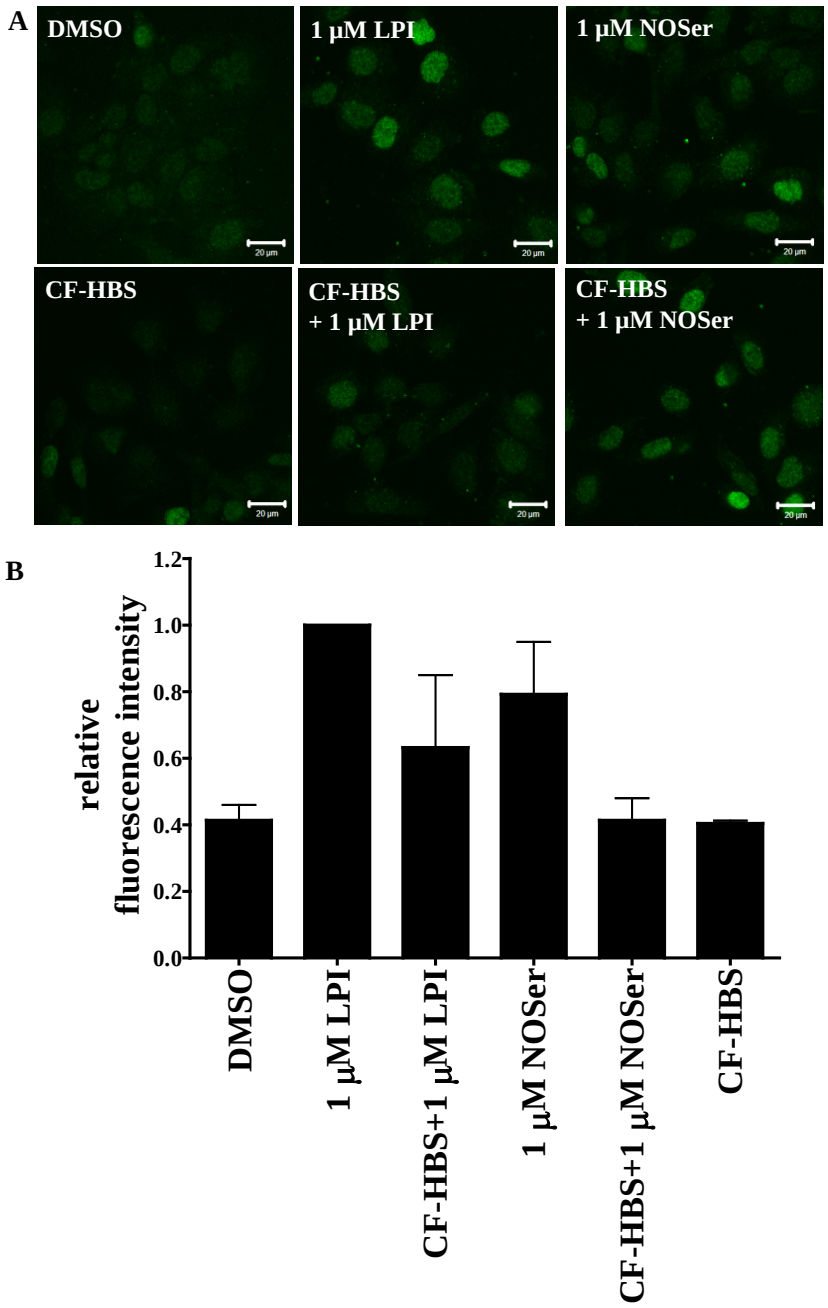

Figure 5.16: Ca^{2+} from extracellular media is required for LPI-mediated nuclear pCREB in DU145s. *Ca^{2+}-free HBS supplemented with 100 µM EGTA (CF-HBS) was applied to DU145 cells 5 min prior to the co-application of the respective lipid for a further 25 min.* ***A****, representative confocal images of nuclear pCREB labelling in DU145 cells are as follows DMSO; 1 µM LPI; 1 µM NOSer; CF-HBS; Ca^{2+} free HBS + 1 µM LPI; Ca^{2+} free HBS + 1 µM NOSer. Scale bars = 20 µM; n = 2.* ***B****, histogram of pooled data, showing the percentage mean of nuclear pCREB fluorescence intensity when DU145 cells were challenged with either 1*

*µM LPI or 1 µM NOSer either in the presence of Ca^{2+} free HBS or alone. * = data compared to vehicle control. Data are the means ± SEM; n = 2. One-way ANOVA.*

DU145 cells were then tested with the PLC inhibitor, U73122 (1 µM). Analysis using a one-way ANOVA highlighted significant differences within the PLC inhibitor experimental data set ($F_{(5,12)}$ = 15.98; P < 0.0001). Responses to LPI were abolished in the presence of U73122 (1 µM), with pCREB labelling similar to DMSO controls (figure 5.17A and B). In contrast, when U73122 was co-applied with NOSer, nuclear pCREB labelling that was similar to that observed in NOSer treated cells. These data suggest that PLC is required for the promotion of nuclear pCREB in DU145 cells challenged with LPI but has no affect in NOSer challenged cells.

PKC is a well-established kinase that can promote CREB phosphorylation (Zanassi *et al.*, 2001). In this PKC was also involved in promoting pCREB in hGPR55-HEK293 cells treated with LPI or NOSer. Using Gö6983 (1 µM), a broad spectrum cell permeable selective PKC inhibitor was tested to uncover the role of PKC in pCREB responses to LPI (1 µM) or NOSer (1 µM) in DU145 cells. A one-way ANOVA revealed significant differences within the Gö6983 experimental data set ($F_{(5,12)}$ = 10.61; P = 0.0004). Moreover a Bonferroni *post hoc* test highlighted that treatment with Gö6983 alone did not effect pCREB levels (figure 5.18A and B). However when LPI was co-applied with Gö6983, pCREB responses to LPI were lowered. Responses to NOSer were inhibited, to a lesser extent than seen with LPI. These data suggest that PKC is likely to be involved in promoting pCREB in DU145 cells challenged with LPI but may not be so important in cells challenged with NOSer.

CaMKII is another kinase implicated in GPR55-CREB signalling in hGPR55-HEK293 cells, therefore KN-62 (2 µM), a CaMKII inhibitor was tested on the DU145 cells. One-way ANOVA analysis highlighted significant differences within the KN-62 data set ($F_{(5,6)}$ = 25.18; P = 0.0006). Furthermore a Bonferroni *post hoc* test revealed that treatment with KN-62 alone did not affect basal levels of pCREB (figure 5.19A and B). However, when KN-62 was co-applied with LPI responses were markedly inhibited. Responses to NOSer were also slightly inhibited in the presence of KN-62 but were not significant. These data suggest that CaMKII is involved in LPI-induced pCREB responses in DU145 cells. However NOSer-induced pCREB in DU145 cells does not require the activation of CAMKII.

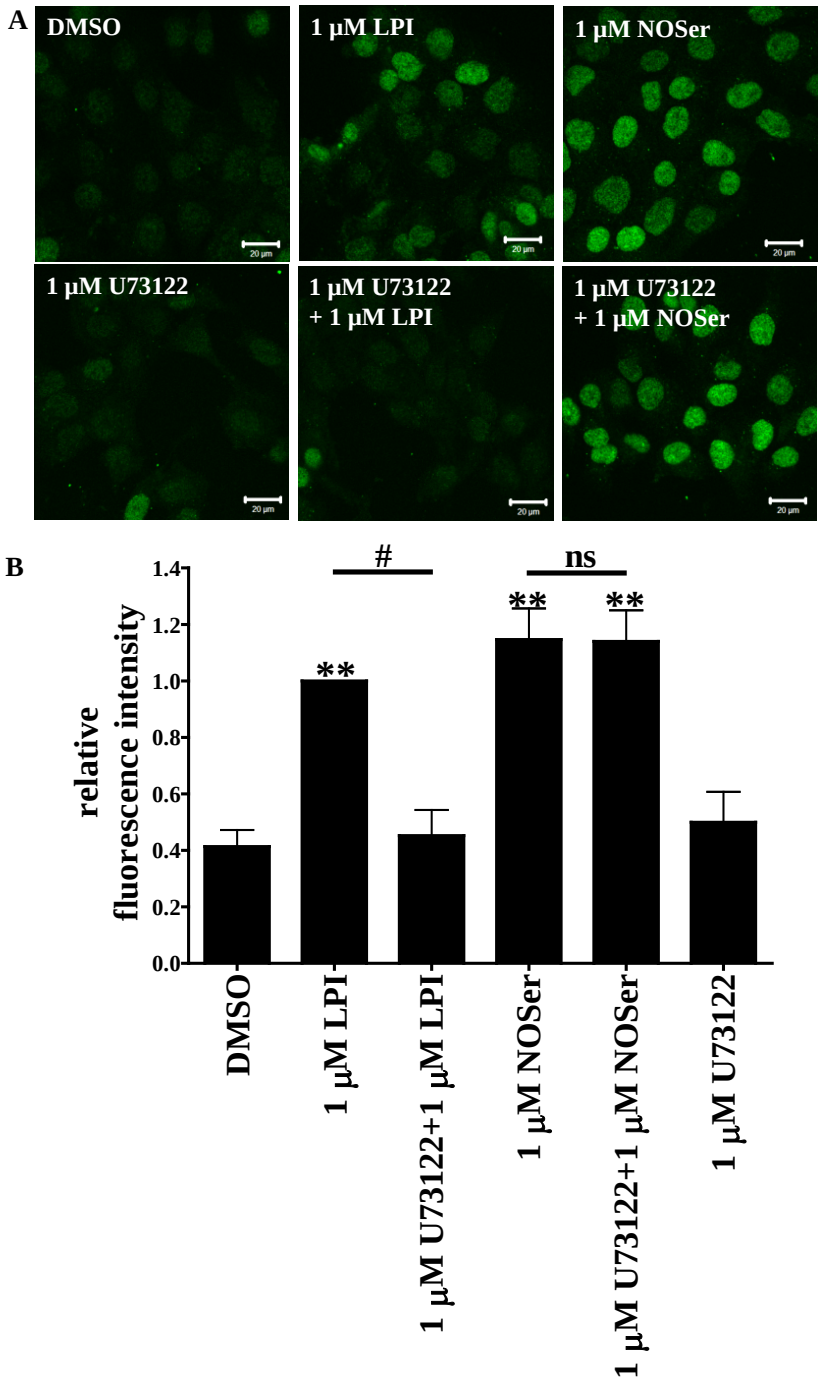

Figure 5.17: A role for PLC in LPI, but not NOSer-mediated nuclear pCREB signalling in DU145s cells. ***A****, representative confocal images of nuclear pCREB labelling in DU145 cells are as follows DMSO; 1 µM LPI; 1 µM NOSer; 1 µM U73122; 1 µM U73122 + 1 µM LPI; 1 µM U73122 + 1 µM NOSer. Scale bars = 20 µm; n = 3.* ***B****, histogram of pooled data; depicting the mean CTNF of nuclear pCREB in DU145 cells treated with either 1 µM LPI, 1 µM NOSer or a lipid co-applied with 1 µM U73122. Analysis revealed that inhibiting PLC significantly decreased the LPI-induced pCREB labelling in the DU145 cells however it had no effect on NOSer-induced pCREB. * = data compared to vehicle control. Data are the means ± SEM; n = 3. One-way ANOVA followed by a Bonferroni post hoc test. **P < 0.01; #P < 0.05; ns = not significant.*

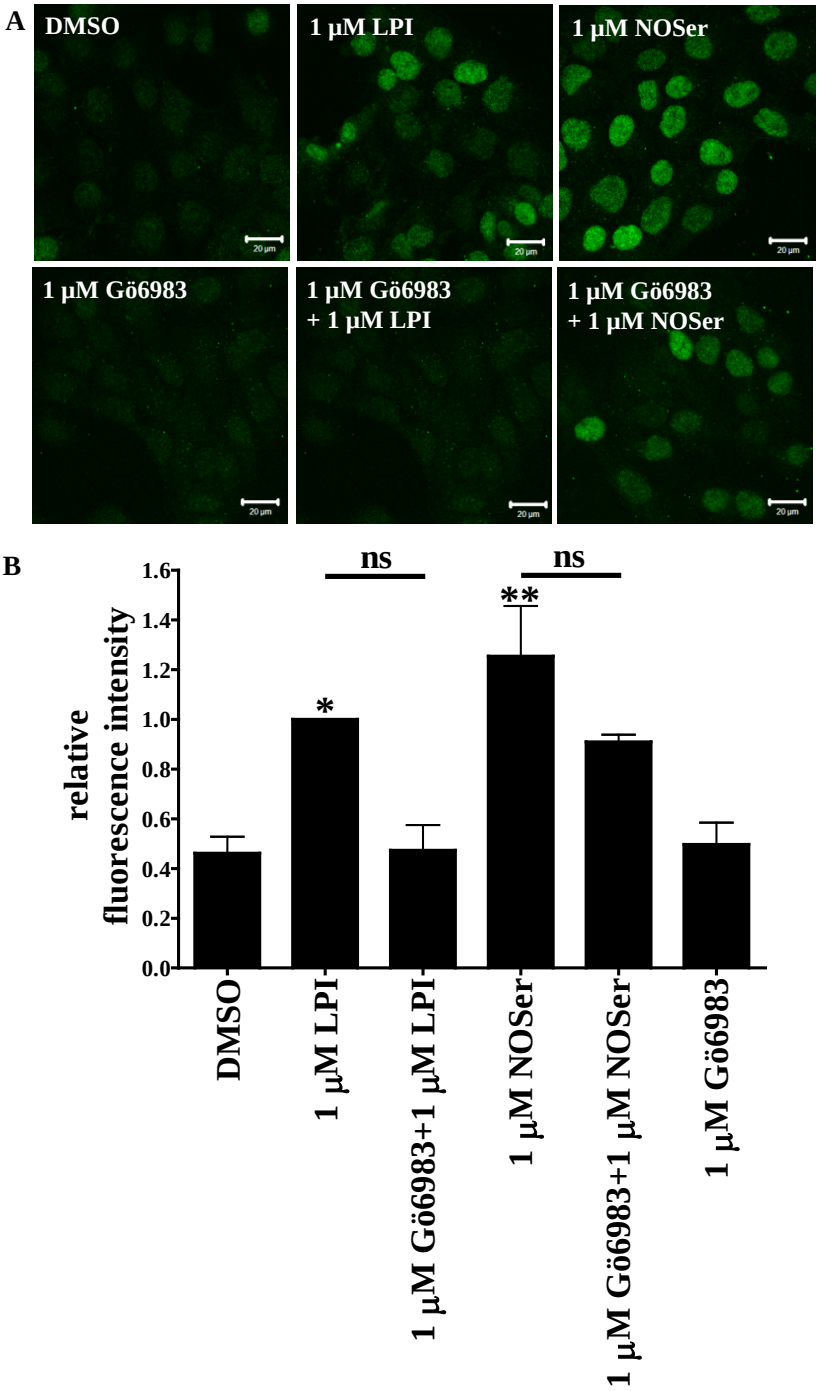

Figure 5.18: PKC signalling is likely to be involved in nuclear pCREB signalling in DU145 cells treated with endogenous lipids. ***A****, representative confocal images of nuclear pCREB labelling in DU145 cells are as follows DMSO; 1 µM LPI; 1 µM NOSer; 1 µM Gö6983; 1 µM Gö6983 + 1 µM LPI; 1 µM Gö6983 + 1 µM NOSer. Scale bars = 20 µm; n = 3.* ***B****, histogram of pooled data; depicting the mean CTNF normalised to 1 µM LPI of nuclear pCREB in DU145 cells treated with either 1 µM LPI, 1 µM NOSer or a lipid co-applied with 1 µM Gö6983. The analysis revealed that PKC inhibition decreased the pCREB labelling in DU145 cells challenged with either of the lipids however to a greater extent with LPI. * = data compared to vehicle control. Data are the means ± SEM; n = 3. One-way ANOVA followed by a Bonferroni post hoc test. *P < 0.05; **P < 0.01; ns = not significant.*

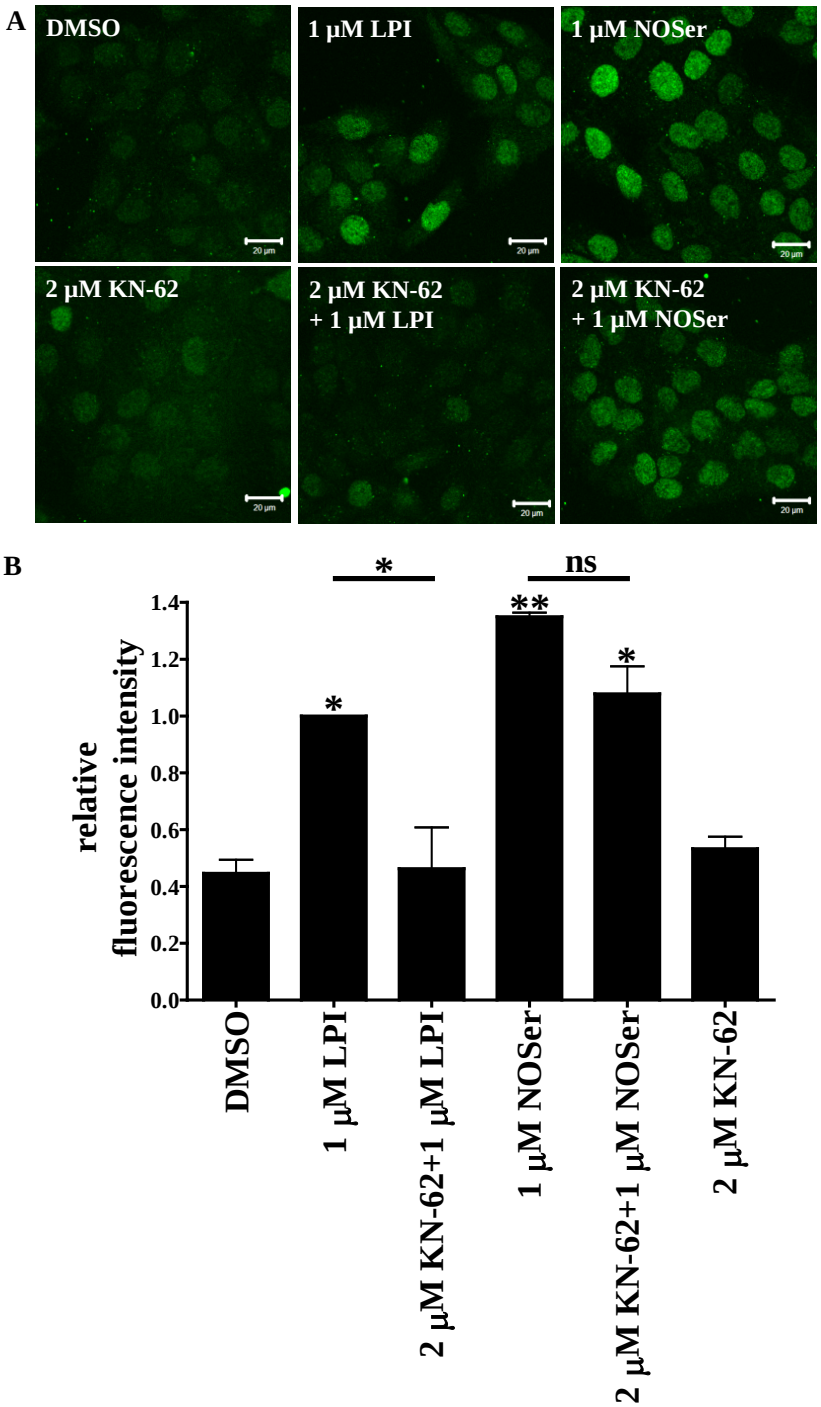

Figure 5.19: CaMKII is involved in GPR55-pCREB signalling in DU145 cells. ***A****, representative confocal images of nuclear pCREB labelling in DU145 cells are as follows DMSO; 1 µM LPI; 1 µM NOSer; 2 µM KN-62; 2 µM KN-62 + 1 µM LPI; 2 µM KN-62 + 1 µM NOSer. Scale bars = 20 µm; n = 2.* ***B****, histogram of pooled data; depicting the mean CTNF of nuclear pCREB in DU145 cells treated with either 1 µM LPI, 1 µM NOSer or a lipid co-applied with 2 µM KN-62. Analysis revealed CaMKII inhibition significantly decreased the pCREB labelling in LPI challenged DU145 cells. * = data compared to vehicle control. Data are the means ± SEM; n = 2. One-way ANOVA followed by a Bonferroni post hoc test. *P < 0.05; **P < 0.01; ns = not significant.*

5.2.2.5. Do DU145 cells challenged with lipids signal through the MAP kinase pathway to induce nuclear pCREB?

Previously LPI (1 µM) was reported to promote ERK1/2 phosphorylation in DU145 cells. The authors also observed that 100 nM LPI phosphorylated ERK1/2, albeit to a lesser extent (Piñeiro *et al.*, 2011). Therefore, PD98059 and U0126, two structurally different MEK1/2 inhibitors, were applied to DU145 cells. One-way ANOVA revealed there were significant differences within the MEK1/2 inhibitor experimental data ($F_{(8,18)} = 37.12$; $P < 0.0001$). Furthermore a Bonferroni post hoc test highlighted that neither of these inhibitors (PD98059, 25 µM; U0126, 5 µM) effected basal pCREB (figure 5.20A and B). However responses to LPI or NOSer were abolished in their presence.

To further confirm the MEK inhibitors results, U0124 (5 µM), an inactive analogue of U0126 was employed. One-way ANOVA revealed significant differences within the experimental data ($F_{(5,12)} = 20.86$; $P < 0.0001$). Moreover a Bonferroni *post hoc* test highlighted that treatment with U0124 did not affect responses to LPI (1 µM) or NOSer (1 µM) (figure 5.20C and D). These data suggest that both LPI and NOSer require activation of MEK1/2 to promote nuclear pCREB labelling in DU145 cells.

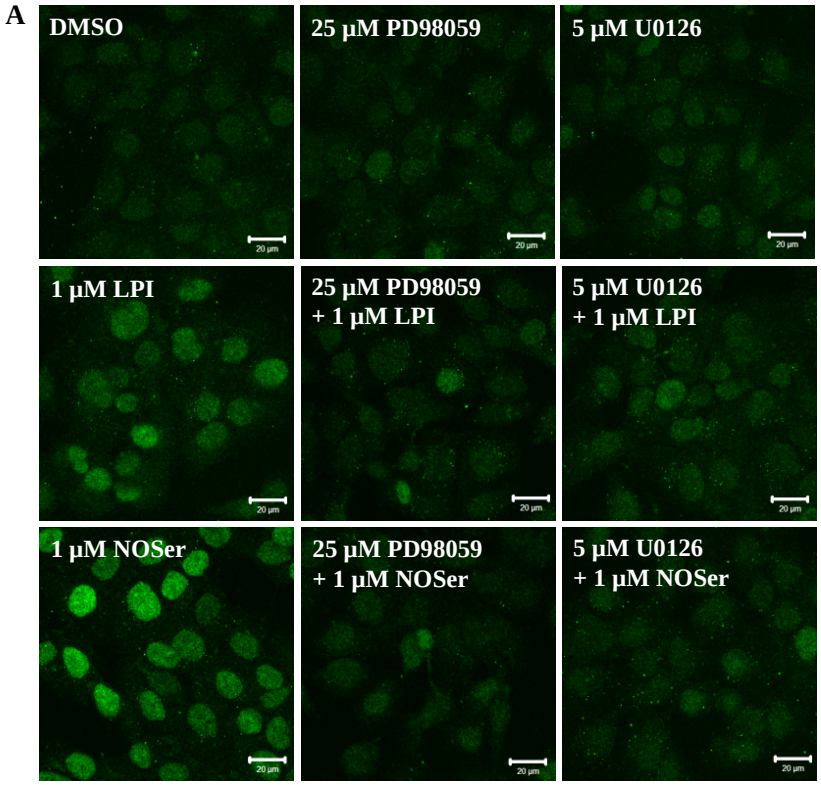
A
DMSO
25 µM PD98059
5 µM U0126
1 µM LPI
25 µM PD98059
+ 1 µM LPI
5 µM U0126
+ 1 µM LPI
1 µM NOSer
25 µM PD98059
+ 1 µM NOSer
5 µM U0126
+ 1 µM NOSer
20 µm

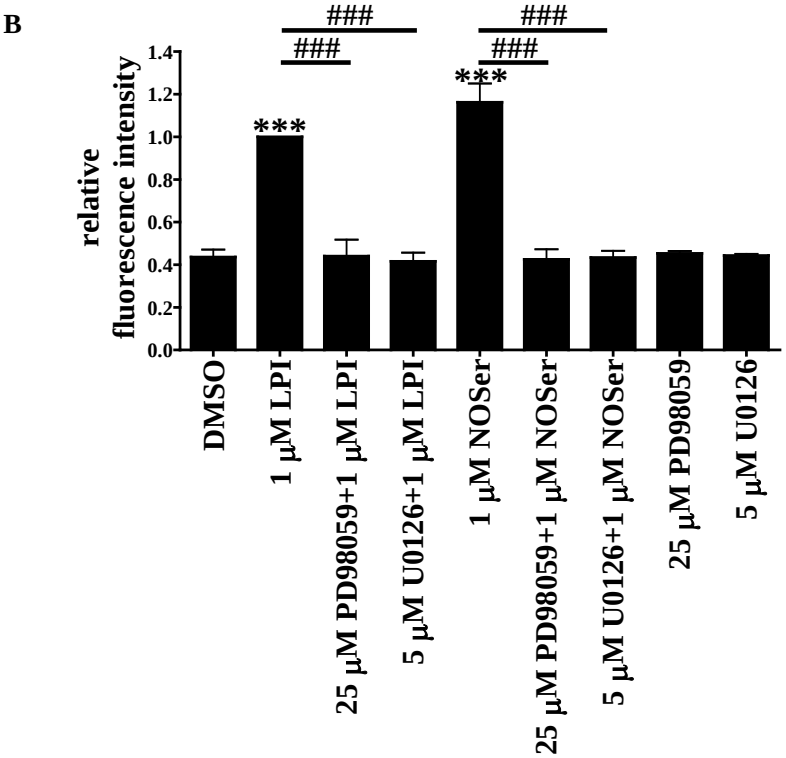
B
relative
fluorescence intensity
1.4
1.2
1.0
0.8
0.6
0.4
0.2
0.0
###
###
###
###
***
***
DMSO
1 µM LPI
25 µM PD98059+1 µM LPI
5 µM U0126+1 µM LPI
1 µM NOSer
25 µM PD98059+1 µM NOSer
5 µM U0126+1 µM NOSer
25 µM PD98059
5 µM U0126

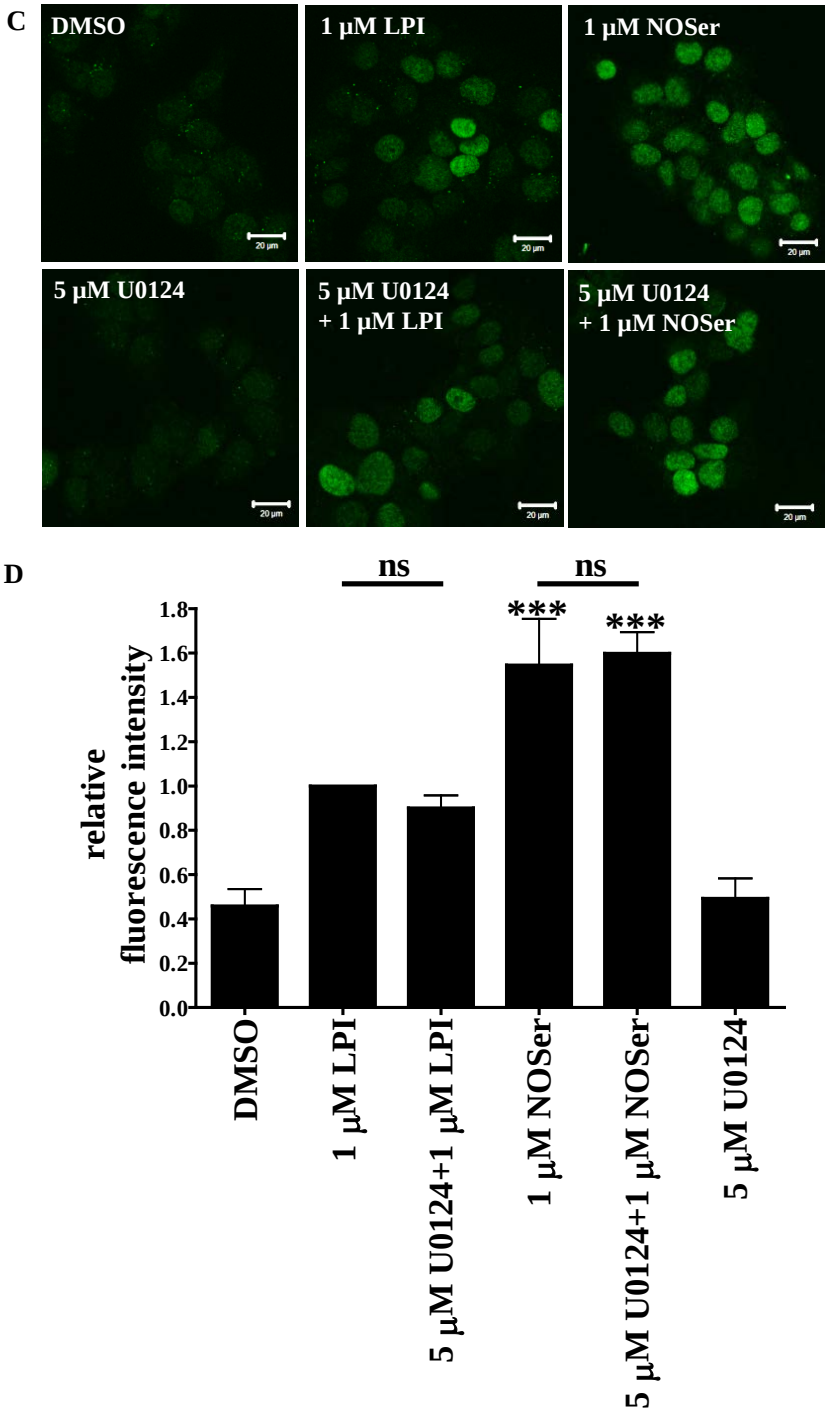

Figure 5.20: MAPK is required for GPR55-pCREB signalling in DU145 cells. *Cells were treated for 30 min with MEK1/2 inhibitors (25 µM PD98059 or 5 µM U0126) prior to co-application of inhibitor with lipid.* ***A****, representative confocal images of nuclear pCREB in DU145 cells treated with active MEK1/2 inhibitors were as follows DMSO; 25 µM PD98059; 5 µM U0126; 1 µM LPI; 25 µM PD98059 + 1 µM LPI; 5 µM U0126 + 1 µM LPI; 1 µM NOSer; 25 µM PD98059 + 1 µM NOSer; 5 µM U0126 + 1 µM NOSer. Scale bars = 20 µm; n = 3.* ***B****, histogram of pooled data, showing the mean CTNF in DU145 cells were challenged with either 1 µM LPI or 1 µM NOSer either with or without MEK1/2 inhibitors; 25 µM PD98059 or 5 µM U0126. Analysis revealed a significant decrease in lipid-induced pCREB labelling in DU145*

cells where the MEK1/2 inhibitors were present. Alternatively cells were treated for 30 min with an inactive form of MEK1/2 inhibitor (5 µM U0124) then the lipids were co-applied. ***C****, representative confocal images of DU145 cells were challenged as follows DMSO; 1 µM LPI; 1 µM NOSer; 5 µM U0124; 5 µM U0124 + 1 µM LPI; 5 µM U0124 + 1 µM NOSer. Scale bars = 20 µm; n=3.* ***D****, histogram of pooled data, highlighting the mean CTNF of pCREB in DU145 cells when treated with either LPI or NOSer either alone or in the presence of U0124. Note there was no significant difference in lipid-induced pCREB labelling in DU145 cells when the inactive MEK1/2 inhibitor was present. Fluorescent intensity is the mean CTNF normalised to 1 µM LPI. Data are means ± SEM; n = 3. * = data compared to vehicle control. One-way ANOVA followed by a Bonferroni post hoc test. ***P < 0.001; ###P < 0.001; ns = not significant.*

5.2.2.6. PI-3-kinase is not required to promote pCREB in DU145 cells.

LPI-induced AKT phosphorylation has been observed previously in DU145 cells (Piñeiro *et al.*, 2011) and a substrate of PI-3-kinase/AKT pathway is CREB (Nicholson and Anderson, 2002). Two structurally different PI-3-kinase inhibitors, LY294002 and wortmannin, were therefore used to assess the potential role PI-3-kinase exerts on GPR55-mediated CREB phosphorylation. An one-way ANOVA revealed significant differences across the LY294002 data set ($F_{(5,12)}$ = 5.236; P = 0.0088). Furthermore a Bonferroni *post hoc* test highlighted treatment with LY294002 (3 µM) did not affect basal pCREB levels. LPI (1 µM) was inhibited but not significantly whereas NOSer was not inhibited when LY294002 was present (figure 5.21A and B).

Application of wortmannin (50 nM) to the DU145 cells was then studied. An one-way ANOVA revealed significant differences across the wortmannin experimental data set ($F_{(5,12)}$ = 10.47; P = 0.0005). Moreover a Bonferroni *post hoc* test highlighted that neither lipid was significantly lowered when the inhibitor was present. These data suggest that in DU145 cells LPI-induced pCREB is likely at least in part through the activation of PI-3 kinase, whereas NOSer does not involve PI-3 kinase activation.

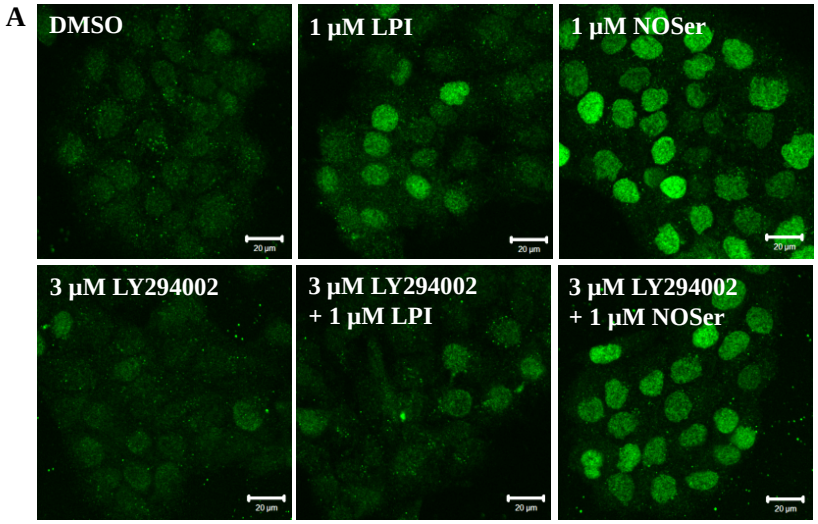
A
DMSO
1 µM LPI
1 µM NOSer
3 µM LY294002
3 µM LY294002
+ 1 µM LPI
3 µM LY294002
+ 1 µM NOSer
20 µm

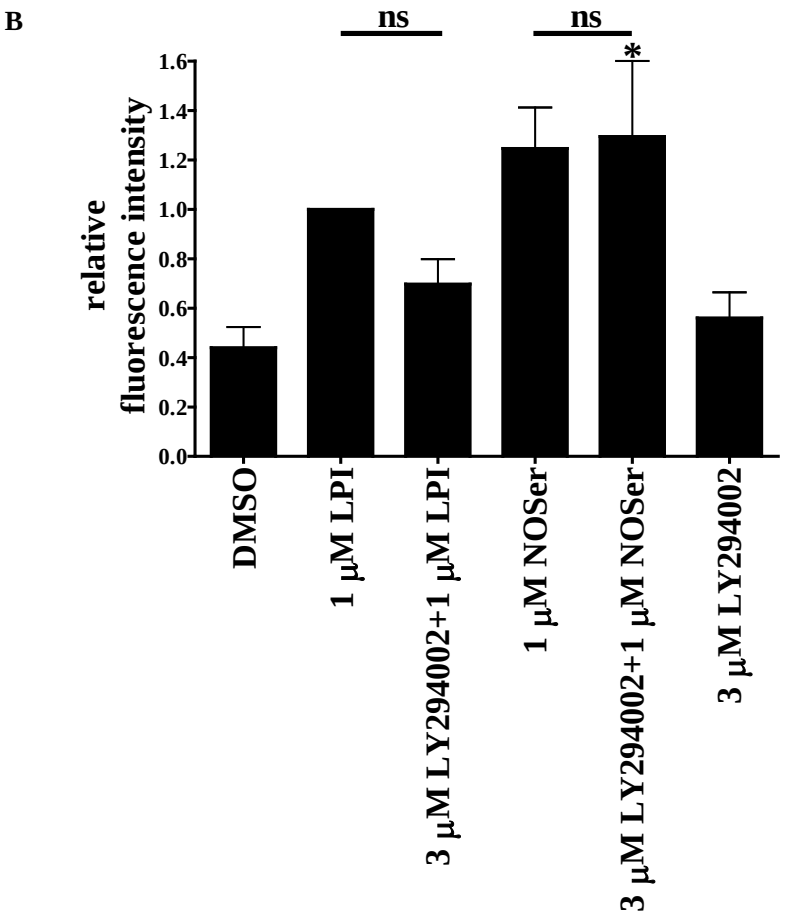
B
ns
ns
*
relative
fluorescence intensity
1.6
1.4
1.2
1.0
0.8
0.6
0.4
0.2
0.0
DMSO
1 µM LPI
3 µM LY294002+1 µM LPI
1 µM NOSer
3 µM LY294002+1 µM NOSer
3 µM LY294002

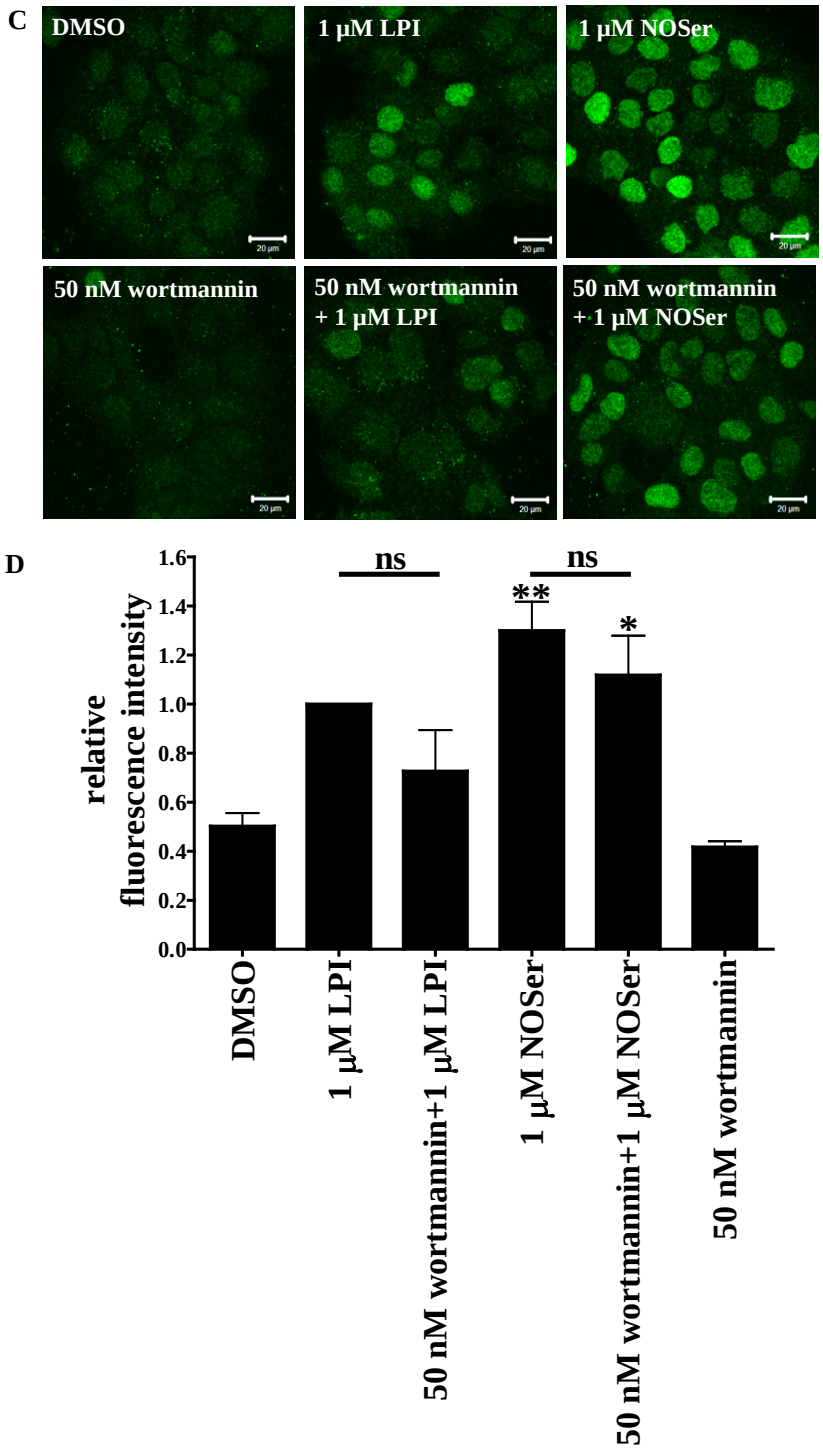

5.21: PI-3-kinase has a role in signalling to nuclear pCREB with LPI but is not required for NOSer responses in DU145s. *Cells were treated for 30 min with MEK1/2 inhibitors (3 µM LY294002 or 50 nM wortmannin) prior to co-application of inhibitor with lipid.* ***A****, representative images of nuclear pCREB in DU145 cells treated with PI-3-kinase inhibitors were as follows DMSO; 1 µM LPI; 1 µM NOSer; 3 µM LY294002; 3 µM LY294002 + 1 µM LPI; 3 µM LY294002 + 1 µM NOSer. Scale bars = 20 µm. n = 3.* ***B****, histogram of pooled data, showing the percentage mean of nuclear pCREB fluorescence when DU145 cells were challenged with either 1 µM LPI or 1 µM NOSer either with or without 3 µM LY294002.* ***C****,*

representative images of DU145 cells were challenged as DMSO; 1 µM LPI; 1 µM NOSer; 50 nM wortmannin; 50 nM wortmannin + 1 µM LPI; 50 nM wortmannin + 1 µM NOSer. Scale bars = 20 µm; n = 3. ***D****, histogram of pooled data, highlighting the fluorescence intensity of nuclear pCREB in hGPR55-HEK293 cells when treated with either 1 µM LPI or 1 µM NOSer either alone or in the presence of 50 nM wortmannin. Analysis revealed LPI-induced pCREB labelling was decreased in DU145 cells treated with the PI-3-kinase inhibitors. Fluorescent intensity is the mean CTNF normalised to 1 µM LPI. Data are means ± SEM; n = 3. * = data compared to vehicle control. One-way ANOVA followed by a Bonferroni post hoc test. *P < 0.05; **P < 0.01; ns = not significant.*

5.2.2.7. mTOR and pCREB in DU145 cells.

Next the involvement of mTOR in pCREB responses was investigated as it is downstream of PI-3 kinase. An one-way ANOVA revealed significant differences within the mTOR inhibitor experimental data ($F_{(5,12)} = 7.587$; $P = 0.0020$). Furthermore a Bonferroni *post hoc* test highlighted that treatment with the mTOR inhibitor rapamycin (50 nM) did not effect pCREB levels (figure 5.22A and B). However, this antagonist did not significantly affect responses to LPI or NOSer. These data suggest that activated mTOR is not a key player in lipid-induced nuclear pCREB in DU145 cells.

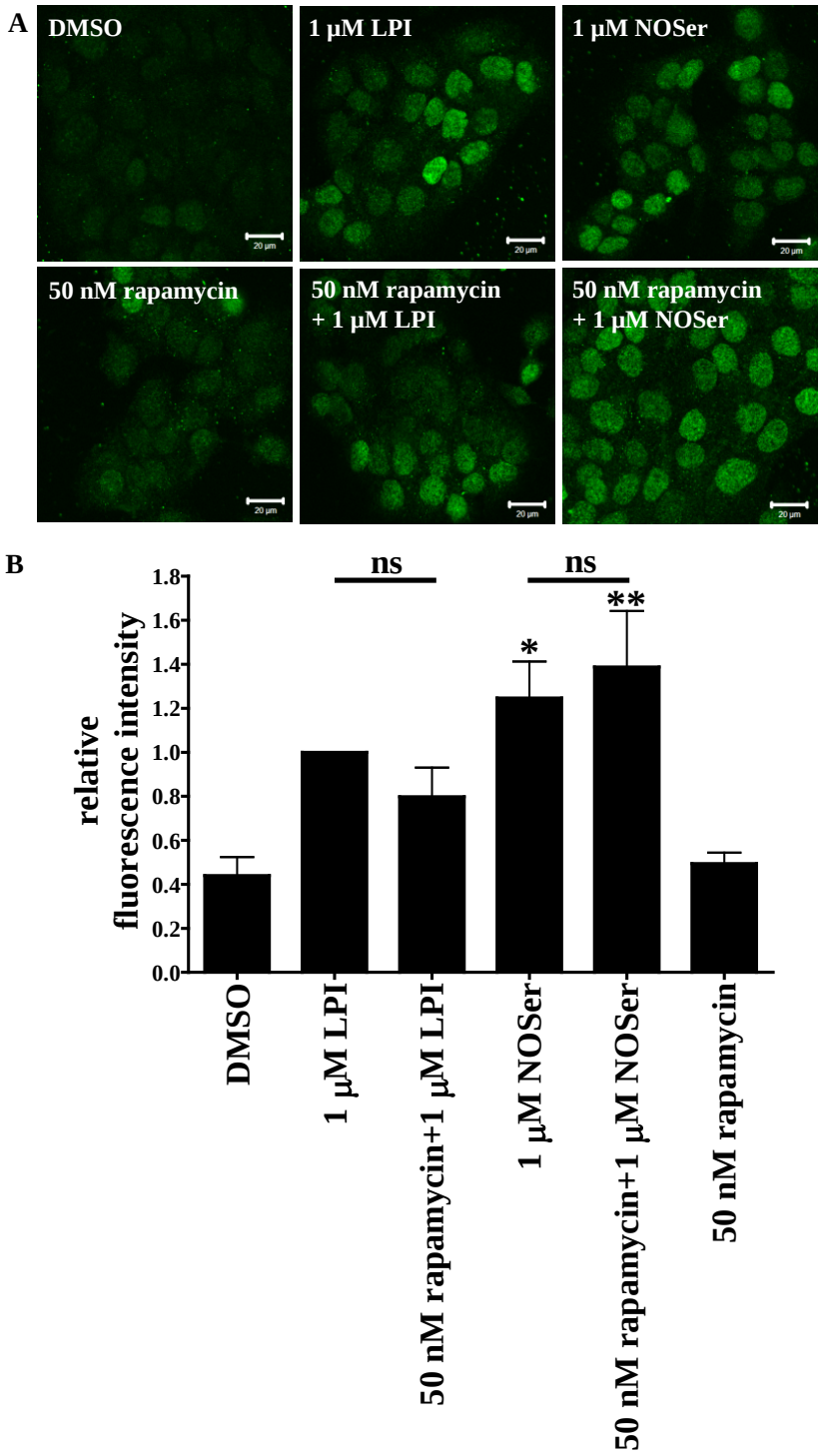

Figure 5.22: mTOR is not required for LPI and NOSer-mediated pCREB signalling in DU145 cells. ***A****, representative confocal images of nuclear pCREB labelling in DU145 cells are as follows DMSO; 1 µM LPI; 1 µM NOSer; 50 nM rapamycin; 50 nM rapamycin + 1 µM LPI; 50 nM rapamycin + 1 µM NOSer. Scale bars = 20 µm; n = 3.* ***B****, histogram of pooled data; depicting the mean CTNF of nuclear pCREB in DU145 cells treated with either 1 µM LPI, 1 µM NOSer or a lipid co-applied with 50 nM rapamycin. Note there was no significant difference between rapamycin treated DU145 cells and lipid alone challenged cells. Data are*

*means ± SEM; n = 3. * = data compared to vehicle control. One-way ANOVA followed by a Bonferroni post hoc test. *P < 0.05; **P < 0.01; ns = not significant.*

5.2.3. The actin cytoskeleton and vinculin, a focal adhesion protein.

5.2.3.1. Changes in cytoskeletal reorganisation and focal adhesion length occur in DU145 cells treated with endogenous lipids.

Both cytoskeletal reorganisation and changes in vinculin were observed in hGPR55-HEK293 cells when challenged with LPI or NOSer. Could similar effects also be seen in DU145 cells treated with the endogenous lipids and are these effects GPR55-mediated? Initially, the temporal-dependence (15, 25, 60, 120 min) of changes in the actin cytoskeleton was evaluated using LPI and NOSer No effect of the lipids was observed at 15 min. However, after 25 min treatment some stress fibres were observed. Likewise after 60 min and 120 min of lipid challenge, stress fibres were present but to a lesser extent (figure 5.23).

Next, DU145 cells were challenged with either LPI or NOSer and changes in FA length were studied at similar time points as used in the cytoskeletal reorganisation study; 15, 30, 60 or 120 min. A two-way ANOVA revealed significant differences within the time points tested ($F_{(3,24)}$ = 11.32; P < 0.0001). A Bonferroni *post hoc* test highlighted that LPI (3 µM; 15 min) and NOSer (3 µM; 15 min) treated DU145 cells were found to have FA lengths that were similar to control cells (DMSO = 2.02 ± 0.03 µm, LPI = 2.19 ± 0.04 µm, NOSer = 2.15 ± 0.07 µm, n = 3, P > 0.05, figure 5.24A and B). Note that the control cells have longer FAs than at other time points in the study. This may be due to the technique of moving the cells thereby adding extra stress to them leading to increased FA activity. Lipid treatment for 25 min promoted a clear increase in FA length compared to control cells (DMSO = 1.56 ± 0.03 µm, LPI = 2.17 ± 0.04 µm, NOSer = 2.16 ± 0.04 µm, n = 3, P < 0.01). Treatment of the cells for 60 min promoted a more robust increase in FA length (DMSO = 1.69 ± 0.03 µm, LPI = 2.48 ± 0.05 µm, NOSer = 2.42 ± 0.05 µm, n = 3, P < 0.01). Finally when the cells were treated for 120 min there was a smaller lipid-induced increase in FA length which were similar to vehicle control (DMSO = 1.60 ± 0.03 µm, LPI = 1.84 ± 0.03 µm, NOSer = 1.80 ± 0.03 µm, n = 3, P > 0.05). These data highlight the dynamic nature of changes in vinculin-containing focal adhesion length.

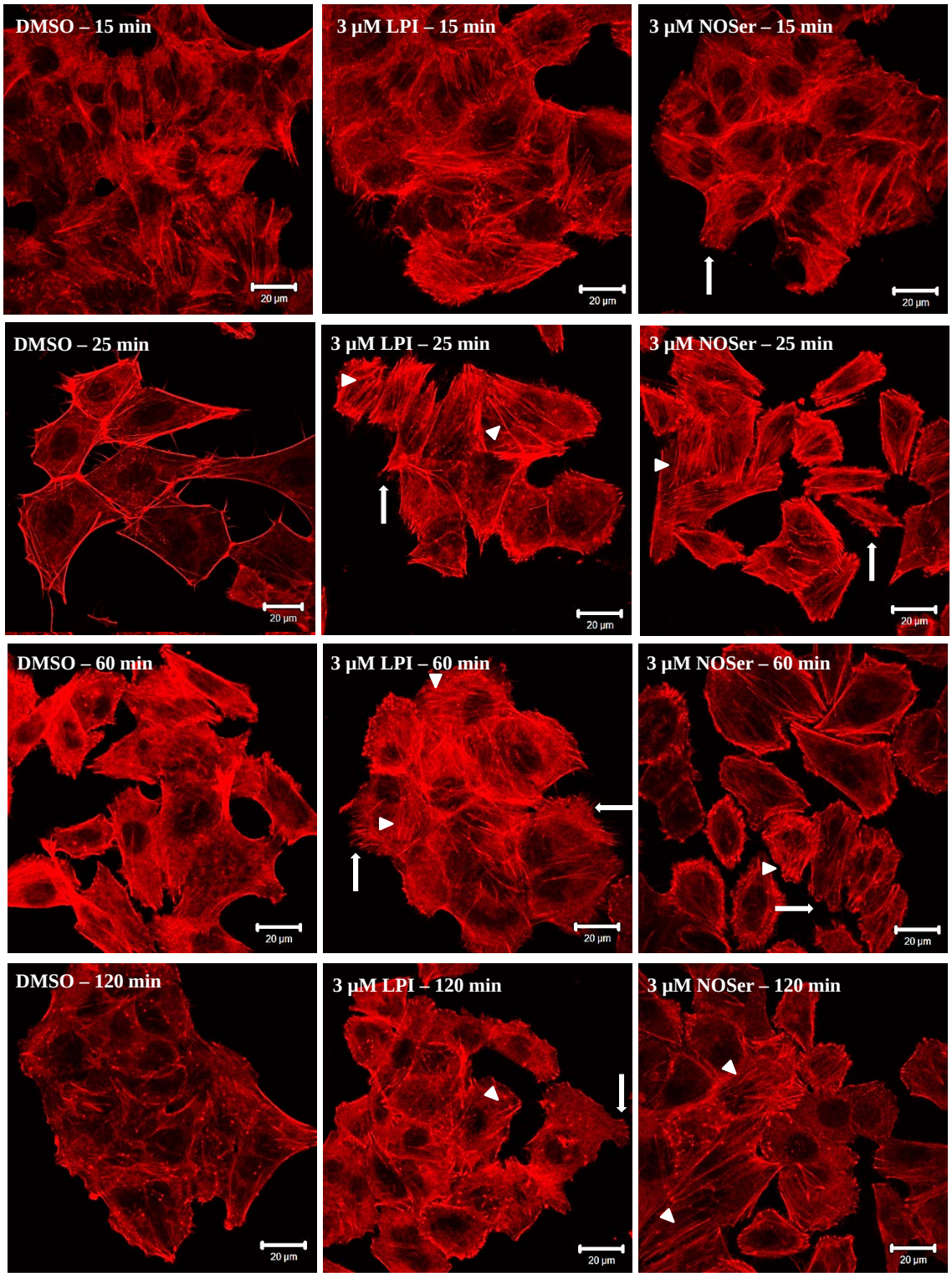

Figure 5.23: Time-course study of the effect of LPI and NOSer on the F-actin cytoskeleton in DU145 cells. *Cells were treated with ligands for times as above. Alexa-fluor® Phalloidin 546 was applied for 20 min to allow visualisation of polymerised F-actin. Scale bars = 20 µm; n = 3. Note the DU145 cell morphology and cytoskeleton are similar to control cells at 15 min. From 25 min cytoskeletal reorganisation is observed in cells treated with the endogenous lipids. Arrows = lamellipodia; arrow heads = stress fibres.*

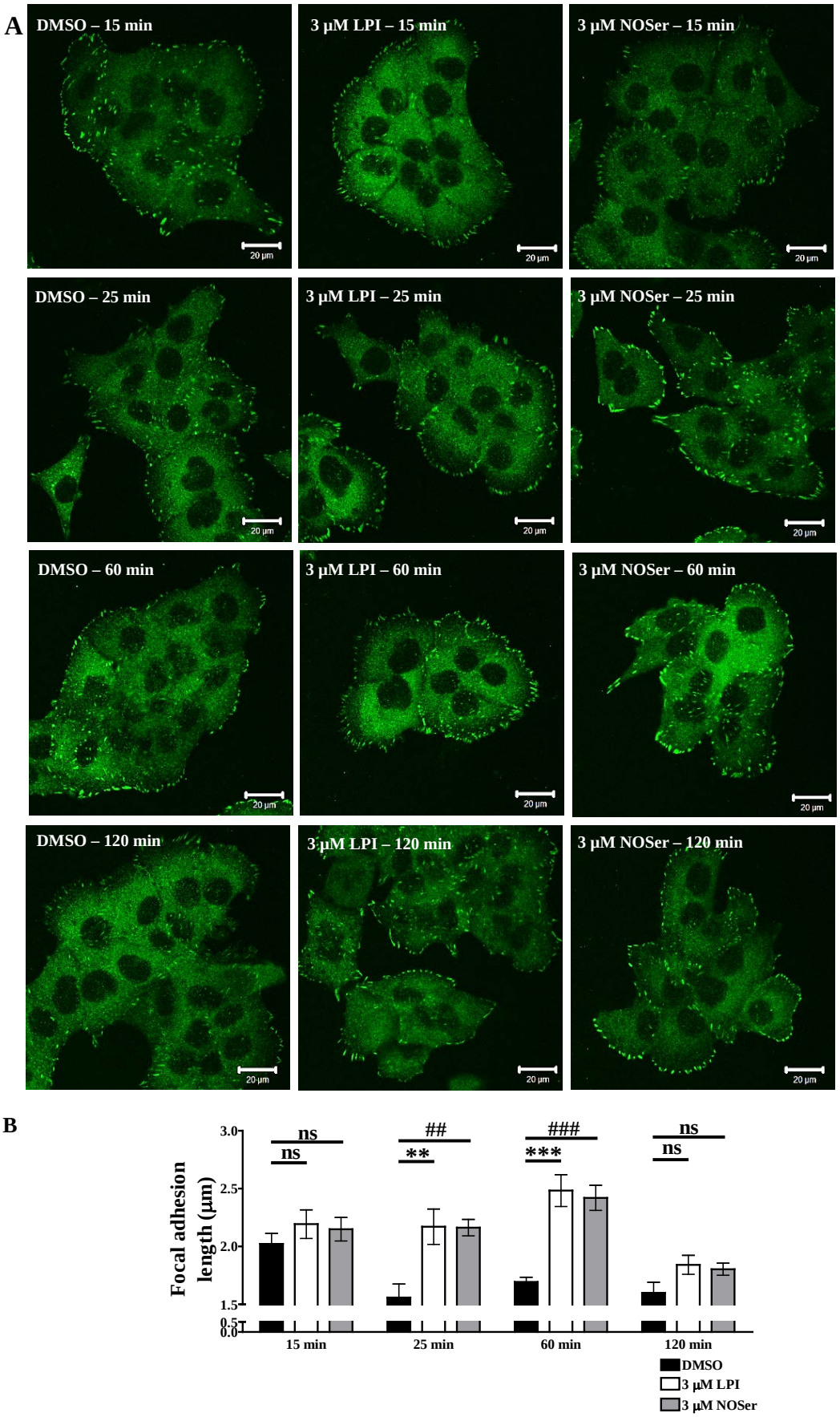

Figure 5.24: Focal adhesion length is dynamic in DU145 cells. *Cells were treated with the endogenous lipids for various times. Vinculin was visualised using an anti-vinculin antibody followed by the appropriate Alexa fluor® 488 secondary antibody.* ***A****, representative confocal*

images of vinculin labelling in DU145s at various time points. Scale bars = 20 µm; n = 3. ***B****, histogram of pooled focal adhesion (FA) length data at various time points; DMSO (black), 3 µM LPI (white) and 3 µM NOSer (grey). * = vehicle control compared to LPI; # = vehicle control compared to NOSer. Data are means ± SEM; n = 3. Two-way ANOVA with a Bonferroni post hoc test; **P < 0.01; ***P < 0.001; ##P < 0.01; ###P < 0.001; ns = not significant.*

5.2.3.2. Cytoskeletal reorganisation and increases in FA length are GPR55-mediated in DU145 cells.

In order to test for GPR55 involvement in cytoskeletal responses to NOSer and LPI, we investigated the effects of lowering GPR55 levels using siRNA techniques. Initially GPR55 siRNA was evaluated in hGPR55-HEK293 cells, which have a triple HA-tag attached to the N-terminus of the receptor, which can be used to visualise GPR55 expression using an antibody against HA. Therefore, hGPR55-HEK293 cells were transiently transfected with either GPR30-siRNA (control) or GPR55-siRNA for 72 hr prior to the commencement of experiments. A one-way ANOVA revealed significant differences within the siRNA data set ($F_{(2,9)}$ = 11.34; P = 0.0035). Moreover a subsequent Bonferroni *post hoc* test highlighted that hGPR55-HEK293 cells that were either untreated or transfected with GPR30-siRNA had bright HA staining that was predominantly localised to the plasma membrane (Untreated = 1029000 ± 50990 units, GPR30-siRNA = 1139000 ± 89490 units, n = 4, one-way ANOVA, P > 0.05). In contrast hGPR55-HEK293 cells transfected with GPR55-siRNA were observed to have HA staining that was lower than seen with untreated (39.5 ± 9.8%; n = 4, P < 0.05) or GPR30-siRNA (44.9 ± 8.9%; n = 4, P < 0.01, figure 5.25A and B).

Having validated that the GPR55-siRNA was effective, we next evaluated it in DU145 cells. DU145 cells were transiently transfected with either GPR30-siRNA (control) or GPR55-siRNA for 72 hr prior to the commencement of experiments. DU145 cells were then treated with either LPI (3 µM) or NOSer (3 µM; 60 min), fixed and permeablised then phalloidin was applied to visualise any cytoskeletal reorganisation. DMSO applied to either untreated or siRNA transiently transfected cells were observed to have a flat, spread-out morphology and with little or no stress fibres. However, LPI challenged control cells (untreated or GPR30-siRNA transfected cells) demonstrated a clear cytoskeletal reorganisation whereby stress fibres were observed in some of the untreated and GPR30-siRNA transfected cells. The untreated cells were also found to have

increased lamellipodia formation following LPI treatment. GPR55-siRNA transfected cells were found to have a similar morphology to vehicle treated (DMSO) cells. However, when NOSer or LPI was applied to untreated or GPR30-siRNA transfected cells, cytoskeletal reorganisation was seen in the form of stress fibres and increased lamellipodia formation was also observed (figure 5.25C). These data suggest that the cytoskeletal reorganisation observed in DU145s challenged with the endogenous lipids is GPR55-mediated.

Next the effect of GRP55 knockdown on FA length was assessed. A two-way ANOVA revealed significant differences within the siRNA treatments ($F_{(2,12)}$ = 14.38; P = 0.0007). DU145 cells that were untreated or transfected with GPR30-siRNA had similar FA lengths in the presence of DMSO, however treatment with NOSer or LPI induced normal FA lengthening (Untreated + DMSO = 1.68 ± 0.03 µm, 30-siRNA + DMSO = 1.72 ± 0.03 µm, untreated + LPI = 2.21 ± 0.04 µm, 30-siRNA + LPI = 2.14 ± 0.04 µm, untreated + NOSer = 2.07 ± 0.04 µm, 30-siRNA+NOSer = 2.10 ± 0.04 µm, n = 3, P > 0.05). However, GPR55-siRNA treated DU145 cells had normal FA lengths at rest, but showed markedly reduced responses to LPI and NOSer (30-siRNA + DMSO = 1.72 ± 0.03 µm, 55-siRNA + DMSO = 1.77 ± 0.03 µm, 30-siRNA + LPI = 2.14 ± 0.04 µm, 55-siRNA + LPI = 1.82 ± 0.03 µm, 30-siRNA + NOSer = 2.10 ± 0.04 µm, 55-siRNA + NOSer = 1.75 ± 0.03 µm, n = 3, two-way ANOVA with a Bonferroni *post hoc* test, P < 0.001). These data suggest that the increases in vinculin-containing FA length are GPR55-mediated.

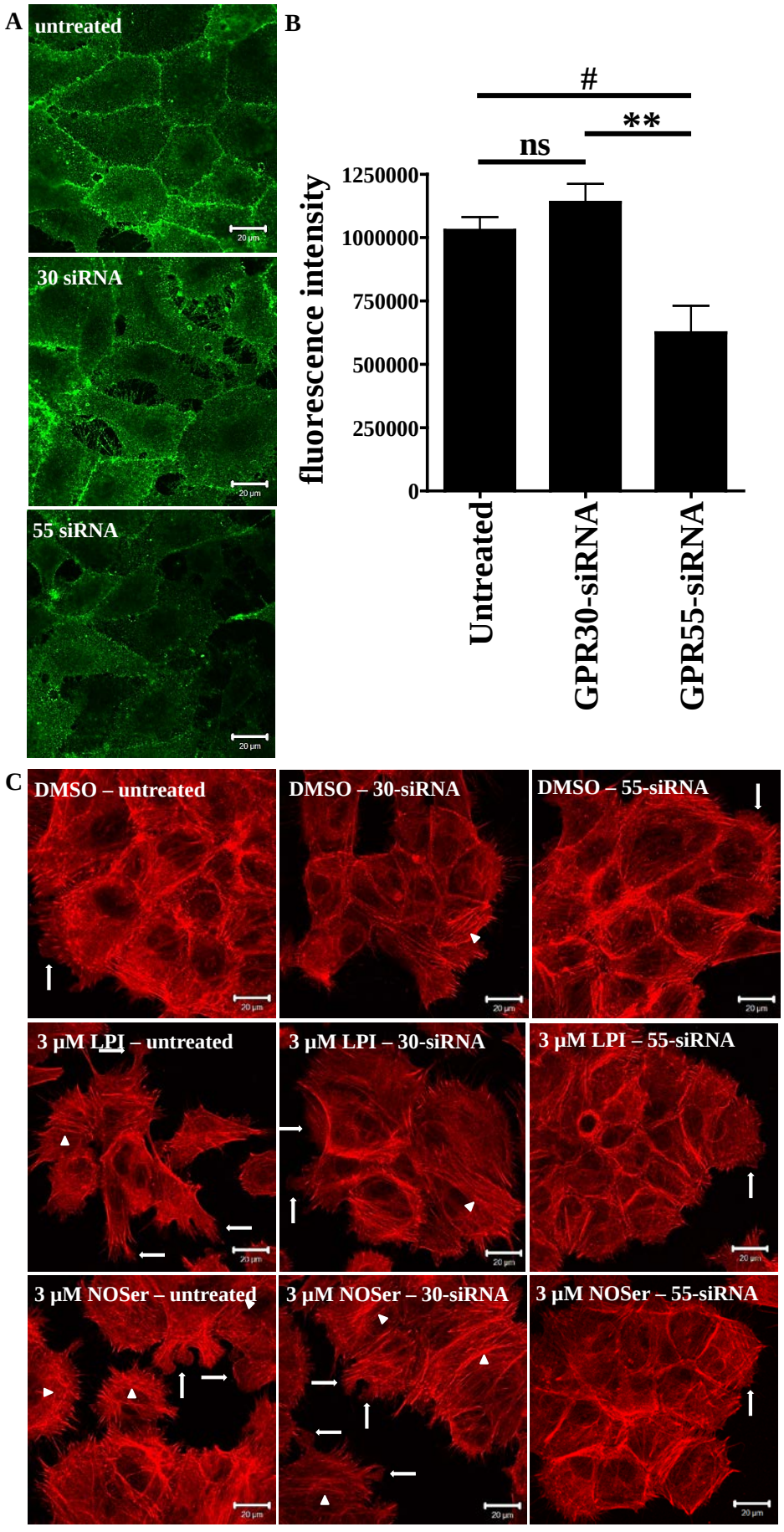

Figure 5.25: Cytoskeletal reorganisation is GPR55-mediated in DU145 cells. *To validate the siRNA; triple HA-tagged, hGPR55-HEK293 cells were transiently transfected with either*

GPR30-siRNA or GPR55-siRNA (72 hr). The cells were fixed and then labelled with HA antibody and visualised with an Alexa fluor® 488 secondary antibody. ***A****, representative confocal images of hGPR55-HEK293 cells either untreated or transiently transfected with GPR30-siRNA or GPR55-siRNA. GPR55 expression was localised to the cell membrane. Decreased HA labelling was observed in GPR55-siRNA transfected cells when compared to the untreated and GPR30-siRNA transfected DU145 cells; n = 4.* ***B****, histogram of pooled data; the HA-immunoreactivity corresponding to GPR55 expression in hGPR55-HEK293 cells. Data are means ± SEM; n = 4. One-way ANOVA with a Bonferroni post hoc test. **P < 0.01; #P < 0.05; ns = not significant.* ***C****, representative confocal images of DU145 cells stained with Alexa Fluor® 546 phalloidin to visualise the actin cytoskeleton; n = 3. Arrows = lamellipodia; arrow heads = stress fibres.*

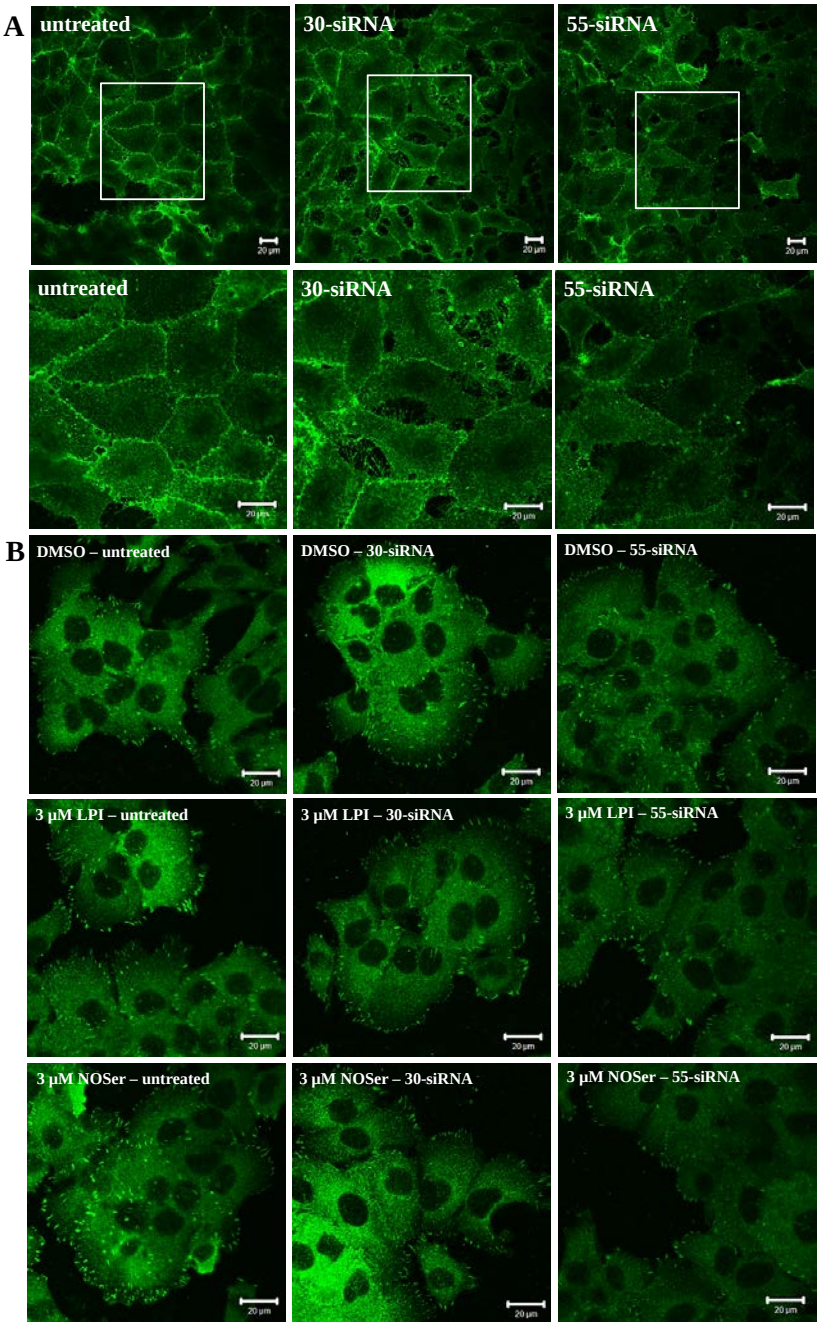

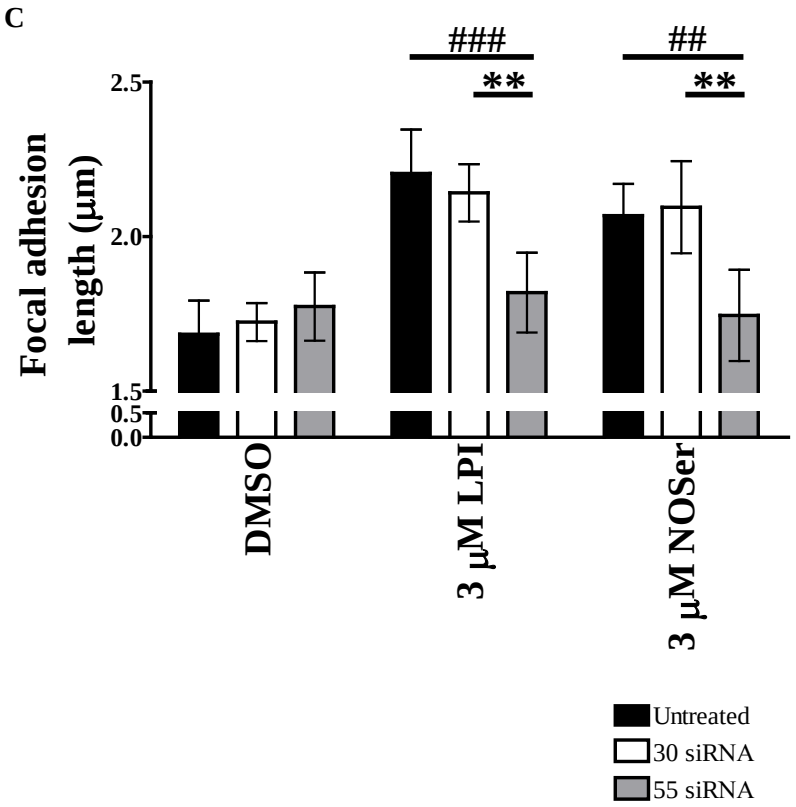

Figure 5.26: Increases in FA length are GPR55-mediated in DU145 cells. *Representative confocal images are **A**, hGPR55-HEK293 cells were either untreated or transfected with GPR30-siRNA or GPR55-siRNA; 72 hr. Note cells that were untreated or transfected with GPR30-siRNA have bright HA labelling that is localised to the plasma membrane (this corresponds to the localisation of GPR55). Cells treated with GPR55-siRNA exhibited decreased HA immunoreactivity therefore suggesting less GPR55 is present in these cells. Scale bars = 20 µm. **B**, DU145 cells were either untreated or transfected with GPR30-siRNA or GPR55-siRNA; 72 hr. The cells were then challenged with DMSO (vehicle control), LPI (3 µM) or NOSer (3 µM) for 60 min. Scale bars = 20 µm; n = 3. **C**, histogram of pooled data, showing FA length (µm) in DU145 cells both untreated with siRNA or transiently transfected with either GPR30-siRNA or GPR55-siRNA and challenged with the endogenous lipids. Note the DU145 cells treated with GPR55-siRNA were found to have shorter FAs lengths when compared to control cells. Data are means ± SEM; n = 3. # = untreated compared to GPR55-siRNA treated DU145 cells; * = GPR30-siRNA compared to GPR55-siRNA treated DU145 cells. Two-way ANOVA with a post hoc Bonferroni test; **P < 0.01; ##P < 0.01; ###P < 0.001.*

5.2.3.3. Cytoskeletal reorganisation and FA length are concentration-dependent in DU145 cells challenged with endogenous lipids.

Marked changes in cytoskeletal structure are seen in DU145 cells treated for 60 min with LPI. Next, the concentration-dependence of these effects on the actin cytoskeleton

was determined at a 60 min period. Cells challenged with DMSO (0.1%) had a typical flattened morphology (figure 5.27). Low concentrations of LPI (< 10 nM) did not have any clear effect on the cytoskeleton. Higher concentrations of LPI (30 nM - 1 µM) induced some cytoskeletal reorganisation in DU145 cells, with some stress fibres observed along with formation of lamellipodia. As the LPI concentration was further increased (3 - 10 µM) the cytoskeletal reorganisation became more pronounced. The cells were also more rounded and lamellipodia had been induced.

Having ascertained that LPI can increase GPR55-mediated vinculin-containing FA length in DU145 cells, the concentration-dependence of this effect was investigated. Low concentrations of LPI (<10 nM) did not effect FA lengths in comparison with control (DMSO) cells (figure 5.28A and B). However higher concentrations of LPI increased FA lengths, with an EC_{50} = 106.3 ± 80.9 nM (95% confidence limits).

The effects of varying concentrations of NOSer on the actin cytoskeleton in DU145 cells were studied next. Treatment with NOSer (10 nM - 10 µM) promoted the formation of stress fibres in the DU145 cells and lamellipodia were also induced (figure 5.29).

The next series of experiments were designed to assess the effect on the length of vinculin-containing FAs challenged with various NOSer concentrations. DMSO (0.1%) was applied as the vehicle control. NOSer (10 nM - 10 µM) applied to DU145 cells promoted an increase in the length of the vinculin-containing FAs (figure 5.30A and B). These increases were concentration-dependent, with an EC_{50} of 71.0 ± 63.5 nM (95% confidence limits). Further experiments are required to clarify if 10 µM NOSer always promotes shorter FAs.

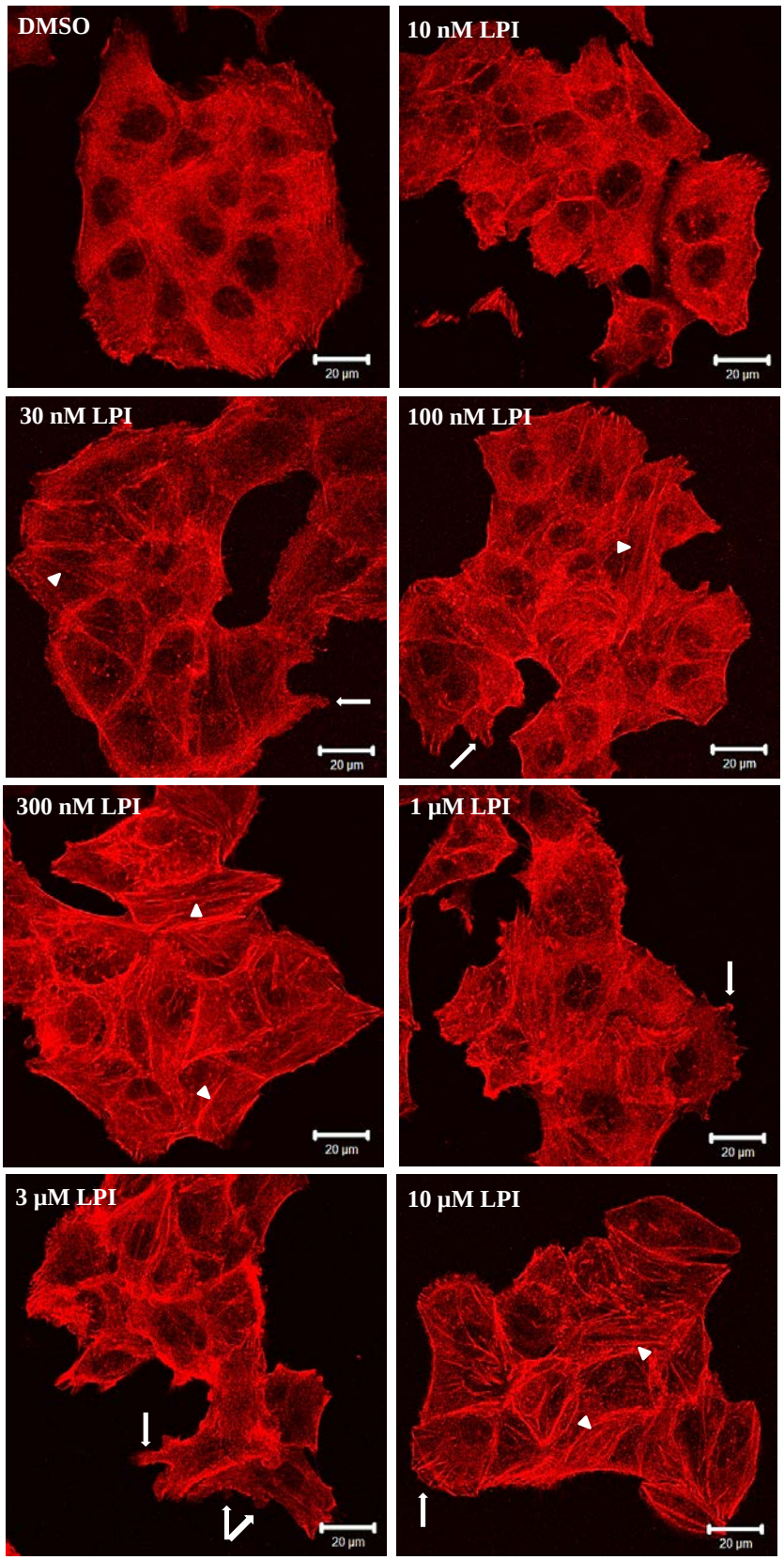

Figure 5.27: Concentration-dependence of cytoskeletal reorganisation in DU145 cells challenged with LPI. *The actin cytoskeleton was visualised with Alexa Fluor 546® phalloidin which binds to the polymerised F-actin. Representative confocal images of phalloidin labelling are illustrated for: DMSO; 10 nM LPI; 30 nM LPI; 100 nM LPI; 300 nM LPI; 1 µM LPI; 3 µM*

LPI; 10 µM LPI. Scale bars = 20 µm; n = 1; note the arrow heads = stress fibres; arrows = lamellipodia.

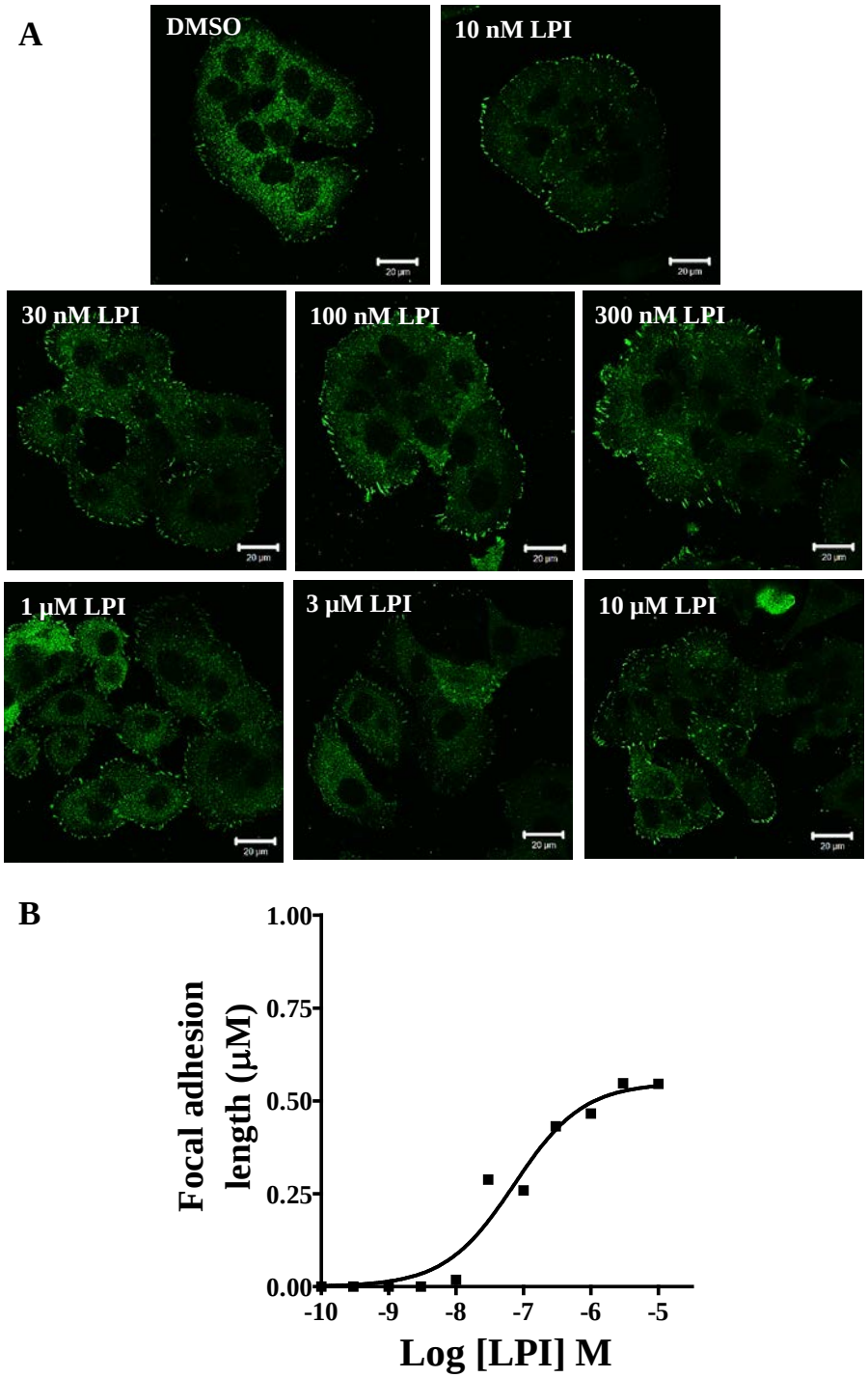

Figure 5.28: LPI-mediated increases in FA length are concentration-dependant in DU145 cells. *LPI was applied to DU145 cells for 60 min then vinculin-containing FA length was analysed.* ***A****, representative confocal images are illustrated for the following treatments: DMSO; 10 nM LPI; 30 nM LPI; 100 nM LPI; 300 nM LPI; 1 µM LPI; 3 µM LPI; 10 µM LPI. Scale bars = 20 µm; n = 1.* ***B****, concentration response curve for LPI-induced FA lengthening in DU145 cells. Mean control (DMSO) lengths have been subtracted. Data are means ± SEM; n = 1.*

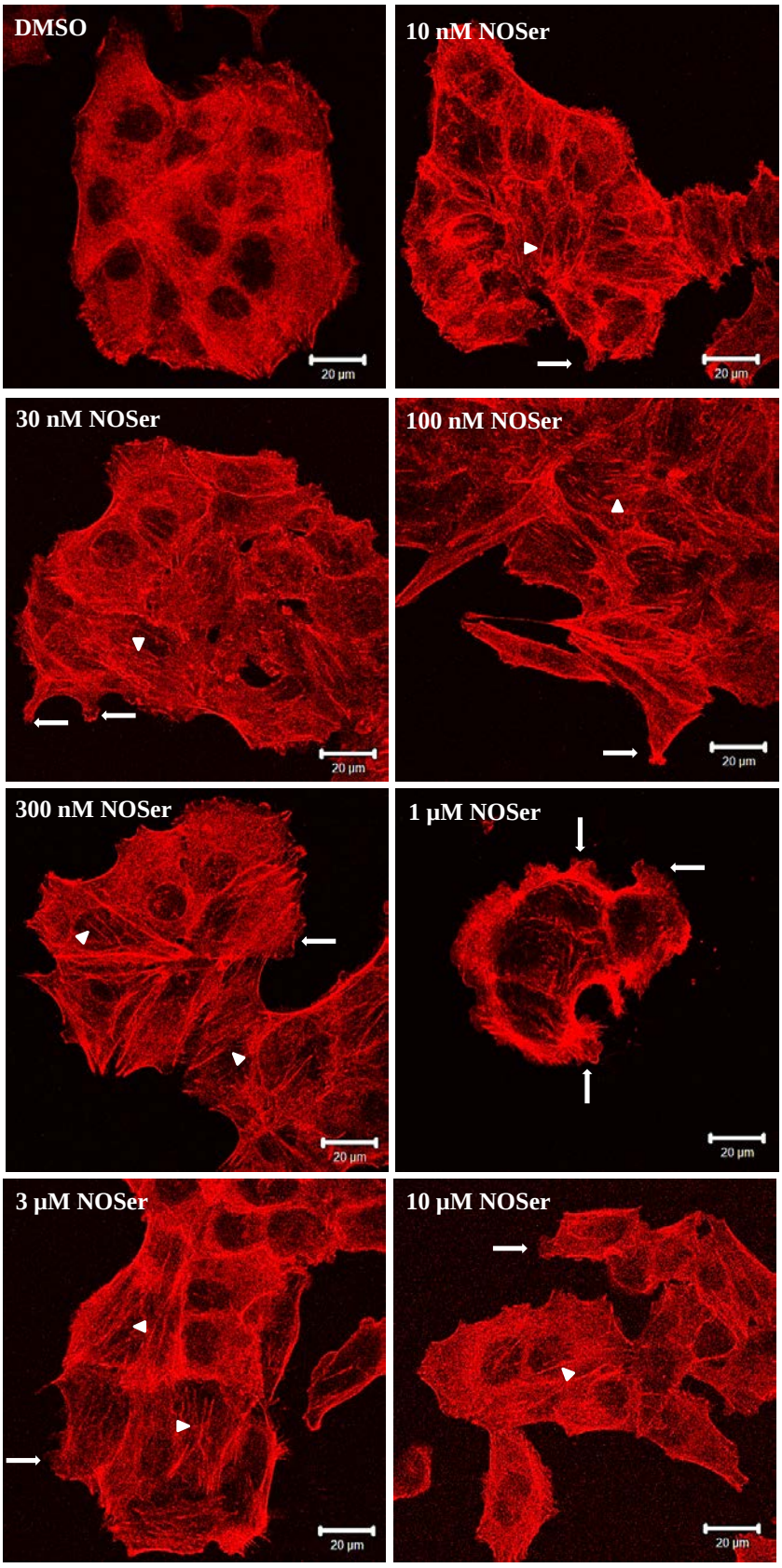

Figure 5.29: NOSer-induced actin reorganisation in DU145 cells. *Various concentrations of NOSer (60 min) were applied to DU145 cells and the actin cytoskeleton was visualised using Alexa Fluor® 546 phalloidin. Representative confocal images of DU145 cells are illustrated for cells treated with: DMSO; 10 nM NOSer; 30 nM NOSer; 100 nM NOSer; 300 nM NOSer; 1*

µM NOSer; 3 µM NOSer; 10 µM NOSer. Scale bars = 20 µm; n = 1; note the arrow heads = stress fibres; arrows = lamellipodia.

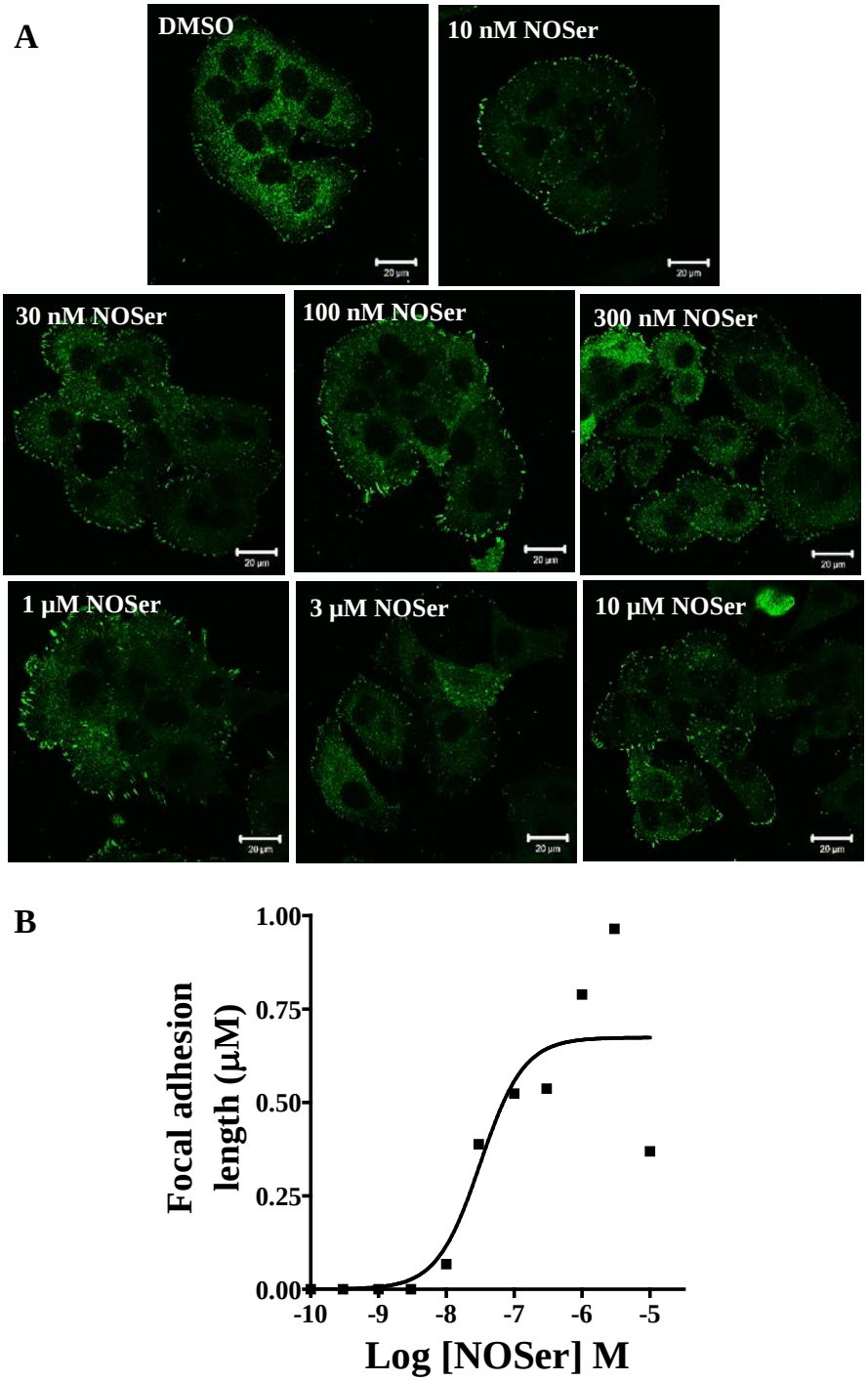

Figure 5.30: FA lengthening in DU145 cells challenged with NOSer. *Vinculin immunolabelling in DU145 cells treated with various concentrations of NOSer for 60 min.* ***A****, representative confocal images are illustrated for the following treatments: DMSO; 10 nM NOSer; 30 nM NOSer; 100 nM NOSer; 300 nM NOSer; 1 µM NOSer; 3 µM NOSer; 10 µM NOSer. Scale bars = 20 µm; n = 1.* ***B****, concentration-response curve for FA lengthening in*

DU145 cells challenged with varying concentrations of NOSer. Mean DMSO value has been removed from each NOSer concentration. Data are means ± SEM; n = 1.

5.2.3.4. Signalling through ROCK is necessary for the formation of vinculin-containing FAs and cytoskeletal reorganisation in DU145 cells.

Cytoskeletal reorganisation in DU145 cells treated with the ROCK inhibitors; Y27632 (10 μM) and H1152 (100 nM) was assessed by looking at changes in F-actin and vinculin-containing FAs. Initially effects on F-actin were determined using phalloidin labelling. Treatment of DU145 cells with Y-27632 induced some changes in the cell morphology compared to control cells with increased lamellipodia being observed (figure 5.31). Cells treated with the ROCK II inhibitor H1152, had more staining in the centre of the cell than seen with Y-27632, ROCK I and II inhibitor with a few stress fibres being observed. Pre-treatment of DU145 cells with either Y-27632 or H1152 prior to co-application with LPI led to a loss of the stress fibres, but with normal lamellipodia formation in comparison with LPI alone. Likewise, NOSer-induced stress fibre formation was also inhibited following treatment with Y-27632 or H1152, such that they were more akin with control cells. However lamellipodia formation was not effected. These data suggest that ROCK-mediated signalling is important for the formation of stress fibres but not lamellipodia in the DU145 cells treated with the endogenous lipids.

DU145 cells were treated for 60 min with either LPI or NOSer alone or each lipid in the presence of either ROCK inhibitor; Y-27632 or H1152. Cells treated with either Y-27632 (10 μM) or H1152 (100 nM) had very few vinculin-containing FAs with many cells completely lacking any vinculin-containing FAs (figure 5.32). Furthermore, no clear increase in vinculin-positive FAs was observed following treatment with LPI or NOSer in DU145 cells pre-treated for 30 min with either Y-27632 or H1152. These data suggest that LPI and NOSer-induced vinculin-containing FAs require signalling through ROCK.

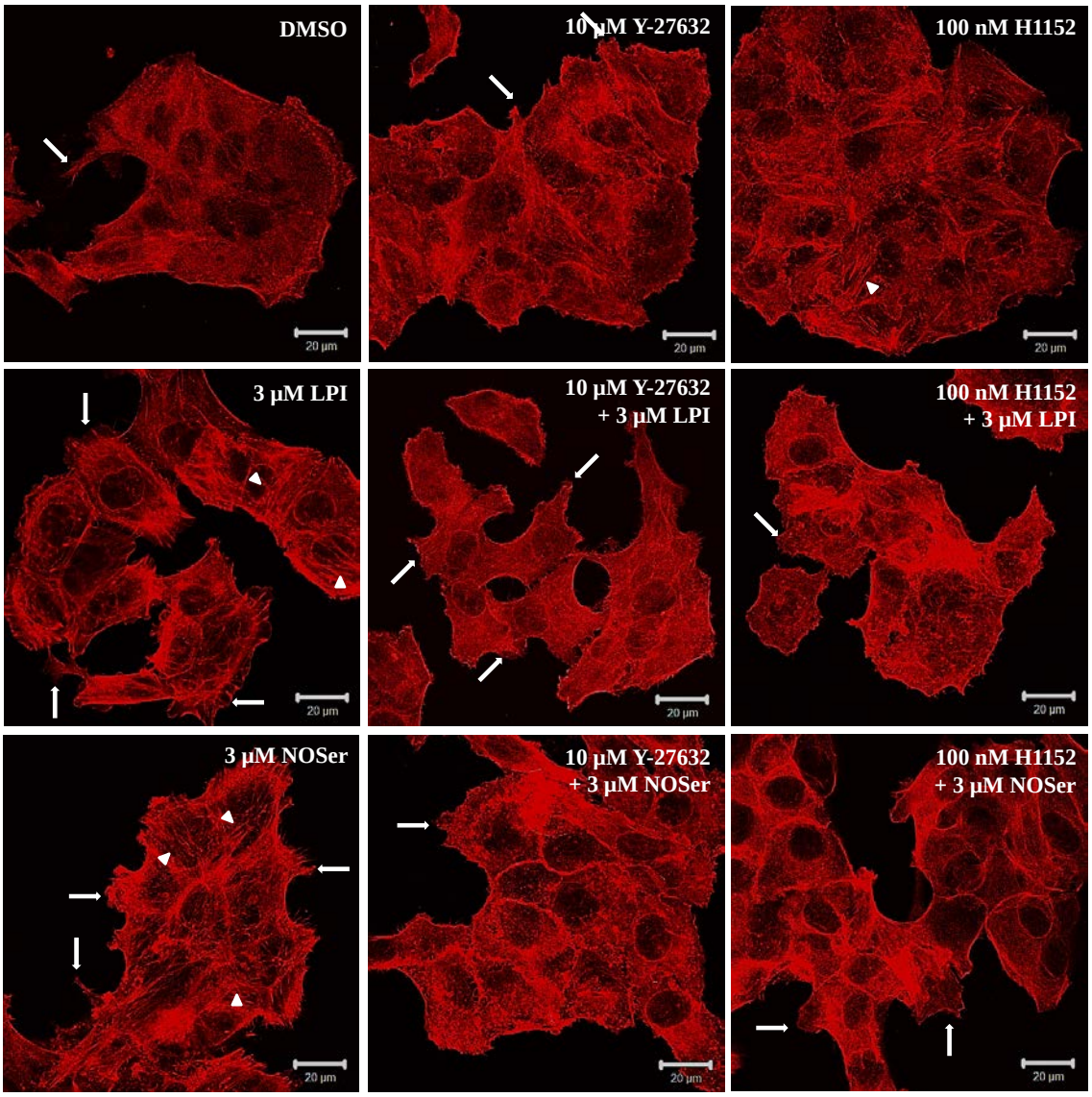

Figure 5.31: DU145 cells require ROCK signalling to promote cytoskeletal reorganisation following treatment with LPI and NOSer. *The actin cytoskeleton was visualised using Alexa Fluor® 546 phalloidin. Representative confocal images are illustrated for DU145 cells with the following treatments: DMSO; 10 µM Y-27632; 100 nM H1152; 3 µM LPI; 10 µM Y-27632 + 3 µM LPI; 100 nM H1152 + 3 µM LPI; 3 µM NOSer; 10 µM Y-27632 + 3 µM NOSer; 100 nM H1152 + 3 µM NOSer. Scale bars = 20 µm. n = 2. Note a loss of the lipid-induced stress fibres with cells pre-treated with either of the ROCK inhibitors. Arrows = lamellipodia; arrow heads = stress fibres.*

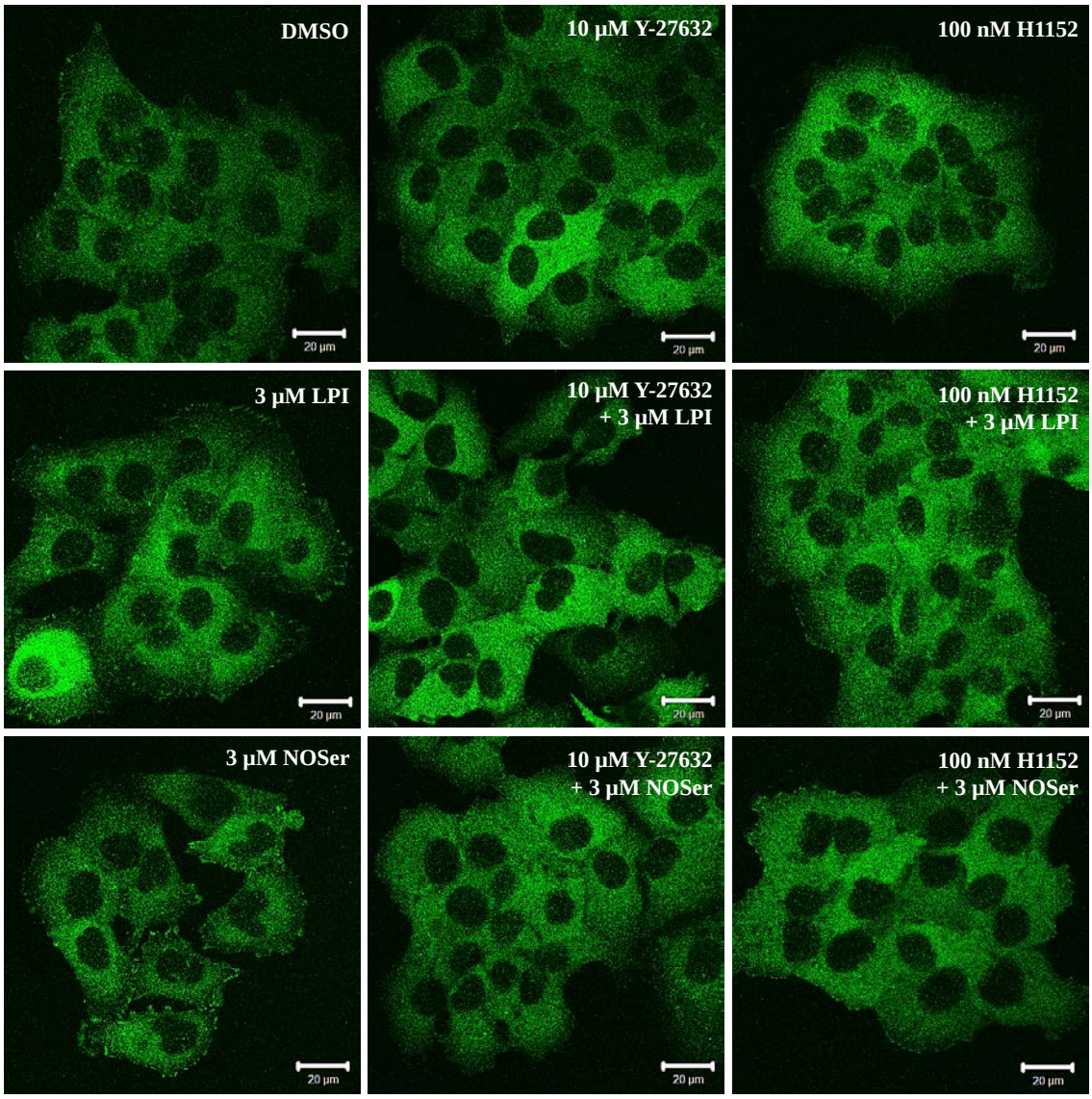

Figure 5.32: Vinculin-containing FAs require signalling through ROCK in DU145 cells treated with endogenous lipids. *DU145 cells were pre-treated with either of the ROCK inhibitors; Y-27632 (10 µM) or H1152 (100 nM) for 30 min prior to co-application with either LPI (3 µM) or NOSer (3 µM). Representative confocal images are illustrated for DU145 cells treated as follows DMSO; 10 µM Y-27632; 100 nM H1152; 3 µM LPI; 10 µM Y-27632 + 3 µM LPI; 100 nM H1152 + 3 µM LPI; 3 µM NOSer; 10 µM Y-27632 + 3 µM NOSer; 100 nM H1152 + 3 µM NOSer. Scale bars = 20 µm. n = 2. Note the ROCK inhibitors decreased the number of vinculin-containing FAs and prevented their up-regulation with either of the endogenous lipids.*

5.3. DISCUSSION

5.3.1. GPR55, lipid ligands and Ca^{2+} signalling in DU145 cells.

This study was designed to consider GPR55-mediated signalling pathways required for Ca^{2+} mobilisation, nuclear pCREB, F-actin cytoskeletal reorganisation and changes in vinculin-containing FAs in the prostate cancer cell line, DU145. Both LPI and NOSer were found to induce GRP55-mediated Ca^{2+} mobilisation in the DU145 cells. LPI has previously been studied in DU145 cells whereby Ca^{2+} mobilisation, pERK1/2, pAKT and proliferation of the cells was observed (Piñeiro *et al.*, 2011). Studies with ovarian cancer have shown that micromolar concentrations of LPI are present (Sutphen *et al.*, 2004) and in this study similar low micromolar concentrations of LPI have led to the Ca^{2+} mobilisation, pCREB, F-actin cytoskeletal reorganisation and increases in FA length in the metastatic DU145 cells. To date there are no reports of NOSer mediated signalling in relation to prostate cancer.

Both LPI and NOSer were found to promote GPR55-mediated Ca^{2+} mobilisation in the DU145 cells. LPI-induced effects were sensitive to CBD, a putative GPR55 antagonist. However the LPI-induced Ca^{2+} mobilisation was only partially decreased in DU145 cells where inhibitors had been applied. There is evidence that LPI can act on $TRPV_2$ channels in a metastatic prostate cancer cell line; PC3 (Monet *et al.*, 2009) and $TRPV_2$ is also expressed in DU145 cells (Monet *et al.*, 2010). Therefore some of the Ca^{2+} mobilisation that is observed with LPI may be due to non-GPR55 specific effects such as LPI acting on TRP channels.

In this study $G_{\alpha q}$ activation was required for the LPI-induced mobilisation of Ca^{2+} in the DU145 cells. Previous research reported that GPR55-mediated $G_{\alpha q}$ activation was necessary for Ca^{2+} mobilisation in both hGPR55-HEK293 cells (Lauckner *et al.*, 2008) and phaeochromocytoma PC12 cells (Obara *et al.*, 2011). $G_{\alpha q}$ can activate Rho (Chikumi *et al.*, 2002) and Rho-ROCK activation is required for LPI-induced Ca^{2+} mobilisation in hGPR55-HEK293 cells (Henstridge *et al.*, 2009). However in DU145 cells challenged with either LPI or NOSer, ROCK activation was not required for Ca^{2+} mobilisation. These results are in agreement with a previous study whereby LPI-induced Ca^{2+} mobilisation in DU145 cells was ROCK-independent (Piñeiro *et al.*, 2011). $G_{\alpha q}$ directly activating PLCβ (Hubbard and Hepler, 2006) promotes the hydrolysis of PIP_2 into IP_3 and DAG, the former promoting Ca^{2+} mobilisation from the ER (Clapham, 2007). In the DU145 cells PLC was required for the mobilisation of Ca^{2+}

adding credence that LPI challenge to DU145 cells initiates signalling through the $G_{\alpha q}$-PLC signalling axis; figure 5.33). At present it remains unknown if NOSer activation of GPR55 recruits $G_{\alpha q}$. Further experiments are required to determine if LPI and NOSer activate $G_{\alpha 13}$ to promote Ca^{2+} mobilisation in DU145 cells. However NOSer does require the activation of PLC to promote Ca^{2+} mobilisation in DU145 cells.

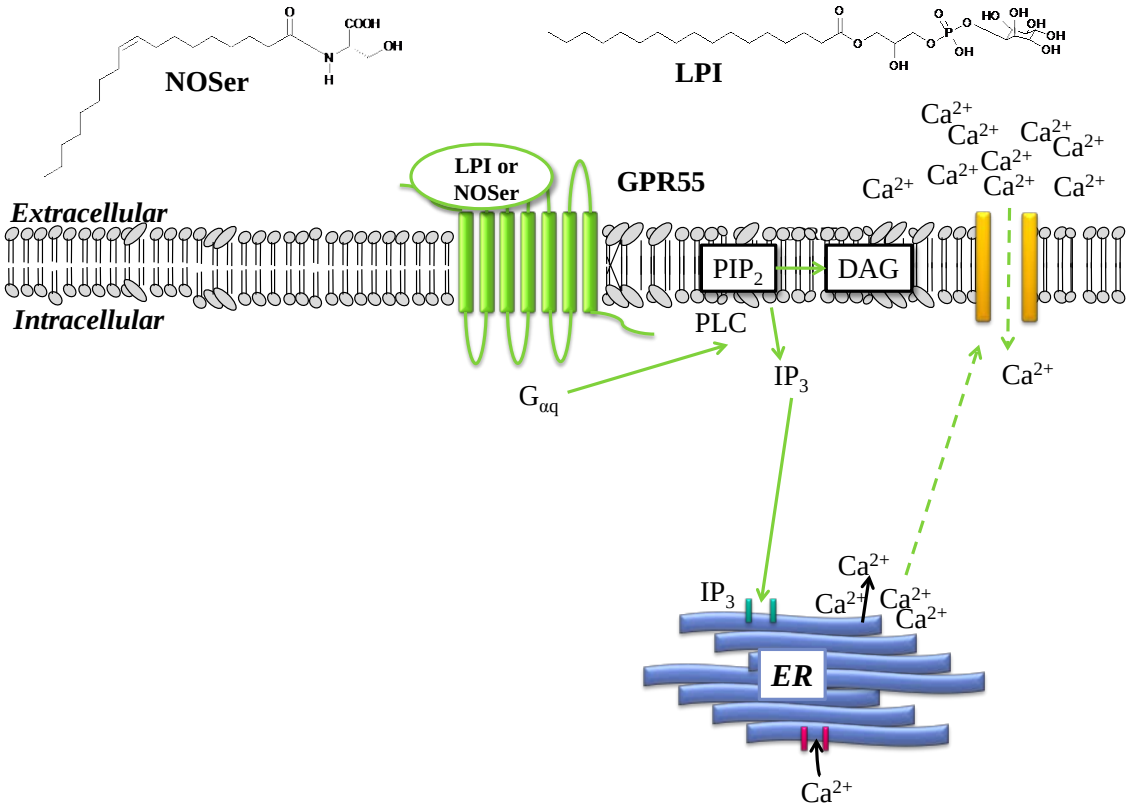

Figure 5.33: Proposed GPR55-mediated Ca^{2+} cascade in LPI challenged DU145 cells. *Agonist binding to GPR55 leads to the activation of $G_{\alpha q}$ the heterotrimeric G-protein which can then activate PLC. PLC activation leads to the hydrolysis of PIP_2 into IP_3 and DAG. IP_3 then translocates and acts on IP_3 receptors localised to the membrane of the ER. The ER being the main Ca^{2+} store found in cells. Subsequently Ca^{2+} is release which may then act on Ca^{2+} channels in the plasma membrane to allow them to open and allow the influx of Ca^{2+} from the extracellular media. GPR55, G-protein coupled receptor 55; LPI, L-α-lysophosphatidylinositol; PLC, Phospholipase C; PIP_2, phosphatidylinositol 4, 5-bisphosphate; DAG, diacylglycerol; IP_3, inositol 1, 4, 5-triphosphate; ER, endoplasmic reticulum.*

5.3.2. GPR55 and pCREB signalling in DU145 cells.

In this study pCREB labelling was increased in DU145 cells treated with either LPI or NOSer. Two heterotrimeric G-proteins; $G_{\alpha 13}$ and $G_{\alpha q}$, were tested for involvement in lipid-induced pCREB responses in these cell. Further studies are required to understand

the role of $G_{\alpha 13}$ in nuclear pCREB signalling in DU145 cells. However there was a trend to inhibit the lipid-induced responses suggesting that it is likely to be required (figure 5.34 and 5.35). Interestingly both $G_{\alpha 13}$ (Kozasa *et al.*, 2011) and $G_{\alpha q}$ (Chikumi *et al.*, 2002) can regulate Rho. However there may be differences in the activation of Rho by these G-proteins. In one study investigating G-protein regulation of RhoA with thrombin, a 2-fold higher concentration of thrombin was required for $G_{\alpha q}$-mediated activation of RhoA compared to concentrations required for $G_{\alpha 13}$-mediated activation (Vogt *et al.*, 2003). Another study described the activation of RhoA with $G_{\alpha q}$ and found the mechanism differed from $G_{\alpha 13}$-mediated regulation depending on which RhoGEF was present (Chikumi *et al*., 2002). Therefore it could be possible for GPR55-mediated $G_{\alpha 13}$ or $G_{\alpha q}$ to regulate RhoA. However further experiments would be required to investigate whether there are similar differences in G-protein signalling via GPR55 in DU145 cells. This would also help to understand any GPR55-induced ligand bias that may be occurring at the level of these G-proteins. Furthermore the Rho-ROCK signalling axis whilst not required for Ca^{2+} mobilisation was required to promote pCREB. In this study both LPI and NOSer required ROCK activation to promote pCREB in DU145 cells.

5.3.2.1. GPR55 and MAPK signalling in DU145 cells

In the present investigation both LPI and NOSer required MAPK signalling to promote pCREB in the DU145 cells. Indeed, the pCREB response promoted by either of the lipids was found to be abolished in the presence of the MEK1/2 inhibitors. These results suggest that MAPK signalling may be the most important pathway to promote pCREB in DU145 cells challenged with either LPI or NOSer. Several studies report GPR55 phosphorylation of ERK1/2 in hGRP55-HEK293 cells (Oka *et al.*, 2007, 2009; Henstridge *et al.*, 2010), osteoclasts (Whyte *et al.*, 2009), in several different cancer cells (Andradas *et al.*, 2011) including prostate cancer cells (Piñeiro *et al.*, 2011). The transcription factor CREB is located downstream of ERK1/2 and previously Rho-ROCK signalling was reported for GPR55-mediated pERK1/2 in DU145 cells treated with LPI (Piñeiro *et al.*, 2011). Furthermore Rho and ROCK may be important mediators of MAPK signalling in DU145 cells. Rho has previously been reported to activate MEKK1; which has p115RhoGAP bound to it in intact murine embryonic fibroblast (NIH 3T3), Madin-Darby Canine Kidney (MDCK) and HEK 293 cells (Christerson *et al.*, 2002). MEKK1 is the protein located upstream of MEK1/2, in HEK293 cells (Gallagher *et al.*, 2004). Also ROCK inhibition has been shown to

decrease pERK1/2 in a glioblastoma cells; LN-18 when treated with fibronectin or platelet derived growth factor (Zohrabian *et al.*, 2009). Therefore it is possible that LPI and NOSer promote pCREB in DU145 cells via a direct route from Rho and ROCK to MAPK signalling.

5.3.2.2. Differences between LPI and NOSer.

LPI was found to be more efficacious and potent than NOSer in the Ca^{2+} mobilisation assay. Extracellular Ca^{2+} was likely to be required for LPI-induced pCREB. In addition, PLC, CaMKII, PKC and possibly PI-3 kinase were all found to be required for LPI-induced pCREB in DU145 cells (figure 5.38). In contrast NOSer did not require PLC, CAMKII and PI-3 kinase to promote the formation of pCREB in the DU145 cells. However PKC may be likely for NOSer-induced pCREB in DU145 cells (figure 5.39). PKCε has been reported as a RhoA effector in a yeast 2-hybrid assay (Wheeler and Ridley, 2004). Furthermore a study using the phospholipid LPA applied to NIH 3T3 murine embryonic fibroblast cells found that Rho activation was required to activate both PKCα and PKCε to promote the activation of serum response element. Interestingly PKCε is a member of the Ca^{2+} independent PKC isoforms (Soh *et al.*, 1999). Therefore it is possible that NOSer activates $G_{\alpha 13}$ or $G_{\alpha q}$ to activate RhoA leading to the subsequent phosphorylation of PKC in the DU145 cells which could be independent of Ca^{2+}. This study however did not differentiate between PKC isoforms.

Only LPI is likely to involve activation of PI-3 kinase to promote pCREB in DU145 cells. The CREB phosphorylation may occur through the activation of AKT; recent research suggests that LPI induced phosphorylation of AKT can be GPR55 mediated in DU145 cells (Piñeiro *et al.*, 2011).

These data suggest NOSer may exert ligand bias with Ca^{2+} mobilisation being less favoured than pCREB in DU145 cells. Both lipids promote pCREB in hGPR55-HEK293 and DU145 cells however, NOSer was found to be more efficacious but less potent when compared to LPI with this pathway in the DU145 cells.

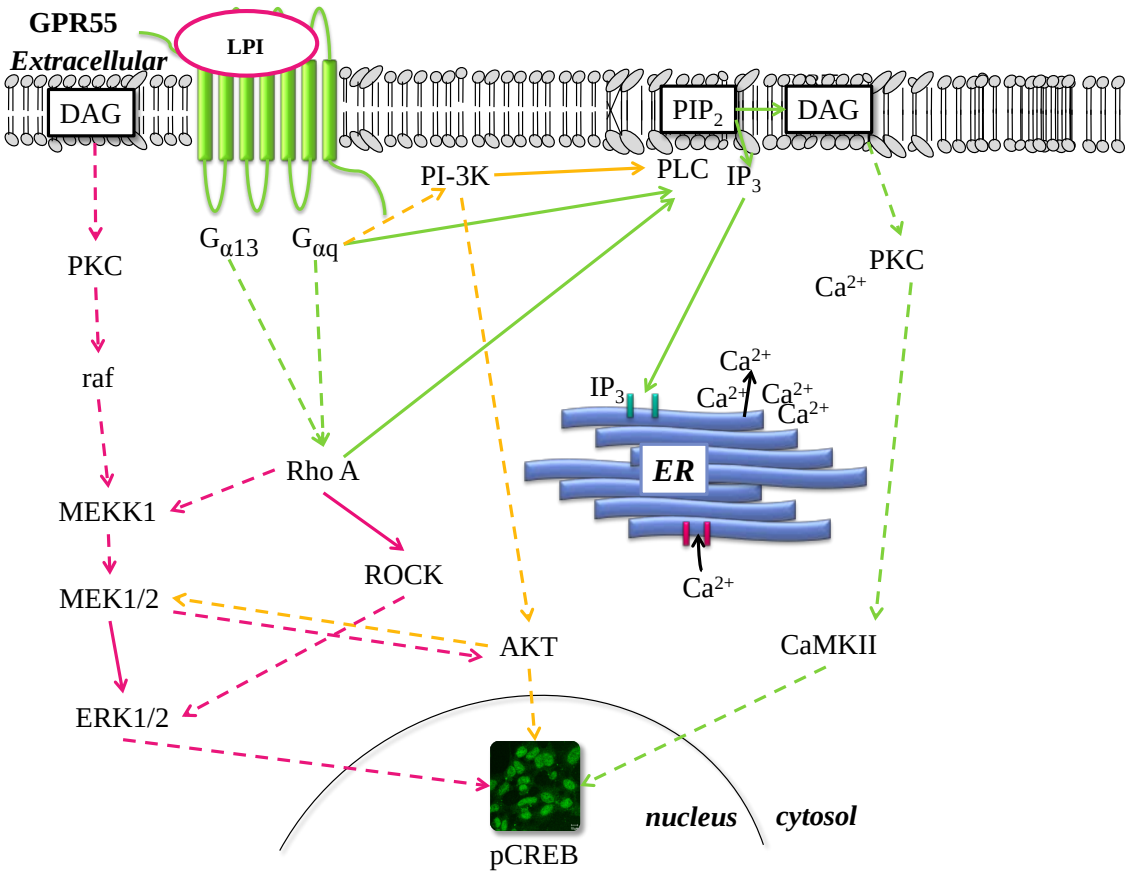

Figure 5.34: Potential signalling pathways required for LPI-induced pCREB in DU145 cells. *Multiple signalling pathways can promote pCREB in hGPR55-HEK293 cells. Potential cross-talk can occur between Ca^{2+} mobilisation, MAPK and PI-3 kinase signalling pathways. LPI, L-α-lysophosphatidylinositol; RhoA, Ras homolog gene, family member A; ROCK, Rho associated protein kinase; PLC, Phospholipase C; PIP_2, phosphatidylinositol 4, 5-bisphosphate; DAG, diacylglycerol; IP_3, inositol 1, 4, 5-triphosphate; PKC, protein kinase C; CaMKII, Ca^{2+}/calmodulin dependent protein kinase II; PI-3K, phosphatidylinositide 3-kinase; mTOR = mammalian Target of Rapamycin; raf = proto-oncogene c-RAF; MEKK1 = mitogen activated protein kinase kinase 1; MEK1 = mitogen activated protein kinase 1; ERK1/2 = extracellular signal-regulated protein kinases 1 and 2; pCREB, phosphorylated cyclic AMP response element binding protein. Green arrows = Ca^{2+} signalling pathway; purple arrows = PI-3 kinase signalling pathway; pink arrows = MAPK signalling pathway. Solid arrows = signalling effectors; dashed arrows = suggested effectors.*

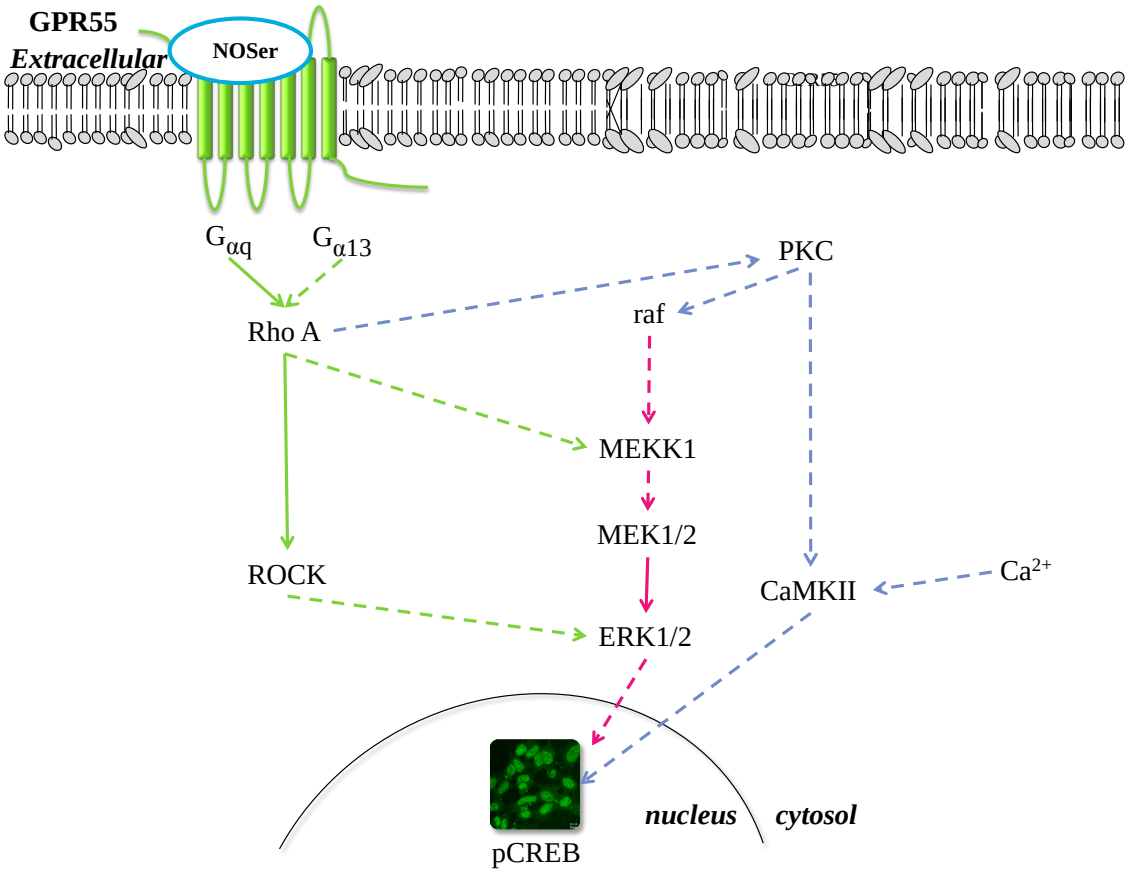

Figure 5.35: Potential signalling pathways required for NOSer-induced pCREB in DU145 cells. *Multiple signalling pathways can promote pCREB in hGPR55-HEK293 cells. Potential cross-talk can occur between ROCK, MAPK and PKC signalling pathways. NOSer, N-oleoyl-L-serine; RhoA, Ras homolog gene, family member A; ROCK, Rho associated protein kinase; PKC, protein kinase C; CaMKII, Ca^{2+}/calmodulin dependent protein kinase II; raf = proto-oncogene c-RAF; MEKK1 = mitogen activated protein kinase kinase 1; MEK1 = mitogen activated protein kinase 1; ERK1/2 = extracellular signal-regulated protein kinases 1 and 2; pCREB, phosphorylated cyclic AMP response element binding protein. Green arrows = ROCK signalling pathway; blue arrows = PKC signalling pathway; pink arrows = MAPK signalling pathway. Solid arrows = signalling effectors; dashed arrows = suggested effectors.*

5.3.3. Cytoskeletal reorganisation and FAs in DU145 cells.

Both LPI and NOSer promoted F-actin cytoskeletal reorganisation and increases in vinculin-containing FA length in the DU145 cells. This is the first study to observe GPR55-mediated effects on FAs. These have a dynamic nature, with co-ordinated assembly and disassembly, to allow the movement of cells (Carisey *et al.*, 2013). In DU145 cells as was also observed in hGPR55-HEK293 cells, the length of the FAs increased with time until 120 min, after which they became shorter suggesting that disassembly may be occurring. The cells in this study were fixed at a time point (60

min) and the treatment was such that the cells would not have a directional polarity as the ligands were applied to a petri dish and the cells were bathed with a uniform concentration of lipid.

Both LPI and NOSer promoted an increase in the stress fibres that was observed to be concentration-dependent. Vinculin-containing FAs were also found to be LPI or NOSer concentration-dependent. Changes in the actin cytoskeleton occur depending on which of the small Rho GTPase that has been activated. Each small Rho GTPase has a specific role in actin cytoskeletal reorganisation. Rho is also reported to be required for the formation of focal adhesion complexes (Ridley and Hall, 1992; Nobes and Hall, 1995). Rac plays a role in the formation of lamellipodia in cells whereas cdc42 activation leads to the formation of filopodia (Nobes and Hall, 1995). Interestingly GPR55 can promote the activation of several small Rho GTPases; RhoA, Rac1 and cdc42 (Ryberg *et al.*, 2007) and Rac2 (Balenga *et al.*, 2011). Lipid-induced lamellipodia were still present when the ROCK inhibitor had been applied to the DU145 cells. Both stress fibre and FA formation were ROCK dependent suggesting that LPI and NOSer induced effects are mediated through the Rho-ROCK signalling axis in the DU145 cells.

In conclusion this study has revealed both LPI and NOSer can exert GPR55-mediated Ca^{2+} mobilisation, F-actin cytoskeletal reorganisation and FA elongation in the prostate cancer cell line; DU145. It however remains to be determined if the LPI and NOSer pCREB responses are GPR55-mediated. Problems with the siRNA assay suggest that more optimisation is required as pCREB was elevated in all cell treatments when using the described siRNA protocol. Also transiently transfecting the cells with serum containing medium and leaving the siRNA-liposome complexes for 60 hr then transferring the cells into serum free medium led to a strange, non-specific labelling in the cells. A potential way to resolve the issue could be to transfect the cells in serum free medium for 24 hr then remove the medium and replace with serum-containing medium and use the cells at 69 - 72 hr. The cells would need to be put in serum free medium overnight prior to the start of the experiments. This allows time for the siRNA-liposome complexes time to enter the cells but does not stress the cells too long which occurs when they are serum starved for 72 hr.

It was also observed that there are subtle differences in the signalling pathways when the lipids were compared in DU145 cells in the pCREB assay. NOSer induced Ca^{2+} mobilisation was not as efficacious as LPI induced responses in the DU145 cells. As such Ca^{2+} mobilisation may not be important to promote pCREB in NOSer challenged DU145 cells. However Ca^{2+} mobilisation was important for pCREB in LPI-challenged DU145 cells. The use of the novel antagonists CID16020046 (Kargl *et al.*, 2013) or ML193 (Yu *et al.*, 2013) would also help to decipher GPR55's role in these signalling assays when challenged with the endogenous lipids.

5.3.4. Breakdown of proposed LPI and NOSer-mediated signalling pathways to promote pCREB in DU145 cells.

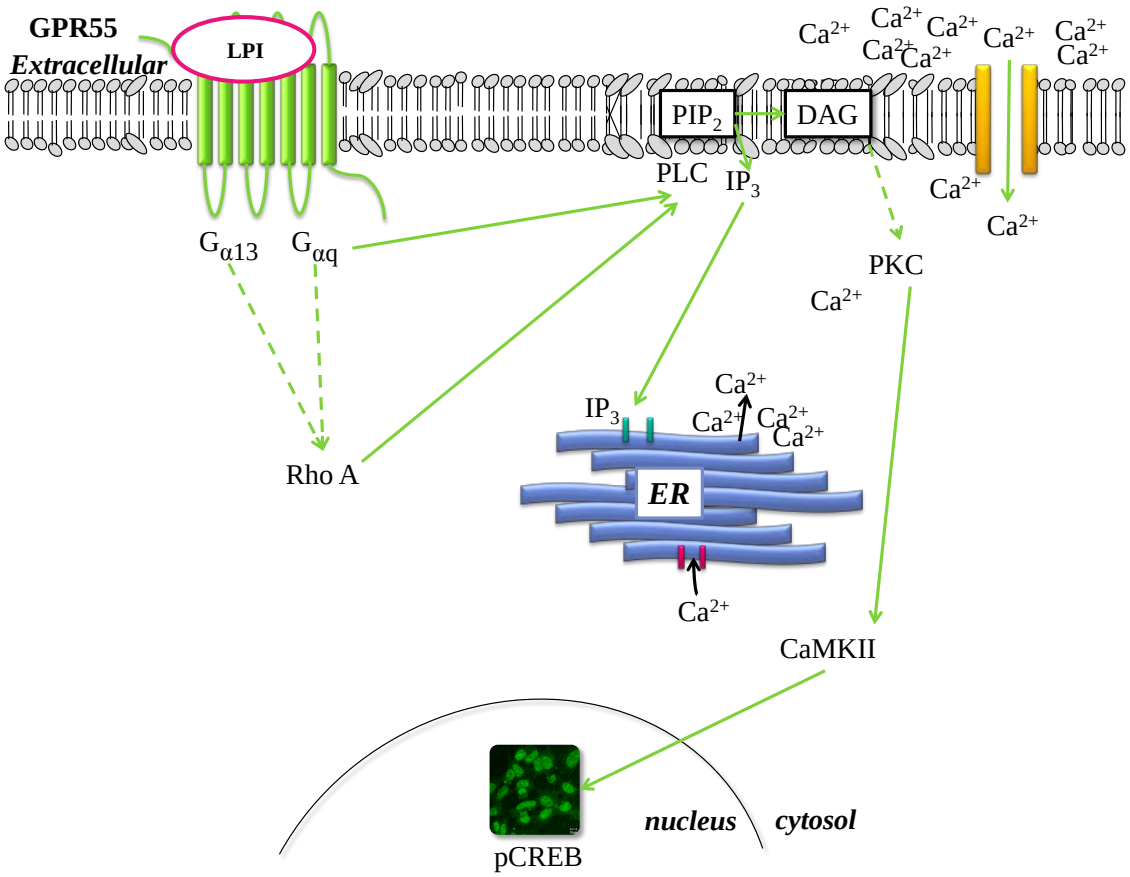

Figure 5.36: Summary of Ca^{2+} cascade require for LPI-induced pCREB in DU145 cells. *LPI binding of GPR55is likely to initiate the activation of $G_{\alpha 13}$ or $G_{\alpha q}$ which in turn activates RhoA and ROCK. This then leads to activation of PLC, which promotes the hydrolysis of PIP_2 into DAG and IP_3. IP_3 activates IP_3 receptors on the ER promoting the release of Ca^{2+}. DAG and/or Ca^{2+} then lead to activation of PKC. Both PKC and Ca^{2+} can activate CAMKII which can then phosphorylate CREB (at either serine 133; positive regulation or 142; negative regulation) Note the antibody in this study was specific for pCREB serine 133. LPI, L-α-lysophosphatidylinositol;; RhoA, Ras homolog gene, family member A; ROCK, Rho associated protein kinase; PLC, Phospholipase C; PIP_2, phosphatidylinositol 4, 5-bisphosphate; DAG, diacylglycerol; IP_3, inositol 1, 4, 5-triphosphate; PKC, protein kinase C; CaMKII, Ca^{2+}/calmodulin dependent protein kinase II; pCREB, phosphorylated cyclic AMP response element binding protein. Solid arrows = signalling effectors; dashed arrows = suggested effectors.*

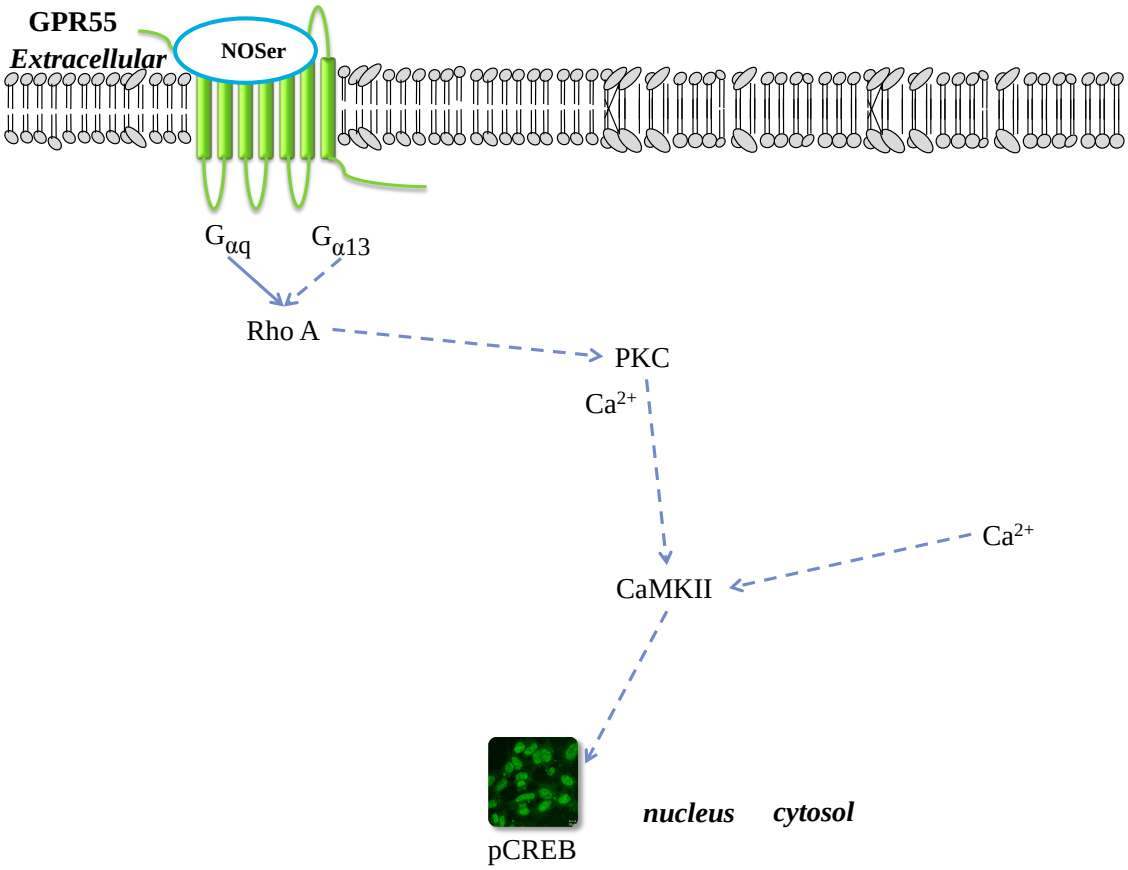

Figure 5.37: Summary of proposed Ca^{2+} cascade require for NOSer-induced pCREB in DU145 cells. *NOSer binding of GPR55 initiates the activation of $G_{\alpha 13}$ or $G_{\alpha q}$ which in turn activates RhoA and ROCK. This may lead to activation of PKC. Both PKC and Ca^{2+} (from the cytosol) could activate CaMKII which can then phosphorylate CREB (at either serine 133; positive regulation or 142; negative regulation) Note the antibody in this study was specific for pCREB serine 133. NOSer, N-oleoyl-L-serine; RhoA, Ras homolog gene, family member A; PKC, protein kinase C; CaMKII, Ca^{2+}/calmodulin dependent protein kinase II; pCREB, phosphorylated cyclic AMP response element binding protein.*

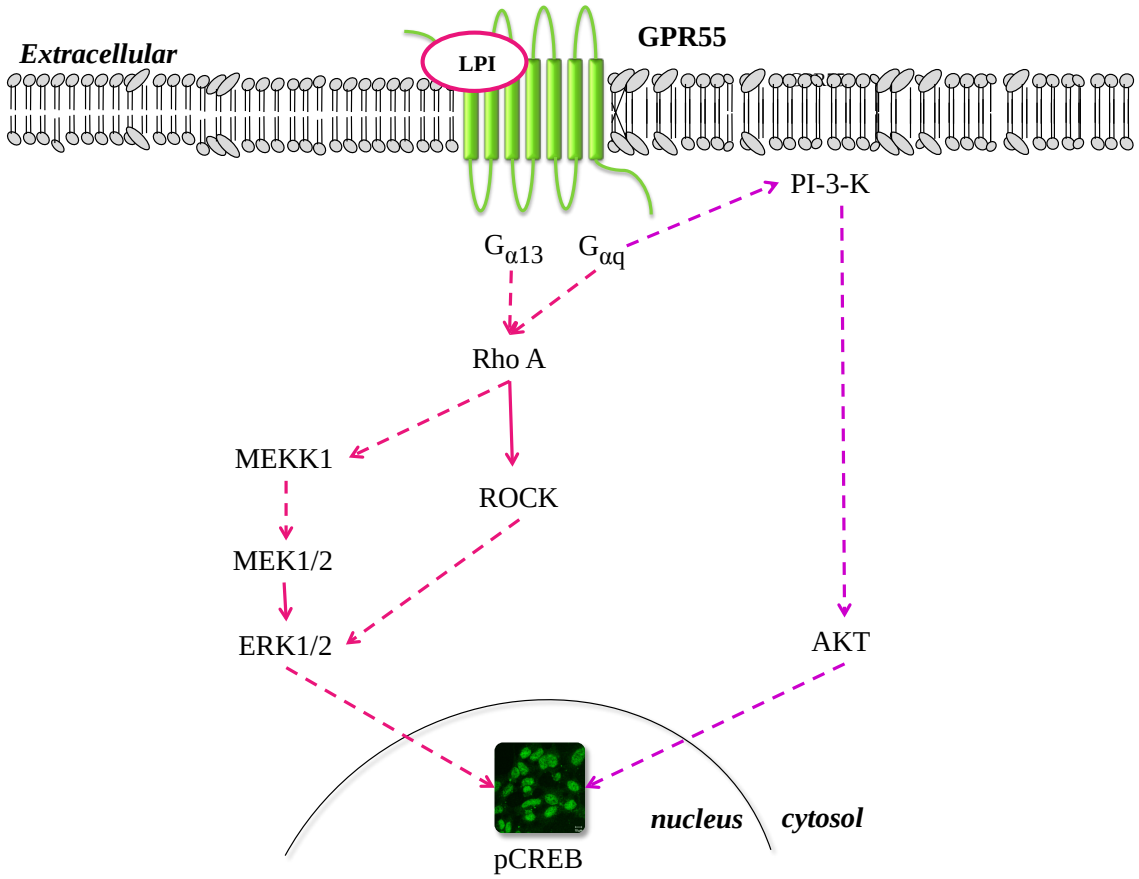

5.38: Summary of the MAPK and PI-3-kinase signalling pathways required to promote LPI-induced nuclear pCREB in DU145 cells. *$G_{\alpha 13}$ or Gαq acting on RhoA could lead to the phosphorylation of MEKK1 which in turn can phosphorylate MEK1/2. MEK1/2 subsequently phosphorylates ERK1/2 which translocates into the nucleus to phosphorylate CREB. Alternatively Rho phosphorylates ROCK which then subsequently phosphorylates ERK1/2. PI-3 kinase could be activated by the $G_{\alpha q}$ which could then phosphorylate AKT which could then phosphorylate CREB. GPR55, G-protein coupled receptor 55; LPI, L-α-lysophosphatidylinositol; RhoA, Ras homolog gene, family member A; ROCK, Rho associated protein kinase; PI-3K, phosphatidylinositide 3-kinase; MEKK1, mitogen-activated protein kinase kinase kinase 1; MEK1, Mitogen-activated protein kinase kinase 1; ERK1/2, extracellular signal-regulated kinase 1/2; pCREB, phosphorylated cyclic AMP response element binding protein. Solid arrows = signalling effectors; dashed arrows = suggested effectors. Pink arrows = MAPK signalling pathway; purple arrows = PI-3 kinase signalling pathway.*

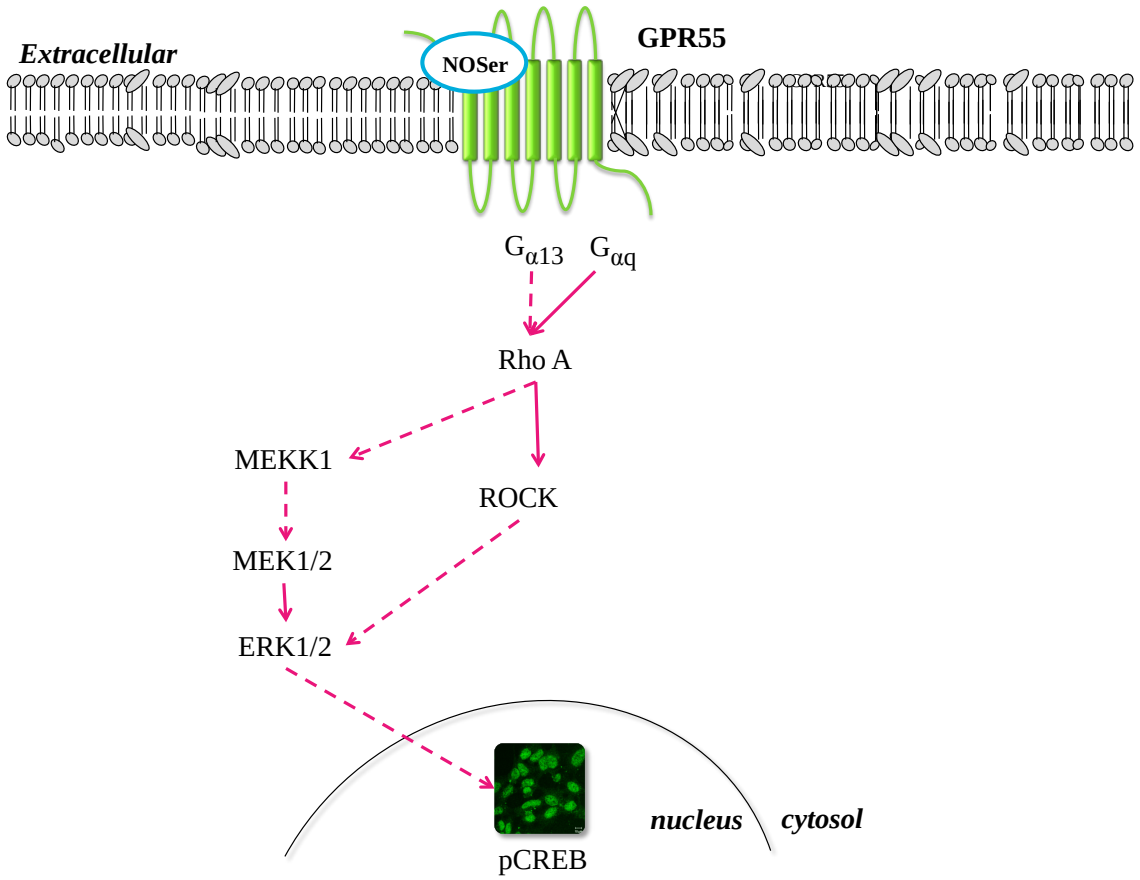

5.39: Summary of the MAPK signalling pathway required to promote NOSer-induced nuclear pCREB in DU145 cells. *$G_{\alpha 13}$ or Gαq acting on RhoA could lead to the phosphorylation of MEKK1 which in turn can phosphorylate MEK1/2. MEK1/2 subsequently phosphorylates ERK1/2 which translocates into the nucleus to phosphorylate CREB. Alternatively Rho phosphorylates ROCK which then subsequently phosphorylates ERK1/2. GPR55, G-protein coupled receptor 55; NOSer, N-oleoyl-L-serine; RhoA, Ras homolog gene, family member A; ROCK, Rho associated protein kinase; MEKK1, mitogen-activated protein kinase kinase kinase 1; MEK1, Mitogen-activated protein kinase kinase 1; ERK1/2, extracellular signal-regulated kinase 1/2; pCREB, phosphorylated cyclic AMP response element binding protein. Solid arrows = signalling effectors; dashed arrows = suggested effectors.*

CHAPTER SIX

Final Discussion

6.1. INTRODUCTION

GPR55 is recognised as a novel lipid sensing receptor where the general consensus is that the endogenous lipid LPI is the natural GPR55 ligand (Oka *et al.,* 2007; Henstridge *et al.,* 2009). However the GPR55 cannabinoid pharmacology is controversial with some groups reporting that cannabinoid ligands can activate the receptor (Ryberg *et al.*, 2007; Lauckner *et al.*, 2008; Henstridge *et al.,* 2010; Sharir *et al.*, 2012) with others contesting these claims (Henstridge *et al*., 2009; Oka *et al*., 2007). Recently a family of lipid mediators, the N-acyl amino acids, are gaining interest due to their structural similarity to the endocannabinoids (Bradshaw *et al*., 2009). They are an intriguing group of endogenous lipids which have little or no affinity for either CB_1 or CB_2 receptors. Some of these lipids have shown biological activity but many remain orphan lipids where no known biological target has been elucidated (Bradshaw *et al.,* 2009). Therefore this study was carried out to investigate potential effects of N-acyl amino acids upon the activation of GPR55.

6.2. SUMMARY OF RESEARCH FINDINGS

6.2.1. N-acyl amino acids induced activation of GPR55 promotes Ca^{2+} mobilisation.

This study has highlighted for the first time that the N-acyl amino acids tested are GPR55 agonist/partial agonists. Using a Ca^{2+} assay in hGPR55-HEK293 cells, N-acyl serines were found to be more potent and efficacious when compared with N-acyl glycines with NASer and NOSer being the most active of these ligands. However LPI remained the most potent and efficacious of all the lipids tested in this assay. Previous research has highlighted that LPI activation of GPR55 requires $G_{\alpha 13}$-Rho-ROCK signalling followed by subsequent activation of PLC to promote a release of Ca^{2+} from internal stores (Lauckner *et al.*, 2008; Henstridge *et al.*, 2009). In agreement this study found that NOSer also required ROCK, PLC activation and Ca^{2+} release from stores in hGPR55-HEK293 cells. However in contrast the present study found that the DU145 prostate cancer cell line, did not require ROCK activation to promote Ca^{2+} mobilisation which confirmed the findings of a previous study (Piñeiro *et al.*, 2011). In support of this, $G_{\alpha q}$ is suggested to be a downstream effector of GPR55 in hGPR55-HEK293 cells (Lauckner *et al.*, 2008) and with phaeochromocytoma PC12 cells (Obara *et al.*, 2011). This is also the first study to report that LPI induced Ca^{2+} mobilisation requires $G_{\alpha q}$ in DU145 cells. Furthermore NOSer was less efficacious in the Ca^{2+} assay in DU145 cells

when compared to LPI. These results suggest that GPR55 may exhibit ligand bias in Ca^{2+} mobilisation in DU145 cells.

6.2.2. CREB phosphorylation, N-acyl amino acids and GPR55.

There were subtle differences when the effects of lipid ligands in hGPR55-HEK293 cells were compared using pCREB and Ca^{2+} assays. NOSer was now found to be the most potent and efficacious lipid tested. Moreover, NOSer exhibited an efficacy which was similar to AM251, which was previously reported to be more efficacious than LPI in a pCREB immunolabelling assay (Henstridge *et al.*, 2010). NOGly was the least potent in the pCREB assay when tested on the hGPR55-HEK293 cells this is contrast to the Ca^{2+} mobilisation assay. These data suggest that NOGly may exert ligand bias in the hGPR55-HEK293 cells with a preference for Ca^{2+} rather than pCREB signalling. Furthermore NASer exhibited ligand bias; certainly in the hGRP55-HEK293 cells as the potency of the lipid acting through GPR55 was different dependent on the assay used (Ca^{2+} > pCREB).

Previously LPI has been shown to activate two kinases upstream of CREB; ERK1/2 and AKT (Piñeiro *et al.*, 2011). However this study is the first time that both LPI and NOSer induced CREB phosphorylation in DU145 cells has been reported. Furthermore this study highlights that LPI requires signalling via Ca^{2+}, MAPK and PI-3 kinase to promote pCREB. In contrast Ca^{2+} is not required for pCREB in DU145 cells challenged with NOSer. A probable reason being NOSer is less effective at promoting Ca^{2+} mobilisation in DU145 cells. Moreover NOSer is less potent but more efficacious in promoting pCREB than LPI in these cells.

6.2.3. N-acyl amino acids promote actin cytoskeletal reorganisation and FA elongation.

Previous studies highlighted that GPR55 can activate members of the Rho family of small GTPases ; RhoA, cdc42, rac1 (Ryberg *et al.*, 2007) and rac2 (Balenga *et al.*, 2011). These Rho GTPases are important for cytoskeletal reorganisation and the formation of FAs (Hall, 1998). This is the first study to highlight that GPR55 can mediate the formation of FAs with either LPI or NOSer. Moreover there was little difference in potency or efficacy for mediating changes in vinculin length in hGPR55-HEK293 cells treated with either LPI or NOSer. Of all the assays tested LPI was the most potent in the vinculin assay measuring FA elongation. NOSer was found to have

an EC_{50} similar as seen in the pCREB assay in hGPR55-HEK293 cells. GPR55-mediated FA formation and actin cytoskeletal reorganisation has not been reported prior to this study in DU145 cells. Stress fibres, filopodia and lamellipodia were all observed in DU145s and hGPR55-HEK293 cells when challenged with either LPI or NOSer. Actin cytoskeletal reorganisation required signalling via Rho and ROCK only in hGPR55-HEK293 cells. The formation of FAs was found to require Rho-ROCK, MAPK and Ca^{2+} signalling in hGPR55-HEK293 cells (figure 6.1).

Whilst the hGPR55-HEK293 cells allow GPR55 to be studied in detail the effects may differ from endogenous expression of the receptor. Indeed the over-expression of GPR55 may mask some of the signalling by forcing signalling down a particular pathway where one G-protein has a higher affinity for the activated GPCR which may then mask other signalling that is occurring (Hermans, 2003). This may be a reason behind the observed differences where hGPR55-HEK293 cells only signalled via $G_{\alpha 13}$ where the DU145 cells activate both $G_{\alpha 13}$ and $G_{\alpha q}$ (figure 6.2). Another explanation may be the levels of each G-protein could be different in differing cell types. Therefore it could be that $G_{\alpha q}$ is expressed at a higher level in DU145 cells.

6.2.4. Potential interactions between the signalling outcomes in this study.

Ca^{2+} is an important second messenger which influences CREB phosphorylation through the activation of Ca^{2+}/CaMKII (Sheng *et al.*, 1990; Impey *et al.*, 1998). Interestingly Ca^{2+} requires an intact actin cytoskeleton to allow capacitance entry of Ca^{2+} in keratinocytes (Korkiamäki *et al.*, 2003). However this is not required for Ca^{2+} capacitance entry in NIH 3T3 cells but the authors report that the disrupted cytoskeleton may affect the spatial relationship between the IP_3 receptors and PLC (Ribeiro *et al.*, 1997). Moreover the actin cytoskeleton is also required for the regulation of interactions between STIM1 (the Ca^{2+} sensor on the ER) and Orai1 and TRPC1 the Ca^{2+} channels in the plasma membrane in HEK293 cells therefore playing a role in Ca^{2+} influx after store depletion (Galán *et al.*, 2011).

Although some of the signalling pathways such as Ca^{2+}, Rho-ROCK and MAPK are required for FA formation and pCREB mediated by GPR55. The two outcomes are thought to be separate as FA formation is likely to be by focal contacts translocating to peripheral regions and combining to form larger focal adhesions rather than being gene regulated. The time scale of ligand treatment (25 min) is not long enough for gene

regulation to play a role, if pCREB were to be involved, as this normally requires several hours for gene transcription to occur.

Vinculin is important adaptor protein allowing the binding of the vinculin head to talin an integrin associated protein and the F-actin cytoskeleton binds to the vinculin tail allowing an anchor to form in the cell (Chen *et al.*, 2006). This anchoring of the cell generates force to allow the cytoskeleton the ability to make the cell contract (Dumbauld *et al.*, 2010). GPR55 is known to signal via Rho (Henstridge *et al.*, 2009). Rho activation of actin filaments can promote vinculin activation leading to the strengthening of vinculin containing adhesions which could then have an effect on cell contractility, migration and shape (Chen *et al.*, 2006).

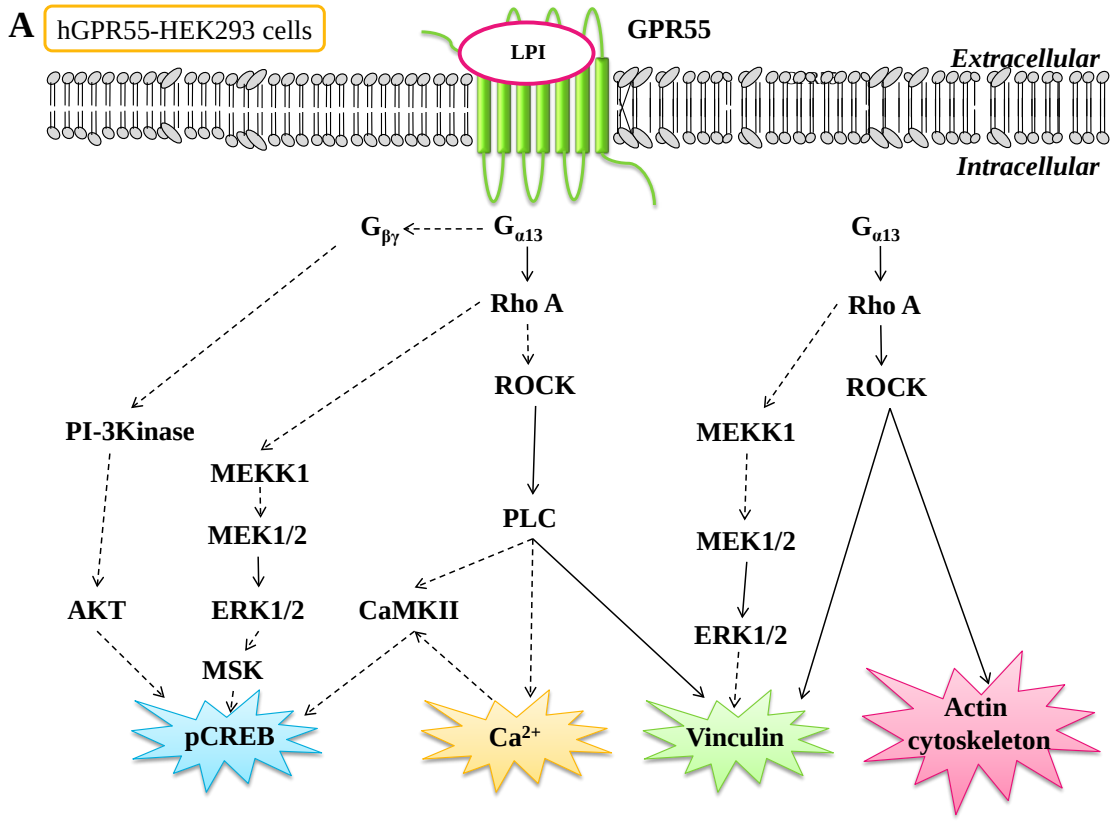

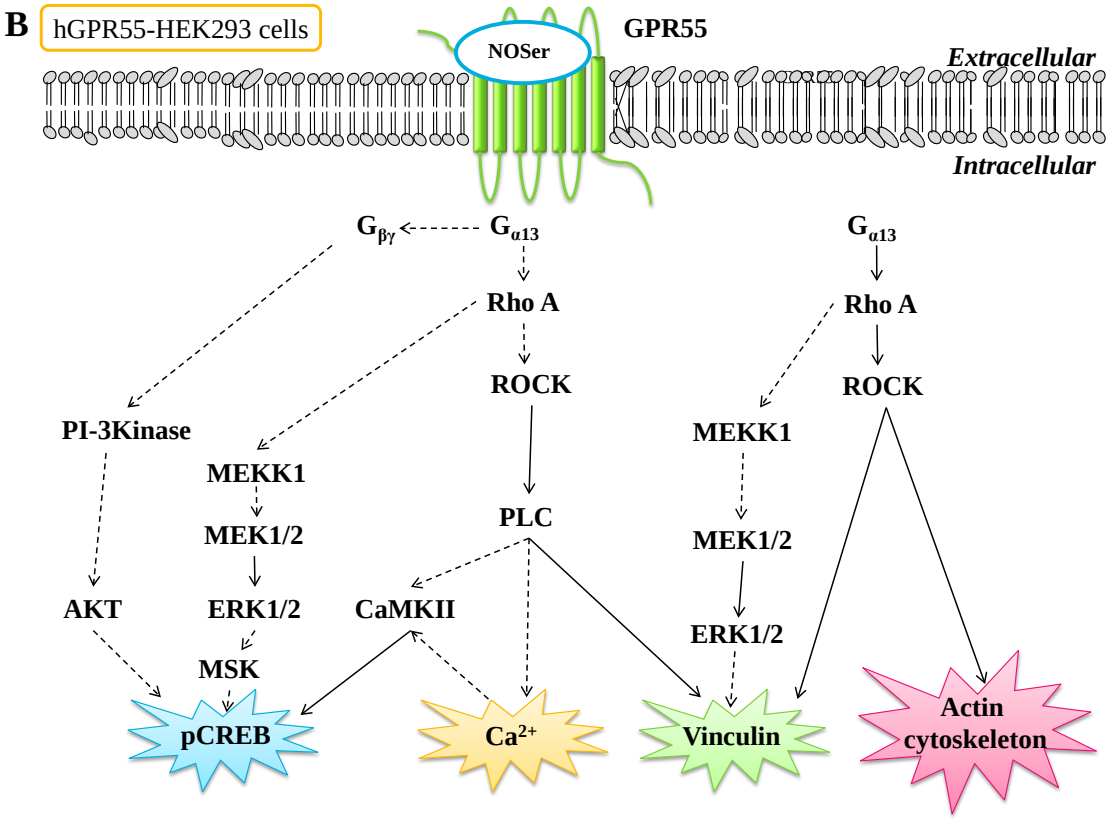

Figure 6.1: Summary of endogenous lipid mediated GPR55 signalling. ***A****, LPI and* ***B****, NOSer mediated signalling pathways in hGPR55-HEK293 cells required to promote pCREB, Ca^{2+} mobilisation, changes in vinculin and actin cytoskeletal reorganisation. Note $G_{\alpha13}$ is activated in hGPR55-HEK293 cells with either LPI or NOSer. Signalling effectors that were activated were similar for both the lipids. Dashed arrows = putative signalling; solid arrows = confirmed signalling (from this study).*

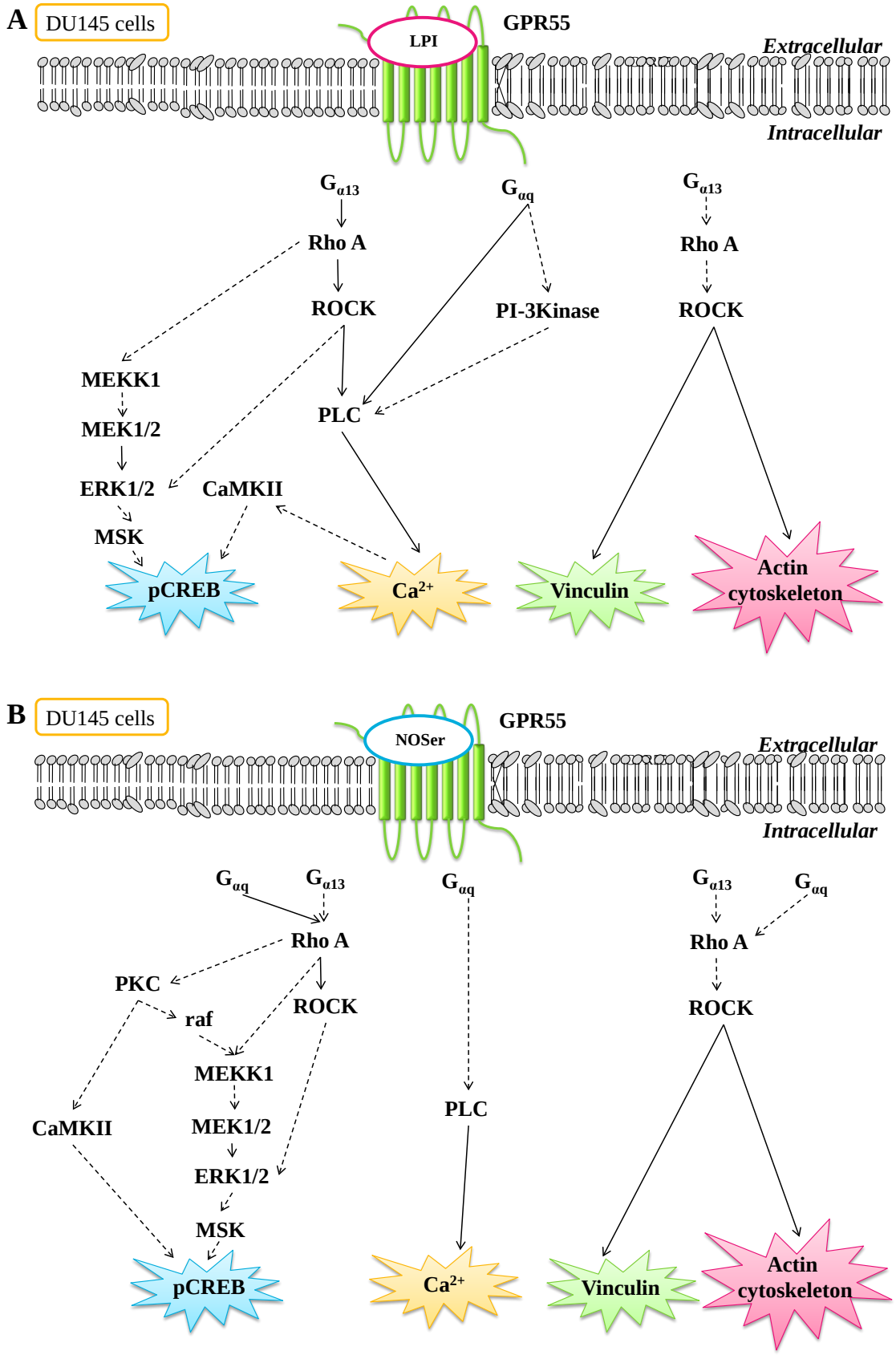

Figure 6.2: Summary of endogenous lipid induced GPR55 signalling in DU145 cells. *LPI promotes signalling to allow pCREB, Ca^{2+} mobilisation, changes in vinculin and actin cytoskeletal reorganisation. Signalling pathways in DU145 cells challenged with* ***A****, LPI or* ***B****, NOSer. Note both $G_{\alpha 13}$ and $G_{\alpha q}$ are recruited in the DU145 cells challenged with either LPI or*

NOSer. Dashed arrows = putative signalling; solid arrows = confirmed signalling (from this study).

6.2.5. Potential physiological roles of NOSer effects mediated by GPR55.

Whist the physiological role of NOSer remains elusive at the present time interactions with GPR55 in a physiological setting are plausible. For example both NOSer and GPR55 are localised to bone (Whyte *et al.*, 2009; Smoum *et al.*, 2010). NOSer acting on GPR55 in bone may have a detrimental effect leading to increased bone loss as was observed $GPR55^{(+/+)}$ mice treated with LPI or O-1602 an effect that was absent in $GPR55^{(-/-)}$ mice (Whyte *et al.*, 2009). Prostate cancer is known as one of the cancers to commonly metastasise to bone (Tantivejkul *et al.*, 2004). Therefore if levels of NOSer were to be increased in the microenvironment surrounding bone this could potentially act upon GPR55 in prostate cancer cells and encourage their migration to the region. Furthermore NOSer could then act on GPR55 present in the prostate cancer cells to allow them to proliferate.

Also NOSer is found in brain and spleen of mice (Smoum *et al.*, 2010), it is interesting to note that these are areas where GPR55 is expressed (Ryberg *et al.*, 2007). The role of GPR55 in the brain is still in its infancy but mEPSCs occur in CA1 pyramidal neurons when the cells were treated with LPI and were sensitive to CBD. It remains to be determined if NOSer is present in the hippocampal region of the brain but if this were to be so then NOSer could exert effects upon the pyramidal neurons. Furthermore GPR55 has been associated with neurotransmitter release that is dependent on Ca^{2+} mobilisation (Sylantyev *et al.*, 2013). The presence of NOSer in the brain may also contribute to effects on microglia (the macrophages of the brain). GPR55 is also localised in microglia and is increased in the murine microglial BV2 cell line when the cells are 'primed' with INFγ. These cells were found to have increases in ERK1/2 phosphorylation when challenged with LPI (Pietr *et al.*, 2009). Therefore it would be possible for NOSer to induce a similar effect.

Until there is knowledge of where NOSer is localised, how it is synthesised and released into plasma or microenvironments a physiological role can only be speculated. However, understanding the localisation of GPR55 and NOSer in a physiological system will help to elucidate the role of NOSer signalling via GPR55.

6.2.6. Limitations within this study.

To improve this study the use of either quantitative polymerase chain reaction (qPCR) or western blotting techniques would be required. This would allow a quantification of GPR55 expression in the endogenously expressing DU145 prostate cancer cell line and in the overexpressing hGPR55-HEK293 cell line. Furthermore these techniques would confirm GPR55 knockdown in cells treated with siRNA.

Time course studies using western blots would allow an insight into GPR55-mediated activation of pCREB. Also increasing the 'n' number of the pCREB experimental data would be advantageous as many of the inhibitor experiments whilst highlighting a general trend of inhibition do not highlight significant differences.

The selectivity of protein kinase inhibitors should also be considered. Kinase inhibitors are known to be promiscuous in nature (Davies *et al.*, 2000; Bain *et al.*, 2007). Therefore validation of the kinase inhibitors would further improve the conclusions in this study. To further validate the kinase inhibitors in this study the use of two structurally unrelated inhibitors would be advantageous. In this study two structurally unrelated MEK1/2 and PI-3 kinase inhibitors were used. Furthermore using inactive analogues of the inhibitor of interest would help confirm the effect of the inhibitor. To allow this and inactive analogue (U0124) of the MEK1/2 inhibitor (U0126) was tested. Also, confirming the effects of the inhibitors on targets that are known to be activated in cells. Applying the inhibitor of interest (eg MEK1/2 inhibitor) to HEK293 cells prior to then applying epidermal growth factor to initiate ERK1/2 signalling and run a Western blot. Untreated cells should produce the relevant phosphoERK1/2 band whereas those treated with the inhibitor should not have a corresponding band. Furthermore data from the International Centre for Kinase Profiling (http://www.kinase-screen.mrc.ac.uk/) based in the Protein Phosphorylation and Ubiquitylation Unit at the University of Dundee allows comparisons of many enzymes to allow the specificity of kinase inhibitors to be evaluated (Cohen, 2010).

6.3. FUTURE DIRECTIONS

6.3.1. GPR55 mediated signalling – other considerations.

This study did not look into the effects of the β-arrestins. These proteins are now known to be important signalling mediators in their own right. Interestingly β-arrestins can play a roles in stress fibre formation (Barnes *et al.*, 2005), ERK1/2 activation (Coffa

et al., 2011) and gene transcription (DeWire *et al.*, 2008). It is not known if GPR55 signalling requires the activation of β-arrestins, although GPR55 exhibits agonist-induced internalization which is likely to be β-arrestin-mediated (Henstridge *et al.*, 2010). Use of siRNA against β-arrestin isoforms could determine if these proteins are important for the lipid mediated GPR55 signalling. Furthermore previous research observed that thrombin concentrations need to be 2 fold higher than that required for $G_{\alpha 12/13}$ to elicit $G_{\alpha q}$-mediated Rho activation of the thromboxane A_2 receptor (Vogt *et al.*, 2003). Therefore it could be possible for GPR55-mediated $G_{\alpha 13}$ or $G_{\alpha q}$ activation to activate RhoA. However further experiments would be required to optimise the LPI or NOSer concentration which promotes signalling through each of the G-proteins as this study just utilised a sub-maximal concentration for each lipid. These sets of experiments would help to elucidate any ligand bias whether G-protein dependent or independent.

To improve our understanding of the signalling pathway data in the DU145 cells, further experiments would help to clarify the exact position of the proteins in the signalling pathway. It is known that AKT can be activated by LPI in DU145 cells (Piñeiro *et al.*, 2011). This kinase can phosphorylate CREB (Du and Montminy, 1998; Das *et al.*, 2005). However NOSer has not been studied in relation to either ERK1/2 or AKT activation. It would be interesting to study where these kinases are in relation to each other and ROCK in the CREB signalling pathways. Further work is required to determine if LPI or NOSer activation of CREB actually induces transcription of genes in DU145 cells. CREB phosphorylation leads to the transcription of genes such as c-FOS in breast cancer cells which is GPR55-mediated (Andradas *et al.*, 2011). CREB mediated gene transcription is temporal in nature and this needs to be confirmed in the DU145 cells. Previous work has highlighted that 25min is the optimal timing for pCREB signalling in hGPR55-HEK293 cells however gene transcription was not studied (Henstridge *et al.*, 2010).

6.3.2. Are there other potential NOSer targets?

A general point to note are that lipids can exert effects on many different targets therefore some care must be taken when evaluated the results. Whilst this study highlights that the lipids act on GPR55 when in hGPR55-HEK293 cells, other targets for LPI or NOSer may exist. Little is known about the NOSer targets within cells however it is documented that NOSer can promote ERK1/2 activation in osteoblasts via

a $G_{\alpha i/o}$ linked GPCR (Smoum *et al.*, 2010). The Abn-CBD receptor, GPR18 is known to activate a $G_{\alpha i/o}$ GPCR (McHugh *et al.*, 2010) and is reported to have some overlap in pharmacology with GPR55 (Ross, 2009). Furthermore GPR18 expression is increased in metastatic melanoma however it remains to be determined if this is the case for prostate cancer (Qin *et al.*, 2011). Another N-acyl amino acid, NAGly, is a GPR18 agonist highlighting this receptor has some sensitivity to this family of proteins (Kohno *et al.*, 2006; McHugh *et al.*, 2012). Therefore application of NOSer to GPR18 would be of interest.

LPI is known to have effects on other GPCRs such as GPR119 (Soga *et al.*, 2005), and certain ion channels such as potassium channels; BK_{Ca} (Bondarenko *et al.*, 2011), TREK and TRAAK (Blondeau *et al.*, 2002) and $TRPV_2$ (Monet *et al.*, 2009). Therefore it is feasible that NOSer will also have additional binding targets. Interestingly oleic acid is able to bind and activate GPR119 (Hansen *et al.*, 2012) also OEA is a GPR119 ligand (Overton *et al.*, 2006). Therefore NOSer may be able to activate GPR119. Also endocannabinoids have the ability to bind and activate members of the PPAR family of nuclear receptors. Furthermore oleic acid is also known to activate PPAR-α therefore compounds with an oleic fatty acid present may be potential ligands for this receptor as was observed with OEA (Fu *et al.*, 2003). It is not known at present if NOSer has affinity for these receptors but could be feasible due to the presence of the oleic fatty acid moiety. Prior application of the antagonists that are available for these receptors (MK886 – PPARα, GW9662 - PPARγ and GSK0660 – PPARδ) would help to determine if NOSer is acting on these receptors (Scuderi *et al.*, 2012; Paterniti *et al.*, 2013). Other GPCRs of interest would be the FFA receptors especially GPR40 which is activated by medium to long chain fatty acids such as oleic acid (Briscoe *et al.*, 2003). Therefore NOSer should be tested as a potential FFA receptor ligand.

6.3.3. Use of novel antagonists.

Application of the novel GPR55 antagonists would allow the validation that the effects in the DU145 cells are GPR55-mediated. Originally CBD was an antagonist for GPR55 however this ligand has several targets such as Abn-CBD (Járai *et al.*, 1999), TRPV1 (Costa *et al.*, 2004) and PPAR-γ (O'Sullivan and Kendall, 2010). Therefore there has been a requirement for a more GPR55-specific antagonist. Recently two novel antagonist; ML193 (Kotsikorou *et al.*, 2013) and CID16020046 (Kargl *et al.*, 2013) have been reported as being GPR55 specific. In this study the use of siRNA in the

DU145 cells to assess GPR55-mediated CREB signalling remains undetermined. The protocol was found to affect pCREB levels in all the cell treatments therefore a comparison with DMSO control cells was not determined. A possible way to reveal the influence of GPR55 in mediating pCREB in the DU145 cells would be to use these novel GPR55 specific antagonists.

6.3.4. Migration studies and DU145 cells.

Migration of cells is important in cancer metastasis (Ridley *et al.*, 2003). Cytoskeletal reorganisation and formation of FAs are important in cell migration particularly to promote directionality on the migrating cell (Machesky and Hall, 1997; Zaidel-Bar *et al.*, 2003). It should also be noted that the presence of stress fibres does not automatically correlate with the migratory ability of cells. For example polymorphonuclear leukocytes do not contain stress fibres but are highly motile cells (Valerius *et al.*, 1981). Therefore future experiments studying migration would be required to understand the effects that cytoskeletal reorganisation and changes in FAs would have in DU145 cells. GPR55 has previously been reported as inducing a migratory phenotype in breast cancer lines where the cells exhibited a directed polarity (Ford *et al.*, 2010). The use of wound assays would allow the migration of cells to be recorded when challenged with either LPI or NOSer. Application of antagonists or siRNA would also help to determine the influence of GPR55 on cell migration. Further studies to understand the signalling effectors required for FA elongation and cytoskeletal reorganisation in the DU145 cells are required.

6.3.5. Physiological properties of NOSer

Physiological concentrations are unknown at present are as the synthesising and degradation processes that are involved with the NOSer. This makes it difficult to understand the physiological role of NOSer when acting on GPR55. For example is NOSer synthesising and degrading enzymes localised in the same regions as GPR55? Furthermore the concentration of NOSer in tissues is in its infancy and further evidence will enhance the field in gaining a better understanding of the concentration and where NOSer is localised.

6.4. CONCLUDING REMARKS

This study adds a further level of complexity to the GPR55-cannabinoid sensitivity debate and further confirms that GPR55 is a novel lipid sensing receptor. This study

has highlighted that the putative cannabinoid receptor; GPR55 is a novel target for a sub-set of N-acyl amino acids. It is the first study to suggest GPR55 as a novel GPCR target for NOSer; in both a recombinant over-expressing hGPR55-HEK293 cell line and in endogenously expressing prostate cancer cell line; DU145. It also demonstrates that NASer is a GPR55 agonist however; results in efficacy and potency are affected by the assay being studied. This therefore emphasises the importance of using different signalling assays to assess effects of novel ligands. Finally there is an importance in having the knowledge of endogenous lipids and the receptors that they target for the development of novel therapeutics. Without an understanding of the effects endogenous lipids exert then assessment of drug interactions is more difficult to predict.

CHAPTER SEVEN

References

Abercrombie M, Heaysman JE, and Pegrum SM (1971) The locomotion of fibroblasts in culture. IV. Electron microscopy of the leading lamella. *Exp Cell Res* **67**:359–367.

Ahluwalia J, Urban L, Capogna M, Bevan S, and Nagy I (2000) Cannabinoid 1 receptors are expressed in nociceptive primary sensory neurons. *Neuroscience* **100**:685–8.

Alessi DR, Gomez N, Moorhead G, Lewis T, Keyse SM, and Cohen P (1995) Inactivation of p42 MAP kinase by protein phosphatase 2A and a protein tyrosine phosphatase, but not CL100, in various cell lines. *Curr Biol* **5**:283–95.

Amano M, Chihara K, Kimura K, Fukata Y, Nakamura N, Matsuura Y, and Kaibuchi K (1997) Formation of actin stress fibers and focal adhesions enhanced by Rho-kinase. *Science* **275**:1308–11.

Anavi-Goffer S, Baillie G, Irving AJ, Gertsch J, Greig IR, Pertwee RG, and Ross RA (2012) Modulation of L-α-lysophosphatidylinositol/GPR55 mitogen-activated protein kinase (MAPK) signaling by cannabinoids. *J Biol Chem* **287**:91–104.

Anavi-Goffer S, and Coutts A a (2003) Cellular distribution of vanilloid VR_1 receptor immunoreactivity in the guinea-pig myenteric plexus. *Eur J Pharmacol* **458**:61–71.

Andersson DA, Nash M, and Bevan S (2007) Modulation of the cold-activated channel $TRPM_8$ by lysophospholipids and polyunsaturated fatty acids. *J Neurosci* **27**:3347–55.

Andradas C, Caffarel MM, Pérez-Gómez E, Salazar M, Lorente M, Velasco G, Guzmán M, and Sánchez C (2011) The orphan G protein-coupled receptor GPR55 promotes cancer cell proliferation via ERK. *Oncogene* **30**:245–52.

Aoki J, Taira A, Takanezawa Y, Kishi Y, Hama K, Kishimoto T, Mizuno K, Saku K, Taguchi R, and Arai H (2002) Serum lysophosphatidic acid is produced through diverse phospholipase pathways. *J Biol Chem* **277**:48737–44.

Arias J, Alberts AS, Brindle P, Claret FX, Smeal T, Karin M, Feramisco J, and Montminy M (1994) Activation of cAMP and mitogen responsive genes relies on a common nuclear factor, *Nature* **370**, 226 - 229.

Ashton JC, Friberg D, Darlington CL, and Smith PF (2006) Expression of the cannabinoid CB_2 receptor in the rat cerebellum: an immunohistochemical study. *Neurosci Lett* **396**:113–6.

Bain J, Plater L, Elliott M, Shpiro N, Hastie CJ, McLauchlan H, Klevernic I, Arthur JSC, Alessi DR, and Cohen P (2007) The selectivity of protein kinase inhibitors: a further update. *Biochem J* **408**:297–315.

Baker D, Pryce G, Davies WL, and Hiley CR (2006) In silico patent searching reveals a new cannabinoid receptor. *Trends Pharmacol Sci* **27**:1–4.

Balenga NAB, Aflaki E, Kargl J, Platzer W, Schröder R, Blättermann S, Kostenis E, Brown AJ, Heinemann A, and Waldhoer M (2011) GPR55 regulates cannabinoid 2 receptor-mediated responses in human neutrophils. *Cell Res* **21**:1452–69.

Baran DT, and Kelly AM (1988) Lysophosphatidylinositol: a potential mediator of 1,25-dihydroxyvitamin D-induced increments in hepatocyte cytosolic calcium. *Endocrinology* **122**:930–934.

Barnes WG, Reiter E, Violin JD, Ren X-R, Milligan G, and Lefkowitz RJ (2005) beta-Arrestin 1 and Galphaq/11 coordinately activate RhoA and stress fiber formation following receptor stimulation. *J Biol Chem* **280**:8041–50.

Bayewitch M, Avidor-Reiss T, Levy R, Barg J, Mechoulam R, and Vogel Z (1995) The peripheral cannabinoid receptor: adenylate cyclase inhibition and G protein coupling. *FEBS Lett* **375**:143–7.

Beaulieu J-M, Sotnikova TD, Marion S, Lefkowitz RJ, Gainetdinov RR, and Caron MG (2005) An Akt/beta-arrestin 2/PP2A signaling complex mediates dopaminergic neurotransmission and behavior. *Cell* **122**:261–73.

Begg M, Pacher P, Bátkai S, Osei-Hyiaman D, Offertáler L, Mo FM, Liu J, and Kunos G (2005) Evidence for novel cannabinoid receptors. *Pharmacol Ther* **106**:133–45.

Bence K, Ma W, Kozasa T, and Huang XY (1997) Direct stimulation of Bruton's tyrosine kinase by G(q)-protein alpha-subunit. *Nature* **389**:296–9.

Berger J, and Moller DE (2002) The mechanisms of action of PPARs. *Annu Rev Med* **53**:409–35.

Berridge MJ, Bootman MD, and Lipp P (1998) Calcium-a life and death signal. *Nature* **395**:645–8.

Berridge MJ, Bootman MD, and Roderick HL (2003) Calcium signalling: dynamics, homeostasis and remodelling. *Nat Rev Mol Cell Biol* **4**:517–29.

Billah MM, and Lapetina EG (1982) Formation of lysophosphatidylinositol in platelets stimulated with thrombin or ionophore A23187. *J Biol Chem* **257**:5196–200.

Bird GSJ, and Putney JW (2005) Capacitative calcium entry supports calcium oscillations in human embryonic kidney cells. *J Physiol* **562**:697–706.

Bisogno T, Howell F, Williams G, Minassi A, Cascio MG, Ligresti A, Matias I, Schiano-Moriello A, Paul P, Williams E-J, Gangadharan U, Hobbs C, Di Marzo V, and Doherty P (2003) Cloning of the first sn1-DAG lipases points to the spatial and temporal regulation of endocannabinoid signaling in the brain. *J Cell Biol* **163**:463–8.

Bisogno T, Melck D, Bobrov MYu, Gretskaya NM, Bezuglov V V, De Petrocellis L, and Di Marzo V (2000) N-acyl-dopamines: novel synthetic CB(1) cannabinoid-receptor ligands and inhibitors of anandamide inactivation with cannabimimetic activity in vitro and in vivo. *Biochem J* **351 Pt 3**:817–24.

Blondeau N, Lauritzen I, Widmann C, Lazdunski M, and Heurteaux C (2002) A potent protective role of lysophospholipids against global cerebral ischemia and glutamate excitotoxicity in neuronal cultures. *J Cereb Blood Flow Metab* **22**:821–34.

Bondarenko A, Waldeck-Weiermair M, Naghdi S, Poteser M, Malli R, and Graier WF (2010) GPR55-dependent and -independent ion signalling in response to lysophosphatidylinositol in endothelial cells. *Br J Pharmacol* **161**:308–20.

Bondarenko AI, Malli R, and Graier WF (2011) The GPR55 agonist lysophosphatidylinositol acts as an intracellular messenger and bidirectionally modulates Ca^{2+} -activated large-conductance K^{+} channels in endothelial cells. *Pflugers Arch* **461**:177–89.

Bondarenko AI, Malli R, and Graier WF (2011) The GPR55 agonist lysophosphatidylinositol directly activates intermediate-conductance Ca^{2+} -activated K^{+} channels. *Pflugers Arch* **462**:245–55.

Bononi A, Agnoletto C, De Marchi E, Marchi S, Patergnani S, Bonora M, Giorgi C, Missiroli S, Poletti F, Rimessi A, and Pinton P (2011) Protein kinases and phosphatases in the control of cell fate. *Enzyme Res* **2011**:329098.

Bonventre J V (1992) Phospholipase A_2 and signal transduction. *J Am Soc Nephrol* **3**:128–50.

Bootman MD, Collins TJ, Peppiatt CM, Prothero LS, MacKenzie L, De Smet P, Travers M, Tovey SC, Seo JT, Berridge MJ, Ciccolini F, and Lipp P (2001) Calcium signalling--an overview. *Semin Cell Dev Biol* **12**:3–10.

Bosier B, and Hermans E (2007) Versatility of GPCR recognition by drugs: from biological implications to therapeutic relevance. *Trends Pharmacol Sci* **28**:438–46.

Bosier B, Hermans E, and Lambert D (2008) Differential modulation of AP-1- and CRE-driven transcription by cannabinoid agonists emphasizes functional selectivity at the CB1 receptor. *Br J Pharmacol* **155**:24–33.

Bosier B, Muccioli GG, Hermans E, and Lambert DM (2010) Functionally selective cannabinoid receptor signalling: therapeutic implications and opportunities. *Biochem Pharmacol* **80**:1–12.

Boyer JL, Waldo GL, and Harden TK (1992) Beta gamma-subunit activation of G-protein-regulated phospholipase C. *J Biol Chem* **267**:25451–6.

Bradshaw HB, Lee SH, and McHugh D (2009) Orphan endogenous lipids and orphan GPCRs: a good match. *Prostaglandins Other Lipid Mediat* **89**:131–4.

Bradshaw HB, Rimmerman N, Hu SS-J, Benton VM, Stuart JM, Masuda K, Cravatt BF, O'Dell DK, and Walker JM (2009) The endocannabinoid anandamide is a precursor for the signaling lipid N-arachidonoyl glycine by two distinct pathways. *BMC Biochem* **10**:14.

Breen C, Brownjohn PW, and Ashton JC (2012) The atypical cannabinoid O-1602 increases hind paw sensitisation in the chronic constriction injury model of neuropathic pain. *Neurosci Lett* **508**:119–22.

Breivogel CS, Griffin G, Di Marzo V, and Martin BR (2001) Evidence for a new G protein-coupled cannabinoid receptor in mouse brain. *Mol Pharmacol* **60**:155–63.

Brindley DN, and Pilquil C (2009) Lipid phosphate phosphatases and signaling. *J Lipid Res* **50 Suppl**:S225–30.

Briscoe CP, Tadayyon M, Andrews JL, Benson WG, Chambers JK, Eilert MM, Ellis C, Elshourbagy NA, Goetz AS, Minnick DT, Murdock PR, Sauls HR, Shabon U, Spinage LD, Strum JC, Szekeres PG, Tan KB, Way JM, Ignar DM, Wilson S, and Muir AI (2003) The orphan G protein-coupled receptor GPR40 is activated by medium and long chain fatty acids. *J Biol Chem* **278**:11303–11.

Brown AJ (2007) Novel cannabinoid receptors. *Br J Pharmacol* **152**:567–75.

Brown AJ, Goldsworthy SM, Barnes A a, Eilert MM, Tcheang L, Daniels D, Muir AI, Wigglesworth MJ, Kinghorn I, Fraser NJ, Pike NB, Strum JC, Steplewski KM, Murdock PR, Holder JC, Marshall FH, Szekeres PG, Wilson S, Ignar DM, Foord SM, Wise A, and Dowell SJ (2003) The Orphan G protein-coupled receptors GPR41 and GPR43 are activated by propionate and other short chain carboxylic acids. *J Biol Chem* **278**:11312–9.

Brown AJ, Wise A, (2001) Identification of modulators of GPR55 activity, Patent number 2001. WO/2001/086305

Bugaj V, Alexeenko V, Zubov A, Glushankova L, Nikolaev A, Wang Z, Kaznacheyeva E, Bezprozvanny I, and Mozhayeva GN (2005) Functional properties of endogenous receptor- and store-operated calcium influx channels in HEK293 cells. *J Biol Chem* **280**:16790–7.

Buhl AM, Johnson NL, Dhanasekaran N, and Johnson GL (1995) G alpha 12 and G alpha 13 stimulate Rho-dependent stress fiber formation and focal adhesion assembly. *J Biol Chem* **270**:24631–4.

Bunzow JR, Van Tol HH, Grandy DK, Albert P, Salon J, Christie M, Machida CA, Neve KA, and Civelli O (1988) Cloning and expression of a rat D_2 dopamine receptor cDNA. *Nature* **336**:783–7.

Burridge K, and Chrzanowska-Wodnicka M (1996) Focal adhesions, contractility, and signaling. *Annu Rev Cell Dev Biol* **12**:463–518.

Burstein SH, McQuain CA, Ross AH, Salmonsen RA, and Zurier RE (2011) Resolution of inflammation by N-arachidonoylglycine. *J Cell Biochem* **112**:3227–33.

Burstein SH, Rossetti RG, Yagen B, and Zurier RB (2000) Oxidative metabolism of anandamide. *Prostaglandins Other Lipid Mediat* **61**:29–41.

Cadas H, di Tomaso E, and Piomelli D (1997) Occurrence and biosynthesis of endogenous cannabinoid precursor, N-arachidonoyl phosphatidylethanolamine, in rat brain. *J Neurosci* **17**:1226–42.

Cadas H, Gaillet S, Beltramo M, Venance L, and Piomelli D (1996) Biosynthesis of an endogenous cannabinoid precursor in neurons and its control by calcium and cAMP. *J Neurosci* **16**:3934–42.

Caldwell MD, Hu SS-J, Viswanathan S, Bradshaw H, Kelly MEM, and Straiker A (2013) A GPR18-based signalling system regulates IOP in murine eye. *Br J Pharmacol* **169**:834–43.

Cantarella G, Scollo M, Lempereur L, Saccani-Jotti G, Basile F, and Bernardini R (2011) Endocannabinoids inhibit release of nerve growth factor by inflammation-activated mast cells. *Biochem Pharmacol* **82**:380–8.

Carafoli E (2003) The calcium-signalling saga: tap water and protein crystals. *Nat Rev Mol Cell Biol* **4**:326–32.

Carisey A, and Ballestrem C (2011) Vinculin, an adapter protein in control of cell adhesion signalling. *Eur J Cell Biol* **90**:157–63.

Carisey A, Tsang R, Greiner AM, Nijenhuis N, Heath N, Nazgiewicz A, Kemkemer R, Derby B, Spatz J, and Ballestrem C (2013) Vinculin regulates the recruitment and release of core focal adhesion proteins in a force-dependent manner. *Curr Biol* **23**:271–81.

Carlezon WA, Duman RS, and Nestler EJ (2005) The many faces of CREB. *Trends Neurosci* **28**:436–45.

Carlisle SJ, Marciano-Cabral F, Staab A, Ludwick C, and Cabral GA (2002) Differential expression of the CB_2 cannabinoid receptor by rodent macrophages and macrophage-like cells in relation to cell activation. *Int Immunopharmacol* **2**:69–82.

Caron MG, Srinivasan Y, Pitha J, Kociolek K, and Lefkowitz RJ (1979) Affinity chromatography of the beta-adrenergic receptor. *J Biol Chem* **254**:2923–7.

Caterina MJ, Schumacher M, Tominaga M, Rosen T, Levine JD, and Julius D (1997) The capsaicin receptor: a heat-activated ion channel in the pain pathway. *Nature* **389**:816–24.

Cavuoto P, McAinch AJ, Hatzinikolas G, Janovská A, Game P, and Wittert G (2007) The expression of receptors for endocannabinoids in human and rodent skeletal muscle. *Biochem Biophys Res Commun* **364**:105–10.

Cescato R, Loesch KA, Waser B, Mäcke HR, Rivier JE, Reubi JC, and Schonbrunn A (2010) Agonist-biased signaling at the sst2A receptor: the multi-somatostatin analogs KE108 and SOM230 activate and antagonize distinct signaling pathways. *Mol Endocrinol* **24**:240–9.

Cha-Molstad H, Keller DM, Yochum GS, Impey S, and Goodman RH (2004) Cell-type-specific binding of the transcription factor CREB to the cAMP-response element. *Proc Natl Acad Sci U S A* **101**:13572–7.

Chaturvedi S, and Driscoll W (2006) In vivo evidence that N-oleoylglycine acts independently of its conversion to oleamide. *Prostaglandins other …* **81**:136–149.

Chawla S, and Bading H (2001) CREB/CBP and SRE-interacting transcriptional regulators are fast on-off switches: duration of calcium transients specifies the magnitude of transcriptional responses. *J Neurochem* **79**:849–58.

Chen H, Choudhury DM, and Craig SW (2006) Coincidence of actin filaments and talin is required to activate vinculin. *J Biol Chem* **281**:40389–98.

Cheng KT, Liu X, Ong HL, Swaim W, and Ambudkar IS (2011) Local Ca^{2+} entry via Orai1 regulates plasma membrane recruitment of TRPC1 and controls cytosolic Ca^{2+} signals required for specific cell functions. *PLoS Biol* **9**:e1001025.

Chikumi H, Vázquez-Prado J, Servitja J-M, Miyazaki H, and Gutkind JS (2002) Potent activation of RhoA by Galpha q and G_q-coupled receptors. *J Biol Chem* **277**:27130–4.

Christerson LB, Gallagher E, Vanderbilt CA, Whitehurst AW, Wells C, Kazempour R, Sternweis PC, and Cobb MH (2002) p115 Rho GTPase activating protein interacts with MEKK1. *J Cell Physiol* **192**:200–8.

Chrivia JC, Kwok RP, Lamb N, Hagiwara M, Montminy MR, and Goodman RH (1993) Phosphorylated CREB binds specifically to the nuclear protein CBP. *Nature* **365**:855–9.

Civelli O, Reinscheid RK, Zhang Y, Wang Z, Fredriksson R, and Schiöth HB (2013) G protein-coupled receptor deorphanizations. *Annu Rev Pharmacol Toxicol* **53**:127–46.

Clapham DE (2007) Calcium signaling. *Cell* **131**:1047–58.

Clarke WP, and Bond RA (1998) The elusive nature of intrinsic efficacy. *Trends Pharmacol Sci* **19**:270–6.

Coffa S, Breitman M, Hanson SM, Callaway K, Kook S, Dalby KN, and Gurevich VV (2011) The effect of arrestin conformation on the recruitment of c-Raf1, MEK1, and ERK1/2 activation. *PLoS One* **6**:e28723.

Cohen P (2010) Guidelines for the effective use of chemical inhibitors of protein function to understand their roles in cell regulation. *Biochem J* **425**:53–4.

Cohen P, Klumpp S, and Schelling DL (1989) An improved procedure for identifying and quantitating protein phosphatases in mammalian tissues. *FEBS Lett* **250**:596–600.

Cohen-Yeshurun A, Trembovler V, Alexandrovich A, Ryberg E, Greasley PJ, Mechoulam R, Shohami E, and Leker RR (2011) N-arachidonoyl-L-serine is neuroprotective after traumatic brain injury by reducing apoptosis. *J Cereb Blood Flow Metab* **31**:1768–77.

Cohen-Yeshurun A, Willner D, Trembovler V, Alexandrovich A, Mechoulam R, Shohami E, and Leker RR (2013) N-arachidonoyl-L-serine (AraS) possesses proneurogenic properties in vitro and in vivo after traumatic brain injury. *J Cereb Blood Flow Metab* **33**:1242–50.

Colton CK, and Zhu MX (2007) 2-Aminoethoxydiphenyl borate as a common activator of TRPV1, TRPV2, and TRPV3 channels. *Handb Exp Pharmacol* 173–87.

Costa B, Giagnoni G, Franke C, Trovato AE, and Colleoni M (2004) Vanilloid $TRPV_1$ receptor mediates the antihyperalgesic effect of the nonpsychoactive cannabinoid, cannabidiol, in a rat model of acute inflammation. *Br J Pharmacol* **143**:247–50.

Costanzi S, Neumann S, and Gershengorn MC (2008) Seven transmembrane-spanning receptors for free fatty acids as therapeutic targets for diabetes mellitus: pharmacological, phylogenetic, and drug discovery aspects. *J Biol Chem* **283**:16269–73.

Coutts AA, Irving AJ, Mackie K, Pertwee RG, and Anavi-Goffer S (2002) Localisation of cannabinoid CB_1 receptor immunoreactivity in the guinea pig and rat myenteric plexus. *J Comp Neurol* **448**:410–22.

Cramer LP, Siebert M, and Mitchison TJ (1997) Identification of novel graded polarity actin filament bundles in locomoting heart fibroblasts: implications for the generation of motile force. *J Cell Biol* **136**:1287–305.

Cravatt BF, and Lichtman AH (2002) The enzymatic inactivation of the fatty acid amide class of signaling lipids. *Chem Phys Lipids* **121**:135–48.

Cristino L, de Petrocellis L, Pryce G, Baker D, Guglielmotti V, and Di Marzo V (2006) Immunohistochemical localization of cannabinoid type 1 and vanilloid transient receptor potential vanilloid type 1 receptors in the mouse brain. *Neuroscience* **139**:1405–15.

Daaka Y, Luttrell LM, Ahn S, Della Rocca GJ, Ferguson SS, Caron MG, and Lefkowitz RJ (1998) Essential role for G protein-coupled receptor endocytosis in the activation of mitogen-activated protein kinase. *J Biol Chem* **273**:685–8.

Dainese E, De Fabritiis G, Sabatucci A, Oddi S, Angelucci CB, Di Pancrazio C, Giorgino T, Stanley N, Del Carlo M, Cravatt B, and Maccarrone M (2014) Membrane lipids are key-modulators of the endocannabinoid-hydrolase FAAH. *Biochem J*, **457**(3):463-72.

Daly CJ, Ross RA, Whyte J, Henstridge CM, Irving AJ, and McGrath JC (2010) Fluorescent ligand binding reveals heterogeneous distribution of adrenoceptors and “cannabinoid-like” receptors in small arteries. *Br J Pharmacol* **159**:787–96.

Damke H, Baba T, Warnock DE, and Schmid SL (1994) Induction of mutant dynamin specifically blocks endocytic coated vesicle formation. *J Cell Biol* **127**:915–34.

Dargan SL, and Parker I (2003) Buffer kinetics shape the spatiotemporal patterns of IP_3-evoked Ca^{2+} signals. *J Physiol* **553**:775–88.

Das S, Tosaki A, Bagchi D, Maulik N, and Das DK (2005) Resveratrol-mediated activation of cAMP response element-binding protein through adenosine A3 receptor by Akt-dependent and -independent pathways. *J Pharmacol Exp Ther* **314**:762–9.

Dash PK, Karl KA, Colicos MA, Prywes R, and Kandel ER (1991) cAMP response element-binding protein is activated by Ca^{2+}/calmodulin- as well as cAMP-dependent protein kinase. *Proc Natl Acad Sci U S A* **88**:5061–5.

Davies SP, Reddy H, Caivano M, and Cohen P (2000) Specificity and mechanism of action of some commonly used protein kinase inhibitors. *Biochem J* **351**:95–105.

De Petrocellis L, Bisogno T, Maccarrone M, Davis JB, Finazzi-AgroA, and Di Marzo V (2001) The activity of anandamide at vanilloid VR1 receptors requires facilitated transport across the cell membrane and is limited by intracellular metabolism. *J Biol Chem* **276**:12856–63.

Delom F, and Fessart D (2011) Role of Phosphorylation in the Control of Clathrin-Mediated Internalization of GPCR. *Int J Cell Biol* **2011**:246954.

Devane WA, Dysarz FA, Johnson MR, Melvin LS, and Howlett AC (1988) Determination and characterization of a cannabinoid receptor in rat brain. *Mol Pharmacol* **34**:605–13.

Devane WA, Hanus L, Breuer A, Pertwee RG, Stevenson LA, Griffin G, Gibson D, Mandelbaum A, Etinger A, and Mechoulam R (1992) Isolation and structure of a brain constituent that binds to the cannabinoid receptor. *Science* **258**:1946–9.

DeWire SM, Kim J, Whalen EJ, Ahn S, Chen M, and Lefkowitz RJ (2008) Beta-arrestin-mediated signaling regulates protein synthesis. *J Biol Chem* **283**:10611–20.

Di Marzo V, Breivogel CS, Tao Q, Bridgen DT, Razdan RK, Zimmer AM, and Martin BR (2000) Levels, metabolism, and pharmacological activity of anandamide in CB_1 cannabinoid receptor knockout mice: evidence for non-CB_1, non-CB_2 receptor-mediated actions of anandamide in mouse brain. *J Neurochem* **75**:2434–44.

Di Marzo V, Fontana A, Cadas H, Schinelli S, Cimino G, Schwartz JC, and Piomelli D (1994) Formation and inactivation of endogenous cannabinoid anandamide in central neurons. *Nature* **372**:686–91.

Díaz-Arteaga a, Vázquez MJ, Vazquez-Martínez R, Pulido MR, Suarez J, Velásquez D a, López M, Ross R a, de Fonseca FR, Bermudez-Silva FJ, Malagón MM, Diéguez C, and Nogueiras R (2012) The atypical cannabinoid O-1602 stimulates food intake and adiposity in rats. *Diabetes Obes Metab* **14**:234–43.

Dinh TP, Carpenter D, Leslie FM, Freund TF, Katona I, Sensi SL, Kathuria S, and Piomelli D (2002) Brain monoglyceride lipase participating in endocannabinoid inactivation. *Proc Natl Acad Sci U S A* **99**:10819–24.

Dixon RA, Kobilka BK, Strader DJ, Benovic JL, Dohlman HG, Frielle T, Bolanowski MA, Bennett CD, Rands E, Diehl RE, Mumford RA, Slater EE, Sigal IS, Caron MG, Lefkowitz RJ, and Strader CD (1986) Cloning of the gene and cDNA for mammalian beta-adrenergic receptor and homology with rhodopsin. *Nature* **321**:75–9.

Dolmetsch RE, Xu K, and Lewis RS (1998) Calcium oscillations increase the efficiency and specificity of gene expression. *Nature* **392**:933–6.

Dorsam RT, and Gutkind JS (2007) G-protein-coupled receptors and cancer. *Nat Rev Cancer* **7**:79–94.

Drmota T, Greasley P, Groblewski T. AstraZeneca (2004) Screening assays for cannabinoid-ligand-type modulators of GPR55, Patent WO2004/074844.

Du K, and Montminy M (1998) CREB is a regulatory target for the protein kinase Akt/PKB. *J Biol Chem* **273**:32377–9.

Dugourd C, Gervais M, Corvol P, and Monnot C (2003) Akt is a major downstream target of PI3-kinase involved in angiotensin II-induced proliferation. *Hypertension* **41**:882–90.

Dumbauld DW, Shin H, Gallant ND, Michael KE, Radhakrishna H, and García AJ (2010) Contractility modulates cell adhesion strengthening through focal adhesion kinase and assembly of vinculin-containing focal adhesions. *J Cell Physiol* **223**:746–56.

Endlich N, Otey CA, Kriz W, and Endlich K (2007) Movement of stress fibers away from focal adhesions identifies focal adhesions as sites of stress fiber assembly in stationary cells. *Cell Motil Cytoskeleton* **64**:966–76.

Euskirchen G, Royce TE, Bertone P, Martone R, Rinn JL, Nelson FK, Sayward F, Luscombe NM, Miller P, Gerstein M, Weissman S, and Snyder M (2004) CREB binds to multiple loci on human chromosome 22. *Mol Cell Biol* **24**:3804–14.

Falasca M, and Corda D (1993) Accumulation and mitogenic activity of lysophosphatidylinositol in k-ras-transformed thyroid cells., in *Mol Oncol Clin Appl* pp 165–171.

Falasca M, and Corda D (1994) Elevated levels and mitogenic activity of lysophosphatidylinositol in k-ras-transformed epithelial cells. *Eur J Biochem* **221**:383–9.

Falasca M, Iurisci C, Carvelli A, Sacchetti A, and Corda D (1998) Release of the mitogen lysophosphatidylinositol from H-Ras-transformed fibroblasts; a possible mechanism of autocrine control of cell proliferation. *Oncogene* **16**:2357–65.

Falasca M, Logan SK, Lehto VP, Baccante G, Lemmon MA, and Schlessinger J (1998) Activation of phospholipase C gamma by PI 3-kinase-induced PH domain-mediated membrane targeting. *EMBO J* **17**:414–22.

Fargin A, Raymond JR, Lohse MJ, Kobilka BK, Caron MG, and Lefkowitz RJ (1988) The genomic clone G-21 which resembles a beta-adrenergic receptor sequence encodes the 5-HT1A receptor, *Nature*, **335** (6188): 358-360.

Faure M, Voyno-Yasenetskaya TA, and Bourne HR (1994) cAMP and beta gamma subunits of heterotrimeric G proteins stimulate the mitogen-activated protein kinase pathway in COS-7 cells. *J Biol Chem* **269**:7851–4.

Feske S, Gwack Y, Prakriya M, Srikanth S, Puppel S-H, Tanasa B, Hogan PG, Lewis RS, Daly M, and Rao A (2006) A mutation in Orai1 causes immune deficiency by abrogating CRAC channel function. *Nature* **441**:179–85.

Fezza F, Bisogno T, Minassi A, Appendino G, Mechoulam R, and Di Marzo V (2002) Noladin ether, a putative novel endocannabinoid: inactivation mechanisms and a sensitive method for its quantification in rat tissues. *FEBS Lett* **513**:294–8.

Finch EA, Turner TJ, and Goldin SM (1991) Calcium as a Coagonist of Inositol 1 , 4 , 5-Trisphosphate-Induced Calcium Release. *Science (80-)* **252**:443–446.

Fincham VJ, James M, Frame MC, and Winder SJ (2000) Active ERK/MAP kinase is targeted to newly forming cell-matrix adhesions by integrin engagement and v-Src. *EMBO J* **19**:2911–23.

Flemming PK, Dedman AM, Xu S-Z, Li J, Zeng F, Naylor J, Benham CD, Bateson AN, Muraki K, and Beech DJ (2006) Sensing of lysophospholipids by $TRPC_5$ calcium channel. *J Biol Chem* **281**:4977–82.

Ford LA, Roelofs AJ, Anavi-Goffer S, Mowat L, Simpson DG, Irving AJ, Rogers MJ, Rajnicek AM, and Ross RA (2010) A role for L-alpha-lysophosphatidylinositol and GPR55 in the modulation of migration, orientation and polarization of human breast cancer cells. *Br J Pharmacol* **160**:762–71.

Fowler CJ (2013) Transport of endocannabinoids across the plasma membrane and within the cell. *FEBS J* **280**:1895–904.

Fredriksson R, Lagerström MC, Lundin L-G, and Schiöth HB (2003) The G-protein-coupled receptors in the human genome form five main families. Phylogenetic analysis, paralogon groups, and fingerprints. *Mol Pharmacol* **63**:1256–72.

Fresno Vara JA, Casado E, de Castro J, Cejas P, Belda-Iniesta C, and González-Barón M (2004) PI3K/Akt signalling pathway and cancer. *Cancer Treat Rev* **30**:193–204.

Fu J, Gaetani S, Oveisi F, Lo Verme J, Serrano A, Rodríguez De Fonseca F, Rosengarth A, Luecke H, Di Giacomo B, Tarzia G, and Piomelli D (2003) Oleylethanolamide regulates feeding and body weight through activation of the nuclear receptor PPAR-alpha. *Nature* **425**:90–3.

Fujisawa K, Fujita A, Ishizaki T, Saito Y, and Narumiya S (1996) Identification of the Rho-binding domain of p160ROCK, a Rho-associated coiled-coil containing protein kinase. *J Biol Chem* **271**:23022–8.

Gagnon a. W, Kallal L, and Benovic JL (1998) Role of clathrin-mediated endocytosis in agonist-induced down-regulation of the beta2-adrenergic receptor. *J Biol Chem* **273**:6976–81.

Galán C, Dionisio N, Smani T, Salido GM, and Rosado JA (2011) The cytoskeleton plays a modulatory role in the association between STIM1 and the Ca^{2+} channel subunits Orai1 and TRPC1. *Biochem Pharmacol* **82**:400–10.

Galandrin S, Oligny-Longpré G, and Bouvier M (2007) The evasive nature of drug efficacy: implications for drug discovery. *Trends Pharmacol Sci* **28**:423–30.

Galiègue S, Mary S, Marchand J, Dussossoy D, Carrière D, Carayon P, Bouaboula M, Shire D, Le Fur G, and Casellas P (1995) Expression of central and peripheral cannabinoid receptors in human immune tissues and leukocyte subpopulations. *Eur J Biochem* **232**:54–61.

Gallagher ED, Gutowski S, Sternweis PC, and Cobb MH (2004) RhoA binds to the amino terminus of MEKK1 and regulates its kinase activity. *J Biol Chem* **279**:1872–7.

Gangadharan V, Selvaraj D, Kurejova M, Njoo C, Gritsch S, Skoricová D, Horstmann H, Offermanns S, Brown AJ, Kuner T, Tappe-Theodor A, and Kuner R (2013) A novel biological role for the phospholipid lysophosphatidylinositol in nociceptive sensitization via activation of diverse G-protein signaling pathways in sensory nerves in vivo. *Pain*, **154**(12):2801-12.

Ganong BR, Loomis CR, Hannun YA, and Bell RM (1986) Specificity and mechanism of protein kinase C activation by sn-1,2-diacylglycerols. *Proc Natl Acad Sci U S A* **83**:1184–8.

Gao Y, Vasilyev D V, Goncalves MB, Howell F V, Hobbs C, Reisenberg M, Shen R, Zhang M-Y, Strassle BW, Lu P, Mark L, Piesla MJ, Deng K, Kouranova E V, Ring RH, Whiteside GT, Bates B, Walsh FS, Williams G, Pangalos MN, Samad TA, and Doherty P (2010) Loss of retrograde endocannabinoid signaling and reduced adult neurogenesis in diacylglycerol lipase knock-out mice. *J Neurosci* **30**:2017–24.

Gaoni Y, and Mechoulam R (1964) Isolation, Structure, and Partial Synthesis of an Active Constituent of Hashish. *J Am Chem Soc* **86**:1646–1647.

Garland SL (2013) Are GPCRs Still a Source of New Targets? *J Biomol Screen* **18**:947–66.

Gavet O, and Pines J (2010) Progressive activation of CyclinB1-Cdk1 coordinates entry to mitosis. *Dev Cell* **18**:533–43.

Georgieva T, Devanathan S, Stropova D, Park CK, Salamon Z, Tollin G, Hruby VJ, Roeske WR, Yamamura HI, and Varga E (2008) Unique agonist-bound cannabinoid CB1 receptor conformations indicate agonist specificity in signaling. *Eur J Pharmacol* **581**:19–29.

Gerard CM, Mollereau IIC, and Parmentier M (1991) Molecular cloning of a human cannabinoid receptor which is also expressed in testis. *Biochem J* **279**:129–134.

Godlewski G, Offertáler L, Osei-Hyiaman D, Mo FM, Harvey-White J, Liu J, Davis MI, Zhang L, Razdan RK, Milman G, Pacher P, Mukhopadhyay P, Lovinger DM, and Kunos G (2009) The endogenous brain constituent N-arachidonoyl L-serine is an activator of large conductance Ca^{2+}-activated K^{+} channels. *J Pharmacol Exp Ther* **328**:351–61.

Golech SA, McCarron RM, Chen Y, Bembry J, Lenz F, Mechoulam R, Shohami E, and Spatz M (2004) Human brain endothelium: coexpression and function of vanilloid and endocannabinoid receptors. *Brain Res Mol Brain Res* **132**:87–92.

Gonsiorek W, Lunn C, Fan X, Narula S, Lundell D, and Hipkin RW (2000) Endocannabinoid 2-arachidonyl glycerol is a full agonist through human type 2 cannabinoid receptor: antagonism by anandamide. *Mol Pharmacol* **57**:1045–50.

Gonzalez GA, and Montminy MR (1989) Cyclic AMP stimulates somatostatin gene transcription by phosphorylation of CREB at serine 133. *Cell* **59**:675–80.

Goodman OB, Krupnick JG, Santini F, Gurevich V V, Penn RB, Gagnon AW, Keen JH, and Benovic JL (1996) Beta-arrestin acts as a clathrin adaptor in endocytosis of the beta2-adrenergic receptor. *Nature* **383**:447–50.

Gu T, Zhang Z, Wang J, Guo J, Shen WH, and Yin Y (2011) CREB is a novel nuclear target of PTEN phosphatase. *Cancer Res* **71**:2821–5.

Guo J, Williams DJ, and Ikeda SR (2008) N-arachidonoyl L-serine, a putative endocannabinoid, alters the activation of N-type Ca^{2+} channels in sympathetic neurons. *J Neurophysiol* **100**:1147–51.

Gurevich E V, Tesmer JJG, Mushegian A, and Gurevich VV (2012) G protein-coupled receptor kinases: more than just kinases and not only for GPCRs. *Pharmacol Ther* **133**:40–69.

Hagiwara M, Alberts A, Brindle P, Meinkoth J, Feramisco J, Deng T, Karin M, Shenolikar S, and Montminy M (1992) Transcriptional attenuation following cAMP induction requires PP-1-mediated dephosphorylation of CREB. *Cell* **70**:105–13.

Hains MD, Wing MR, Maddileti S, Siderovski DP, and Harden TK (2006) Galpha12/13- and rho-dependent activation of phospholipase C-epsilon by lysophosphatidic acid and thrombin receptors. *Mol Pharmacol* **69**:2068–75.

Hall A (1998) Rho GTPases and the Actin Cytoskeleton. *Science (80-)* **279**:509–514.

Hall B, Limaye A, and Kulkarni AB (2009) Overview: generation of gene knockout mice. *Curr Protoc Cell Biol* **Chapter 19**:Unit 19.12 19.12.1–17.

Hannedouche SE RM (2010) US Patent Application, Patent number US 7,824,866 B2.

Hansen HS, Rosenkilde MM, Holst JJ, and Schwartz TW (2012) GPR119 as a fat sensor. *Trends Pharmacol Sci* **33**:374–81.

Hanus L, Abu-Lafi S, Fride E, Breuer a, Vogel Z, Shalev DE, Kustanovich I, and Mechoulam R (2001) 2-arachidonyl glyceryl ether, an endogenous agonist of the cannabinoid CB1 receptor. *Proc Natl Acad Sci U S A* **98**:3662–5.

Hanus LO (2009) Pharmacological and therapeutic secrets of plant and brain (endo)cannabinoids. *Med Res Rev* **29**:213–71.

Hart MJ, Jiang X, Kozasa T, Roscoe W, Singer WD, Gilman AG, Sternweis PC, and Bollag G (1998) Direct stimulation of the guanine nucleotide exchange activity of p115 RhoGEF by Galpha13. *Science* **280**:2112–4.

Heng BC, Aubel D, and Fussenegger M (2013) An overview of the diverse roles of G-protein coupled receptors (GPCRs) in the pathophysiology of various human diseases. *Biotechnol Adv* **31**:1676–1694.

Henstridge CM, Balenga NAB, Ford LA, Ross RA, Waldhoer M, and Irving AJ (2009) The GPR55 ligand L-alpha-lysophosphatidylinositol promotes RhoA-dependent Ca^{2+} signaling and NFAT activation. *FASEB J* **23**:183–93.

Henstridge CM, Balenga NA, Schröder R, Kargl JK, Platzer W, Martini L, Arthur S, Penman J, Whistler JL, Kostenis E, Waldhoer M, and Irving AJ (2010) GPR55 ligands promote receptor coupling to multiple signalling pathways. *Br J Pharmacol* **160**:604–14.

Herkenham M, Lynn AB, Little MD, Johnson MR, Melvin LS, de Costa BR, and Rice KC (1990) Cannabinoid receptor localization in brain. *Proc Natl Acad Sci U S A* **87**:1932–6.

Hermans E (2003) Biochemical and pharmacological control of the multiplicity of coupling at G-protein-coupled receptors. *Pharmacol Ther* **99**:25–44.

Hollinger S, and Hepler JR (2002) Cellular regulation of RGS proteins: modulators and integrators of G protein signaling. *Pharmacol Rev* **54**:527–59.

Howlett AC, Barth F, Bonner TI, Cabral G, Casellas P, Devane WA, Felder CC, Herkenham M, Mackie K, Martin BR, Mechoulam R, and Pertwee RG (2002) International Union of Pharmacology. XXVII. Classification of cannabinoid receptors. *Pharmacol Rev* **54**:161–202.

Hu C, van der Heijden R, Wang M, van der Greef J, Hankemeier T, and Xu G (2009) Analytical strategies in lipidomics and applications in disease biomarker discovery. *J Chromatogr B Analyt Technol Biomed Life Sci* **877**:2836–46.

Huang L, Ramirez JC, Frampton GA, Golden LE, Quinn MA, Pae HY, Horvat D, Liang L, and DeMorrow S (2011) Anandamide exerts its antiproliferative actions on cholangiocarcinoma by activation of the GPR55 receptor. *Lab Invest* **91**:1007–17.

Huang SM, Bisogno T, Petros TJ, Chang SY, Zavitsanos P a, Zipkin RE, Sivakumar R, Coop A, Maeda DY, De Petrocellis L, Burstein S, Di Marzo V, and Walker JM (2001) Identification of a new class of molecules, the arachidonyl amino acids, and characterization of one member that inhibits pain. *J Biol Chem* **276**:42639–44.

Huang SM, Bisogno T, Trevisani M, Al-Hayani A, De Petrocellis L, Fezza F, Tognetto M, Petros TJ, Krey JF, Chu CJ, Miller JD, Davies SN, Geppetti P, Walker JM, and Di Marzo V (2002) An endogenous capsaicin-like substance with high potency at recombinant and native vanilloid VR1 receptors. *Proc Natl Acad Sci U S A* **99**:8400–5.

Hubbard KB, and Hepler JR (2006) Cell signalling diversity of the Gqalpha family of heterotrimeric G proteins. *Cell Signal* **18**:135–50.

Hudson BD, Hébert TE, and Kelly MEM (2010) Ligand- and heterodimer-directed signaling of the CB_1 cannabinoid receptor. *Mol Pharmacol* **77**:1–9.

Humphries JD, Wang P, Streuli C, Geiger B, Humphries MJ, and Ballestrem C (2007) Vinculin controls focal adhesion formation by direct interactions with talin and actin. *J Cell Biol* **179**:1043–57.

Hunter T (1995) Protein kinases and phosphatases: the yin and yang of protein phosphorylation and signaling. *Cell* **80**:225–36.

Ichimura A, Hirasawa A, Poulain-Godefroy O, Bonnefond A, Hara T, Yengo L, Kimura I, Leloire A, Liu N, Iida K, Choquet H, Besnard P, Lecoeur C, Vivequin S, Ayukawa K, Takeuchi M, Ozawa K, Tauber M, Maffeis C, Morandi A, Buzzetti R, Elliott P, Pouta A, Jarvelin M-R, Körner A, Kiess W, Pigeyre M, Caiazzo R, Van Hul W, Van Gaal L, Horber F, Balkau B, Lévy-Marchal C, Rouskas K, Kouvatsi A, Hebebrand J, Hinney A, Scherag A, Pattou F, Meyre D, Koshimizu T, Wolowczuk I, Tsujimoto G, and Froguel P (2012) Dysfunction of lipid sensor GPR120 leads to obesity in both mouse and human. *Nature* **483**:350–4.

Impey S, Obrietan K, Wong ST, Poser S, Yano S, Wayman G, Deloulme JC, Chan G, and Storm DR (1998) Cross talk between ERK and PKA is required for Ca^{2+} stimulation of CREB-dependent transcription and ERK nuclear translocation. *Neuron* **21**:869–83.

Ishii I, Fukushima N, Ye X, and Chun J (2004) Lysophospholipid receptors: signaling and biology. *Annu Rev Biochem* **73**:321–54.

Ishii S, Noguchi K, and Yanagida K (2009) Non-Edg family lysophosphatidic acid (LPA) receptors. *Prostaglandins Other Lipid Mediat* **89**:57–65.

Ishizaki T, Uehata M, Tamechika I, Keel J, Nonomura K, Maekawa M, and Narumiya S (2000) Pharmacological properties of Y-27632, a specific inhibitor of Rho-associated kinases. *Mol Pharmacol* **57**:976–83.

Iversen L (2003) Cannabis and the brain. *Brain* **126**:1252–1270.

Jacoby E, Bouhelal R, Gerspacher M, and Seuwen K (2006) The 7 TM G-protein-coupled receptor target family. *ChemMedChem* **1**:761–82.

Janefjord E, Mååg JL V, Harvey BS, and Smid SD (2013) Cannabinoid Effects on β Amyloid Fibril and Aggregate Formation, Neuronal and Microglial-Activated Neurotoxicity In Vitro. *Cell Mol Neurobiol*, doi: 10.1007/s10571-013-9984-x.

Járai Z, Wagner JA, Varga K, Lake KD, Compton DR, Martin BR, Zimmer AM, Bonner TI, Buckley NE, Mezey E, Razdan RK, Zimmer A, and Kunos G (1999) Cannabinoid-induced mesenteric vasodilation through an endothelial site distinct from CB_1 or CB_2 receptors. *Proc Natl Acad Sci U S A* **96**:14136–41.

Jin X-H, Okamoto Y, Morishita J, Tsuboi K, Tonai T, and Ueda N (2007) Discovery and characterization of a Ca^{2+}-independent phosphatidylethanolamine N-acyltransferase generating the anandamide precursor and its congeners. *J Biol Chem* **282**:3614–23.

Johannessen M, Delghandi MP, and Moens U (2004) What turns CREB on? *Cell Signal* **16**:1211–27.

Johns DG, Behm DJ, Walker DJ, Ao Z, Shapland EM, Daniels DA, Riddick M, Dowell S, Staton PC, Green P, Shabon U, Bao W, Aiyar N, Yue T-L, Brown AJ, MorrisonAD, and Douglas SA (2007) The novel endocannabinoid receptor GPR55 is activated by atypical cannabinoids but does not mediate their vasodilator effects. *Br J Pharmacol* **152**:825–31.

Jones NP, Peak J, Brader S, Eccles SA, and Katan M (2005) PLCgamma1 is essential for early events in integrin signalling required for cell motility. *J Cell Sci* **118**:2695–706.

Jung J, Hwang SW, Kwak J, Lee SY, Kang CJ, Kim WB, Kim D, and Oh U (1999) Capsaicin binds to the intracellular domain of the capsaicin-activated ion channel. *J Neurosci* **19**:529–38.

Kallendrusch S, Kremzow S, Nowicki M, Grabiec U, Winkelmann R, Benz A, Kraft R, Bechmann I, Dehghani F, and Koch M (2013) The G Protein-Coupled Receptor 55 Ligand l-α-Lysophosphatidylinositol Exerts Microglia-Dependent Neuroprotection After Excitotoxic Lesion. *Glia* 1–10.

Kano M, Ohno-Shosaku T, Hashimotodani Y, Uchigashima M, and Watanabe M (2009) Endocannabinoid-mediated control of synaptic transmission. *Physiol Rev* **89**:309–80.

Kaplan BLF, Springs AEB, and Kaminski NE (2008) The profile of immune modulation by cannabidiol (CBD) involves deregulation of nuclear factor of activated T cells (NFAT). *Biochem Pharmacol* **76**:726–37.

Kapur A, Zhao P, Sharir H, Bai Y, Caron MG, Barak LS, and Abood ME (2009) Atypical responsiveness of the orphan receptor GPR55 to cannabinoid ligands. *J Biol Chem* **284**:29817–27.

Kargl J, Brown AJ, Andersen L, Dorn G, Schicho R, Waldhoer M, and Heinemann A (2013) A selective antagonist reveals a potential role of G protein-coupled receptor 55 in platelet and endothelial cell function. *J Pharmacol Exp Ther*, **346** (1):54-66.

Katoh K, Kano Y, Amano M, Kaibuchi K, and Fujiwara K (2001) Stress fiber organization regulated by MLCK and Rho-kinase in cultured human fibroblasts. *Am J Physiol Cell Physiol* **280**:C1669–79.

Katoh K, Kano Y, and Ookawara S (2007) Rho-kinase dependent organization of stress fibers and focal adhesions in cultured fibroblasts. *Genes Cells* **12**:623–38.

Kaverina I, Krylyshkina O, and Small JV (2002) Regulation of substrate adhesion dynamics during cell motility. *Int J Biochem Cell Biol* **34**:746–61.

Kaya H, Patton GM, and Hong SL (1989) Bradykinin-induced activation of phospholipase A_2 is independent of the activation of polyphosphoinositide-hydrolyzing phospholipase C. *J Biol Chem* **264**:4972–7.

Keenan RW, And Hokin LE (1964) The Enzymatic Acylation Of Lysophosphatidylinositol. *J Biol Chem* **239**:2123–9.

Kelley GG, Reks SE, and Smrcka A V (2004) Hormonal regulation of phospholipase Cepsilon through distinct and overlapping pathways involving G_{12} and Ras family G-proteins. *Biochem J* **378**:129–39.

Kelly P, Stemmle LN, Madden JF, Fields TA, Daaka Y, and Casey PJ (2006) A role for the G_{12} family of heterotrimeric G proteins in prostate cancer invasion. *J Biol Chem* **281**:26483–90.

Kenakin T (2011) Functional selectivity and biased receptor signaling. *J Pharmacol Exp Ther* **336**:296–302.

Kenakin T, Watson C, Muniz-Medina V, Christopoulos A, and Novick S (2012) A simple method for quantifying functional selectivity and agonist bias. *ACS Chem Neurosci* **3**:193–203.

Keyse SM (2000) Protein phosphatases and the regulation of mitogen-activated protein kinase signalling. *Curr Opin Cell Biol* **12**:186–92.

Klabunde T, and Hessler G (2002) Drug design strategies for targeting G-protein-coupled receptors. *Chembiochem* **3**:928–44.

Kobayashi T, Kishimoto M, and Okuyama H (1996) Phospholipases involved in lysophosphatidylinositol metabolism in rat brain. *J Lipid Mediat Cell Signal* **14**:33–37.

Kohno M, Hasegawa H, Inoue A, Muraoka M, Miyazaki T, Oka K, and Yasukawa M (2006) Identification of N-arachidonylglycine as the endogenous ligand for orphan G-protein-coupled receptor GPR18. *Biochem Biophys Res Commun* **347**:827–32.

Kondoh K, and Nishida E (2007) Regulation of MAP kinases by MAP kinase phosphatases. *Biochim Biophys Acta* **1773**:1227–37.

Korkiamäki T, Ylä-Outinen H, Koivunen J, and Peltonen J (2003) An intact actin-containing cytoskeleton is required for capacitative calcium entry, but not for ATP-induced calcium-mediated cell signaling in cultured human keratinocytes. *Med Sci Monit* **9**:BR199–207.

Kostenis E, Waelbroeck M, and Milligan G (2005) Techniques: promiscuous Galpha proteins in basic research and drug discovery. *Trends Pharmacol Sci* **26**:595–602.

Kotarsky K, Boketoft A, Bristulf J, Nilsson NE, Norberg A, Hansson S, Owman C, Sillard R, Leeb-Lundberg LMF, and Olde B (2006) Lysophosphatidic acid binds to and activates GPR92, a G protein-coupled receptor highly expressed in gastrointestinal lymphocytes. *J Pharmacol Exp Ther* **318**:619–28.

Kotsikorou E, Sharir H, Shore DM, Hurst DP, Lynch DL, Madrigal KE, Heynen-Genel S, Milan LB, Chung TDY, Seltzman HH, Bai Y, Caron MG, Barak LS, Croatt MP, Abood ME, and Reggio PH (2013) Identification of the GPR55 Antagonist Binding Site Using a Novel Set of High Potency GPR55 Selective Ligands. *Biochemistry*, **52** (52):9456-69.

Kovacs G, Montalbetti N, Simonin A, Danko T, Balazs B, Zsembery A, and Hediger MA (2012) Inhibition of the human epithelial calcium channel $TRPV_6$ by 2-aminoethoxydiphenyl borate (2-APB). *Cell Calcium* **52**:468–80.

Kozak KR, Gupta RA, Moody JS, Ji C, Boeglin WE, DuBois RN, Brash AR, and Marnett LJ (2002) 15-Lipoxygenase metabolism of 2-arachidonylglycerol. Generation of a peroxisome proliferator-activated receptor alpha agonist. *J Biol Chem* **277**:23278–86.

Kozak KR, Rowlinson SW, and Marnett LJ (2000) Oxygenation of the endocannabinoid, 2-arachidonylglycerol, to glyceryl prostaglandins by cyclooxygenase-2. *J Biol Chem* **275**:33744–9.

Kozasa T, Hajicek N, Chow CR, and Suzuki N (2011) Signalling mechanisms of RhoGTPase regulation by the heterotrimeric G proteins G12 and G13. *J Biochem* **150**:357–69.

Kozasa T, Jiang X, Hart MJ, Sternweis PM, Singer WD, Gilman AG, Bollag G, and Sternweis PC (1998) p115 RhoGEF, a GTPase activating protein for Galpha12 and Galpha13. *Science* **280**:2109–11.

Kunkel GT, Maceyka M, Milstien S, and Spiegel S (2013) Targeting the sphingosine-1-phosphate axis in cancer, inflammation and beyond. *Nat Rev Drug Discov* **12**:688–702.

Kwok RP, Lundblad JR, Chrivia JC, Richards JP, Bächinger HP, Brennan RG, Roberts SG, Green MR, and Goodman RH (1994) Nuclear protein CBP is a coactivator for the transcription factor CREB. *Nature* **370**:223–6.

Langhans-Rajasekaran SA, Wan Y, and Huang XY (1995) Activation of Tsk and Btk tyrosine kinases by G protein beta gamma subunits. *Proc Natl Acad Sci U S A* **92**:8601–5.

Lauckner JE, Jensen JB, Chen H-Y, Lu H-C, Hille B, and Mackie K (2008) GPR55 is a cannabinoid receptor that increases intracellular calcium and inhibits M current. *Proc Natl Acad Sci U S A* **105**:2699–704.

Lebovitz HE, and Banerji MA (2005) Point: visceral adiposity is causally related to insulin resistance. *Diabetes Care* **28**:2322–5.

Lee C-W, Rivera R, Dubin AE, and Chun J (2007) LPA(4)/GPR23 is a lysophosphatidic acid (LPA) receptor utilizing G(s)-, G(q)/G(i)-mediated calcium signaling and G(12/13)-mediated Rho activation. *J Biol Chem* **282**:4310–7.

Lee C-W, Rivera R, Gardell S, Dubin AE, and Chun J (2006) GPR92 as a new G12/13- and Gq-coupled lysophosphatidic acid receptor that increases cAMP, LPA5. *J Biol Chem* **281**:23589–97.

Lee M, Choi S, Hallde G, Yo SJ, Schichnes D, Aponte GW, Sj Y, and Gw A (2009) P2Y5 is a Gα i , Gα 12 / 13 G protein-coupled receptor activated by lysophosphatidic acid that reduces intestinal cell adhesion. *Am J Physiol Gastrointest Liver Physiol*, **297** (4): G641–G654.

Lee MJ, Van Brocklyn JR, Thangada S, Liu CH, Hand AR, Menzeleev R, Spiegel S, and Hla T (1998) Sphingosine-1-phosphate as a ligand for the G protein-coupled receptor EDG-1. *Science* **279**:1552–5.

Lee SF, Newton C, Widen R, Friedman H, and Klein TW (2001) Differential expression of cannabinoid CB(2) receptor mRNA in mouse immune cell subpopulations and following B cell stimulation. *Eur J Pharmacol* **423**:235–41.

Lehmann DM, Seneviratne AMPB, and Smrcka A V (2008) Small molecule disruption of G protein beta gamma subunit signaling inhibits neutrophil chemotaxis and inflammation. *Mol Pharmacol* **73**:410–8.

Leung D, Saghatelian A, Simon GM, and Cravatt BF (2006) Inactivation of N-acyl phosphatidylethanolamine phospholipase D reveals multiple mechanisms for the biosynthesis of endocannabinoids. *Biochemistry* **45**:4720–6.

Li K, Fichna J, Schicho R, Saur D, Bashashati M, Mackie K, Li Y, Zimmer A, Göke B, Sharkey KA, and Storr M (2013) A role for O-1602 and G protein-coupled receptor GPR55 in the control of colonic motility in mice. *Neuropharmacology* **71**:1–9, Elsevier Ltd.

Li M, Jiang J, and Yue L (2006) Functional characterization of homo- and heteromeric channel kinases TRPM6 and TRPM7. *J Gen Physiol* **127**:525–37.

Libert F, Parmentier M, Lefort A, Dinsart C, Van Sande J, Maenhaut C, Simons MJ, Dumont JE, and Vassart G (1989) Selective amplification and cloning of four new members of the G protein-coupled receptor family. *Science* **244**:569–72.

Lichtman AH, Hawkins EG, Griffin G, and Cravatt BF (2002) Pharmacological activity of fatty acid amides is regulated, but not mediated, by fatty acid amide hydrolase in vivo. *J Pharmacol Exp Ther* **302**:73–9.

Lin X-H, Yuece B, Li Y-NY-Y, Feng Y-J, Feng J-Y, Yu L-Y, Li K, and Storr M (2011) A novel CB receptor GPR55 and its ligands are involved in regulation of gut movement in rodents. *Neurogastroenterol Motil* **23**:862–e342.

Liu J, Gao B, Mirshahi F, Sanyal AJ, Khanolkar AD, Makriyannis A, and Kunos G (2000) Functional CB_1 cannabinoid receptors in human vascular endothelial cells. *Biochem J* **346 Pt 3**:835–40.

Liu J, Wang L, Harvey-White J, Osei-Hyiaman D, Razdan R, Gong Q, Chan AC, Zhou Z, Huang BX, Kim H-Y, and Kunos G (2006) A biosynthetic pathway for anandamide. *Proc Natl Acad Sci U S A* **103**:13345–50.

Logothetis DE, Kurachi Y, Galper J, Neer EJ, and Clapham DE (1987) The beta gamma subunits of GTP-binding proteins activate the muscarinic K^+ channel in heart. *Nature* **325**:321–6.

Luttrell LM, and Lefkowitz RJ (2002) The role of beta-arrestins in the termination and transduction of G-protein-coupled receptor signals. *J Cell Sci* **115**:455–65.

Luttrell LM, Roudabush FL, Choy EW, Miller WE, Field ME, Pierce KL, and Lefkowitz RJ (2001) Activation and targeting of extracellular signal-regulated kinases by beta-arrestin scaffolds. *Proc Natl Acad Sci U S A* **98**:2449–54.

Lutz S, Freichel-Blomquist A, Yang Y, Rümenapp U, Jakobs KH, Schmidt M, and Wieland T (2005) The guanine nucleotide exchange factor p63RhoGEF, a specific link between Gq/11-coupled receptor signaling and RhoA. *J Biol Chem* **280**:11134–9.

Lytton J, Westlin M, and Hanley MR (1991) Thapsigargin inhibits the sarcoplasmic or endoplasmic reticulum Ca-ATPase family of calcium pumps. *J Biol Chem* **266**:17067–71.

Machesky LM, and Hall A (1997) Role of actin polymerization and adhesion to extracellular matrix in Rac- and Rho-induced cytoskeletal reorganization. *J Cell Biol* **138**:913–26.

Maingret F (2000) Lysophospholipids Open the Two-pore Domain Mechano-gated K^+ Channels TREK-1 and TRAAK. *J Biol Chem* **275**:10128–10133.

Marazzi J, Kleyer J, Paredes JMV, and Gertsch J (2011) Endocannabinoid content in fetal bovine sera - unexpected effects on mononuclear cells and osteoclastogenesis. *J Immunol Methods* **373**:219–28.

Mariggiò S, Sebastià J, Filippi BM, Iurisci C, Volonté C, Amadio S, De Falco V, Santoro M, and Corda D (2006) A novel pathway of cell growth regulation mediated by a PLA2alpha-derived phosphoinositide metabolite. *FASEB J* **20**:2567–9.

Marinissen MJ, and Gutkind JS (2001) G-protein-coupled receptors and signaling networks: emerging paradigms. *Trends Pharmacol Sci* **22**:368–76.

Márquez MG, Del Carmen Fernández-Tome M, Favale NO, Pescio LG, and Sterin-Speziale NB (2008) Bradykinin modulates focal adhesions and induces stress fiber remodeling in renal papillary collecting duct cells. *Am J Physiol Renal Physiol* **294**:F603–13.

Marrion N V (1997) Control of M-current. *Annu Rev Physiol* **59**:483–504.

Maruyama T, Kanaji T, Nakade S, Kanno T, and Mikoshiba K (1997) 2APB, 2-aminoethoxydiphenyl borate, a membrane-penetrable modulator of Ins(1,4,5)P3-induced Ca^{2+} release. *J Biochem* **122**:498–505.

Matsui T, Amano M, Yamamoto T, Chihara K, Nakafuku M, Ito M, Nakano T, Okawa K, Iwamatsu A, and Kaibuchi K (1996) Rho-associated kinase, a novel serine/threonine kinase, as a putative target for small GTP binding protein Rho. *EMBO J* **15**:2208–16.

McCue JM, Driscoll WJ, and Mueller GP (2008) Cytochrome c catalyzes the in vitro synthesis of arachidonoyl glycine. *Biochem Biophys Res Commun* **365**:322–7.

McCue JM, Driscoll WJ, and Mueller GP (2009) In vitro synthesis of arachidonoyl amino acids by cytochrome c. *Prostaglandins Other Lipid Mediat* **90**:42–8.

McDonald PH, Chow CW, Miller WE, Laporte SA, Field ME, Lin FT, Davis RJ, and Lefkowitz RJ (2000) Beta-arrestin 2: a receptor-regulated MAPK scaffold for the activation of JNK3. *Science* **290**:1574–7.

McHugh D, Hu SSJ, Rimmerman N, Juknat A, Vogel Z, Walker JM, and Bradshaw HB (2010) N-arachidonoyl glycine, an abundant endogenous lipid, potently drives directed cellular migration through GPR18, the putative abnormal cannabidiol receptor. *BMC Neurosci* **11**:44.

McHugh D, Page J, Dunn E, and Bradshaw HB (2012) Δ(9) -Tetrahydrocannabinol and N-arachidonyl glycine are full agonists at GPR18 receptors and induce migration in human endometrial HEC-1B cells. *Br J Pharmacol* **165**:2414–24.

McHugh D, Tanner C, Mechoulam R, Pertwee RG, and Ross RA (2008) Inhibition of human neutrophil chemotaxis by endogenous cannabinoids and phytocannabinoids: evidence for a site distinct from CB_1 and CB_2. *Mol Pharmacol* **73**:441–50.

McKillop AM, Moran BM, Abdel-Wahab YHA, and Flatt PR (2013) Evaluation of the insulin releasing and antihyperglycaemic activities of GPR55 lipid agonists using clonal beta-cells, isolated pancreatic islets and mice. *Br J Pharmacol*, doi: 10.1111/bph.12356.

Mechoulam R, Ben-Shabat S, Hanus L, Ligumsky M, Kaminski NE, Schatz AR, Gopher A, Almog S, Martin BR, and Compton DR (1995) Identification of an endogenous 2-monoglyceride, present in canine gut, that binds to cannabinoid receptors. *Biochem Pharmacol* **50**:83–90.

Mechoulam R, and Gaoni Y (1967) The absolute configuration of delta-1-tetrahydrocannabinol, the major active constituent of hashish. *Tetrahedron Lett* **8**:1109–11.

Merkler DJ, Chew GH, Gee AJ, Merkler KA, Sorondo JO, Johnson ME, March R V, Re V, Recei M, and August V (2004) Oleic acid derived metabolites in mouse neuroblastoma N18TG2 cells. *Biochemistry* **43**:12667–74.

Metz SA (1986) Lysophosphatidylinositol, but not lysophosphatidic acid, stimulates insulin release. A possible role for phospholipase A_2 but not de novo synthesis of lysophospholipid in pancreatic islet function. *Biochem Biophys Res Commun* **138**:720–727.

Meyer zu Heringdorf D, and Jakobs KH (2007) Lysophospholipid receptors: signalling, pharmacology and regulation by lysophospholipid metabolism. *Biochim Biophys Acta* **1768**:923–40.

Michalik L, Auwerx J, Berger JP, Chatterjee VK, Glass CK, Gonzalez FJ, Grimaldi PA, Kadowaki T, Lazar MA, O'Rahilly S, Palmer CNA, Plutzky J, Reddy JK, Spiegelman BM, Staels B, and Wahli W (2006) International Union of Pharmacology. LXI. Peroxisome proliferator-activated receptors. *Pharmacol Rev* **58**:726–41.

Milligan G, and Kostenis E (2006) Heterotrimeric G-proteins: a short history. *Br J Pharmacol* **147 Suppl** :S46–55.

Milman G, Maor Y, Abu-Lafi S, Horowitz M, Gallily R, Batkai S, Mo F, Offertaler L, Pacher P, Kunos G, and Mechoulam R (2006) N-arachidonoyl L-serine, an endocannabinoid-like brain constituent with vasodilatory properties. *Proc Natl Acad Sci U S A* **103**:2428–33.

Moldrich G, and Wenger T (2000) Localization of the CB_1 cannabinoid receptor in the rat brain. An immunohistochemical study. *Peptides* **21**:1735–42.

Monet M, Gkika D, Lehen'kyi V, Pourtier A, Vanden Abeele F, Bidaux G, Juvin V, Rassendren F, Humez S, and Prevarsakaya N (2009) Lysophospholipids stimulate prostate cancer cell migration via $TRPV_2$ channel activation. *Biochim Biophys Acta* **1793**:528–39.

Monet M, Lehen'kyi V, Gackiere F, Firlej V, Vandenberghe M, Roudbaraki M, Gkika D, Pourtier A, Bidaux G, Slomianny C, Delcourt P, Rassendren F, Bergerat J-P, Ceraline J, Cabon F, Humez S, and Prevarskaya N (2010) Role of cationic channel $TRPV_2$ in promoting prostate cancer migration and progression to androgen resistance. *Cancer Res* **70**:1225–35.

Moolenaar WH (1999) Bioactive lysophospholipids and their G protein-coupled receptors. *Exp Cell Res* **253**:230–8.

Moreno-Navarrete JM, Catalán V, Whyte L, Díaz-Arteaga A, Vázquez-Martínez R, Rotellar F, Guzmán R, Gómez-Ambrosi J, Pulido MR, Russell WR, Imbernón M, Ross RA, Malagón MM, Dieguez C, Fernández-Real JM, Frühbeck G, and Nogueiras R (2012) The L-α-lysophosphatidylinositol/GPR55 system and its potential role in human obesity. *Diabetes* **61**:281–91.

Mueller GP, and Driscoll WJ (2007) In vitro synthesis of oleoylglycine by cytochrome c points to a novel pathway for the production of lipid signaling molecules. *J Biol Chem* **282**:22364–9.

Mukherjee A, Wu J, Barbour S, and Fang X (2012) Lysophosphatidic acid activates lipogenic pathways and de novo lipid synthesis in ovarian cancer cells. *J Biol Chem* **287**:24990–5000.

Munro S, Thomas KL, and Abu-Shaar M (1993) Molecular characterization of a peripheral receptor for cannabinoids. *Nature* **365**:61–5.

Naderi N, Majidi M, Mousavi Z, Khoramian Tusi S, Mansouri Z, and Khodagholi F (2012) The interaction between intrathecal administration of low doses of palmitoylethanolamide and AM251 in formalin-induced pain related behavior and spinal cord IL1-β expression in rats. *Neurochem Res* **37**:778–85.

Nagasaki H, Kondo T, Fuchigami M, Hashimoto H, Sugimura Y, Ozaki N, Arima H, Ota A, Oiso Y, and Hamada Y (2012) Inflammatory changes in adipose tissue enhance expression of GPR84, a medium-chain fatty acid receptor: TNFα enhances GPR84 expression in adipocytes. *FEBS Lett* **586**:368–72.

Neer EJ (1994) G proteins: critical control points for transmembrane signals. *Protein Sci* **3**:3–14.

Neves SR, Ram PT, and Iyengar R (2002) G protein pathways. *Science* **296**:1636–9.

Nicholson KM, and Anderson NG (2002) The protein kinase B/Akt signalling pathway in human malignancy. *Cell Signal* **14**:381–95.

Nishimura A, Kitano K, Takasaki J, Taniguchi M, Mizuno N, Tago K, Hakoshima T, and Itoh H (2010) Structural basis for the specific inhibition of heterotrimeric G_q protein by a small molecule. *Proc Natl Acad Sci U S A* **107**:13666–71.

Nobes CD, and Hall A (1995) Rho, rac, and cdc42 GTPases regulate the assembly of multimolecular focal complexes associated with actin stress fibers, lamellipodia, and filopodia. *Cell* **81**:53–62.

Noguchi K, Ishii S, and Shimizu T (2003) Identification of p2y9/GPR23 as a novel G protein-coupled receptor for lysophosphatidic acid, structurally distant from the Edg family. *J Biol Chem* **278**:25600–6.

Núñez E, Benito C, Pazos MR, Barbachano A, Fajardo O, González S, Tolón RM, and Romero J (2004) Cannabinoid CB_2 receptors are expressed by perivascular microglial cells in the human brain: an immunohistochemical study. *Synapse* **53**:208–13.

O'Sullivan SE (2007) Cannabinoids go nuclear: evidence for activation of peroxisome proliferator-activated receptors. *Br J Pharmacol* **152**:576–82.

O'Sullivan SE, and Kendall D (2010) Cannabinoid activation of peroxisome proliferator-activated receptors: potential for modulation of inflammatory disease. *Immunobiology* **215**:611–6.

Oakley RH, Laporte SA, Holt JA, Barak LS, and Caron MG (1999) Association of beta-arrestin with G protein-coupled receptors during clathrin-mediated endocytosis dictates the profile of receptor resensitization. *J Biol Chem* **274**:32248–57.

Obara Y, Ueno S, Yanagihata Y, and Nakahata N (2011) Lysophosphatidylinositol Causes Neurite Retraction via GPR55, G(13) and RhoA in PC12 Cells. *PLoS One* **6**:10.

Offermanns S (2013) Free Fatty Acid (FFA) and Hydroxy Carboxylic Acid (HCA) Receptors. *Annu Rev Pharmacol Toxicol* 1–28.

Offertáler L, Mo F-M, Bátkai S, Liu J, Begg M, Razdan RK, Martin BR, Bukoski RD, and Kunos G (2003) Selective ligands and cellular effectors of a G protein-coupled endothelial cannabinoid receptor. *Mol Pharmacol* **63**:699–705.

Oh DY, Yoon JM, Moon MJ, Hwang J-I, Choe H, Lee JY, Kim J Il, Kim S, Rhim H, O'Dell DK, Walker JM, Na HS, Lee MG, Kwon HB, Kim K, and Seong JY (2008) Identification of farnesyl pyrophosphate and N-arachidonylglycine as endogenous ligands for GPR92. *J Biol Chem* **283**:21054–64.

Oka S, Kimura S, Toshida T, Ota R, Yamashita A, and Sugiura T (2010) Lysophosphatidylinositol induces rapid phosphorylation of p38 mitogen-activated protein kinase and activating transcription factor 2 in HEK293 cells expressing GPR55 and IM-9 lymphoblastoid cells. *J Biochem* **147**:671–8.

Oka S, Nakajima K, Yamashita A, Kishimoto S, and Sugiura T (2007) Identification of GPR55 as a lysophosphatidylinositol receptor. *Biochem Biophys Res Commun* **362**:928–34.

Oka S, Ota R, Shima M, Yamashita A, and Sugiura T (2010) GPR35 is a novel lysophosphatidic acid receptor. *Biochem Biophys Res Commun* **395**:232–7.

Oka S, Toshida T, Maruyama K, Nakajima K, Yamashita A, and Sugiura T (2009) 2-Arachidonoyl-sn-glycero-3-phosphoinositol: a possible natural ligand for GPR55. *J Biochem* **145**:13–20.

Oka S, Tsuchie A, Tokumura A, Muramatsu M, Suhara Y, Takayama H, Waku K, and Sugiura T (2003) Ether-linked analogue of 2-arachidonoylglycerol (noladin ether) was not detected in the brains of various mammalian species. *J Neurochem* **85**:1374–1381.

Okamoto Y, Wang J, Morishita J, and Ueda N (2007) Biosynthetic pathways of the endocannabinoid anandamide. *Chem Biodivers* **4**:1842–57.

Oldham WM, and Hamm HE (2008) Heterotrimeric G protein activation by G-protein-coupled receptors. *Nat Rev Mol Cell Biol* **9**:60–71.

Oldham WM, and Hamm HE (2006) Structural basis of function in heterotrimeric G proteins. *Q Rev Biophys* **39**:117–66.

Ovchinnikov YUA (1982) Rhodopsin and bacteriorhodopsin: structure-function relationships. *FEBS Lett* **148**:179–91.

Overton HA, Babbs AJ, Doel SM, Fyfe MCT, Gardner LS, Griffin G, Jackson HC, Procter MJ, Rasamison CM, Tang-Christensen M, Widdowson PS, Williams GM, and Reynet C (2006) Deorphanization of a G protein-coupled receptor for oleoylethanolamide and its use in the discovery of small-molecule hypophagic agents. *Cell Metab* **3**:167–75.

Palczewski K, Kumasaka T, Hori T, Behnke CA, Motoshima H, Fox BA, Le Trong I, Teller DC, Okada T, Stenkamp RE, Yamamoto M, and Miyano M (2000) Crystal structure of rhodopsin: A G protein-coupled receptor. *Science* **289**:739–45.

Park B, Gibbons HM, Mitchell MD, and Glass M (2003) Identification of the CB_1 cannabinoid receptor and fatty acid amide hydrolase (FAAH) in the human placenta. *Placenta* **24**:990–5.

Park CY, Hoover PJ, Mullins FM, Bachhawat P, Covington ED, Raunser S, Walz T, Garcia KC, Dolmetsch RE, and Lewis RS (2009) STIM1 clusters and activates CRAC channels via direct binding of a cytosolic domain to Orai1. *Cell* **136**:876–90.

Pasternack SM, von Kügelgen I, Al Aboud K, Lee Y-A, Rüschendorf F, Voss K, Hillmer AM, Molderings GJ, Franz T, Ramirez A, Nürnberg P, Nöthen MM, and Betz RC (2008) G protein-coupled receptor P2Y5 and its ligand LPA are involved in maintenance of human hair growth. *Nat Genet* **40**:329–34.

Paterniti I, Impellizzeri D, Crupi R, Morabito R, Campolo M, Esposito E, and Cuzzocrea S (2013) Molecular evidence for the involvement of PPAR-δ and PPAR-γ in anti-inflammatory and neuroprotective activities of palmitoylethanolamide after spinal cord trauma. *J Neuroinflammation* **10 (1)**:1-13.

Pérez-Gómez E, Andradas C, Flores JM, Quintanilla M, Paramio JM, Guzmán M, and Sánchez C (2013) The orphan receptor GPR55 drives skin carcinogenesis and is upregulated in human squamous cell carcinomas. *Oncogene* **32**:2534–42.

Pertwee RG (2006) The pharmacology of cannabinoid receptors and their ligands: an overview. *Int J Obes (Lond)* **30 Suppl 1**:S13–8.

Pertwee RG, Fernando SR, Nash JE, and Coutts a a (1996) Further evidence for the presence of cannabinoid CB1 receptors in guinea-pig small intestine. *Br J Pharmacol* **118**:2199–205.

Pertwee RG, Howlett AC, Abood ME, Alexander SPH, Marzo V Di, Elphick MR, Greasley PJ, Hansen HS, and Kunos G (2010) International Union of Basic and Clinical Pharmacology . LXXIX . Cannabinoid Receptors and Their Ligands : Beyond CB_1 and CB_2. *Pharmacol Rev* **62**:588–631.

Petersen OH, Michalak M, and Verkhratsky A (2005) Calcium signalling: past, present and future. *Cell Calcium* **38**:161–9.

Petitet F, Donlan M, and Michel A (2006) GPR55 as a new cannabinoid receptor: still a long way to prove it. *Chem Biol Drug Des* **67**:252–3.

Pietr M, Kozela E, Levy R, Rimmerman N, Lin YH, Stella N, Vogel Z, and Juknat A (2009) Differential changes in GPR55 during microglial cell activation. *FEBS Lett* **583**:2071–6.

Piñeiro R, and Falasca M (2012) Lysophosphatidylinositol signalling: new wine from an old bottle. *Biochim Biophys Acta* **1821**:694–705.

Piñeiro R, Maffucci T, and Falasca M (2011) The putative cannabinoid receptor GPR55 defines a novel autocrine loop in cancer cell proliferation. *Oncogene* **30**:142–52.

Piomelli D, Astarita G, and Rapaka R (2007) A neuroscientist's guide to lipidomics. *Nat Rev Neurosci* **8**:743–54.

Porter AC, Sauer J-M, Knierman MD, Becker GW, Berna MJ, Bao J, Nomikos GG, Carter P, Bymaster FP, Leese AB, and Felder CC (2002) Characterization of a novel endocannabinoid, virodhamine, with antagonist activity at the CB_1 receptor. *J Pharmacol Exp Ther* **301**:1020–4.

Potapova TA, Sivakumar S, Flynn JN, Li R, and Gorbsky GJ (2011) Mitotic progression becomes irreversible in prometaphase and collapses when Wee1 and Cdc25 are inhibited. *Mol Biol Cell* **22**:1191–206.

Pouysségur J, Volmat V, and Lenormand P (2002) Fidelity and spatio-temporal control in MAP kinase (ERKs) signalling. *Biochem Pharmacol* **64**:755–63.

Prakriya M, Feske S, Gwack Y, Srikanth S, Rao A, and Hogan PG (2006) Orai1 is an essential pore subunit of the CRAC channel. *Nature* **443**:230–3.

Price MR, Baillie GL, Thomas A, Stevenson LA, Easson M, Goodwin R, McLean A, McIntosh L, Goodwin G, Walker G, Westwood P, Marrs J, Thomson F, Cowley P, Christopoulos A, Pertwee RG, and Ross RA (2005) Allosteric modulation of the cannabinoid CB_1 receptor. *Mol Pharmacol* **68**:1484–95.

Pullikuth AK, and Catling AD (2010) Extracellular signal-regulated kinase promotes Rho-dependent focal adhesion formation by suppressing p190A RhoGAP. *Mol Cell Biol* **30**:3233–48.

Qin Y, Verdegaal EME, Siderius M, Bebelman JP, Smit MJ, Leurs R, Willemze R, Tensen CP, and Osanto S (2011) Quantitative expression profiling of G-protein-coupled receptors (GPCRs) in metastatic melanoma: the constitutively active orphan GPCR GPR18 as novel drug target. *Pigment Cell Melanoma Res* **24**:207–18.

Radhika V, and Dhanasekaran N (2001) Transforming G proteins. *Oncogene* **20**:1607–14.

Rao GK, and Kaminski NE (2006) Cannabinoid-mediated elevation of intracellular calcium: a structure-activity relationship. *J Pharmacol Exp Ther* **317**:820–9.

Rappoport JZ, Heyman KP, Kemal S, and Simon SM (2008) Dynamics of dynamin during clathrin mediated endocytosis in PC12 cells. *PLoS One* **3**:e2416.

Rask-Andersen M, Almén MS, and Schiöth HB (2011) Trends in the exploitation of novel drug targets. *Nat Rev Drug Discov* **10**:579–90.

Ribeiro CM, Reece J, and Putney JW (1997) Role of the cytoskeleton in calcium signaling in NIH 3T3 cells. An intact cytoskeleton is required for agonist-induced $[Ca^{2+}]_i$ signaling, but not for capacitative calcium entry. *J Biol Chem* **272**:26555–61.

Richardson D, Ortori CA, Chapman V, Kendall DA, and Barrett DA (2007) Quantitative profiling of endocannabinoids and related compounds in rat brain using liquid chromatography-tandem electrospray ionization mass spectrometry. *Anal Biochem* **360**:216–26.

Ridley AJ, and Hall A (1992) The small GTP-binding protein Rho regulates the assembly of focal adhesions and actin stress fibers in response to growth factors. *Cell* **70**:389–99.

Ridley AJ, Schwartz MA, Burridge K, Firtel RA, Ginsberg MH, Borisy G, Parsons JT, and Horwitz AR (2003) Cell migration: integrating signals from front to back. *Science* **302**:1704–9.

Rimmerman N, Bradshaw HB, Hughes HV, Chen JS, Hu SS, McHugh D, Vefring E, Jahnsen JA, Thompson EL, Masuda K, Cravatt BF, Burstein S, Vasko MR, Prieto AL, O'Dell DK, and Walker JM (2008) N-palmitoyl glycine, a novel endogenous lipid that acts as a modulator of calcium influx and nitric oxide production in sensory neurons. *Mol Pharmacol* **74**:213–24.

Ringer S (1883) A further Contribution regarding the influence of the different Constituents of the Blood on the Contraction of the Heart. *J Physiol* **4**:29–42.3.

Rodbell M, Birnbaumer L, Pohl SL, and Krans HM (1971) The glucagon-sensitive adenyl cyclase system in plasma membranes of rat liver. V. An obligatory role of guanylnucleotides in glucagon action. *J Biol Chem* **246**:1877–82.

Rojo ML, Rodriguez-Gaztelumendi A, and Fowler CJ (2012) Lysophosphatidylinositol stimulates [^{35}S]GTPγS binding in the rat prefrontal cortex and hippocampus. *Neurochem Res* **37**:1037–42.

Romero-Zerbo SY, Rafacho A, Díaz-Arteaga A, Suárez J, Quesada I, Imbernon M, Ross RA, Dieguez C, Rodríguez de Fonseca F, Nogueiras R, Nadal A, and Bermúdez-Silva FJ (2011) A role for the putative cannabinoid receptor GPR55 in the islets of Langerhans. *J Endocrinol* **211**:177–85.

Roos J, DiGregorio PJ, Yeromin A V, Ohlsen K, Lioudyno M, Zhang S, Safrina O, Kozak JA, Wagner SL, Cahalan MD, Veliçelebi G, and Stauderman K a (2005) STIM1, an essential and conserved component of store-operated Ca2+ channel function. *J Cell Biol* **169**:435–45.

Ross GR, Lichtman A, Dewey WL, and Akbarali HI (2012) Evidence for the putative cannabinoid receptor (GPR55)-mediated inhibitory effects on intestinal contractility in mice. *Pharmacology* **90**:55–65.

Ross RA (2011) L-α-lysophosphatidylinositol meets GPR55: a deadly relationship. *Trends Pharmacol Sci* **32**:265–9.

Ross RA (2009) The enigmatic pharmacology of GPR55. *Trends Pharmacol Sci* **30**:156–63.

Ruiz-Llorente L, Sánchez MG, Carmena MJ, Prieto JC, Sánchez-Chapado M, Izquierdo A, and Díaz-Laviada I (2003) Expression of functionally active cannabinoid receptor CB_1 in the human prostate gland. *Prostate* **54**:95–102.

Russo EB (2007) History of cannabis and its preparations in saga, science, and sobriquet. *Chem Biodivers* **4**:1614–48.

Ryberg E, Larsson N, Sjögren S, Hjorth S, Hermansson N-O, Leonova J, Elebring T, Nilsson K, Drmota T, and Greasley PJ (2007) The orphan receptor GPR55 is a novel cannabinoid receptor. *Br J Pharmacol* **152**:1092–101.

Sands WA, and Palmer TM (2008) Regulating gene transcription in response to cyclic AMP elevation. *Cell Signal* **20**:460–6.

Sawzdargo M, George SR, Nguyen T, Xu S, Kolakowski LF, and O'Dowd BF (1997) A cluster of four novel human G protein-coupled receptor genes occurring in close proximity to CD22 gene on chromosome 19q13.1. *Biochem Biophys Res Commun* **239**:543–547.

Sawzdargo M, Nguyen T, Lee DK, Lynch KR, Cheng R, Heng HH, George SR, and O'Dowd BF (1999) Identification and cloning of three novel human G protein-coupled receptor genes GPR52, PsiGPR53 and GPR55: GPR55 is extensively expressed in human brain. *Brain Res Mol Brain Res* **64**:193–8.

Schicho R, Bashashati M, Bawa M, McHugh D, Saur D, Hu H, Zimmer A, Lutz B, Mackie K, Bradshaw HB, McCafferty D-M, Sharkey KA, and Storr M (2011) The atypical cannabinoid O-1602 protects against experimental colitis and inhibits neutrophil recruitment. *Inflamm Bowel Dis* **17**:1651–64.

Schlyer S, and Horuk R (2006) I want a new drug: G-protein-coupled receptors in drug development. *Drug Discov Today* **11**:481–93.

Schuelert N, and McDougall JJ (2011) The abnormal cannabidiol analogue O-1602 reduces nociception in a rat model of acute arthritis via the putative cannabinoid receptor GPR55. *Neurosci Lett* **500**:72–6.

Schwaninger M, Lux G, Blume R, Oetjen E, Hidaka H, and Knepel W (1993) Membrane depolarization and calcium influx induce glucagon gene transcription in pancreatic islet cells through the cyclic AMP-responsive element. *J Biol Chem* **268**:5168–77.

Scuderi C, Valenza M, Stecca C, Esposito G, Carratù MR, and Steardo L (2012) Palmitoylethanolamide exerts neuroprotective effects in mixed neuroglial cultures and organotypic hippocampal slices via peroxisome proliferator-activated receptor-α. *J Neuroinflammation* **9**:49.

Sedláková I, Vávrová J, Tošner J, and Hanousek L (2011) Lysophosphatidic acid (LPA)—a perspective marker in ovarian cancer. *Tumour Biol* **32**:311–6.

Sergeeva M, Ubl JJ, and Reiser G (2000) Disruption of actin cytoskeleton in cultured rat astrocytes suppresses ATP- and bradykinin-induced $[Ca^{(2+)}]_{(i)}$ oscillations by reducing the coupling efficiency between $Ca^{(2+)}$ release, capacitative $Ca^{(2+)}$ entry, and store refilling. *Neuroscience* **97**:765–9.

Sharir H, Console-Bram L, Mundy C, Popoff SN, Kapur A, and Abood ME (2012) The endocannabinoids anandamide and virodhamine modulate the activity of the candidate cannabinoid receptor GPR55. *J Neuroimmune Pharmacol* **7**:856–65.

Shen Z, Wu M, Elson P, Kennedy a W, Belinson J, Casey G, and Xu Y (2001) Fatty acid composition of lysophosphatidic acid and lysophosphatidylinositol in plasma from patients with ovarian cancer and other gynecological diseases. *Gynecol Oncol* **83**:25–30.

Sheng M, McFadden G, and Greenberg ME (1990) Membrane depolarization and calcium induce c-fos transcription via phosphorylation of transcription factor CREB. *Neuron* **4**:571–82.

Sheng M, Thompson MA, and Greenberg ME (1991) CREB: a Ca^{2+}-regulated transcription factor phosphorylated by calmodulin-dependent kinases. *Science* **252**:1427–30.

Shenoy SK, Drake MT, Nelson CD, Houtz DA, Xiao K, Madabushi S, Reiter E, Premont RT, Lichtarge O, and Lefkowitz RJ (2006) beta-arrestin-dependent, G protein-independent ERK1/2 activation by the beta2 adrenergic receptor. *J Biol Chem* **281**:1261–73.

Sheskin T, Hanus L, Slager J, Vogel Z, and Mechoulam R (1997) Structural requirements for binding of anandamide-type compounds to the brain cannabinoid receptor. *J Med Chem* **40**:659–67.

Shinomura T, Asaoka Y, Oka M, Yoshida K, and Nishizuka Y (1991) Synergistic action of diacylglycerol and unsaturated fatty acid for protein kinase C activation: its possible implications. *Proc Natl Acad Sci U S A* **88**:5149–53.

Shoemaker JL, Joseph BK, Ruckle MB, Mayeux PR, and Prather PL (2005) The endocannabinoid noladin ether acts as a full agonist at human CB_2 cannabinoid receptors. *J Pharmacol Exp Ther* **314**:868–75.

Shrestha SS, Parmar M, Kennedy C, and Bushell TJ (2010) Two-pore potassium ion channels are inhibited by both $G_{q/11}$- and G_i-coupled P2Y receptors. *Mol Cell Neurosci* **43**:363–9.

Simon GM, and Cravatt BF (2008) Anandamide biosynthesis catalyzed by the phosphodiesterase GDE1 and detection of glycerophospho-N-acyl ethanolamine precursors in mouse brain. *J Biol Chem* **283**:9341–9.

Simon GM, and Cravatt BF (2010) Characterization of mice lacking candidate N-acyl ethanolamine biosynthetic enzymes provides evidence for multiple pathways that contribute to endocannabinoid production in vivo. *Mol Biosyst* **6**:1411–8.

Singer SJ, and Nicolson GL (1972) The fluid mosaic model of the structure of cell membranes. *Science* **175**:720–31.

Singer SJ, and Nicolson GL (1971) The structure and chemistry of mammalian cell membranes. *Am J Pathol* **65**:427–37.

Sisay S, Pryce G, Jackson SJ, Tanner C, Ross RA, Michael GJ, Selwood DL, Giovannoni G, and Baker D (2013) Genetic Background Can Result in a Marked or Minimal Effect of Gene Knockout (GPR55 and CB_2 Receptor) in Experimental Autoimmune Encephalomyelitis Models of Multiple Sclerosis. *PLoS One* **8** (10):e76907.

Small J V, Kaverina I, Krylyshkina O, and Rottner K (1999) Cytoskeleton cross-talk during cell motility. *FEBS Lett* **452**:96–9.

Small-Howard AL, Shimoda LMN, Adra CN, and Turner H (2005) Anti-inflammatory potential of CB1-mediated cAMP elevation in mast cells. *Biochem J* **388**:465–73.

Smart D, Gunthorpe MJ, Jerman JC, Nasir S, Gray J, Muir AI, Chambers JK, Randall AD, and Davis JB (2000) The endogenous lipid anandamide is a full agonist at the human vanilloid receptor (hVR1). *Br J Pharmacol* **129**:227–30.

Smilenov LB (1999) Focal Adhesion Motility Revealed in Stationary Fibroblasts. *Science*, **286**:1172–1174.

Smoum R, Bar A, Tan B, Milman G, Attar-Namdar M, Ofek O, Stuart JM, Bajayo A, Tam J, Kram V, O'Dell D, Walker MJ, Bradshaw HB, Bab I, and Mechoulam R (2010) Oleoyl serine, an endogenous N-acyl amide, modulates bone remodeling and mass. *Proc Natl Acad Sci U S A* **107**:17710–5.

Soga T, Ohishi T, Matsui T, Saito T, Matsumoto M, Takasaki J, Matsumoto S-I, Kamohara M, Hiyama H, Yoshida S, Momose K, Ueda Y, Matsushime H, Kobori M, and Furuichi K (2005) Lysophosphatidylcholine enhances glucose-dependent insulin secretion via an orphan G-protein-coupled receptor. *Biochem Biophys Res Commun* **326**:744–51.

Soh JW, Lee EH, Prywes R, and Weinstein IB (1999) Novel roles of specific isoforms of protein kinase C in activation of the c-fos serum response element. *Mol Cell Biol* **19**:1313–24.

Southern C, Cook JM, Neetoo-Isseljee Z, Taylor DL, Kettleborough CA, Merritt A, Bassoni DL, Raab WJ, Quinn E, Wehrman TS, Davenport AP, Brown AJ, Green A, Wigglesworth MJ, and Rees S (2013) Screening β-arrestin recruitment for the identification of natural ligands for orphan G-protein-coupled receptors. *J Biomol Screen* **18**:599–609.

Spiegel S, and Milstien S (2003) Sphingosine-1-phosphate: an enigmatic signalling lipid. *Nat Rev Mol Cell Biol* **4**:397–407.

Stadel JM, Wilson S, and Bergsma DJ (1997) Orphan G protein-coupled receptors: a neglected opportunity for pioneer drug discovery. *Trends Pharmacol Sci* **18**:430–7.

Starowicz K, Nigam S, and Di Marzo V (2007) Biochemistry and pharmacology of endovanilloids. *Pharmacol Ther* **114**:13–33.

Staton PC, Hatcher JP, Walker DJ, Morrison AD, Shapland EM, Hughes JP, Chong E, Mander PK, Green PJ, Billinton A, Fulleylove M, Lancaster HC, Smith JC, Bailey LT, Wise A, Brown AJ, Richardson JC, and Chessell IP (2008) The putative cannabinoid receptor GPR55 plays a role in mechanical hyperalgesia associated with inflammatory and neuropathic pain. *Pain* **139**:225–36.

Steelman LS, Chappell WH, Abrams SL, Kempf RC, Long J, Laidler P, Mijatovic S, Maksimovic-Ivanic D, Stivala F, Mazzarino MC, Donia M, Fagone P, Malaponte G, Nicoletti F, Libra M, Milella M, Tafuri A, Bonati A, Bäsecke J, Cocco L, Evangelisti C, Martelli AM, Montalto G, Cervello M, and McCubrey JA (2011) Roles of the Raf/MEK/ERK and PI3K/PTEN/Akt/mTOR pathways in controlling growth and sensitivity to therapy-implications for cancer and aging. *Aging (Albany NY)* **3**:192–222.

Stella N, Schweitzer P, and Piomelli D (1997) A second endogenous cannabinoid that modulates long-term potentiation. *Nature* **388**:773–8.

Stoddart LA, Smith NJ, and Milligan G (2008) International Union of Pharmacology. LXXI. Free fatty acid receptors FFA1, -2, and -3: pharmacology and pathophysiological functions. *Pharmacol Rev* **60**:405–17.

Succar R, Mitchell VA, and Vaughan CW (2007) Actions of N-arachidonyl-glycine in a rat inflammatory pain model. *Mol Pain* **3**:24.

Sugiura T, Kondo S, Kishimoto S, Miyashita T, Nakane S, Kodaka T, Suhara Y, Takayama H, and Waku K (2000) Evidence That 2-Arachidonoylglycerol but Not N-Palmitoylethanolamine or Anandamide Is the Physiological Ligand for the Cannabinoid CB2 Receptor. Comparison Of The Agonistic Activities Of Various Cannabinoid Receptor Ligands In Hl-60 Cells. *J Biol Chem* **275**:605–12.

Sugiura T, Kondo S, Sukagawa A, Nakane S, Shinoda A, Itoh K, Yamashita A, and Waku K (1995) 2-Arachidonoylglycerol: A Possible Endogenous Cannabinoid Receptor Ligand in Brain, *Biochem Biophys Res Commun* **215** (1):89-97.

Sun P, Enslen H, Myung PS, and Maurer RA (1994) Differential activation of CREB by Ca^{2+}/calmodulin-dependent protein kinases type II and type IV involves phosphorylation of a site that negatively regulates activity. *Genes Dev* **8**:2527–39.

Sutherland EW (1972) Studies on the mechanism of hormone action. *Science* **177**:401–8.

Sutherland EW, And Wosilait WD (1955) Inactivation and Activation of Liver Phosphorylase. *Nature* **175**:169–170.

Sutphen R, Xu Y, Wilbanks GD, Fiorica J, Grendys EC, LaPolla JP, Arango H, Hoffman MS, Martino M, Wakeley K, Griffin D, Blanco RW, Cantor AB, Xiao Y, and Krischer JP (2004) Lysophospholipids are potential biomarkers of ovarian cancer. *Cancer Epidemiol Biomarkers Prev* **13**:1185–91.

Suzuki N, Nakamura S, Mano H, and Kozasa T (2003) Galpha 12 activates Rho GTPase through tyrosine-phosphorylated leukemia-associated RhoGEF. *Proc Natl Acad Sci U S A* **100**:733–8.

Svoboda P, Teisinger J, Novotný J, Bourová L, Drmota T, Hejnová L, Moravcová Z, Lisý V, Rudajev V, Stöhr J, Vokurková A, Svandová I, and Durchánková D (2004) Biochemistry of transmembrane signaling mediated by trimeric G proteins. *Physiol Res* **53 Suppl 1**:S141–52.

Sylantyev S, Jensen TP, Ross RA., and Rusakov DA. (2013) Cannabinoid- and lysophosphatidylinositol-sensitive receptor GPR55 boosts neurotransmitter release at central synapses. *Proc Natl Acad Sci*, **110**(13):5193-8.

Takasaki J, Saito T, Taniguchi M, Kawasaki T, Moritani Y, Hayashi K, and Kobori M (2004) A novel Galphaq/11-selective inhibitor. *J Biol Chem* **279**:47438–45.

Takashima S-I, Sugimoto N, Takuwa N, Okamoto Y, Yoshioka K, Takamura M, Takata S, Kaneko S, and Takuwa Y (2008) G12/13 and Gq mediate $S1P_2$-induced inhibition of Rac and migration in vascular smooth muscle in a manner dependent on Rho but not Rho kinase. *Cardiovasc Res* **79**:689–97.

Tamura M, Nakao H, Yoshizaki H, Shiratsuchi M, Shigyo H, Yamada H, Ozawa T, Totsuka J, and Hidaka H (2005) Development of specific Rho-kinase inhibitors and their clinical application. *Biochim Biophys Acta* **1754**:245–52.

Tan B, O'Dell DK, Yu YW, Monn MF, Hughes HV, Burstein S, and Walker JM (2010) Identification of endogenous acyl amino acids based on a targeted lipidomics approach. *J Lipid Res* **51**:112–9.

Tang X, Sun Z, Runne C, Madsen J, Domann F, Henry M, Lin F, and Chen S (2011) A critical role of Gbetagamma in tumorigenesis and metastasis of breast cancer. *J Biol Chem* **286**:13244–54.

Taniguchi M, Nagai K, Arao N, Kawasaki T, Saito T, Moritani Y, Takasaki J, Hayashi K, Fujita S, Suzuki K, and Tsukamoto S (2003) YM-254890, a novel platelet aggregation inhibitor produced by Chromobacterium sp. QS3666. *J Antibiot (Tokyo)* **56**:358–63.

Tantivejkul K, Kalikin LM, and Pienta KJ (2004) Dynamic process of prostate cancer metastasis to bone. *J Cell Biochem* **91**:706–17.

Thastrup O, Cullen PJ, Drøbak BK, Hanley MR, and Dawson a P (1990) Thapsigargin, a tumor promoter, discharges intracellular Ca^{2+} stores by specific inhibition of the endoplasmic reticulum $Ca^{2(+)}$-ATPase. *Proc Natl Acad Sci U S A* **87**:2466–70.

Thomas A, Baillie GL, Phillips a M, Razdan RK, Ross RA, and Pertwee RG (2007) Cannabidiol displays unexpectedly high potency as an antagonist of CB_1 and CB_2 receptor agonists in vitro. *Br J Pharmacol* **150**:613–23.

Tigyi G, and Miledi R (1992) Lysophosphatidates bound to serum albumin activate membrane currents in Xenopus oocytes and neurite retraction in PC12 pheochromocytoma cells. *J Biol Chem* **267**:21360–7.

Tohgo A, Pierce KL, Choy EW, Lefkowitz RJ, and Luttrell LM (2002) beta-Arrestin scaffolding of the ERK cascade enhances cytosolic ERK activity but inhibits ERK-mediated transcription following angiotensin AT1a receptor stimulation. *J Biol Chem* **277**:9429–36.

Tokumitsu H, Chijiwa T, Hagiwara M, Mizutani A, Terasawa M, and Hidaka H (1990) KN-62, 1-[N,O-bis(5-isoquinolinesulfonyl)-N-methyl-L-tyrosyl]-4-phenylpiperazine, a specific inhibitor of Ca^{2+}/calmodulin-dependent protein kinase II. *J Biol Chem* **265**:4315–20.

Tominaga M, Caterina MJ, Malmberg a B, Rosen TA, Gilbert H, Skinner K, Raumann BE, Basbaum a I, and Julius D (1998) The cloned capsaicin receptor integrates multiple pain-producing stimuli. *Neuron* **21**:531–43.

Tsutsumi T, Kobayashi T, Ueda H, Yamauchi E, Watanabe S, and Okuyama H (1994) Lysophosphoinositide-specific phospholipase C in rat brain synaptic plasma membranes. *Neurochem Res* **19**:399–406.

Ubersax JA, and Ferrell JE (2007) Mechanisms of specificity in protein phosphorylation. *Nat Rev Mol Cell Biol* **8**:530–41.

Uhlén P, and Fritz N (2010) Biochemistry of calcium oscillations. *Biochem Biophys Res Commun* **396**:28–32.

Urban JD, Clarke WP, von Zastrow M, Nichols DE, Kobilka B, Weinstein H, Javitch JA, Roth BL, Christopoulos A, Sexton PM, Miller KJ, Spedding M, and Mailman RB (2007) Functional selectivity and classical concepts of quantitative pharmacology. *J Pharmacol Exp Ther* **320**:1–13.

Vaccani A, Massi P, Colombo A, Rubino T, and Parolaro D (2005) Cannabidiol inhibits human glioma cell migration through a cannabinoid receptor-independent mechanism. *Br J Pharmacol* **144**:1032–6.

Vaiskunaite R, Adarichev V, Furthmayr H, Kozasa T, Gudkov a, and Voyno-Yasenetskaya T a (2000) Conformational activation of radixin by G_{13} protein alpha subunit. *J Biol Chem* **275**:26206–12.

Valerius NH, Stendahl O, Hartwig JH, and Stossel TP (1981) Distribution of actin-binding protein and myosin in polymorphonuclear leukocytes during locomotion and phagocytosis. *Cell* **24**:195–202.

Van Sickle MD, Duncan M, Kingsley PJ, Mouihate A, Urbani P, Mackie K, Stella N, Makriyannis A, Piomelli D, Davison JS, Marnett LJ, Di Marzo V, Pittman QJ, Patel KD, and Sharkey K a (2005) Identification and functional characterization of brainstem cannabinoid CB2 receptors. *Science* **310**:329–32.

Veale EL, Kennard LE, Sutton GL, MacKenzie G, Sandu C, and Mathie A (2007) G(alpha)q-mediated regulation of TASK3 two-pore domain potassium channels: the role of protein kinase C. *Mol Pharmacol* **71**:1666–75.

Vogt PK (2001) PI 3-kinase, mTOR, protein synthesis and cancer. *Trends Mol Med* **7**:482–4.

Vogt S, Grosse R, Schultz G, and Offermanns S (2003) Receptor-dependent RhoA activation in G12/G13-deficient cells: genetic evidence for an involvement of Gq/G11. *J Biol Chem* **278**:28743–9.

Vriens J, Appendino G, and Nilius B (2009) Pharmacology of vanilloid transient receptor potential cation channels. *Mol Pharmacol* **75**:1262–79.

Vuong L a Q, Mitchell V a, and Vaughan CW (2008) Actions of N-arachidonyl-glycine in a rat neuropathic pain model. *Neuropharmacology* **54**:189–93.

Wacker D, Wang C, Katritch V, Han GW, Huang X-P, Vardy E, McCorvy JD, Jiang Y, Chu M, Siu FY, Liu W, Xu HE, Cherezov V, Roth BL, and Stevens RC (2013) Structural features for functional selectivity at serotonin receptors. *Science* **340**:615–9.

Wade CB (2003) Estrogen Activation of Cyclic Adenosine 5'-Monophosphate Response Element-Mediated Transcription Requires the Extracellularly Regulated Kinase/Mitogen-Activated Protein Kinase Pathway. *Endocrinology* **144**:832–838.

Wadzinski BE, Wheat WH, Jaspers S, Peruski LF, Lickteig RL, Johnson GL, and Klemm DJ (1993) Nuclear protein phosphatase $_{2A}$ dephosphorylates protein kinase A-phosphorylated CREB and regulates CREB transcriptional stimulation. *Mol Cell Biol* **13**:2822–34.

Waldeck-Weiermair M, Zoratti C, Osibow K, Balenga N, Goessnitzer E, Waldhoer M, Malli R, and Graier WF (2008) Integrin clustering enables anandamide-induced Ca^{2+} signaling in endothelial cells via GPR55 by protection against CB1-receptor-triggered repression. *J Cell Sci* **121**:1704–17.

Walter L, Franklin A, Witting A, Wade C, Xie Y, Kunos G, Mackie K, and Stella N (2003) Nonpsychotropic cannabinoid receptors regulate microglial cell migration. *J Neurosci* **23**:1398–405.

Waxham MN, and Aronowski J (1993) Ca2+/calmodulin-dependent protein kinase II is phosphorylated by protein kinase C in vitro. *Biochemistry* **32**:2923–30.

Webb DJ, Donais K, Whitmore LA, Thomas SM, Turner CE, Parsons JT, and Horwitz AF (2004) FAK-Src signalling through paxillin, ERK and MLCK regulates adhesion disassembly. *Nat Cell Biol* **6**:154–61.

Wehrle-Haller B, and Imhof BA (2003) Actin, microtubules and focal adhesion dynamics during cell migration. *Int J Biochem Cell Biol* **35**:39–50.

Wenk MR (2005) The emerging field of lipidomics. *Nat Rev Drug Discov* **4**:594–610.

Werth DK, and Pastan I (1984) Vinculin phosphorylation in response to calcium and phorbol esters in intact cells. *J Biol Chem* **259**:5264–70.

Wheeler AP, and Ridley AJ (2004) Why three Rho proteins? RhoA, RhoB, RhoC, and cell motility. *Exp Cell Res* **301**:43–9.

White JF, Noinaj N, Shibata Y, Love J, Kloss B, Xu F, Gvozdenovic-Jeremic J, Shah P, Shiloach J, Tate CG, and Grisshammer R (2012) Structure of the agonist-bound neurotensin receptor. *Nature* **490**:508–13.

Whyte LS, Ford L, Ridge SA, Cameron GA, Rogers MJ, and Ross RA (2012) Cannabinoids and bone: endocannabinoids modulate human osteoclast function in vitro. *Br J Pharmacol* **165**:2584–97.

Whyte LS, Ryberg E, Sims NA, Ridge SA, Mackie K, Greasley PJ, Ross RA, and Rogers MJ (2009) The putative cannabinoid receptor GPR55 affects osteoclast function in vitro and bone mass in vivo. *Proc Natl Acad Sci U S A* **106**:16511–6.

Woodward DF, Carling RWC, Cornell CL, Fliri HG, Martos JL, Pettit SN, Liang Y, and Wang JW (2008) The pharmacology and therapeutic relevance of endocannabinoid derived cyclo-oxygenase (COX)-2 products. *Pharmacol Ther* **120**:71–80.

Worzfeld T, Wettschureck N, and Offermanns S (2008) G(12)/G(13)-mediated signalling in mammalian physiology and disease. *Trends Pharmacol Sci* **29**:582–9.

Wu C-S, Chen H, Sun H, Zhu J, Jew CP, Wager-Miller J, Straiker A, Spencer C, Bradshaw H, Mackie K, and Lu H-C (2013) GPR55, a G-protein coupled receptor for lysophosphatidylinositol, plays a role in motor coordination. *PLoS One* **8**:e60314.

Wu MM, Buchanan J, Luik RM, and Lewis RS (2006) Ca^{2+} store depletion causes STIM1 to accumulate in ER regions closely associated with the plasma membrane. *J Cell Biol* **174**:803–13.

Wymann MP, and Schneiter R (2008) Lipid signalling in disease. *Nat Rev Mol Cell Biol* **9**:162–76.

Xiao YJ, Schwartz B, Washington M, Kennedy a, Webster K, Belinson J, and Xu Y (2001) Electrospray ionization mass spectrometry analysis of lysophospholipids in human ascitic fluids: comparison of the lysophospholipid contents in malignant vs nonmalignant ascitic fluids. *Anal Biochem* **290**:302–13.

Yamamoto KK, Gonzalez GA, Biggs WH, and Montminy MR (1988) Phosphorylation-induced binding and transcriptional efficacy of nuclear factor CREB. *Nature* **334**:494–8.

Yamashita a, Sugiura T, and Waku K (1997) Acyltransferases and transacylases involved in fatty acid remodeling of phospholipids and metabolism of bioactive lipids in mammalian cells. *J Biochem* **122**:1–16.

Yamashita A, Kumazawa T, Koga H, Suzuki N, Oka S, and Sugiura T (2010) Generation of lysophosphatidylinositol by DDHD domain containing 1 (DDHD1): Possible involvement of phospholipase D/phosphatidic acid in the activation of DDHD1. *Biochim Biophys Acta* **1801**:711–20.

Yamashita A, Oka S, Tanikawa T, Hayashi Y, Nemoto-Sasaki Y, and Sugiura T (2013) The actions and metabolism of lysophosphatidylinositol, an endogenous agonist for GPR55. *Prostaglandins Other Lipid Mediat*, **107**:103-16.

Yanagida K, Ishii S, Hamano F, Noguchi K, and Shimizu T (2007) LPA4/p2y9/GPR23 mediates Rho-dependent morphological changes in a rat neuronal cell line. *J Biol Chem* **282**:5814–24.

Yang X, Zhou G, Ren T, Li H, Zhang Y, Yin D, Qian H, and Li Q (2012) β-Arrestin prevents cell apoptosis through pro-apoptotic ERK1/2 and p38 MAPKs and anti-apoptotic Akt pathways. *Apoptosis* **17**:1019–26.

Yates ML, and Barker EL (2009) Inactivation and biotransformation of the endogenous cannabinoids anandamide and 2-arachidonoylglycerol. *Mol Pharmacol* **76**:11–7.

Yatomi Y, Ruan F, Hakomori S, and Igarashi Y (1995) Sphingosine-1-phosphate: a platelet-activating sphingolipid released from agonist-stimulated human platelets. *Blood* **86**:193–202.

Yeromin A V, Roos J, Stauderman K a, and Cahalan MD (2004) A store-operated calcium channel in Drosophila S2 cells. *J Gen Physiol* **123**:167–82.

Yin H, Chu A, Li W, Wang B, Shelton F, Otero F, Nguyen DG, Caldwell JS, and Chen YA (2009) Lipid G protein-coupled receptor ligand identification using beta-arrestin PathHunter assay. *J Biol Chem* **284**:12328–38.

Yoneda A, Multhaupt H a B, and Couchman JR (2005) The Rho kinases I and II regulate different aspects of myosin II activity. *J Cell Biol* **170**:443–53.

Yu J, Deliu E, Zhang X-Q, Hoffman NE, Carter RL, Grisanti L a, Brailoiu GC, Madesh M, Cheung JY, Force T, Abood ME, Koch WJ, Tilley DG, and Brailoiu E (2013) Differential Activation of Cultured Neonatal Cardiomyocytes by Plasmalemmal vs Intracellular G Protein-Coupled Receptor 55. *J Biol Chem* **288**(31):22481-92.

Zaidel-Bar R, Ballestrem C, Kam Z, and Geiger B (2003) Early molecular events in the assembly of matrix adhesions at the leading edge of migrating cells. *J Cell Sci* **116**:4605–13.

Zamir E, and Geiger B (2001) Molecular complexity and dynamics of cell-matrix adhesions. *J Cell Sci* **114**:3583–90.

Zanassi P, Paolillo M, Feliciello A, Avvedimento E V, Gallo V, and Schinelli S (2001) cAMP-dependent protein kinase induces cAMP-response element-binding protein phosphorylation via an intracellular calcium release/ERK-dependent pathway in striatal neurons. *J Biol Chem* **276**:11487–95.

Zhang H, Desai NN, Olivera A, Seki T, Brooker G, and Spiegel S (1991) Sphingosine-1-phosphate, a novel lipid, involved in cellular proliferation. *J Cell Biol* **114**:155–67.

Zhang SL, Yu Y, Roos J, Kozak JA, Deerinck TJ, Ellisman MH, Stauderman KA, and Cahalan MD (2005) STIM1 is a Ca2+ sensor that activates CRAC channels and migrates from the Ca^{2+} store to the plasma membrane. *Nature* **437**:902–5.

Zhang X, Maor Y, Wang JF, Kunos G, and Groopman JE (2010) Endocannabinoid-like N-arachidonoyl serine is a novel pro-angiogenic mediator. *Br J Pharmacol* **160**:1583–94.

Zhao P, and Abood ME (2013) GPR55 and GPR35 and their relationship to cannabinoid and lysophospholipid receptors. *Life Sci* **92**:453–7.

Ziegler WH, Liddington RC, and Critchley DR (2006) The structure and regulation of vinculin. *Trends Cell Biol* **16**:453–60.

Ziembicki J, Tandon R, Schelling JR, Sedor JR, Miller RT, and Huang C (2005) Mechanical force-activated phospholipase D is mediated by Galpha12/13-Rho and calmodulin-dependent kinase in renal epithelial cells. *Am J Physiol Renal Physiol* **289**:F826–34.

Zoeller R a, Wightman PD, Anderson MS, and Raetz CR (1987) Accumulation of lysophosphatidylinositol in RAW 264.7 macrophage tumor cells stimulated by lipid A precursors. *J Biol Chem* **262**:17212–20.

Zohrabian VM, Forzani B, Chau Z, Murali R, and Jhanwar-Uniyal M (2009) Rho/ROCK and MAPK signaling pathways are involved in glioblastoma cell migration and proliferation. *Anticancer Res* **29**:119–23.

Zuardi AW (2006) History of cannabis as a medicine: a review. *Rev Bras Psiquiatr* **28**:153–7.

Zygmunt PM, Petersson J, Andersson DA, Chuang H, Sørgård M, Di Marzo V, Julius D, and Högestätt ED (1999) Vanilloid receptors on sensory nerves mediate the vasodilator action of anandamide. *Nature* **400**:452–7.